frontiers | Research Topics

Emerging and reemerging plant viruses in a context of global change

Edited by
Giuseppe Parrella, Paul Leslie Guy and Toufic Elbeaino

Published in
Frontiers in Plant Science
Frontiers in Microbiology

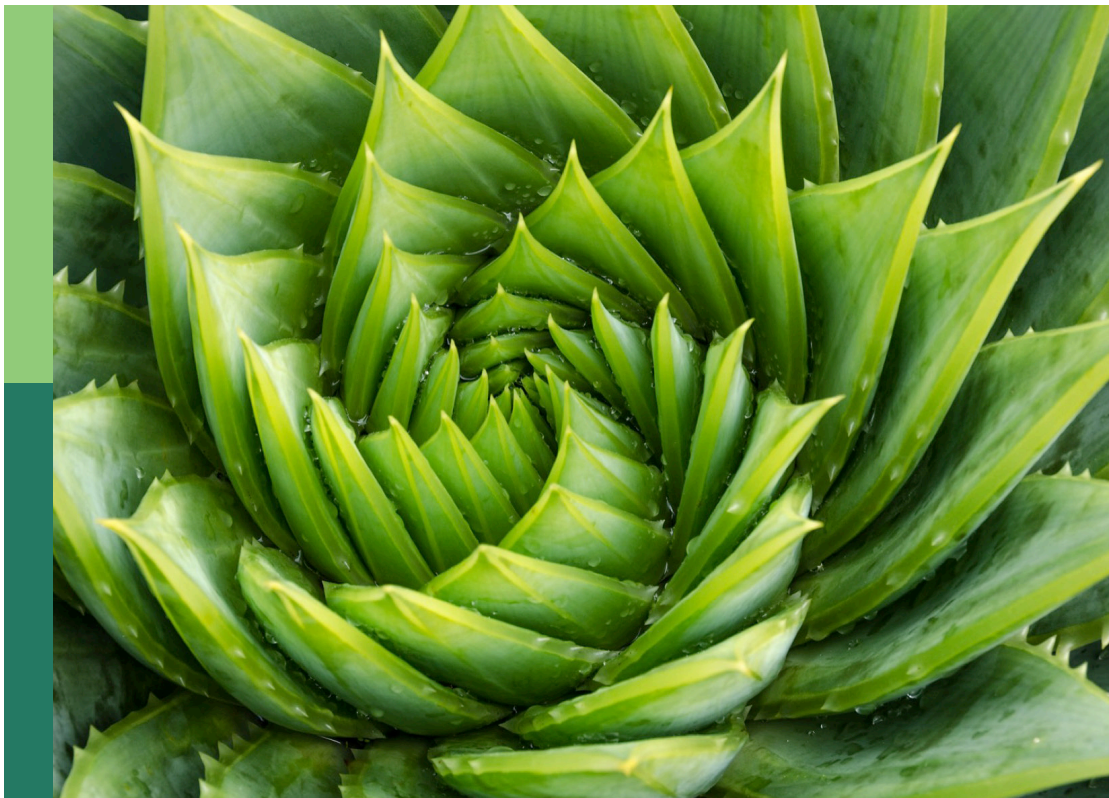

ISSN 1664-8714
ISBN 978-2-83251-316-3
DOI 10.3389/978-2-83251-316-3

About Frontiers

Frontiers is more than just an open access publisher of scholarly articles: it is a pioneering approach to the world of academia, radically improving the way scholarly research is managed. The grand vision of Frontiers is a world where all people have an equal opportunity to seek, share and generate knowledge. Frontiers provides immediate and permanent online open access to all its publications, but this alone is not enough to realize our grand goals.

Frontiers journal series

The Frontiers journal series is a multi-tier and interdisciplinary set of open-access, online journals, promising a paradigm shift from the current review, selection and dissemination processes in academic publishing. All Frontiers journals are driven by researchers for researchers; therefore, they constitute a service to the scholarly community. At the same time, the *Frontiers journal series* operates on a revolutionary invention, the tiered publishing system, initially addressing specific communities of scholars, and gradually climbing up to broader public understanding, thus serving the interests of the lay society, too.

Dedication to quality

Each Frontiers article is a landmark of the highest quality, thanks to genuinely collaborative interactions between authors and review editors, who include some of the world's best academicians. Research must be certified by peers before entering a stream of knowledge that may eventually reach the public - and shape society; therefore, Frontiers only applies the most rigorous and unbiased reviews. Frontiers revolutionizes research publishing by freely delivering the most outstanding research, evaluated with no bias from both the academic and social point of view. By applying the most advanced information technologies, Frontiers is catapulting scholarly publishing into a new generation.

What are Frontiers Research Topics?

Frontiers Research Topics are very popular trademarks of the *Frontiers journals series*: they are collections of at least ten articles, all centered on a particular subject. With their unique mix of varied contributions from Original Research to Review Articles, Frontiers Research Topics unify the most influential researchers, the latest key findings and historical advances in a hot research area.

Find out more on how to host your own Frontiers Research Topic or contribute to one as an author by contacting the Frontiers editorial office: frontiersin.org/about/contact

Emerging and reemerging plant viruses in a context of global change

Topic editors

Giuseppe Parrella — Institute for Sustainable Plant Protection of the National Research Council (IPSP-CNR), Italy

Paul Leslie Guy — University of Otago, New Zealand

Toufic Elbeaino — International Centre for Advanced Mediterranean Agronomic Studies, Italy

Citation

Parrella, G., Guy, P. L., Elbeaino, T., eds. (2023). *Emerging and reemerging plant viruses in a context of global change*. Lausanne: Frontiers Media SA.

doi: 10.3389/978-2-83251-316-3

Table of contents

frontiers | Frontiers in Plant Science

TYPE Editorial
PUBLISHED 29 December 2022
DOI 10.3389/fpls.2022.1108211

OPEN ACCESS

EDITED AND REVIEWED BY
Rajarshi Kumar Gaur,
Deen Dayal Upadhyay Gorakhpur University, India

*CORRESPONDENCE
Giuseppe Parrella
giuseppe.parrella@ipsp.cnr.it

SPECIALTY SECTION
This article was submitted to Plant Pathogen Interactions, a section of the journal Frontiers in Plant Science

RECEIVED 25 November 2022
ACCEPTED 14 December 2022
PUBLISHED 29 December 2022

CITATION
Parrella G, Elbeaino T and Guy PL (2022) Editorial: Emerging and reemerging plant viruses in a context of global change. *Front. Plant Sci.* 13:1108211. doi: 10.3389/fpls.2022.1108211

Editorial: Emerging and reemerging plant viruses in a context of global change

Giuseppe Parrella[1]*, Toufic Elbeaino[2] and Paul Leslie Guy[3]

[1]Institute for Sustainable Plant Protection, National Research Council (IPSP-CNR), Portici, Italy, [2]Mediterranean Agronomic Institute of Bari (Centre International de Hautes Études Agronomiques Méditerranéennes (CIHEAM)-Istituto Agronomico Mediterraneo di Bari (IAMB)), Valenzano, Italy, [3]Department of Botany, University of Otago, Dunedin, New Zealand

KEYWORDS

emerging viruses, climate change, globalization, invasive plants, plant viruses, vector introduction

Editorial on the Research Topic:
Emerging and reemerging plant viruses in a context of global change

Emerging and reemerging plant diseases can be defined as those diseases caused by new or reappearing pathogens which, due to their intrinsic characteristics, have the ability to spread rapidly and cause epidemics in certain agro-climatic contexts. In recent years, both DNA and RNA viruses have been implicated in important disease outbreaks in plants. The different forms of mutation, recombination and other types of genetic exchange, considered as the basis of the evolutionary forces of viruses, have undoubtedly given rise tothe genetic diversity found in plant virus populations. In this context, environmental factors play an important role in driving virus evolution. In addition, the rapid expansion of human activity in the world of commerce, agriculture, anthropization of natural ecosystems and climate change have further contributed to the instability between hosts and virus populations, favouring the emergence of viruses with mutant and/or recombinant forms, with potentially negative impacts on plants, vectors and ecosystems.

Organization of the Research Topic

This Research Topic includes three comprehensive reviews that describe different aspects related to some emerging plant viruses. The first review provides an overview ofnanoviruses (Lal et al.), an important group of emerging viruses with a destructive potential on many crops; capable of causing serious social and economic losses (Johnstone and Mclean, 1987; Hull, 2014). This review deals with nanoviruses features, providing knowledge on their genome organization, replication and their transmission mediated by different aphid species. In addition, the review focuses on the recent emergence of new nanovirus species, often associated with the expansion of their natural host range.

The second review addresses the problem of yellow mottle rice virus (YMRV) (Odongo et al.), currently causing major losses in rice production mainly in sub-Saharan Africa (SSA). This review deals with the molecular characteristics of RYMV: the genomic structure, function and gene diversity, and RYMV-host interactions. In particular, the review sheds light on mechanisms related to the qualitative resistances, controlled by three recessive genes RYMV1, RYMV2 and RYMV3, and quantitative resistances, with the description of several QTLs found in *Oryza* germplasm. Finally, since RYMV shows high genetic variability and some Oryza germplasm has low or non-durable resistance, the review suggests possible genetic improvement strategies for a significant enhancement of rice protection through the use of assisted selection with molecular markers and by employing genome editing to impair susceptibility.

The final review concerns the progress on tomato virome research (Rivarez et al.), with particular reference to the contribution provided by high-throughput sequencing (HTS). The work takes into consideration the period 2011-2020, during which 45 new viruses have been described in tomato, 14 of these identified by HTS. Based on the data present in the literature and in the databases, the authors list 312 viruses, satellite viruses, or viroid species (in 22 families and 39 genera) identified in tomato. This represents the highest number of viral and viral-like agents described in a single botanical species. The work also underlines the importance of the application of HTS for epidemiological studies, in particular for the identification of the virome of weeds and other wild plants, or for the identification of viruses in vectors, irrigation water or wastewater and soil. The HTS analysis of environmental samples helps to greatly improve the understanding of epidemiology and ecology of tomato-infecting viruses and can facilitate virus disease forecasting in order to prevent virus disease outbreaks in tomato. Finally, the review outlines the main tomato viruses, highlighting their potential threat and impact. Newly emerged viruses, such as tomato brown rugose fruit virus (ToBRFV), are capable of overcoming the *Tm*-2^2 resistance gene used to contain tobacco mosaic virus (TMV) and tomato mosaic virus (ToMV) infections in greenhouse tomatoes. Tomato spotted wilt virus (TSWV) easily overcomes the resistance mediated by the *Tsw* hypersensitivity gene in pepper with increasing temperatures. A group of emerging geminiviruses, of subtropical and tropical origins, including tomato leaf curl New Delhi virus (ToLCNDV) and tomato leaf curl virus (TYLCV), mostly are virulent at high temperatures. Their vector, *Bemisia tabaci*, is notoriously thermophilic and a highly invasive species.

This special issue also contains two articles concerning diagnostic methods for two emerging solanaceous viruses: the first work concerns the setup of loop-mediated isothermal amplification (LAMP) assays, both real time and visual, for the diagnosis of ToBRFV on leaf samples and seeds of tomato and bell pepper (Rizzo et al.). The work also highlights progress in the detection of ToBRFV, mainly regarding sensitivity, compared to previous methods. This paper also emphasizes the practical advantages deriving from the use of LAMP, since it can be applied by poorly equipped laboratories and unskilled persons at official country points of entry, providing a new diagnostic tool for phytosanitary investigations and management of ToBRFV. The second work describes an RT-qPCR assay for the diagnosis of parietaria mottle virus (PMoV), based on a specific TaqMan® probe (Panno et al.),. PMoV is considered an emerging pathogen in the Mediterranean basin on tomatoes and peppers. This virus has recently expanded its natural host range (Parrella et al., 2021). Symptoms on tomato leaves and fruits can be easily confused with those induced by cucumber mosaic virus (CMV) with necrogenic satellite RNA (CMV-satRNA), TSWV or ToMV, and since there are no commercial diagnostic kits available (serological and molecular) on the market, the incidence of PMoV has probably been underestimated up to now in both tomatoes and peppers. Although other molecular diagnostic methods for the detection of PMoV have been previously described and applied for various applications (Parrella, 2020), the diagnostic method proposed in the present work represents an important improvement in the efficiency and applicability of an easily manageable protocol. The improved sensitivity of the method detects 10 copies of ssRNA of PMoV in infected tomato.

The Research Topic also contains eight additional original research works concerning different aspects on some emerging viruses.

The paper of Fiallo-Olivè and Navas-Castillo, identifies the complete genome sequences of two novel virus-satellite complex in *Corchorus siliquosus* collected in Cuba: the begomoviruses corchorus yellow vein Cuba virus (CoYVCUV) and desmodium leaf distortion virus (DesLDD) and two deltasatellite. This is the first report of (i) a monopartite New World begomovirus found in a host other than tomato and (ii) deltasatellites found in *C. siliquosus*, thus extending the host and helper virus ranges of this recently recognized class of DNA satellites.

Tomato chlorosis virus (genus *Crinivirus*, family *Closteroviridae*) (ToCV) is expanding its geographical and host ranges associated with the emergence of whiteflies of the *Bemisia tabaci* complex (Parrella et al., 2014; Bertin et al., 2018). Fortes et al., demonstrated that it is possible to reduce the incidence of ToCV in tomato by selecting for acylsugar-producing *B. tabaci*-resistant tomatoes with type IV glandular trichomes. Candidate resistance genes in melon to the *B. tabaci*-transmitted worldwide emerging begomovirus-ToLCNDV, were identified by Sáez et al., by transcriptome analysis of the resistant WM-7 genotype and the susceptible cultivar Piñonet Piel de Sapo. Transcriptome analysis was also applied by Han et al., to identify responsible host factors for symptom enhancement in the broad bean wilt virus 2 (BBWV2) (genus *Fabavirus* in the family *Comoviridae*), an emerging virus in economically important crops worldwide. They investigated the BBWV2-pepper (*Capsicum annuum* L.)

pathosystem, using two distinct BBWV2 strains, PAP1 (a severe strain) and RP1 (a mild strain). Upregulation of several genes associated with pathogen-associated molecular pattern (PAMP)-triggered immunity (PTI) and ethylene signaling were associated only with the severe PAP1 strain, with high ethylene emission detected. Authors conclude that the activation of PTI-associated defense responses increase symptom development during BBWV2 infection in a virus strain-specific manner.

HTS analysis has been applied to study the diversity of virus (es) associated with common bean (*Phaseolus vulgaris* L.) in the North-Western Himalayan region of India by Rashid et al. Three viruses were identified: bean common mosaic virus (BCMV), bean common mosaic necrosis virus (BCMNV), and clover yellow vein virus (ClYVV), with BCMV more widespread and BCMNV and ClYVV new records from India. In another paper (Li et al.), applied HTS to characterize the virome of *Pseudostellaria heterophylla*, generated data on three novel carlaviruses and one novel amalgavirus.

Peng et al., identified and characterized interspecific recombinant viruses between zucchini tigre mosaic virus (ZTMV) and papaya ringspot virus (PRSV) in cucurbits with a novel recombination pattern detected in the HC-pro. Despite the origin from interspecific recombination, they proposed that these viruses still belong to ZTMV according to their genome characteristics; their results provide insights into the prevalence and evolution of ZTMV and PRSV in cucurbits.

The last paper concerns a complementation phenomenon between TYLCV and ToLCNDV-ES, first observed in the field and then demonstrated in the laboratory with agro-inoculations of infectious clones (Vo et al.). ToLCNDV-ES hardly infects tomato and some isolates would not at all. Nonetheless, ToLCNDV-ES in the presence of TYLCV proves to be able to multiply and infect tomatoes. In addition to the known risk of formation of recombinants between geminiviruses, this work highlights the risks of a possible expansion of the natural hosts for this group of emerging viruses thanks to the phenomena of assistance and complementation between viruses.

Conclusions

In summary, this Research Topic provides cutting-edge methodologies, research, observations and knowledge on the current scenario of *Emerging and Reemerging Viruses in the Context of Global Change*. We are deeply grateful to all the authors and reviewers who with their exceptional work have made possible the realization of this special issue. We believe that this collection will increase knowledge and awareness about the importance of emerging and reemerging viral diseases in order to improve the monitoring and the possible control that derives from them, with the aim to prevent epidemics in agricultural crops.

Author contributions

All authors listed have made a substantial, direct, and intellectual contribution to the work and approved it for publication.

Funding

This work was partially supported by the Campania Region-funded URCoFi project (Unità Regionale di Coordinamento Fitosanitario-Strengthening of the supervision activities and control of pests).

Conflict of interest

The authors declare that the research was conducted in the absence of any commercial or financial relationships that could be construed as a potential conflict of interest.

Publisher's note

References

Bertin, S., Luigi, M., Parrella, G., Giorgini, M., Davino, S., and Tomassoli, L. (2018). Survey of the distribution of *Bemisia tabaci* (Hemiptera: Aleyrodidae) in Lazio region (central italy): a threat for the northward expansion of tomato leaf curl new Delhi virus (*Begomovirus*: Geminiviridae) infection. *Phytoparasitica* 46, 171–182. doi: 10.1007/s12600-018-0649-7

Hull, R. (2014). *Plant virology. 5th edition* (London: Academic Press), 854 p.

Johnstone, G. R., and Mclean, G. D. (1987). Virus diseases of subterranean clover. *Ann. Appl. Biol.* 110, 421–440. doi: 10.1111/j.1744-7348.1987.tb03274.x

Parrella, G. (2020). Sources of resistance in wild *Solanum* germplasm (section *Lycopersicon*) to parietaria mottle virus, an emerging virus in the Mediterranean basin. *Plant Pathol.* 69, 1018–1025. doi: 10.1111/ppa.13194

Parrella, G., Nappo, A. G., Manco, E., Greco, B., and Giorgini, M. (2014). Invasion of the Q2 mitochondrial variant of Mediterranean *Bemisia tabaci* in southern Italy: possible role of bacterial endosymbionts. *Pest Manage. Sci.* 70, 1514–1523. doi: 10.1002/ps.3686

Parrella, G., Troiano, E., Stinca, A., and Pozzi, M. I. (2021). Molecular and serological detection of parietaria mottle virus in *Phytolacca americana*, a new host of the virus. *Phytopathol. Mediterr.* 60 (1), 101–104. doi: 10.36253/phyto-12207

frontiers in Microbiology

ORIGINAL RESEARCH
published: 23 July 2020
doi: 10.3389/fmicb.2020.01755

Molecular and Biological Characterization of a New World Mono-/Bipartite Begomovirus/Deltasatellite Complex Infecting *Corchorus siliquosus*

Elvira Fiallo-Olivé and Jesús Navas-Castillo**

Instituto de Hortofruticultura Subtropical y Mediterránea "La Mayora", Consejo Superior de Investigaciones Científicas - Universidad de Málaga (IHSM-CSIC-UMA), Málaga, Spain

OPEN ACCESS

Edited by:
Giuseppe Parrella,
Institute for Sustainable Plant Protection (CNR), Italy

Reviewed by:
Arvind Varsani,
Arizona State University, United States
Anders Kvarnheden,
Swedish University of Agricultural Sciences, Sweden
Emanuela Noris,
National Research Council (CNR), Italy

***Correspondence:**
Elvira Fiallo-Olivé
efiallo@eelm.csic.es
Jesús Navas-Castillo
jnavas@eelm.csic.es

Specialty section:
This article was submitted to Virology, a section of the journal Frontiers in Microbiology

Received: *01 May 2020*
Accepted: *06 July 2020*
Published: *23 July 2020*

Citation:
Fiallo-Olivé E and Navas-Castillo J (2020) Molecular and Biological Characterization of a New World Mono-/Bipartite Begomovirus/Deltasatellite Complex Infecting Corchorus siliquosus. Front. Microbiol. 11:1755. doi: 10.3389/fmicb.2020.01755

The genus *Begomovirus* (family *Geminiviridae*) is the largest genus in the entire virosphere, with more than 400 species recognized. Begomoviruses are single-stranded DNA plant viruses transmitted by whiteflies of the *Bemisia tabaci* complex and are considered one of the most important groups of emerging plant viruses in tropical and subtropical regions. Several types of DNA satellites have been described to be associated with begomoviruses: betasatellites, alphasatellites, and deltasatellites. Recently, a family of single-stranded DNA satellites associated with begomoviruses has been created, *Tolecusatellitidae*, including the genera *Betasatellite* and *Deltasatellite*. In this work, we analyzed the population of begomoviruses and associated DNA satellites present in *Corchorus siliquosus*, a malvaceous plant growing wild in Central America, southeastern North America and the Caribbean, collected in Cuba. The genomes of isolates of two New World begomoviruses [(Desmodium leaf distortion virus (DesLDV) and Corchorus yellow vein Cuba virus (CoYVCUV)] and two deltasatellites [tomato yellow leaf distortion deltasatellite 2 (TYLDD2) and Desmodium leaf distortion deltasatellite (DesLDD)] have been cloned and sequenced from plants showing yellow vein symptoms. Isolates of one of the begomoviruses, CoYVCUV, and one of the deltasatellites, DesLDD, represent novel species. Experiments with infectious clones showed the monopartite nature of CoYVCUV and that DesLDD utilizes the bipartite DesLDV as helper virus, but not the monopartite CoYVCUV. Also, CoYVCUV was shown to infect common bean in addition to *Nicotiana benthamiana*. This is the first time that (i) a monopartite New World begomovirus is found in a host other than tomato and (ii) deltasatellites have been found in *C. siliquosus*, thus extending the host and helper virus ranges of this recently recognized class of DNA satellites.

Keywords: geminiviruses, begomoviruses, DNA satellites, deltasatellites, *Corchorus siliquosus*, Malvaceae, virus taxonomy, phylogenetic analysis

INTRODUCTION

Virus diseases that have emerged in the past three decades limit the production of important vegetable and fiber crops in tropical, subtropical, and temperate regions worldwide. Many of the causal viruses are transmitted by whiteflies (Hemiptera: Aleyrodidae), mainly by those belonging to the *Bemisia tabaci* cryptic species complex. Viruses known to be transmitted by whiteflies include members of the genera *Begomovirus*, *Crinivirus*, *Ipomovirus*, *Torradovirus*, and *Carlavirus* (Navas-Castillo et al., 2011), and two poleroviruses (genus *Polerovirus*) recently reported to be transmitted by *B. tabaci* (Ghosh et al., 2019; Costa et al., 2020).

The genus *Begomovirus* (family *Geminiviridae*) is the largest genus in the entire virosphere, with more than 400 species officially recognized. Begomoviruses are transmitted by whiteflies of the *Bemisia tabaci* complex (Navas-Castillo et al., 2011; Zerbini et al., 2017) and are considered among the most important emerging plant viruses. They infect a wide range of crops and wild plants in tropical and subtropical regions (Navas-Castillo et al., 2011). Begomoviruses are circular single-stranded DNA plant viruses with twin (geminate) quasi-icosahedral virions (Zerbini et al., 2017). Begomovirus genomes can be monopartite or bipartite depending on the presence of one or two (DNA-A and DNA-B) components, each of about 2.7 kb in size. Monopartite begomoviruses are widely spread in the Old World, but only a few examples have been reported from the New World. The genomes of monopartite begomoviruses resemble the DNA-A component. The DNA-A virion-sense strand encodes the coat and pre-coat proteins; the latter being present only in begomoviruses from the Old World. The DNA-A complementary-sense strand encodes the replication-associated protein (Rep), a transcriptional activator protein, a replication enhancer protein and C4 protein. DNA-B encodes a nuclear shuttle protein on the virion-sense strand and a movement protein on the complementary-sense strand. DNA-A and DNA-B share ∼200 nt in a common region (CR), located within the intergenic region that includes the replication origin. The Rep initiates viral DNA replication by binding to reiterated motifs (iterons) present in the CR and introducing a nick into the conserved non-anucleotide TAATATTAC. The CR shows a high level of nucleotide identity between both genome components of bipartite begomoviruses. Based on the phylogenetic analysis of full-length begomovirus genomic sequences (or DNA-A sequences), begomoviruses are classified into four lineages, Old World begomoviruses, New World begomoviruses, sweepoviruses and legumoviruses (Briddon et al., 2010).

Three types of DNA satellites have been described to be associated with begomoviruses, betasatellites (Briddon et al., 2003), alphasatellites (Briddon et al., 2004), and deltasatellites (Lozano et al., 2016). Recently, the International Committee on Taxonomy of Viruses (ICTV) modified the International Code of Virus Classification and Nomenclature to enable the classification of satellite nucleic acids (Adams et al., 2017). This change makes official the creation of a family of single-stranded DNA satellites associated with begomoviruses, *Tolecusatellitidae* (Briddon et al., 2016; Adams et al., 2017). The family *Tolecusatellitidae* includes two genera, *Betasatellite* and *Deltasatellite*. The genus *Betasatellite* includes DNA satellites about half the size of begomovirus genome components. Betasatellites encode the βC1 protein in the complementary-sense strand, which has important roles in symptom induction and suppression of transcriptional and post-transcriptional gene silencing (Zhou, 2013). Betasatellites have been found associated with monopartite begomoviruses in the Old World. Deltasatellites are non-coding DNA satellites associated with begomoviruses, of about a quarter size of begomoviral genome components (Fiallo-Olivé et al., 2012; Lozano et al., 2016). Tomato leaf curl deltasatellite, formerly ToLCV-sat, was the first DNA satellite identified in association with a plant virus, the monopartite Old World begomovirus tomato leaf curl virus (ToLCV) originating from Australia (Dry et al., 1997). Deltasatellites have been also found associated with bipartite New World begomoviruses infecting malvaceous weeds (Fiallo-Olivé et al., 2012, 2016) and sweepoviruses (Hassan et al., 2016; Lozano et al., 2016; Rosario et al., 2016). Also, the sequences of two uncharacterized deltasatellites from Philippines (KF433066) and India (AJ968684) have been deposited in GenBank. All deltasatellites contain common features; they share a small region with some sequence identity to a conserved region present in the betasatellites, an A-rich sequence, a predicted stem-loop structure containing the nonanucleotide TAATATTAC, and a predicted secondary stem-loop (Fiallo-Olivé et al., 2012; Lozano et al., 2016).

The genus *Deltasatellite* comprises 11 species (Briddon et al., 2016; Adams et al., 2017), five of them reported associated with bipartite New World begomoviruses. Until now, New World deltasatellites have been found only in the malvaceous plants *Malvastrum coromandelianum* and *Sidastrum micranthum* and only associated with two helper begomoviruses, Sida golden yellow vein virus and tomato yellow leaf distortion virus (Fiallo-Olivé et al., 2012, 2016). Recently, biological evidence has been obtained that New World deltasatellites depend on a limited range of begomoviruses for maintenance *in planta* (Fiallo-Olivé et al., 2016). In addition to the helper bipartite begomoviruses that the New World deltasatellites are associated with in nature, they can be transreplicated by the monopartite New World begomovirus tomato leaf deformation virus. In contrast, they cannot be maintained by the Old World begomoviruses tomato yellow leaf curl virus, tomato yellow leaf curl Sardinia virus and African cassava mosaic virus or the curtovirus beet curly top virus. New World deltasatellites do not affect the symptoms induced by the helper begomoviruses but in some instances they are able to reduce virus accumulation. Also, one New World deltasatellite has been shown to be transmitted by the whitefly *B. tabaci*, the natural vector of begomoviruses (Fiallo-Olivé et al., 2016).

In this study we analyzed the population of begomoviruses and associated DNA satellites present in wild *Corchorus siliquosus* plants collected in Cuba. The genomes of two New World begomoviruses (one bipartite and one monopartite) and two deltasatellites have been cloned and sequenced from plants showing yellow vein symptoms, the monopartite begomovirus and one of the deltasatellites representing novel species. Experiments with infectious clones showed that the

monopartite begomovirus is also able to infect common bean and that the novel deltasatellite is maintained only by the bipartite begomovirus. This is the first time that a monopartite begomovirus native to the New World and deltasatellites have been found in *C. siliquosus*, extending the ranges of plant hosts and helper viruses for these recently recognized DNA satellites.

MATERIALS AND METHODS

Plant Samples

Leaves of *Corchorus siliquosus* plants (family Malvaceae) showing yellow vein symptoms (**Figure 1**) were collected in the province of Matanzas, Cuba, on December 2013 (**Table 1**). Each sample consisted of a few leaves which were dried, transported to the laboratory and held at 4°C. Morphological identification of the plants was confirmed at the molecular level by DNA barcoding using chloroplast rbcL and matK genes (Hollingsworth et al., 2009).

DNA Extraction and Cloning

Total DNA was extracted from leaf samples using a cetyltrimethylammonium bromide-based method (Permingeat et al., 1998) and then used as a template in rolling-circle amplification (RCA) using ϕ29 DNA polymerase (TempliPhi kit, GE Healthcare). Amplified RCA products were first digested with *Hpa*II, a 4-bp restriction enzyme, for preliminary restriction fragment length polymorphism (RFLP) analysis on 1.5% agarose gels. Then, RCA products were digested with a set of 6-bp restriction enzymes (*Eco*RI, *Bam*HI, *Hin*dIII, *Nco*I, *Sac*I). Putative full-length begomovirus genome components (∼2.6 kb) and deltasatellites (∼0.7 kb) obtained after digestion were size-selected and cloned into the appropriate sites of pBluescriptII SK(+) (Stratagene) or pGEM-T Easy Vector (Promega). Recombinant plasmid DNAs were transformed into *Escherichia coli* DH5α by electroporation and selected clones were sequenced in both directions by the Sanger method using M13 forward and reverse [for pBluescriptII SK(+)] or T7 promoter and SP6 promoter (for pGEM-T Easy Vector) primers and then by primer-walking (Macrogen Inc., Seoul, South Korea).

Sequence Analysis

Sequences were assembled with SeqMan software included in the DNASTAR package (Lasergene). Open reading frames were identified using Open Reading Frame Finder (NCBI) and confirmed by a BLAST analysis[1] of their deduced amino acid sequences. Initial sequence identity comparison was performed using the BLAST program, sequences were aligned with MUSCLE (Edgar, 2004), and pairwise identity scores were calculated using SDT (Sequence demarcation tool) (Muhire et al., 2014). *In silico* digestion analysis of cloned begomovirus and deltasatellite sequences was performed with SnapGene (Insightful Science, available at snapgene.com).

[1]https://blast.ncbi.nlm.nih.gov/Blast.cgi

Phylogenetic Analysis

For phylogenetic analysis of begomoviruses and deltasatellites, the maximum likelihood method was used after selecting the best-fit model of nucleotide substitution based on corrected Akaike Information Criterion and Bayesian Information Criterion as implemented in MEGA 7 (Kumar et al., 2016). For analysis of begomoviruses, the most closely related DNA-A and DNA-B components were selected as well as sequences belonging to different clades of New World begomoviruses. For phylogenetic analysis of deltasatelites, the deltasatellites isolates described in this work and one isolate belonging to each deltasatellite species (Briddon et al., 2016; Adams et al., 2017) were included.

Recombination Analysis

Recombination analysis of sequences reported in this study was performed using RDP4 (Martin et al., 2015) after alignment with MUSCLE (Edgar, 2004). Only recombination events detected with at least five methods were considered. To carry out the recombination analysis of the begomoviruses, the sequences with highest SWeBLAST scores (window size of 200 and step size of 200) were selected (Fourment et al., 2008). For deltasatellites, all the sequences available in GenBank were included in the analysis.

Construction of Infectious Clones

Infectious dimeric clones of the begomovirus genomic components and one of the deltasatellites characterized in this work were constructed as previously described (Fiallo-Olivé et al., 2016). Inserts from monomeric clones of each viral component or deltasatellite were released from the plasmids, religated and subjected to RCA. RCA products were partially digested to produce dimeric molecules which were subsequently cloned in a plasmid vector. The inserts of the dimeric clones were excised and subcloned in the binary vector pCAMBIA0380. Details of the restriction enzymes and vectors used in each cloning step are given in **Supplementary Table 1**. Ligation reactions were transformed into *Escherichia coli* DH5α by electroporation (25 μF, 200 Ω, 2500 V) in a Gene Pulser XCell (Bio-Rad). In each cloning step, clones were verified by digestion. Clones in the binary vector with inserts of the expected size were sequenced (Macrogen Inc., Seoul, South Korea) and transformed into *Agrobacterium tumefaciens* C58C1 by electroporation (25 μF, 200 Ω, 2500 V).

Plant Inoculation and Begomovirus and Deltasatellite Detection

For agroinoculation assays, *A. tumefaciens* cultures harboring each dimeric construct were grown and inoculated as previously described (Fiallo-Olivé et al., 2016). Plant species used for agroinoculation assays were *Nicotiana benthamiana*, *Corchorus olitorius* (seeds purchased from B&T World Seeds), common bean (*Phaseolus vulgaris*) cv. Donna, tomato (*Solanum lycopersicum*) cv. Moneymaker, pepper (*Capsicum annuum*) cv. California Wonder and zucchini (*Cucurbita pepo*) cv. Milenio. Plants were inoculated with *A. tumefaciens* cultures containing clones of viral DNA components and deltasatellites

FIGURE 1 | *Corchorus siliquosus* plants showing vein yellowing symptoms. **(A)** Sample 679. **(B)** Sample 705.

TABLE 1 | Location of *Corchorus siliquosus* plants showing yellow vein symptoms sampled in the province of Matanzas, Cuba.

Sample	Municipality	Geographical coordinates
679	Matanzas	23°03.868′N 81°33.517′W
680	Matanzas	23°03.877′N 81°33.521′W
704	Jovellanos	22°53.152′N 81°17.163′W
705	Jovellanos	22°53.159′N 81°17.170′W
706	Jovellanos	22°53.167′N 81°17.178′W

by stem puncture inoculation. *N. benthamiana* plants were inoculated at the four-leaf stage and the rest of the plants at the two-leaf stage. Plants were maintained in an insect-free growth chamber (25°C during the day and 18°C at night, 70% relative humidity, with a 16-h photoperiod at 250 μmol s^{-1} m^{-2} of photosynthetically active radiation) until analyzed. All agroinoculation experiments were repeated twice and each contained 12 plants, with the exception of Exp. 2 with *C. olitorius* in which eight plants were inoculated. Plants that served as negative controls were mock inoculated with *A. tumefaciens* C58C1 cultures containing empty vector.

For biolistic inoculation, the monomeric clone of CoYVCuV obtained in this work was used to inoculate *N. benthamiana* and *C. olitorius* plants. Viral DNA insert was released from the vector by digestion with *Sac*I, circularized using T4 DNA ligase (Roche Diagnostics) and then subjected to RCA. The RCA product was precipitated onto 1.0 μm gold microcarriers (Bio-Rad) which were resuspended in ethanol. Plants were inoculated with a "Bim-Lab" instrument (Bio-Oz Biotechnologies). Both third and fourth leaves of each plant were shot twice with 5 μL of the RCA product-coated microcarriers. Biolistic inoculation experiments were repeated twice and each contained 12 (*N. benthamiana*) or 10 (*C. olitorius*) plants. Plants that served as negative controls were mock inoculated with the microcarriers in ethanol.

Apical leaves were used for tissue blots of petiole cross-sections (tissue printing) performed on positively charged nylon membranes (Roche Diagnostics) at 33 days post-inoculation. In the case of *N. benthamiana*, stem cross-sections were employed instead. Hybridization was carried out using digoxigenin-labeled DNA probes specific to each viral genomic component and deltasatellites. The probes were prepared by PCR with primers specifically designed for each begomovirus genomic component and one of the deltasatellites (**Supplementary Table 2**) according to the DIG-labeling detection kit (Roche Diagnostics). Hybridization was carried out under high stringency conditions [washing steps at 65°C in 0.1× SSC (15 mM NaCl, 1.5 mM sodium citrate) and 0.1% sodium dodecyl sulfate] following standard procedures. Hybridization signals were detected on X-ray film after treatment with CDP-Star (Roche Diagnostics).

RESULTS

A Bipartite and a Monopartite Begomovirus, the Latter Representing a Novel Species, Infect *Corchorus siliquosus* in Cuba

Digestion with *Hpa*II of RCA-amplified products from the five *C. siliquosus* leaf samples yielded restriction patterns

(**Supplementary Figure 1**) supporting the suspected begomovirus infections based on the symptomatology observed in the field, consisting of yellow veins (**Figure 1**). The complexity of the restriction patterns was suggestive of mixed infections. Sequencing of cloned DNA fragments following digestion with 6-bp enzymes confirmed the presence of DNA-A and DNA-B genomic components in the five samples. In total, 15 DNA-A and 21 DNA-B full-length clones were sequenced (**Table 2**). All of them showed the organization of typical New World begomoviruses.

Pairwise comparison analysis carried out with SDT showed that 10 of the DNA-As (isolated from the five samples as *Bam*HI or *Sac*I fragments, GenBank acc. no. MF773881-MF773890) (**Table 2**) showed a nucleotide identity of 97.3–100% between them and the highest identity (94.1–94.3%) with Desmodium leaf distortion virus (DesLDV) DNA-A (DQ875870). In accordance with the current taxonomic guidelines for the genus *Begomovirus* (a new DNA-A sequence with ≥91% pairwise identity to an available begomovirus DNA-A sequence will belong to the same species) (Brown et al., 2015), the isolates described here belong to the species *Desmodium leaf distortion virus*. DesLDV is a bipartite New World begomovirus previously found infecting only the wild fabaceous *Desmodium glabrum* in Yucatán, Mexico (Hernández-Zepeda et al., 2009). DNA-Bs (also isolated from the five samples as *Eco*RI, *Hin*dIII or *Sac*I fragments, MF773891-MF773911) (**Table 2**) showed nucleotide identity of 90.2–100% between them and the highest identity (87.9–88.9%) with DesLDV DNA-B from Mexico (DQ875871). A common region of 161 nt was identified in the cloned DNA-As and DNA-Bs of DesLDV which showed an identity of 93.8–96.9% between both components. Also, four copies of identical iterons, two of them inverted, were present in both genome components (**Figure 2**), thus supporting that they constitute cognate pairs. Phylogenetic analysis showed that both DNA-A and DNA-B components of DesLDV isolates cloned from *C. siliquosus* plants, as expected, grouped with the DesLDV isolate from *D. glabrum* characterized in Mexico (Hernández-Zepeda et al., 2009; **Figure 3**). Recombination analysis of a representative isolate of DesLDV (Cuba-Corchorus 706-2-2013), showed the recombinant nature of the DNA-A. Interestingly, the major parent of the only recombination event detected is Corchorus yellow spot virus, a begomovirus isolated from *C. siliquosus* in Mexico (Hernández-Zepeda et al., 2007) and the minor parent an isolate of cabbage leaf curl virus from Florida (Abouzid et al., 1992; **Table 3**). No recombination events were detected in the DNA-B.

The other five full-length DNA-A components (isolated from samples 705 and 706 and cloned as *Eco*RI or *Sac*I fragments, MF773912-MF773916) (**Table 2**) showed an identity of 99.8–100% between them and only 76.6–77.4% with the cloned DesLDV isolates. The highest identity (81.9%) was with the DNA-A of two begomoviruses from the Caribbean, tobacco yellow crinkle virus (FJ213931) (Fiallo-Olivé et al., 2009) and Jatropha mosaic virus (KJ174331) (Melgarejo et al., 2015). In accordance with the above-mentioned taxonomic guidelines for the genus *Begomovirus*, the isolates described here represent a novel species for which we propose the name *Corchorus yellow vein Cuba virus* (CoYVCUV). Phylogenetic analysis showed that the DNA-As of CoYVCUV isolates were highly divergent and grouped in a single cluster with a high bootstrap value, thus supporting that this begomovirus constitutes a novel species (**Figure 3A**). Recombination analysis of a representative CoYVCUV DNA-A (Cuba-Corchorus 706-1-2013), also showed its recombinant nature. The three recombination events detected involved begomoviruses infecting wild plants, Jatropha mosaic virus, Dalechampia chlorotic mosaic virus and DesLDV from Dominican Republic, Venezuela and Mexico, respectively (Hernández-Zepeda et al., 2009; Fiallo-Olivé et al., 2013; Melgarejo et al., 2015; **Table 3**).

The CR of the DesDLDV DNA-B and the equivalent region of the CoYVCUV DNA-A present in the same samples showed a low identity (65.8–68.0%) and dissimilar iterons (**Figure 2**). Based on this, the DNA-A of CoYVCUV and the DNA-B of DesLDV would not constitute a cognate pair. On the other hand, although the DNA-A of CoYVCUV showed the typical genome organization of a bipartite New World begomovirus DNA-A, no DNA-B could be found for this virus in the two samples analyzed despite repeated attempts to clone full-length or partial genome components different from the described above. This was done using the above-mentioned set of restriction enzymes as well as other 6-bp restriction enzymes whose recognition sequences were not present in the cloned genome components (data not shown). Also, *in silico* digestion analysis of cloned begomovirus and deltasatellite (see next section) sequences produced a RCA-RFLP pattern from samples 705 and 706 similar to those experimentally obtained (**Figure 4**). This analysis supports that no additional begomovirus genome components are present in an amplifiable amount in these samples. Taking together, these results suggested the possibility that CoYVCUV could be a monopartite New World begomovirus.

To assess the putative monopartite nature of CoYVCUV, a dimeric clone obtained for its DNA-A component was agroinoculated alone or in combination with a dimeric clone of DesLDV DNA-B in *Nicotiana benthamiana* and *Corchorus olitorius* plants. In four independent experiments, tissue printing hybridization of apical leaves showed that CoYVCUV was infectious in *N. benthamiana*, all the inoculated plants becoming infected (**Table 4** and **Supplementary Figure 2A**) although they remained asymptomatic (data not shown). This included the two experiments in which CoYVCUV DNA-A was co-inoculated with DesLDV DNA-B, whose replication was not supported based on the tissue printing hybridization analysis (**Table 4** and **Supplementary Figure 2A**). In contrast, *C. olitorius* plants were not infected in any of the four independent experiments (**Table 4** and **Supplementary Figure 2**). Biolistic inoculation of *C. olitorius* plants was also assayed with CoYVCUV DNA-A for which RCA products obtained from circularized monomer genomes were employed. In two independent experiments, *C. olitorius* was not infected as determined by tissue printing hybridization analysis (**Table 4** and **Supplementary Figure 2B**). However, about 50% of the *N. benthamiana* plants inoculated in the same experiments were infected (**Table 4** and **Supplementary Figure 2B**) but remained asymptomatic.

TABLE 2 | Begomoviruses and deltasatellites isolated from *Corchorus siliquosus* plants showing yellow vein symptoms sampled in the province of Matanzas, Cuba.

Sample	Begomovirus/deltasatellite	Genome component	Isolate	Restriction enzyme	Size (nt)	GenBank acc. no.
679	DesLDV	DNA-A	CU-Co679-1-13	*Sac*I	2569	MF773881
	DesLDV	DNA-A	CU-Co679-2-13	*Bam*HI	2570	MF773882
	DesLDV	DNA-B	CU-Co679-1-13	*Sac*I	2497	MF773891
	DesLDV	DNA-B	CU-Co679-2-13	*Sac*I	2497	MF773892
680	DesLDV	DNA-A	CU-Co680-1-13	*Sac*I	2570	MF773883
	DesLDV	DNA-A	CU-Co680-2-13	*Sac*I	2570	MF773884
	DesLDV	DNA-A	CU-Co680-3-13	*Sac*I	2569	MF773885
	DesLDV	DNA-B	CU-Co680-1-13	*Sac*I	2498	MF773893
	DesLDV	DNA-B	CU-Co680-2-13	*Sac*I	2497	MF773894
	DesLDV	DNA-B	CU-Co680-3-13	*Eco*RI	2498	MF773895
	DesLDV	DNA-B	CU-Co680-4-13	*Eco*RI	2498	MF773896
	DesLDV	DNA-B	CU-Co680-5-13	*Eco*RI	2498	MF773897
	ToYLDD2		CU-Co680-S8-13	*Sac*I	692	MF773917
	ToYLDD2		CU-Co680-S11-13	*Sac*I	692	MF773918
	ToYLDD2		CU-Co680-S17-13	*Sac*I	692	MF773919
704	DesLDV	DNA-A	CU-Co704-1-13	*Sac*I	2570	MF773886
	DesLDV	DNA-A	CU-Co704-2-13	*Sac*I	2570	MF773887
	DesLDV	DNA-B	CU-Co704-1-13	*Hin*dIII	2499	MF773898
	DesLDV	DNA-B	CU-Co704-2-13	*Hin*dIII	2499	MF773899
	DesLDV	DNA-B	CU-Co704-3-13	*Hin*dIII	2499	MF773900
	DesLDV	DNA-B	CU-Co704-4-13	*Sac*I	2498	MF773901
	DesLDD		CU-Co704-H1-13	*Hin*dIII	666	MF773920
	DesLDD		CU-Co704-H6-13	*Hin*dIII	666	MF773921
	DesLDD		CU-Co704-H7-13	*Hin*dIII	666	MF773922
	DesLDD		CU-Co704-H8-13	*Hin*dIII	666	MF773923
	DesLDD		CU-Co704-H9-13	*Hin*dIII	666	MF773924
	DesLDD		CU-Co704-H10-13	*Hin*dIII	666	MF773925
705	DesLDV	DNA-A	CU-Co705-1-13	*Sac*I	2569	MF773888
	DesLDV	DNA-B	CU-Co705-1-13	*Eco*RI	2531	MF773902
	DesLDV	DNA-B	CU-Co705-2-13	*Sac*I	2530	MF773903
	DesLDV	DNA-B	CU-Co705-3-13	*Eco*RI	2531	MF773904
	DesLDV	DNA-B	CU-Co705-4-13	*Sac*I	2530	MF773905
	DesLDV	DNA-B	CU-Co705-5-13	*Eco*RI	2531	MF773906
	DesLDV	DNA-B	CU-Co705-6-13	*Sac*I	2531	MF773907
	DesLDV	DNA-B	CU-Co705-7-13	*Sac*I	2530	MF773908
	DesLDV	DNA-B	CU-Co705-8-13	*Eco*RI	2531	MF773909
	CoYVCUV		CU-Co705-1-13	*Eco*RI	2576	MF773912
	CoYVCUV		CU-Co705-2-13	*Eco*RI	2576	MF773913
	CoYVCUV		CU-Co705-3-13	*Sac*I	2576	MF773914
	CoYVCUV		CU-Co705-4-13	*Sac*I	2576	MF773915
	DesLDD		CU-Co705-H1-13	*Hin*dIII	666	MF773926
	DesLDD		CU-Co705-H2-13	*Hin*dIII	665	MF773927
	DesLDD		CU-Co705-H3-13	*Hin*dIII	666	MF773928
	DesLDD		CU-Co705-H4-13	*Hin*dIII	665	MF773929
	DesLDD		CU-Co705-H5-13	*Hin*dIII	665	MF773930
	DesLDD		CU-Co705-H6-13	*Hin*dIII	665	MF773931
	DesLDD		CU-Co705-H7-13	*Hin*dIII	665	MF773932
	DesLDD		CU-Co705-H8-13	*Hin*dIII	665	MF773933
	DesLDD		CU-Co705-H11-13	*Hin*dIII	666	MF773934
706	DesLDV	DNA-A	CU-Co706-1-13	*Sac*I	2570	MF773889
	DesLDV	DNA-A	CU-Co706-2-13	*Sac*I	2570	MF773890
	DesLDV	DNA-B	CU-Co706-1-13	*Sac*I	2530	MF773910
	DesLDV	DNA-B	CU-Co706-2-13	*Sac*I	2531	MF773911
	CoYVCUV		CU-Co706-1-13	*Sac*I	2576	MF773916

DesLDV, Desmodium leaf distortion virus; CoYVCUV, Corchorus yellow vein Cuba virus; ToYLDD2, tomato yellow leaf distortion deltasatellite 2, DesLDD; Desmodium leaf distortion deltasatellite.

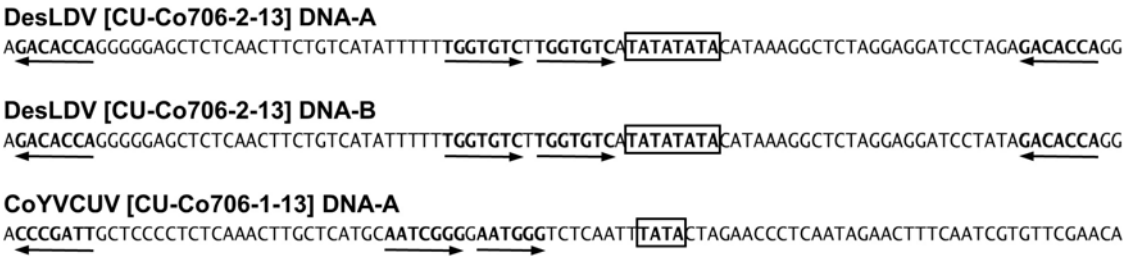

FIGURE 2 | Iterons (arrows) of genome components of begomoviruses Desmodium leaf distortion virus (DesLDV) and Corchorus yellow vein Cuba virus (CoYVCUV). TATA motifs of the Rep promoter are highlighted with boxes.

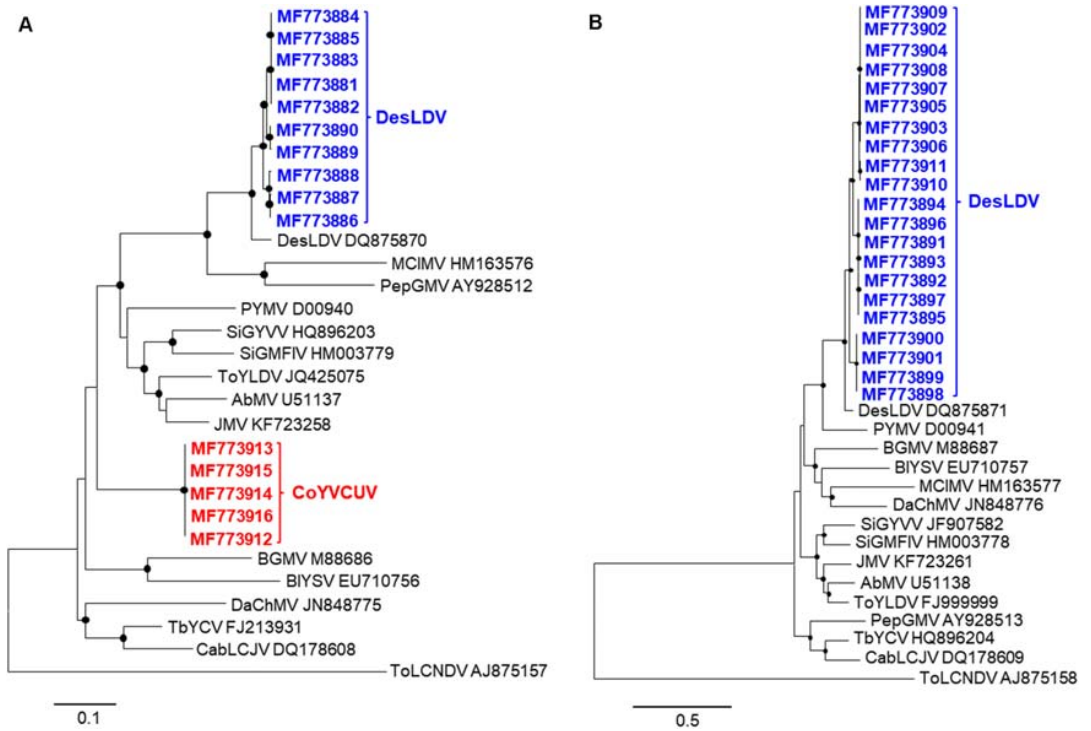

FIGURE 3 | Phylogenetic trees illustrating the relationships of isolates of Desmodium leaf distortion virus (DesLDV) DNA-A **(A)** and DNA-B **(B)** (bold in blue) and Corchorus yellow vein Cuba virus (CoYVCUV) DNA-A (bold in red) isolates with other New World begomoviruses. The trees were constructed by the maximum likelihood method (1000 replicates) with the MEGA 7 program using the best fit model, TN93 + G + I for DNA-A and HKY + G for DNA-B. AbMV, Abutilon mosaic virus; BGMV, bean golden mosaic virus; BIYSV, Blainvillea yellow spot virus; CabLCJV, cabbage leaf curl Jamaica virus; DaChMV, Dalechampia chlorotic mosaic virus; JMV, Jatropha mosaic virus; MCIMV, melon chlorotic mosaic virus; PepGMV, pepper golden mosaic virus; PYMV, potato yellow mosaic virus; SiGMFIV, Sida golden mosaic Florida virus; SiGYVV, Sida golden yellow vein virus; TbYCV, tobacco yellow crinckle virus; ToYLDV, tomato yellow leaf distortion virus. The Old World begomovirus tomato leaf curl New Delhi virus (ToLCNDV) was used as an outgroup. The bars below the trees indicate the number of nucleotide substitutions per site. Nodes with bootstrap values higher than 50% are marked with filled circles.

To further confirm the monopartite nature of CoYVCUV and to get insight on its possible host range, several plant species were inoculated with the CoYVCUV infectious clone. Two independent assays showed that CoYVCUV DNA-A was infectious in common bean, accumulating at detectable levels in apical leaves (**Table 4** and **Supplementary Figure 2A**), but not in tomato, pepper and zucchini. Symptoms developed in common bean plants consisted of leaf crinkle and mild yellowing (**Figure 5**). These results confirm that CoYVCUV is a monopartite New World begomovirus.

Two Deltasatellites, One Representing a Novel Species, Are Associated With the Begomoviruses Infecting *Corchorus siliquosus*

Eighteen deltasatellite molecules were cloned and sequenced from three of the five *C. siliquosus* samples showing yellow vein symptoms analyzed in this work (**Table 2**). Identification of such molecules as deltasatellites was based on their size (665–692 nt) and genome organization, including the features

TABLE 3 | Recombinant fragments detected in the DNA-A sequences of Desmodium leaf distortion virus – (Cuba-Corchorus 706-2-2013) (DesLDV) and Corchorus yellow vein Cuba virus – (Cuba-Corchorus 706-1-2013) (CoYVCUV) by at least five methods included in the RDP4 package.

Recombinant virus	Recombination breakpoints	Parent-like sequences		*p*-value	Methods that detected recombination[a]
		Major	Minor		
DesLDV	1917–2561	CoYSV DQ875868	CabLCV U65529	7.224×10^{-58}	R, G, B, M, C, S, 3S
CoYVCUV	68–262	Unknown	DesLDV DQ875870	7.330×10^{-15}	R, G, B, M, C, S
CoYVCUV	1186–1281	JMV KJ174331	DaChMV JN848775	3.841×10^{-6}	R, G, B, S, 3S
CoYVCUV	1416–1605	JMV KJ174331	DaChMV JN848775	3.818×10^{-10}	R, G, B, S, 3S

[a] *The method with the lower p-value obtained for each fragment is underlined. CabLCV, cabbage leaf curl virus; CoYSV, Corchorus yellow spot virus; DaChMV, Dalechampia chlorotic mosaic virus; JMV, Jatropha mosaic virus. R, RDP; G, GENCONV; B, BootScan; M, MaxChi; C, Chimaera; S, SiScan; 3S, 3Seq.*

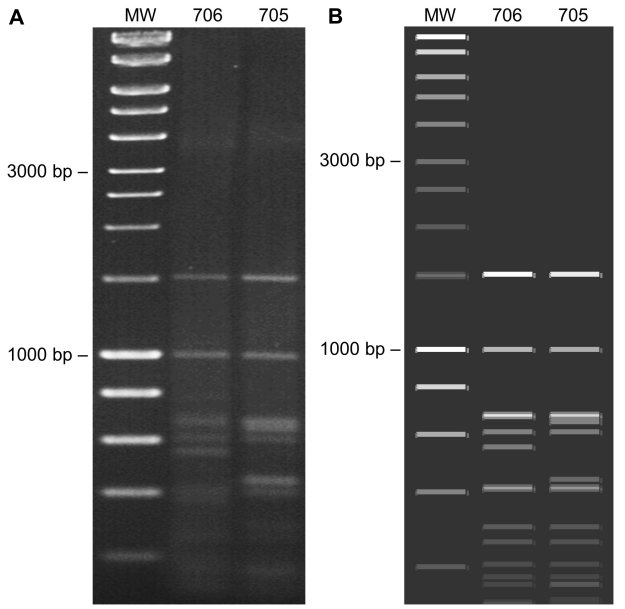

FIGURE 4 | Restriction fragment length polymorphism (RFLP) analysis of begomoviruses and deltasatellites infecting *Corchorus siliquosus* (samples 705 and 706). **(A)** RFLP performed by digestion of rolling circle amplification (RCA) products obtained from DNA extracts with the restriction enzyme *Hpa*II revealed on a 1.5% agarose gel. **(B)** *In silico* RFLP analysis (*Hpa*II) of the begomovirus and deltasatellite sequences obtained from each sample, performed with SnapGene (Insightful Science, available at snapgene.com). MW: molecular weight marker (HyperLadder 1 kb, Bioline).

common to all deltasatellites: a small region with some sequence identity to the conserved region present in the betasatellites, an A-rich sequence, a predicted stem-loop structure containing the non-anucleotide TAATATTAC, and a predicted secondary stem-loop. Pairwise comparison between these deltasatellites and all the deltasatellite sequences available in GenBank showed that the deltasatellites from *C. siliquosus* can be readily separated into two groups consisting of those molecules isolated from sample 680 (n = 3, 99.7–100% nucleotide identity between them, cloned as *Sac*I fragments, MF773917-MF773919) and samples 704 and 705 (n = 15, 96.4–100% nucleotide identity between them, cloned as *Hin*dIII fragments, MF773920-MF773934), respectively. Nucleotide identity between isolates from both groups are only 73.0–74.9%. According to the proposed 91% deltasatellite species demarcation criteria (Briddon et al., 2016), the deltasatellites isolated in this work belong to two different species. The three deltasatellites isolated from sample 680 belong to the species *Tomato yellow leaf distortion deltasatellite 2*, as having the highest nucleotide identity of 97.4% with the only previously known isolate of this species (KU232893) (Fiallo-Olivé et al., 2016). The 15 deltasatellites isolated from samples 704 and 705 showed the highest nucleotide identity (74.4–75.7%) with the five isolates of *Sida golden yellow vein deltasatellite 2* (JN819490-JN819494) (Fiallo-Olivé et al., 2012), thus indicating that they constitute a novel deltasatellite species. Based on the presence of DesLDV in both samples where the novel deltasatellite was found, the name *Desmodium leaf distortion deltasatellite* (DesLDD) is proposed for this species.

Phylogenetic analysis of all deltasatellites known to date, including those described in this work, showed two main clusters (**Figure 6**). One of these clusters contains deltasatellites associated with bipartite New World begomoviruses, Sida golden yellow vein deltasatellite 1 (SiGYVD1), SiGYVD2, SiGYVD3, tomato yellow leaf distortion deltasatellite 1 (ToYLDD1), ToYLDD2 and the novel deltasatellite described in this study, DesLDD. All DesLDD isolates clustered together and are separated from the rest of New World deltasatellites, supporting that this deltasatellite constitutes a novel species. No recombination events were detected in the genomes of the deltasatellites described here.

Desmodium Leaf Distortion Deltasatellite Is Replicated by the Bipartite Desmodium Leaf Distortion Virus but Not by the Monopartite Corchorus Yellow Vein Cuba Virus

Agroinoculation experiments were carried out to asses which begomovirus could act as a helper for DesLDD. For this, a dimeric clone obtained for DesLDD was co-inoculated on *N. benthamiana* and *C. olitorius* plants with dimeric clones of DesLDV DNA-A and DNA-B or of CoYVCUV. As it has been stated above, DesLDV and CoYVCUV did not infect *C. olitorius* in two different experiments. Thus, as expected, DesLDD did not infect this plant. In contrast, both begomoviruses were able to infect *N. benthamiana* (**Table 5**). In this host, tissue printing hybridization of petiole cross-sections showed that all

TABLE 4 | Infectivity of CoYVCUV in several plant species.

Inoculation method	Virus component	Plant	No. infected plants/No. inoculated plants	
			Expt. 1	Expt. 2
Agroinoculation	CoYVCUV	*N. benthamiana*	12/12	12/12
	CoYVCUV + DesLDV DNA-B	*N. benthamiana*	12/12*	12/12*
	CoYVCUV	*C. olitorius*	0/12	0/8
	CoYVCUV + DesLDV DNA-B	*C. olitorius*	0/12	0/8
	CoYVCUV	Zucchini	0/12	0/12
	CoYVCUV	Common bean	5/12	8/12
	CoYVCUV	Pepper	0/12	0/12
	CoYVCUV	Tomato	0/12	0/12
Biolistics	CoYVCUV	*N. benthamiana*	5/12	6/12
	CoYVCUV	*C. olitorius*	0/10	0/10

**Only CoYVCUV was detected in the coinoculated plants.*

TABLE 5 | Infectivity of Desmodium leaf distortion deltasatellite (DesLDD) in the presence of Corchorus yellow vein Cuba virus (CoYVCUV) and Desmodium leaf distortion virus (DesLDV).

Plant species	Helper virus components	Deltasatellite	No. infected plants/No. agroinoculated plants			
			Expt. 1		Expt. 2	
			Virus	Deltasatellite	Virus	Deltasatellite
N. benthamiana	CoYVCUV	None	12/12	0/12	12/12	0/12
	CoYVCUV	DesLDD	12/12	0/12	11/12	0/12
	DesLDV A + B	None	12/12	0/12	12/12	0/12
	DesLDV A + B	DesLDD	12/12	6/12	12/12	6/12
	None	None	0/12	0/12	0/12	0/12
C. olitorius	CoYVCUV	None	0/12	0/12	0/8	0/8
	CoYVCUV	DesLDD	0/12	0/12	0/8	0/8
	DesLDV A + B	None	0/12	0/12	0/8	0/8
	DesLDV A + B	DesLDD	0/12	0/12	0/8	0/8
	None	None	0/12	0/12	0/8	0/8

agroinoculated plants became infected with DesLDV (DNA-A plus DNA-B) or CoYVCUV (**Supplementary Figure 3**). In two independent experiments, DesLDD replicated and accumulated only in the presence of DesLDV (50% of the plants in both experiments) but not of CoYVCUV (**Table 5** and **Supplementary Figure 3**), thus showing that the former acts as the helper virus.

N. benthamiana plants infected with DesLDV showed symptoms of leaf distortion and a significant reduction in plant growth (**Figure 7**). The presence of DesLDD did not affect the symptoms caused by DesLDV (**Figure 7**). The fact that DesLDV is the helper virus of this deltasatellite supports the proposal to name the novel species *Desmodium leaf distortion deltasatellite*.

DISCUSSION

In this work, a complex of begomoviruses and associated deltasatellites has been characterized from *C. siliquosus* plants showing yellow vein symptoms in Cuba. Isolates of two New World begomovirus species, *Desmodium leaf distortion virus* and *Corchorus yellow vein Cuba virus* have been cloned and sequenced. DesLDV (DNA-A and DNA-B) was found in single infection in several samples, whereas CoYVCUV (DNA-A) was found only in mixed infection with DesLDV. DNA-A from both begomoviruses had the typical genome organization of bipartite New World begomoviruses, but despite repeated attempts, a DNA-B could not be detected for CoYVCUV. Thus, the question remained whether CoYVCUV could be a monopartite begomovirus or it would utilize the DNA-B of DesLDV. Although CoYVCUV DNA-A and DesLDV DNA-B have different iterons, the possibility of forming pseudorecombinants cannot be ruled out. A few cases are known of both New World and Old World begomovirus pairs that form viable pseudorecombinants, at least experimentally, even if their iterons are not identical (Andrade et al., 2006; Chakraborty et al., 2008). Agroinoculation assays carried out in this work showed that (i) CoYVCUV DNA-A alone was infectious in *N. benthamiana* and common bean plants and (ii) DesLDV DNA-B is not replicated in the presence of CoYVCUV DNA-A in *N. benthamiana* plants. Although DNA-As of some bipartite begomoviruses have been shown to be able to infect *N. benthamiana* (Fiallo-Olivé et al., 2016), the fact that CoYVCUV DNA-A was able to

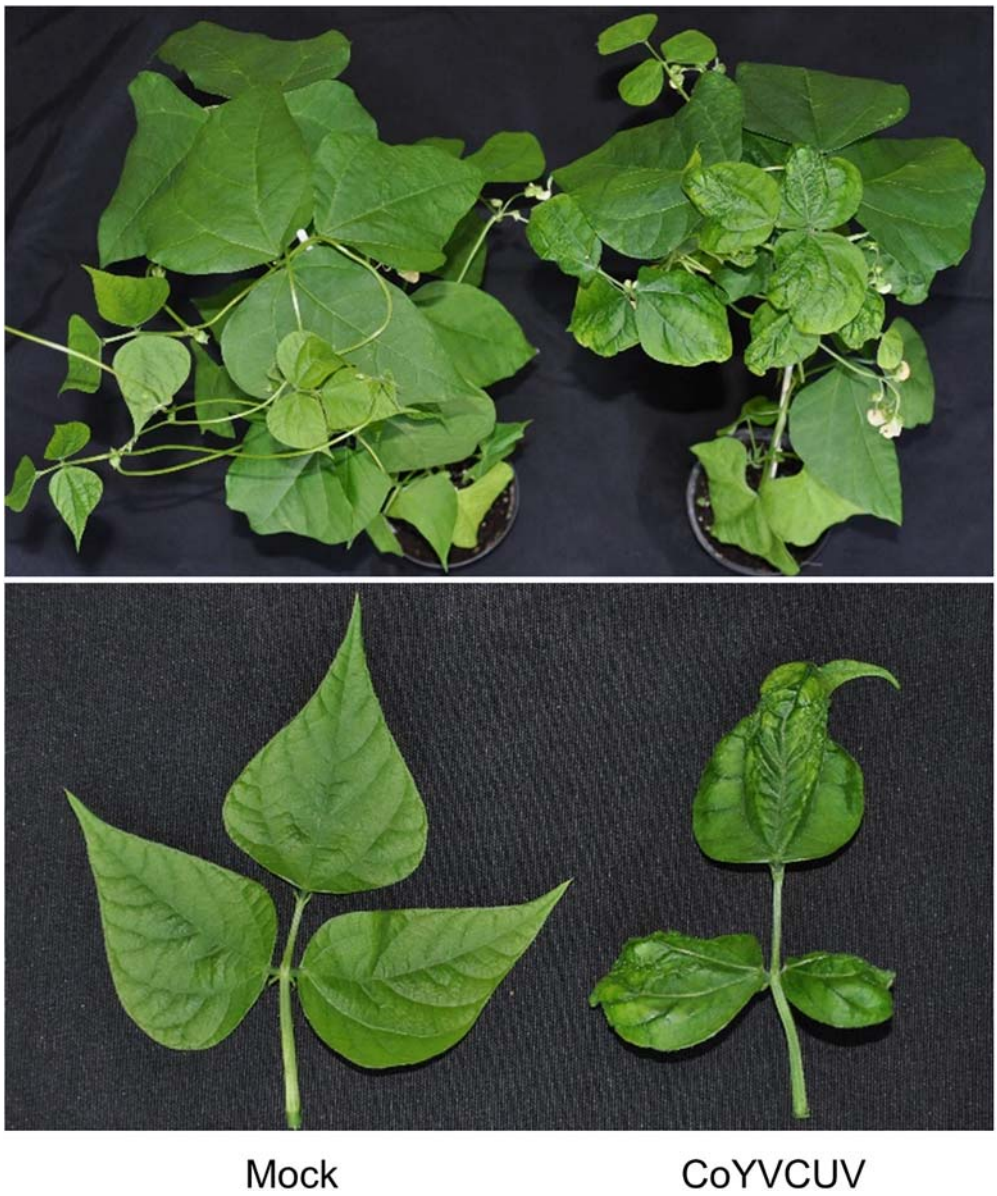

FIGURE 5 | Symptoms of leaf crinkle and mild yellowing developed in common bean plants agroinoculated with Corchorus yellow vein Cuba virus (CoYVCUV) DNA-A. Mock-inoculated controls are shown at the left of each panel.

infect common bean definitely revealed the monopartite nature of this begomovirus. Although comparison of experimental RCA-RFLP data and *in silico* digestion analysis suggested that no additional begomovirus genome components are present in the studied samples, it does not escape our attention that a deep sequencing approach would have precisely defined if other viruses and/or subviral molecules were present at low concentration.

New World begomoviruses are classically bipartite (Brown et al., 2015; Zerbini et al., 2017). However, in 2011 a monopartite begomovirus native to the Americas was described infecting tomato plants in Peru and Ecuador (Márquez-Martín et al., 2011; Melgarejo et al., 2013; Sánchez-Campos et al., 2013). Later, four additional monopartite begomoviruses have been described from the Americas, all of them infecting tomato: tomato latent virus (TLV) in Cuba (Fuentes et al., 2016), tomato mottle leaf curl virus and tomato leaf curl purple vein virus in Brazil (Vu et al., 2015; Macedo et al., 2018), and tomato twisted leaf virus in Venezuela (Romay et al., 2019). TLV is in fact a recombinant consisting of a moiety from the monopartite Old World tomato yellow leaf curl virus (introduced into the Americas in the early 1990s) and a moiety from an unidentified bipartite New World begomovirus DNA-A (Fuentes et al., 2016). The results obtained in this work expands the number of New World begomoviruses

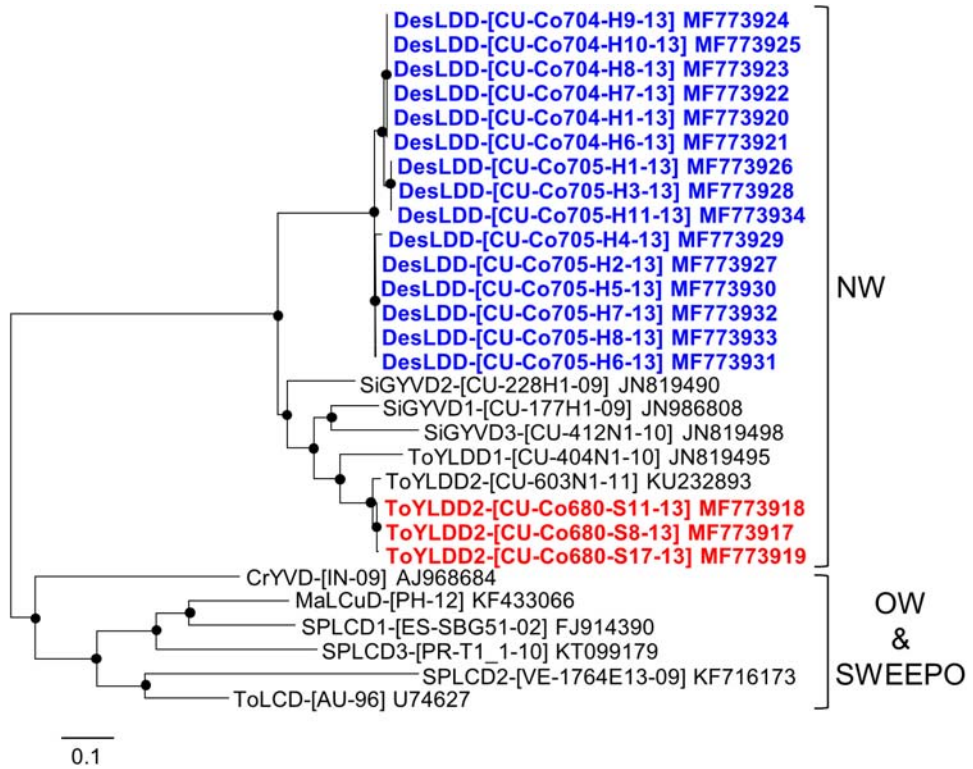

FIGURE 6 | Phylogenetic tree illustrating the relationships of Desmodium leaf distortion deltasatellite (DesLDD) (bold in blue) and tomato yellow leaf distortion deltasatellite 2 (ToYLDD2) (bold in red) isolates obtained in this work with representative isolates of other deltasatellite species. The tree was constructed by the maximum-likelihood method (1000 replicates) with the MEGA 7 program using the best fit model, T92 + G. CrYVD, Croton yellow vein deltasatellite; MaLCuD, Malvastrum leaf curl deltasatellite; SiGYVD1, Sida golden yellow vein deltasatellite 1; SiGYVD2, Sida golden yellow vein deltasatellite 2; SiGYVD3, Sida golden yellow vein deltasatellite 3; SPLCD1, sweet potato leaf curl deltasatellite 1; SPLCD2, sweet potato leaf curl deltasatellite 2; SPLCD3, sweet potato leaf curl deltasatellite 3; ToLCD, tomato leaf curl deltasatellite; ToYLDD1, tomato yellow leaf distortion deltasatellite 1; ToYLDD2, tomato yellow leaf distortion deltasatellite 2. Major deltasatellite clusters associated with bipartite New World begomoviruses (NW) and monopartite Old World begomoviruses and sweepoviruses (OW and SWEEPO) are indicated. The bar below the tree indicates the number of nucleotide substitutions per site. Nodes with bootstrap values higher than 50% are marked with filled circles.

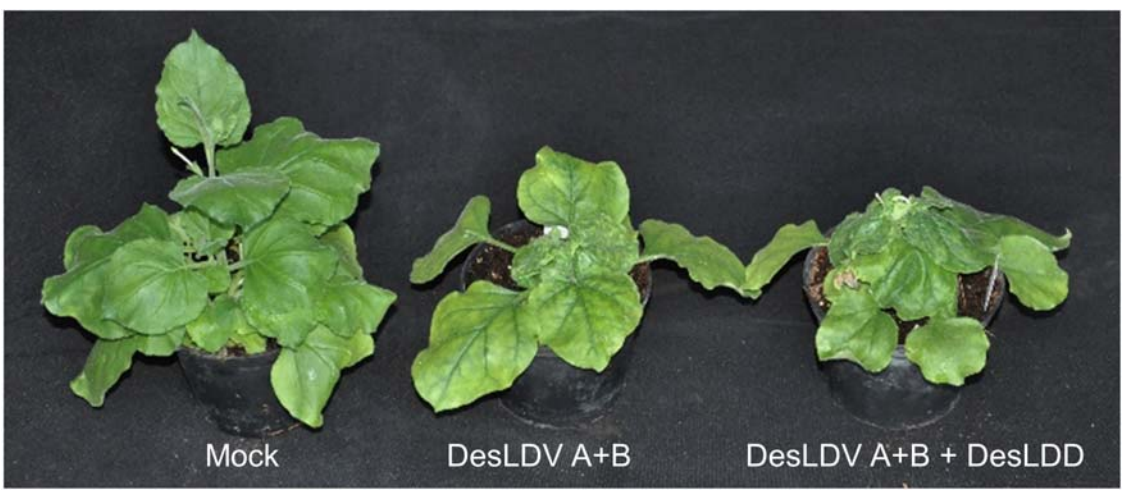

FIGURE 7 | Symptoms of leaf distortion and a significant reduction in plant growth developed in *Nicotiana benthamiana* plants agroinoculated with Desmodium leaf distortion virus (DesLDV) DNA-A and DNA-B, alone or in combination with Desmodium leaf distortion deltasatellite (DesLDD). Mock-inoculated control is shown at the left of the photograph.

whose monopartite nature has been shown experimentally to six, which is a very low number considering that there are about 170 New World begomovirus species recognized to date. It is generally believed that the first begomoviruses were monopartite (Briddon et al., 2010) and that the bipartite genome likely evolved before continental drift because bipartite begomoviruses occur in the Old and New World (Rojas et al., 2005). It has been suggested that the low number of indigenous monopartite begomoviruses in the New World could be explained by the predominance of bipartite progenitors in the areas of Pangea that gave rise to the Americas or by a later introduction (Melgarejo et al., 2013). The emergence of monopartite begomoviruses infecting tomato in the New World has been hypothesized to represent an evolutionary process which could have occurred due to a combination of factors including: (i) the extensive cultivation of this crop in which monopartite begomoviruses could evolve on their own, (ii) the existence of a local progenitor bipartite begomovirus in wild or cultivated plants, and (iii) the introduction of this local progenitor begomovirus into tomato crops by the invasive and polyphagous Middle East-Asia Minor 1 species (formerly B biotype) of the *Bemisia tabaci* complex (Melgarejo et al., 2013). In contrast to the rest of monopartite New World begomoviruses, CoYVCUV was not found infecting tomato but a wild malvaceous plant and tomato plants could not be experimentally infected by agroinoculation either. Thus, this could represent an additional evolutionary path in generating monopartite New World begomoviruses which could emerge in cultivated plants. Also, the facts that common bean became experimentally infected by CoYVCUV and showed symptoms of leaf crinkle and mild yellowing are relevant since this important crop could be threatened by this begomovirus in Cuba.

Since we were not successful in obtaining *C. siliquosus* seeds, *C. olitorius*, one of the two cultivated species in the genus *Corchorus*, was used in the agroinoculation and biolistics assays. *C. olitorius* was not infected by DesLDV or CoYVCUV, but it should be mentioned that this species is only distantly related to *C. siliquosus* (Benor, 2018).

Other partners in the viral complex found in *C. siliquosus* were subviral molecules, deltasatellites, which are the smallest DNA satellites associated with begomoviruses known to date. Deltasatellites have been previously found associated with two bipartite New World begomoviruses in Cuba, Sida golden yellow vein virus infecting *M. coromandelianum* and tomato yellow leaf distortion virus infecting *S. micranthum* (Fiallo-Olivé et al., 2012, 2016). Here, we have described the presence of two deltasatellites in a third malvaceous plant species, *C. siliquosus*, also from Cuba. One of these deltasatellites, Desmodium leaf distortion deltasatellite (DesLDD), constitutes a novel species, the twelfth of the genus *Deltasatellite*. This finding extends the ranges of natural hosts and helper viruses for these subviral molecules only recently recognized as a novel class of DNA satellites included in the family *Tolecusatellitidae* (Lozano et al., 2016; Adams et al., 2017).

Agroinoculation assays also showed that the novel deltasatellite described here, DesLDD, accumulated in *N. benthamiana* plants in the presence of DesLDV, but not CoYVCUV. Also, the presence of the deltasatellite did not modify the symptoms of leaf distortion and significant reduction in plant growth caused by DesLDV. This result is in agreement with those obtained with the two New World deltasatellites for which infectious clones were available to date, tomato yellow leaf distortion deltasatellite 2 and Sida golden yellow vein deltasatellite 1. Neither of the deltasatellites influenced the symptoms caused by their natural helper begomoviruses in *N. benthamiana* or in their natural hosts (Fiallo-Olivé et al., 2016). In contrast, deltasatellites associated with sweet potato leaf curl virus, a sweepovirus, usually reduced symptom severity caused by its natural helper virus and by tomato leaf curl virus, a monopartite Old World begomovirus (Hassan et al., 2016).

Recombination analysis of representative isolates of the two begomoviruses described in this study showed the recombinant nature of both DNA-As. With the exception of cabbage leaf curl virus (Florida isolate) (Abouzid et al., 1992), all begomoviruses involved in the detected recombination events infect wild plants (*C. siliquosus*, *Desmodium glabrum*, *Jatropha* sp., *Dalechampia* sp., and *Boerhavia diffusa*) in countries from the Caribbean and surrounding areas, from Venezuela to Florida (Hernández-Zepeda et al., 2007, 2009; Fiallo-Olivé et al., 2013; Polston et al., 2014; Melgarejo et al., 2015).

In this work, an additional begomovirus-deltasatellite complex has been characterized in a wild malvaceous plant, with known and novel partners which (i) have been shown to have interacted via recombination with other begomoviruses infecting both cultivated and wild plants and (ii) are able to infect new crops as common bean. In addition, the discovery of a deltasatellite that constitutes a novel species increases the complexity of a recently established, and still poorly understood, class of DNA satellites. This in an example which illustrates the phenomenon of emergence of plant viruses at the interface between natural vegetation and cultivated plants, which can cause outbreaks in nearby crops as well as in new areas driven by whitefly transmission, climate change and global trade.

DATA AVAILABILITY STATEMENT

The datasets generated for this study can be found in the online repositories. The names of the repository/repositories and accession number(s) can be found here: https://www.ncbi.nlm.nih.gov/genbank/, MF773881–MF773934.

AUTHOR CONTRIBUTIONS

EF-O and JN-C collected the *Corchorus siliquosus* leaf samples in the frame of the Ibero-American Network on Integrated Management of Vegetable Virus Diseases (CYTED 111RT0433), analyzed the data, and wrote the manuscript. EF-O and JN-C conceived the experiments that were performed by EF-O. Both authors contributed to the article and approved the submitted version.

FUNDING

This work was supported by the Ministerio de Economía y Competitividad (MINECO, Spain) (Grants AGL2013-48913-C2-1-R and AGL2016-75819-C2-2-R), co-financed by the European Regional Development Fund (ERDF), and the Programa Iberoamericano de Ciencia y Tecnología para el Desarrollo (CYTED) (network 111RT0433). EF-O was the recipient of a "Juan de la Cierva-Incorporación" postdoctoral contract from MINECO.

ACKNOWLEDGMENTS

We thank Remedios Tovar and José M. Cid for technical assistance.

SUPPLEMENTARY MATERIAL

The Supplementary Material for this article can be found online at: https://www.frontiersin.org/articles/10.3389/fmicb.2020.01755/full#supplementary-material

REFERENCES

Abouzid, A. M., Hiebert, E., and Strandberg, J. O. (1992). Cloning, identification, and partial sequencing of the genomic components of a geminivirus infecting the Brassicaceae. *Phytopathology* 82:1070.

Adams, M. J., Kefkowitz, E. J., King, A. M. Q., Harrach, B., Harrison, R. L., Knowles, N. J., et al. (2017). Changes to taxonomy and the international code of virus classification and nomenclature ratified by the international committee on taxonomy of viruses. *Arch. Virol.* 162, 2505–2538.

Andrade, E. C., Manhani, G. G., Alfenas, P. F., Calegario, R. F., Fontes, E. P. B., and Zerbini, F. M. (2006). Tomato yellow spot virus, a tomato-infecting begomovirus from Brazil with a closer relationship to viruses from Sida sp., forms pseudorecombinants with begomoviruses from tomato but not from Sida. *J. Gen. Virol.* 87, 3687–3696. doi: 10.1099/vir.0.82279-0

Benor, S. (2018). Molecular phylogeny of the genus corchorus (Grewioideae, Malvaceae s.l.) based on nuclear rDNA ITS sequences. *Crop J.* 6, 552–563. doi: 10.1016/j.cj.2018.03.007

Briddon, R. W., Bull, S. E., Amin, I., Idris, A. M., Mansoor, S., Bedford, I. A., et al. (2003). Diversity of DNA β, a satellite molecule associated with some monopartite begomoviruses. *Virology* 312, 106–121. doi: 10.1016/s0042-6822(03)00200-9

Briddon, R. W., Bull, S. E., Amin, I., Mansoor, S., Bedford, I. D., Rishi, N., et al. (2004). Diversity of DNA 1: a satellite-like molecule associated with monopartite begomovirus-DNA β complexes. *Virology* 324, 462–474. doi: 10.1016/j.virol.2004.03.041

Briddon, R. W., Navas-Castillo, J., and Fiallo-Olivé, E. (2016). *ICTV taxonomic Proposal 2016.021a-kP.A.v2.Tolecusatellitidae. Create the Tolecusatellitidae, a New Family Of Single-Stranded DNA Satellites With Two Genera*. Available online at: http://www.ictv.global/proposals-16/2016.021a-kP.A.v2.Tolecusatellitidae.pdf (accessed March 28, 2020).

Briddon, R. W., Patil, B. L., Bagewadi, B., Nawaz-ul-Rehman, M. S., and Fauquet, C. M. (2010). Distinct evolutionary histories of the DNA-A and DNA-B components of bipartite begomoviruses. *BMC Evol. Biol.* 10:97. doi: 10.1186/1471-2148-10-97

Brown, J. K., Zerbini, F. M., Navas-Castillo, J., Moriones, E., Ramos-Sobrinho, R., Silva, J. C. F., et al. (2015). Revision of begomovirus taxonomy based on pairwise sequence comparisons. *Arch. Virol.* 160, 1593–1619. doi: 10.1007/s00705-015-2398-y

Chakraborty, S., Vanitharani, R., Chattopadhyay, B., and Fauquet, C. M. (2008). Supervirulent pseudorecombination and asymmetric synergism between genomic components of two distinct species of begomovirus associated with severe tomato leaf curl disease in India. *J. Gen. Virol.* 89, 818–828. doi: 10.1099/vir.0.82873-0

Costa, T. M., Inoue-Nagata, A. K., Vidal, A. H., Ribeiro, S. G., and Nagata, T. (2020). The recombinant isolate of cucurbit aphid-borne yellows virus from Brazil is a polerovirus transmitted by whiteflies. *Plant Pathol.* 69, 1042–1050. doi: 10.1111/ppa.13186

Dry, I. B., Krake, L. R., Rigden, J. E., and Rezaian, M. A. (1997). A novel subviral agent associated with a geminivirus: the first report of a DNA satellite. *Proc. Natl. Acad. Sci. U.S.A.* 94, 7088–7093. doi: 10.1073/pnas.94.13.7088

Edgar, R. C. (2004). MUSCLE: multiple sequence alignment with high accuracy and high throughput. *Nucleic Acids Res.* 32, 1792–1797. doi: 10.1093/nar/gkh340

Fiallo-Olivé, E., Chirinos, D. T., Geraud-Pouey, F., Moriones, E., and Navas-Castillo, J. (2013). Complete genome sequences of two begomoviruses infecting weeds in Venezuela. *Arch. Virol.* 158, 277–280. doi: 10.1007/s00705-012-1451-3

Fiallo-Olivé, E., Martínez-Zubiaur, Y., Moriones, E., and Navas-Castillo, J. (2012). A novel class of DNA satellites associated with new world begomoviruses. *Virology* 426, 1–6. doi: 10.1016/j.virol.2012.01.024

Fiallo-Olivé, E., Rivera-Bustamante, R., and Martínez-Zubiaur, Y. (2009). Tobacco yellow crinkle virus, a new bipartite begomovirus infecting tobacco and pepper in Cuba. *Plant Pathol.* 58:785. doi: 10.1111/j.1365-3059.2009.02078.x

Fiallo-Olivé, E., Tovar, R., and Navas-Castillo, J. (2016). Deciphering the biology of deltasatellites from the new world: maintenance by New World begomoviruses and whitefly transmission. *New Phytol.* 212, 680–692. doi: 10.1111/nph.14071

Fourment, M., Gibbs, A. J., and Gibbs, M. J. (2008). SWeBLAST: a sliding window web-based BLAST tool for recombinant analysis. *J. Virol. Methods* 152, 98–101. doi: 10.1016/j.jviromet.2008.06.009

Fuentes, A., Carlos, N., Ruíz, Y., Callard, D., Sánchez, Y., Ochagavía, M. E., et al. (2016). Field trial and molecular characterization of RNAi-transgenic tomato plants that exhibit resistance to tomato yellow leaf curl geminivirus. *Mol. Plant Microbe Int.* 29, 197–209. doi: 10.1094/mpmi-08-15-0181-r

Ghosh, S., Kanakala, S., Lebedev, G., Kontsedalov, S., Silverman, D., Alon, T., et al. (2019). Transmission of a new polerovirus infecting pepper by the whitefly *Bemisia tabaci*. *J. Virol.* 93:e0488-19.

Hassan, I., Orílio, A. F., Fiallo-Olivé, E., Briddon, R. W., and Navas-Castillo, J. (2016). Infectivity, effects on helper viruses and whitefly transmission of the deltasatellites associated with sweepoviruses (genus Begomovirus, family Geminiviridae). *Sci. Rep.* 6:30204.

Hernández-Zepeda, C., Argüello-Astorga, G., Idris, A. M., Carnevali, G., Brown, J. K., and Moreno-Valenzuela, O. A. (2009). Molecular characterization and phylogenetic relationships of desmodium leaf distortion virus (DeLDV): a new begomovirus infecting *Desmodium glabrum* in Yucatan, Mexico. *Virus Genes* 39, 371–374. doi: 10.1007/s11262-009-0398-2

Hernández-Zepeda, C., Idris, A. M., Carnevali, G., Brown, J. K., and Moreno-Valenzuela, O. A. (2007). Molecular characterization and phylogenetic relationships of two new bipartite begomovirus infecting malvaceous plants in Yucatan, Mexico. *Virus Genes* 35, 369–377. doi: 10.1007/s11262-007-0080-5

Hollingsworth, P. M., Forrest, L. L., Spouge, J. L., Hajibabaei, M., Ratnasingham, S., van der Bank, M., et al. (2009). A DNA barcode for land plants. *Proc. Natl. Acad. Sci. U.S.A.* 106, 12794–12797.

Kumar, S., Stecher, G., and Tamura, K. (2016). MEGA7: molecular evolutionary genetics analysis version 7.0 for bigger datasets. *Mol. Biol. Evol.* 33, 1870–1874. doi: 10.1093/molbev/msw054

Lozano, G., Trenado, H. P., Fiallo-Olivé, E., Chirinos, D., Geraud-Pouey, F., Briddon, R. W., et al. (2016). Characterization of non-coding DNA satellites associated with sweepoviruses (genus Begomovirus, Geminiviridae) - definition of a distinct class of begomovirus-associated satellites. *Front. Microbiol.* 7:162. doi: 10.3389/fmicb.2016.00162

Macedo, M. A., Albuquerque, L. C., Maliano, M. R., Souza, J. O., Rojas, M. R., Inoue-Nagata, A. K., et al. (2018). Characterization of tomato leaf curl purple vein virus, a new monopartite New World begomovirus infecting tomato

in Northeast Brazil. *Arch. Virol.* 163, 737–743. doi: 10.1007/s00705-017-3662-0

Márquez-Martín, B., Aragón-Caballero, L., Fiallo-Olivé, E., Navas-Castillo, J., and Moriones, E. (2011). Tomato leaf deformation virus, a novel begomovirus associated with a severe disease of tomato in Peru. *Eur. J. Plant Pathol.* 129, 1–7. doi: 10.1007/s10658-010-9699-5

Martin, D. P., Murrell, B., Golden, M., Khoosal, A., and Muhire, B. (2015). RDP4: detection and analysis of recombination patterns in virus genomes. *Virus Evol.* 1:vev003.

Melgarejo, T. A., Kon, T., and Gilbertson, R. L. (2015). Molecular and biological characterization of distinct strains of Jatropha mosaic virus from the dominican republic reveal a potential to infect crop plants. *Phytopathology* 105, 141–153. doi: 10.1094/phyto-05-14-0135-r

Melgarejo, T. A., Kon, T., Rojas, M. R., Paz-Carrasco, L., Zerbini, F. M., and Gilbertson, R. L. (2013). Characterization of a new world monopartite begomovirus causing leaf curl disease of tomato in Ecuador and Peru reveals a new direction in geminivirus evolution. *J. Virol.* 87, 5397–5413. doi: 10.1128/jvi.00234-13

Muhire, B., Varsani, A., and Martin, D. P. (2014). SDT: a virus classification tool based on pairwise sequence alignment and identity calculation. *PLoS One* 9:e108277. doi: 10.1371/journal.pone.0108277

Navas-Castillo, J., Fiallo-Olivé, E., and Sánchez-Campos, S. (2011). Emerging virus diseases transmitted by whiteflies. *Annu. Rev. Phytopathol.* 49, 219–248. doi: 10.1146/annurev-phyto-072910-095235

Permingeat, H. R., Romagnoli, M. V., Sesma, J. I., and Vallejos, R. H. (1998). A simple method for isolating high yield and quality DNA from cotton (*Gossypium hirsutum* L.) leaves. *Plant Mol. Biol. Rep.* 16:89.

Polston, J. E., Londoño, M. A., and Capobianco, H. (2014). The complete genome sequence of the New World jatropha mosaic virus. *Arch. Virol.* 159, 3131–3136. doi: 10.1007/s00705-014-2132-1

Rojas, M. R., Hagen, C., Lucas, W. J., and Gilbertson, R. L. (2005). Exploiting chinks in the plant's armor: evolution and emergence of geminiviruses. *Annu. Rev. Phytopathol.* 43, 361–394. doi: 10.1146/annurev.phyto.43.040204.135939

Romay, G., Geraud-Pouey, F., Chirinos, D. T., Mahillon, M., Gillis, A., Mahillon, J., et al. (2019). Tomato twisted leaf virus: a novel indigenous new world monopartite begomovirus infecting tomato in Venezuela. *Viruses* 11:327. doi: 10.3390/v11040327

Rosario, K., Marr, C., Varsani, A., Kraberger, S., Stainton, D., Moriones, E., et al. (2016). Begomovirus-associated satellite DNA diversity captured through vector-enabled metagenomic (VEM) surveys using whiteflies (Aleyrodidae). *Viruses* 8:36. doi: 10.3390/v8020036

Sánchez-Campos, S., Martínez-Ayala, A., Márquez-Martín, B., Aragón-Caballero, L., Navas-Castillo, J., and Moriones, E. (2013). Fulfilling Koch's postulates confirms the monopartite nature of tomato leaf deformation virus: a begomovirus native to the New World. *Virus Res.* 173, 286–293. doi: 10.1016/j.virusres.2013.02.002

Vu, S., Melgarejo, T. A., Chen, L., Souza, J. O., Macedo, M. A., Inoue-Nagata, A. K., et al. (2015). Evidence that tomato mottle leaf curl virus from Northeastern Brazil is an indigenous New World monopartite begomovirus. *Phytopathology* 105:143.

Zerbini, F. M., Briddon, R. W., Idris, A., Martin, D. P., Moriones, E., Navas-Castillo, J., et al. (2017). ICTV virus taxonomy profile: geminiviridae. *J. Gen. Virol.* 98, 131–133. doi: 10.1099/jgv.0.000738

Zhou, X. P. (2013). Advances in understanding begomovirus satellites. *Annu. Rev. Phytopathol.* 51, 357–381. doi: 10.1146/annurev-phyto-082712-102234

Conflict of Interest: The authors declare that the research was conducted in the absence of any commercial or financial relationships that could be construed as a potential conflict of interest.

frontiers in Plant Science

ORIGINAL RESEARCH
published: 14 October 2020
doi: 10.3389/fpls.2020.585510

Host Plant Resistance to *Bemisia tabaci* to Control Damage Caused in Tomato Plants by the Emerging Crinivirus Tomato Chlorosis Virus

*Isabel M. Fortes, Rafael Fernández-Muñoz and Enrique Moriones**

Instituto de Hortofruticultura Subtropical y Mediterránea "La Mayora", Universidad de Málaga-Consejo Superior de Investigaciones Científicas (IHSM-UMA-CSIC), Estación Experimental "La Mayora", Málaga, Spain

Tomato chlorosis virus (genus *Crinivirus*, family *Closteroviridae*) (ToCV) is rapidly emerging, causing increased damage to tomato production worldwide. The virus is transmitted in a semipersistent manner by several whitefly (Hemiptera: Aleyrodidae) species and is expanding its geographical and host ranges associated with the emergence of whiteflies of the *Bemisia tabaci* complex. Control is based essentially on intensive insecticide applications against the insect vector but is largely ineffective. No virus-resistant or tolerant commercial tomato cultivars are available. Recently, a *B. tabaci*-resistant tomato line based on the introgression of type IV leaf glandular trichomes and secretion of acylsucroses from the wild tomato *Solanum pimpinellifolium* was shown to effectively control the spread of tomato yellow leaf curl virus, a begomovirus (genus *Begomovirus*, family *Geminiviridae*) persistently transmitted by *B. tabaci*. As short acquisition and transmission periods are associated to the semipersistent transmission of ToCV, its possible control by means of the *B. tabaci*-resistant tomato could be compromised. Moreover, if the antixenosis effect of the resistance trait present in those tomato plants results in increased *B. tabaci* mobility, an increased ToCV spread might even occur. We demonstrated, however, that the use of acylsugar-producing *B. tabaci*-resistant tomatoes effectively controls ToCV spread compared to a near-isogenic line without type IV trichomes and acylsugar secretion. No increase in the primary ToCV spread is observed, and secondary spread could be reduced significantly decreasing the incidence of this virus. The possible use of host plant resistance to whiteflies to limit spread of ToCV opens up new alternatives for a more effective control of this virus to reduce the damage caused in tomato crops.

Keywords: tomato chlorosis virus, tomato yellow leaf curl virus, crinivirus, begomovirus, *Bemisia tabaci*, whitefly resistance, tomato

OPEN ACCESS

Edited by:
Giuseppe Parrella,
Italian National Research Council, Italy

Reviewed by:
Jorge A. M. Rezende,
University of São Paulo, Brazil
Fengming Yan,
Henan Agricultural University, China

****Correspondence:***
Enrique Moriones
moriones@eelm.csic.es

Specialty section:
This article was submitted to Plant Pathogen Interactions, a section of the journal Frontiers in Plant Science

Received: *20 July 2020*
Accepted: *24 September 2020*
Published: *14 October 2020*

Citation:
Fortes IM, Fernández-Muñoz R and Moriones E (2020) Host Plant Resistance to Bemisia tabaci to Control Damage Caused in Tomato Plants by the Emerging Crinivirus Tomato Chlorosis Virus. Front. Plant Sci. 11:585510. doi: 10.3389/fpls.2020.585510

INTRODUCTION

Plant virus infections represent a severe constraint to tomato (*Solanum lycopersicum* L.) production worldwide. Among them, emerging whitefly (Hemiptera: Aleyrodidae)-transmitted viruses such as the crinivirus (genus *Crinivirus*, family *Closteroviridae*) tomato chlorosis virus (ToCV) or begomoviruses (genus *Begomovirus*, family *Geminiviridae*) causing the tomato yellow

leaf curl disease (tomato yellow leaf curl virus, TYLCV, the most widespread type), severely damage tomato crops worldwide (Hanssen et al., 2010; Rybicki, 2015; Rojas et al., 2018; Fiallo-Olivé and Navas-Castillo, 2019). Emergence of ToCV and TYLCV has been associated with the global spread of the whitefly *Bemisia tabaci* (Gennadius) in tropical and warm regions worldwide (Tzanetakis et al., 2013; Fereres, 2015; Gilbertson et al., 2015; Rojas et al., 2018; Fiallo-Olivé and Navas-Castillo, 2019). ToCV is transmitted in a semipersistent manner (short acquisition and inoculation periods) and TYLCV in a persistent manner (long acquisition and inoculation periods), respectively (Cohen and Antignus, 1994; Wintermantel, 2016; Fiallo-Olivé and Navas-Castillo, 2019).

Control of whitefly-transmitted viruses in tomato crops relies frequently on intensive chemical applications against the insect vector to reduce virus spread (Lapidot et al., 2014; Rojas et al., 2018; Fiallo-Olivé and Navas-Castillo, 2019). In fact, control of ToCV is mainly based in insecticide applications against whiteflies but has proven largely ineffective (Fiallo-Olivé and Navas-Castillo, 2019). Virus-resistant tomatoes are widely used commercially to effectively reduce the damage caused by TYLCV (Lapidot and Friedmann, 2002; Vidavski et al., 2008). However, although resistance of tomato plants to ToCV infection has been explored with sources from wild tomato relatives localized (García-Cano et al., 2010), no resistant/tolerant commercial tomato cultivar is yet available. Therefore, the recent report of a *B. tabaci*-resistant tomato line based on the introgression of type IV leaf glandular trichomes bred from the wild tomato *S. pimpinellifolium* useful to control the persistently transmitted begomovirus TYLCV (Rodríguez-López et al., 2011) offered new possibilities for the control of ToCV infections in tomato crops. Type IV trichomes in tomato are known to have acylsugars in their exudates which have been associated with negative effects on hemipteran pests (Simmons and Gurr, 2005). Nevertheless, the rapid acquisition and inoculation periods characteristic of semipersistent transmission of criniviruses, ToCV among others (Whitfield et al., 2015; Wintermantel, 2016), might compromise the control of this virus using *B. tabaci*-resistant tomatoes. Moreover, if the antixenosis effect of the resistance trait present in those acylsugar-producing tomato plants (Rodríguez-López et al., 2011) results in higher *B. tabaci* mobility, an increased ToCV spread might even occur. Therefore, the potential use of *B. tabaci*-resistant tomatoes to control ToCV spread is still an open question. Here, we provide evidence that support the use of *B. tabaci* resistance based on trichome production of acylsucroses as a management alternative to reduce ToCV spread during epidemics in tomato crops.

MATERIALS AND METHODS

Tomato Plants

Two tomato lines were used in this work, the whitefly and virus susceptible tomato cv. Moneymaker and its near-isogenic genotype, the advanced backcross line ABL 14-8. The latter was generated from the initial cross *S. lycopersicum* cv. Moneymaker (without type IV leaf glandular trichomes) x *S. pimpinellifolium* accession TO-937 (with type IV leaf glandular trichomes, IHSM-CSIC germplasm collection) (Fernández-Muñoz et al., 2003). Three cycles of combined recurrent crosses toward "Moneymaker" and subsequent selfing steps with selection for high type-IV leaf glandular trichome density and acylsugar production traits were done followed by two additional final selfing steps. Seedlings were individually sown in plastic pots of 12 cm containing a mixture of 50% soil (54% sand, 24% silt, 22% clay), 30% horticultural substrate, 15% coconut-fiber substrate and 5% litonite. Until used, plants were grown within an insect-proof glasshouse under natural lighting with loose temperature control (22–27°C day, 17–20°C night) and supplied weekly with nutrient solution. Experiments were conducted taking into account the plant growth stage because significant difference in acylsucrose production between "Moneymaker" and ABL 14-8 is only achieved after plants reach the 10-leaf growth stage (Rodríguez-López et al., 2011).

Virus Isolates, Whitefly Colony, and Virus Inoculation

ToCV isolate Pl-1-2 was used. This isolate was obtained from a naturally infected tomato plant collected during 1997 in Málaga (southern Spain) from a commercial tomato crop and maintained at IHSM in tomato cv. Moneymaker by periodic transmission with *B. tabaci* (García-Cano et al., 2010). The infectious clone of isolate [ES:Alm:Pep:99] of the Israel strain of TYLCV (hereafter, TYLCV), has been described elsewhere (Morilla et al., 2005). Virus-free *B. tabaci* (Mediterranean species) individuals were obtained from a colony originating from individuals collected during field visits in Málaga (Spain) and reared on melon (*Cucumis melo* L. cv. ANC42, IHSM seedbank collection) plants within wooden cages covered with insect-proof nets, in an insect-proof glasshouse with temperature control (22–27°C day and 17–20°C night) and light supplementation when needed.

ToCV-infected tomato plants were obtained by *B. tabaci*-mediated inoculation using viruliferous whiteflies. TYLCV-infected tomato plants were obtained either by *B. tabaci*-mediated inoculation using viruliferous whiteflies or by *Agrobacterium tumefaciens*-mediated inoculation (agroinoculation) using the infectious clone (see above) and the stem puncture method described by Monci et al. (2005). Plants were inoculated at the three-leaf growth stage. Mock inoculated control plants were obtained following the same inoculation procedures but using virus-free whiteflies or virus-free *A. tumefaciens*.

For *B. tabaci*-mediated inoculation, viruliferous whiteflies were obtained by mass feeding of virus-free *B. tabaci* adults (48-h acquisition access period, within insect-proof cages) on tomato cv. Moneymaker plants infected with ToCV or TYLCV 30 days before used for virus acquisition. For whitefly inoculation of individual plants, clip-on cages containing 25 viruliferous whiteflies were used on each test plant for a 48-h inoculation access period (IAP). Following IAP, the plants were sprayed with insecticide and maintained until used in an insect-proof glasshouse with temperature control (22–27°C day and 17–20°C night) and light supplementation when needed.

Primary Spread Experiments

Primary spread, i.e., virus spread to healthy plants from external source viruliferous insect vectors (Campbell and Madden, 1990), was simulated in medium-scale field experiments conducted within whitefly-proof net (10 × 22 threads/cm^2) walk-in structures (5 × 5 × 2 m) built within a tunnel net house at IHSM Experimental Station (Málaga, southern coastal Spain). Experiments were conducted by releasing 15 adult viruliferous whiteflies per test plant for a 48-h IAP. Viruliferous whiteflies were placed in the center of a circle (2 m diameter) of 22 healthy tomato test plants in a no-choice test design (**Figure 1A**). Experiments were conducted during summer with test plants at 10-leaf growth stage. Three independently repeated experiments were conducted with three replications per treatment in each one. After the IAP, plants were treated with insecticide and then transferred to an insect-proof glasshouse until analyzed. Type IV trichome density and acylsucrose accumulation on leaves were evaluated in assayed plants (see below). Virus presence was scored on the youngest newly emerged leaf of each test plant at weekly intervals until 28 days post inoculation (dpi) by tissue blot hybridization (see below). Propensity of the genotypes to be whitefly-infected was estimated by the percentage of infected plants. Data in the form of numbers of infected and non-infected plants were subjected to a generalized linear model analysis (Logit as the link function and Binomial as the underlying distribution) to perform statistical comparisons between the two genotypes by least-squares (LS) means test by using IBM SPSS Statistics for Windows, v. 26.0 (IBM Corp., Armonk, NY, United States).

Secondary Spread Experiments

Secondary spread, i.e., virus spread from virus-infected source plants to healthy plants (Campbell and Madden, 1990), was simulated in medium-scale field experiments conducted within insect-proof net walk-in structures (see above). In each treatment three virus-infected source plants were used which were placed forming a triangle with 60 cm separation from each other, in the center of a circle (2 m diameter) of 22 healthy test plants (**Figure 1B**). Excess number of potential virus-infected source plants were prepared by agroinoculation (TYLCV) or by clip-on-cage viruliferous whitefly-mediated inoculation (ToCV) at the three-leaf stage. Then, the virus-infected source plants to be used in the experiments were selected for showing similar virus hybridization signals in apical leaves (see below). Virus-free *B. tabaci* adult individuals (30 whiteflies per test plant) were released in the center of the triangle of virus source plants and after 96 h, test plants were treated with insecticide and transferred to an insect-proof glasshouse until analyzed. Experiments were conducted during summer with test and virus-infected source plants at the 10-leaf growth stage. Two independently repeated experiments were performed with three replications per treatment in each one. Test plants were analyzed and statistical analyses of results were conducted as for primary spread experiments.

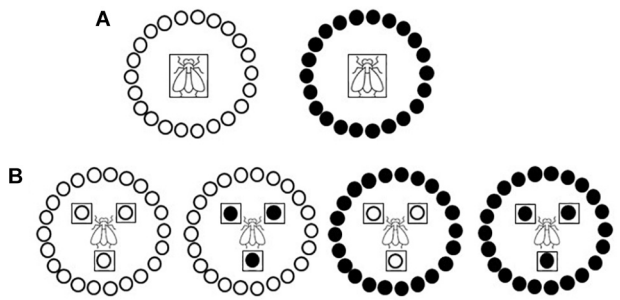

FIGURE 1 | Schematic diagramof the primary and secondary spread experiments. Two near-isogenic tomato genotypes with or without type IV leaf glandular trichomes and acylsucrose secretions (ABL 14-8 and cv. Moneymaker, respectively) were used. **(A)** Primary spread to healthy "Moneymaker" or ABL 14-8 test plants (22 plants in a no-choice test) at 10-leaf growth stage using 15 viruliferous *Bemisia tabaci* Mediterranean (Med) species adult whiteflies per test plant and a 48-h feeding access period. **(B)** Secondary spread from 10-leaf growth stage "Moneymaker" or ABL 14-8 virus source plants to 10-leaf growth stage "Moneymaker" or ABL 14-8 healthy test plants (22 plants in a no-choice test) using 30 virus-free *B. tabaci* Med adult whiteflies per test plant and 96-h feeding access period. Virus source plants and viruliferous whiteflies are boxed; "Moneymaker" plants are represented with open circles, and ABL 14-8 plants with solid circles.

Virus Detection by Molecular Hybridization

Presence of ToCV viral RNAs was analyzed in tomato plants by tissue blot hybridization. For this, freshly made cross-sections of petioles of the youngest newly emerged leaf of test plants were squash-blotted on positively charged nylon membranes (Roche Diagnostics GmbH, Mannheim, Germany). After blotting, nucleic acids were UV-cross-linked and hybridized with a ToCV-specific probe as described (García-Cano et al., 2006). For TYLCV detection, tissue blot hybridizations were also conducted as above using a TYLCV-specific probe (Monci et al., 2002). Although tissue-blotting is not a quantitative technique to determine virus accumulation, it was demonstrated to be useful in differentiating relative viral susceptibility among materials with different levels of resistance (Picó et al., 1999).

Trichome Observation and Acylsucrose Accumulation Quantification

Leaf trichome density and targeted associated secretions were measured on leaflets of the third youngest leaf on 10-leaf growth stage plants. Type-IV trichome density was calculated following the indications by Alba et al. (2009). Previous analysis of TO-937 (the *S. pimpinellifolium* accession source of type IV leaf glandular trichomes introgressed in ABL 14-8) and the derived *S. lycopersicum* introgression line indicated that these produced sucrosyl esters. Epicuticular leaf acylsucroses were extracted and quantified according to Escobar-Bravo et al. (2016). To normalize the data and stabilize the variance, trichome density and acylsucrose production were Log $(x + 1)$ transformed prior to analysis. Statistical differences between the means of trichome IV density and acylsucrose production in the two genotypes were analyzed by one-way ANOVA and the Fisher's least significant difference (LSD) test by using IBM SPSS Statistics for Windows, Version 26.0 (IBM Corp., Armonk, NY, United States).

RESULTS

Presence of Type-IV Leaf Glandular Trichome and Secretion of Acyl Sugars in ABL 14-8 Plants

Whereas type-I and type-VI glandular, and type-V non-glandular trichomes are present in both "Moneymaker" and its near-isogenic line ABL 14-8, the acylsucrose-producing type-IV leaf glandular trichomes, introgressed from *S. pimpinellifolium* accession TO-937, are absent in "Moneymaker" but densely cover the abaxial surface of ABL 14-8 leaves. As a result, in 10-leaf growth stage plants, significant differences were observed in the density of type IV trichomes and the acylsucrose production of "Moneymaker" and ABL 14-8 plants (**Figure 2**).

Virus Susceptibility of "Moneymaker" and ABL 14-8

For a correct assessment of the effect of insect resistance on the spread of ToCV (and TYLCV control), the ABL 14-8 and "Moneymaker" genotypes to be compared should be equally susceptible to the virus. This was inspected and similar ToCV and TYLCV susceptibility was observed for both genotypes based on hybridization analyses (**Supplementary Figure S1**).

No Increase of Primary ToCV Spread in ABL 14-8

The results of the medium-scale field experiments conducted to determine the possible effect of *B. tabaci*-resistance on primary ToCV spread are summarized in **Figure 3**. In no case was an increased ToCV spread observed owing to the presence of type IV glandular trichomes in ABL 14-8. As shown, in the three repeated experiments, ABL 14-8 plants exhibited an equal or lower propensity to be infected by ToCV compared to "Moneymaker," even at statistically supported differences in some cases (**Figure 3**, Experiment 2). A significantly reduced primary spread of the persistently-transmitted begomovirus TYLCV in ABL 14-8 versus "Moneymaker" was observed in the control treatments included (**Figure 3**) in every experiment and as previously reported (Rodríguez-López et al., 2011). The latter confirmed the optimum expression and accumulation of acylsucroses from type IV leaf glandular trichomes present in the ABL 14-8 plants used. The lower primary spread propensity observed for ToCV in ABL 14-8 was less pronounced than that observed for TYLCV.

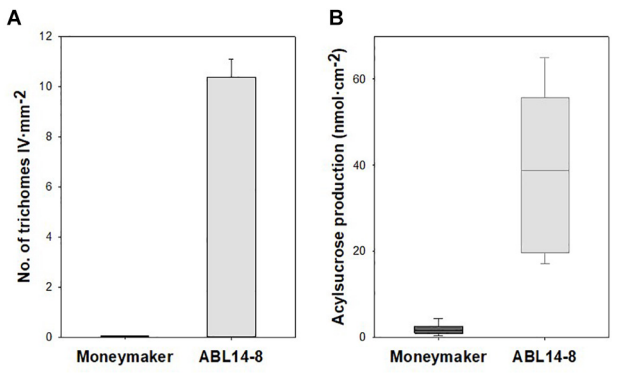

FIGURE 2 | Type-IV leaf glandular trichome density and acylsucrose production in ABL 14-8 and "Moneymaker" near-isogenic tomato lines. **(A)**, mean values of type-IV leaf glandular trichome densities (+ SEM, $n = 10$) measured in "Moneymaker" and ABL 14-8 10-leaf growth stages plants. **(B)** Box-and-Whisker plots showing acylsucrose accumulation in young leaves of "Moneymaker" and ABL 14-8 plants ($n = 10$) at 10-leaf growth stage; the box represents the interquartile range, the horizontal line in the box shows the value of the median, and bars below and above the box mark the 10th and 90th percentiles. Plants were grown in warm (summer) conditions. Both type IV trichome densities and acylsucrose production were significantly different ($P < 0.001$) between the two lines.

Reduced Secondary ToCV Spread in ABL 14-8

Given that the previous results indicated that ABL 14-8 plants could be infected by ToCV, it was important to assess whether the *B. tabaci* resistance could help to limit the secondary spread of the virus from the infected source plants. As for the primary spread, in no case was an increased ToCV secondary spread observed owing to the presence of type IV glandular trichomes in ABL 14-8. As summarized in **Figure 4**, infected ABL 14-8 plants resulted in significantly less efficient virus sources for secondary ToCV spread at any time assessed compared to "Moneymaker." About 20% to 40% less ToCV-incidence was detected at the end of the test period when ABL 14-8 was the virus source plant. No significant differences were observed for ABL 14-8 or "Moneymaker" as test plants (**Figure 4**). As expected from already reported studies (Rodríguez-López et al., 2011), significantly reduced secondary spread was also observed from ABL 14-8 source plants for the persistently-transmitted begomovirus TYLCV in the control treatments included (**Figure 4**). The latter confirmed the optimum expression and accumulation of acylsucroses from type IV leaf glandular trichomes present in the ABL 14-8 plants used. Therefore, the *B. tabaci* resistance present in ABL 14-8 was effective to impair secondary spread of the semipersistently transmitted ToCV.

DISCUSSION

Here a clue is given on the possibility to apply insect-resistant host plant to control a vectored plant virus. Control of ToCV infections in tomato crops is a challenge as yield losses of up to 50% of the tomato production have been reported (Mansilla-Córdova et al., 2018). In the absence of effective control measures the possibility to interfere with virus uptake and transmission (Dietzgen et al., 2016) was explored as an alternative management strategy. The results demonstrated that the use of the *B. tabaci*-resistance present in the ABL 14-8 tomato genotype based on type IV leaf glandular trichomes and acylsucrose exudates helps to impair ToCV spread which might be useful in controlling the damage caused by this virus.

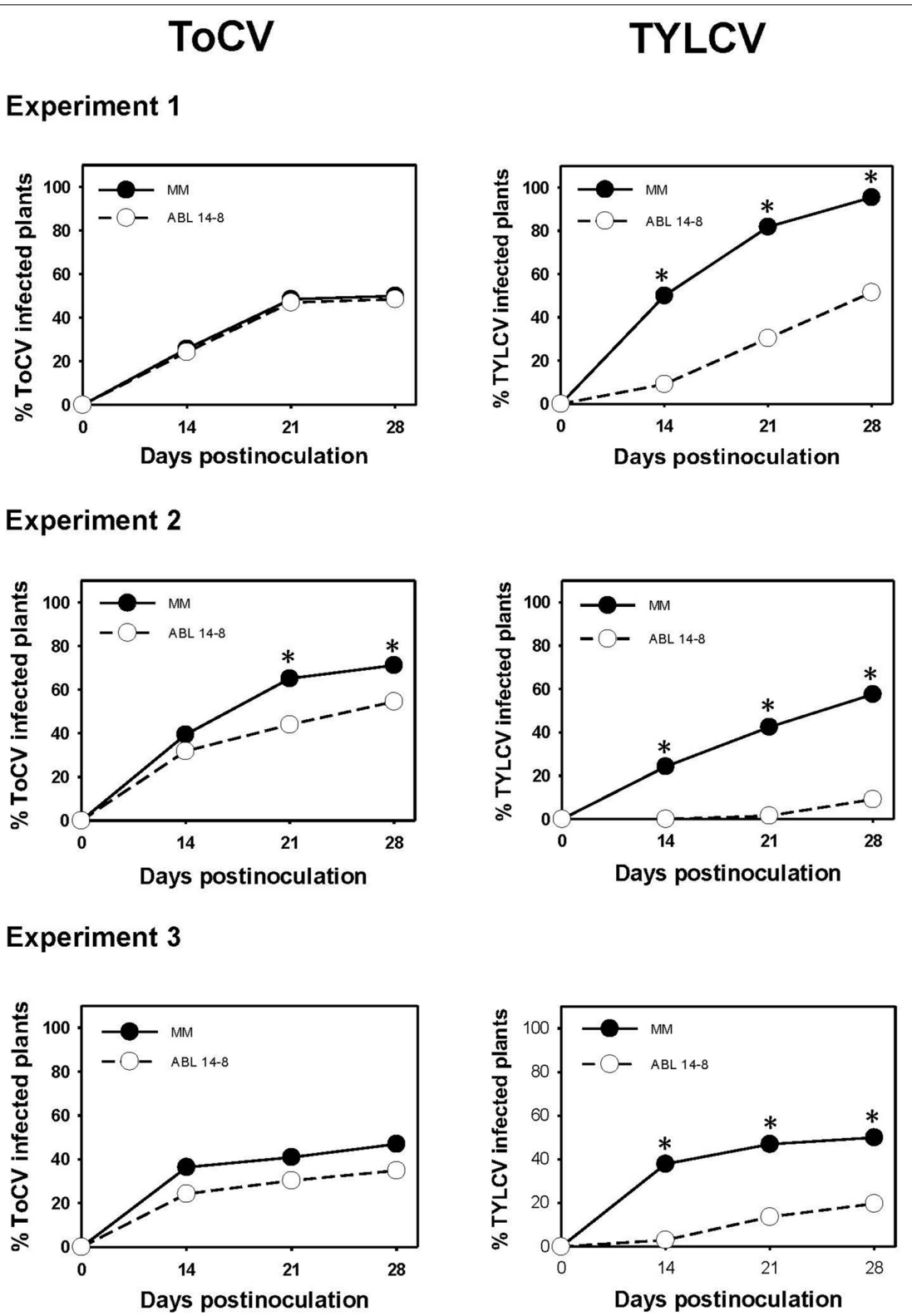

FIGURE 3 | Primary spread of tomato chlorosis virus. Primary spread of tomato chlorosis virus (ToCV) and control tomato yellow leaf curl virus (TYLCV) to near isogenic healthy tomato test plants (22 plants in a no-choice test) with (ABL 14-8) or without ("Moneymaker," MM) type IV leaf glandular trichomes and acylsucrose secretions at 10-leaf growth stage in medium-scale field experiments (three independently repeated experiments) conducted under warm-season conditions. ToCV and TYLCV transmission to test plants was measured several times after viruliferous whiteflies (15 *Bemisia tabaci* adult whiteflies per test plant) were given a 48-h feeding access period. Asterisk indicates significant differences in virus incidence between the two genotypes at a specific time (LS mean tests, $P < 0.05$).

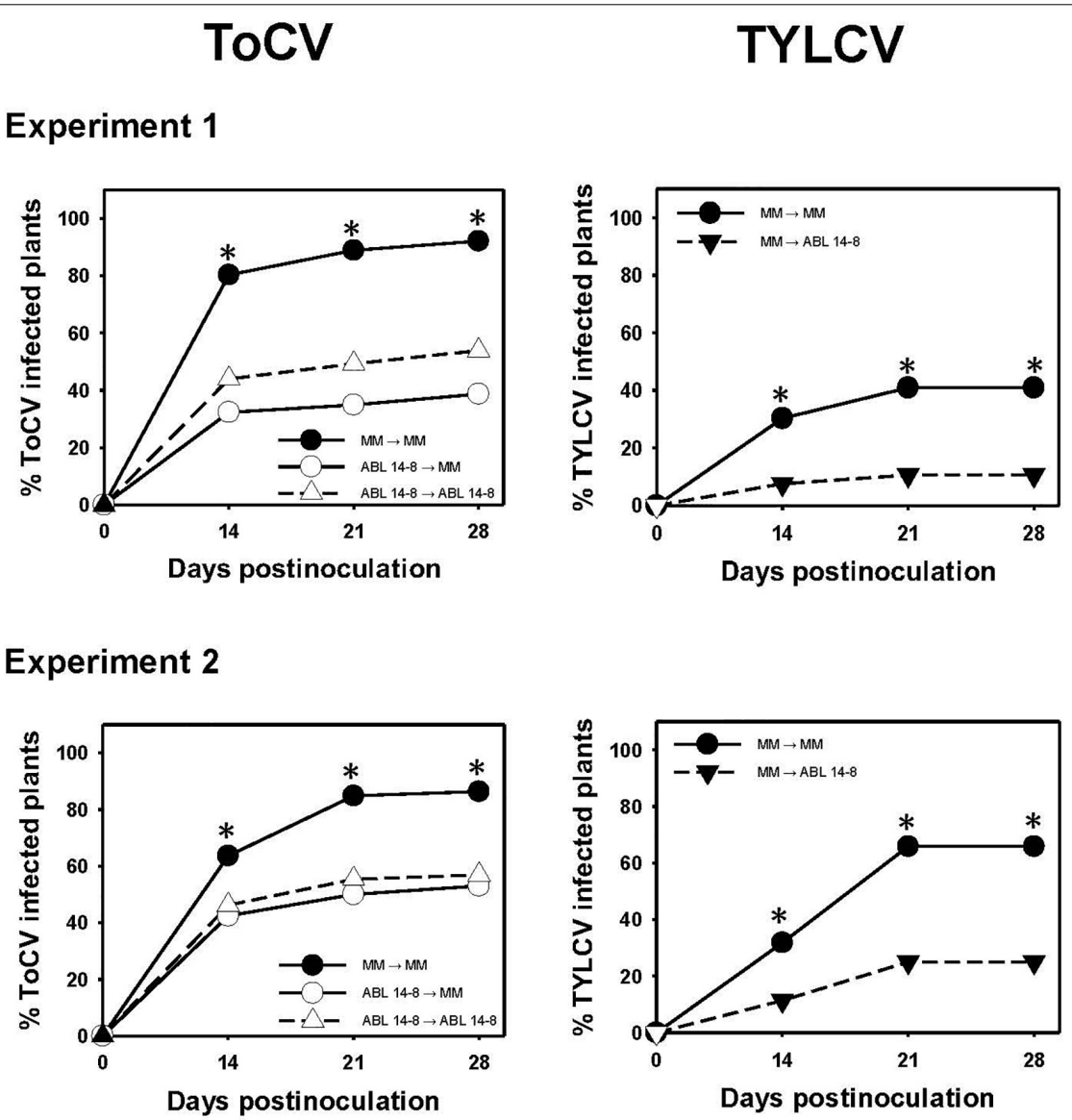

FIGURE 4 | Secondary spread of tomato chlorosis virus. Secondary spread of tomato chlorosis virus (ToCV) and control tomato yellow leaf curl virus (TYLCV) from 10-leaf growth stage near isogenic tomato infected source plants with (ABL 14-8) or without ("Moneymaker," MM) type IV leaf glandular trichomes and acylsucrose secretions to healthy ABL 14-8 or "Moneymaker" test plants (22 plants in a no-choice test) in medium-scale field experiments (two independently repeated experiments) conducted under warm-season conditions. Virus transmission to test plants was measured several times after virus-free whiteflies (30 *Bemisia tabaci* adult whiteflies per test plant) were given a 96-h feeding access period. Virus source (first) and test (second) plants are indicated in the figure legends. Asterisk indicates significant differences in virus incidence between the two genotypes at a specific time (LS mean tests, $P < 0.05$), which appeared only between the combination "Moneymaker" (source)-"Moneymaker" (test) and the other combinations.

The specific factors that determine ToCV transmission are complex, involving not only the virus and the insect vector but also the host plant and the environmental conditions. However, in addition to the nature of virus association with the vector, vector landing and probing on the plant as well as vector feeding patterns might condition the efficiency of virus transmission (Fereres and Moreno, 2009). Evidence is provided here supporting the idea that the presence of type IV leaf glandular trichomes and acylsucrose secretions in the tomato host can alter *B. tabaci* behavior in a way that can lead to changes in ToCV transmission. Alteration of virus transmission can then result in changes of virus spread dynamics (Jeger et al., 2004). No increase of primary ToCV spread was observed in ABL 14-8 in the experiments conducted in the present work. Moreover, a tendency to less efficient ToCV spread was observed in some cases. We had previously demonstrated that the *B. tabaci*-resistance traits present in ABL 14-8, in addition to deterring insect landing, affected insect feeding behavior (Rodríguez-López et al., 2011). The possibility of using insect deterrence to reduce virus-associated crop losses

has been highlighted (Mutschler and Wintermantel, 2006). Then, the less efficient ToCV primary virus spread shown in the *B. tabaci*-resistant tomato genotype could have been the result of a restricted *B. tabaci* interaction with these plants owing to their reduced attractiveness to the insect landing (Rodríguez-López et al., 2011). However, the relevance of *B. tabaci* feeding behavior after landing on a plant and the possible effects on virus transmission has also been discussed (Peñalver-Cruz et al., 2020). ToCV is a phloem-restricted virus in tomato and its inoculation is mainly associated with effective stylet activities in phloem sieve elements (Prado Maluta et al., 2017). Thus, the tendency to reduced primary spread observed in ABL 14-8 might also have been the result of the longer non-probe periods and shorter salivation times in the phloem reported for *B. tabaci* in ABL 14-8 (Rodríguez-López et al., 2011) which may have contributed to a less efficient ToCV inoculation. Therefore, both the *B. tabaci* restricted landing and the altered phloem feeding behavior in ABL 14-8 might contribute to a less effective primary virus spread.

For secondary virus spread, both virus acquisition from virus-infected source plants and virus inoculation in healthy plants should occur (Campbell and Madden, 1990). Therefore, an impaired secondary spread is expected in the *B. tabaci*-resistant ABL 14-8 tomato plants, as was observed. On the one hand, the *B. tabaci* deterrence reported in ABL 14-8 (Rodríguez-López et al., 2011) may have affected both virus uptake and virus transmission which might have resulted in the significantly decreased ToCV secondary spread observed. On the other hand, the reported altered feeding behavior of *B. tabaci* in this tomato genotype may also have affected ToCV secondary spread. The combination of an impaired virus acquisition expected from the longer non-probe periods and lower number of phloematic ingestions reported for *B. tabaci* in ABL 14-8 (Rodríguez-López et al., 2011), and an impaired ToCV inoculation that may result from the less efficient *B. tabaci* phloem salivation in the resistant plants (Rodríguez-López et al., 2011; Prado Maluta et al., 2017) might also support a less efficient secondary spread. Therefore, as for primary spread, the sum of the effects of the *B. tabaci* restricted landing and the altered phloem feeding behavior in ABL 14-8 might have resulted in the less effective secondary virus spread observed.

Madden et al. (2000) have stressed that the effect of vector resistance on disease development can strongly depend on the virus transmission mode. ToCV is a semipersistently transmitted virus (Wintermantel, 2016), with short acquisition and transmission periods. If these periods were enough for virus spread in ABL 14-8 and the *B. tabaci*-resistance traits present in plants of this tomato genotype stimulate greater movement of the whiteflies, an increased ToCV spread might have been feared. In fact, increased spread of non-persistently transmitted viruses (very short acquisition and transmission periods) has been reported in insect vector resistant plants in which the virus can be transmitted during the insect's short feeding probes for suitable feeding sites (Atiri et al., 1984). Also, a similar increased virus spread has been observed for non-persistently transmitted viruses with the use of some insecticides that agitate the insects and encourage movement to and feeding on greater numbers of plants before the time they die (Dent, 2001). The results obtained here, however, did not support an increased spread associated with the *B. tabaci*-resistance in ABL 14-8 which is strongly relevant for ToCV control purposes. In addition, a reduced secondary spread of ToCV was shown, mimicking the already reported response for the case of the persistently transmitted TYLCV (Rodríguez-López et al., 2011). Then, the effective reduced spread of the semipersistently transmitted ToCV obtained here by using the *B. tabaci*-resistant ABL 14-8 genotype might help to manage this virus in tomato crops. Future field testing can help in consolidating the results obtained here. Intensive tomato production mostly done under greenhouse conditions can be the perfect scenario for such field trials based on the results obtained. In these conditions, passive insect containment is conducted using screen nets in windows to minimize *B. tabaci* influx into the crop. In these conditions, the primary virus spread due to the continuous influx of viruliferous insects is mostly contained and secondary spread from initial virus foci is especially relevant. Conducting field tests under greenhouse conditions, might then allow the evaluation of the effect of the tomato plants ABL 14-8 on the reduction of secondary transmissions of ToCV, for which experimental data are robust. Moreover, if mixed ToCV-TYLCV infections occur during field trials, periodic monitoring of the exposed plants using molecular techniques will allow assessing single and mixed infections for an extended period. This can help to obtain more general conclusions about the benefits of the use of resistance to the vector, conferred by the glandular trichomes, to reduce the spread of these two viruses.

Management of viruses through alteration of vector efficiency as shown here for *B. tabaci* and ToCV is an interesting control alternative that might help to reduce dependence on intensive insecticide use (Zitter and Simons, 1980). This is especially important in cases in which no host-plant resistance to the virus is commercially available, as is the case for ToCV. Moreover, the use of insect-resistance in the host is also valuable for improving the management of *B. tabaci* as a pest, because it has been shown that insecticide pressure rapidly results in the development of resistant populations (Horowitz et al., 2020). As a result, the *B. tabaci* resistance described here would also be useful for supplementing *B. tabaci* control measures (Perring et al., 2018) in order to reduce the dependence on insecticide applications.

CONCLUSION

In conclusion, the *B. tabaci*-resistance derived from the presence of type IV leaf glandular trichomes and acylsucrose production present in ABL 14-8 tomato plants significantly helps to reduce ToCV spread even though this tomato genotype is fully susceptible to the virus. This resistance might then be an interesting tool to be included in integrated management of ToCV epidemics. As ToCV-resistance sources have also been reported from tomato relatives (García-Cano et al., 2010) it may be expected that ToCV-resistance will soon be bred in commercial tomatoes. It has been shown that the use of vector resistant lines to reduce virus spread helps to exert minimal

selection pressure on the virus to evolve more harmful strains (van den Bosch et al., 2006). Then, the alternative of combining *B. tabaci*-resistance with virus-resistance genes (gene pyramids) will offer future alternatives for a more effective, sustainable and durable control of ToCV (Gómez et al., 2009; Mundt, 2014).

DATA AVAILABILITY STATEMENT

All datasets presented in this study are included in the article/**Supplementary Material**.

AUTHOR CONTRIBUTIONS

EM conceived and developed the concept, supervised the experiments, and wrote the manuscript. RF-M contributed to the data analysis and interpretation, discussions, and writing of the manuscript. IF performed the experiments. All the authors contributed to the manuscript revision, read, and approved the final manuscript.

FUNDING

EM was supported by the grants AGL2016-75819-C2-2-R and PID2019-107657RB-C21 and RF-M by the grant AGL2015-65246-R, funded by the Agencia Estatal de Investigación-Ministerio de Economía, Industria y Competitividad and Ministerio de Ciencia e Innovación, Spain. EM and RF-M were supported by the grant P18-RT-1249 from Consejería de Economía, Conocimiento y Universidad, Junta de Andalucía, Spain. Both AGL2016-75819-C2-2 and P18-RT-1249 grants have the assistance of the European Regional Development Fund (ERDF) and the European Social Fund (ESF).

ACKNOWLEDGMENTS

We acknowledge support of the publication fee by the CSIC Open Access Publication Support Initiative through its Unit of Information Resource for Research (URICI).

SUPPLEMENTARY MATERIAL

The Supplementary Material for this article can be found online at: https://www.frontiersin.org/articles/10.3389/fpls.2020.585510/full#supplementary-material

Supplementary Figure 1 | Accumulation of tomato chlorosis virus and tomato yellow leaf curl virus in isogenic tomato genotypes ABL 14-8 and "Moneymaker." Molecular hybridization of squash blots of freshly cross-sectioned young leaves petioles performed at 30 days post-inoculation for nine plants of each of the "Moneymaker" or ABL 14-8 near-isogenic tomato lines inoculated by using tomato chlorosis virus (ToCV) **(A,B)** or tomato yellow leaf curl virus (TYLCV) **(D,E)** with clip-on-caged viruliferous whiteflies; short **(A,D)** and long **(B,E)** exposition of autoradiographs are shown. In order to prevent interference of the *Bemisia tabaci* resistance of ABL 14-8 in the assessment of the host-plant susceptibility to the viruses of the two nearly isogenic lines, the plants were inoculated at the three-leaf growth stage when acylsucrose production of type IV leaf glandular trichomes is still very low (Rodríguez-López et al., 2011). For monitoring of virus accumulation, one leaf petiole was tested per test plant performing two squash blots. Molecular hybridization was conducted with probes specific to ToCV or TYLCV. Numbers on top of the autoradiographs refer to the plant number. The two genotypes were equally susceptible to each virus in terms of both the number of infected plants and the estimation of viral accumulation done by densitometry measure of hybridization signals obtained in digitized imaging of autoradiographs. The comparison of the hybridization signals for the short exposition autoradiographs obtained from ToCV and TYLCV infected "Moneymaker" and ABL 14-8 plants is shown in **(C)** and **(F)**. respectively. Densitometry measurements were expressed as adjusted pixel densities calculated using Quantity One Software v 4.6.7 (VersaDoc MP 4000 Imaging System; Bio-Rad). Values were then represented in Box-and-Whisker plots and compared by One way ANOVA by using IBM SPSS Statistics for Windows, v. 26.0 (IBM Corp., Armonk, NY, United States). NS = non-significant differences.

REFERENCES

Alba, J. M., Montserrat, M., and Fernández-Munoz, R. (2009). Resistance to the two-spotted spider mite (*Tetranychus urticae*) by acylsucroses of wild tomato (*Solanum pimpinellifolium*) trichomes studied in a recombinant inbred line population. *Exp. Appl. Acarol.* 47, 35–47. doi: 10.1007/s10493-008-9192-4

Atiri, G. I., Ekpot, E. J. A., and Thottappilly, G. (1984). The effect of aphid-resistance in cowpea on infestation and development *of Aphis craccivora* and the transmission of cowpea aphid-borne mosaic virus. *Ann. Appl. Biol.* 104, 339–346. doi: 10.1111/j.1744-7348.1984.tb05619.x

Campbell, C. L., and Madden, L. V. (1990). *Introduction to Plant Disease Epidemiology*. New York, NY: John Wiley & Sons.

Cohen, S., and Antignus, Y. (1994). "Tomato yellow leaf curl virus, a whitefly-borne geminivirus of tomatoes," in *Advances in Disease Vector Research*, Vol. 10, ed. K. F. Harris (Springer), 259–288. doi: 10.1007/978-1-4612-2590-4_10

Dent, D. (2001). *Insect Pest Management*. Wallingford: CABI Publishing.

Dietzgen, G. R., Mann, S. K., and Johnson, N. K. (2016). Plant virus-insect vector interactions: current and potential future research directions. *Viruses* 8:303. doi: 10.3390/v8110303

Escobar-Bravo, R., Alba, J. M., Pons, C., Granell, A., Kant, M. R., Moriones, E., and Fernández-Munoz, R. (2016). A jasmonate-inducible defense trait transferred from wild into cultivated tomato establishes increased whitefly resistance and reduced viral disease incidence. *Front. Plant Sci.* 7:1732. doi: 10.3389/fpls.2016.01732

Fereres, A. (2015). Insect vectors as drivers of plant virus emergence. *Curr. Opin. Virol.* 10, 42–46. doi: 10.1016/j.coviro.2014.12.008

Fereres, A., and Moreno, A. (2009). Behavioural aspects influencing plant virus transmission by homopteran insects. *Virus Res.* 141, 158–168. doi: 10.1016/j.virusres.2008.10.020

Fernández-Muñoz, R., Salinas, M., Alvarez, M., and Cuartero, J. (2003). Inheritance of resistance to two-spotted spider mite and glandular leaf trichomes in wild tomato *Lycopersicon pimpinellifolium* (Jusl.) . *Mill. J. Am. Soc. Hortic. Sci.* 128, 188–195. doi: 10.21273/JASHS.128.2.0188

Fiallo-Olivé, E., and Navas-Castillo, J. (2019). Tomato chlorosis virus, an emergent plant virus still expanding its geographical and host ranges. *Mol. Plant Pathol.* 20, 1307–1320. doi: 10.1111/mpp.12847

García-Cano, E., Navas-Castillo, J., Moriones, E., and Fernández-Munoz, R. (2010). Resistance to *Tomato chlorosis virus* in wild tomato species that impair virus accumulation and disease symptom expression. *Phytopathology* 100, 582–592. doi: 10.1094/PHYTO-100-6-0582

García-Cano, E., Resende, R. O., Fernández-Munoz, R., and Moriones, E. (2006). Synergistic interaction between *Tomato chlorosis virus* and *Tomato spotted wilt virus* results in breakdown of resistance in tomato. *Phytopathology* 96, 1263–1269. doi: 10.1094/PHYTO-96-1263

Gilbertson, R. L., Batuman, O., Webster, C. G., and Adkins, S. (2015). Role of the insect supervectors *Bemisia tabaci* and *Frankliniella occidentalis* in the

emergence and global spread of plant viruses. *Ann. Rev. Virol.* 2, 67–93. doi: 10.1146/annurev-virology-031413-085410

Gómez, P., Rodríguez-Hernández, A. M., Moury, B., and Aranda, M. A. (2009). Genetic resistance for the sustainable control of plant virus diseases: breeding, mechanisms and durability. *Eur. J. Plant Pathol.* 125, 1–22. doi: 10.1007/s10658-009-9468-5

Hanssen, I. M., Lapidot, M., and Thomma, B. P. H. J. (2010). Emerging viral diseases of tomato crops. *Mol. Plant Microbe Int.* 23, 539–548. doi: 10.1094/MPMI-23-5-0539

Horowitz, A. R., Ghanim, M., Roditakis, E., Nauen, R., and Ishaaya, I. (2020). Insecticide resistance and its management in *Bemisia tabaci* species. *J. Pest Sci.* 93, 893–910. doi: 10.1007/s10340-020-01210-0

Jeger, M. J., Holt, J., van den Bosch, F., and Madden, L. V. (2004). Epidemiology of insect-transmitted plant viruses: modelling disease dynamics and control interventions. *Physiol. Entomol.* 29, 291–304. doi: 10.1111/j.0307-6962.2004.00394.x

Lapidot, M., and Friedmann, M. (2002). Breeding for resistance to whitefly-transmitted geminiviruses. *Ann. Appl. Biol.* 140, 109–127. doi: 10.1111/j.1744-7348.2002.tb00163.x

Lapidot, M., Legg, J. P., Wintermantel, W. M., and Polston, J. E. (2014). Management of whitefly-transmitted viruses in open-field production systems. *Adv. Virus Res.* 90, 147–206. doi: 10.1016/B978-0-12-801246-8.00003-2

Madden, L. V., Jeger, M. J., and van den Bosch, F. (2000). A theoretical assessment of the effects of vector-virus transmission mechanism on plant virus disease epidemics. *Phytopathology* 90, 576–594. doi: 10.1094/PHYTO.2000.90.6.576

Mansilla-Córdova, P. J., Bampi, D., Rondinel-Mendoza, N. V., Melo, P. C. T., Lourenção, A. L., and Rezende, J. A. M. (2018). Screening tomato genotypes for resistance and tolerance to *Tomato chlorosis virus*. *Plant Pathol.* 67, 1231–1237. doi: 10.1111/ppa.12826

Monci, F., García-Andrés, S., Maldonado, J. A., and Moriones, E. (2005). Resistance to monopartite begomoviruses associated with the bean leaf crumple disease in *Phaseolus vulgaris* controlled by a single dominant gene. *Phytopathology* 95, 819–826. doi: 10.1094/PHYTO-95-0819

Monci, F., Sánchez-Campos, S., Navas-Castillo, J., and Moriones, E. (2002). A natural recombinant between the geminiviruses *Tomato yellow leaf curl Sardinia virus* and *Tomato yellow leaf curl virus* exhibits a novel pathogenic phenotype and is becoming prevalent in Spanish populations. *Virology* 303, 317–326. doi: 10.1006/viro.2002.163

Morilla, G., Janssen, D., García-Andrés, S., Moriones, E., Cuadrado, I. M., and Bejarano, E. R. (2005). Pepper (*Capsicum annuum*) is a dead-end host for Tomato yellow leaf curl virus. *Phytopathology* 95, 1089–1097. doi: 10.1094/PHYTO-95-1089

Mundt, C. C. (2014). Durable resistance: a key to sustainable management of pathogens and pests. *Infect. Genet. Evol.* 27, 446–455. doi: 10.1016/j.meegid.2014.01.011

Mutschler, M. A., and Wintermantel, W. M. (2006). "Reducing virus associated crop loss through resistance to insect vectors," in *Natural Resistance Mechanisms of Plant Viruses*, eds G. Loebenstein and J. P. Carr (The Netherlands: Springer), 241–260. doi: 10.1007/1-4020-3780-5_11

Peñalver-Cruz, A., Garzo, E., Prieto-Ruiz, I., Díaz-Carro, M., Winters, A., and Moreno, A. (2020). Feeding behavior, life history, and virus transmission ability of *Bemisia tabaci* Mediterranean species (*Hemiptera*: *Aleyrodidae*) under elevated CO2. *Insect Sci.* 27, 558–570. doi: 10.1111/1744-7917.12661

Perring, T. M., Stansly, P. A., Liu, T. X., Smith, H. A., and Andreason, S. A. (2018). "Whiteflies: biology, ecology, and management," in *Sustainable Management of Arthropod Pests of Tomato*, eds W. Wakil, G. E. Brust, and T. M. Perring (San Diego, CA: Academic Press), 73–110.

Picó, B., Ferriol, M., Díez, M., and Nuez, F. (1999). Developing tomato breeding lines resistant to tomato yellow leaf curl virus. *Plant Breed.* 118, 537–542. doi: 10.1046/j.1439-0523.1999.00427.x

Prado Maluta, N., Garzo, E., Moreno, A., Navas-Castillo, J., Fiallo-Olivé, E., and Spotti Lopez, J. (2017). Stylet penetration activities of the whitefly *Bemisia tabaci* associated with inoculation of the crinivirus *Tomato chlorosis virus*. *J. Gen. Virol.* 98, 1515–1520. doi: 10.1099/jgv.0.000783

Rodríguez-López, M. J., Garzo, E., Bonani, J. P., Fereres, A., Fernández-Muñoz, R., and Moriones, E. (2011). Whitefly resistance traits derived from the wild tomato *Solanum pimpinellifolium* affect the preference and feeding behavior of *Bemisia tabaci* and reduce the spread of Tomato yellow leaf curl virus. *Phytopathology* 101, 1191–1201. doi: 10.1094/PHYTO-01-11-0028

Rojas, M. R., Macedo, M. A., Maliano, M. R., Soto-Aguilar, M., Souza, J. O., and Briddon, R. W. (2018). World management of geminiviruses. *Annu. Rev. Phytopathol.* 56, 637–677. doi: 10.1146/annurev-phyto-080615-100327

Rybicki, E. P. (2015). A Top Ten list for economically important plant viruses. *Arch. Virol.* 160, 17–20. doi: 10.1007/s00705-014-2295-9

Simmons, A. T., and Gurr, G. M. (2005). Trichomes of *Lycopersicon* species and their hybrids: effects on pests and natural enemies. *Agric. Forest Entomol.* 7, 265–276. doi: 10.1111/j.1461-9555.2005.00271.x

Tzanetakis, I. E., Martin, R. R., and Wintermantel, W. (2013). Epidemiology of criniviruses, an emerging problem in world agriculture. *Front. Microbiol.* 4:119. doi: 10.3389/fmicb.2013.00119

van den Bosch, F., Akudibilah, G., Seal, S., and Jeger, M. (2006). Host resistance and the evolutionary response of plant viruses. *J. Appl. Ecol.* 43, 503–516. doi: 10.1111/j.1365-2664.2006.01159.x

Vidavski, F., Czosnek, H., Gazit, S., Levy, D., and Lapidot, M. (2008). Pyramiding of genes conferring resistance to *Tomato yellow leaf curl virus* from different wild tomato species. *Plant Breed.* 127, 625–631. doi: 10.1111/j.1439-0523.2008.01556.x

Whitfield, A. E., Falk, B. W., and Rotenberg, D. (2015). Insect vector-mediated transmission of plant viruses. *Virology* 479-480, 278–289. doi: 10.1016/j.virol.2015.03.026

Wintermantel, W. M. (2016). "Semipersistent whitefly-transmitted viruses: criniviruses," in *Vector-Mediated Transmission of Plant Pathogens*, ed. J. K. Brown (College Park, MA: APS Publications),), 111–119. doi: 10.1094/9780890545355.008

Zitter, T. A., and Simons, J. N. (1980). Management of viruses by alteration of vector efficiency and by cultural practices. *Annu. Rev. Phytopathol.* 18, 289–310. doi: 10.1146/annurev.py.18.090180.001445

Conflict of Interest: The authors declare that the research was conducted in the absence of any commercial or financial relationships that could be construed as a potential conflict of interest.

frontiers in Plant Science

REVIEW
published: 19 November 2020
doi: 10.3389/fpls.2020.558403

Nanovirus Disease Complexes: An Emerging Threat in the Modern Era

Aamir Lal[1], Thuy Thi Bich Vo[1], I Gusti Ngurah Prabu Wira Sanjaya[1], Phuong Thi Ho[1], Ji-Kwang Kim[2], Eui-Joon Kil[1,3] and Sukchan Lee[1]**

[1] Department of Integrative Biotechnology, Sungkyunkwan University, Suwon, South Korea, [2] Research and Development Bureau, Chungcheongnam-do Agricultural Research and Extension Services, Yesan, South Korea, [3] Department of Plant Medicals, Andong National University, Andong, South Korea

Multipartite viruses package their genomic segments independently and mainly infect plants; few target animals. *Nanoviridae* is a family of multipartite single-stranded DNA plant viruses that individually encapsidate single-stranded DNAs of approximately 1 kb and transmit them through aphids without replication in the aphid vectors, thereby causing important diseases of leguminous crops and banana. Significant findings regarding nanoviruses have recently been made on important features, such as their multicellular way of life, the transmission of distinct encapsidated genome segments through the vector body, evolutionary ambiguities, mode of infection, host range and geographical distribution. This review deals with all the above-mentioned features in view of recent advances with special emphasis on the emergence of new species and recognition of new host range of nanoviruses and aims to shed light on the evolutionary linkages, the potentially devastating impact on the world economy, and the future challenges imposed by nanoviruses.

Keywords: nanoviruses, multipartite virus, evolution, host range, geographical distribution, geminiviruses

OPEN ACCESS

Edited by:
Toufic Elbeaino, International Centre for Advanced Mediterranean Agronomic Studies, Italy

Reviewed by:
Stéphane Blanc, Institut National de la Recherche Agronomique de Montpellier, France
Ana Grande-Pérez, Institute of Subtropical and Mediterranean Horticulture "La Mayora", Spain
Heiko Ziebell, Julius Kühn-Institut, Germany

****Correspondence:***
Eui-Joon Kil
viruskil@anu.ac.kr
Sukchan Lee
cell4u@skku.edu

Specialty section:
This article was submitted to Plant Pathogen Interactions, a section of the journal Frontiers in Plant Science

Received: *02 May 2020*
Accepted: *28 October 2020*
Published: *19 November 2020*

Citation:
Lal A, Vo TTB, Sanjaya IGNPW, Ho PT, Kim J-K, Kil E-J and Lee S (2020) Nanovirus Disease Complexes: An Emerging Threat in the Modern Era. Front. Plant Sci. 11:558403. doi: 10.3389/fpls.2020.558403

INTRODUCTION

Among viruses, single-stranded (ss) DNA viruses are a considerable threat to all living organisms. These ssDNA viruses infect both plants and animals. Circoviruses (Tischer et al., 1986; Cheung, 2006), bidensoviruses (Hayakawa et al., 2000), small circular (smaco) viruses (Ng et al., 2015), redondoviruses (Abbas et al., 2019), anelloviruses (Biagini et al., 2006; Blatter et al., 2018), genomoviruses (Krupovic et al., 2016), and circular replication-associated protein (Rep)-encoding single-stranded (CRESS) DNA viruses (Dayaram et al., 2014; Rosario et al., 2015) are some of the important ssDNA viruses, which infect animals, silkworm, human beings, fungi, insects and marine invertebrates, respectively. ssDNA viruses are largely known for their devastating effects on the plant world (Goodman, 1977; Kenyon et al., 2014; Malathi and Renuka Devi, 2019b). Among these ssDNA viruses, monopartite and bipartite viruses, with one and two segments, respectively, are very common. In these viruses, nucleic acid segments are encapsidated into a single virion (viral particle) which propagates as a whole. Some viruses are multipartite and have two or more segmented genomes packaged into separate virions, each of them capable of propagating independently (Randles et al., 2000; Sicard et al., 2016).

Based on their genomic organization, the International Committee on the Taxonomy of Viruses (ICTV) categorized ssDNA plant viruses into two families: (i) *Geminiviridae* (Zerbini et al., 2017) and (ii) *Nanoviridae* (Randles et al., 2000; Vetten et al., 2012). *Geminiviridae* is the largest family of plant viruses which can infect a large number of hosts belonging to several plant genera and

families. *Nanoviridae*, the focal point of this study, comprises plant viruses possessing very small virions which contain a multipartite (6–8), circular, single stranded DNA genome of approximately 1 kb in length, along with a few satellite molecules, each possessing a specific function (Vetten et al., 2012; Briddon et al., 2018; Malathi and Dasgupta, 2019a). Highly diversified host ranges are ascribed to *Nanoviridae* members which induce symptoms such as stunting, dwarfism, necrosis, mosaic, and leaf rolling in host plants and may eventually lead to plant death as well (Mandal, 2010; Grigoras et al., 2014; Hull, 2014; Gaafar et al., 2017, 2018). Viral replication occurs in the nucleus of infected cells via ssDNA rolling circle amplification (Rosario et al., 2012; Jeske, 2018). In addition, aphid transmission is a key characteristic for viruses belonging to the *Nanoviridae* family (Sano et al., 1998; Franz et al., 1999). Here we outline the *Nanoviridae* family and delve into the recent developments while identifying its impact on the agricultural world.

NANOVIRIDAE FAMILY: CLASSIFICATION, GENOMIC-STRUCTURE, AND FUNCTION

The *International Committee on Taxonomy of Viruses (ICTV)* categorized the *Nanoviridae* family into two genera, *Nanovirus* and *Babuvirus,* based on their genome organization and transmission vectors, along with categorization of coconut foliar decay virus (CFDV) as an unassigned species (Mandal, 2010; **Table 1**). Nanoviruses are non-enveloped with icosahedral and round geometries, and $T = 1$ symmetry with a diameter of 18–19 nm (**Figures 1A,B**). Contrary to geminiviruses, nanoviruses are multipartite viruses with 8–10 circular ssDNA components of approximately 1 kb in size (Sano et al., 1998; Gronenborn, 2004), while babuviruses contain six components with a size of approximately 1–1.1 kb (Halbert and Baker, 2015) and 12 DNAs of approximately 1.2–1.4 kb in size in association with CFDV (Gronenborn et al., 2018). Additional circular, ssDNA molecules (∼1–1.4 kb) that encode Rep protein, referred to as satellite molecules, have also been reported along with nanoviruses and babuviruses recently and categorized as *nano alphasatellites*. Those in the unassigned CFDV are categorized into unassigned species in the family *alphasatellitidae* (Briddon et al., 2018).

Whilst the genomes of geminiviruses are encoded by one or two circular ssDNA molecules, the genomes of Nanoviridae members are encoded by six or eight components (**Figure 1B**). Furthermore, these components are encapsidated separately into individual virions each with a specific role (Harrison, 1985; Randles et al., 2000; Saunders et al., 2003). DNA R encodes the master replication (M-Rep) initiator protein (Timchenko et al., 2000; Horser et al., 2001), DNA M encodes the movement protein, DNA C encodes the cell-cycle-link (clink) protein (Aronson et al., 2000), DNA S encodes the capsid protein (CP) (Wanitchakorn et al., 1997), and DNA N encodes the nuclear shuttle protein (NSP) (Wanitchakorn et al., 2000; Gronenborn, 2004) (Function of CP, Rep and NSP explained in following sections). Despite the numerous attempts to investigate U1, U2, and U4 of nanoviruses and U3 of babuviruses as well as the satellite molecules associated with nanoviruses, their biological functions remain unclear (**Figures 2A–C**).

GEOGRAPHICAL DISTRIBUTION OF *NANOVIRIDAE* MEMBERS

There have been increasing reports of the presence of *Nanoviridae* members from different regions of the world. Between the genera of the family *Nanoviridae*, babuviruses are highly ubiquitous viruses, e.g., banana bunchy top virus (BBTV) has been reported almost throughout the world (Sun, 1961; Burns et al., 1995; Beetham et al., 1997; Amin et al., 2008; Almeida et al., 2009; Blomme et al., 2013). Abaca bunchy top virus (ABTV) and cardamom bushy dwarf virus (CBDV) are found in the Philippines and Malaysia (Sharman et al., 2008) and India, respectively (Mandal et al., 2004; Ghosh et al., 2015). *Nanoviridae* members have marked their presence in major continents: Asia, Europe, Africa, and Australia. Among these nanoviruses, some were observed to be limited to certain areas or particular countries within a continent, while some exhibited high diversity through their presence across many continents, such as cow vetch latent virus (CVLV) in France; sophora yellow stunt-associated virus (SYSaV) and milk vetch chlorotic dwarf virus (MVCDV) in Iran; and faba bean yellow leaf virus (FBYLV) reported only in Ethiopia (Abraham et al., 2012; Heydarnejad et al., 2017; Hassan-Sheikhi et al., 2020); milk vetch dwarf virus (MDV) and subterranean clover stunt virus (SCSV) in Asia (Boevink et al., 1995; Sano et al., 1998; Lal et al., 2018); pea necrotic yellow dwarf virus (PNYDV), black medic leafroll virus (BMLRV), parsley severe stunt associated virus (PSSaV) and pea yellow stunt virus (PYSV) in Europe (Grigoras et al., 2014; Gaafar et al., 2016; Vetten et al., 2019); faba bean necrotic yellows virus (FBNYV) and faba bean necrotic stunt virus (FBNSY) in Asia, Europe, and Africa (Katul et al., 1998; Grigoras et al., 2010b); and CFDV unassigned species detected from Vanuatu, located near the South Pacific Ocean (Gronenborn et al., 2018; **Figure 3**). Interestingly, no nanoviruses have been identified in the new world to date. Though some of these viruses could be invasive, while others may have been there for ages and have been increasingly identified in these regions due to an increasing number of metagenomic studies (Gaafar et al., 2018; Gronenborn et al., 2018; Vetten et al., 2019; Hassan-Sheikhi et al., 2020; Lal et al., 2020), data scarcity confines our analysis. The purpose of listing the species at different locations around the world is simply to reflect the regions in which the specific nanoviruses were identified.

HOST RANGE AND SYMPTOMS

Nanoviruses are considered as viral agents with limited host range. Among nanoviruses, babuviruses infect only the monocot species, *Musaceae* and *Zingiberaceae* (Burns et al., 1995; Mandal et al., 2004; Amin et al., 2008). No other plant families

TABLE 1 | Introduction to *Nanoviridae*: occurrence, transmission, host ranges and symptoms development.

Genus	Species	Family	Host Species	Symptoms	Transmission	References
Nanovirus	*Subterranean clover stunt virus* (SCSV)	*Fabaceae*	*Trifolium subterraneum* *Medicago hispida* *Macroptilium lathyroides*	Chlorosis and stunting	*Aphis craccivora, A. gossypii,*	Boevink et al., 1995
	Faba bean necrotic yellows virus (FBNYV)	*Fabaceae*	*Cicer arietinum,* *Vicia faba* *Phaseolus vulgaris*	Necrosis and leaf rolling	*Acyrthosiphon pisum*	Katul et al., 1998
	Faba bean necrotic stunt virus (FBNSY)	*Fabaceae*	*Lens culinaris* *Vicia sativa*	Necrosis and stunting	*Acyrthosiphon pisum* *Aphis craccivora*	Grigoras et al., 2010a
	Pea necrotic yellow dwarf virus (PNYDV)	*Fabaceae*	*Pisum sativum* *Vicia faba, V. sativa* and *Lens culinaris*	Stunting, dwarfing, yellowing and leaf rolling	*Acyrthosiphon pisum*	Gaafar et al., 2016
	Milk Vetch Dwarf Virus (MDV)	*Fabaceae* *Caricaceae* *Solanaceae*	*Astragalus sinicus* *Glycine max* *Carica papaya* *Solanum lycopersicum* *Capsicum annuum*	Stunting, dwarfing, vein yellowing	*Aphis craccivora*	Sano et al., 1998
	Faba bean yellow leaf virus (FBYLV)	*Fabaceae*	*Vicia faba*	Yellowing, stunting, necrosis and leaf deformation	*Acyrthosiphon pisum*	Abraham et al., 2012
	Black medic leaf roll virus (BMLRV)	*Fabaceae*	*Medicago lupulina* *Pisum sativum*	Leaf rolling	–	Grigoras et al., 2014
	Pea yellow stunt virus (PYSV)	*Fabaceae*	*Pisum sativum*	Stunting, yellowing	–	Grigoras et al., 2014
	Cow vetch latent virus (CvLV)	*Fabaceae*	*Vicia cracca*	–	–	Gallet et al., 2018
	Sophora yellow stunt associated virus (SYSaV)	*Fabaceae*	*Sophora alopecuroides L.*	Dwarfing, yellowing, stunted leaves and yellow vein banding.	–	Heydarnejad et al., 2017
	Parsley severe stunt associated virus (PSSaV)	*Apiaceae*	*Petroselinum crispum (Mill.) Fuss*	Stunting, leaf yellowing and leaf curling.	–	Vetten et al., 2019
	Milk vetch chlorotic dwarf virus (MVCDV)	*Fabaceae*	*Astragalus myriacanthus Boiss.*	Leaf chlorosis, little leaves and dwarfism	–	Hassan-Sheikhi et al., 2020
Babuvirus	*Banana bunchy top virus* (BBTV)	*Musaceae*	*Musa* spp.	Dark green streaks plant stunting	*Pentalonia nigronervosa*	Burns et al., 1995
	Abaca bunchy top virus (ABTV)	*Musaceae*	*Musa* spp.	Mosaic	–	Sharman et al., 2008
	Cardamom bushy dwarf virus (CBDV)	*Zingiberaceae*	*Amomum subulatum*	Streak mosaic Bushy appearance	*Micromyzus-kalimpongensis*	Mandal et al., 2004
Coconut foliar decay virus	*Coconut foliar decay virus* (CFDV)	*Arecaceae*	*Cocos nucifera*	foliar decay	*Myndus tiffany*	Gronenborn et al., 2018

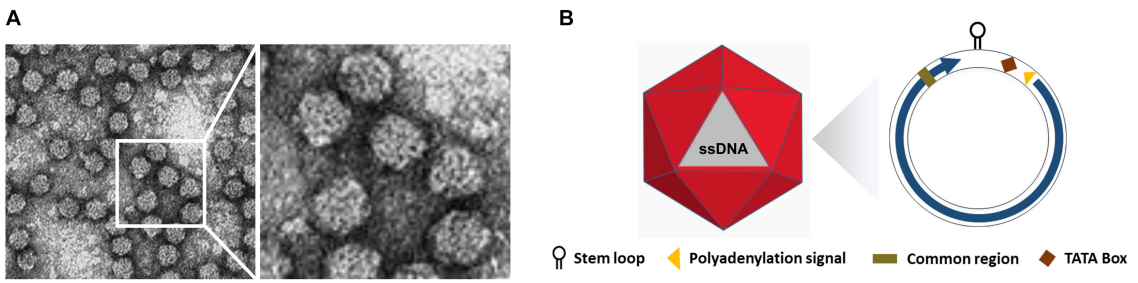

FIGURE 1 | Structure of Nanoviruses. **(A)** Negative contrast electron micrograph of particles of Faba bean necrotic yellows virus (FBNYV). The bar represents 50 nm. (Courtesy of L. Katul and D.-E. Lesemann.) **(B)** Non-enveloped ssDNA with icosahedral and round geometries, and T = 1 symmetry. The diameter is around 18–19 nm. The encoded protein (ORF) is indicated inside circles by arrow.

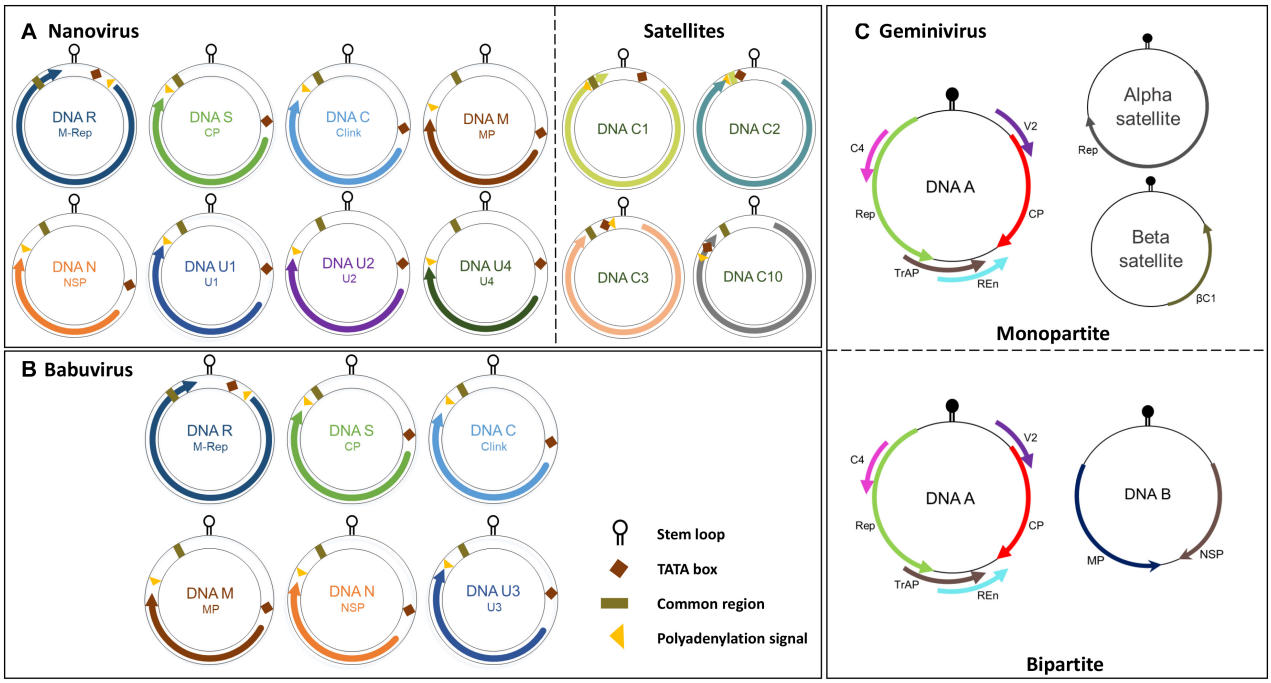

FIGURE 2 | Genome organization of the nanovirus, babuvirus and geminivirus. **(A)** Nanovirus and babuvirus comprises of eight ssDNA components along with three or four satellite molecules. **(B)** Babuvirus comprises of six ssDNA components. In both nanoviruses and babuviruses, the name of each genome segment and the name of the encoded protein is indicated inside circles in respective colors: Clink, Cell-cycle linked protein; MP, movement protein; NSP, nuclear shuttle protein; M-Rep, master rep; CP, coat protein; U1, U2, U4 (nanovirus) and U3 (babuvirus). **(C)** Geminiviruses are categorized in monopartite and bipartite based on genome organization. Monopartite geminiviruses contains a main ssDNA (DNA A) component in which six ORFs are present which encodes specific proteins to perform different functions: replication-associated protein (Rep), coat protein (CP), replication enhancer protein (REn), transcriptional activator protein (TrAP), proteins involved in virus movement (AV2), pathogenicity determinant and a suppressor of RNA silencing (AC4). Monopartite geminiviruses contain alphasatellites which encode for Rep protein (Rep) or betasatellites which have a βC1 gene, satellite conserved region (SCR) or both. Bipartite viruses contain DNA B along with DNA A which encodes for MP and NSP. Stem loop, TATA box, common region and polyadenylation signal are also highlighted.

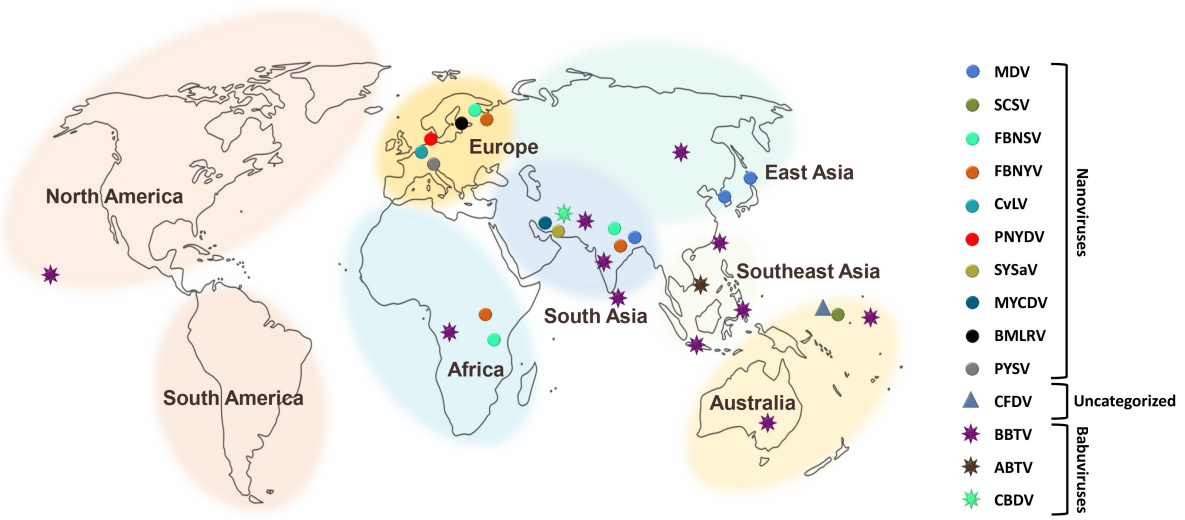

FIGURE 3 | Geographical distribution of *Nanoviridae* members. Eight different centers at continent and subcontinent levels were marked: South America, North America, Africa, Europe, South Asia, Southeast Asia, East Asia, and Australia. Circles represent the species of the genus, *Nanovirus* whereas, species of the genus, *Babuvirus* are shown by the eight-point star. Triangle represents the uncategorized species i.e., *Coconut foliar decay virus*. To differentiate the species, circles, stars and triangles have been highlighted with different colors respectively.

have been reported to be infected by babuviruses. BBTV mainly infects *Musa acuminata*, *M. coccinea*, *M. balbisiana*, *M. ornata*, *M. jackeyi*, *M. textilis*, and *M. velutina* (Burns et al., 1995; Sharman et al., 2008; Qazi, 2016). Nanoviruses were considered to affect only the legumes (Franz et al., 1997; Abraham et al., 2010; Grigoras et al., 2010a). Fabaceae, also known as Leguminosae, a legume family, is an ideal target for infection by nanovirus members (Abraham et al., 2010, 2012; Grigoras et al., 2014). About 50 Fabaceae species are infected by these members, and this number continues to increase (Franz et al., 1997; Gaafar et al., 2016) (nanoviruses with respective host ranges are listed in detail in **Table 1**). Nanoviruses limitation to narrow host ranges was a major factor in considering them as low impact viruses with an exiguous domain. This is why geminiviruses with the infection severity and outbreaks in broad host range have always been a preferred research area among ssDNA viruses compared to nanoviruses (Harrison, 1985; Mansoor et al., 2003; Jeske, 2009; Kenyon et al., 2014; Kil et al., 2016; Rodrigues et al., 2019). Recent developments have contributed to the discovery of new nanovirus hosts by confirming their presence in various important plant families including both dicots as well as monocots. For example, MDV was recently reported in dicots families i.e., Caricaceae (*Carica papaya*) (Lal et al., 2018), Solanaceae (*Solanum lycopersicum, Capsicum annuum*) (Lal et al., 2020) and in monocots family i.e., Liliaceae (*Lilium candidum*) (Lal et al., 2018). Moreover, the unassigned species, CFDV has been reported in a monocot family i.e., Arecaceae (*Cocos nucifera*) (Gronenborn et al., 2018). Recent identification of new nanoviruses in new host plants is an intriguing aspect to be focused on. PSSaV was recently reported in Apiaceae [*Petroselinum crispum* (Mill.) Fuss] (Vetten et al., 2019) whereas, MVCDV was reported in Fabaceae (*A. myriacanthus Boiss*) (Hassan-Sheikhi et al., 2020). Recent discoveries show the ongoing surge of viral infection evidence in various new host plant species owing to the growing number of metagenomics studies.

Generally, symptom development in nanovirid-infected plant species resembles that observed in *Geminiviridae* infections, such as chlorosis, necrosis, leaf rolling, dwarfing, stunting, leaf yellowing, vein yellowing, leaf deformation, and plant death (Mansoor et al., 2003; Spence et al., 2007; Jeske, 2009; Hull, 2014; Kenyon et al., 2014; Gaafar et al., 2016; Rodrigues et al., 2019; Saucke et al., 2019; Vetten et al., 2019; **Figures 4A–D**). However, *Geminiviridae* has a much more diverse assortment of associated symptoms. *Nanoviruses* induce almost all of the symptoms mentioned above in their respective hosts (**Table 1**). Each nanovirus has been named according to its major symptom; for example, FBNYV, MVCDV, MDV, and BMLRV show leaf yellowing, leaf chlorosis, dwarfism, and leaf rolling, respectively. Babuviruses also show a slight deviation in symptom development, inducing dark green streaks, streak mosaicism and a bushy appearance in hosts infected by the BBTV, ABTV, and CBDV, respectively. Coconut foliar decay is observed in the case of unassigned species CFDV (Merits et al., 2000). Mostly, clear symptoms can be observed in parts of the plant infected by any member of the *Nanoviridae* family. but in few recently reported cases,

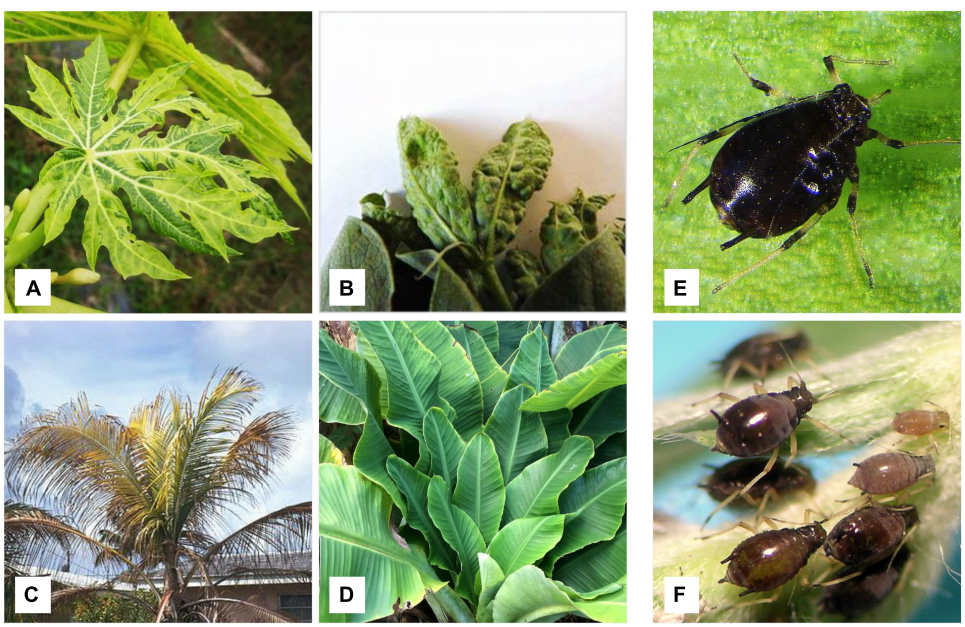

FIGURE 4 | Symptomatic host plants of nanovirus and babuviruses along with insect vectors. **(A)** Papaya plant showing leaf yellowing and dwarfism and found infected with MDV (nanovirus). **(B)** Faba bean showing necrosis and infected with FBNYV (nanovirus). **(C)** Coconut tree exhibiting foliar decay due to CFDV (uncategorized). **(D)** Banana plant showing bunchy top disease symptoms and infected with BBTV. Insect vectors, **(E)** *Pentalonia nigronervosa* transmits babuviruses and **(F)** *Aphis craccivora* responsible for the transmission of nanoviruses.

no significant symptoms were observed i.e., MDV infection in Solanaceous members (Lal et al., 2020). Nanoviruses do not exhibit any phenotypic difference with other viruses and no symptom can be associated specifically with the nanoviruses to date.

DIVERGENCE OF *NANOVIRIDAE* FROM *GEMINIVIRIDAE* AND *CIRCOVIRIDAE*

Nanoviridae are more closely related to *Geminiviridae* and *Circoviridae* among the seven families of ssDNA viruses in the phylum Cressdnaviricota (Krupovic et al., 2020). *Geminiviridae* is one of the largest families of plant viruses belonging to the order *Geplafuvirales* of the *Repensiviricetes* class. Replication occurs via a rolling circle mechanism, highly conserved sequences TARTATTAC (geminiviruses), TANTATTAC (nanoviruses) in the loop of a putative stem-loop structure within the IR, and the association with satellite molecules (especially alphasatellites in) are common features of the plant virus families *Geminiviridae* and *Nanoviridae* (Burns et al., 1995; Sano et al., 1998; Timchenko et al., 2000; Buchmann et al., 2009). Based on these resemblances, the members of these viral families are considered cousin viruses (Koonin et al., 2015).

The family *Circoviridae* involves a community of diverse animal viruses with small, closed-circular, ssDNA that belongs to the order *Cirlivirales* of the *Arfiviricetes* class. *Nanoviridae* shares the same class but different order i.e., Mulpavirales with *Circoviridae*. Their genome size is ∼1.7–2.1 kb and consists of two ORFs in the opposite direction with NANTATTAC as highly conserved sequences. These animal circoviruses are closely related to plant nanoviruses, as the Rep of circoviruses shows high similarity to the Rep of nanoviruses (Simmonds et al., 2017). The origin of replication (ori) in both the circovirus and nanovirus DNA is adjacent to the N-terminal part of the Rep gene (Niagro et al., 1998). This similarity between circovirus and nanovirus ori sequences indicates that these sequences have evolved from a common ancestral sequence (Katul et al., 1998), and that the circovirus has evolved to infect a vertebrate in various intermediate stages over time (Gibbs and Weiller, 1999). Another study showed that Rep proteins of marine ssDNA viruses show high resemblance with nanoviruses. A high copy number viral genome has been isolated from an algal cell identifying protists as the possible origin of nanoviruses, circoviruses and geminiviruses (Yoon et al., 2011). Despite some common factors, *Nanoviridae* exhibit certain contradictions to *Geminiviridae* and *Circoviridae* in terms of their genome organization, way of transmission, mode of infection, host range, and symptoms development (see details in **Table 2**; Sano et al., 1998; Gronenborn, 2004; Sharman et al., 2008; Iranzo and Manrubia, 2012; Halbert and Baker, 2015; Sicard et al., 2015; Di Mattia et al., 2020).

MULTICELLULAR WAY OF LIFE FOR *NANOVIRIDAE*

In viruses, multipartitism may exert benefits by conferring greater stability due to the genome compartmentalization of smaller-sized segments (Ojosnegros et al., 2011), by increasing the possibility of faster replication of small genomic segments (Nee, 1987), by generating non-mutated offspring (Pressing and Reanney, 1984), or by increasing genome shuffling (Chao, 1988, 1991). In contrast, multipartitism has drawbacks, such as the necessity to either package all the segments together or to

TABLE 2 | Divergence of *Nanoviridae* from *Geminiviridae* and *Circoviridae*.

Type	Attributes	*Nanoviridae*		*Geminiviridae*	*Circoviridae*
		Nanovirus	**Babuvirus**	**Begomovirus**	**Circovirus**
DNA	Shape	Circular, ssDNA	Circular, ssDNA	Circular, ssDNA	Circular, ssDNA
	Partite	Multipartite (8–11 segments)	Multipartite (6 segments)	Monopartite or Bipartite	Monopartite
	ORFs	1 ORF in each component	1 or 2 ORFs in components	6–7 in DNA A 2 in DNA B	2 ORFs in opposite direction
	Stem loop (5'- 3)'	TANTATTAC	TATTATTAC	TATTATTAC	NANTATTAC
	Satellite molecules	∼3–4	1	2 (1 alpha and 1 Beta)	0
Size	Length	∼1 kb	∼1–1.1 kb	∼2.5–3 kb	∼1.7–2.1 kb
	Diameter	18–19 nm	17–20 nm	18–20 nm	∼20 nm
Transmission	Vector	Aphids	Aphids	Whitefly, Leafhopper, Tree- hopper, Aphid	Fecal, oral
	Tissue tropism	Phloem	Phloem	Phloem, Mesophyll	Thymocytes, erythroblastoid cells, embryonal tissues
Infection	Host Range	Plants families: *Fabaceae, Caricaceae, Solanaceae*	Plants family: *Musaceae Zingiberaceae*	Plants families: *Fabaceae, Caricaceae, Solanaceae, Convolvulaceae*	Animal families: Birds, pigs, freshwater fish Dogs and humans
	Symptoms	Yellows, stunting, mosaic, leaf rolling	Streak mosaic, bushy appearance	Chlorosis, stunting, curling, leaf curling, mottling, leaf distortion	Enlarged lymph nodes, difficulty in breathing, diarrhea, pale skin, jaundice

ensure the co-entry of an ensemble of virus particles containing at least one copy of each genomic segment, (Chao, 1988; Escriu et al., 2007; Ojosnegros et al., 2011). Moreover, there are serious challenges regarding certain features of these viruses that should be fully elucidated, such as replication, genetic expression, genome encapsidation, method of localization within host cells, transport system (i.e., within-host cell-to-cell or long-distance spread), transmission patterns from one host to another by insect vectors, and evolution of multipartite viruses. Recently efforts were made to understand the intriguing multicellular way of life nanoviruses, but it has been demonstrated thus far only one species of the genus *Nanovirus* i.e., FBNSV, not all species of the family *Nanoviridae*.

GENE EXPRESSION AND VIRAL INFECTION

Multipartite viruses have a set of 8–10 nucleic acid segments, each encapsidated separately. Each segment has a specific number in the host cell to ensure infection. Some viral genes accumulate at low frequency, whereas others dominate at a high frequency (Sicard et al., 2013). This copy number variation in specific genes within individual cells may considerably affect gene expression in most of the organisms (Stranger et al., 2007; Hastings et al., 2009). Each ssDNA segment accumulates in a reproducible manner with a specific relative copy number in a specific host. These copy numbers, each associated with a specific segment, are defined as the "genome formula" and have proved to be specific to the host plant species. The genome formulae in two different host species i.e., *Vicia faba* and *Medicago truncatula* showed clear variations in the relative frequencies of the eight FBNSV segments calculated in within-host viral populations (Sicard et al., 2013). Although the discovery of the genome formula is remarkable in the biology of multipartite viruses, certain gaps need to be addressed; whether the genome formula is also controlled in the same manner as that in other multipartite viruses, whether it has a role in genetic and phenotypic expression, and whether it is an adaptive and evolvable trait.

The mechanism by which multipartite viruses manage to efficiently infect individual cells with all their segments with whole-genome information is a long-standing mystery. Initially, two possibilities were considered: (i) the particles could penetrate the cells massively with any probability independent of the identity of the contained segment, and (ii) multipartite viruses could somehow sort the particles that enter a cell depending on the encapsidated segment and promote the selective entry of the complete set of the viral genetic information (Sicard et al., 2013, 2016; Dall'ara et al., 2016). This mystery was solved by localizing and quantifying the genome segments of a nanovirus in host plant tissues. It was identified that the segments rarely co-occurred within individual cells; instead, distinct segments accumulated independently in different cells, and that the viral system was functional through complementation across cells (Sicard et al., 2016). These findings deviate from the classical conceptual framework in virology and suggest that various viral particles can localize themselves in separate neighboring cells to produce infection at a multicellular tissue level, thus revealing that the collective presence of all viral genomes in a particular cell is not the basis for infectivity (Sicard et al., 2019). However, these findings are limited to only one nanovirus species i.e., FBNSV. Whether all nanovirus behave like FBNSV is still a question yet to be answered.

SHORT AND LONG DISTANCE MOVEMENT

Generally, monopartite viruses transfer their genome information either when moving from cell-to-cell or across long distances to systemically colonize their host. In contrast, multipartite viruses bundle their genetic information in separate virus particles, which must somehow come together to cause infection, as viral trafficking within the host plant is multifarious (Hipper et al., 2013). Three models of movements within the host have been suggested in both monopartite and multipartite viruses. Some plant virus species demonstrate both cell-to-cell movement and movement across long distances as mature virus particles. Some can move from cell-to-cell as nucleoprotein complexes (Lazarowitz and Beachy, 1999) but are not capable of long-distance movement because of their inability to assemble into mature virus particles. Finally, some viral species can spread both by cell-to-cell movement and movement in the plant vasculature as nucleoprotein complexes even without containing the protein coat (Carluccio and Stavolone, 2014). There exists a considerable gap in the literature on the differentiation between multipartite virus movement mechanisms, including those of *Nanoviridae* members and other viruses, however, for multipartite viruses, it is predicted that the multiplicity of cellular infection (MOI) should reach very high values (up to hundreds) for the maintenance of genome integrity (Iranzo and Manrubia, 2012). Owing to the lack of data regarding the movement of multipartite viruses, more investigation is needed with focus on species with multiple segments.

VECTOR TRANSMISSION

Transmission of viruses, either monopartite or multipartite, mostly requires a particular insect vector (Goodman, 1977; Hogenhout et al., 2008; Hull, 2014; Sicard et al., 2015). In the case of *Nanoviridae* members, aphids transmit nanoviruses and babuviruses (Vetten et al., 2005; Almeida et al., 2009; Sicard et al., 2015), while *Myndus tiffany*, a planthopper, transmits CFDV and is considered a major factor in categorizing CFDV as a separate, unassigned species (Gronenborn et al., 2018). No reports regarding the transmission of *Nanoviridae* members either mechanically or through seeds exist to date because of their restriction to the phloem of infected host plants (Grigoras et al., 2018). Babuviruses are transmitted through finite aphid vectors *Pentalonia nigronervosa* and *Micromyzus kalimpongensis* (Almeida et al., 2009; Bressan and Watanabe, 2011; Ghosh et al., 2015; Halbert and Baker, 2015; Qazi, 2016; **Figure 4E**). In contrast, nanoviruses can be transmitted by various aphid

species, in particular *Aphis craccivora*, *A. gossypii*, *Acyrthosiphon pisum*, *Myzus persicae*, and *Macrosiphum euphorbiae* are the most effective vector species for nanoviruses (Sano et al., 1998; Sicard et al., 2015; Gaafar et al., 2016; Richet et al., 2019; **Figure 4F**). Among these aphid species, *A. craccivora* is the most abundant and efficient vector, which transmits MDV, SCSV, FBNYV and FBNSV from plant to plant (Franz et al., 1998; Sicard et al., 2015; Gallet et al., 2018; Webster et al., 2018). Some nanoviruses are transmitted by more than one aphid species, but transmission efficiency varies accordingly, e.g., *A. craccivora* transmits SCSV more efficiently than *M. persicae* (Franz et al., 1998; Sicard et al., 2015). In this way, these nanoviruses can have far-reaching effects outside their pivoting areas.

TRANSLOCATION OF NANOVIRUSES WITHIN APHID VECTORS

Similar to luteoviruses and geminiviruses, nanoviruses are transmitted in a circular non-propagative manner in their insect vectors (Hogenhout et al., 2008). Virus particles acquired from the infected plant need to cross from the aphids' gut into the hemolymph; within the hemolymph they are transported to the salivary glands (Blanc et al., 2014), followed by injection into new plants during probing. To ensure successful passage of the integral genome to a new host plant, especially in the case of multipartite viruses such as nanoviruses, it is assumed that at least one functional particle of each type must be transmitted (Iranzo and Manrubia, 2012). Several factors e.g., the accumulation of distinct genome segments at different frequencies (Sicard et al., 2013; Sánchez-Navarro et al., 2013), the stability variations within the host plants (Vaughan et al., 2014), along with the degradation and the relative frequency changes in the segments during the passage within the insect vectors (Sicard et al., 2015) and the impacts of transmission-related bottlenecks (Gallet et al., 2018) may result in the loss of genetic information. It was a highly contentious issue that how the most labile particles can be transmitted as efficiently as the others.

Franz et al. (1999) proposed an aphid helping factor to facilitate virus transport which was confirmed and recognized as NSP (Grigoras et al., 2018). Recently, its potential function investigated as distinct proteins and genome segments of the nanovirus FBNSV were remarkably monitored during transcytosis through the gut and salivary gland cells of its aphid vector *Acyrthosiphon pisum* using a combination of fluorescence *in situ* hybridization and immunofluorescence (Di Mattia et al., 2020). FBNSV follows a route similar to that of the geminiviruses but distinct from that of the luteoviruses, as demonstrated by transportation through cells of the anterior midgut and principal salivary gland. A large number of virus particles enter each susceptible cell to keep distinct genome segments together (Di Mattia et al., 2020; Gaafar and Ziebell, 2020). Previously, similar studies were conducted to track the BBTV (genus *Babuvirus*) within its aphid vector by monitoring the coat protein (Bressan and Watanabe, 2011; Watanabe and Bressan, 2013; Watanabe et al., 2016).

ROLE OF NUCLEAR SHUTTLE PROTEIN IN THE TRANSMISSION

Vector transmission of nanoviruses requires a viral factor or a helper component in addition to the virus particles (Franz et al., 1999). DNA N is the most variable genome component among all components of nanovirus (FBNSV) (Grigoras et al., 2010b). The FBNSV was reconstituted successfully as a fully infectious and sustainably insect-transmissible nanovirus from its multiple cloned DNAs (Grigoras et al., 2009). Recently, the preclusion of aphid transmission was observed when the agroinfectious clones of all segments of FBNSV, except the segment N, were inoculated in a plant though this plant showed similar symptoms as plants that were inoculated with all the eight viral components (Grigoras et al., 2018). The virions that were produced within the plants inoculated with the seven components, excluding DNA-N, abolished the aphid transmission as well when a mutated NSP with a 13-amino acid tag at the carboxyl-terminus was introduced but restored aphid transmission with the introduction of DNA-N of another nanovirus PNYDV (Grigoras et al., 2018), which reinforced the mandatory role of NSP in viral accumulation into the gut cells of the aphid. Co-localization of NSP and coat protein with other viral genome segments, suggest that NSP-virus particle complexes are the viral form that cycles within the aphid body (Di Mattia et al., 2020; Gaafar and Ziebell, 2020). Vector transmission is the major and best-documented mode of transmission of plant viruses, but many gaps i.e., purpose of self interactions between NSPs during translocation, impact of the changes in virus formulas on virus transmission etc., need to be addressed.

PHYLOGENETIC ANALYSIS OF CP AND REP

Little has been known about the variability and molecular evolution of nanoviruses. The nucleotide substitution rate of 1.78×10^{-3} substitutions per nucleotide per year was observed in FBNSV (Grigoras et al., 2010b) whereas 1.4×10^{-4} substitutions per nucleotide per year was determined in local evolution of BBTV in Hawaii (based only on a single base change) (Almeida et al., 2009). Phylogenetic relationships and pairwise sequence identity calculations also depict the linkages and variations among various types of viruses in a better way (Howarth and Vandemark, 1989). In our study, phylogenetic analysis of DNA R (Rep protein) and DNA S (coat protein) was conducted using different nanovirus and babuvirus species. Master Rep is the most similar segment in nanoviruses as well as in babuviruses and is responsible for replication while CP plays a key role in many steps of the infection cycle i.e., translation, targeting of the viral genome to its site of replication, cell-to-cell and/or systemic movement of the virus, symptomatology and virulence of the infection etc., to ensure viral infection (Bol, 2008). Phylogenetic relationships were analyzed using the iTOL (Letunic and Bork, 2019). The Nevick file for iTOL was generated using the MEGA7 program where the multiple sequence alignment tool MUSCLE used to align all sequences. Genome segments of about 60

reported species i.e., both nanoviruses and babuviruses were analyzed. In case of DNA R, circoviruses were taken into consideration as well owing to their similarity with the Rep protein of nanoviruses (Gibbs and Weiller, 1999; **Figures 5A,B**). Phylogenetic analysis reveals that each species members share same clade in both cases i.e., DNA R and DNA S due to high similarity within the species members than other species members. As, the isolates of each virus were grouped among virus species, and it was confirmed that nanoviruses and babuviruses were also clearly distinguished.

NANOVIRIDAE AS AN ECONOMIC THREAT

Agriculture is assumed to be one of the sectors most vulnerable to plant viruses, owing to the potential of viruses to affect plants on a significant scale. Agriculture is considered a fundamental pillar in the world economy and society at large, as it remains a key sector in food supply and is a major source of income. According to the Food and Agriculture Organization of the United Nations, estimated crop losses due to pathogens including plant viruses have been reported to be 20–40% at national and regional levels. Severe damage by plant viruses as well as other pests can significantly decrease the yield of crops as well as their quality, resulting in compromised financial returns due to less produce and lower quality. Plant virus outbreaks, specifically those due to *Geminiviridae* members, have already proven to be a huge setback to the economy in different countries. However, the substantial and devastating consequences of emerging *Nanoviridae* members on crops (Johnstone and Mclean, 1987; Hull, 2014), and the associated economic and social impacts, have largely been underestimated in the agricultural world. In the early 2000s, a sporadic outbreak of FBNYV was reported in Spain (Ortiz et al., 2006). In 2016, a survey of 33 symptomatic faba bean sites in central Germany was conducted toward the end of the growing season to analyze the suspected virus spectrum, and PNYDV was found as the major causal agent in all the sites. A close relationship was observed between PNYDV abundance, symptom-intensity, and a corresponding yield decline in grain weight and crude protein. Combining the relative yield level for each symptom category with its respective appearance, the overall yield gap at the field scale was extrapolated to 4.1 and 9.2% for grain yield and 3.9 and 1.2% for crude protein (Saucke et al., 2019). Furthermore, in the epidemic that occurred in central Germany in 2016, the focal appearance with a blackish core can be regarded as a PNYDV-specific feature for temperate faba beans (Ziebell, 2017; Saucke et al., 2019).

Considering the importance of host species infected by babuviruses and nanoviruses categorically may help in the development of broad-scale adversary agents. Bananas are among the top 10 food plants, especially valued in the tropics and are the source of staple food, nutrition and income for millions of banana farmers worldwide. These factors have led to its high demand and the ultimate increase in production over the last decade. BBTV outbreaks alone across 2007–2010 in different states of India caused production losses of at least US$50 million (Balasubramanian and Selvarajan, 2014). *Vicia faba*, a bean family member found in the Middle East, the Mediterranean region, China, and Ethiopia, is a multipurpose crop used for both food and fodder (hay, silage, and straw). More than 50 species of the bean family are used in human food production as seeds, as an important livestock feed, and for economic benefit owing to their value and consideration as a cash crop in Egypt and

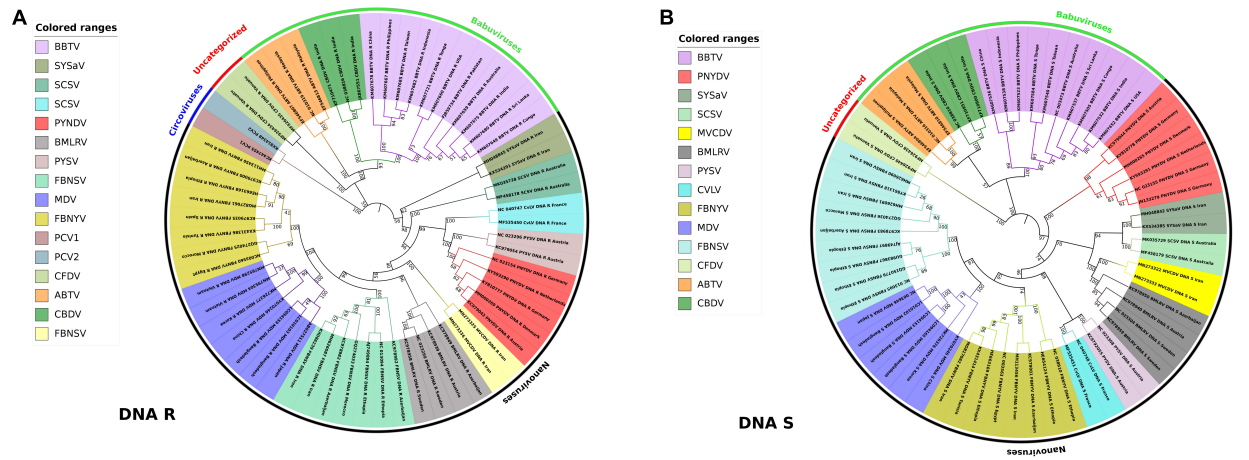

FIGURE 5 | Phylogenetic analysis of DNA-R and DNA-S detected from *Nanoviridae* members. Phylogenetic relationships were generated using the iTOL software. Nevick file for iTOL was generated using MEGA7 program. Virus abbreviations: *Subterranean clover stunt virus* (SCSV), *Black medic leaf roll virus* (BMLRV), *Faba bean necrotic yellows virus* (FBNYV), *Milk Vetch Dwarf Virus* (MDV), *Faba bean necrotic stunt virus* (FBNSY), *Pea yellow stunt virus* (PYSV), *Pea necrotic yellow dwarf virus* (PNYDV), *Cow vetch latent virus* (CvLV), *Sophora yellow stunt-associated virus* (SYSaV), *Milk vetch chlorotic dwarf virus* (MVCDV), *Banana bunchy top virus* (BBTV), *Abaca bunchy top virus* (ABTV), *Cardamom bushy dwarf virus* (CBDV), and *Coconut foliar decay virus* (CFDV). **(A)** Phylogenetic tree of DNA-R generated from around 60 complete genome segments of DNA-R of all members of *Nanoviridae*. Circoviruses: *Porcine circovirus* 1 (PCV1), *Porcine circovirus* 2 (PCV2) were also analyzed due to similarity with Rep protein of nanoviruses. **(B)** Phylogenetic tree of DNA-S generated from around 60 complete genome segments of DNA-S of all members of *Nanoviridae*.

Sudan. Along with bean family members, recent developments clearly outline the expansion in the host range of nanoviruses (as mentioned above). Among these new hosts, papaya, tomato and pepper are the most important ones (though parsley is a valuable member as well). Papaya (*C. papaya* L.) is the third most cultivated fruit in the world and found in both tropical and subtropical zones. It is produced in about 60 countries, mainly in developing countries, with an estimated production of 11.22 Mt (annual growth rate 4.35 percent between 2002 and 2010). The high nutritional and medicinal content of papaya make it an attractive crop for farmers to grow. Tomato (*S. lycopersicum*) is an extremely important Solanaceae member along with pepper (*C. annum*); both are produced and consumed by people across the world and are used in many cuisines worldwide. In 2017, the worldwide production of tomatoes totaled 170.8 million tons, while pepper production was 576,949 tons in 2018. These high numbers of production are directly and indirectly connected with food security and economic growth in the countries that produce them. Thus, one can speculates that nanoviruses might have the ability for significant impact on these newly reported food crops by affecting their yield (Grigoras et al., 2008; Rosario et al., 2012; Lal et al., 2018, 2020). So, expanding host range threatens to develop into unexpected and serious epidemics but this prediction is still somewhat obscure.

FUTURE CHALLENGES REGARDING *NANOVIRIDAE*

Recent developments highlight the diversity in host ranges of the *Nanoviridae* members, with strong evidence indicating that an increasing number of host species will be reported with time. Along with *Geminiviridae*, *Nanoviridae* members also play a notable role in the plant world, which necessitates equal attention to geminiviruses in understanding their complexities. Particularly, their mode of infection, method of localization, evolutionary history, host ranges, multicellular way of life, preferred hosts and environment, and transmission pattern are all features which remain to be investigated in detail. The agriculture sector has a new emerging threat of *Nanoviridae* infection. It is the collective responsibility of the scientific community to develop a thorough plan and policy to counteract this before a devastating effect on food security and the global economy is realized.

AUTHOR CONTRIBUTIONS

AL, E-JK, and SL outlined and conceptualized the review theme. AL wrote the first draft of the manuscript. J-KK, TV, IS, PH, E-JK, and SL contributed to manuscript preparation and revision, and also read and approved the submitted version. All authors contributed to the article and approved the submitted version.

FUNDING

This work was supported by the National Research Foundation of Korea grant funded by the Korean government (MSIT) (NRF-2020R1A2C2009946).

REFERENCES

Abbas, A. A., Taylor, L. J., Dothard, M. I., Leiby, J. S., Fitzgerald, A. S., Khatib, L. A., et al. (2019). Redondoviridae, a family of small, circular DNA viruses of the human oro-respiratory tract associated with periodontitis and critical illness. *Cell Host Microbe* 25, 719–729.e714.

Abraham, A. D., Bencharki, B., Torok, V., Katul, L., Varrelmann, M., and Vetten, H. J. (2010). Two distinct nanovirus species infecting faba bean in Morocco. *Arch. Virol.* 155, 37–46. doi: 10.1007/s00705-009-0548-9

Abraham, A. D., Varrelmann, M., and Josef Vetten, H. (2012). Three distinct nanoviruses, one of which represents a new species, infect faba bean in Ethiopia. *Plant Dis.* 96, 1045–1053. doi: 10.1094/pdis-09-11-0734-re

Almeida, R. P., Bennett, G. M., Anhalt, M. D., Tsai, C.-W., and O'grady, P. (2009). Spread of an introduced vector-borne banana virus in Hawaii. *Mol. Ecol.* 18, 136–146. doi: 10.1111/j.1365-294x.2008.04009.x

Amin, I., Qazi, J., Mansoor, S., Ilyas, M., and Briddon, R. W. (2008). Molecular characterisation of banana bunchy top virus (BBTV) from Pakistan. *Virus Genes* 36, 191–198. doi: 10.1007/s11262-007-0168-y

Aronson, M. N., Meyer, A. D., Györgyey, J., Katul, L., Vetten, H. J., Gronenborn, B., et al. (2000). Clink, a nanovirus-encoded protein, binds both pRB and SKP1. *J. Virol.* 74, 2967–2972. doi: 10.1128/jvi.74.7.2967-2972.2000

Balasubramanian, V., and Selvarajan, R. (2014). Genetic diversity and recombination analysis in the coat protein gene of banana bract mosaic virus. *Virus Genes* 48, 509–517. doi: 10.1007/s11262-014-1056-x

Beetham, P. R., Hafner, G. J., Harding, R. M., and Dale, J. L. (1997). Two mRNAs are transcribed from banana bunchy top virus DNA-1. *J. Gen. Virol.* 78, 229–236. doi: 10.1099/0022-1317-78-1-229

Biagini, P., De Micco, P., and De Lamballerie, X. (2006). Identification of a third member of the Anellovirus genus ("small anellovirus") in French blood donors. *Arch. Virol.* 151, 405–408. doi: 10.1007/s00705-005-0660-4

Blanc, S., Drucker, M., and Uzest, M. (2014). Localizing viruses in their insect vectors. *Annu. Rev. Phytopathol.* 52, 403–425. doi: 10.1146/annurev-phyto-102313-045920

Blatter, J. A., Sweet, S. C., Conrad, C., Danziger-Isakov, L. A., Faro, A., Goldfarb, S. B., et al. (2018). Anellovirus loads are associated with outcomes in pediatric lung transplantation. *Pediatr. Transplant* 22

Blomme, G., Ploetz, R., Jones, D., De Langhe, E., Price, N., Gold, C., et al. (2013). A historical overview of the appearance and spread of *Musa* pests and pathogens on the African continent: highlighting the importance of clean *Musa* planting materials and quarantine measures. *Ann. Appl. Biol.* 162, 4–26. doi: 10.1111/aab.12002

Boevink, P., Chu, P. W. G., and Keese, P. (1995). Sequence of subterranean clover stunt virus DNA: affinities with the geminiviruses. *J. Virol.* 207, 354–361. doi: 10.1006/viro.1995.1094

Bol, J. F. (2008). Role of capsid proteins. *Methods Mol. Biol.* 451, 21–31. doi: 10.1007/978-1-59745-102-4_2

Bressan, A., and Watanabe, S. (2011). Immunofluorescence localisation of banana bunchy top virus (family *Nanoviridae*) within the aphid vector, *Pentalonia nigronervosa*, suggests a virus tropism distinct from aphid-transmitted luteoviruses. *Virus Res.* 155, 520–525. doi: 10.1016/j.virusres.2010.12.005

Briddon, R. W., Martin, D. P., Roumagnac, P., Navas-Castillo, J., Fiallo-Olivé, E., Moriones, E., et al. (2018). *Alphasatellitidae*: a new family with two subfamilies for the classification of geminivirus-and nanovirus-associated alphasatellites. *Arch. Virol.* 163, 2587–2600. doi: 10.1007/s00705-018-3854-2

Buchmann, R. C., Asad, S., Wolf, J. N., Mohannath, G., and Bisaro, D. M. (2009). Geminivirus AL2 and L2 proteins suppress transcriptional gene silencing and cause genome-wide reductions in cytosine methylation. *J. Virol.* 83, 5005–5013. doi: 10.1128/jvi.01771-08

Burns, T. M., Harding, R. M., and Dale, J. L. (1995). The genome organization of banana bunchy top virus: analysis of six ssDNA components. *J. Gen. Virol.* 76, 1471–1482. doi: 10.1099/0022-1317-76-6-1471

Carluccio, A. V., and Stavolone, L. (2014). Interference of Brefeldin A in viral movement protein tubules assembly. *Plant Signal. Behav.* 9:e29121. doi: 10.4161/psb.29121

Chao, L. (1988). Evolution of sex in RNA viruses. *J. Theor. Biol.* 133, 99–112. doi: 10.1016/s0022-5193(88)80027-4

Chao, L. (1991). Levels of selection, evolution of sex in RNA viruses, and the origin of life. *J. Theor. Biol.* 153, 229–246. doi: 10.1016/s0022-5193(05)80424-2

Cheung, A. K. (2006). Rolling-circle replication of an animal circovirus genome in a theta-replicating bacterial plasmid in *Escherichia coli*. *J. Virol.* 80, 8686–8694. doi: 10.1128/jvi.00655-06

Dall'ara, M., Ratti, C., Bouzoubaa, S. E., and Gilmer, D. (2016). Ins and outs of multipartite positive-strand RNA plant viruses: packaging versus systemic spread. *Viruses* 8:228. doi: 10.3390/v8080228

Dayaram, A., Galatowitsch, M., Harding, J. S., Argüello-Astorga, G. R., and Varsani, A. (2014). Novel circular DNA viruses identified in *Procordulia grayi* and *Xanthocnemis zealandica* larvae using metagenomic approaches. *Infect. Genet. Evol.* 22, 134–141. doi: 10.1016/j.meegid.2014.01.013

Di Mattia, J., Vernerey, M. S., Yvon, M., Pirolles, E., Villegas, M., Gaafar, Y., et al. (2020). Route of a multipartite nanovirus across the body of its aphid vector. *J. Virol.* 94:e01998-19.

Escriu, F., Fraile, A., and García-Arenal, F. (2007). Constraints to genetic exchange support gene coadaptation in a tripartite RNA virus. *PLoS Pathog.* 3:e8. doi: 10.1371/journal.ppat.0030008

Franz, A., Makkouk, K. M., and Vetten, H. J. (1997). Host range of faba bean necrotic yellows virus and potential yield loss in infected faba bean. *Phytopathol. Mediterr.* 36, 94–103.

Franz, A., Makkouk, K. M., and Vetten, H. J. (1998). Acquisition, retention and transmission of faba bean necrotic yellows virus by two of its aphid vectors, *Aphis craccivora* (Koch) and *Acyrthosiphon pisum* (Harris). *Phytopathology* 146, 347–355. doi: 10.1111/j.1439-0434.1998.tb04703.x

Franz, A. W. E., Van Der Wilk, F., Verbeek, M., Dullemans, A. M., and Van Den Heuvel, J. F. J. M. (1999). Faba bean necrotic yellows virus (Genus *Nanovirus*) requires a helper factor for its aphid transmission. *J. Virol.* 262, 210–219. doi: 10.1006/viro.1999.9904

Gaafar, Y., Cordsen Nielsen, G., and Ziebell, H. (2018). Molecular characterisation of the first occurrence of pea necrotic yellow dwarf virus in Denmark. *New Dis. Rep.* 37, 16–16. doi: 10.5197/j.2044-0588.2018.037.016

Gaafar, Y., Grausgruber-Gröger, S., and Ziebell, H. (2016). *Vicia Faba*, *V. Sativa* and *Lens Culinaris* as new hosts for *pea necrotic yellow dwarf virus* in Germany and Austria. *New Dis. Rep.* 34:28. doi: 10.5197/j.2044-0588.2016.034.028

Gaafar, Y., Timchenko, T., and Ziebell, H. (2017). First report of pea necrotic yellow dwarf virus in the Netherlands. *New Dis. Rep.* 35:23. doi: 10.5197/j.2044-0588.2017.035.023

Gaafar, Y. Z. A., and Ziebell, H. (2020). Aphid transmission of nanoviruses. *Arch. Insect Biochem. Physiol.* 104:e21668.

Gallet, R., Fabre, F., Thébaud, G., Sofonea, M. T., Sicard, A., Blanc, S., et al. (2018). Small bottleneck size in a highly multipartite virus during a complete infection cycle. *J. Virol.* 92:e00139-18.

Ghosh, A., Das, A., Vijayanandraj, S., and Mandal, B. (2015). Cardamom bushy dwarf virus infection in large cardamom alters plant selection preference, life stages, and fecundity of aphid vector, *Micromyzus kalimpongensis* (Hemiptera: Aphididae). *Environ. Entomol.* 45, 178–184. doi: 10.1093/ee/nvv161

Gibbs, M. J., and Weiller, G. F. (1999). Evidence that a plant virus switched hosts to infect a vertebrate and then recombined with a vertebrate-infecting virus. *Proc. Natl. Acad. Sci. U.S.A.* 96, 8022–8027. doi: 10.1073/pnas.96.14.8022

Goodman, R. M. (1977). Single-stranded DNA genome in a whitefly-transmitted plant virus. *J. Virol.* 83, 171–179. doi: 10.1016/0042-6822(77)90220-3

Grigoras, I., Del Cueto Ginzo, A. I., Martin, D. P., Varsani, A., Romero, J., Mammadov, A. C., et al. (2014). Genome diversity and evidence of recombination and reassortment in nanoviruses from Europe. *J. Gen. Virol.* 95, 1178–1191. doi: 10.1099/vir.0.063115-0

Grigoras, I., Gronenborn, B., and Vetten, H. (2010a). First report of a nanovirus disease of pea in Germany. *Plant Dis.* 94, 642–642. doi: 10.1094/pdis-94-5-0642c

Grigoras, I., Timchenko, T., Grande-Pérez, A., Katul, L., Vetten, H.-J., and Gronenborn, B. (2010b). High variability and rapid evolution of a nanovirus. *J. Virol.* 84:9105. doi: 10.1128/jvi.00607-10

Grigoras, I., Timchenko, T., and Gronenborn, B. (2008). Transcripts encoding the nanovirus master replication initiator proteins are terminally redundant. *J. Gen. Virol.* 89, 583–593. doi: 10.1099/vir.0.83352-0

Grigoras, I., Timchenko, T., Katul, L., Grande-Pérez, A., Vetten, H.-J., and Gronenborn, B. (2009). Reconstitution of authentic nanovirus from multiple cloned DNAs. *J. Virol.* 83, 10778–10787. doi: 10.1128/jvi.01212-09

Grigoras, I., Vetten, H.-J., Commandeur, U., Ziebell, H., Gronenborn, B., and Timchenko, T. (2018). Nanovirus DNA-N encodes a protein mandatory for aphid transmission. *J. Virol.* 522, 281–291. doi: 10.1016/j.virol.2018.07.001

Gronenborn, B. (2004). Nanoviruses: genome organisation and protein function. *Vet. Microbiol.* 98, 103–109. doi: 10.1016/j.vetmic.2003.10.015

Gronenborn, B., Randles, J. W., Knierim, D., Barrière, Q., Vetten, H. J., Warthmann, N., et al. (2018). Analysis of DNAs associated with coconut foliar decay disease implicates a unique single-stranded DNA virus representing a new taxon. *Sci. Rep.* 8:5698.

Halbert, S. E., and Baker, C. A. (2015). *Banana bunchy top virus* and its vector *Pentalonia nigronervosa* (Hemiptera: Aphididae). *Pathol. Circ.* 47:8.

Harrison, B. D. (1985). Advances in geminivirus research. *Annu. Rev. Phytopathol.* 23, 55–82. doi: 10.1146/annurev.py.23.090185.000415

Hassan-Sheikhi, P., Heydarnejad, J., Massumi, H., Kraberger, S., and Varsani, A. (2020). Novel nanovirus and associated alphasatellites identified in milk vetch plants with chlorotic dwarf disease in Iran. *Virus Res.* 276:197830. doi: 10.1016/j.virusres.2019.197830

Hastings, P. J., Lupski, J. R., Rosenberg, S. M., and Ira, G. (2009). Mechanisms of change in gene copy number. *Nat. Rev. Genet.* 10, 551–564. doi: 10.1038/nrg2593

Hayakawa, T., Kojima, K., Nonaka, K., Nakagaki, M., Sahara, K., Asano, S.-I., et al. (2000). Analysis of proteins encoded in the bipartite genome of a new type of parvo-like virus isolated from silkworm — structural protein with DNA polymerase motif. *Virus Res.* 66, 101–108. doi: 10.1016/s0168-1702(99)00129-x

Heydarnejad, J., Kamali, M., Massumi, H., Kvarnheden, A., Male, M. F., Kraberger, S., et al. (2017). Identification of a nanovirus-alphasatellite complex in *Sophora alopecuroides*. *Virus Res.* 235, 24–32. doi: 10.1016/j.virusres.2017.03.023

Hipper, C., Brault, V., Ziegler-Graff, V., and Revers, F. (2013). Viral and cellular factors involved in phloem transport of plant viruses. *Front. Plant Sci.* 4:154. doi: 10.3389/fpls.2013.00154

Hogenhout, S. A., Ammar, E.-D., Whitfield, A. E., and Redinbaugh, M. G. (2008). Insect vector interactions with persistently transmitted viruses. *Annu. Rev. Phytopathol.* 46, 327–359. doi: 10.1146/annurev.phyto.022508.092135

Horser, C. L., Harding, R. M., and Dale, J. L. (2001). *Banana bunchy top nanovirus* DNA-1 encodes the 'master'replication initiation protein. *J. Gen. Virol.* 82, 459–464. doi: 10.1099/0022-1317-82-2-459

Howarth, A. J., and Vandemark, G. J. (1989). Phylogeny of geminiviruses. *J. Gen. Virol.* 70, 2717–2727. doi: 10.1099/0022-1317-70-10-2717

Hull, R. (2014). *Plant Virology*. Cambridge, MA: Academic press.

Iranzo, J., and Manrubia, S. C. (2012). Evolutionary dynamics of genome segmentation in multipartite viruses. *Proc. R. Soc. B.* 279, 3812–3819. doi: 10.1098/rspb.2012.1086

Jeske, H. (2009). "Geminiviruses," in *TT Viruses: The Still Elusive Human Pathogens*, eds E.-M. De Villiers, and H. Z. Hausen (Berlin: Springer Berlin Heidelberg), 185–226.

Jeske, H. (2018). Barcoding of plant viruses with circular single-stranded DNA based on rolling circle amplification. *Viruses* 10:469. doi: 10.3390/v10090469

Johnstone, G. R., and Mclean, G. D. (1987). Virus diseases of subterranean clover. *Ann. Appl. Biol.* 110, 421–440.

Katul, L., Timchenko, T., Gronenborn, B., and Vetten, H. J. (1998). Ten distinct circular ssDNA components, four of which encode putative replication-associated proteins, are associated with the faba bean necrotic yellows virus genome. *J. Gen. Virol.* 79, 3101–3109. doi: 10.1099/0022-1317-79-12-3101

Kenyon, L., Tsai, W.-S., Shih, S.-L., and Lee, L.-M. (2014). Emergence and diversity of begomoviruses infecting solanaceous crops in East and Southeast Asia. *Virus Res.* 186, 104–113. doi: 10.1016/j.virusres.2013.12.026

Kil, E.-J., Kim, S., Lee, Y.-J., Byun, H.-S., Park, J., Seo, H., et al. (2016). *Tomato yellow leaf curl virus* (TYLCV-IL): a seed-transmissible geminivirus in tomatoes. *Sci. Rep.* 6:19013.

Koonin, E. V., Dolja, V. V., and Krupovic, M. (2015). Origins and evolution of viruses of eukaryotes: the ultimate modularity. *J. Virol.* 479, 2–25. doi: 10.1016/j.virol.2015.02.039

Krupovic, M., Ghabrial, S. A., Jiang, D., and Varsani, A. (2016). Genomoviridae: a new family of widespread single-stranded DNA viruses. *Arch. Virol.* 161, 2633–2643. doi: 10.1007/s00705-016-2943-3

Krupovic, M., Varsani, A., Kazlauskas, D., Breitbart, M., Delwart, E., Rosario, K., et al. (2020). *Cressdnaviricota*: a virus phylum unifying 7 families of Rep-encoding viruses with single-stranded, circular DNA genomes. *J. Virol.* 94:e00582-20.

Lal, A., Kil, E.-J., Byun, H.-S., Zarghami, D. S., Kim, J.-K., and Lee, S. (2018). First report of milk vetch dwarf virus associated with dwarfism in papaya in Korea. *Plant Dis.* 102:2666. doi: 10.1094/pdis-01-18-0190-pdn

Lal, A., Kil, E.-J., Thuy, V. T. B., Fadhila, C., Ho, P. T., Byun, H.-S., et al. (2020). Milk vetch dwarf virus infection in the *Solanaceae* and *Caricaceae* families in Southeast Asia. *Plant Pathol.* 69, 1026–1033. doi: 10.1111/ppa.13196

Lazarowitz, S. G., and Beachy, R. N. (1999). Viral movement proteins as probes for intracellular and intercellular trafficking in plants. *Plant Cell* 11:535. doi: 10.2307/3870882

Letunic, I., and Bork, P. (2019). Interactive Tree Of Life (iTOL) v4: recent updates and new developments. *Nucleic Acids Res.* 47, W256–W259.

Malathi, V. G., and Dasgupta, I. (2019a). Insights into the world of ssDNA viruses. *Virusdisease* 30, 1–2. doi: 10.1007/s13337-019-00529-2

Malathi, V. G., and Renuka Devi, P. (2019b). ssDNA viruses: key players in global virome. *Virusdisease* 30, 3–12. doi: 10.1007/s13337-019-00519-4

Mandal, B. (2010). Advances in small isometric multicomponent ssDNA viruses infecting plants. *Indian J. Virol.* 21, 18–30. doi: 10.1007/s13337-010-0010-3

Mandal, B., Mandal, S., Pun, K. B., and Varma, A. (2004). First report of the association of a nanovirus with foorkey disease of large cardamom in India. *Plant Dis.* 88, 428–428. doi: 10.1094/pdis.2004.88.4.428a

Mansoor, S., Briddon, R. W., Zafar, Y., and Stanley, J. (2003). Geminivirus disease complexes: an emerging threat. *Trends Plant Sci.* 8, 128–134. doi: 10.1016/s1360-1385(03)00007-4

Merits, A., Fedorkin, O. N., Guo, D., Kalinina, N. O., and Morozov, S. Y. (2000). Activities associated with the putative replication initiation protein of coconut foliar decay virus, a tentative member of the genus *Nanovirus*. *J. Gen. Virol.* 81, 3099–3106. doi: 10.1099/0022-1317-81-12-3099

Nee, S. (1987). The evolution of multicompartmental genomes in viruses. *J. Mol. Evol.* 25, 277–281.

Ng, T. F. F., Zhang, W., Sachsenröder, J., Kondov, N. O., Da Costa, A. C., Vega, E., et al. (2015). A diverse group of small circular ssDNA viral genomes in human and non-human primate stools. *Virus Evol.* 1:vev017. doi: 10.1093/ve/vev017

Niagro, F. D., Forsthoefel, A. N., Lawther, R. P., Kamalanathan, L., Ritchie, B. W., Latimer, K. S., et al. (1998). Beak and feather disease virus and porcine circovirus genomes: intermediates between the geminiviruses and plant circoviruses. *Arch. Virol.* 143, 1723–1744. doi: 10.1007/s007050050412

Ojosnegros, S., García-Arriaza, J., Escarmís, C., Manrubia, S. C., Perales, C., Arias, A., et al. (2011). Viral genome segmentation can result from a trade-off between genetic content and particle stability. *PLoS Genet.* 7:e1001344. doi: 10.1371/journal.pgen.1001344

Ortiz, V., Navarro, E., Castro, S., Carazo, G., and Romero, J. (2006). Incidence and transmission of *Faba bean necrotic yellows virus* (FBNYV) in Spain. *Span. J. Agric. Res.* 4, 255–260. doi: 10.5424/sjar/2006043-200

Pressing, J., and Reanney, D. (1984). Divided genomes and intrinsic noise. *J. Mol. Evol.* 20, 135–146. doi: 10.1007/bf02257374

Qazi, J. (2016). Banana bunchy top virus and the bunchy top disease. *J. Gen. Plant Pathol.* 82, 2–11. doi: 10.1007/s10327-015-0642-7

Randles, J., Chu, P., Dale, J., Harding, R., Hu, J., Katul, L., et al. (2000). "Nanoviridae," in *Virus Taxonomy: Classification and Nomenclature of Viruses. Seventh Report of the International Committee on Taxonomy of Viruses*, eds M. H. V. van Regenmortel, et al. (London: Elsevier/Academic Press).

Richet, C., Kraberger, S., Filloux, D., Bernardo, P., Harkins, G. W., Martin, D. P., et al. (2019). Novel circular DNA viruses associated with *Apiaceae* and *Poaceae* from South Africa and New Zealand. *Arch. Virol.* 164, 237–242. doi: 10.1007/s00705-018-4031-3

Rodrigues, G. B., Rocha Sobrinho, G. G., Mituti, T., Bergamin Filho, A., Amorim, L., Rezende, J. A. M., et al. (2019). Etiology, occurrence and epidemiology of a begomovirus disease in passionflower in the southwest of Bahia. *Sci. Agric.* 76, 337–343. doi: 10.1590/1678-992x-2017-0272

Rosario, K., Duffy, S., and Breitbart, M. (2012). A field guide to eukaryotic circular single-stranded DNA viruses: insights gained from metagenomics. *Arch. Virol.* 157, 1851–1871. doi: 10.1007/s00705-012-1391-y

Rosario, K., Schenck, R. O., Harbeitner, R. C., Lawler, S. N., and Breitbart, M. (2015). Novel circular single-stranded DNA viruses identified in marine invertebrates reveal high sequence diversity and consistent predicted intrinsic disorder patterns within putative structural proteins. *Front. Microbiol.* 6:696.

Sánchez-Navarro, J. A., Zwart, M. P., and Elena, S. F. (2013). Effects of the number of genome segments on primary and systemic infections with a multipartite plant RNA virus. *J. Virol.* 87:10805. doi: 10.1128/jvi.01402-13

Sano, Y., Wada, M., Hashimoto, Y., Matsumoto, T., and Kojima, M. (1998). Sequences of ten circular ssDNA components associated with the milk vetch dwarf virus genome. *J. Gen. Virol.* 79, 3111–3118. doi: 10.1099/0022-1317-79-12-3111

Saucke, H., Uteau, D., Brinkmann, K., and Ziebell, H. (2019). Symptomology and yield impact of pea necrotic yellow dwarf virus (PNYDV) in faba bean (*Vicia faba* L. minor). *Eur. J. Plant Pathol.* 153, 1299–1315. doi: 10.1007/s10658-018-01643-5

Saunders, K., Bedford, I. D., Yahara, T., and Stanley, J. (2003). The earliest recorded plant virus disease. *Nature* 422:831. doi: 10.1038/422831a

Sharman, M., Thomas, J., Skabo, S., and Holton, T. (2008). Abaca bunchy top virus, a new member of the genus *Babuvirus* (family *Nanoviridae*). *Arch. Virol.* 153, 135–147. doi: 10.1007/s00705-007-1077-z

Sicard, A., Michalakis, Y., Gutiérrez, S., and Blanc, S. (2016). The strange lifestyle of multipartite viruses. *PLoS Pathog.* 12:e1005819. doi: 10.1371/journal.ppat.1005819

Sicard, A., Pirolles, E., Gallet, R., Vernerey, M.-S., Yvon, M., Urbino, C., et al. (2019). A multicellular way of life for a multipartite virus. *eLife* 8:e43599.

Sicard, A., Yvon, M., Timchenko, T., Gronenborn, B., Michalakis, Y., Gutierrez, S., et al. (2013). Gene copy number is differentially regulated in a multipartite virus. *Nat. Commun.* 4:2248.

Sicard, A., Zeddam, J.-L., Yvon, M., Michalakis, Y., Gutiérrez, S., and Blanc, S. (2015). Circulative nonpropagative aphid transmission of nanoviruses: an oversimplified view. *J. Virol.* 89, 9719–9726. doi: 10.1128/jvi.00780-15

Simmonds, P., Adams, M. J., Benkő, M., Breitbart, M., Brister, J. R., Carstens, E. B., et al. (2017). Consensus statement: virus taxonomy in the age of metagenomics. *Nat. Rev. Microbiol.* 15, 161–168.

Spence, N. J., Phiri, N. A., Hughes, S. L., Mwaniki, A., Simons, S., Oduor, G., et al. (2007). Economic impact of turnip mosaic virus, cauliflower mosaic virus and beet mosaic virus in three Kenyan vegetables. *Plant Pathol.* 56, 317–323. doi: 10.1111/j.1365-3059.2006.01498.x

Stranger, B. E., Forrest, M. S., Dunning, M., Ingle, C. E., Beazley, C., Thorne, N., et al. (2007). Relative impact of nucleotide and copy number variation on gene expression phenotypes. *J. Sci.* 315, 848–853. doi: 10.1126/science.1136678

Sun, S.-K. (1961). Studies on the bunchy top disease of bananas. *Spec. Publ.* 10, 82–109.

Timchenko, T., Katul, L., Sano, Y., De Kouchkovsky, F., Vetten, H. J., and Gronenborn, B. (2000). The master rep concept in nanovirus replication: identification of missing genome components and potential for natural genetic reassortment. *J. Virol.* 274, 189–195. doi: 10.1006/viro.2000.0439

Tischer, I., Mields, W., Wolff, D., Vagt, M., and Griem, W. (1986). Studies on epidemiology and pathogenicity of porcine circovirus. *Arch. Virol.* 91, 271–276. doi: 10.1007/bf01314286

Vaughan, R., Tragesser, B., Ni, P., Ma, X., Dragnea, B., and Kao, C. C. (2014). The tripartite virions of the brome mosaic virus have distinct physical properties that affect the timing of the infection process. *J. Virol.* 88:6483. doi: 10.1128/jvi.00377-14

Vetten, H., Chu, P., Dale, J., Harding, R., Hu, J., Katul, L., et al. (2005). *Nanoviridae*. Cambridge, MA: Elsevier-Academic Press.

Vetten, H. J., Dale, J. L., Grigoras, I., Gronenborn, B., Harding, R., Randles, J. W., et al. (2012). *Family Nanoviridae in virus Taxonomy: Ninth Report of the International Committee on Taxonomy of Viruses*. Amsterdam: Elsevier.

Vetten, H. J., Knierim, D., Rakoski, M. S., Menzel, W., Maiss, E., Gronenborn, B., et al. (2019). Identification of a novel nanovirus in parsley. *Arch. Virol.* 164, 1883–1887. doi: 10.1007/s00705-019-04280-3

Wanitchakorn, R., Hafner, G. J., Harding, R. M., and Dale, J. L. (2000). Functional analysis of proteins encoded by banana bunchy top virus DNA-4 to -6. *Virus Res.* 81, 299–306. doi: 10.1099/0022-1317-81-1-299

Wanitchakorn, R., Harding, R., and Dale, J. (1997). *Banana bunchy top virus* DNA-3 encodes the viral coat protein. *Arch. Virol.* 142, 1673–1680. doi: 10.1007/s007050050188

Watanabe, S., Borthakur, D., and Bressan, A. (2016). Localization of banana bunchy top virus and cellular compartments in gut and salivary gland tissues of the aphid vector *Pentalonia nigronervosa*. *Insect Sci.* 23, 591–602. doi: 10.1111/1744-7917.12211

Watanabe, S., and Bressan, A. (2013). Tropism, compartmentalization and retention of banana bunchy top virus (*Nanoviridae*) in the aphid vector *Pentalonia nigronervosa*. *J. Gen. Virol.* 94, 209–219. doi: 10.1099/vir.0.047308-0

Webster, C. G., Pichon, E., Van Munster, M., Monsion, B., Deshoux, M., Gargani, D., et al. (2018). Identification of plant virus receptor candidates in the stylets of their aphid vectors. *J. Virol.* 92:e00432-18.

Yoon, H. S., Price, D. C., Stepanauskas, R., Rajah, V. D., Sieracki, M. E., Wilson, W. H., et al. (2011). Single-cell genomics reveals organismal interactions in uncultivated marine protists. *Science* 332:714. doi: 10.1126/science.1203163

Zerbini, F. M., Briddon, R. W., Idris, A., Martin, D. P., Moriones, E., Navas-Castillo, J., et al. (2017). ICTV Virus Taxonomy profile: *Geminiviridae*. *J. Gen. Virol.* 98, 131–133.

Ziebell, H. (2017). Die virusepidemie an leguminosen 2016 eine folge des klimawandels? *J. Kultpflanzen* 69, 64–68.

Conflict of Interest: The authors declare that the research was conducted in the absence of any commercial or financial relationships that could be construed as a potential conflict of interest.

frontiers in Microbiology

METHODS
published: 21 April 2021
doi: 10.3389/fmicb.2021.640932

Rapid and Sensitive Detection of Tomato Brown Rugose Fruit Virus in Tomato and Pepper Seeds by Reverse Transcription Loop-Mediated Isothermal Amplification Assays (Real Time and Visual) and Comparison With RT-PCR End-Point and RT-qPCR Methods

*Domenico Rizzo[1], Daniele Da Lio[2], Alessandra Panattoni[2], Chiara Salemi[2], Giovanni Cappellini[1], Linda Bartolini[1] and Giuseppe Parrella[3]**

[1]*Laboratory of Phytopathological Diagnostics and Molecular Biology, Plant Protection Service of Tuscany, Pistoia, Italy,* [2]*Department of Agricultural, Food and Agro-Environmental Sciences, University of Pisa, Pisa, Italy,* [3]*Institute for Sustainable Plant Protection of National Research Council (IPSP-CNR), Portici, Italy*

Tomato brown rugose fruit virus (ToBRFV) represents an emerging viral threat to the productivity of tomato and pepper protected cultivation worldwide. This virus has got the status of quarantine organism in the European Union (EU) countries. In particular, tomato and pepper seeds will need to be free of ToBRFV before entering the EU and before coming on the market. Thus, lab tests are needed. Here, we develop and validate a one-step reverse transcription LAMP platform for the detection of ToBRFV in tomato and pepper leaves, by real-time assay [reverse transcription loop-mediated isothermal amplification (RT-LAMP)] and visual screening (visual RT-LAMP). Moreover, these methods can also be applied successfully for ToBRFV detection in tomato and pepper seeds. The diagnostic specificity and sensitivity of both RT-LAMP and visual RT-LAMP are both 100%, with a detection limit of nearly 2.25 fg/μl, showing the same sensitivity as RT-qPCR Sybr Green, but 100 times more sensitive than end-point RT-PCR diagnostic methods. In artificially contaminated seeds, the proposed LAMP assays detected ToBRFV in 100% of contaminated seed lots, for up to 0.025–0.033% contamination rates in tomato and pepper, respectively. Our results demonstrate that the proposed LAMP assays are simple, inexpensive, and sensitive enough for the detection of ToBRFV, especially in seed health testing. Hence, these methods have great potential application in the routine detection of ToBRFV, both in seeds and plants, reducing the risk of epidemics.

Keywords: virus diagnostic, seeds contamination, seed testing, tomato brown rugose fruit virus, RT-LAMP assay

OPEN ACCESS

Edited by:
Ralf Georg Dietzgen, The University of Queensland, Australia

Reviewed by:
Krzysztof Treder, Plant Breeding and Acclimatization Institute, Poland
Baswaraj Raigond, Central Potato Research Institute (ICAR), India

****Correspondence:***
Giuseppe Parrella
giuseppe.parrella@ipsp.cnr.it

Specialty section:
This article was submitted to Microbe and Virus Interactions With Plants, a section of the journal Frontiers in Microbiology

Received: *14 December 2020*
Accepted: *15 March 2021*
Published: *21 April 2021*

Citation:
Rizzo D, Da Lio D, Panattoni A, Salemi C, Cappellini G, Bartolini L and Parrella G (2021) Rapid and Sensitive Detection of Tomato Brown Rugose Fruit Virus in Tomato and Pepper Seeds by Reverse Transcription Loop-Mediated Isothermal Amplification Assays (Real Time and Visual) and Comparison With RT-PCR End-Point and RT-qPCR Methods. Front. Microbiol. 12:640932. doi: 10.3389/fmicb.2021.640932

INTRODUCTION

Tomato brown rugose fruit virus (ToBRFV), a member of the genus *Tobamovirus*, family *Virgaviridae*, is an emerging and highly virulent virus, mainly affecting tomato crops worldwide. ToBRFV presents a genome organization common to tobamoviruses, with a single-strand positive-sense RNA of ~6,400 nucleotides (nt) with four open reading frames (ORFs) that encode two replication-related proteins (Salem et al., 2016). Since the first report of ToBRFV outbreak in tomato in Jordan (Salem et al., 2016), the virus has been identified within recent years in other countries on different continents: Israel (Luria et al., 2017), Mexico (Cambrón-Crisantos et al., 2018), United States (Chitambar, 2018; Ling et al., 2019), Germany (Menzel et al., 2019), Italy (Panno et al., 2019), Palestine (Alkowni et al., 2019), Turkey (Fidan, 2020), China (Yan et al., 2019), the United Kingdom (Skelton et al., 2019) and, more recently, in Greece (Beris et al., 2020). Likely occurrences have also been reported (but not confirmed) in Chile, Ethiopia, Sudan, and Netherlands.

Tomato brown rugose fruit virus constitutes an emerging threat of global concern to tomato crops, as it is able to overcome the resistance gene *Tm-2*^{2} routinely used by breeders for the constitution of tomato hybrids, with special reference to those destined for protected cultivation, as it is effective in controlling other tomato tobamoviruses, such as tobacco mosaic virus (TMV) and tomato mosaic virus (ToMV; Zhang et al., 2013). On the other hand, pepper varieties harboring the *L1*, *L3*, or the *L4* alleles of the *L* resistance gene to tobamoviruses have displayed hypersensitivity response (HR) when inoculated with ToBRFV, allowing for some control of the virus. More recently, a severe outbreak of ToBRFV in a red sweet pepper (*Capsicum annum*) variety not harboring the resistance gene, has been recorded in Sicily (south Italy), with an incidence of the viral disease of about 85% (Panno et al., 2020b).

Seeds provide an efficient means for disseminating many plant diseases across the world. In particular, it has been widely documented that seed-transmitted viruses are often introduced into new countries and continents through infected germplasm, due to the global trade involving large-scale movements of seeds. Tobamoviruses are seed-borne, mechanically transmitted stable viruses (Dombrovsky and Elisheva, 2017). By analogy with other tobamoviruses infecting tomato and pepper (i.e., TMV and ToMV), the seed transmission of ToBRFV is strongly suspected but has not yet been definitely demonstrated (Dombrovsky and Elisheva, 2017). Nevertheless, the long-distance movement of ToBRFV by means of infected seeds could explain how this virus emerged so rapidly and simultaneously in different countries. Moreover, it is important to underline that, even if most of the tobamoviruses display a low percentage of seed transmission (primary infection), such very low occurrence of seed transmission is enough to cause an outbreak of the disease, as these viruses are easily transmitted mechanically through wounding, which is often caused by human activity during agronomic crop management, by contact with infected plants or facilitated by pollinator activity (secondary infection), as demonstrated recently just for ToBRFV (Levitzky et al., 2019; Panno et al., 2020a).

Given its rapid spread and potential harm to tomatoes and peppers, ToBRFV has been included in EPPO's *Alert list* and has been regulated in the European Union since November 2019 (Commission Implementing Decision EU 2019/1615). In addition, ToBRFV has also been included in the list of quarantine bodies (Commission regulation – EU – 2019/2072), as well as included in the priorities of the European Union (Commission regulation – EU – 2019/1702). In light of European legislation, the cultivation of host plants must be subjected to territorial monitoring every year, in order to check for the presence of the virus. In particular, for tomato and bell pepper, specific measures have been approved, with the introduction and movement of the virus in the EU being prohibited. In particular, considering that the virus can be spread through the movement of seeds, tomato, and pepper seeds must be free of ToBRFV or originate from ToBRFV-free areas, both before entering the EU and before coming onto the market. Current ToBRFV outbreaks in different parts of the world highlight that early detection is crucial to prevent the spread of the virus, to control outbreaks and, eventually, to quickly begin appropriate eradication interventions. Therefore, rapid and effective detection methods are needed, particularly at entry points or during monitoring investigations, to prevent outbreaks in new environments with negative ecological and economic consequences. Phytosanitary certification systems have been established all over the world, in order to certify the propagation of virus-free plant material (EPPO, 2009). Implementing these disease control schemes requires techniques with high sensitivity and specificity, such as biomolecular methods.

Different techniques have been proposed to detect ToBRFV in seeds, leaves, or petioles, including biological indexing, serology, and nucleic acid-based detection techniques with specific primers such as reverse transcription polymerase chain reaction (RT-PCR), real-time RT-PCR, and *reverse transcription* loop-mediated isothermal amplification (RT-LAMP; Dombrovsky and Elisheva, 2017; Almeida et al., 2018; Panno et al., 2019). Although real-time RT-PCR assay presents increased sensitivity and stability, compared to conventional RT-PCR, this method still requires sophisticated and expensive equipment and reagents, which may not be available in laboratories with limited resources. This status has prompted motivation for the investigation and development of a sensitive but cost-effective alternative technique. Loop-mediated isothermal amplification (LAMP) is a sensitive and rapid nucleic acid amplification technology, first reported by Notomi et al. (2000). To date, LAMP has reached many fields of application, including plant pathology (Panno et al., 2020c). In particular, RT-LAMP is a valid substitute for RT-PCR, due to its simplicity, rapidity, specificity, and sensitivity, as only a water bath or thermoblock capable of ensuring a constant temperature (60–65°C) is required. The LAMP reaction is an auto-cycling strand amplification reaction based on the *Bacillus stearothermophilus* (*Bst*) DNA polymerase, which possesses strand-displacement activity, and two or three pairs of specific primers that recognize four or six stem-loop DNA regions with various lengths. The product of the LAMP reaction can

be detected using agarose gel or an intercalator that emits fluorescence in the case of amplification in RT-LAMP. The latter can be visualized by monitoring either the turbidity using a photometer, the fluorescence using a fluorimeter, or by the naked eye under a UV lamp when using an intercalating dye which changes color (Panno et al., 2020c).

In this study, we have developed a rapid and sensitive RT-LAMP and a visual RT-LAMP assay for the specific detection of ToBRFV RNA for the first time in tomato and pepper seeds using a single-tube one-step RT-LAMP and visual RT-LAMP, as well as comparing the sensitivity and specificity of the developed methods with those of RT-PCR and real-time RT-PCR.

MATERIALS AND METHODS

Virus Isolates and Plant Material

Four biologically and molecularly characterized ToBRFV isolates were used to evaluate the RT-LAMP assay. Isolates were obtained as lyophilized infected tomato leaves from various sources, both institutional and commercial: Isolate Sic1/19, from the University of Palermo (Italy); isolate T1101, from the Institute of Sustainable Plant Protection of the National Research Council (IPSP-CNR), Torino (Italy); isolate TBRFV-Ps1, from the An-Najah National University (Palestine); and isolate PC-1236, from North Rhine-Westphalia, Germany (DSMZ – German Collection of Micro-organisms and Cell Cultures).

All isolates were maintained, in an insect-proof greenhouse, on the tomato line Momor carrying the *Tm-2*^{2} gene of resistance to tobamoviruses (Dombrovsky and Elisheva, 2017), and on the pepper ecotype Friariello, without any resistance gene. Healthy tomato and pepper plants were also maintained in a separate greenhouse compartment and used as controls. To check the specificity of the RT-LAMP assay, additional tobamoviruses, obtained from the DSMZ collection as dehydrated leaves, were included in the trials for method validation. In particular, bell pepper mottle virus (BPeMV, isolate PC-0170), odontoglossum ringspot virus (ORSV, isolate PC 0625), paprika mild mottle virus (PaMMV, isolate PC 0606), pepper mild mottle virus (PMMoV, isolate PC 0165), streptocarpus flower break virus (SFBV, isolate PC 1058), tobacco mild green mosaic virus (TMGMV, isolate PC 0887), ToMV (isolate PC 15705), TMV (isolate PC 0107), turnip vein clearing virus (TVCV, isolate PC 0148), youcai mosaic virus (YMoV, isolate PC 0527), and watermelon chlorotic stunt virus (WmCSV, isolate PC 0830) were used.

Finally, several batches of uncontaminated tomato and pepper seeds were used for specific ToBRFV detection tests in tomato and pepper seeds (see below).

LAMP Primer Design

Nine complete ToBRFV genome sequences available in the NCBI GenBank[1] were downloaded and aligned using the MAFFT v. 7.450 alignment software (Katoh and Standley, 2013) in Geneious version 10.2.6 (Kearse et al., 2012) for preliminary identification of the most conserved ToBRFV genomic regions. Then, a set of ToBRFV-specific primers was designed using the LAMP Designer software (OptiGene Limited, Horsham, United Kingdom). The 5' region of the RNA-dependent RNA polymerase gene (*RdRp*) was chosen as the amplification target. The primer set included two external primers (forward outer primer F3 and backward outer primer B3), two internal primers (forward inner primer FIP and backward inner primer BIP), and two additional loop primers (backward loop primer LB and forward loop primer LF) to augment the number of loops in the LAMP reaction, thus enhancing the reaction speed. The sequences and binding sites of the primers are shown in **Table 1** and **Figure 1**.

Primers were synthesized by Eurofins Genomics (Ebersberg, Germany), dissolved in qPCR-grade water (Promega, United States) to produce 100 µM solutions, and stored at −20°C. The specificity of each primer was verified by comparing the primer sequences against the NCBI GenBank nucleotide and genome databases using the BLASTn tool. The specificity of the primer set was evaluated using Geneious software by *in silico* analysis of the sequences corresponding to ToBRFV genomic regions defined by the F3/B3 LAMP primers of the ToBRFV reference strain (GenBank Acc. Number MN013188) and the most similar sequences found in GenBank after BLASTn search using the F3/B3 sequence of the reference strain. The selected sequences were imported into Geneious and aligned using the MAFFT software with default settings (**Supplementary Figure S1A**). In addition, the F3/B3 sequence of the reference strain was also aligned with the sequences of eight tobamoviruses downloaded from GenBank: TMV (Acc. Number. V01408), ToMV (Acc. Number. AF332868), tomato mottle mosaic virus (ToMMV; Acc. Number. KF477193), BPeMV (BPeMV; Acc. Number. DQ355023), TMGMV (TMGMV; Acc. Number. M34077), PMMoV (Acc. Number. M81413), paprica mild mottle virus (PaMMV; Acc. Number. AB089381), and obuda pepper virus (ObPV; Acc. Number. D13438; **Supplementary Figure S1B**). Further, the F3/B3 amplicon obtained in RT-PCR end-point was sequenced, in order to confirm the identity of the amplicon by BLASTn search.

RNA Extraction

Total RNA was extracted from fresh leaves, dehydrated leaves, and seeds using the RNeasy plant mini kit (Qiagen, United States), according to the manufacturer's instructions with minor modification (Foissac et al., 2001). In the case of leaves (both fresh and dehydrated), they were placed in nylon mesh U-shaped bags (Bioreba, Reinach, Switzerland) and homogenized with Homex 6.0 (Promega) in presence of 7 ml (100 mg tissue/1 ml buffer) of GBF (Grinding Buffer Foissac; 4 M Guanidine Isothiocyanate, Sodium acetate 0.2 M, disodium EDTA, 0.025 M, Potassium acetate 1 M and PVP 40 K 2.5%). One milliliter of lysate was withdrawn and 200 microliters of 10% N – Lauril Sarcosine (Sarkosil) were added and mixed. After centrifugation at maximum speed for 2 min (13,000 rpm), 500 µl of the supernatant was recovered and transferred to

[1]https://www.ncbi.nlm.nih.gov/

TABLE 1 | RT-LAMP primers for detection of ToBRFV designed in this study.

Primer name	Length (nt)	Sequence 5'–3'	Nucleotide position	Product size (bp)	Reference sequence
ToBRFV_B3	20	GGACACCGTCAACTAGGA	2,576–2,558	278 (from F3 to B3); 163 (from F2 to B2)	MN815773
ToBRFV_BIP (B1c + B2)	43	CCGTGAGTTCTGAGTCAATGGTT – ATGAGGCTCACCATCTCTTA	2,359–2,382 and 2,457–2,437		
ToBRFV_F3	18	TTGGAGTCTTAGATGTTGCG	2,298–2,318		
ToBRFV_FIP (F1c + F2)	43	CCTTCTCCAACTGTCGCAAGTTA – CACATGCTAGGAAGTACCAC	2,452–2,429 and 2,376–2,396		
ToBRFV_LoopB	22	GCTCAGAACACTGAGGAGATT	2,497–2,518		
ToBRFV_LoopF	21	CTCCATGCTCATCATACTCCAA	2,426–2,404		

For each primer, the nucleotide position related to the reference sequence is reported.

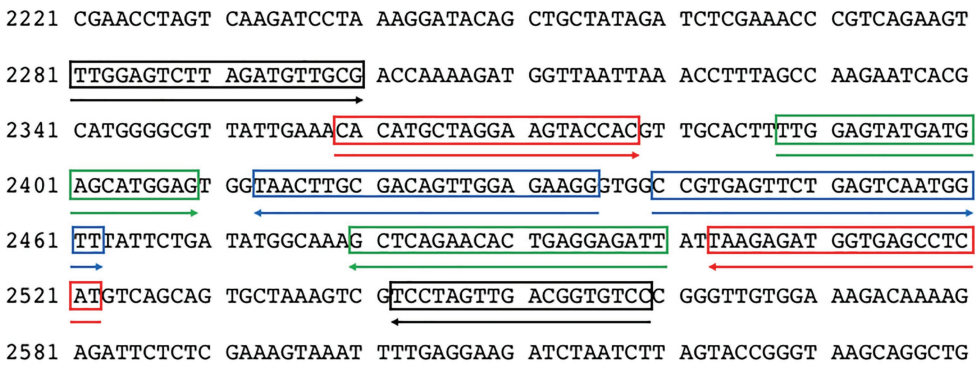

FIGURE 1 | Distribution of the LAMP primers on the nucleotide sequence of ToBRFV (GenBank Acc. Number MN815773). F3/B3 primers are highlighted in black, F2/B2 in red, LoopF/LoopB in green, and F1c/B1c in blue.

the QIAshredder sieve columns (Qiagen, United States). Subsequently, the extraction protocol took place in accordance with the kit manual. In the case of the seeds, the same procedure was used but the homogenization step was carried out with the aid of a Mixer Mill MM 200 (Retsch, Torre Boldone, Italy) homogenizer in 10 ml steel jars at a high speed (30 oscillations/s) for 30 s.

To check the quality and integrity of the RNA extracted from leaves and seeds, a one-step real-time RT-PCR reaction using starting concentrations of 10 ng/µl of RNA and a TaqMan dual-labeled probe targeting a highly conserved portion of the plant 18S rRNA was employed, as described by Osman et al. (2017). Results showed a mean Cq value of 12.8 ± 2.6 and 16.8 ± 3.5 for the RNA extracted from the leaves and seeds, respectively. Reactions were performed with a CFX96 (Biorad) thermocycler, following the protocol described by Osman et al. (2017). The RNA quality and quantity were further assessed using a QIAxpert spectrophotometer (Qiagen, Hilden, Germany) and the final concentration was adjusted to ~100 ng/µl.

RT-LAMP and Visual RT-LAMP Assay

Reverse transcription loop-mediated isothermal amplification reactions were performed and optimized on a CFX96 (Biorad) thermocycler using Isothermal Master Mix (ISO-001) from OptiGene (Horsham, United Kingdom). RNA samples were amplified in 0.2 ml strips of eight tubes for Real-Time PCR (Starlab, Milan, Italy). Each isothermal reaction was performed in duplicate, with a final volume of 20 µl. The optimization of the LAMP protocol took into account the isothermal amplification times (from 20 to 40 min), the mix quantities of Reverse Transcription 5× Master Mix kit (GeneSpin, Italy; from 0.5 to 1.5 µl), and the LAMP primer mixture 10X (2.0–5.0 µl), as well as the individual concentrations of the groups of LAMP primers (at concentrations of 0.2–0.4 µM each of F3 and B3, 0.4–0.8 µM each of LoopF and LoopB, and 0.8–1.2 µM each of FIP and BIP). The cDNA was produced for all RNA targets extracted and was tested in RT-LAMP for all the matrices under investigation, with the aim to have a double operational possibility and relative verification of the results (i.e., both in one-step and two-step RT-LAMP). The cDNA synthesis was performed at 25°C for 5 min and 42°C for 10 min, followed by LAMP amplification cycle. To find the optimal temperature for the LAMP amplification, the reactions were carried out at 58–65°C in a thermal gradient using a CFX96 thermal cycler. In order to evaluate the diagnostic selectivity, the optimized protocol was also applied using a LAMP-dedicated Genie II (OptiGene, Horsham, United Kingdom) thermocycler.

With respect to the visual RT-LAMP protocol, reactions were carried out in duplicate using *Bst* 3.0 DNA polymerase

(New England Biolabs, Ipswich, Massachusetts, United States) in a total volume of 20 µl. Optimization of the visual assay was carried out in a similar manner to the real-time assay. In particular, several parameters were taken into account: 1.5–1.8× Isothermal Amplification Buffer, 8–12 U of *Bst* 3.0 DNA polymerase, 6–8 mM $MgSO_4$, 1.2–1.6 mM deoxynucleotide triphosphates (dNTPs; GeneSpin, Milan, Italy), 0.15–0.3 µM of HNB, Betaine 0.8–1.2 M (GeneSpin, Milan, Italy), 0.2–0.4 µM of F3 and B3 primers, 0.8–1.2 µM of FIP and BIP primers, 0.4–0.8 µM of LoopF and LoopB primers, and 2 µl test sample [no template control (NTC), or extracted RNA]. Set-up and execution of all LAMP reactions was done on a conventional lab bench using designated pipettes and filter tips, while imaging analysis took place in separate rooms. All experiments were independently replicated at least six times.

Visual RT-LAMP results were observed by the naked eye under natural light and photographed using a conventional smartphone camera. A color change to light blue indicated positive samples, while negative samples remained purple. Moreover, to verify the occurrence of LAMP amplification, RT-LAMP amplicons were analyzed by 1.7% agarose gel electrophoresis in 1x TAE buffer, followed by GelRed (Biotium, Hayward, United States) staining and DNA visualization using a transilluminator. Four microliters of 100 bp DNA ladder (GeneSpin, Milan, Italy) was used as a DNA size marker.

Specificity and Sensitivity of the LAMP Assays and Comparison With End-Point RT-PCR and RT-qPCR

The specificity of the LAMP primers was validated against four different ToBRFV isolates and by testing cross-reactivity with other tobamoviruses, used as non-target samples (see Section "Virus isolates and plant material"). All samples were tested in duplicate in RT-LAMP and values of threshold, baseline, and reaction efficiency were calculated using the CFX Maestro software (Biorad, United States). Samples with a threshold cycle value (Cq/min) above 30 were ignored.

The diagnostic specificity, for both RT-LAMP and visual RT-LAMP, were calculated using the following formula: D/D + C × 100, where C indicates false positives and D indicates true negatives (EPPO, 2019). The diagnostic sensitivity of both methods was calculated using the formula: % diagnostic sensitivity = A/(A+B) × 100, where A is the obtained positives/expected positives (True positives) and B is the obtained negatives/expected positives (False negatives; EPPO, 2019). The analytical sensitivity (limit of detection, LoD) of both methods was verified using 10-fold RNA extract serial dilutions ranging from 22.5 ng/µl to 0.0225 fg/µl, repeated three times. The same dilutions used to calculate the LoD of the assay were also used in end-point RT-PCR (Alkowni et al., 2019; Ling et al., 2019) and SybrGreen RT-qPCR, in order to compare the degree of sensitivity of the three methods (**Tables 2**, **3**).

TABLE 2 | Primers used for conventional RT-PCR and RT-qPCR amplification for comparison with the RT-LAMP method proposed in this study.

Primers	Sequence (5'–3')	Length (bp)	Annealing (°C)	Protocol	Reference
ToBRFV-F	AATGTCCATGTTTGTTACGCC	560	58	RT-PCR end point	Alkowni et al., 2019
ToBRFV-R	CGAATGTGATTTAAAACTGTGAAT				
ToBRFV_B3	GGACACCGTCAACTAGGA	278	58	RT-qPCR SybrGreen	This study
ToBRFV_F3	TTGGAGTCTTAGATGTTGCG				
ToBRFV-F (5503)	GAAGTCCCGATGTCTGTAAGG	842	55	RT-PCR end point	Ling et al., 2019
ToBRFV-R (6344)	GTGCCTACGGATGTGTATGA				

TABLE 3 | Sensitivity of LAMP used for the ToBRFV detection with different techniques.

Dilutions	RT-LAMP	Visual RT- LAMP	RT-PCR[1]	RT-PCR[2]	RT-qPCR SybrGreen[3]
	Cq means ± SD	Positive (+)/negative (–)	Positive (+)/negative (–)	Positive (+)/negative (–)	Cq means ± SD
22.5 ng/µl	3.80 ± 0.15	+	+	+	5.99 ± 0.34
2.25 ng/µl	5.47 ± 0.11	+	+	+	10.05 ± 0.36
0.225 ng/µl	6.57 ± 0.13	+	+	+	13.81 ± 1.95
22.5 pg/µl	7.71 ± 0.37	+	+	+	18.46 ± 2.20
2.25 pg/µl	8.59 ± 0.07	+	+	+	21.86 ± 1.87
0.225 pg/µl	10.34 ± 0.48	+	+	–	25.18 ± 2.03
22.5 fg/µl	12.22 ± 0.86	+	–	–	28.47 ± 2.14
2.25 fg/µl	16.04 ± 2.75	+	–	–	32.43 ± 1.99
0.225 fg/µl	n/a[4]	–	–	–	n/a
0.0225 fg/µl	n/a	–	–	–	n/a

Mean Cq ± SD = mean of the three threshold cycles of each dilution (Cq) ± standard deviation (SD). Cq values above 30 were considered as negative results.

[1]*Based on Alkowni et al. (2019).*

[2]*Based on Ling et al. (2019).*

[3]*Based on F3 and B3 primer pair.*

[4]*n/a = not applicable.*

The SybrGreen RT-qPCR was performed in a total volume of 20 µl, with a concentration of 0.4 µM of F3 and B3 primers and 10 µl of SsoAdvanced Universal SYBR Green Supermix (Biorad, Hercules, United States), using the same CFX96 thermal cycler used for the RT-LAMP.

The results obtained with gel electrophoresis, capillary electrophoresis using a Qiaxcel (Qiagen, United States), and for the RT-PCR end-point and melt-curve analyses for RT-qPCR with the F3 and B3 LAMP primers were compared (**Table 3**).

Detection of ToBRFV Using RT-LAMP and Visual RT-LAMP Assays on Artificially and Naturally Contaminated Seeds

Tomato and pepper seeds were artificially contaminated with the ToBRFV isolate Sic1/19 by the following method: seeds were disinfected using a diluted solution of sodium hypochlorite, as previously described (Prohens et al., 2008). Then, 100 seeds for each species/variety were contaminated with a leaf extract obtained by macerating 50 mg of infected tomato dehydrated leaves in 1 ml of sterile water in a sterile mortar. Seeds were left in the mortar to macerate for 2 h and then air-dried. Naturally contaminated seeds were obtained from fruits of plants infected by ToBRFV identified in a tomato protected crop from southern Italy (Sicily). Before testing the seeds using the two LAMP assays, seed contamination was verified by checking the presence of viral RNA and virus infectivity, using the total RNA extracted separately from 10 seeds, by end-point RT-PCR, using the method described by Alkowni et al. (2019), and by mechanical inoculation on *Nicotiana tabacum* cv. Xanthi nc. Contaminated tomato and pepper seeds were mixed with clean seeds to generate seed lots with 0% (0/1,000 seeds), 2% (1/50 seeds), 1% (1/100 seeds), 0.1% (1/1,000 seeds), 0.05% (1/2,000 seeds), 0.033% (1/3,000 seeds), 0.025% (1/4,000 seeds), 0.02% (1/5,000 seeds), 0.017% (1/6,000 seeds), 0.014% (1/7,000 seeds), 0.012% (1/8,000 seeds), 0.011% (1/9,000 seeds), and 0.01% (1/10,000 seeds) contamination. Seed lots were ground in a mixer mill and the powder was transferred into sterile plastic bags. Total RNA was extracted and used in the RT-LAMP and visual RT-LAMP assays, as described above. The same seed dilutions used for the two LAMP assays were used for end-point RT-PCR assay (Alkowni et al., 2019; Ling et al., 2019) and SybrGreen RT-qPCR using the F3/B3 primer pair, in order to compare the diagnostic sensitivity in relation to the two LAMP assays. Seeds obtained from tomato and pepper plants found to be infected with ToBRFV were also tested as single seeds or seed lots of 5, 10, or 30 seeds.

RESULTS

Optimization of the ToBRFV LAMP Assay

A one-step LAMP assay for the rapid detection of ToBRFV was developed using a set of six primers designed from a highly conserved region of the *RdRp* gene (**Table 1**). Sequencing F3/B3 amplicons of the four ToBRFV reference isolates revealed 100% nucleotide sequence identity with the corresponding genomic region of the virus isolate used to design the LAMP primers (Acc. Number MN815773).

During the optimization of the RT-LAMP assay, significant differences in the Cq values were obtained for all ToBRFV RNA and cDNA with temperatures ranging from 58 to 65°C, resulting in an optimal annealing temperature of 60°C, while negligible differences in Cq values with different concentrations of LAMP primers were observed. The optimal thermal cycle protocol included 5 min of incubation at 25°C, 10 min at 42°C, and 30 min at 60°C, followed a melting curve increasing the temperature from 65 to 95°C with a 1-s interval for every 0.5°C increment. For all the reactions, the melting peak was reached around 86.5 ± 0.5°C. The optimized reaction mix contained 10 µl Isothermal Master Mix, 0.5 µl of Reverse Transcription 5× Master Mix kit, 2.0 µl LAMP primer mixture 10× (final concentrations of 0.2 µM each of F3 and B3, 0.4 µM each of LF and LB, and 0.8 µM each of FIP and BIP), and 2 µl of template RNA diluted 1:10 in sterile water or 2 µl dd-water used as NTC. The results obtained concerning amplification curves, melting curves, and melting peaks by RT-LAMP are shown in **Figures 2A–C**, respectively.

In terms of reaction performance and color change rate, the optimal visual RT-LAMP reaction mixture was as follows: 2.5 µl Isothermal Buffer 10×, 0.6 mM of dNTPs, 2 mM of MgSO4, 0.2 M of Betaine, 0.5 µl of Reverse Transcription 5× Master Mix kit, 2.0 µl LAMP primer mixture 10× (at final concentrations of 0.2 µM each of F3 and B3, 0.4 µM each of LF and LB, and 0.8 µM each of FIP and BIP), 8 U of *Bst* 3.0, 150 µM of hydroxynapthol blue (HNB) dye as a visual indicator, and 2 µl of template RNA diluted 1:10 in sterile water or 2 µl sterile water used as NTC. The optimal thermal cycle consisted of 25°C for 5 min and 42°C for 10 min, followed by one cycle of 60°C for 30 min, and a final cycle of 80°C for 2 min to inactivate the polymerase and terminate the reaction. Using HNB dye as a visual indicator, positive samples produced an intense blue color, while negative samples presented a pale purple coloration (**Figure 3**).

Diagnostic Specificity and Sensitivity of the LAMP Assay

The RT-LAMP assay detected all ToBRFV isolates, while none of the non-target tobamoviruses produced any amplification throughout the entire 30 min test (**Supplementary Figure S2**). A distinct peak on the melting temperature curve (86.5 ± 0.5°C), resulting from the melting curve analysis in RT-LAMP, was found only for ToBRFV isolates, confirming the specificity of the RT-LAMP assay (**Figures 2A–C**).

For the *Bst* 3.0-based visual RT-LAMP assay using HNB as a colorimetric indicator, all positive reactions showed a color change from purple to blue, while the negative ones remained purple. Thus, the positive and negative results were easily distinguishable by the naked eye. The typical ladder-like pattern of LAMP products was observed only for the ToBRFV

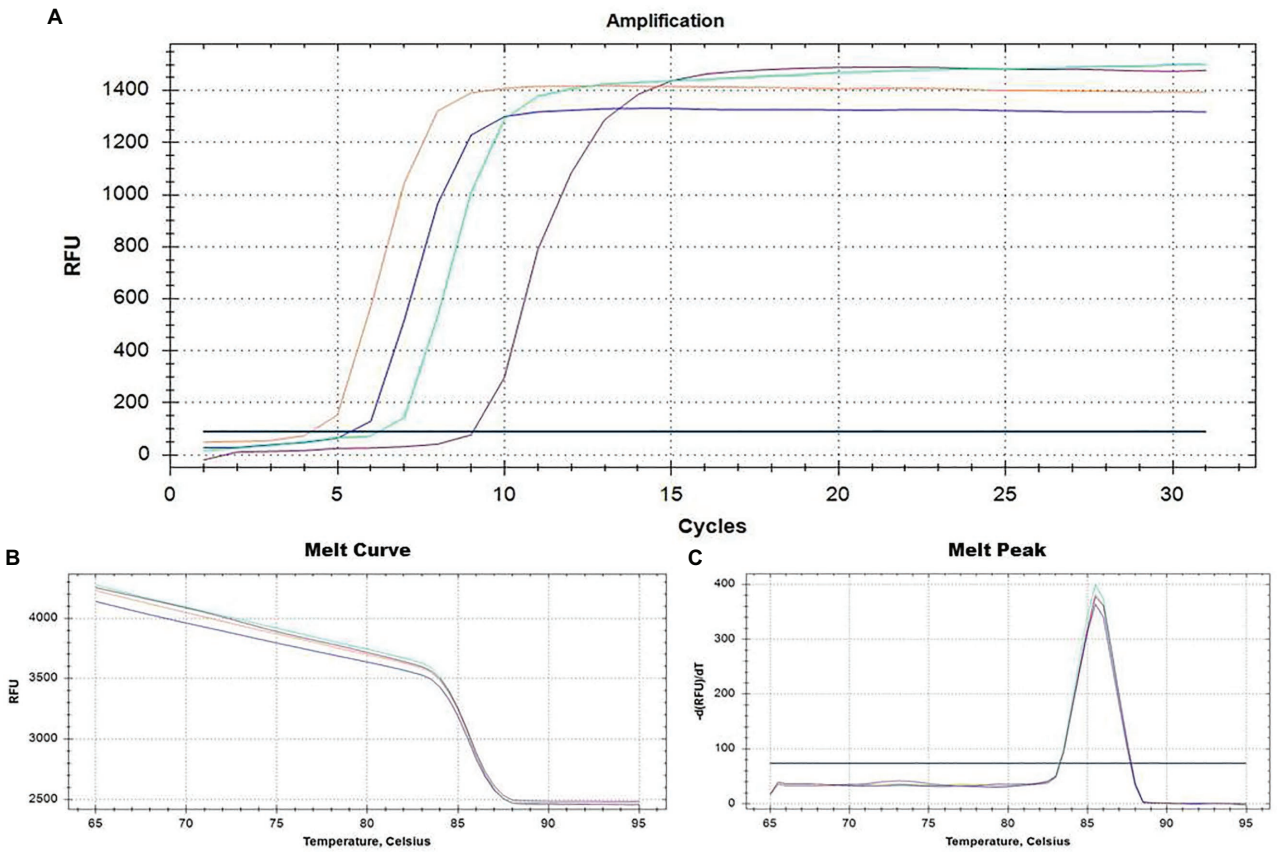

FIGURE 2 | Real-time monitoring of the RT-LAMP result assay for ToBRFV detection based on primer pairs designed on the 5' region of the RNA-dependent RNA polymerase gene (*RdRp*; **Table 1**). Amplification plots and the two dissociation curves, melting curve and melting peak, are shown in **(A-C)**, respectively. ToBRFV isolates used as positive controls, including Italian isolates Sic1/19 (blue curve) and T1101 (green curve), the Palestinian isolate TBRFV-Ps1 (purple curve), and the German isolate PC-1236 (orange curve). Negative controls (black line) consisted of a no-template control (NTC). Healthy tomato plants and other different tobamoviruses (see section "Virus isolates and plant material") were also used as negative controls (not shown).

isolates in gel electrophoresis, confirming the specificity of the LAMP assay (**Figure 3**).

Based on the diagnostic specificity tests, performed either using the RT-LAMP or the visual RT-LAMP, the percentage of diagnostic specificity resulted as 100%. The same results were observed for the diagnostic sensitivity, which was equal to 100%.

To assess the analytic sensitivity (LoD) of RT-LAMP and visual RT-LAMP assay, using the set of primers and to compare the LoD with that of end-point RT-PCR and qPCR SybrGreen, we compared all four methods using 10-fold serial dilutions of total RNA extracted from Sic1/19-infected leaves. In particular, the threshold cycle of each reaction increased along with the dilution degree, and the average values of Cq of three replicates were calculated (**Table 3**). The Cq values showed a linear relationship with the log value of the RNA concentrations in the 10-fold dilution series (R^2 = 0.99). For the 10-fold dilution series, starting from 22.5 ng/µl to a value of 0.0225 fg/µl, we observed that the highest dilution at which LAMP showed positive results for ToBRFV was 2.25 fg/µl (**Table 3**; **Figure 4**). The RT-LAMP and visual RT-LAMP assays, were perfectly comparable and 100 times more sensitive than RT-PCR, based on the method described by Alkowni et al. (2019) and 1,000 times more sensitive than RT-PCR, based on the data of Ling et al. (2019), whose LoD results were 0.225 and 2.25 pg/µl, respectively (**Figure 5**). Finally, the qPCR assay based on SybrGreen and using the F3 and B3 primers showed high performance, with values consistent with those obtained by LAMP assays, thus supporting their specificity and sensitivity (**Figure 6**).

Detection of ToBRFV in Tomato and Pepper Seeds

To evaluate the efficiency and feasibility of both LAMP methods in detecting ToBRFV in tomato and pepper seeds, artificially and naturally contaminated seed samples were tested and compared with RT-PCR, based on the results of Alkowni et al. (2019) and Ling et al. (2019), and with qPCR SybrGreen assay based on the F3/B3 primer pair.

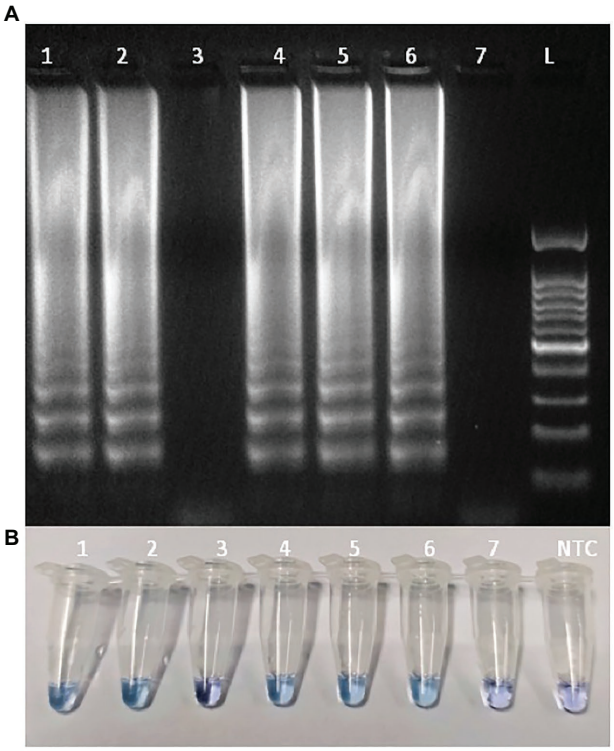

FIGURE 3 | Detection of ToBRFV isolates in tomato leaves samples using loop-mediated isothermal amplification (LAMP) assay: **(A)** Agarose gel electrophoresis analysis of the LAMP products; **(B)** Detecting LAMP products by adding hydroxynapthol blue (HNB) as dye. Lane L: 100 bp ladder (GeneSpin); line 1: isolate Sic1/19; line 2: isolate T1101; line 3: ToMV (isolate PC15705); line 4: isolate TBRFV-Ps1; lines 5 and 6: isolate PC-1236; line 7: tomato healthy leaves; NTC: no template control.

With artificially contaminated seeds, the RT-LAMP and visual RT-LAMP assay detected ToBRFV up to 0.025% of contamination in tomato seeds (one contaminated seed per 3,000 healthy seeds; **Table 4**; **Figure 7A**, right) and 0.033% of contamination in pepper seeds (one contaminated seed per 4,000 healthy seeds; **Table 5**; **Figure 7A**, left). Comparable results to the LAMP assays were also observed when the LAMP external primers F3 and B3 were used with the qPCR SybrGreen assay (**Tables 4** and **5**).

The detection limits for conventional RT-PCR were found to be below that obtained with the LAMP and SybrGreen assays: 0.10% of contamination for both pepper and tomato seeds, based on Ling et al. (2019; **Figure 7B**, left), and 0.10 and 0.05% of contamination of pepper and tomato seeds, respectively, based on Alkowni et al. (2019; **Figure 7B**, right).

Tomato brown rugose fruit virus was also detected in all seed samples obtained from naturally infected plants of tomato and pepper, both with LAMP methods and by qPCR (data not shown).

The 10-fold serial dilution of total RNA extracted from artificially contaminated seed lots, as inoculated on *N. tabacum* cv. Xanthi nc, led to hypersensitive reaction on the inoculated leaves within 1 week at up to 1:4,000 serial dilution of RNA (data not shown).

DISCUSSION

Two LAMP assays were developed in this work (RT-LAMP and visual RT-LAMP), with the aim of designing a simple, fast, and also, in the case of visual RT-LAMP assay, cheap diagnostic method, for screening tomato and pepper seeds for the presence of ToBRFV.

These two approaches are both characterized by advantages and disadvantages, and can be combined to adapt the LAMP methodology to various situations (Panno et al., 2020c). For an end-point-based LAMP method – in particular, the visual RT-LAMP developed herein – the most remarkable advantages are its ease to use, and the possibility to use it directly in the field or in laboratories which do not possess specialized personnel and equipment (e.g., thermocyclers). On the other hand, the proposed RT-LAMP method possesses two important advantages: there is no need to check the amplification product at the end of the reaction by the naked eye, and it is easy to read the results though an increase in fluorescence during the amplification reaction. Moreover, by determining the melting temperature of the final reaction product, the result can be further confirmed, thus excluding non-specific products or primer-dimer products. This method showed the same results as conventional qPCR, with the advantage of being more rapid and easy to use. The reaction can be carried out using a typical real-time PCR thermocycler, generating results in <30 min for most samples (Panno et al., 2020c). Considering these aspects, the diagnostic protocols presented in this study were developed based on both RT-LAMP and visual RT-LAMP assays.

Very recently, another LAMP assay for the detection of ToBRFV has been proposed by Sarkes et al. (2020). This assay was applied to plant matrices and gene constructs (gBlocks) to verify their diagnostic specificity. Our work differs for several substantial aspects, including the starting matrices (pepper and tomato seeds), with the relative peculiarities concerning nucleic acid extraction, presence of inhibitors, and diagnostic sensitivity. Furthermore, by developing two LAMP methods in parallel, one in real-time and one visual, it was possible to verify any doubtful or uncertain diagnostic cases through the cross-use of the two techniques. The diagnostic specificity is also confirmed by the use of the melting point (peaks and graphs of the melting curves) of the RT-LAMP, which cannot be verified with the visual RT-LAMP alone.

Finally, in the work presented by Sarkes et al. (2020), specificity was evaluated with respect to only two tobamoviruses, ToMV and TMV, while we used a total of eight different tobamoviruses, including, in addition to ToMV and TMV, other important tomato and pepper viruses, such as ToMMV, BPeMV, TMGMV, PMMoV, PaMMV, and ObPV. It is important to remember that ToMMV, like ToBRFV, has been reported on resistant tomato genotypes (Li et al., 2013; Turina et al., 2016),

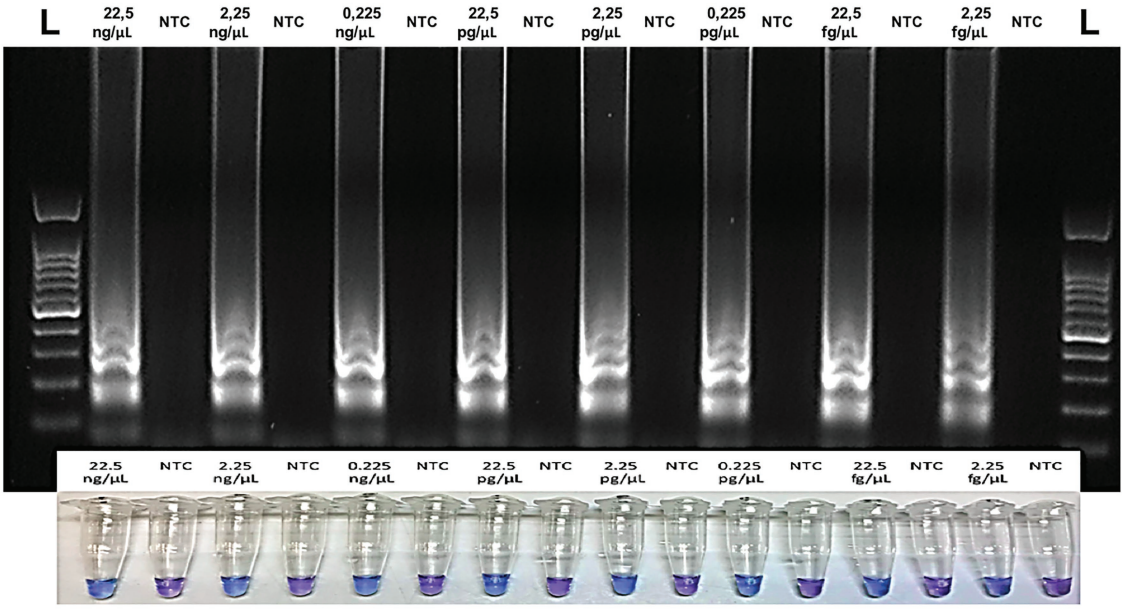

FIGURE 4 | Analytical sensitivity of the Visual RT-LAMP based on the HNB colorimetric assay showing the relative reaction tubes: purple color indicates negative samples, while blue color indicates the positive ones. For each reaction tube, the corresponding agarose gel is shown above. L = 100 bp DNA Ladder (GeneSpin).

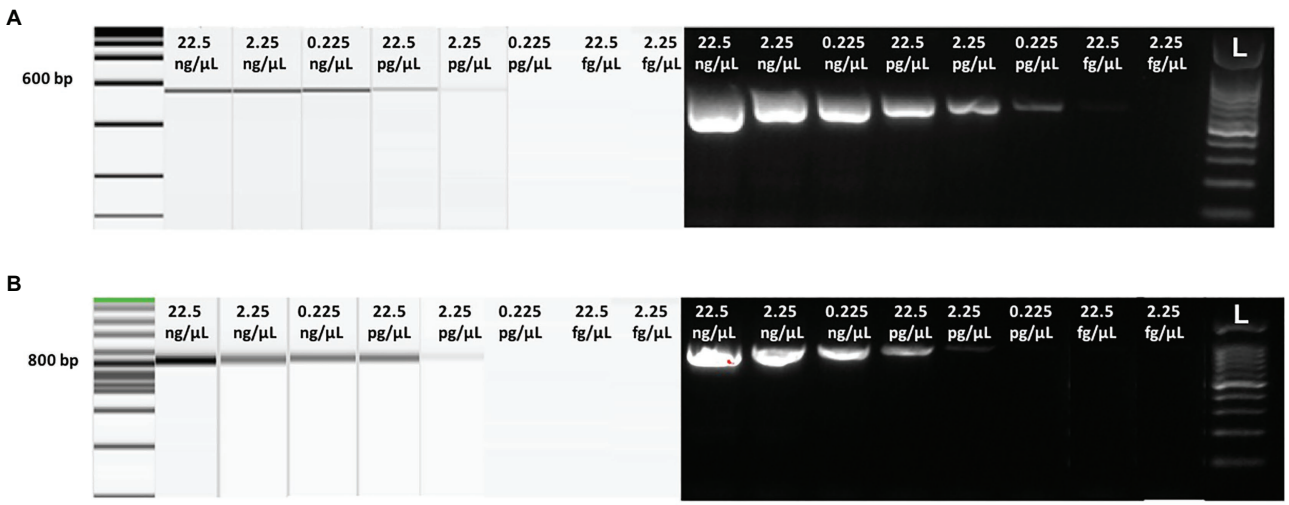

FIGURE 5 | Analytical sensitivity of conventional RT-PCR detected by capillarity and gel electrophoresis using 10-fold serial dilution of purified total RNAs extracted from tomato leaves infected with Sic1/19 isolate of ToBRFV, based on the end-point RT-PCR protocols described by Alkowni et al. (2019; **A**) and Ling et al. (2019; **B**), respectively. On the top of each lane, total RNA concentration is reported. L = 100 bp ladder (GeneSpin).

and therefore, certified and verified LAMP methods are needed to specifically identify only ToBRFV.

Our method based on the two above-mentioned protocols resulted in high specificity, being able to distinguish ToBRFV from the other tobamoviruses with no cross-reactions between the RNA extracts of tomato and pepper and viral RNA. The performance characteristics of the LAMP protocol developed in real-time showed the highest degree of inclusiveness, exclusivity, and diagnostic specificity. These results were also confirmed by the repeatability and reproducibility obtained with different operators (data not shown).

Unlike most of the LAMP protocols that use thermostable polymerases for which a single amplification cycle at high temperatures is adopted, we adopted lower initial temperatures (25°C for 5 min followed by 42°C for 10 min) with the aim

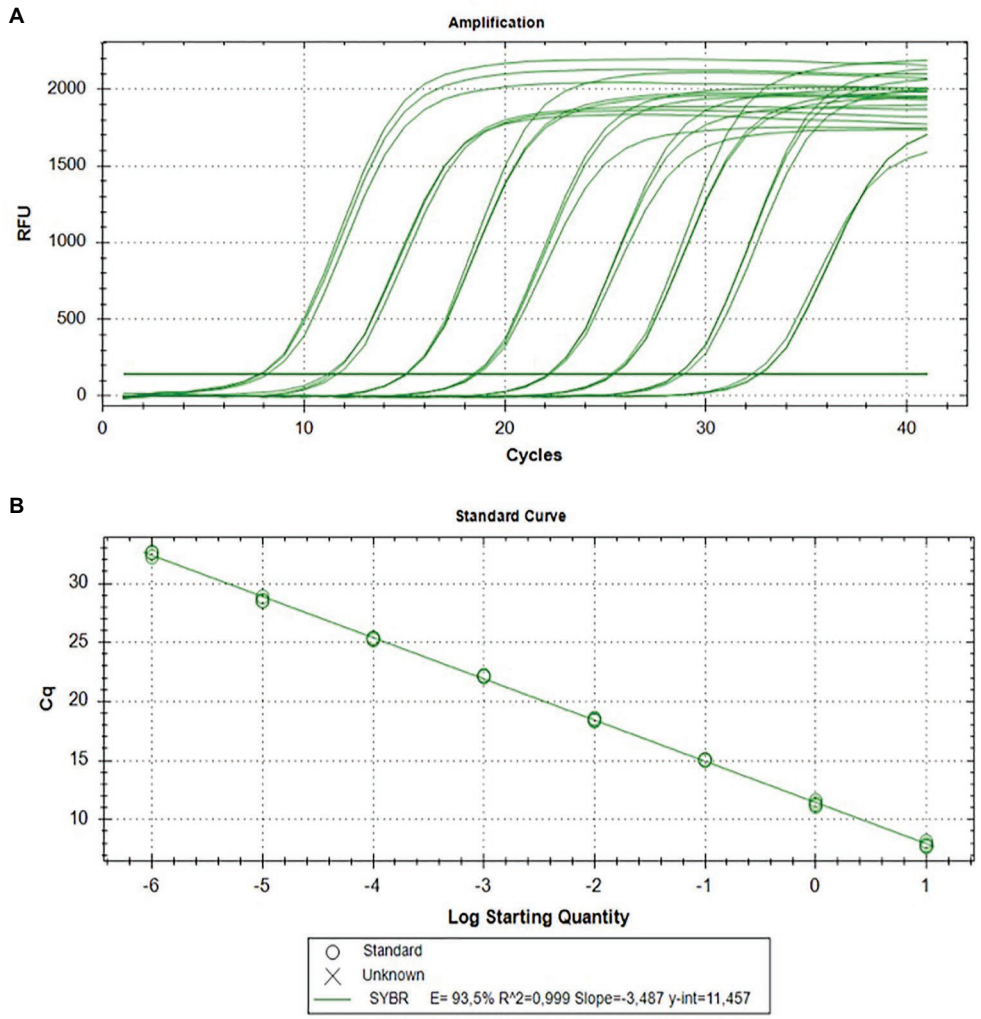

FIGURE 6 | Analytical sensitivity of the qPCR SybrGreen assay using the F3/B3 primer pair for ToBRFV detection. Amplification curves in triplicate **(A)** and the resulting standard curve **(B)** are shown.

of favoring the cDNA synthesis in this phase, probably allowing to reach high sensitivities.

The optimization conditions of the method, based on the use of different reagents and thermocyclers and testing different annealing temperatures and reagent concentrations, did not show any significant differences, in terms of diagnostic results, indicating the robustness of the developed method. Moreover, LAMP assays have shown higher robustness, in terms of pH change, temperature stability, and the use of plant extracts which commonly inhibit PCR reactions (Francois et al., 2011; Kogovsek et al., 2015).

In our experiments, comparison between conventional RT-PCR and the LAMP protocols we developed, demonstrated the higher sensitivity of the LAMP methods. In particular, our LAMP methods were 100 and 1,000 times more sensitive than the RT-PCR methods described by Alkowni et al. (2019) and Ling et al. (2019), respectively (**Figures 4, 5**). This was demonstrated using both plant leaf (fresh or dehydrated) and seed samples of tomato or pepper (**Figure 7**). The qPCR SybrGreen method using the F3/B3 LAMP external primers gave similar results to those obtained by RT-LAMP assay, with optimal reaction efficiency parameters (R^2, slope, and E), indirectly supporting the specificity and sensitivity of the RT-LAMP assay (**Figure 6**).

The LAMP methods developed herein were able to detect as little as 2.25 fg/μl of ToBRFV RNA from host plants, either by RT-LAMP or visual RT-LAMP (**Table 3**; **Figure 4**). In addition, LAMP assays performed on pepper and tomato seeds gave good results, in terms of analytic sensitivity, considering the percentage of infected seeds over the healthy ones. The LAMP assays proposed in this study were able to detect ToBRFV to 0.025% of contamination in tomato seeds (**Table 4**; **Figure 7A**, right) and 0.033% of contamination in pepper seeds (one contaminated seed per 3,000 and 4,000 healthy seeds, respectively; **Table 5**; **Figure 7A**, left), while the detection limits for conventional RT-PCR, were 0.10% of contamination for both

TABLE 4 | Detection of ToBRFV in seed-lots of tomato with different techniques.

Seedlots of Tomato	RT-LAMP	Visual RT- LAMP	RT-PCR[1]	RT-PCR[2]	RT-qPCR SybrGreen[3]
	Cq means ± SD	Positive (+)/negative (–)	Positive (+)/negative (–)	Positive (+)/negative (–)	Cq means ± SD
0/1,000	n/a[4]	–	–	–	n/a
1/50	11.10 ± 0.93	+	+	+	26.85 ± 0.2
1/100	12.15 ± 0.67	+	+	+	26.40 ± 0.25
1/500	5.50 ± 0.64	+	+	+	27.12 ± 0.05
1/1,000	8.67 ± 4.55	+	+	+	22.95 ± 0.12
1/2,000	15.13 ± 2.32	+	+	–	23.59 ± 0.08
1/3,000	17.4 ± 0.13	+	–	–	25.10 ± 0.10
1/4,000	15.15 ± 0.70	+	–	–	27.42 ± 0.19
1/5,000	n/a	–	–	–	n/a
1/6,000	n/a	–	–	–	n/a
1/7,000	n/a	–	–	–	n/a
1/8,000	n/a	–	–	–	n/a
1/9,000	n/a	–	–	–	n/a
1/10,000	n/a	–	–	–	n/a

Mean Cq ± SD of seed-lots of tomato = mean of the three threshold cycles of each dilution (Cq) ± standard deviation (SD). Cq values above 30 were considered as negative results.
[1]Based on Alkowni et al. (2019).
[2]Based on Ling et al. (2019).
[3]Based on F3 and B3 primer pair.
[4]n/a = not applicable.

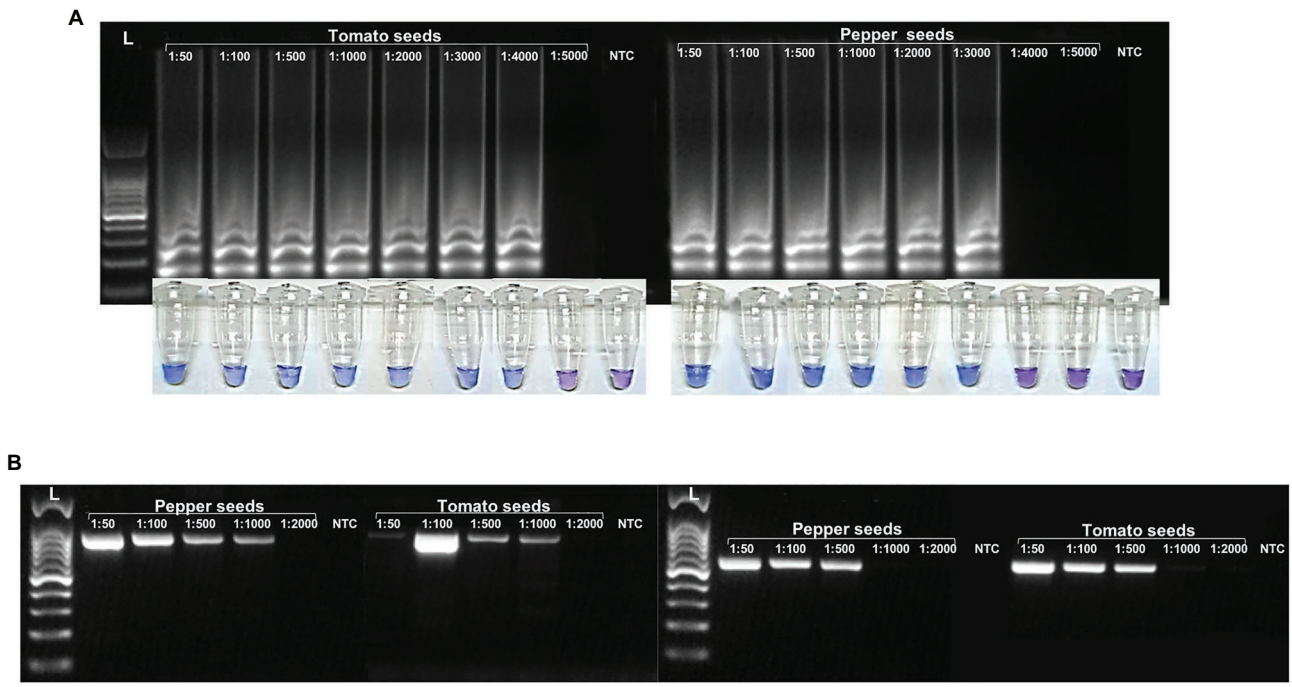

FIGURE 7 | Comparison of ToBRFV sensitivity detection between RT-LAMP **(A)** and RT-PCR, based on the results of Ling et al. (2019; **B**, left) and Alkowni et al. (2019; **B**, right) using 10-fold serial dilutions of purified total RNA extracted in contaminated pepper and tomato seeds.

pepper and tomato seeds, based on Ling et al. (2019; **Figure 7B**, left); 0.10 and 0.05% of contamination of pepper and tomato seeds, respectively, based on Alkowni et al. (2019; **Figure 7B**, right).

In conclusion, the results obtained in the present study show that, using the rapid and versatile LAMP methods developed, accurate and reliable diagnosis of ToBRFV can be performed in leaves and, for the first time, in tomato and pepper seeds. This approach offers a new diagnostic tool in phytosanitary investigations, which can be used to support plant and seed inspection and early diagnosis of ToBRFV infection at official entry points, nurseries, during

TABLE 5 | Detection of ToBRFV in seed-lots of pepper with different techniques.

Seedlots of Pepper	RT-LAMP	Visual RT- LAMP	RT-PCR[1]	RT-PCR[2]	RT-qPCR SybrGreen[3]
	Cq means ± SD	Positive (+)/negative (–)	Positive (+)/negative (–)	Positive (+)/negative (–)	Cq means ± SD
0/1,000	n/a[4]	–	–	–	n/a
1/50	8.54 ± 1.70	+	+	+	24.55 ± 0.19
1/100	11.59 ± 1.37	+	+	+	25.80 ± 0.22
1/500	3.51 ± 0.94	+	+	+	26.54 ± 0.16
1/1,000	12.41 ± 0.64	+	+	+	25.87 ± 0.17
1/2,000	13.97 ± 0.42	+	–	–	26.67 ± 0.28
1/3,000	16.24 ± 2.84	+	–	–	27.25 ± 0.16
1/4,000	n/a	–	–	–	n/a
1/5,000	n/a	–	–	–	n/a
1/6,000	n/a	–	–	–	n/a
1/7,000	n/a	–	–	–	n/a
1/8,000	n/a	–	–	–	n/a
1/9,000	n/a	–	–	–	n/a
1/10,000	n/a	–	–	–	n/a

Mean Cq ± SD of seed-lots of pepper = mean of the three threshold cycles of each dilution (Cq) ± standard deviation (SD). Cq values above 30 were considered as negative results.
[1]Based on Alkowni et al. (2019).
[2]Based on Ling et al. (2019).
[3]Based on F3 and B3 primer pair.
[4]n/a = not applicable.

plant and seed trade, and for the correct implementation of the phytosanitary management of ToBRFV.

DATA AVAILABILITY STATEMENT

The original contributions presented in the study are included in the article/**Supplementary Material**, further inquiries can be directed to the corresponding author.

AUTHOR CONTRIBUTIONS

DR and GP conceived the work and supervised the experiments. Experiments were performed by AP, DL, GC, LB, and GP. The article was drafted by DR, AP, DL, and GP. All authors contributed to manuscript revision, read, and approved the final manuscript.

ACKNOWLEDGMENTS

We thank Prof. S. Davino of the University of Palermo (Italy) for providing the isolate Sic1/19 of ToBRFV, Dr. M. Ciuffo of the Institute of Sustainable Plant Protection of Torino (Italy) for providing the isolate T1101, and Prof. R. Alkowni of the An-Najah National University (Palestine) for providing the isolate TBRFV-Ps1. We also thank R. Martellucci, M. Matteoni, A. Consani, N. Tedde, E. Marcucci, F. Bertelli, and E. Silvestri of the Phytosanitary Service of the Tuscany Region for their contribution in collecting field samples of tomato and pepper.

SUPPLEMENTARY MATERIAL

The Supplementary Material for this article can be found online at: https://www.frontiersin.org/articles/10.3389/fmicb.2021.640932/full#supplementary-material

REFERENCES

Alkowni, R., Alabdallah, O., and Fadda, Z. (2019). Molecular identification of tomato brown rugose fruit virus in tomato in Palestine. *J. Plant Pathol.* 101, 719–723. doi: 10.1007/s42161-019-00240-7

Almeida, J. E. M., Figueira, A. D. R., Duarte, P. D. S. G., Lucas, M. A., and Alencar, N. E. (2018). Procedure for detecting tobamovirus in tomato and pepper seeds decreases the cost analysis. *Bragantia* 77, 590–598. doi: 10.1590/1678-4499.2017317

Beris, D., Malandraki, I., Kektsidou, O., Theologidis, I., Vassilakos, N., and Varveri, C. (2020). First report of tomato brown rugose fruit virus infecting tomato in Greece. *Plant Dis.* 104:2035. doi: 10.1094/PDIS-01-20-0212-PDN

Cambrón-Crisantos, J. M., Rodríguez-Mendoza, J., Valencia-Luna, J. B., Alcasio-Rangel, S., García-Ávila, C. J., López-Buenfil, J. A., et al. (2018). First report of *Tomato brown rugose fruit virus* (ToBRFV) in Michoacan, Mexico. *MJP* 37, 185–192. doi: 10.18781/R.MEX.FIT.1810-5

Chitambar, J. (2018). Tomato brown rugose fruit virus. Available at: https://blogs.cdfa.ca.gov/Section3162/?p=5843 (Accessed June 7, 2020).

Dombrovsky, A., and Elisheva, S. (2017). "Seed transmission of tobamoviruses: Aspects of global disease distribution" in *Advances in seed biology*. ed. J. C. Jimenez-Lopez (IntechOpen).

EPPO (2009). PM 4 production of healthy plants for planting. *Bull. OEPP* 39, 267–270. doi: 10.1111/j.1365-2338.2009.02307.x

EPPO (2019). PM 7/98 specific requirements for laboratories preparing accreditation for a plant pest diagnostic activity. *EPPO Bull.* 49, 530–563. doi: 10.1111/epp.12629

Fidan, H. (2020). Tomato brown rugose fruit virus (ToBRFV): current situation and future prospects. *Mediterr. Agric. Sci.* 33, 43–49. doi: 10.29136/mediterranean.705740

Foissac, X., Svanella-Dumas, L., Dulucq, M. J., Gentit, P., and Candresse, T. (2001). Polyvalent detection of fruit tree tricho, capillo and foveaviruses by nested RT-PCR using degenerated and inosine containing primers (PDO

nested RT-PCR). *Acta Hort.* 550, 37–44. doi: 10.17660/ActaHortic.2001.550.2

Francois, P., Tangomo, M., Hibbs, J., Bonetti, E. J., Boehme, C. C., Notomi, T., et al. (2011). Robustness of a loop-mediated isothermal amplification reaction for diagnostic applications. *FEMS Immunol. Med. Microbiol.* 62, 41–48. doi: 10.1111/j.1574695X.2011.00785.x

Katoh, K., and Standley, D. M. (2013). MAFFT multiple sequence alignment software version 7: improvements in performance and usability. *Mol. Biol. Evol.* 30, 772–780. doi: 10.1093/molbev/mst010

Kearse, M., Moir, R., Wilson, A., Stones-Havas, S., Cheung, M., Sturrock, S., et al. (2012). Geneious basic: an integrated and extendable desktop software platform for the organization and analysis of sequence data. *Bioinformatics* 28, 1647–1649. doi: 10.1093/bioinformatics/bts199

Kogovsek, P., Hodgetts, J., Hall, J., Prezelj, N., Nikolic, P., Mehle, N., et al. (2015). LAMP assay and rapid sample preparation method for on-site detection of flavescence doree phytoplasma in grapevine. *Plant Pathol.* 64, 286–296. doi: 10.1111/ppa.12266

Levitzky, N., Smith, E., Lachman, O., Luria, N., Mizrahi, Y., Bakelman, H., et al. (2019). The bumblebee *Bombus terrestris* carries a primary inoculum of *Tomato brown rugose fruit virus* contributing to disease spread in tomatoes. *PLoS One* 14:e0210871. doi: 10.1371/journal.pone.0210871

Li, R., Gao, S., Fei, Z., and Ling, K.-S. (2013). Complete genome sequence of a new tobamovirus naturally infecting tomatoes in Mexico. *Genome Announc.* 1:e00794-e13. doi: 10.1128/genomeA.00794-13

Ling, K.-S., Tian, T., Gurung, S., Salati, R., and Gilliard, A. (2019). First report of tomato brown rugose fruit virus infecting greenhouse tomato in the United States. *Plant Dis.* 103:1439. doi: 10.1094/PDIS-11-18-1959-PDN

Luria, N., Smith, E., Reingold, V., Bekelman, I., Lapidot, M., Levin, I., et al. (2017). A new israeli tobamovirus isolate infects tomato plants harboring *Tm-2*^{2} resistance genes. *PLoS One* 12:e0170429. doi: 10.1371/journal.pone.0170429

Menzel, W., Knierim, D., Winter, S., Hamacher, J., and Heupel, M. (2019). First report of tomato brown rugose fruit virus infecting tomato in Germany. *New Dis. Rep.* 39:1. doi: 10.5197/j.2044-0588.2019.039.001

Notomi, T., Okayama, H., Masubuchi, H., Yonekawa, T., Watanabe, K., Amino, N., et al. (2000). Loop-mediated isothermal amplification of DNA. *Nucleic Acids Res.* 28:e63. doi: 10.1093/nar/28.12.e63

Osman, F., Al Rwahnjn, M., and Rowhani, A. (2017). Real-time RT-qPCR detection of cherry rasp leaf virus, cherry green ring mottle virus, cherry necrotic rusty mottle virus, cherry virus a and apple chlorotic leaf spot virus in stone fruits. *J. Plant Path.* 99, 279–285. doi: 10.4454/jpp.v99i1.3789

Panno, S., Caruso, A. G., Barone, S., Lo Bosco, G., Rangel, E. A., and Davino, S. (2020a). Spread of tomato brown rugose fruit virus in sicily and evaluation of the spatiotemporal dispersion in experimental conditions. *Agronomy* 10: 834. doi: 10.3390/agronomy10060834

Panno, S., Caruso, A. G., Blanco, G., and Davino, S. (2020b). First report of tomato brown rugose fruit virus infecting sweet pepper in Italy. *New Dis. Rep.* 41:20. doi: 10.5197/j.2044-0588.2020.041.020

Panno, S., Caruso, A. G., and Davino, S. (2019). First report of tomato brown rugose fruit virus on tomato crops in Italy. *Plant Dis.* 103:1443. doi: 10.1094/PDIS-12-18-2254-PDN

Panno, S., Matić, S., Tiberini, A., Caruso, A. G., Bella, P., Torta, L., et al. (2020c). Loop mediated isothermal amplification: principles and applications in plant virology. *Plants* 9:461. doi: 10.3390/plants9040461

Prohens, J., Soler, S., and Nuez, F. (2008). The effects of thermotherapy and sodium hypochlorite treatments on Pepino seed germination, a crucial step in breeding programmes. *Ann. Appl. Biol.* 134, 299–305. doi: 10.1111/j.1744-7348.1999.tb05268.x

Salem, N., Mansour, A., Ciuffo, M., Falk, B. W., and Turina, M. (2016). A new tobamovirus infecting tomato crops in Jordan. *Arch. Virol.* 161, 503–506. doi: 10.1007/s00705-015-2677-7

Sarkes, A., Fu, H., Feindel, D., Harding, M., and Feng, J. (2020). Development and evaluation of a loop-mediated isothermal amplification (LAMP) assay for the detection of *Tomato brown rugose fruit virus* (ToBRFV). *PLoS One* 15:e0230403. doi: 10.1371/journal.pone.0230403

Skelton, A., Buxton-Kirk, A., Ward, R., Harju, V., Frew, L., Fowkes, A., et al. (2019). First report of *Tomato brown rugose fruit virus* in tomato in the United Kingdom. *New Dis. Rep.* 40:12. doi: 10.5197/j.2044-0588.2019.040.012

Turina, M., Geraats, B. P. J., and Ciuffo, M. (2016). First report of tomato mottle mosaic virus in tomato crops in Israel. *New Dis. Rep.* 33:1. doi: 10.5197/j.2044-0588.2016.033.001

Yan, Z.-Y., Ma, H.-Y., Han, S.-L., Geng, C., Tian, Y.-P., and Li, X.-D. (2019). First report of tomato brown rugose fruit virus infecting tomato in China. *Plant Dis.* 103:2973. doi: 10.1094/PDIS-05-19-1045-PDN

Zhang, H., Zhao, J., Liu, S., Zhang, D.-P., and Liu, Y. (2013). *Tm-2*^{2} confers different resistance responses against *Tobacco mosaic virus* dependent on its expression level. *Mol. Plant* 6, 971–974. doi: 10.1093/mp/sss153

Conflict of Interest: The authors declare that the research was conducted in the absence of any commercial or financial relationships that could be construed as a potential conflict of interest.

frontiers in Microbiology

REVIEW
published: 21 May 2021
doi: 10.3389/fmicb.2021.671925

Global Advances in Tomato Virome Research: Current Status and the Impact of High-Throughput Sequencing

*Mark Paul Selda Rivarez[1,2], Ana Vučurović[1,3], Nataša Mehle[1], Maja Ravnikar[1,4] and Denis Kutnjak[1]**

[1] Department of Biotechnology and Systems Biology, National Institute of Biology, Ljubljana, Slovenia, [2] Jožef Stefan International Postgraduate School, Ljubljana, Slovenia, [3] Faculty of Agriculture, University of Belgrade, Belgrade, Serbia, [4] School for Viticulture and Enology, University of Nova Gorica, Nova Gorica, Slovenia

OPEN ACCESS

Edited by:
Giuseppe Parrella, Institute for Sustainable Plant Protection of the National Research Council (IPSP-Consiglio Nazionale delle Ricerche (CNR)), Italy

Reviewed by:
Vicente Pallas, Polytechnic University of Valencia, Spain
Aviv Dombrovsky, Agricultural Research Organization (ARO), Israel

***Correspondence:**
Denis Kutnjak
denis.kutnjak@nib.si

Specialty section:
This article was submitted to Virology, a section of the journal Frontiers in Microbiology

Received: 24 February 2021
Accepted: 12 April 2021
Published: 21 May 2021

Citation:
Rivarez MPS, Vučurović A, Mehle N, Ravnikar M and Kutnjak D (2021) Global Advances in Tomato Virome Research: Current Status and the Impact of High-Throughput Sequencing. Front. Microbiol. 12:671925. doi: 10.3389/fmicb.2021.671925

Viruses cause a big fraction of economically important diseases in major crops, including tomato. In the past decade (2011–2020), many emerging or re-emerging tomato-infecting viruses were reported worldwide. In this period, 45 novel viral species were identified in tomato, 14 of which were discovered using high-throughput sequencing (HTS). In this review, we first discuss the role of HTS in these discoveries and its general impact on tomato virome research. We observed that the rate of tomato virus discovery is accelerating in the past few years due to the use of HTS. However, the extent of the post-discovery characterization of viruses is lagging behind and is greater for economically devastating viruses, such as the recently emerged tomato brown rugose fruit virus. Moreover, many known viruses still cause significant economic damages to tomato production. The review of databases and literature revealed at least 312 virus, satellite virus, or viroid species (in 22 families and 39 genera) associated with tomato, which is likely the highest number recorded for any plant. Among those, here, we summarize the current knowledge on the biology, global distribution, and epidemiology of the most important species. Increasing knowledge on tomato virome and employment of HTS to also study viromes of surrounding wild plants and environmental samples are bringing new insights into the understanding of epidemiology and ecology of tomato-infecting viruses and can, in the future, facilitate virus disease forecasting and prevention of virus disease outbreaks in tomato.

Keywords: tomato, virome, high-throughput sequencing, metagenomics, virus diversity, virus discovery, virus ecology, virus epidemiology

INTRODUCTION

Tomato (*Solanum lycopersicum* L.) is one of the most economically valuable fruit or vegetable crops worldwide, valued at 93.9 billion US dollars in 2018, with yield estimated at 180.8 million tons in 2019 (FAOSTAT, 2020). Tomato production is affected by numerous diseases and, among them, viruses are considered an important production-limiting factor (Hanssen et al., 2010b; Souiri et al., 2019; Hančinský et al., 2020; Ong et al., 2020). It was estimated that almost half of the emerging

crop diseases can be attributed to plant viruses (Anderson et al., 2004), which could amount up to around a quarter of the overall attainable yields in major crops, including tomato (Oerke, 2006). Worldwide economic damages caused by viruses in crops are difficult to estimate; however, rough approximations indicate yield losses range from 30 to 50 billion US dollars annually (Sastry, 2013). Yield and economic losses due to virus diseases in tomato vary greatly and are often dependent on the virus species and growing region.

Until a decade ago, viruses were mostly analyzed using targeted detection techniques such as ELISA, PCR, and Sanger sequencing (Katsarou et al., 2019). These methods are widely available in molecular biology labs, but they require *a priori* information on viral genomes or serological properties of viral species that might be present in a sample. The study of a whole community of viruses (i.e., viromes), including unknown ones, became possible due to the rapid decrease in high-throughput sequencing (HTS) costs (NIH-NHGRI, 2019) and the availability of the improved data analysis tools (Villamor et al., 2019). This circumvented challenges of targeted detection of plant viruses and contributed useful ecological and epidemiological insights. First examples of the use of HTS for detection of plant viruses are now over a decade old (Adams et al., 2009a; Al Rwahnih et al., 2009; Donaire et al., 2009; Kreuze et al., 2009). Currently, HTS is used for discovery of many novel viruses and is now establishing its position as one of the classical approaches in plant virology research and diagnostics laboratories (Massart et al., 2019). HTS is often employed with one of the possible nucleic acid preparation approaches, such as sequencing of double-stranded (ds)RNA, small (s)RNAs, total (tot)DNA after rolling circle amplification, virion-associated RNA (VANA), and total (tot)RNA after ribosomal (r)RNA depletion (Pecman et al., 2017; Ma et al., 2019; de Nazaré Almeida dos Reis et al., 2020; Gaafar and Ziebell, 2020). Each method has its pros and cons (Roossinck, 2017) and should be selected according to the aims of the study; e.g., sequencing rRNA depleted totRNA or sRNA might be the most straightforward and generic approaches for detection of a wide range of viruses in single samples or relatively small sample pools (Pecman et al., 2017). On the other hand, dsRNA or VANA might be beneficial, when trying to enrich for viruses in, e.g., large pools of starting plant material (Ma et al., 2019).

Both classical (Sanger) sequencing and HTS are regularly used for discovery of new viruses in tomato; however, the usage of the latter is evidently increasing in the past few years. In the first part of this review, we discuss the discovery of 45 novel virus species in tomato within the 2011–2020 period and contextualize the role of HTS in these findings. Moreover, a post-discovery characterization of new viruses represents an important step toward understanding their biological and/or economical relevance (Massart et al., 2017; Hou et al., 2020); thus, we also systematically reviewed to which extent such characterization have been performed for newly discovered viruses associated with tomato. Beyond discovering and detecting viruses in tomato, HTS can enable a broader look into the virome of tomato on a defined geographical scale, a virome of surrounding plants and vectors, and possible exchanges among those communities. HTS-based virome studies of tomato and surrounding wild plant species (which can serve as reservoirs for viruses) (Hančinský et al., 2020; Ma et al., 2020), and environmental samples, such as water (which might serve as transmission pathway) (Bačnik et al., 2020), can also bring important insights into the understanding of the epidemiology of some tomato viruses.

Review of the past and recent discoveries of viruses in tomato shows that tomato is currently associated with at least 312 different viral species, which is likely, according to our knowledge, the largest recorded number known for any cultivated plant. Among those, many known and several recently discovered viruses cause significant economic damage in tomato production in different parts of the world. In the second part of this review, we focus on important tomato viruses, which caused significant economic losses in tomato production in the past decade and new virus discoveries in tomato, for which limited or no knowledge about potential impact on tomato health is available.

HTS HAS BECOME AN IMPORTANT TOOL IN TOMATO VIRUS DISCOVERY AND EPIDEMIOLOGY STUDIES

Forty-five novel virus species were discovered in tomato in the recent decade (2011–2020) (**Table 1**). Majority of these discoveries were made in Neotropic and Palearctic countries and just in recent years (**Figure 1**). Out of this set, 14 were discovered using HTS, and in 2020 alone, seven novel species were discovered just by three HTS-based studies (Ciuffo et al., 2020; de Nazaré Almeida dos Reis et al., 2020; Ma et al., 2020). In this period, also four viral families were associated with tomato for the first time, in four HTS-based studies, i.e., *Iflaviridae* (Saqib et al., 2015), *Phenuiviridae* (Lecoq et al., 2019), *Kitaviridae* (Ciuffo et al., 2020), and *Genomoviridae* (de Nazaré Almeida dos Reis et al., 2020). Specifically, more than half of the RNA viruses were discovered using HTS (7/13), while most of the DNA viruses (including satellite virus species) were discovered using a non-HTS approach (24/32). Overall, non-HTS-based discovery approaches remain widely used for targeted, single species plant virus discoveries, while HTS has become a tool to discover multiple species, without *a priori* knowledge about possibly present viruses. In this section, the impact of HTS as an important tool in tomato viromics is further contextualized, from the discovery of viruses in individual plants, through the post-discovery characterization of new viruses, to the holistic analysis of plant viromes in agroecosystems.

Discovery and Generic Detection of Viruses in Tomato Using HTS

Fourteen new tomato viruses or virus satellites were detected using HTS in recent years (**Table 1**). As an example, HTS was used to characterize the diversity of viruses and viroids in tomato-growing areas of Mexico, where a novel tobamovirus, tomato mild mottle virus (ToMMV), and a novel potyvirus, tomato necrotic stunt virus (ToNStV), were discovered (Li et al., 2012, 2013). In the extensive study of the diversity of tomato viruses

TABLE 1 | Novel virus species discovered from 2011 to 2020 and associated with tomato.

Family	Genus	Virus name	Acronym	Baltimore Group[1]	HTS-based discovery?	Sample and library preparation approach[2]/ Sequencing platform	Country(ies) where first reported	Publication
Alphasatellitidae	Unspecified	"New alphasatellite"	–	ssDNA	Yes	Total DNA-RCA/HiSeq 2500	Brazil	de Nazaré Almeida dos Reis et al., 2020
	Colecusatellite	Tomato leaf curl Cameroon alphasatellite	ToLCCMA	ssDNA	No	–	Cameroon	Leke et al., 2011
Bromoviridae	*Ilarvirus*	Solanum nigrum ilarvirus 1	SnIV1	(+)ssRNA	Yes	dsRNA/HiSeq 3000	France	Ma et al., 2020
		Tomato necrotic streak virus	TomNSV	(+)ssRNA	No	–	USA	Adkins et al., 2015
Geminiviridae	*Begomovirus*	"New begomovirus species #1"	–	ssDNA	Yes	Total DNA-RCA/HiSeq 2500	Brazil	de Nazaré Almeida dos Reis et al., 2020
		"New begomovirus species #2"	–	ssDNA	Yes	Total DNA-RCA/HiSeq 2500	Brazil	de Nazaré Almeida dos Reis et al., 2020
		"New begomovirus species #3"	–	ssDNA	Yes	Total DNA-RCA/HiSeq 2500	Brazil	de Nazaré Almeida dos Reis et al., 2020
		Pepper leafroll virus	PepLRV	ssDNA	No	–	Peru	Martínez-Ayala et al., 2014
		Pepper yellow leaf curl Aceh virus	PepYLCAV	ssDNA	No	–	Indonesia	Kesumawati et al., 2019
		Tomato apical leaf curl virus	ToALCV	ssDNA	No	–	Argentina	Vaghi Medina et al., 2018
		Tomato chlorotic leaf curl virus	ToCLCV	ssDNA	No	–	Brazil	Quadros et al., 2019
		Tomato chlorotic leaf distortion virus	TCLDV	ssDNA	No	–	Venezuela	Zambrano et al., 2011
		Tomato dwarf leaf virus	ToDLV	ssDNA	No	–	Argentina	Vaghi Medina and López Lambertini, 2012
		Tomato interveinal chlorosis virus	ToICV	ssDNA	No	–	Brazil	Albuquerque et al., 2012
		Tomato interveinal chlorosis virus-2	ToICV2	ssDNA	Yes	Total DNA-RCA/HiSeq 2000	Brazil	Rego-Machado et al., 2019
		Tomato latent virus	TLV	ssDNA	No	–	Cuba	Fuentes et al., 2016
		Tomato leaf curl Burkina Faso virus	ToLCBFV	ssDNA	No	-	Burkina Faso	Ouattara et al., 2017
		Tomato leaf curl Cameroon virus	ToLCCMV	ssDNA	No	–	Cameroon	Leke et al., 2011
		Tomato leaf curl Kunene virus	ToLCKunV	ssDNA	No	–	Namibia	Lett et al., 2020
		Tomato leaf curl Liwa virus	ToLCLV	ssDNA	No	–	Oman	Khan et al., 2014
		Tomato leaf curl Mahé virus	ToLCMahV	ssDNA	No	–	Seychelles	Scussel et al., 2018
		Tomato leaf curl Oman virus	ToLCOMV	ssDNA	No	–	Oman	Idris et al., 2011
		Tomato leaf curl purple vein virus	ToLCPVV	ssDNA	No	–	Brazil	Macedo et al., 2018

(Continued)

TABLE 1 | Continued

Family	Genus	Virus name	Acronym	Baltimore Group[1]	HTS-based discovery?	Sample and library preparation approach[2]/ Sequencing platform	Country(ies) where first reported	Publication
		Tomato leaf deformation virus	ToLDeV	ssDNA	No	–	Peru	Márquez-Martín et al., 2011
		Tomato mottle wrinkle virus	ToMoWV	ssDNA	No	–	Argentina	Vaghi Medina et al., 2015
		Tomato rugose yellow leaf curl virus	ToRYLCV	ssDNA	No	–	Uruguay	Márquez-Martín et al., 2012
		Tomato twisted leaf virus	ToTLV	ssDNA	No	–	Venezuela	Romay et al., 2019
		Tomato vein clearing leaf deformation virus	ToVCLDeV	ssDNA	No	–	Argentina	Vaghi Medina et al., 2020
		Tomato wrinkled mosaic virus	ToWMV	ssDNA	No	–	Venezuela	Romay et al., 2018
		Tomato yellow margin leaf curl virus	TYMLCV	ssDNA	No	–	Venezuela	Nava et al., 2013
	Unassigned	"Tomato associated geminivirus 1"	TaGV1	ssDNA	Yes	Total DNA-RCA/HiSeq 2500	Brazil	Fontenele et al., 2017
Genomoviridae	*Gemycirculavirus*	"Plant-associated genomovirus 2"	–	ssDNA	Yes	Total DNA-RCA/HiSeq 2500	Brazil	de Nazaré Almeida dos Reis et al., 2020
Iflaviridae	*Iflavirus*	Tomato matilda virus	TMaV	(+)ssRNA	Yes	Total RNA/GA IIx	Australia	Saqib et al., 2015
Kitaviridae	*Blunervirus*	Tomato fruit blotch virus	ToFBV	(+)ssRNA	Yes	Total RNA-RD/unspecified	Italy, Australia	Ciuffo et al., 2020
Phenuiviridae	*Tenuivirus*	Melon chlorotic spot virus	MeCSV	(–)ssRNA	Yes	Small RNA/HiSeq	France	Lecoq et al., 2019
Potyviridae	*Potyvirus*	Tomato necrotic stunt virus	ToNStV[3]	(+)ssRNA	Yes	Small RNA/GA IIx	Mexico	Li et al., 2012
Rhabdoviridae	*Cytorhabdovirus*	Tomato yellow mottle-associated virus	TYMaV	(–)ssRNA	Yes	Small RNA/HiSeq 2500	China	Xu et al., 2017
Tollecusatellitidae	*Betasatellite*	Tomato leaf curl Hajipur betasatellite	ToLCHLB	ssDNA	No	–	India	Kumar et al., 2013
		Tomato leaf curl Togo betasatellite	ToLCTGB	ssDNA	No	–	Togo	Kon and Gilbertson, 2012
Tospoviridae	*Orthotospovirus*	Pepper necrotic spot virus	PNSV	(–)ssRNA	No	–	Peru	Torres et al., 2012
		Tomato necrotic ringspot virus	TNRSV	(-)ssRNA	No	–	Thailand	Seepiban et al., 2011
		Tomato necrotic spot virus[4]	TNSV	(–)ssRNA	No	–	China	Yin et al., 2014
Tymoviridae	*Tymovirus*	Tomato blistering mosaic tymovirus	ToBMV	(+)ssRNA	No	–	Brazil	De Oliveira et al., 2013
Virgaviridae	*Tobamovirus*	Tomato brown rugose fruit virus	ToBRFV	(+)ssRNA	No	–	Jordan	Salem et al., 2016
		Tomato mottle mosaic virus	ToMMV	(+)ssRNA	Yes	Small RNA/HiSeq 2000	Mexico	Li et al., 2013

Viruses are grouped according to virus family and genus, with its genome type indicated. The sample and library preparation approach and sequencing platform used are indicated for viruses discovered using HTS. Lastly, the country where the virus was first discovered and the corresponding publication and year are also indicated. [1]ssDNA: circular, positive sense, single-stranded DNA (Group I), (+)ssRNA: linear, positive sense, single-stranded RNA (Group IV), (–)ssRNA: linear, negative sense, single-stranded RNA (Group V); [2]total DNA-RCA: total DNA with rolling circle amplification, total RNA-RD: total RNA with rRNA depletion; [3]Taken from recent literature, ToNSV and TNSV were previously also used in literature; however, they are also used for other viruses. [4]The same name is used also for another virus from the genus Ilarvirus (family Bromoviridae).

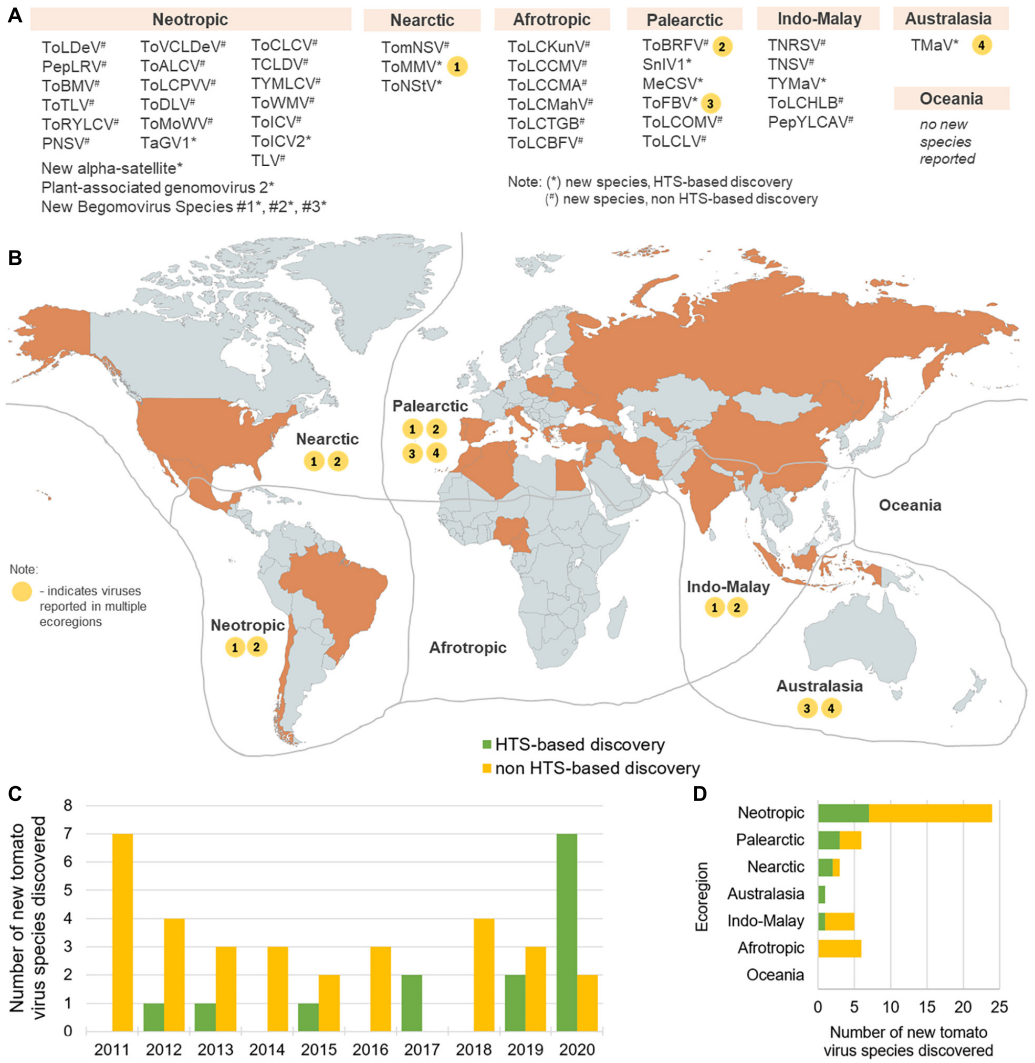

FIGURE 1 | Global distribution of virus species newly discovered in the 2011 to 2020 period. Abbreviated virus names (see **Table 1**) are shown in groups corresponding to the ecozones in which they were discovered (Antarctic is not shown, for simplicity, China and Indonesia are included in Indo-Malay, and Mexico is included in the Neotropic ecoregion) **(A)**. In the map **(B)**, ecoregions are delimited by gray lines and countries colored in orange are top producers of tomato in the 2008–2018 period, recording at least 8.14 million tons of total tomato produced (FAOSTAT, 2020). Viruses detected in more than one ecozone are shown on the map as number-coded yellow circles (1–4) corresponding to the virus species designated in the list in **(A)**. The numbers of annual new tomato virus discoveries in the 2011–2020 period are shown in **(C)** and the numbers of new tomato virus discoveries per ecoregion in this time period are shown in **(D)**. The map was created using www.mapchart.net under the CC BY-SA 4.0 license.

in China, a novel cytorhabdovirus, named tomato yellow mottle-associated virus (TYMaV), was discovered (Xu et al., 2017). In France, a novel ilarvirus was found in tomatoes and *Solanum nigrum*, named Solanum nigrum ilarvirus 1 (SnIV1) (Ma et al., 2020). Three begomoviruses, a gemycircularvirus, and a new alpha satellite were discovered by HTS in tomatoes in Brazil (de Nazaré Almeida dos Reis et al., 2020). A novel begomovirus named tomato-associated geminivirus 1 (TaGV1) was discovered using HTS in Brazil and was suggested as a member of a putative new genus closely related to *Capulavirus* (Fontenele et al., 2017). In Italy and Australia, a new blunervirus (*Kitaviridae*), named tomato fruit blotch virus (ToFBV), was discovered by HTS (Ciuffo et al., 2020). Tomato matilda virus (TMaV) (*Iflaviridae*), first detected in Australia using HTS (Saqib et al., 2015), was also detected in tomatoes grown in Italy, based on sequences deposited in GenBank (accession number MK517476) (**Table 1** and **Figure 1**). The infectivity of ToFBV and TMaV in tomato, other biological characteristics, and their impact on tomato yield are not yet known.

Aside from discovery of new viruses, HTS was also used to detect known viruses for the first time in tomato. In China, six known viruses, namely, potato virus A, tobacco vein banding mosaic virus (*Potyviridae*), potato virus H, potato virus S, potato virus M (*Betaflexiviridae*), and turnip yellows virus (*Luteoviridae*) were reported for the first time in tomato (Xu et al., 2017). In Germany, Physostegia chlorotic mottle virus (PhCMoV)

was detected for the first time in tomato using HTS (Gaafar et al., 2018), and in the United States, cherry rasp leaf virus was detected (Bratsch et al., 2020) in tomato. In a survey of tomato and pepper viruses in Vietnam, pepper chlorotic spot orthotospovirus (*Tospoviridae*) and Lindernia anagallis yellow vein virus (*Geminiviridae*) were associated with tomato for the first time (Choi et al., 2020). A known virus, discovered in henbane in 1932 in England, called henbane mosaic virus (HMV), but later on rarely detected, was found using HTS for the first time in tomatoes from Slovenia (Pecman et al., 2018). In the same study, HTS was also used to reconstruct complete genomic sequences of the isolate from tomato and historic isolates from virus collections, since only partial genomic sequence of the virus was available before.

Post-discovery Characterization of New Tomato Viruses

Even though HTS advanced our ability for generic detection and discovery of novel viruses, it can only provide us with genomic information of the virus. For a meaningful biological characterization, classical virology tools are still very much needed, which include plant bioassays (i.e., infectivity and transmission assays), electron microscopy, and targeted diagnostics. Virus characterization is a time- and resource-intensive task that often requires efforts from different institutions, sometimes at an international scale. A framework for biological characterization of viruses discovered by HTS was proposed to facilitate this part of the research pipeline (Massart et al., 2017). We used this framework to review how the 45 new viruses discovered in tomato, both through HTS and through other methods, were characterized. The same approach was recently employed for fruit tree infecting viruses (Hou et al., 2020), where fulfillment of 14 characterization categories were reviewed. We analyzed 53 publications on novel tomato viruses (41 reporting viruses for the first time and 12 follow-up studies) from the 2011–2020 period contributing to characterization of newly discovered viruses associated with tomato, reviewing the fulfillment of 14 characterization categories (**Figure 2A**; for details, see **Supplementary Table 1**).

Our review showed that, e.g., for majority (>60%) of the HTS-based new virus discoveries, whole genome sequence was determined, primers for detection of the virus with PCR were designed, local survey of prevalence was done, and co-infection with other viruses was checked (**Figure 2A**). Comparing HTS-based and non-HTS-based virus discoveries, there were fewer infectivity studies done on the original host and other natural or indicator hosts for HTS-based discoveries compared to that of non-HTS discoveries. Moreover, vector transmission was studied in very few cases and possibility of latent infections has not been studied for any of the newly discovered viruses. Practically, completeness of virus characterization greatly depended on the phytosanitary priority level of a virus. For tomato brown rugose fruit virus (ToBRFV), which is an emerging virus with significant economic importance, 13 of 14 characterization criteria were fulfilled in less than 4 years after the discovery, included in five publications after its first report. On the other hand,

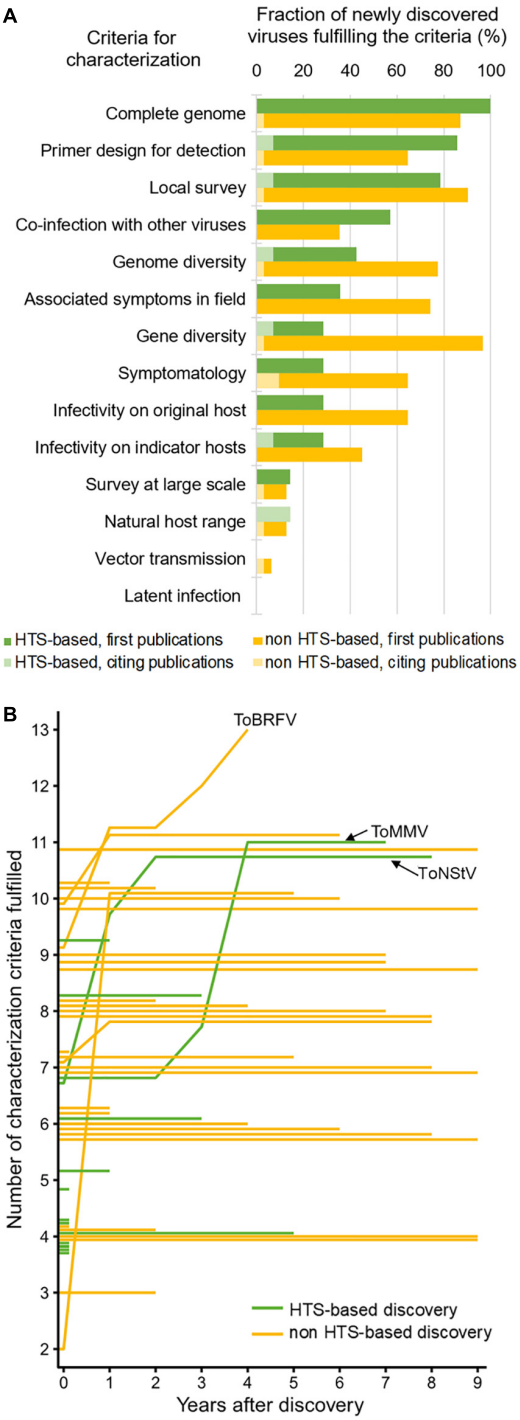

FIGURE 2 | Post-discovery characterization of new tomato-infecting viruses according to the literature review. Percentages of newly discovered virus species fulfilling each of the 14 characterization criteria are shown for viruses discovered by HTS or other methods **(A)**. Fulfillment of characterization criteria plotted through the years elapsed since the first report is shown as a line plot **(B)**, wherein each line represents a single virus and the evolution of its characterization; the lines corresponding to the emerging tomato brown rugose fruit virus (ToBRFV), and the first two tomato viruses discovered through HTS, tomato mottle mosaic virus (ToMMV) and tomato necrotic stunt virus (ToNStV), are labeled.

ToNStV and ToMMV, which were the first tomato-infecting viruses discovered using small RNA sequencing, were more extensively characterized after 7–8 years. Finally, many viruses were not followed up at all after the initial discovery and first publication (**Figure 2B**).

Looking Outside Tomato: Vectors, Weeds, Water, and Epidemiological Implications of HTS

Spatially, crop lands are always in conjunction with the wild or urban ecosystems bound by an agroecological interface, which is characterized by active biological interactions and exchange of materials, including pests and pathogens (Alexander et al., 2014). Nevertheless, it was just in the recent decade that plant virologists started to explore more intensively the diversity of viruses in wild ecosystems. Plant virus ecology and epidemiology include studies on viruses infecting weeds and other wild plants (Malmstrom and Alexander, 2016; Shates et al., 2019) as well as water as potential channel for plant virus spread (Mehle and Ravnikar, 2012). In this context, HTS is a well-suited tool, which allows generic investigation of viromes in a diverse set of sample matrices, from an array of different plant species to environmental samples, such as water and soil.

Weeds and other wild plants could act as reservoirs from which plant viruses can spill to crops, or vice versa (Malmstrom and Alexander, 2016). The association of tomato viruses with weeds also implies increased chances of survival for the viruses because weeds have high reproductive rates and are environmentally persistent (Cooper and Jones, 2006). These findings imply importance of weeds in plant-virus pathosystems and the importance of their inclusion in epidemiological studies. A recent review of viruses infecting plants from the *Solanaceae* family highlights the importance of studying the virome of both wild and cultivated plants to fully understand the plant virus impact on the agroecological scale (Hančinský et al., 2020). For tomato-infecting viruses, several studies were done to elucidate the role of wild plants as virus reservoirs, more specifically referred to in Section "Emerging and endemic viruses and viroids causing significant economic damages in tomato production in the past decade."

The first extensive tomato virome HTS-based study was done in major tomato-growing areas in China (Xu et al., 2017), resulting in a lot of new knowledge about occurrence of tomato viruses in the region and revealed several previously unknown associations of known plant viruses with tomato. It also suggested that some viruses originally associated with insect hosts (Wuhan insect virus 4, 5, and 6) (Li et al., 2015) might in fact be plant viruses, since they were found in tomato and they cluster with other plant viruses in phylogenetic analysis (Xu et al., 2017). This study did not look into virome of wild plants growing nearby. On the other hand, a recent large-scale virome study of tomato in France also included its wild relative, *S. nigrum* or European black nightshade (Ma et al., 2020). The study suggested the likely exchange of some viruses between tomato and *S. nigrum*; a newly discovered SnIV1 was found in both species, as well as potato virus Y (PVY), for which there was a strong evidence for a likely spillover from tomato to *S. nigrum*. On the other hand, a possible biological and ecological barrier was proposed for a spread of broad bean wilt virus (known to be able to infect both hosts) from *S. nigrum* to tomato, since high incidence and diversity of this virus was observed in *S. nigrum*; however, the virus was not detected in tomato in this study. Moreover, discovery of Euphorbia caput-medusae latent virus by HTS in South Africa in wild plant *Euphorbia caput-medusae*, which was shown to be infective in tomato and *Nicotiana benthamiana*, led to the establishment of a new genus, *Capulavirus*, in the family *Geminiviridae* (Bernardo et al., 2013).

Even prior to the application of HTS-based methods for detection of plant viruses, several studies detected plant viruses outside of the host, in environmental samples, such as water (Mehle and Ravnikar, 2012) and in soil (Fillhart et al., 1998). Several plant viruses are stable in the environment and can survive long periods of time outside the host (Mehle et al., 2018). Water can serve as virus transmission channel that have the potential to create new infection foci and to spread viruses in a wide range of host species and at long distances (Jones, 2018). HTS-based virome studies of different environmental waters all over the world reported the presence of plant virus nucleic acids in various types of samples. With the use of HTS, viruses in wastewater, irrigation water, and potable water can be monitored in extended areas over a regular period of time, which can provide a useful info for predicting or following disease outbreaks (Mehle et al., 2018). A recent virome study focusing on plant viruses in wastewater in Slovenia gave insights into diverse economically important plant viruses that might be circulating in the area. Wastewater treatment plant influents and effluents contained nucleic acids of at least 47 viruses, both previously known and also unknown to be present in the region. Tobamoviruses were highly represented in the samples, and for three of them, all of which can infect tomato [pepper mild mottle virus, tobacco mild green mosaic virus and tomato mosaic virus (ToMV)], the infectivity was confirmed (Bačnik et al., 2020). Alongside other detected plant viruses, nucleic acids of ToBRFV, which is currently one of the major threats in tomato production worldwide, were also detected in this study; however, ToBRFV was still not detected in the plants in the area. Moreover, pollinators, specifically honeybees (*Apis mellifera*), were studied as possible effective ecological "samplers" of plant viruses. HTS was employed in a recent study of honeybee-assisted surveillance in Australia to investigate the presence of plant viruses, and cucumber green mottle mosaic virus was detected on bees in several states of Australia before its subsequent detection in diseased plant material (Roberts et al., 2018).

High-throughput sequencing can also be used to rapidly obtain complete genome sequences of many viral isolates of the same species and thus follow the molecular epidemiology of viruses in real time. As such, HTS was used in a recent comprehensive study of whole genome sequences of ToBRFV from the Netherlands, which revealed the existence of three virus phylogenetic clusters in the country, which are hypothesized

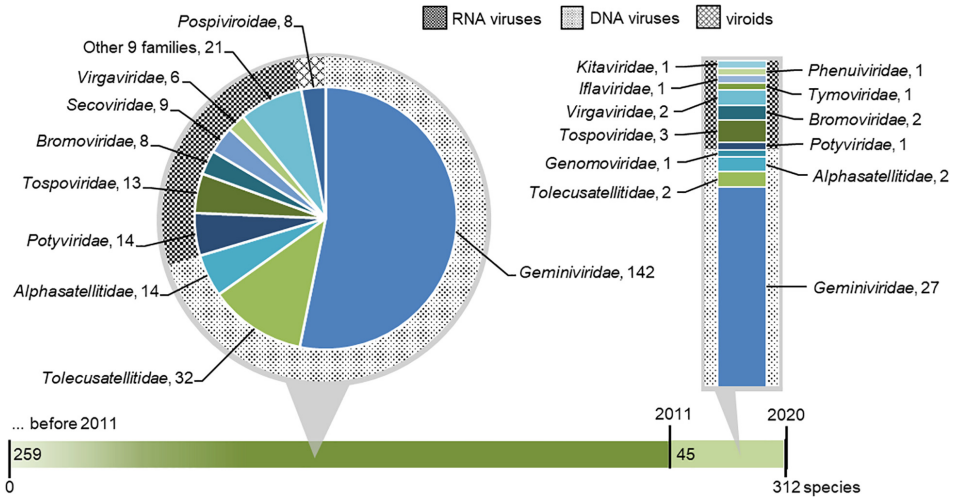

FIGURE 3 | Taxonomic distribution of virus and viroid species that were reported to infect or were associated with tomato. The green horizontal bar represents tomato viruses discovered before 2011 and within the 2011–2020 period. Known species reported before 2011 (including all known viruses that were first associated in tomato within the 2011–2020 period) are shown in the dark green portion on the left and extended in pie chart callout, where their distribution across viral families is shown. Species newly discovered in 2011–2020 are shown in the light green portion of the bar and extended in bar chart callout, where their distribution across viral families is shown. In both callouts, families of DNA viruses, RNA viruses, and viroids are designated with differently hatched backgrounds.

to represent three different introduction sources of the virus (van de Vossenberg et al., 2020).

EMERGING AND ENDEMIC VIRUSES AND VIROIDS CAUSING SIGNIFICANT ECONOMIC DAMAGES IN TOMATO PRODUCTION IN THE PAST DECADE

We collected a list of viruses and viroids with tomato indicated as host (**Supplementary Table 2**). A total of 312 species of tomato viruses (including satellite viruses) and viroids were verified. They are classified across 39 genera and 22 families (**Figure 3**). Among the species in the list, 220 species of tomato viruses (including satellite viruses) have DNA genomes and are classified in three families. Due to the high species count within a genus, the majority of viral species infecting tomato belongs to the *Begomovirus* genus (DNA viruses) and associated satellites. On the other hand, a greater richness of tomato viruses is found for RNA viruses, for which 84 known species are classified in 18 families. Finally, eight viroids, from a single family, are known to infect tomato (**Figure 3**).

Virus can be considered as emerging if it recently has changed or appeared to occupy and spread within a new niche (Rojas and Gilbertson, 2008). In general, emergence is connected to ecological change or intensive agricultural practices (Elena et al., 2014). Complex virus epidemiology, especially insect transmission (by, e.g., whiteflies, aphids, and thrips), and constant evolution of virus populations are key factors associated with emergence and outbreaks of viruses. Emerging pathogens and pests in crop plants are often accompanied by significant yield or economic losses (Savary et al., 2019). In addition, changes in global climate conditions, e.g., increasing temperatures, are predicted to generally exacerbate spread of plant virus diseases in many regions and can cause changes in the severity of the disease symptoms (Canto et al., 2009; Jones, 2016, 2021; Trebicki, 2020). As an example, tomato yellow leaf curl virus (TYLCV) invasion risk analysis under different climate scenarios predicted emergence of the virus and its primary vector, *B. tabaci*, in tomatoes cultivated in open fields worldwide (Ramos et al., 2019). Another study showed that, indeed, heat stress accompanied by the infection of TYLCV resulted in lower stress response efficiency in tomatoes and higher aggregation of TYLCV proteins and DNA (Anfoka et al., 2016). Higher day–night temperature regimes were also shown to favor virion accumulation of tomato spotted wilt orthotospovirus (TSWV) in solanaceous weeds (Llamas-Llamas et al., 1998), and pepper plants that are heterozygous for the *Tsw* resistance gene showed susceptibility at higher temperatures (Moury et al., 1998). Pepper plants with tobamovirus resistance genes were also shown to be susceptible to ToBRFV, when grown in infected soil at 32°C (Luria et al., 2017).

Over the past decades, significant damages to tomato production were caused by viruses described as emerging or re-emerging, such as a few criniviruses, pepino mosaic virus (PepMV), tomato torrado virus (ToTV), tomato leaf curl New Delhi virus (ToLCNDV), and ToBRFV (Hanssen et al., 2010b; Navas-Castillo et al., 2011; Gómez et al., 2012; Moodley et al., 2019, 2020; Oladokun et al., 2019). On the other hand, significant yield losses in tomato could also be associated with widespread, endemic viruses, such as PVY or cucumber mosaic virus (CMV) (Quenouille et al., 2013; Tepfer and García-Arenal, 2019). In the following sections, we review the available information about an array of important emergent or endemic viruses and viroids

in tomato, as well as some recently discovered viruses with yet unclear role in tomato health.

Begomoviruses and Their Satellite Viruses

Begomovirus (*Geminiviridae*) is the biggest and one of the most studied genera of plant viruses, comprising 162 known species infecting tomato. Seven viral species belonging to other genera from the family *Geminiviridae* are also known to infect tomato (**Figure 3**). Virions of viruses belonging to *Geminiviridae* are typically twinned ("geminate"). Begomoviruses have monopartite or bipartite genomes (Zerbini et al., 2017). The most important way of the transmission of begomoviruses is by the whiteflies *Bemisia tabaci,* a cryptic species complex, which can infest many crops and is now globally widespread (Stansly et al., 2010; Fiallo-Olivé et al., 2020).

Among the tomato-infecting begomoviruses, ToLCNDV and TYLCV are the most widespread and economically important (Zaidi et al., 2017; Prasad et al., 2020). ToLCNDV is a re-emerging bipartite begomovirus known to infect around 47 different plant species, predominantly crops and weeds from *Solanaceae* and *Cucurbitaceae* (Moriones et al., 2017) families. ToLCNDV, distinct species with two strains (ToLCNDV and ToLCNDV-ES), was first described in India (Padidam et al., 1995) and it is mainly present in Asia where many host plants and various isolates were described (Zaidi et al., 2017). In the Mediterranean basin, the ToLCNDV-ES recombinant strain was identified in tomatoes showing stunting, yellowing, and/or curling in apical leaves (Fortes et al., 2016). ToLCNDV was then reported to spread in Africa and in European countries (e.g., Spain, Italy, Greece, Portugal) (EPPO GD, 2020). Furthermore, the monopartite TYLCV has several widespread strains that are altogether considered as most devastating for tomato production in the tropical and subtropical tomato-growing regions (Mabvakure et al., 2016). Severe yield losses of up to 100% were frequently recorded in tomato yellow leaf curl virus-infected susceptible cultivars showing typical symptoms, such as stunting, upward curling of leaves, chlorosis, and reduction in leaf size (Prasad et al., 2020). For instance, losses due to TYLCV outbreaks in the Dominican Republic were estimated at over 10 million US dollars (Gilbertson et al., 2007), and in China, the virus was reported to be widely spreading and causing unprecedented losses (Pan et al., 2012). Several resistance genes (e.g., *Ty-1, Ty-2, Ty-3*) identified from wild tomato relatives are used to breed for tolerant varieties against ToLCNDV, TYLCV, and other begomoviruses and multi-gene resistance is currently considered to increase the level of resistance and prevent its breakdown (Zaidi et al., 2017; Prasad et al., 2020).

Circular ssDNA satellite viruses (i.e., alphasatellites, betasatellites, and deltasatellites) are often associated with begomoviruses (Rao and Kalantidis, 2015). They can influence helper virus (i.e., begomovirus) multiplication and disease severity (Gnanasekaran and Chakraborty, 2018). Their replication, cell-to-cell movement and vector transmission are dependent on helper virus, except for independently replicating alphasatellites (Gnanasekaran and Chakraborty, 2018). Several betasatellites were connected with enhancement of symptom severity of TYLCV, e.g., cotton leaf curl Gezira betasatellite, tobacco leaf curl Japan betasatellite, honey-suckle yellow vein mosaic betasatellite (Ito et al., 2009), and tomato leaf curl Philippines betasatellite (Sharma et al., 2011). Co-inoculation experiments of several betasatellites with ToLCNDV resulted in enhancement of symptom severity (Jyothsna et al., 2013), while, in one experiment, co-inoculation of an alphasatellite, betasetellite, and TYLCV resulted in reduction of the accumulation of betasatellite and symptoms induced by TYLCV (Idris et al., 2011) in *N. benthamiana*.

In the last 10 years, several novel begomovirus species were described in different parts of the world (**Table 1** and **Figure 1**). From the Afrotropic ecoregion, tomato leaf curl Kunene virus (Lett et al., 2020), tomato leaf curl Mahé virus (Scussel et al., 2018), and tomato leaf curl Burkina Faso virus (Ouattara et al., 2017) were recently discovered. Numerous begomoviruses were discovered in Neotropic countries, which include four novel species: tomato leaf deformation virus (ToLDeV; Márquez-Martín et al., 2011), tomato apical leaf curl virus (Vaghi Medina et al., 2018), tomato twisted leaf virus (Romay et al., 2019), and pepper leafroll virus (PepLRV; Melgarejo et al., 2013; Martínez-Ayala et al., 2014). Initial surveys suggest that ToLDeV and PepLRV are the predominant pathogens causing the tomato leaf curl disease complex in the Ecuadorian and Peruvian regions (Melgarejo et al., 2013). In Brazil, tomato severe rugose fruit virus (ToSRV) and tomato mottle leaf curl virus (ToMoLCV) were found to be prevalent in tomato crops (Souza et al., 2020).

Reports were made on the potential of wild plants to act as hosts for important tomato-infecting begomoviruses (Prajapat et al., 2014). In Cyprus, a large-scale survey of more than a hundred weed species in major tomato-growing areas revealed the presence of TYLCV in 49 species (in 15 families), suggesting inclusion of these possible reservoir hosts in control measures (Papayiannis et al., 2011). A recent study focused on ToLCNDV found the virus in 5 out of 24 investigated wild plant species in Spain. In that study, HTS was used to characterize the genomes of 80 isolates from different plant species and analyze within-plant virus population diversities for some of them, hinting at some differences between the isolates from wild and cultivated (cucurbit) plants. Tomato chlorotic mottle virus (TCMV) was also found in several weed species in Brazil (Ambrozevicius et al., 2002). In Spain, *S. nigrum* was shown to harbor four known begomoviruses associated with tomato yellow leaf curl disease. Through infectivity assays, tomato severe rugose virus was shown to be infective and harbored in common weeds, such as *Nicandra physaloides*, *Datura stramonium*, and *Sida* sp., which are found surrounding the tomato-growing areas in Brazil (Barreto et al., 2013; Gorayeb et al., 2020).

Tobamoviruses

Tobamoviruses (*Virgaviridae*) are among the most environmentally stable viruses that remain viable for a long time outside of their host plant in various environmental media (e.g., water, soil) (Fillhart et al., 1998; Mehle and Ravnikar, 2012).

A positive-sense single-stranded RNA [(+)ssRNA] genome of tobamoviruses is around 6.5 kb long and coated in rigid rod virion (Adams et al., 2009b). They are efficiently transmitted mechanically (e.g., by wounding and contact) and can be spread also passively through water and soil, and vertically through seeds (Dombrovsky and Smith, 2017; Mehle et al., 2018). Six tobamoviruses are known to infect tomato, and two of them are known to be globally widespread for many years, namely, tobacco mosaic virus (TMV) and ToMV. Since the discovery and deployment of three resistance genes, *Tm-1*, *Tm-2,* and *Tm-2*^{2}, the economic damages caused by these two viruses reduced dramatically (Pfitzner, 2006).

The most recent virus outbreaks with significant losses in tomato production worldwide were connected to the emergence of two new tobamovirus species, ToMMV (Li et al., 2013, 2017; Sui et al., 2016) and ToBRFV (Salem et al., 2016; Luria et al., 2017). Many research efforts are directed in studies of these viruses, particularly ToBRFV, and significant efforts are directed to limit their spread with appropriate quarantine and phytosanitary measurements (EPPO, 2020a,b).

ToBRFV was first detected in field-cultivated tomatoes showing typical mosaic symptoms as well as narrowing of leaves (Luria et al., 2017) and strong brown rugose spots on fruits (Salem et al., 2016). ToBRFV was found in tomatoes in Jordan in 2015 (Salem et al., 2016) and in 2014 in tomatoes from Israel, where ToBRFV was also shown to break the *Tm-2*^{2} resistance in some tomato cultivars (Luria et al., 2017). ToBRFV likely emerged as a recombinant between TMV and ToMMV (Salem et al., 2016). It can infect up to 100% of plants at a location and amounts to around 70% tomato yield losses due to symptoms expressed in the fruits (EPPO, 2020a). After its first detection in Israel and in Jordan, it has rapidly spread into many other countries (**Figure 1**). It was recently reported in the United States (Ling et al., 2019), Mexico (Camacho-Beltrán et al., 2019), China (Yan et al., 2019), Palestine (Alkowni et al., 2019), Turkey (Fidan et al., 2019), Germany (Menzel et al., 2019), Netherlands (van de Vossenberg et al., 2020), France (Verdin et al., 2020), Greece (Beris et al., 2020), Italy (Panno et al., 2019), the United Kingdom (Skelton et al., 2019), Egypt (Amer and Mahmoud, 2020), and Spain (Alfaro-Fernández et al., 2021). ToBRFV can be easily transmitted through mechanical contact or can be transmitted by bumblebees (Levitzky et al., 2019), similar to what was reported for TMV (Okada et al., 2000). ToBRFV can overcome known resistance genes against tobamoviruses and there are currently no commercially available ToBRFV-resistant tomato varieties; thus, it remains an imminent threat to tomato production worldwide (EPPO, 2020a). Currently, the only possible control measures are the ones directed at eradication and containment of the infections, such as restriction of access to the production site, disposal of infested plant material, and sanitation measures (EPPO, 2020a). Moreover, a recent research reported that co-infection of ToBRFV with mild strain PepMV resulted in enhanced PepMV accumulation and symptoms characteristic for an aggressive PepMV strain (Klap et al., 2020), bringing additional concerns about the impact of ToBRFV on tomato production.

ToMMV was first isolated from infected greenhouse-grown tomatoes showing mosaic and leaf distortion in Mexico in 2013 (Li et al., 2013). Later on, ToMMV was reported to occur across three ecoregions, specifically in the United States (Padmanabhan et al., 2015a), Israel (Turina et al., 2016a), Spain (Ambrós et al., 2017), China (Che et al., 2018), Brazil (Nagai et al., 2019), Iran, and Czech Republic (EPPO GD, 2020). Interception of ToMMV introduction in Australia through infected pepper seeds was made in biosecurity checks (Lovelock et al., 2020), highlighting the importance of preventive measures in preventing virus spread. ToMMV was shown to successfully infect a small portion of ToMV-resistant plants (Sui et al., 2016) but did not successfully infect some cultivars with *Tm-2*^{2} gene, (Nagai et al., 2019). Further assessment is needed to ascertain yield loss and economic impact of ToMMV.

Through mechanical inoculation, ToBFRV was shown to be able to infect various hosts, aside from crops from genus *Solanum*, also *Chenopodium* spp., *Petunia hybrida*, and wild relative of tomato, *S. nigrum* (Luria et al., 2017; Alkowni et al., 2019; Yan et al., 2019). ToMMV was experimentally shown to infect various species from family Solanaceae (Ambrós et al., 2017), causing systemic necrosis and death in *Datura stramonium* (Sui et al., 2016). No further studies were conducted yet on the possibility of these alternative hosts to act as natural reservoir of these viruses.

Orthotospoviruses

The genus *Orthotospovirus* (*Tospoviridae*) is currently composed of 26 species and is the only plant-infecting genus in the order *Bunyavirales* (Oliver and Whitfield, 2016; ICTV, 2020). Orthotospoviruses have a single-stranded negative-sense RNA [(−)ssRNA] genome, divided into three segments, and are capable of replication both in the plant host and in thrips (Riley et al., 2011). Economically, the most important orthotospovirus infecting tomato is the re-emerging TSWV. In the case of TSWV outbreaks, up to 95% losses in total market value can be recorded due to tomato fruits showing typical necrotic spots and concentric rings (Sherwood et al., 2003; Sevik and Arli-Sokmen, 2012).

TSWV has one of the widest host ranges of all plant viruses with more than 1000 known host species from 85 families (Parrella et al., 2003). In large-scale surveys of weeds in United States, several were proven to harbor TSWV, and, among them, *Sonchus asper*, *Taraxacum officinale*, *Ranunculus sardous*, *Aster* sp., *Senecio vulgaris*, and *S. nigrum* were shown to have the highest potential to be an inoculum source of TSWV (Chatzivassiliou et al., 2001; Groves et al., 2002). Four weed species surrounding tomato-growing areas in Kenya were also shown to be hosts of TSWV (Macharia et al., 2016). TSWV was found in all known ecozones of the world, affecting numerous crops (Butković et al., 2021). Orthotospoviruses are transmitted in a persistent propagative and circulative manner by thrips, the most important of which is western flower thrips (*Frankliniella occidentalis*). This insect vector remains a global problem due to inefficient insecticidal control (Riley et al., 2011), thus contributing to continuous emergence of orthotospoviruses worldwide (Oliver and Whitfield, 2016).

Several resistance genes have been identified and employed to confer resistance against TSWV in tomato, *Sw-5b* offering the most durable and broad resistance to different orthotospovirus species (Turina et al., 2016b).

Tomato spotted wilt orthotospovirus resistance-breaking (RB) strains were first discovered in the early 2000s, and since then, they are occurring sporadically in many regions causing significant damages. These strains overcome TSWV resistance regulated by hypersensitivity genes: *Tsw* (in pepper) and *Sw-5* (in tomato). This further worsened the economic losses caused by TSWV in tomato and pepper, which were previously estimated at more than 1 billion US dollars annually (Prins and Goldbach, 1998). Currently, there is no new resistance gene discovered against TSWV (Turina et al., 2016b).

Among other orthotospoviruses, important viruses reported in tomato in the past decade are tomato chlorotic spot virus (TCSV), groundnut ringspot virus (GRSV), capsicum chlorosis virus (CaCV), and tomato yellow ring virus (TYRV) (**Table 1** and **Figure 1**). TCSV was reported to be actively spreading in the Nearctic countries such as United States (Sui et al., 2017; Poudel et al., 2019), Puerto Rico (Webster et al., 2013) and GRSV was reported in tomatoes and other vegetables in the United States (Webster et al., 2010, 2014). CaCV is expanding its distribution in Indo-Malay and Australasian ecoregions as it was detected in Taiwan (Huang et al., 2010), China (Yin et al., 2015), and Australia (Sharman et al., 2020). TYRV was reported in Kenya (Birithia et al., 2012) and Poland (Zarzyńska-Nowak et al., 2016). Other novel orthotospoviruses recently identified are tomato necrotic ring virus (TNRV) from Thailand (Hassani-Mehraban et al., 2011), pepper necrotic spot virus (PNSV) from Peru (Torres et al., 2012), and tomato necrotic spot virus (TNSV; as a word of caution, an ilarvirus was named identically, but has another acronym: ToNSV) from China (Yin et al., 2014). These viruses were not yet associated with significant or large-scale outbreaks.

Potyviruses

Potyvirus (*Potyviridae*) is one of the largest genera of plant-infecting viruses, with 183 recognized species (ICTV, 2020), 15 of which are known to infect tomato (**Figure 3**). Potyviruses are characterized by a (+)ssRNA genome (∼9.7 kb), which is coated in a flexible filamentous virion. PVY is an economically important potyvirus infecting solanaceous crops. It is efficiently transmitted by *Myzus persicae* and other aphid species (Revers and García, 2015; Gadhave et al., 2020). PVY is widespread in several tomato-growing regions worldwide, based on recent large-scale studies (Soler et al., 2010; Al-Kuwaiti et al., 2016; Xu et al., 2017; Nikolić et al., 2018; Ignatov et al., 2020; Ma et al., 2020). Recently, PVY strain C was detected in tomatoes showing leaf necrosis in Kenya (Chikh-Ali et al., 2015). Symptoms of PVY infection in tomato ranges from faint mottling to necrosis but varies depending on plant age, environmental conditions, PVY strain, and co-infecting viruses (Sastry et al., 2019). Aside from tomato, PVY was shown to infect weed species from *Asteraceae, Chenopodiaceae, Geraniaceae,* and *Lamiaceae* families (Kaliciak and Syller, 2009).

In recent years, three other potyviruses infecting tomato were reported, namely, chili veinal mottle virus (ChiVMV), pepper mottle virus (PepMoV), and pepper veinal mottle virus (PVMV). PepMoV infection in tomatoes in Hawaii resulted in unmarketable fruits with mottling symptoms (Melzer et al., 2012) and, recently, the virus was detected in India (Sharma et al., 2019). ChiVMV was detected in several provinces in southwest China, with recorded incidence of up to 90% in some areas (Zhao et al., 2014; Zhu et al., 2017). PVMV was reported to cause considerable epidemics in tomato-growing areas in Mali in 2010 and is now under consideration in tomato disease resistance breeding programs (Tsai et al., 2010). HMV was recently reported to naturally infect field tomatoes in Slovenia (Pecman et al., 2018).

Cucumoviruses and Other Members of Family *Bromoviridae*

Cucumber mosaic virus (genus *Cucumovirus*, family *Bromoviridae*) is an important tomato-infecting virus. Cucumoviruses have a spherical virion encapsidating a tripartite (+)ssRNA genome. Some CMV strains encapsidate subviral RNAs termed satellite RNAs (satRNAs) (Masuta, 2014). In nature, CMV and other cucumoviruses are non-persistently transmitted by aphid species, the most important of which are *Myzus persicae* and *Aphis gossypii*. They were also shown to be transmitted through seeds of some species, but not tomato (Palukaitis and García-Arenal, 2003). CMV has a very broad host range, able to infect more than 1200 plant species across 100 botanical families (Mochizuki and Ohki, 2012). Several weed species surrounding tomato production areas were shown to harbor CMV and could serve as reservoir or alternative host of the virus. Such weeds include, e.g., *Convolvulus arvensis*, *Malva sylvestris*, and *Sonchus tenerrimus*, reported from Spain (Lavina et al., 1996), and other nine diverse weeds from Pakistan (Akhtar et al., 2019). Due to its very broad host range, transmissibility through seeds of some species, and ubiquitous presence of its aphid vectors (Jacquemond, 2012), CMV became a globally distributed species that still causes significant damages in many crops, especially in tomato.

Outbreaks of CMV infection in tomato-growing areas were reported, and some of these were associated with satellite RNAs (satRNAs) that induce systemic necrotic symptoms, referred to as lethal necrosis (Garcìa-Arenal and Palukaitis, 1999; Xu et al., 2003). This disease was reported in Italy between 1988 and 1993 (Cillo et al., 1994; Grieco et al., 1997) and in Croatia in 1993 (Škoric et al., 1996). Recently, CMV-satRNA infection was reported in legume crops in Greece (Chatzivassiliou et al., 2016), and was shown to cause lethal necrosis in tomato through mechanical inoculation (Giakountis et al., 2018). Also, during a 4-year survey in Serbia (2012–2015), CMV satRNAs were identified from collected tomato samples showing systemic necrosis accompanied by fruit malformation (Stanković et al., 2021). Cultivated crops are important reservoir of CMV satRNAs (Gallitelli, 2000), and thus, strategic intercropping should be taken into consideration to prevent devastating CMV lethal necrosis outbreaks in tomato.

Tomato aspermy virus (TAV) is another cucumovirus that naturally infects tomato. TAV was recently reported in tomato samples from China; however, its economic impact was not

recorded (Xu et al., 2017). TAV was reported as a major pathogen of ornamentals such as chrysanthemums that are grown in subtropical Asia (Verma et al., 2009; Maddahian et al., 2017).

Tomato necrotic spot virus (ToNSV) and the novel species named tomato necrotic streak virus (TomNSV) are tomato-infecting ilarviruses within *Bromoviridae* family. Detections of these viruses were reported in the United States (Batuman et al., 2009; Adkins et al., 2015; Badillo-Vargas et al., 2016; Bratsch et al., 2018, 2019). Both viruses caused necrotic symptoms in leaves, stem or fruits of tomatoes. In France, a novel ilarvirus, named SnIV1, was discovered in both tomato and its wild relative, *S. nigrum* (Ma et al., 2020). However, the transmission routes, possible reservoir or alternative hosts, and economic impact are yet to be determined for ToNSV, TomNSV, and SnIV1 (Badillo-Vargas et al., 2016; Bratsch et al., 2019; Ma et al., 2020). Moreover, a re-emerging ilarvirus named parietaria mottle virus (PMoV) was suggested to be a threat to tomatoes, which showed rings and bright necrotic mosaic on young leaves upon infection. It was reported in Europe, particularly in the Mediterranean countries such as Italy, France, Greece, and Spain (Aparicio et al., 2018). Outbreaks of PMoV were recently reported in Sardinia, Italy (Parrella et al., 2020) and research on possible sources of resistance against the virus already started (Parrella, 2020). Lastly, two other members of *Bromoviridae* known to infect tomato and a variety of other crops are alfalfa mosaic virus (*Alfamovirus*), causing necrotic yellows disease on tomato (Finetti Sialer et al., 1997; Nikolić et al., 2018) and pelargonium zonate spot virus causing mild mosaic, leaf malformation, and severe stunting of the plants (Finetti-Sialer and Gallitelli, 2003; Lapidot et al., 2010).

Potexvirus: Pepino Mosaic Virus (PepMV)

PepMV belongs to genus *Potexvirus* (*Alphaflexiviridae*) and has an unsegmented (+)ssRNA genome coated in a flexuous rod virion. PepMV was first described in Peru, and since its first detection in tomato in Netherlands in 1999, it quickly spread in Europe (van der Vlugt et al., 2000; Hanssen and Thomma, 2010). It is efficiently transmitted mechanically (e.g., contaminated tools and whitefly feeding) (Hanssen and Thomma, 2010; Noël et al., 2014) with occasional transmission through seeds (Hanssen et al., 2010c), as well as through water (Mehle et al., 2014). PepMV was originally discovered to infect pepino (*Solanum muricatum*) (Jones et al., 1980), and it quickly became endemic in tomato since its first discovery in this plant in 1999 (van der Vlugt et al., 2000; van der Vlugt and Stijger, 2021). In tomato, fruit marbling symptoms are considered as the most important cause of significant economic losses around the world (Hanssen and Thomma, 2010; Hanssen et al., 2010b). PepMV is present in major tomato-growing areas of the Mediterranean (Gómez et al., 2012) and was recently reported in United States and Mexico (Ling and Zhang, 2011), South Africa (Carmichael et al., 2011), Spain and Morocco (Gómez-Aix et al., 2019), and Serbia (Stanković et al., 2020).

To date, there are five strains identified for PepMV, namely, (1) the Peruvian (LP) strain, originally found infecting pepino (*S. muricatum*) and wild *Solanum* spp.; (2) the European EU-tomato (EU) strain; (3) the American US1 strain; (4) the Chilean-2 (CH2) strain; and (5) the PES strain, described in wild tomato populations in Peru (Moreno-Perez et al., 2014). PepMV was reported to infect a wide range of crops and weed species (Gómez et al., 2012); its infectivity and symptom expression are also dependent on the virus strain and host species or cultivar (Kazinczi et al., 2005; Hanssen et al., 2009; Blystad et al., 2015).

Due to the extensive damages caused by PepMV infections, and since there are currently no commercially available PepMV-resistant tomato varieties available, efforts have been made to produce efficient cross-protection strategies against the virus, particularly for the strains circulating in Europe (Pechinger et al., 2019). Other than host resistance, cross-protection is one of the most effective methods of virus disease management, which entails "pre-immunization" of susceptible genotypes by inoculation of mild strain of a particular virus (Ziebell and Carr, 2010). Successful applications of PepMV mild strain cross-protection were reported in the laboratory or greenhouse in the past years (Hanssen et al., 2010a; Schenk et al., 2010; Vermunt and Kaarsemaker, 2017). Recently, successful protection of field tomatoes against PepMV were reported using two mild strains of the virus (Agüero et al., 2018).

Criniviruses

Criniviruses from genus *Crinivirus* (*Closteroviridae*) are whitefly transmitted viruses with bipartite genome composed of two (+)ssRNA genome segments that are separately coated in filamentous virions (Kiss et al., 2013). Their infection in plants can be mistaken for nutritional disorders and phytotoxicity because of the obvious interveinal leaf yellowing and leaf brittleness, resulting in reduced overall yield (Tzanetakis et al., 2013). Two widespread tomato-infecting criniviruses are tomato infectious chlorosis virus (TICV) and tomato chlorosis virus (ToCV). TICV was first described in 1996 in the United States (Duffus et al., 1996), and recently reported to cause yield losses in Mexico (Méndez-Lozano et al., 2012), Greece (Orfanidou et al., 2014), and Serbia (Vučurović et al., 2019). ToCV was first described in 1998 (Wisler et al., 1998) and is now present globally causing yield losses due to fruit size reduction (Fiallo-Olivé and Navas-Castillo, 2019). ToCV was shown to infect 25 species of crops and weeds (Fariña et al., 2019), while TICV was shown to be infective in 22 species of weeds that may serve as reservoir of the virus (Alfaro-Fernández et al., 2008). Lastly, another crinivirus that was first reported to infect tomato in China is lettuce chlorosis virus; however, its economic impact has not yet been assessed (Zhang et al., 2017).

Rhabdoviruses

Rhabdoviruses (*Rhabdoviridae*) can propagate inside either a leafhopper, an aphid, or mite vector or a plant. Rhabdoviruses are composed of large bacilliform virions encapsulating an (−)ssRNA genome of around 13–15 kbp. There are currently three known species of rhabdoviruses that infect or are associated with tomato: the newly discovered TYMaV in genus *Cytorhabdovirus* (Xu et al., 2017) and, in genus *Alphanucleorhabdovirus*, the eggplant mottled dwarf virus (Mavrič et al., 2006) and the recently discovered PhCMoV. PhCMoV was first detected in *Physostegia* sp. sampled in 2014 in Austria (Menzel et al., 2018) and was recently detected

in Germany from two tomato samples 12 years apart (2003 and 2015) that showed typical fruit marbling and discoloration symptoms (Gaafar et al., 2018). Within this period, PhCMoV was also detected in tomato samples showing leaf and fruit mottling and uneven ripening of fruits collected in 2012 at three locations in Serbia (Vučurović et al., 2021), indicating extended presence of the virus in the country. Findings of PhCMoV in three different countries in two different plant species in recent years could indicate the emerging status, and the presence of this virus needs to be assessed in the future, to determine its potential impact on tomato production.

Secoviridae: Nepoviruses and Torradoviruses

Family *Secoviridae* contains insect or nematode transmitted viruses, nine of which are known to infect tomato. These viruses have mono- or bipartite 9- to 13.7-kbp-long (+)ssRNA genomes encapsidated in an icosahedral virion (Thompson et al., 2017). Several viruses of this group were reported in recent years, namely, tomato black ring virus (TBRV) from genus *Nepovirus* and ToTV and tomato marchitez virus (ToMarV), both from genus *Torradovirus*. TBRV was recently reported infecting tomatoes in Poland showing chlorotic and/or necrotic ringspots and was found to be associated with eight satellite RNAs, but no assessment about economic losses were made (Rymelska et al., 2013; Zarzyńska-Nowak et al., 2020). Moreover, ToTV is reported to spread globally since its discovery in 2007 in tomatoes from Spain showing systemic necrosis or burnt-like symptoms (Verbeek et al., 2007). ToTV was recently reported to be present in South Africa (Moodley et al., 2016, 2020) and Colombia (Verbeek and Dullemans, 2012), which are first reports of the virus in the Afrotropic and Neotropic ecoregions. ToTV was also reported in tomato-growing areas in the Mediterranean basin (e.g., Spain and Italy), in Poland, Hungary, and Australia (Hanssen et al., 2010a; Hanssen and Lapidot, 2012) and recently in Serbia (Vučurović et al., 2021). On the contrary, since the discovery of ToMarV in tomatoes from Mexico showing severe leaf necrosis and necrotic rings on fruits in 2007 (Verbeek et al., 2008), natural infection of ToMarV was only reported in pepper in Mexico (Camacho-Beltrán et al., 2015).

Other Known Viruses Associated With Tomato

Several other tomato viruses were recently reported worldwide. Necrotic foliar symptoms in greenhouse grown tomatoes in Poland were associated with an alphanecrovirus (*Tombusviridae*) named olive latent virus 1 (OLV1); however, its economic impact has not been assessed (Borodynko et al., 2010). Aside from its original host, olive, OLV1 was also reported to infect citrus and tulip (Varanda et al., 2014).

In 2015, TMaV, classified in the family *Iflaviridae*, which is currently known to contain members that infect arthropod hosts (Valles et al., 2017), was reported to be associated with tomato (Saqib et al., 2015). The virus was discovered in a single asymptomatic tomato sample in which no presence of a probable arthropod pest was observed under the microscope and in BLAST search of the assembled contigs from small RNA sequencing. Among the artificially inoculated plants, TMaV was detected in non-inoculated leaves, reported to cause symptomless infection in *S. lycopersicum* and *S. melongena*, but showed mild symptomatic infection in *Capsicum annum* (Saqib et al., 2015). Further research is needed to ascertain the role of TMaV in tomato and also to investigate its possible replication in arthropod hosts.

In Brazil, tomato blistering mosaic virus (ToBMV) (*Tymoviridae*) was discovered in field tomatoes that exhibited severe leaf mosaic and blistering symptoms (De Oliveira et al., 2013). Later, analyses confirmed the presence of ToBMV in the tobacco sample from 1986 (Melo et al., 2014). ToBMV was also reported in tomatoes from Argentina (Ferrand et al., 2016) and in a weed relative of tomato, *Solanum violaefolium* (Blawid et al., 2016). These studies may imply possible emergent status of ToBMV in the Neotropics and further investigations are therefore needed.

Southern tomato virus (STV) (family *Amalgaviridae*, genus *Amalgavirus*), a double-stranded (ds) RNA virus, was first detected in tomato plants in United States and Mexico exhibiting stunting of the growing tips, fruit discoloration, and reduced fruit size (Sabanadzovic et al., 2009). Since then, it was also reported in several European countries (Iacono et al., 2015; Verbeek et al., 2015; Pecman et al., 2018; Gaafar et al., 2019; HortDaily, 2019; WUR, 2019), Bangladesh (Padmanabhan et al., 2015c), China (Padmanabhan et al., 2015b), and South Korea (Oh et al., 2018), and so far only in tomato plants. STV co-infections with other viruses are frequent, as well as detections of STV in asymptomatic tomatoes (Alcalá-Briseño et al., 2017). STV virions were not yet observed (Tzanetakis et al., 2020), and the epidemiology of STV remains unclear, as it is only known to be vertically transmitted through seeds at high rates (70–90%) (Sabanadzovic et al., 2009). A recent study showed that STV infection alone did not induce symptoms and cellular ultrastructure changes; however, it modified expression of certain microRNAs (Elvira-González et al., 2020).

Pospiviroids

Viroids are naked, non-coding, circular (+)ssRNA molecules, around 246–401 bp long, and are the smallest entities known to infect any living organisms. They are known to infect only plants (Kovalskaya and Hammond, 2014). They can induce disease symptoms, resulting in significant economic damages in different crops and ornamentals (Navarro et al., 2012). Viroid infection in tomatoes results in growth reduction or stunting accompanied by leaf distortion or epinasty, although symptoms vary greatly among viroid strains and tomato cultivars (Mackie et al., 2019). Aside from tomato and other crops and ornamentals (van Brunschot et al., 2014a), pospiviroids were also found to be harbored in several weed species, which were reported as their natural reservoir (Van Bogaert et al., 2015; Mackie et al., 2016). Majority of viroids are transmitted mechanically through infected tools and seldom through seeds or pollen; however, the most efficient transmission of viroids is through vegetative propagation of infected material (Flores et al., 2005). Viroids were reported to cause significant losses in tomato

production in a few countries over the last decade. Out of the nine recognized pospiviroids (*Pospiviroidae*), eight are known to infect tomato. Among these viroids, potato spindle tuber viroid (PSTVd) and tomato chlorotic dwarf viroid (TCDVd) are the most prevalent and economically important (Verhoeven et al., 2010; van Brunschot et al., 2014b). Several introductions of viroids were reported recently, such as in Italy and Norway, where phytosanitary authorities were able to eradicate PSTVd and TCDVd upon the detection in established tomato crops (Navarro et al., 2009; Fox et al., 2013). In order to prevent introduction of viroids, all imported lots of tomato and pepper seeds are tested in Australia (Constable et al., 2019). Since testing of seeds is needed to prevent the introduction of pospiviroids into new areas, many efforts have already been done to optimize diagnostic protocols that enable their detection at low concentration, which is expected in case of seed infestation (Mehle et al., 2017).

CONCLUSION AND FUTURE PROSPECTS

New discoveries and studies on emergence of tomato viruses in the recent decade contributed to our understanding of the tomato virome, its diversity, virus ecology, and epidemiology. Tomato is likely associated with the highest number of viruses and viroids known for any plant species to date, currently amounting to at least 312 known species. Because of the absence of resistant varieties for some viruses, global spread of insect vectors, emergence of RB viral strains, increased global movement of plant materials, such as seeds, and high stability and environmental persistence of some viruses, viral diseases in tomato cause massive yield and economic losses. Begomoviruses and associated satellite viruses represent the most numerous group of tomato viruses. ToLCNDV and TYLCV are two of the most important begomoviruses, with ToLCNDV currently prevailing as an emergent and damaging species worldwide (Zaidi et al., 2017; Prasad et al., 2020). On the other hand, a diverse array of RNA viruses cause high economic losses in tomato globally. The most striking example is the recent emergence of ToBRFV that quickly caused outbreaks in several regions all around the world, within just few years after its discovery. According to our review, 45 novel virus species have been discovered in tomato in the past decade and several known viruses have been associated with tomato for the first time. The discovery and first detections of viruses in tomato are increasing in recent years also because of the prevalent use of HTS as a generic virus detection technique. This faster discovery rate is often not paralleled with virus characterization studies, biological or ecological, for newly discovered tomato viruses. In-depth characterization studies are mostly performed for viruses with high phytosanitary and economic importance. At the agroecological scale, the first extensive HTS-based tomato virome studies were conducted in China (Xu et al., 2017) and France (Ma et al., 2020), the latter also addressing the link between the virome of tomato and wild plants. In addition, by the use of HTS, viable tomato-infecting tobamoviruses were detected in the environment outside their hosts, specifically in untreated and treated wastewater (Bačnik et al., 2020).

The increasing knowledge on the virome of tomato, the environment, and the surrounding wild plants contributes to better understanding of virus disease emergence and epidemiology of viruses associated with tomato. Moreover, an increase in viral sequence information in databases can enable more rapid development of targeted diagnostic tests. A tailored approach in studies of plant virus diseases is needed because each crop species or family has its distinctive virome (McLeish et al., 2020b). At the agroecological scale, a holistic view of the virome would include viruses in crops, wild plants, vectors, or in the surrounding environment. This is important to consider for tomato that is associated with a very high number of virus species, which are transmitted by numerous vectors and harbored in wild plants and some remain stable in the environment. HTS-based viromics approach enables collection of ecosystem-level genomic data in extended spatiotemporal scales (McLeish et al., 2020a,b). Furthermore, the use of long-read (or single molecule) portable sequencing platforms, such as Oxford Nanopore Technologies MinIon, is expected to bring HTS even closer to the end-users (e.g., small research and diagnostics laboratories) and contribute to new viral discoveries in plants, including tomato (Bronzato Badial et al., 2018; Boykin et al., 2019; Chalupowicz et al., 2019). Approaches such as virome network analysis can finally be used to, e.g., associate viromes of the crops to that of the insect vectors or wild plants and can consider biogeographical features of the cropping area (Alcalá-Briseño et al., 2020). With such analyses, new insights can be generated that could be useful in possible forecasting and eventual prevention of virus disease emergence and outbreaks in the future (Garrett et al., 2018; McLeish et al., 2020a).

AUTHOR CONTRIBUTIONS

MPSR and DK conceptualized the review topic. MPSR did the data mining and analysis and wrote the first draft of the manuscript, including the table, figures, and **Supplementary Material**. DK contributed in making and editing the table and figures. DK and AV edited initial drafts of the manuscript. DK, AV, NM, and MR edited the final draft of the manuscript. All authors significantly contributed to the writing and editing of the manuscript.

FUNDING

This work was supported by the funding from Horizon 2020 Marie Skłodowska-Curie Actions Innovative Training Network (H2020 MSCA-ITN) project "INEXTVIR" (GA 813542) under the management of the European Commission-Research Executive Agency and from the Slovenian Research Agency (ARRS), Republic of Slovenia project (L7-2632), and core financing (P4-0407 and P4-0165).

SUPPLEMENTARY MATERIAL

The Supplementary Material for this article can be found online at: https://www.frontiersin.org/articles/10.3389/fmicb.2021.671925/full#supplementary-material

Supplementary Table 1 | Meta-analysis of the extent of characterization of novel viruses discovered in tomato from 2011 to 2020.

Supplementary Table 2 | Summary list of all viruses with tomato indicated as host based on review of literature and different databases.

REFERENCES

Adams, I. P., Glover, R. H., Monger, W. A., Mumford, R., Jackeviciene, E., Navalenskiene, M., et al. (2009a). Next-generation sequencing and metagenomic analysis: a universal diagnostic tool in plant virology. *Mol. Plant Pathol.* 10, 537–545. doi: 10.1111/j.1364-3703.2009.00545.x

Adams, M. J., Antoniw, J. F., and Kreuze, J. (2009b). Virgaviridae: a new family of rod-shaped plant viruses. *Arch. Virol.* 154, 1967–1972. doi: 10.1007/s00705-009-0506-6

Adkins, S., Baker, C. A., Badillo-Vargas, I. E., Frantz, G., Mellinger, H. C., Roe, N., et al. (2015). Necrotic streak disease of tomato in florida caused by a new ilarvirus species related to tulare apple mosaic virus. *New Dis. Rep.* 31:16. doi: 10.5197/j.2044-0588.2015.031.016

Agüero, J., Gómez-Aix, C., Sempere, R. N., García-Villalba, J., García-Núñez, J., Hernando, Y., et al. (2018). Stable and broad spectrum cross-protection against pepino mosaic virus attained by mixed infection. *Front. Plant Sci.* 9:1810. doi: 10.3389/fpls.2018.01810

Akhtar, K. P., Anwer, M., Saleem, M. Y., Yousaf, S., Ullah, N., Cheema, H. M. N., et al. (2019). Identification of natural weed hosts of cucumber mosaic virus subgroup-I and the absence of seed transmission in weed hosts in pakistan. *J. Hortic. Sci. Biotechnol.* 94, 468–474. doi: 10.1080/14620316.2019.1565947

Al Rwahnih, M., Daubert, S., Golino, D., and Rowhani, A. (2009). Deep sequencing analysis of RNAs from a grapevine showing syrah decline symptoms reveals a multiple virus infection that includes a novel virus. *Virology* 387, 395–401. doi: 10.1016/j.virol.2009.02.028

Albuquerque, L. C., Varsani, A., Fernandes, F. R., Pinheiro, B., Martin, D. P., de Tarso Oliveira Ferreira, P., et al. (2012). Further characterization of tomato-infecting begomoviruses in Brazil. *Arch. Virol.* 157, 747–752. doi: 10.1007/s00705-011-1213-7

Alcalá-Briseño, R. I., Casarrubias-Castillo, K., López-Ley, D., Garrett, K. A., and Silva-Rosales, L. (2020). Network analysis of the papaya orchard virome from two agroecological regions of chiapas, mexico. *mSystems* 5, e419–e423. doi: 10.1128/msystems.00423-19

Alcalá-Briseño, R. I., Coşkan, S., Londoño, M. A., and Polston, J. E. (2017). Genome sequence of southern tomato virus in asymptomatic tomato 'Sweet Hearts'. *Genome Announc.* 5, e1316–e1374. doi: 10.1128/genomeA.01374-16

Alexander, H. M., Mauck, K. E., Whitfield, A. E., Garrett, K. A., and Malmstrom, C. M. (2014). Plant-virus interactions and the agro-ecological interface. *Eur. J. Plant Pathol.* 138, 529–547. doi: 10.1007/s10658-013-0317-1

Alfaro-Fernández, A., Castillo, P., Sanahuja, E., Rodríguez-Salido, M. C., and Font, M. I. (2021). First report of tomato brown rugose fruit virus in tomato in spain. *Plant Dis.* 105, 515–515. doi: 10.1094/PDIS-06-20-1251-PDN

Alfaro-Fernández, A., Córdoba-Sellés, C., Cebrián, M. C., Herrera-Vásquez, J. A., Sánchez-Navarro, J. A., Juárez, M., et al. (2008). First report of tomato torrado virus on weed hosts in Spain. *Plant Dis.* 92, 831. doi: 10.1094/PDIS-92-5-0831B

Alkowni, R., Alabdallah, O., and Fadda, Z. (2019). Molecular identification of tomato brown rugose fruit virus in tomato in Palestine. *J. Plant Pathol.* 101, 719–723. doi: 10.1007/s42161-019-00240-7

Al-Kuwaiti, N. A., Maruthi, M. N., and Seal, S. E. (2016). Molecular characterization of potyviruses infecting potato and vegetables in Iraq. *J. Plant Pathol.* 98, 603–606.

Ambrós, S., Martínez, F., Ivars, P., Hernández, C., de la Iglesia, F., and Elena, S. F. (2017). Molecular and biological characterization of an isolate of Tomato mottle mosaic virus (ToMMV) infecting tomato and other experimental hosts in eastern Spain. *Eur. J. Plant Pathol.* 149, 261–268. doi: 10.1007/s10658-017-1180-2

Ambrozevicius, L. P., Calegario, R. F., Fontes, E. P. B., De Carvalho, M. G., and Zerbini, F. M. (2002). Genetic diversity of begomovirus infecting tomato and associated weeds in southeastern Brazil. *Fitopatol. Bras.* 27, 372–377. doi: 10.1590/s0100-41582002000400006

Amer, M. A., and Mahmoud, S. Y. (2020). First report of tomato brown rugose fruit virus on tomato in Egypt. *New Dis. Rep.* 41:24. doi: 10.5197/j.2044-0588.2020.041.024

Anderson, P. K., Cunningham, A. A., Patel, N. G., Morales, F. J., Epstein, P. R., and Daszak, P. (2004). Emerging infectious diseases of plants: pathogen pollution, climate change and agrotechnology drivers. *Trends Ecol. Evol.* 19, 535–544. doi: 10.1016/j.tree.2004.07.021

Anfoka, G., Moshe, A., Fridman, L., Amrani, L., Rotem, O., Kolot, M., et al. (2016). Tomato yellow leaf curl virus infection mitigates the heat stress response of plants grown at high temperatures. *Sci. Rep.* 6:19715. doi: 10.1038/srep19715

Aparicio, F., Aramburu, J., Herranz, M. C., Pallás, V., and López, C. (2018). Parietaria mottle virus: a potential threat for tomato crops? *Acta Hortic.* 1207, 261–268. doi: 10.17660/ActaHortic.2018.1207.36

Bačnik, K., Kutnjak, D., Pecman, A., Mehle, N., Tušek Žnidarič, M., Gutiérrez Aguirre, I., et al. (2020). Viromics and infectivity analysis reveal the release of infective plant viruses from wastewater into the environment. *Water Res.* 177:115628. doi: 10.1016/j.watres.2020.115628

Badillo-Vargas, I. E., Baker, C. A., Turechek, W. W., Frantz, G., Mellinger, H. C., Funderburk, J. E., et al. (2016). Genomic and biological characterization of tomato necrotic streak virus, a novel subgroup 2 ilarvirus infecting tomato in Florida. *Plant Dis.* 100, 1046–1053. doi: 10.1094/PDIS-12-15-1437-RE

Barreto, S. S., Hallwass, M., Aquino, O. M., and Inoue-Nagata, A. K. (2013). A study of weeds as potential inoculum sources for a tomato-infecting begomovirus in central Brazil. *Phytopathology* 103, 436–444. doi: 10.1094/PHYTO-07-12-0174-R

Batuman, O., Miyao, G., Kuo, Y. W., Chen, L. F., Davis, R. M., and Gilbertson, R. L. (2009). An outbreak of a necrosis disease of tomato in california in 2008 was caused by a new ilarvirus species related to parietaria mottle virus. *Plant Dis.* 93:546. doi: 10.1094/PDIS-93-5-0546C

Beris, D., Malandraki, I., Kektsidou, O., Theologidis, I., Vassilakos, N., and Varveri, C. (2020). First report of tomato brown rugose fruit virus infecting tomato in Greece. *Plant Dis.* 104:2035. doi: 10.1094/PDIS-01-20-0212-PDN

Bernardo, P., Golden, M., Akram, M., Naimuddin, K., Nadarajan, N., Fernandez, E., et al. (2013). Identification and characterisation of a highly divergent geminivirus: evolutionary and taxonomic implications. *Virus Res.* 177, 35–45. doi: 10.1016/j.virusres.2013.07.006

Birithia, R., Subramanian, S., Villinger, J., Muthomi, J. W., Narla, R. D., and Pappu, H. R. (2012). First report of tomato yellow ring virus (tospovirus, bunyaviridae) infecting tomato in kenya. *Plant Dis.* 96, 1384–1384. doi: 10.1094/PDIS-05-12-0462-PDN

Blawid, R., Hayashi, E. A. I., Rezende, J. A. M., Kitajima, E. W., and Nagata, T. (2016). A highly divergent isolate of tomato blistering mosaic virus from solanum violaefolium. *Virus Genes* 52, 294–298. doi: 10.1007/s11262-016-1288-z

Blystad, D. R., van der Vlugt, R., Alfaro-Fernández, A., del Carmen Córdoba, M., Bese, G., Hristova, D., et al. (2015). Host range and symptomatology of pepino mosaic virus strains occurring in Europe. *Eur. J. Plant Pathol.* 143, 43–56. doi: 10.1007/s10658-015-0664-1

Borodynko, H., Hasiów-Jaroszewska, B., and Pospieszny, H. (2010). Identification and characterization of an olive latent virus 1 isolate from a new host: solanum lycopersicum. *J. Plant Pathol.* 92, 789–792. doi: 10.4454/jpp.v92i3.328

Boykin, L. M., Sseruwagi, P., Alicai, T., Ateka, E., Mohammed, I. U., Stanton, J. A. L., et al. (2019). Tree lab: portable genomics for early detection of plant viruses and pests in sub-saharan africa. *Genes (Basel).* 10:632. doi: 10.3390/genes10090632

Bratsch, S. A., Creswell, T. C., and Ruhl, G. E. (2018). First report of tomato necrotic spot virus infecting tomato in indiana. *Plant Heal. Prog.* 19, 224–225. doi: 10.1094/PHP-05-18-0019-BR

Bratsch, S. A., Grinstead, S., Creswell, T. C., Ruhl, G. E., and Mollov, D. (2019). Characterization of tomato necrotic spot virus, a subgroup 1 ilarvirus causing

necrotic foliar, stem, and fruit symptoms in tomatoes in the united states. *Plant Dis.* 103, 1391–1396. doi: 10.1094/PDIS-11-18-2112-RE

Bratsch, S. A., Grinstead, S., Lockhart, B., and Mollov, D. (2020). Biological properties and genomic sequence of an isolate of cherry rasp leaf virus from tomato. *J. Plant Pathol.* 102, 843–848. doi: 10.1007/s42161-020-00522-5

Bronzato Badial, A., Sherman, D., Stone, A., Gopakumar, A., Wilson, V., Schneider, W., et al. (2018). Nanopore sequencing as a surveillance tool for plant pathogens in plant and insect tissues. *Plant Dis.* 102, 1648–1652. doi: 10.1094/PDIS-04-17-0488-RE

Butković, A., González, R., and Elena, S. F. (2021). Revisiting orthotospovirus phylogeny using full-genome data and testing the contribution of selection, recombination and segment reassortment in the origin of members of new species. *Arch. Virol.* 166, 491–499. doi: 10.1007/s00705-020-04902-1

Camacho-Beltrán, E., Armenta-Chávez, R., Romero-Romero, J. L., Magallanes-Tapia, M. A., Leyva-López, N. E., Apodaca-Sánchez, M. Á, et al. (2015). First report of pepper as a natural new host for tomato marchitez virus in sinaloa, mexico. *Can. J. Plant Pathol.* 37, 384–389. doi: 10.1080/07060661.2015.1078412

Camacho-Beltrán, E., Pérez-Villarreal, A., Leyva-López, N. E., Rodríguez-Negrete, E. A., Ceniceros-Ojeda, E. A., and Méndez-Lozano, J. (2019). Occurrence of tomato brown rugose fruit virus infecting tomato crops in mexico. *Plant Dis.* 103, 1440–1440. doi: 10.1094/PDIS-11-18-1974-PDN

Canto, T., Aranda, M. A., and Fereres, A. (2009). Climate change effects on physiology and population processes of hosts and vectors that influence the spread of hemipteran-borne plant viruses. *Glob. Chang. Biol.* 15, 1884–1894. doi: 10.1111/j.1365-2486.2008.01820.x

Carmichael, D. J., Rey, M. E. C., Naidoo, S., Cook, G., and van Heerden, S. W. (2011). First report of pepino mosaic virus infecting tomato in south africa. *Plant Dis.* 95:767. doi: 10.1094/PDIS-01-11-0036

Chalupowicz, L., Dombrovsky, A., Gaba, V., Luria, N., Reuven, M., Beerman, A., et al. (2019). Diagnosis of plant diseases using the nanopore sequencing platform. *Plant Pathol.* 68, 229–238. doi: 10.1111/ppa.12957

Chatzivassiliou, E. K., Boubourakas, I., Drossos, E., Eleftherohorinos, I., Jenser, G., Peters, D., et al. (2001). Weeds in greenhouses and tobacco fields are differentially infected by tomato spotted wilt virus and infested by its vector species. *Plant Dis.* 85, 40–46. doi: 10.1094/PDIS.2001.85.1.40

Chatzivassiliou, E. K., Giakountis, A., Kumari, S. G., and Makkouk, K. M. (2016). Viruses affecting lentil (lens culinaris medik.) in greece; incidence and genetic variability of bean leafroll virus and pea enation mosaic virus. *Phytopathol. Mediterr.* 55, 239–252. doi: 10.2307/44809330

Che, H. Y., Luo, D. Q., and Cao, X. R. (2018). First report of tomato mottle mosaic virus in tomato crops in china. *Plant Dis.* 102:2051. doi: 10.1094/PDIS-03-18-0538-PDN

Chikh-Ali, M., Naidu, R. A., and Karasev, A. V. (2015). First report of potato virus Y (PVY) strain PVY C associated with a tomato disease in kenya. *Plant Dis.* 100:864. doi: 10.1094/PDIS-08-15-0890-PDN

Choi, H., Jo, Y., Cho, W. K., Yu, J., Tran, P.-T., Salaipeth, L., et al. (2020). Identification of viruses and viroids infecting tomato and pepper plants in vietnam by metatranscriptomics. *Int. J. Mol. Sci.* 21:7565. doi: 10.3390/ijms21207565

Cillo, F., Barbarossa, L., Grieco, F., and Gallitelli, D. (1994). Lethal necrosis, fruit necrosis and top stunting: molecular- biological aspects of three cucumber mosaic virus-induced diseases of processing tomatoes in Italy. *Acta Hortic.* 379, 369–376. doi: 10.17660/ActaHortic.1994.376.51

Ciuffo, M., Kinoti, W. M., Tiberini, A., Forgia, M., Tomassoli, L., Constable, F. E., et al. (2020). A new blunervirus infects tomato crops in italy and australia. *Arch. Virol.* 165, 2379–2384. doi: 10.1007/s00705-020-04760-x

Constable, F., Chambers, G., Penrose, L., Daly, A., Mackie, J., Davis, K., et al. (2019). Viroid-infected tomato and capsicum seed shipments to Australia. *Viruses* 11:98. doi: 10.3390/v11020098

Cooper, I., and Jones, R. A. C. (2006). Wild plants and viruses: under-investigated ecosystems. *Adv. Virus Res.* 67, 1–47. doi: 10.1016/S0065-3527(06)67001-2

de Nazaré Almeida dos Reis, L., Fonseca, M. E. N., Ribeiro, S. G., Naito, F. Y. B., Boiteux, L. S., and Pereira-Carvalho, R. C. (2020). Metagenomics of neotropical single-stranded DNA viruses in tomato cultivars with and without the Ty-1 gene. *Viruses* 12:819. doi: 10.3390/v12080819

De Oliveira, V. C., Nagata, T., Guimarães, F. C., Ferreira, F. A., Kitajima, E. W., Nicolini, C., et al. (2013). Characterization of a novel tymovirus on tomato plants in Brazil. *Virus Genes* 46, 190–194. doi: 10.1007/s11262-012-0830-x

Dombrovsky, A., and Smith, E. (2017). "Seed Transmission of Tobamoviruses: Aspects of Global Disease Distribution," in *Advances in Seed Biology*, ed. J. C. Jimenez-Lopez (London: InTech).

Donaire, L., Wang, Y., Gonzalez-Ibeas, D., Mayer, K. F., Aranda, M. A., and Llave, C. (2009). Deep-sequencing of plant viral small RNAs reveals effective and widespread targeting of viral genomes. *Virology* 392, 203–214. doi: 10.1016/j.virol.2009.07.005

Duffus, J. E., Liu, H.-Y., and Wisler, G. C. (1996). Tomato infectious chlorosis virus — a new clostero-like virus transmitted by trialeurodes vaporariorum. *Eur. J. Plant Pathol.* 102, 219–226. doi: 10.1007/BF01877960

Elena, S. F., Fraile, A., and García-Arenal, F. (2014). *"Evolution and Emergence of Plant Viruses," in Advances in Virus Research*. Amsterdam: Elsevier, 161–191.

Elvira-González, L., Medina, V., Rubio, L., and Galipienso, L. (2020). The persistent southern tomato virus modifies miRNA expression without inducing symptoms and cell ultra-structural changes. *Eur. J. Plant Pathol.* 156, 615–622. doi: 10.1007/s10658-019-01911-y

EPPO (2020a). *Tomato brown rugose fruit virus (TOBRFV)[Datasheet]| EPPO Global Database*. Available Online at: https://gd.eppo.int/taxon/TOBRFV/datasheet [Accessed January 5, 2021].

EPPO (2020b). *Tomato mottle mosaic virus*. Available Online at: https://www.eppo.int/ACTIVITIES/plant_quarantine/alert_list_viruses/tomato_mottle_mosaic_virus [Accessed January 5, 2021]

EPPO GD (2020). *EPPO Global Database*. Available Online at: https://gd.eppo.int [Accessed January 5, 2021].

FAOSTAT (2020). *Statistics Division of the Food and Agricultural Organization of the United Nations*. Availabe Online at: http://www.fao.org/faostat/en/ Accessed December 31, 2020

Fariña, A. E., Rezende, J. A. M., and Wintermantel, W. M. (2019). Expanding knowledge of the host range of *Tomato chlorosis virus* and host plant preference of *Bemisia tabaci* MEAM1. *Plant Dis.* 103, 1132–1137. doi: 10.1094/PDIS-11-18-1941-RE

Ferrand, L., Nome, C., Orílio, A. F., García, M. L., Nagata, T., Ronco, L. B., et al. (2016). First report of tomato blistering mosaic virus infecting tomato in Argentina. *Plant Dis.* 100:1026. doi: 10.1094/PDIS-07-15-0782-PDN

Fiallo-Olivé, E., and Navas-Castillo, J. (2019). Tomato chlorosis virus, an emergent plant virus still expanding its geographical and host ranges. *Mol. Plant Pathol.* 20, 1307–1320. doi: 10.1111/mpp.12847

Fiallo-Olivé, E., Pan, L.-L., Liu, S.-S., and Navas-Castillo, J. (2020). Transmission of begomoviruses and other whitefly-borne viruses: dependence on the vector species. *Phytopathology* 110, 10–17. doi: 10.1094/PHYTO-07-19-0273-FI

Fidan, H., Sarikaya, P., and Calis, O. (2019). First report of tomato brown rugose fruit virus on tomato in Turkey. *New Dis. Rep.* 39:18. doi: 10.5197/j.2044-0588.2019.039.018

Fillhart, R. C., Bachand, G. D., and Castello, J. D. (1998). Detection of infectious tobamoviruses in forest soils. *Appl. Environ. Microbiol.* 64, 1430–1435. doi: 10.1128/aem.64.4.1430-1435.1998

Finetti Sialer, M., Di Franco, A., Papanice, M. A., and Gallitelli, D. (1997). Tomato necrotic yellows induced by a novel strain of alfalfa mosaic virus. *J. Plant Pathol.* 79, 115–120.

Finetti-Sialer, M., and Gallitelli, D. (2003). Complete nucleotide sequence of pelargonium zonate spot virus and its relationship with the family bromoviridae. *J. Gen. Virol.* 84, 3143–3151. doi: 10.1099/vir.0.19391-0

Flores, R., Hernández, C., Alba, A. E. M., de Daròs, J.-A., and Serio, F. D. (2005). Viroids and viroid-host interactions. *Annu. Rev. Phytopathol.* 43, 117–139. doi: 10.1146/annurev.phyto.43.040204.140243

Fontenele, R. S., Lamas, N. S., Lacorte, C., Lacerda, A. L. M., Varsani, A., and Ribeiro, S. G. (2017). A novel geminivirus identified in tomato and cleome plants sampled in Brazil. *Virus Res.* 240, 175–179. doi: 10.1016/j.virusres.2017.08.007

Fortes, I. M., Sánchez-Campos, S., Fiallo-Olivé, E., Díaz-Pendón, J. A., Navas-Castillo, J., and Moriones, E. (2016). A novel strain of tomato leaf curl new delhi virus has spread to the mediterranean basin. *Viruses* 8:307. doi: 10.3390/v8110307

Fox, A., Daly, M., Nixon, T., Brurberg, M. B., Blystad, D.-R., Harju, V., et al. (2013). First report of tomato chlorotic dwarf viroid (TCDVd) in tomato in norway and subsequent eradication. *New Dis. Rep.* 27:8. doi: 10.5197/j.2044-0588.2013.027.008

Fuentes, A., Carlos, N., Ruiz, Y., Callard, D., Sánchez, Y., Ochagavía, M. E., et al. (2016). Field trial and molecular characterization of RNAi-transgenic tomato plants that exhibit resistance to tomato yellow leaf curl geminivirus. *Mol. Plant-Microbe Interact.* 29, 197–209. doi: 10.1094/MPMI-08-15-0181-R

Gaafar, Y., Lüddecke, P., Heidler, C., Hartrick, J., Sieg-Müller, A., Hübert, C., et al. (2019). First report of southern tomato virus in german tomatoes. *New Dis. Rep.* 40:1. doi: 10.5197/j.2044-0588.2019.040.001

Gaafar, Y. Z. A., Abdelgalil, M. A. M., Knierim, D., Richert-Pöggeler, K. R., Menzel, W., Winter, S., et al. (2018). First report of physostegia chlorotic mottle virus on tomato (*Solanum lycopersicum*) in germany. *Plant Dis.* 102, 255–255. doi: 10.1094/PDIS-05-17-0737-PDN

Gaafar, Y. Z. A., and Ziebell, H. (2020). Comparative study on three viral enrichment approaches based on RNA extraction for plant virus/viroid detection using high-throughput sequencing. *PLoS One* 15:e0237951. doi: 10.1371/journal.pone.0237951

Gadhave, K. R., Gautam, S., Rasmussen, D. A., and Srinivasan, R. (2020). Aphid transmission of Potyvirus: the largest plant-infecting RNA virus genus. *Viruses* 12:773. doi: 10.3390/v12070773

Gallitelli, D. (2000). The ecology of cucumber mosaic virus and sustainable agriculture. *Virus Res.* 71, 9–21. doi: 10.1016/S0168-1702(00)00184-2

Garcìa-Arenal, F., and Palukaitis, P. (1999). Structure and functional relationships of satellite RNAs of cucumber mosaic virus. *Curr. Top. Microbiol. Immunol.* 239, 37–63. doi: 10.1007/978-3-662-09796-0_3

Garrett, K. A., Alcalá-Briseño, R. I., Andersen, K. F., Buddenhagen, C. E., Choudhury, R. A., Fulton, J. C., et al. (2018). Network analysis: a systems framework to address grand challenges in plant pathology. *Annu. Rev. Phytopathol.* 56, 559–580. doi: 10.1146/annurev-phyto-080516-035326

Giakountis, A., Tsarmpopoulos, I., and Chatzivassiliou, E. K. (2018). Cucumber mosaic virus isolates from greek legumes are associated with satellite RNAs that are necrogenic for tomato. *Plant Dis.* 102, 2268–2276. doi: 10.1094/PDIS-08-17-1259-RE

Gilbertson, R. L., Rojas, M. R., Kon, T., and Jaquez, J. (2007). "Introduction of Tomato Yellow Leaf Curl Virus into the Dominican Republic: the Development of a Successful Integrated Pest Management Strategy," in *Tomato Yellow Leaf Curl Virus Disease: Management, Molecular Biology, Breeding for Resistance*, ed. H. Czosnek (Dordrecht: Springer), 279–303.

Gnanasekaran, P., and Chakraborty, S. (2018). Biology of viral satellites and their role in pathogenesis. *Curr. Opin. Virol.* 33, 96–105. doi: 10.1016/j.coviro.2018.08.002

Gómez, P., Sempere, R., and Aranda, M. A. (2012). Pepino mosaic virus and tomato torrado virus: two emerging viruses affecting tomato crops in the mediterranean basin. *Adv. Virus Res.* 84, 505–532. doi: 10.1016/B978-0-12-394314-9.00014-2

Gómez-Aix, C., Alcaide, C., Agüero, J., Faize, M., Juárez, M., Díaz-Marrero, C. J., et al. (2019). Genetic diversity and population structure of pepino mosaic virus in tomato crops of spain and morocco. *Ann. Appl. Biol.* 174, 284–292. doi: 10.1111/aab.12491

Gorayeb, E. S., Bello, V. H., Cruciol, G. C. D., Watanabe, L. F. M., Dovigo, L. H., Sartori, M. M. P., et al. (2020). Evaluation of datura stramonium and nicandra physaloides as reservoirs of tomato severe rugose virus and whiteflies. *Plant Pathol.* 69, 569–575. doi: 10.1111/ppa.13139

Grieco, F., Lanave, C., and Gallitelli, D. (1997). Evolutionary dynamics of cucumber mosaic virus satellite RNA during natural epidemics in Italy. *Virology* 229, 166–174. doi: 10.1006/viro.1996.8426

Groves, R. L., Walgenbach, J. F., Moyer, J. W., and Kennedy, G. G. (2002). The role of weed hosts and tobacco thrips, *Frankliniella fusca*, in the epidemiology of tomato spotted wilt virus. *Plant Dis.* 86, 573–582. doi: 10.1094/PDIS.2002.86.6.573

Hančinský, R., Mihálik, D., Mrkvová, M., Candresse, T., and Glasa, M. (2020). Plant viruses infecting solanaceae family members in the cultivated and wild environments: a review. *Plants* 9:667. doi: 10.3390/plants9050667

Hanssen, I. M., Gutiérrez-Aguirre, I., Paeleman, A., Goen, K., Wittemans, L., Lievens, B., et al. (2010a). Cross-protection or enhanced symptom display in greenhouse tomato co-infected with different pepino mosaic virus isolates. *Plant Pathol.* 59, 13–21. doi: 10.1111/j.1365-3059.2009.02190.x

Hanssen, I. M., Lapidot, M., and Thomma, B. P. H. J. (2010b). Emerging viral diseases of tomato crops. *Mol. Plant-Microbe Interact.* 23, 539–548. doi: 10.1094/MPMI-23-5-0539

Hanssen, I. M., Mumford, R., Blystad, D.-R., Cortez, I., Hasiów-Jaroszewska, B., Hristova, D., et al. (2010c). Seed transmission of pepino mosaic virus in tomato. *Eur. J. Plant Pathol.* 126, 145–152. doi: 10.1007/s10658-009-9528-x

Hanssen, I. M., and Lapidot, M. (2012). Major tomato viruses in the mediterranean basin. *Adv. Virus Res.* 84, 31–66. doi: 10.1016/B978-0-12-394314-9.00002-6

Hanssen, I. M., Paeleman, A., Vandewoestijne, E., Van Bergen, L., Bragard, C., Lievens, B., et al. (2009). Pepino mosaic virus isolates and differential symptomatology in tomato. *Plant Pathol.* 58, 450–460. doi: 10.1111/j.1365-3059.2008.02018.x

Hanssen, I. M., and Thomma, B. P. H. J. (2010). Pepino mosaic virus: a successful pathogen that rapidly evolved from emerging to endemic in tomato crops. *Mol. Plant Pathol.* 11, 179–189. doi: 10.1111/j.1364-3703.2009.00600.x

Hassani-Mehraban, A., Cheewachaiwit, S., Relevante, C., Kormelink, R., and Peters, D. (2011). Tomato necrotic ring virus (TNRV), a recently described tospovirus species infecting tomato and pepper in Thailand. *Eur. J. Plant Pathol.* 130, 449–456. doi: 10.1007/s10658-011-9771-9

HortDaily (2019). *Southern Tomato Virus reported in the UK*. Available Online at: https://www.hortidaily.com/article/9103907/southern-tomato-virus-reported-in-the-uk/ [Accessed August 3, 2020]

Hou, W., Li, S., and Massart, S. (2020). Is there a "biological desert" with the discovery of new plant viruses? a retrospective analysis for new fruit tree viruses. *Front. Microbiol.* 11:592816. doi: 10.3389/fmicb.2020.592816

Huang, C.-H., Zheng, Y.-X., Cheng, Y.-H., Lee, W.-S., and Jan, F.-J. (2010). First report of capsicum chlorosis virus infecting tomato in Taiwan. *Plant Dis.* 94:1263. doi: 10.1094/PDIS-04-10-0275

Iacono, G., Hernandez-Llopis, D., Alfaro-Fernandez, A., Davino, M., Font, M., Panno, S., et al. (2015). First report of southern tomato virus in tomato crops in Italy. *New Dis. Rep.* 32, 27–27. doi: 10.5197/j.2044-0588.2015.032.027

ICTV (2020). *ICTV Master Species List 2019.v1*. Available Online at: https://talk.ictvonline.org/files/master-species-lists/m/msl/9601 (accessed June 1, 2020).

Idris, A. M., Shahid, M. S., Briddon, R. W., Khan, A. J., Zhu, J. K., and Brown, J. K. (2011). An unusual alphasatellite associated with monopartite begomoviruses attenuates symptoms and reduces betasatellite accumulation. *J. Gen. Virol.* 92, 706–717. doi: 10.1099/vir.0.025288-0

Ignatov, A. N., Gritsenko, V. V., and Dzhalilov, F. S. (2020). Risks of new tomato virus diseases spreading in the russian federation. *Potato Veg.* 5:3. doi: 10.25630/PAV.2020.80.51.001

Ito, T., Kimbara, J., Sharma, P., and Ikegami, M. (2009). Interaction of tomato yellow leaf curl virus with diverse betasatellites enhances symptom severity. *Arch. Virol.* 154, 1233–1239. doi: 10.1007/s00705-009-0431-8

Jacquemond, M. (2012). "Cucumber Mosaic Virus," in *Viruses and Virus Diseases of Vegetables in the Mediterranean Basin*, eds G. Loebenstein and H. Lecoq (Cambridge,MA: Academic Press), 439–504.

Jones, R. A. C. (2016). *"Future Scenarios for Plant Virus Pathogens as Climate Change Progresses," in Advances in Virus Research*. Cambridge,MA: Academic Press Inc, 87–147.

Jones, R. A. C. (2018). *"Plant and Insect Viruses in Managed and Natural Environments: Novel and Neglected Transmission Pathways," in Advances in Virus Research*. Cambridge,MA: Academic Press Inc, 149–187.

Jones, R. A. C. (2021). Global plant virus disease pandemics and epidemics. *Plants* 10:233. doi: 10.3390/plants10020233

Jones, R. A. C., Koenig, R., and Lasemann, D. E. (1980). Pepino mosaic virus, a new potexvirus from pepino (solanum muricatum). *Ann. Appl. Biol.* 94, 61–68. doi: 10.1111/j.1744-7348.1980.tb03896.x

Jyothsna, P., Haq, Q. M. I., Singh, P., Sumiya, K. V., Praveen, S., Rawat, R., et al. (2013). Infection of tomato leaf curl New Delhi virus (ToLCNDV), a bipartite begomovirus with betasatellites, results in enhanced level of helper virus components and antagonistic interaction between DNA B and betasatellites. *Appl. Microbiol. Biotechnol.* 97, 5457–5471. doi: 10.1007/s00253-012-4685-9

Kaliciak, A., and Syller, J. (2009). New hosts of potato virus Y (PVY) among common wild plants in Europe. *Eur. J. Plant Pathol.* 124, 707–713. doi: 10.1007/s10658-009-9452-0

Katsarou, K., Bardani, E., Kallemi, P., and Kalantidis, K. (2019). Viral detection: past, present, and future. *Bioessays* 41:e1900049. doi: 10.1002/bies.201900049

Kazinczi, G., Takács, A. P., Horváth, J., Gáborjányi, R., and Béres, I. (2005). Susceptibility of some weed species to pepino mosaic virus (PepMV). *Commun. Agric. Appl. Biol. Sci.* 70, 489–491.

Kesumawati, E., Okabe, S., Homma, K., Fujiwara, I., Zakaria, S., Kanzaki, S., et al. (2019). Pepper yellow leaf curl aceh virus: a novel bipartite begomovirus isolated from chili pepper, tomato, and tobacco plants in indonesia. *Arch. Virol.* 164, 2379–2383. doi: 10.1007/s00705-019-04316-8

Khan, A. J., Akhtar, S., Singh, A. K., Al-Shehi, A. A., Al-Matrushi, A. M., Ammara, U., et al. (2014). Recent evolution of a novel begomovirus causing tomato leaf curl disease in the Al-batinah region of oman. *Arch. Virol.* 159, 445–455. doi: 10.1007/s00705-013-1853-x

Kiss, Z. A., Medina, V., and Falk, B. W. (2013). Crinivirus replication and host interactions. *Front. Microbiol.* 4:99. doi: 10.3389/fmicb.2013.00099

Klap, C., Luria, N., Smith, E., Hadad, L., Bakelman, E., Sela, N., et al. (2020). Tomato brown rugose fruit virus contributes to enhanced pepino mosaic virus titers in tomato plants. *Viruses* 12:879. doi: 10.3390/v12080879

Kon, T., and Gilbertson, R. L. (2012). Two genetically related begomoviruses causing tomato leaf curl disease in togo and nigeria differ in virulence and host range but do not require a betasatellite for induction of disease symptoms. *Arch. Virol.* 157, 107–120. doi: 10.1007/s00705-011-1139-0

Kovalskaya, N., and Hammond, R. W. (2014). Molecular biology of viroid–host interactions and disease control strategies. *Plant Sci.* 228, 48–60. doi: 10.1016/j.plantsci.2014.05.006

Kreuze, J. F., Perez, A., Untiveros, M., Quispe, D., Fuentes, S., Barker, I., et al. (2009). Complete viral genome sequence and discovery of novel viruses by deep sequencing of small RNAs: a generic method for diagnosis, discovery and sequencing of viruses. *Virology* 388, 1–7. doi: 10.1016/j.virol.2009.03.024

Kumar, J., Gunapati, S., Singh, S. P., Kumar, A., Lalit, A., Sharma, N. C., et al. (2013). A new betasatellite associated with cotton leaf curl burewala virus infecting tomato in india: influence on symptoms and viral accumulation. *Arch. Virol.* 158, 1349–1353. doi: 10.1007/s00705-013-1613-y

Lapidot, M., Guenoune-Gelbart, D., Leibman, D., Holdengreber, V., Davidovitz, M., MacHbash, Z., et al. (2010). Pelargonium zonate spot virus is transmitted vertically via seed and pollen in tomato. *Phytopathology* 100, 798–804. doi: 10.1094/PHYTO-100-8-0798

Lavina, A., Aramburu, J., and Moriones, E. (1996). Occurrence of tomato spotted wilt and cucumber mosaic viruses in field-grown tomato crops and associated weeds in northeastern Spain. *Plant Pathol.* 45, 837–842. doi: 10.1111/j.1365-3059.1996.tb02893.x

Lecoq, H., Wipf-Scheibel, C., Verdin, E., and Desbiez, C. (2019). Characterization of the first tenuivirus naturally infecting dicotyledonous plants. *Arch. Virol.* 164, 297–301. doi: 10.1007/s00705-018-4057-6

Leke, W. N., Kvarnheden, A., Ngane, E. B., Titanji, V. P. K., and Brown, J. K. (2011). Molecular characterization of a new begomovirus and divergent alphasatellite from tomato in Cameroon. *Arch. Virol.* 156, 925–928. doi: 10.1007/s00705-011-0957-4

Lett, J.-M., Ncho, J., Claverie, S., Hoareau, M., Lefeuvre, P., De Cauwer, V., et al. (2020). Tomato leaf curl kunene virus: a novel tomato-infecting monopartite begomovirus from namibia. *Arch. Virol.* 165, 1887–1889. doi: 10.1007/s00705-020-04666-8

Levitzky, N., Smith, E., Lachman, O., Luria, N., Mizrahi, Y., Bakelman, H., et al. (2019). The bumblebee bombus terrestris carries a primary inoculum of tomato brown rugose fruit virus contributing to disease spread in tomatoes. *PLoS One* 14:e0210871. doi: 10.1371/journal.pone.0210871

Li, C. X., Shi, M., Tian, J. H., Lin, X. D., Kang, Y. J., Chen, L. J., et al. (2015). Unprecedented genomic diversity of RNA viruses in arthropods reveals the ancestry of negative-sense RNA viruses. *Elife* 4:e05378. doi: 10.7554/eLife.05378

Li, R., Gao, S., Fei, Z., and Ling, K.-S. (2013). Complete genome sequence of a new tobamovirus naturally infecting tomatoes in Mexico. *Genome Announc.* 1, e713–e794. doi: 10.1128/genomeA.00794-13

Li, R., Gao, S., Hernandez, A. G., Wechter, W. P., Fei, Z., and Ling, K.-S. (2012). Deep sequencing of small RNAs in tomato for virus and viroid identification and strain differentiation. *PLoS One* 7:e37127. doi: 10.1371/journal.pone.0037127

Li, Y., Wang, Y., Hu, J., Xiao, L., Tan, G., Lan, P., et al. (2017). The complete genome sequence, occurrence and host range of tomato mottle mosaic virus chinese isolate. *Virol. J.* 14:15. doi: 10.1186/s12985-016-0676-2

Ling, K.-S., Tian, T., Gurung, S., Salati, R., and Gilliard, A. (2019). First report of tomato brown rugose fruit virus infecting greenhouse tomato in the united states. *Plant Dis.* 103:1439. doi: 10.1094/pdis-11-18-1959-pdn

Ling, K.-S., and Zhang, W. (2011). First report of pepino mosaic virus infecting tomato in Mexico. *Plant Dis.* 95, 1035–1035. doi: 10.1094/PDIS-04-11-0334

Llamas-Llamas, M. E., Zavaleta-Mejia, E., Gonzalez-Hernandez, V. A., Cervantes-Diaz, L., Santizo-Rincon, J. A., and Ochoa-Martinez, D. L. (1998). Effect of temperature on symptom expression and accumulation of tomato spotted wilt virus in different host species. *Plant Pathol.* 47, 341–347. doi: 10.1046/j.1365-3059.1998.00249.x

Lovelock, D. A., Kinoti, W. M., Bottcher, C., Wildman, O., Dall, D., Rodoni, B. C., et al. (2020). Tomato mottle mosaic virus intercepted by australian biosecurity in capsicum annuum seed. *Aust. Plant Dis. Notes* 15:8. doi: 10.1007/s13314-020-0378-x

Luria, N., Smith, E., Reingold, V., Bekelman, I., Lapidot, M., Levin, I., et al. (2017). A new Israeli tobamovirus isolate infects tomato plants harboring Tm-22 resistance genes. *PLoS One* 12:e0170429. doi: 10.1371/journal.pone.0170429

Ma, Y., Marais, A., Lefebvre, M., Faure, C., and Candresse, T. (2020). Metagenomic analysis of virome cross-talk between cultivated *Solanum lycopersicum* and wild *Solanum nigrum*. *Virology* 540, 38–44. doi: 10.1016/j.virol.2019.11.009

Ma, Y., Marais, A., Lefebvre, M., Theil, S., Svanella-Dumas, L., Faure, C., et al. (2019). Phytovirome analysis of wild plant populations: comparison of double-stranded RNA and virion-associated nucleic acid metagenomic approaches. *J. Virol.* 94, e1419–e1462. doi: 10.1128/JVI.01462-19

Mabvakure, B., Martin, D. P., Kraberger, S., Cloete, L., van Brunschot, S., Geering, A. D. W., et al. (2016). Ongoing geographical spread of tomato yellow leaf curl virus. *Virology* 498, 257–264. doi: 10.1016/j.virol.2016.08.033

Macedo, M. A., Albuquerque, L. C., Maliano, M. R., Souza, J. O., Rojas, M. R., Inoue-Nagata, A. K., et al. (2018). Characterization of tomato leaf curl purple vein virus, a new monopartite new world begomovirus infecting tomato in northeast Brazil. *Arch. Virol.* 163, 737–743. doi: 10.1007/s00705-017-3662-0

Macharia, I., Backhouse, D., Wu, S. B., and Ateka, E. M. (2016). Weed species in tomato production and their role as alternate hosts of tomato spotted wilt virus and its vector frankliniella occidentalis. *Ann. Appl. Biol.* 169, 224–235. doi: 10.1111/aab.12297

Mackie, A. E., Barbetti, M. J., Rodoni, B., McKirdy, S. J., and Jones, R. A. C. (2019). Effects of a potato spindle tuber viroid tomato strain on the symptoms, biomass, and yields of classical indicator and currently grown potato and tomato cultivars. *Plant Dis.* 103, 3009–3017. doi: 10.1094/PDIS-02-19-0312-RE

Mackie, A. E., Rodoni, B. C., Barbetti, M. J., McKirdy, S. J., and Jones, R. A. C. (2016). Potato spindle tuber viroid: alternative host reservoirs and strain found in a remote subtropical irrigation area. *Eur. J. Plant Pathol.* 145, 433–446. doi: 10.1007/s10658-016-0857-2

Maddahian, M., Massumi, H., Heydarnejad, J., Hosseini Pour, A., and Varsani, A. (2017). Characterization of iranian tomato aspermy virus isolates with a variant 2b gene sequence. *Trop. Plant Pathol.* 42, 475–484. doi: 10.1007/s40858-017-0173-1

Malmstrom, C. M., and Alexander, H. M. (2016). Effects of crop viruses on wild plants. *Curr. Opin. Virol.* 19, 30–36. doi: 10.1016/j.coviro.2016.06.008

Márquez-Martín, B., Aragón-Caballero, L., Fiallo-Olivé, E., Navas-Castillo, J., and Moriones, E. (2011). Tomato leaf deformation virus, a novel begomovirus associated with a severe disease of tomato in Peru. *Eur. J. Plant Pathol.* 129, 1–7. doi: 10.1007/s10658-010-9699-5

Márquez-Martín, B., Maeso, D., Martínez-Ayala, A., Bernal, R., Teresa Federici, M., Vincelli, P., et al. (2012). Diverse population of a new bipartite begomovirus infecting tomato crops in uruguay. *Arch. Virol.* 157, 1137–1142. doi: 10.1007/s00705-012-1262-6

Martínez-Ayala, A., Sánchez-Campos, S., Cáceres, F., Aragón-Caballero, L., Navas-Castillo, J., and Moriones, E. (2014). Characterisation and genetic diversity of pepper leafroll virus, a new bipartite begomovirus infecting pepper, bean and tomato in Peru. *Ann. Appl. Biol.* 164, 62–72. doi: 10.1111/aab.12074

Massart, S., Candresse, T., Gil, J., Lacomme, C., Predajna, L., Ravnikar, M., et al. (2017). A framework for the evaluation of biosecurity, commercial, regulatory, and scientific impacts of plant viruses and viroids identified by NGS technologies. *Front. Microbiol.* 8:45. doi: 10.3389/fmicb.2017.00045

Massart, S., Chiumenti, M., De Jonghe, K., Glover, R., Haegeman, A., Koloniuk, I., et al. (2019). Virus detection by high-throughput sequencing of small RNAs: Large-scale performance testing of sequence analysis strategies. *Phytopathology* 109, 488–497. doi: 10.1094/PHYTO-02-18-0067-R

Masuta, C. (2014). Molecular biology of cucumber mosaic virus and its satellite RNA. *J. Gen. Plant Pathol.* 80, 514–518. doi: 10.1007/s10327-014-0547-x

Mavrič, I., Tušek Žnidarič, M., Virščck Marn, M., Dolničar, P., Mehle, N., Lesemann, D.-E., et al. (2006). First report of eggplant mottled dwarf virus in potato and tomato in Slovenia. *Plant Pathol.* 55, 566. doi: 10.1111/j.1365-3059.2006.01414.x

McLeish, M. J., Fraile, A., and García-Arenal, F. (2020a). Population genomics of plant viruses: the ecology and evolution of virus emergence. *Phytopathology* 111, 32–39. doi: 10.1094/PHYTO-08-20-0355-FI

McLeish, M. J., Fraile, A., and García-Arenal, F. (2020b). Trends and gaps in forecasting plant virus disease risk. *Ann. Appl. Biol.* 176, 102–108. doi: 10.1111/aab.12553

Mehle, N., Gutiérrez-Aguirre, I., Kutnjak, D., and Ravnikar, M. (2018). Water-mediated transmission of plant, animal, and human viruses. *Adv. Virus Res.* 101, 85–128. doi: 10.1016/bs.aivir.2018.02.004

Mehle, N., Gutiérrez-Aguirre, I., Prezelj, N., Delić, D., Vidic, U., and Ravnikar, M. (2014). Survival and transmission of potato virus Y, pepino mosaic virus, and potato spindle tuber viroid in water. *Appl. Environ. Microbiol.* 80, 1455–1462. doi: 10.1128/AEM.03349-13

Mehle, N., Kogovšek, P., Rački, N., Jakomin, T., Gutiérrez-Aguirre, I., Kramberger, P., et al. (2017). Filling the gaps in diagnostics of *Pepino mosaic virus* and *Potato spindle tuber viroid* in water and tomato seeds and leaves. *Plant Pathol.* 66, 1191–1201. doi: 10.1111/ppa.12710

Mehle, N., and Ravnikar, M. (2012). Plant viruses in aqueous environment - survival, water mediated transmission and detection. *Water Res.* 46, 4902–4917. doi: 10.1016/j.watres.2012.07.027

Melgarejo, T. A., Kon, T., Rojas, M. R., Paz-Carrasco, L., Zerbini, F. M., and Gilbertson, R. L. (2013). Characterization of a new world monopartite begomovirus causing leaf curl disease of tomato in ecuador and peru reveals a new direction in geminivirus evolution. *J. Virol.* 87, 5397–5413. doi: 10.1128/jvi.00234-13

Melo, F. L., Fernandes, J. E. A., Ribeiro, B. M., and Ribeiro, S. G. (2014). Complete genome sequence of a tobacco-infecting, tomato blistering mosaic virus. *Genome Announc.* 2, 701–715. doi: 10.1128/genomeA.00701-14

Melzer, M. J., Sugano, J. S., Cabanas, D., Dey, K. K., Kandouh, B., Mauro, D., et al. (2012). First report of pepper mottle virus infecting tomato in Hawaii. *Plant Dis.* 96:917. doi: 10.1094/PDIS-02-12-0147-PDN

Méndez-Lozano, J., Magallanes-Tapia, M. A., Romero-Romero, J. L., Camacho-Beltrán, E., Vega, W. L. O., Leyva-López, N. E., et al. (2012). Tomato infectious chlorosis virus associated with tomato diseases in baja california, mexico. *Plant Dis.* 96:1229. doi: 10.1094/PDIS-02-12-0196-PDN

Menzel, W., Knierim, D., Winter, S., Hamacher, J., and Heupel, M. (2019). First report of tomato brown rugose fruit virus infecting tomato in Germany. *New Dis. Rep.* 39:1. doi: 10.5197/j.2044-0588.2019.039.001

Menzel, W., Richert-Pöggeler, K. R., Winter, S., and Knierim, D. (2018). Characterization of a nucleorhabdovirus from physostegia. *Acta Hortic.* 1193, 29–38. doi: 10.17660/ActaHortic.2018.1193.5

Mochizuki, T., and Ohki, S. T. (2012). Cucumber mosaic virus: viral genes as virulence determinants. *Mol. Plant Pathol.* 13, 217–225. doi: 10.1111/j.1364-3703.2011.00749.x

Moodley, V., Gubba, A., and Mafongoya, P. L. (2016). First report of tomato torrado virus on tomato (*Solanum lycopersicum*) in south africa. *Plant Dis.* 100:231. doi: 10.1094/PDIS-06-15-0683-PDN

Moodley, V., Gubba, A., and Mafongoya, P. L. (2019). A survey of whitefly-transmitted viruses on tomato crops in south africa. *Crop Prot.* 123, 21–29.

Moodley, V., Gubba, A., and Mafongoya, P. L. (2020). Emergence and full genome analysis of tomato torrado virus in south africa. *Viruses* 12:1167. doi: 10.3390/v12101167

Moreno-Perez, M. G., Pagan, I., Aragon-Caballero, L., Caceres, F., Fraile, A., and Garcia-Arenal, F. (2014). Ecological and genetic determinants of pepino mosaic virus emergence. *J. Virol.* 88, 3359–3368. doi: 10.1128/JVI.02980-13

Moriones, E., Praveen, S., and Chakraborty, S. (2017). Tomato leaf curl new delhi virus: an emerging virus complex threatening vegetable and fiber crops. *Viruses* 9:264. doi: 10.3390/v9100264

Moury, B., Gebre Selassie, K., Marchoux, G., Daubčze, A. M., and Palloix, A. (1998). High temperature effects on hypersensitive resistance to tomato spotted wilt tospovirus (TSWV) in pepper (capsicum chinense jacq.). *Eur. J. Plant Pathol.* 104, 489–498. doi: 10.1023/A:1008618022144

Nagai, A., Duarte, L. M. L., Chaves, A. L. R., Peres, L. E. P., and dos Santos, D. Y. A. C. (2019). Tomato mottle mosaic virus in brazil and its relationship with Tm-22 gene. *Eur. J. Plant Pathol.* 155, 353–359. doi: 10.1007/s10658-019-01762-7

Nava, A., Londoño, A., and Polston, J. E. (2013). Characterization and distribution of tomato yellow margin leaf curl virus, a begomovirus from venezuela. *Arch. Virol.* 158, 399–406. doi: 10.1007/s00705-012-1501-x

Navarro, B., Gisel, A., Rodio, M.-E., Delgado, S., Flores, R., and Di Serio, F. (2012). Viroids: how to infect a host and cause disease without encoding proteins. *Biochimie* 94, 1474–1480. doi: 10.1016/j.biochi.2012.02.020

Navarro, B., Silletti, M. R., Trisciuzzi, V. N., and Di Serio, F. (2009). Identification and characterization of potato spindle tuber viroid infecting tomato in italy. *J. Plant Pathol.* 91, 723–726.

Navas-Castillo, J., Fiallo-Olivé, E., and Sánchez-Campos, S. (2011). Emerging virus diseases transmitted by whiteflies. *Annu. Rev. Phytopathol.* 49, 219–248. doi: 10.1146/annurev-phyto-072910-095235

NIH-NHGRI (2019). *DNA sequencing costs: data*. Available Online at: https://www.genome.gov/about-genomics/fact-sheets/DNA-Sequencing-Costs-Data [Accessed July 8, 2020]

Nikolić, D., Vučurović, A., Stanković, I., Radović, N., Zečević, K., Bulajić, A., et al. (2018). Viruses affecting tomato crops in Serbia. *Eur. J. Plant Pathol.* 152, 225–235. doi: 10.1007/s10658-018-1467-y

Noël, P., Hance, T., and Bragard, C. (2014). Transmission of the pepino mosaic virus by whitefly. *Eur. J. Plant Pathol.* 138, 23–27. doi: 10.1007/s10658-013-0313-5

Oerke, E. C. (2006). Crop losses to pests. *J. Agric. Sci.* 144, 31–43. doi: 10.1017/S0021859605005708

Oh, J., Lee, H.-K., Park, C.-Y., Yeom, Y.-A., Min, H.-G., Yang, H.-J., et al. (2018). First report of southern tomato virus in tomato (*Solanum lycopersicum*) in Korea. *Plant Dis.* 102:1467. doi: 10.1094/PDIS-09-17-1499-PDN

Okada, K., Kusari, S., Kawaratani, M., Negoro, J., Ohki, S. T., and Osaki, T. (2000). Tobacco mosaic virus is transmissible from tomato to tomato by pollinating bumblebees. *J. Gen. Plant Pathol.* 66, 71–74. doi: 10.1007/pl00012924

Oladokun, J. O., Halabi, M. H., Barua, P., and Nath, P. D. (2019). Tomato brown rugose fruit disease: current distribution, knowledge and future prospects. *Plant Pathol.* 68, 1579–1586. doi: 10.1111/ppa.13096

Oliver, J. E., and Whitfield, A. E. (2016). The genus tospovirus: emerging bunyaviruses that threaten food security. *Annu. Rev. Virol.* 3, 101–124. doi: 10.1146/annurev-virology-100114-055036

Ong, S. N., Taheri, S., Othman, R. Y., and Teo, C. H. (2020). Viral disease of tomato crops (*Solanum lycopesicum* L.): an overview. *J. Plant Dis. Prot.* 127, doi: 10.1007/s41348-020-00330-0

Orfanidou, C. G., Dimitriou, C., Papayiannis, L. C., Maliogka, V. I., and Katis, N. I. (2014). Epidemiology and genetic diversity of criniviruses associated with tomato yellows disease in Greece. *Virus Res.* 186, 120–129. doi: 10.1016/j.virusres.2013.12.013

Ouattara, A., Tiendrébéogo, F., Lefeuvre, P., Claverie, S., Hoareau, M., Traoré, E. V., et al. (2017). Tomato leaf curl burkina faso virus: a novel tomato-infecting monopartite begomovirus from burkina faso. *Arch. Virol.* 162, 1427–1429. doi: 10.1007/s00705-017-3231-6

Padidam, M., Beachy, R. N., and Fauquet, C. M. (1995). Tomato leaf curl geminivirus from India has a bipartite genome and coat protein is not essential for infectivity. *J. Gen. Virol.* 76, 25–35. doi: 10.1099/0022-1317-76-1-25

Padmanabhan, C., Zheng, Y., Li, R., Martin, G. B., Fei, Z., and Ling, K. S. (2015a). Complete genome sequence of a tomato-infecting tomato mottle mosaic virus in New York. *Genome Announc.* 3, 151–152. doi: 10.1128/genomeA.01523-15

Padmanabhan, C., Zheng, Y., Li, R., Sun, S.-E., Zhang, D., Liu, Y., et al. (2015b). Complete genome sequence of southern tomato virus identified in china using next-generation sequencing. *Genome Announc.* 3, 1226–1241. doi: 10.1128/genomeA.01226-15

Padmanabhan, C., Zheng, Y., Li, R., Fei, Z., and Ling, K.-S. (2015c). Complete genome sequence of southern tomato virus Naturally infecting tomatoes in bangladesh. *Genome. Announc.* 3, 1522–1537. doi: 10.1128/genomeA.01522-15

Palukaitis, P., and García-Arenal, F. (2003). Cucumoviruses. *Adv. Virus Res.* 62, 241–323. doi: 10.1016/S0065-3527(03)62005-1

Pan, H., Chu, D., Yan, W., Su, Q., Liu, B., Wang, S., et al. (2012). Rapid spread of tomato yellow leaf curl virus in china is aided differentially by two invasive whiteflies. *PLoS One* 7:e34817. doi: 10.1371/journal.pone.0034817

Panno, S., Caruso, A. G., and Davino, S. (2019). First report of tomato brown rugose fruit virus on tomato crops in italy. *Plant Dis.* 103:1443. doi: 10.1094/PDIS-12-18-2254-PDN

Papayiannis, L. C., Katis, N. I., Idris, A. M., and Brown, J. K. (2011). Identification of weed hosts of tomato yellow leaf curl virus in cyprus. *Plant Dis.* 95, 120–125. doi: 10.1094/PDIS-05-10-0346

Parrella, G. (2020). Sources of resistance in wild solanum germplasm (*Section lycopersicon*) to parietaria mottle virus, an emerging virus in the mediterranean basin. *Plant Pathol.* 69, 1018–1025. doi: 10.1111/ppa.13194

Parrella, G., Gognalons, P., Gebre-Selassie, K., Vovlas, C., and Marchoux, G. (2003). An update of the host range of tomato spotted wilt virus. *J. Plant Pathol.* 85, 227–264.

Parrella, G., Troiano, E., Cherchi, C., and Giordano, P. (2020). Severe outbreaks of parietaria mottle virus in tomato in sardinia, southern Italy. *J. Plant Pathol.* 102:915. doi: 10.1007/s42161-020-00492-8

Pechinger, K., Chooi, K. M., Macdiarmid, R. M., Ziebell, H., and Harper, S. J. (2019). A new era for mild strain cross-protection. *Viruses* 11, 1–17. doi: 10.3390/v11070670

Pecman, A., Kutnjak, D., Gutiérrez-Aguirre, I., Adams, I., Fox, A., Boonham, N., et al. (2017). Next generation sequencing for detection and discovery of plant viruses and viroids: comparison of two approaches. *Front. Microbiol.* 8:1998. doi: 10.3389/fmicb.2017.01998

Pecman, A., Kutnjak, D., Mehle, N., Žnidarič, M. T., Gutiérrez-Aguirre, I., Pirnat, P., et al. (2018). High-throughput sequencing facilitates characterization of a "forgotten" plant virus: the case of a henbane mosaic virus infecting tomato. *Front. Microbiol.* 9:2739. doi: 10.3389/fmicb.2018.02739

Pfitzner, A. J. P. (2006). ""Resistance to Tobacco Mosaic Virus and Tomato Mosaic Virus in Tomato," in *Natural Resistance Mechanisms of Plants to Viruses*, eds G. Loebenstein and J. P. Carr (Dordrecht: Springer), 399–413.

Poudel, B., Abdalla, O. A., Liu, Q., Wang, Q., McAvoy, E., Seal, D., et al. (2019). Field distribution and disease incidence of tomato chlorotic spot virus, an emerging virus threatening tomato production in south Florida. *Trop. Plant Pathol.* 44, 430–437. doi: 10.1007/s40858-019-00305-z

Prajapat, R., Marwal, A., and Gaur, R. K. (2014). Begomovirus associated with alternative host weeds: a critical appraisal. *Arch. Phytopathol. Plant Prot.* 47, 157–170. doi: 10.1080/03235408.2013.805497

Prasad, A., Sharma, N., Hari-Gowthem, G., Muthamilarasan, M., and Prasad, M. (2020). Tomato yellow leaf curl virus: impact, challenges, and management. *Trends Plant Sci.* 25, 897–911. doi: 10.1016/j.tplants.2020.03.015

Prins, M., and Goldbach, R. (1998). The emerging problem of tospovirus infection and nonconventional methods of control. *Trends Microbiol.* 6, 31–35. doi: 10.1016/S0966-842X(97)01173-6

Quadros, A. F. F., Silva, J. P., Xavier, C. A. D., Zerbini, F. M., and Boari, A. J. (2019). Two new begomoviruses infecting tomato and hibiscus sp. in the amazon region of Brazil. *Arch. Virol.* 164, 1897–1901. doi: 10.1007/s00705-019-04245-6

Quenouille, J., Vassilakos, N., and Moury, B. (2013). Potato virus Y: a major crop pathogen that has provided major insights into the evolution of viral pathogenicity. *Mol. Plant Pathol.* 14, 439–452. doi: 10.1111/mpp.12024

Ramos, R. S., Kumar, L., Shabani, F., and Picanço, M. C. (2019). Risk of spread of tomato yellow leaf curl virus (TYLCV) in tomato crops under various climate change scenarios. *Agric. Syst.* 173, 524–535. doi: 10.1016/j.agsy.2019.03.020

Rao, A. L. N., and Kalantidis, K. (2015). Virus-associated small satellite RNAs and viroids display similarities in their replication strategies. *Virology* 479–480, 627–636. doi: 10.1016/j.virol.2015.02.018

Rego-Machado, C. M., Nakasu, E. Y. T., Blawid, R., Nagata, T., and Inoue-Nagata, A. K. (2019). Complete genome sequence of a new bipartite begomovirus infecting tomato in Brazil. *Arch. Virol.* 164, 2873–2875. doi: 10.1007/s00705-019-04380-0

Revers, F., and García, J. A. (2015). Chapter three - molecular biology of potyviruses. *Adv. Virus Res.* 92, 101–199. doi: 10.1016/bs.aivir.2014.11.006

Riley, D. G., Joseph, S. V., Srinivasan, R., and Diffie, S. (2011). Thrips vectors of tospoviruses. *J. Integr. Pest Manag.* 2, I1–I10. doi: 10.1603/IPM10020

Roberts, J. M. K., Ireland, K. B., Tay, W. T., and Paini, D. (2018). Honey bee-assisted surveillance for early plant virus detection. *Ann. Appl. Biol.* 173, 285–293. doi: 10.1111/aab.12461

Rojas, M. R., and Gilbertson, R. L. (2008). *"Emerging plant viruses: a diversity of mechanisms and opportunities," in Plant virus evolution*. Amsterdam: Springer, 27–51.

Romay, G., Chirinos, D. T., Geraud-Pouey, F., Gillis, A., Mahillon, J., and Bragard, C. (2018). Complete genome sequence of two tomato-infecting begomoviruses in Venezuela: evidence of a putative novel species and a novel recombinant strain. *Arch. Virol.* 163, 555–558. doi: 10.1007/s00705-017-3611-y

Romay, G., Geraud-Pouey, F., Chirinos, D., Mahillon, M., Gillis, A., Mahillon, J., et al. (2019). Tomato twisted leaf virus: a novel indigenous new world monopartite begomovirus infecting tomato in Venezuela. *Viruses* 11:327. doi: 10.3390/v11040327

Roossinck, M. J. (2017). Deep sequencing for discovery and evolutionary analysis of plant viruses. *Virus Res.* 239, 82–86. doi: 10.1016/j.virusres.2016.11.019

Rymelska, N., Borodynko, N., Pospieszny, H., and Hasiów-Jaroszewska, B. (2013). Analysis of the biological and molecular variability of the polish isolates of tomato black ring virus (TBRV). *Virus Genes* 47, 338–346. doi: 10.1007/s11262-013-0941-z

Sabanadzovic, S., Valverde, R. A., Brown, J. K., Martin, R. R., and Tzanetakis, I. E. (2009). Southern tomato virus: the link between the families totiviridae and partitiviridae. *Virus Res.* 140, 130–137. doi: 10.1016/j.virusres.2008.11.018

Salem, N., Mansour, A., Ciuffo, M., Falk, B. W., and Turina, M. (2016). A new tobamovirus infecting tomato crops in Jordan. *Arch. Virol.* 161, 503–506. doi: 10.1007/s00705-015-2677-7

Saqib, M., Wylie, S. J., and Jones, M. G. K. (2015). Serendipitous identification of a new Iflavirus -like virus infecting tomato and its subsequent characterization. *Plant Pathol.* 64, 519–527. doi: 10.1111/ppa.12293

Sastry, K. S. (2013). *Plant Virus and Viroid Diseases in the Tropics*. Dordrecht: Springer.

Sastry, K. S., Mandal, B., Hammond, J., Scott, S. W., and Briddon, R. W. (2019). *Encyclopedia of Plant Viruses and Viroids*. New Delhi: Springer.

Savary, S., Willocquet, L., Pethybridge, S. J., Esker, P., McRoberts, N., and Nelson, A. (2019). The global burden of pathogens and pests on major food crops. *Nat. Ecol. Evol.* 3, 430–439. doi: 10.1038/s41559-018-0793-y

Schenk, M. F., Hamelink, R., van der Vlugt, R. A. A., Vermunt, A. M. W., Kaarsenmaker, R. C., and Stijger, I. C. C. M. M. (2010). The use of attenuated isolates of pepino mosaic virus for cross-protection. *Eur. J. Plant Pathol.* 127, 249–261. doi: 10.1007/s10658-010-9590-4

Scussel, S., Claverie, S., Hoareau, M., Moustache, R., Delatte, H., Lefeuvre, P., et al. (2018). Tomato leaf curl mahé virus: a novel tomato-infecting monopartite begomovirus from the seychelles. *Arch. Virol.* 163, 3451–3453. doi: 10.1007/s00705-018-4007-3

Seepiban, C., Gajanandana, O., Attathom, T., and Attathom, S. (2011). Tomato necrotic ringspot virus, a new tospovirus isolated in Thailand. *Arch. Virol.* 156, 263–274. doi: 10.1007/s00705-010-0856-0

Sevik, M. A., and Arli-Sokmen, M. (2012). Estimation of the effect of Tomato spotted wilt virus (TSWV) infection on some yield components of tomato. *Phytoparasitica* 40, 87–93. doi: 10.1007/s12600-011-0192-2

Sharma, P., Matsuda, N., Bajet, N. B., and Ikegami, M. (2011). Molecular analysis of new isolates of tomato leaf curl philippines virus and an associated betasatellite occurring in the Philippines. *Arch. Virol.* 156, 305–312. doi: 10.1007/s00705-010-0837-3

Sharma, S., Sharma, A., and Kaur, S. I. (2019). Occurrence of pepper mottle virus on tomato in India. *Virus Dis.* 30, 474–475. doi: 10.1007/s13337-019-00543-4

Sharman, M., Thomas, J. E., Tree, D., and Persley, D. M. (2020). Natural host range and thrips transmission of capsicum chlorosis virus in Australia. *Aust. Plant Pathol.* 49, 45–51. doi: 10.1007/s13313-019-00675-7

Shates, T. M., Sun, P., Malmstrom, C. M., Dominguez, C., and Mauck, K. E. (2019). Addressing research needs in the field of plant virus ecology by defining knowledge gaps and developing wild dicot study systems. *Front. Microbiol.* 9:3305. doi: 10.3389/fmicb.2018.03305

Sherwood, J. L., German, T. L., Moyer, J. W., and Ullman, D. E. (2003). Tomato spotted wilt. *Plant Heal. Instr.* doi: 10.1094/PHI-I-2003-0613-02

Skelton, A., Buxton-Kirk, A., Ward, R., Harju, V., Frew, L., Fowkes, A., et al. (2019). First report of Tomato brown rugose fruit virus in tomato in the united kingdom. *New Dis. Rep.* 40:12. doi: 10.5197/j.2044-0588.2019.040.012

Škoric, D., Krajacic, M., Barbarossa, L., Cillo, F., Grieco, F., Šaric, A., et al. (1996). Occurrence of cucumber mosaic cucumovirus with satellite RNA in lethal necrosis affected tomatoes in croatia. *J. Phytopathol.* 144, 543–549. doi: 10.1111/j.1439-0434.1996.tb00296.x

Soler, S., Prohens, J., López, C., Aramburu, J., Galipienso, L., and Nuez, F. (2010). Viruses infecting tomato in valčncia, spain: occurrence, distribution and effect of seed origin. *J. Phytopathol.* 158, 797–805. doi: 10.1111/j.1439-0434.2010.01706.x

Souiri, A., Khataby, K., Kasmi, Y., Zemzami, M., Amzazi, S., and Ennaji, M. M. (2019). "Emerging and reemerging viral diseases of solanaceous crops and management strategies for detection and eradication," in *Emerging and Reemerging Viral Pathogens*, ed. M. M. Ennaji (Cambridge, MA: Elsevier), 847–877.

Souza, T. A., Silva, J. M. F., Nagata, T., Martins, T. P., Nakasu, E. Y. T., and Inoue-Nagata, A. K. (2020). A temporal diversity analysis of brazilian begomoviruses in tomato reveals a decrease in species richness between 2003 and 2016. *Front. Plant Sci.* 11:1201. doi: 10.3389/fpls.2020.01201

Stanković, I., Vučurović, A., Zečević, K., Petrović, B., Nikolić, D., and Delibašić, G. (2021). Characterization of cucumber mosaic virus and its satellite RNAs associated with tomato lethal necrosis in Serbia. *Eur. J. Plant Pathol.* doi: 10.1007/s10658-021-02241-8

Stanković, I., Vučurović, A., Zečević, K., Petrović, B., Ristic, D., Vucurovic, I., et al. (2020). Short communication: pepino mosaic virus, a new threat for Serbia's tomatoes. *Spanish J. Agric. Res.* 18:e10SC05. doi: 10.5424/sjar/2020184-16244

Stansly, P. A., Naranjo, S. E., Brown, J. K., Horowitz, A. R., Legg, J. P., Polston, J. E., et al. (2010). *Bemisia: Bionomics and Management of a Global Pest*. Netherlands: Springer.

Sui, X., McGrath, M. T., Zhang, S., Wu, Z., and Ling, K.-S. (2017). First report of tomato chlorotic spot virus infecting tomato in New York. *Plant Dis.* 102:460. doi: 10.1094/PDIS-07-17-0991-PDN

Sui, X., Zheng, Y., Li, R., Padmanabhan, C., Tian, T., Groth-Helms, D., et al. (2016). Molecular and biological characterization of tomato mottle mosaic virus and development of RT-PCR detection. *Plant Dis.* 101, 704–711. doi: 10.1094/PDIS-10-16-1504-RE

Tepfer, M., and García-Arenal, F. (2019). "Chapter 3: Epidemiology and Ecology," in *Cucumber Mosaic Virus*, (Saint Paul,MN: The American Phytopathological Society), 37–45.

Thompson, J. R., Dasgupta, I., Fuchs, M., Iwanami, T., Karasev, A. V., Petrzik, K., et al. (2017). ICTV virus taxonomy profile: secoviridae. *J. Gen. Virol.* 98, 529–531. doi: 10.1099/jgv.0.000779

Torres, R., Larenas, J., Fribourg, C., and Romero, J. (2012). Pepper necrotic spot virus, a new tospovirus infecting solanaceous crops in Peru. *Arch. Virol.* 157, 609–615. doi: 10.1007/s00705-011-1217-3

Trebicki, P. (2020). Climate change and plant virus epidemiology. *Virus Res.* 286:198059. doi: 10.1016/j.virusres.2020.198059

Tsai, W. S., Abdourhamane, I. K., and Kenyon, L. (2010). First report of pepper veinal mottle virus associated with mosaic and mottle diseases of tomato and pepper in Mali. *Plant Dis.* 94, 378–378. doi: 10.1094/PDIS-94-3-0378B

Turina, M., Geraats, B. P. J., and Ciuffo, M. (2016a). First report of tomato mottle mosaic virus in tomato crops in Israel. *New Dis. Rep.* 33:1. doi: 10.5197/j.2044-0588.2016.033.001

Turina, M., Kormelink, R., and Resende, R. O. (2016b). Resistance to tospoviruses in vegetable crops: epidemiological and molecular aspects. *Annu. Rev. Phytopathol.* 54, 347–371. doi: 10.1146/annurev-phyto-080615-095843

Tzanetakis, I. E., Martin, R. R., and Wintermantel, W. M. (2013). Epidemiology of criniviruses: an emerging problem in world agriculture. *Front. Microbiol.* 4:119. doi: 10.3389/fmicb.2013.00119

Tzanetakis, I. E., Sabanadzovic, S., and Valverde, R. A. (2020). *"Amalgaviruses (Amalgaviridae)," in Reference Module in Life Sciences*. Amsterdam: Elsevier.

Vaghi Medina, C. G., Bornancini, V. A., and López Lambertini, P. M. (2020). Tomato vein clearing leaf deformation virus, a new begomovirus species infecting tomato in Argentina. *Eur. J. Plant Pathol.* 156, 285–290. doi: 10.1007/s10658-019-01835-7

Vaghi Medina, C. G., and López Lambertini, P. M. (2012). Tomato dwarf leaf virus, a new world begomovirus infecting tomato in Argentina. *Arch. Virol.* 157, 1975–1980. doi: 10.1007/s00705-012-1355-2

Vaghi Medina, C. G., Martin, D. P., and López Lambertini, P. M. (2015). Tomato mottle wrinkle virus, a recombinant begomovirus infecting tomato in Argentina. *Arch. Virol.* 160, 581–585. doi: 10.1007/s00705-014-2216-y

Vaghi Medina, C. G., Teppa, E., Bornancini, V. A., Flores, C. R., Marino-Buslje, C., and López Lambertini, P. M. (2018). Tomato apical leaf curl virus: a novel, monopartite geminivirus detected in tomatoes in Argentina. *Front. Microbiol.* 8:2665. doi: 10.3389/fmicb.2017.02665

Valles, S. M., Chen, Y., Firth, A. E., Guérin, D. M. A., Hashimoto, Y., Herrero, S., et al. (2017). ICTV virus taxonomy profile: iflaviridae. *J. Gen. Virol.* 98, 527–528. doi: 10.1099/jgv.0.000757

Van Bogaert, N., Smagghe, G., and De Jonghe, K. (2015). The role of weeds in the epidemiology of pospiviroids. *Weed Res.* 55, 631–638. doi: 10.1111/wre.12173

van Brunschot, S. L., Persley, D. M., Roberts, A., and Thomas, J. E. (2014a). First report of pospiviroids infecting ornamental plants in australia: potato spindle tuber viroid in solanum laxum (synonym S. jasminoides) and citrus exocortis viroid in petunia spp. *New Dis. Rep.* 29:3. doi: 10.5197/j.2044-0588.2014.029.003

van Brunschot, S. L., Verhoeven, J. T. J., Persley, D. M., Geering, A. D. W., Drenth, A., and Thomas, J. E. (2014b). An outbreak of potato spindle tuber viroid in tomato is linked to imported seed. *Eur. J. Plant Pathol.* 139, 1–7. doi: 10.1007/s10658-014-0379-8

van de Vossenberg, B. T. L. H., Visser, M., Bruinsma, M., Koenraadt, H. M. S., Westenberg, M., and Botermans, M. (2020). Real-time tracking of tomato brown rugose fruit virus (ToBRFV) outbreaks in the netherlands using nextstrain. *PLoS One* 15:e0234671. doi: 10.1371/journal.pone.0234671

van der Vlugt, R. A. A., Stijger, C., Verhoeven, J. T. J., and Lesemann, D.-E. (2000). First report of pepino mosaic virus on tomato. *Plant Dis.* 84:103. doi: 10.1094/pdis.2000.84.1.103c

van der Vlugt, R. A. A., and Stijger, C. C. M. M. (2021). *Pepino Mosaic Virus (Alphaflexiviridae), in Encyclopedia of Virology*. Amsterdam: Elsevier, 539–544.

Varanda, C. M. R., Nolasco, G., Clara, M. I., and Félix, M. R. (2014). Genetic diversity of the coat protein of olive latent virus 1 isolates. *Arch. Virol.* 159, 1351–1357. doi: 10.1007/s00705-013-1953-7

Verbeek, M., and Dullemans, A. M. (2012). First report of tomato torrado virus infecting tomato in colombia. *Plant Dis.* 96, 592–592. doi: 10.1094/PDIS-11-11-1000

Verbeek, M., Dullemans, A. M., Espino, A., Botella, M., Alfaro-Fernández, A., and Font, M. I. (2015). First report of southern tomato virus in tomato in the canary islands, spain. *J. Plant Pathol.* 97:392. doi: 10.4454/JPP.V97I2.038

Verbeek, M., Dullemans, A. M., Van Den Heuvel, J. F. J. M., Maris, P. C., and Van Der Vlugt, R. A. A. (2007). Identification and characterisation of tomato torrado virus, a new plant picorna-like virus from tomato. *Arch. Virol.* 152, 881–890. doi: 10.1007/s00705-006-0917-6

Verbeek, M., Dullemans, A. M., van den Heuvel, J. F. J. M., Maris, P. C., and van der Vlugt, R. A. A. (2008). Tomato marchitez virus, a new plant picorna-like virus from tomato related to tomato torrado virus. *Arch. Virol.* 153, 127–134. doi: 10.1007/s00705-007-1076-0

Verdin, E., Gentit, P., Steyer, S., Wetzel, T., Le Bourgeois, T., Balesdent, M.-H., et al. (2020). *Évaluation du risque simplifiée du tomato brown rugose fruit virus pour la France métropolitaine*. Available online at: https://hal.archives-ouvertes.fr/hal-02473673 [Accessed July 28, 2020].

Verhoeven, J. T. J., Jansen, C. C. C., Botermans, M., and Roenhorst, J. W. (2010). Epidemiological evidence that vegetatively propagated, *Solanaceous* plant species act as sources of potato spindle tuber viroid inoculum for tomato. *Plant Pathol.* 59, 3–12. doi: 10.1111/j.1365-3059.2009.02173.x

Verma, N., Kumar, K., Kulshrestha, S., Raikhy, G., Hallan, V., Ram, R., et al. (2009). Molecular studies on tomato aspermy virus isolates infecting chrysanthemums. *Arch. Phytopathol. Plant Prot.* 42, 99–111. doi: 10.1080/03235400600951779

Vermunt, A. M. W., and Kaarsemaker, R. C. (2017). Multi-genotype cross-protection against pepino mosaic virus in tomato. *Crop Prot.* 96, 116–122. doi: 10.1016/j.cropro.2017.02.007

Villamor, D. E. V., Ho, T., Al Rwahnih, M., Martin, R. R., and Tzanetakis, I. E. (2019). High throughput sequencing for plant virus detection and discovery. *Phytopathology* 109, 716–725. doi: 10.1094/PHYTO-07-18-0257-RVW

Vučurović, A., Kutnjak, D., Mehle, N., Stanković, I., Pecman, A., Bulajić, A., et al. (2021). Detection of four new tomato viruses in serbia using post-hoc high-throughput sequencing analysis of samples from a large-scale field survey. *Plant Dis.*

Vučurović, A., Stanković, I., Zečević, K., Petrović, B., Delibašić, G., and Krstić, B. (2019). *First report of Tomato infectious chlorosis virus on tomato in Serbia. B. Abstr. VIII Congr. Plant Prot. Integr. Plant Prot. Sustain. Crop Prod. For. Novemb. 25-29.2019., Zlatibor, Serbia, 188.*

Webster, C. G., de Jensen, C. E., Rivera-Vargas, L. I., Rodrigues, J. C. V., Mercado, W., Frantz, G., et al. (2013). First report of tomato chlorotic spot virus (TCSV) in tomato, pepper, and jimsonweed in puerto rico. *Plant Heal. Prog.* 14:47. doi: 10.1094/PHP-2013-0812-01-BR

Webster, C. G., Frantz, G., Reitz, S. R., Funderburk, J. E., Mellinger, H. C., McAvoy, E., et al. (2014). Emergence of groundnut ringspot virus and tomato chlorotic spot virus in vegetables in Florida and the southeastern united states. *Phytopathology* 105, 388–398. doi: 10.1094/PHYTO-06-14-0172-R

Webster, C. G., Perry, K. L., Lu, X., Horsman, L., Frantz, G., Mellinger, C., et al. (2010). First report of groundnut ringspot virus infecting tomato in south Florida. *Plant Heal. Prog.* 11:49. doi: 10.1094/PHP-2010-0707-01-BR

Wisler, G. C., Li, R. H., Liu, H.-Y., Lowry, D. S., and Duffus, J. E. (1998). Tomato chlorosis virus: a new whitefly-transmitted, phloem-limited, bipartite closterovirus of tomato. *Phytopathology* 88, 402–409. doi: 10.1094/PHYTO.1998.88.5.402

WUR (2019). *Southern tomato virus: hype or a real threat? - WUR*. Available Online at: https://www.wur.nl/en/newsarticle/Southern-tomato-virus-hype-or-a-real-threat.htm [Accessed August 3, 2020]

Xu, C., Sun, X., Taylor, A., Jiao, C., Xu, Y., Cai, X., et al. (2017). Diversity, distribution, and evolution of tomato viruses in china uncovered by small RNA sequencing. *J. Virol.* 91, e117–e173. doi: 10.1128/JVI.00173-17

Xu, P., Blancaflor, E. B., and Roossinck, M. J. (2003). In spite of induced multiple defense responses, tomato plants infected with cucumber mosaic virus and D satellite RNA succumb to systemic necrosis. *Mol. Plant-Microbe Interact.* 16, 467–476. doi: 10.1094/MPMI.2003.16.6.467

Yan, Z.-Y., Ma, H.-Y., Han, S.-L., Geng, C., Tian, Y.-P., and Li, X.-D. (2019). First report of tomato brown rugose fruit virus infecting tomato in china. *Plant Dis.* 103, 2973–2973. doi: 10.1094/PDIS-05-19-1045-PDN

Yin, Y., Zheng, K., Dong, J., Fang, Q., Wu, S., Wang, L., et al. (2014). Identification of a new tospovirus causing necrotic ringspot on tomato in china. *Virol. J.* 11:213. doi: 10.1186/s12985-014-0213-0

Yin, Y. Y., Li, T. T., Lu, X., Fang, Q., Ding, M., and Zhang, Z. K. (2015). First report of capsicum chlorosis virus infecting tomato in yunnan, southwest of china. *Plant Dis.* 100:230. doi: 10.1094/PDIS-01-15-0088-PDN

Zaidi, S. S.-E.-A., Martin, D. P., Amin, I., Farooq, M., and Mansoor, S. (2017). Tomato leaf curl new delhi virus: a widespread bipartite begomovirus in the territory of monopartite begomoviruses. *Mol. Plant Pathol.* 18, 901–911. doi: 10.1111/mpp.12481

Zambrano, K., Geraud-Pouey, F., Chirinos, D., Romay, G., and Marys, E. (2011). Tomato chlorotic leaf distortion virus, a new bipartite begomovirus infecting *Solanum lycopersicum* and capsicum chinense in venezuela. *Arch. Virol.* 156, 2263–2266. doi: 10.1007/s00705-011-1093-x

Zarzyñska-Nowak, A., Rymelska, N., Borodynko, N., and Hasiów-Jaroszewska, B. (2016). The occurrence of tomato yellow ring virus on tomato in Poland. *Plant Dis.* 100, 234–234. doi: 10.1094/PDIS-05-15-0521-PDN

Zarzyñska-Nowak, A., Hasiów-Jaroszewska, B., Budzyñska, D., and Trzmiel, K. (2020). Genetic variability of polish tomato black ring virus isolates and their satellite RNAs. *Plant Pathol.* 69, 1034–1041. doi: 10.1111/ppa.13188

Zerbini, F. M., Briddon, R. W., Idris, A., Martin, D. P., Moriones, E., Navas-Castillo, J., et al. (2017). ICTV virus taxonomy profile: geminiviridae. *J. Gen. Virol.* 98, 131–133. doi: 10.1099/jgv.0.000738

Zhang, S. B., Zhang, D. Y., Liu, Y., Luo, X. W., Liu, M. Y., Du, J., et al. (2017). First report of lettuce chlorosis virus infecting tomato in china. *Plant Dis.* 101, 846–846. doi: 10.1094/PDIS-09-16-1315-PDN

Zhao, F.-F., Xi, D.-H., Liu, J., Deng, X.-G., and Lin, H.-H. (2014). First report of chilli veinal mottle virus infecting tomato (*Solanum lycopersicum*) in China. *Plant Dis.* 98, 1589–1589. doi: 10.1094/PDIS-11-13-1188-PDN

Zhu, F., Che, Y.-P., Qian, K., Zhou, Y.-K., Xu, Y.-J., Zhao, Y.-Q., et al. (2017). First report of chilli veinal mottle virus infecting *Lycopersicon esculentum* in jiangsu province in China. *Plant Dis.* 102:462. doi: 10.1094/PDIS-07-17-1100-PDN

Ziebell, H., and Carr, J. P. (2010). *Cross-Protection*. 1st Edn. Amsterdam: Elsevier Inc.

Conflict of Interest: The authors declare that the research was conducted in the absence of any commercial or financial relationships that could be construed as a potential conflict of interest.

frontiers in Plant Science

REVIEW
published: 29 June 2021
doi: 10.3389/fpls.2021.671355

Insights Into Natural Genetic Resistance to Rice Yellow Mottle Virus and Implications on Breeding for Durable Resistance

*Patrick J. Odongo[1,2], Geoffrey Onaga[2,3], Oliver Ricardo[4], Keiko T. Natsuaki[5], Titus Alicai[2] and Koen Geuten[1]**

[1]Molecular Biotechnology of Plants and Micro-Organisms, Institute of Botany and Microbiology, KU Leuven, Leuven, Belgium, [2]National Crops Resources Research Institute, National Agriculture Research Organization, Kampala, Uganda, [3]M'bé Research Station, Africa Rice Center (AfricaRice), Bouaké, Côte d'Ivoire, [4]Breeding Innovations Platform, International Rice Research Institute, Metro Manila, Philippines, [5]Graduate School of Agriculture, Tokyo University of Agriculture, Tokyo, Japan

OPEN ACCESS

Edited by:
Paul Leslie Guy, University of Otago, New Zealand

Reviewed by:
Wen-Ming Wang, Sichuan Agricultural University, China
Mihir Kumar Mandal, Claflin University, United States

***Correspondence:**
Koen Geuten
koen.geuten@kuleuven.be

Specialty section:
This article was submitted to Plant Pathogen Interactions, a section of the journal Frontiers in Plant Science

Received: *23 February 2021*
Accepted: *14 May 2021*
Published: *29 June 2021*

Citation:
Odongo PJ, Onaga G, Ricardo O, Natsuaki KT, Alicai T and Geuten K (2021) Insights Into Natural Genetic Resistance to Rice Yellow Mottle Virus and Implications on Breeding for Durable Resistance. Front. Plant Sci. 12:671355. doi: 10.3389/fpls.2021.671355

Rice is the main food crop for people in low- and lower-middle-income countries in Asia and sub-Saharan Africa (SSA). Since 1982, there has been a significant increase in the demand for rice in SSA, and its growing importance is reflected in the national strategic food security plans of several countries in the region. However, several abiotic and biotic factors undermine efforts to meet this demand. Rice yellow mottle virus (RYMV) caused by *Solemoviridae* is a major biotic factor affecting rice production and continues to be an important pathogen in SSA. To date, six pathogenic strains have been reported. RYMV infects rice plants through wounds and rice feeding vectors. Once inside the plant cells, viral genome-linked protein is required to bind to the rice translation initiation factor [eIF(iso)4G1] for a compatible interaction. The development of resistant cultivars that can interrupt this interaction is the most effective method to manage this disease. Three resistance genes are recognized to limit RYMV virulence in rice, some of which have nonsynonymous single mutations or short deletions in the core domain of eIF(iso)4G1 that impair viral host interaction. However, deployment of these resistance genes using conventional methods has proved slow and tedious. Molecular approaches are expected to be an alternative to facilitate gene introgression and/or pyramiding and rapid deployment of these resistance genes into elite cultivars. In this review, we summarize the knowledge on molecular genetics of RYMV-rice interaction, with emphasis on host plant resistance. In addition, we provide strategies for sustainable utilization of the novel resistant sources. This knowledge is expected to guide breeding programs in the development and deployment of RYMV resistant rice varieties.

Keywords: RYMV, rice-RYMV interaction, resistance mechanisms, durable resistance, rice improvement

INTRODUCTION

Food security is a primary concern for many economies around the world because the human population is increasing, and food production must increase to keep pace (Food and Agriculture Organization of the United Nations, 2010; Boyd et al., 2013; Savary et al., 2019). According to Valin et al. (2014), a 74% increase in food demand is expected by 2050, which would affect consumers worldwide. Meeting this demand is a daunting task, and will require major improvements in agricultural production systems, including improved strategies to minimize crop losses to biotic and abiotic stresses (Das and Rao, 2015). Cereal crops account for more than 60% of food intake and will continue to contribute significantly to global food security. This contribution is reflected in projected increases in the consumption of wheat, corn, and rice by an average of 53, 106, and 47%, respectively, by 2050 (Valin et al., 2014; FAOSTAT, 2018). Of these three main crops, rice is the most important food crop for people in low- and lower-middle-income countries. In sub-Saharan Africa (SSA), where most of the population falls within the category of low incomes, the demand for rice has increased considerably since 1982. This increased demand is due to improving economies, rising household incomes, and growing population and urbanization that have led to increased consumption of rice as a major staple (Balasubramanian et al., 2007). To meet the increased demand, the region is continuously pushing for coordinated efforts to increase rice self-sufficiency in several rice-producing countries (Seck et al., 2013). However, the prospects for rice self-sufficiency are being subverted by abiotic and biotic factors, including plant diseases. Several important rice diseases have emerged recently in SSA (Séré et al., 2013). The most notorious of these has been Rice yellow mottle virus (RYMV), which is restricted to only Africa (Bakker, 1974; Kouassi et al., 2005; Savary et al., 2019).

RYMV was first identified in East Africa in 1966 (Bakker, 1974), from where it is believed to have spatially spread westward into West Africa (Pinel et al., 2000). The virus has now spread to all rice-growing countries in the region, and as such is described as an emerging disease (Fargette et al., 2006). The natural hosts of RYMV are limited to *Oryza sativa*, *Oryza glaberrima*, and wild rice, including *Oryza logistiminata* and *Oryza barthi* (Bakker, 1970; Allarangaye et al., 2007). Recently, some wild accessions from the primary gene pool (AA genome), including *Oryza glumaepatula*, *Oryza breviligulata*, *Oryza meridionalis*, *Oryza rufipogon*, and *Oryza nivara*, have also shown susceptibility in screening experiments (Allarangaye et al., 2007; Odongo et al., 2019), which indicate that RYMV is capable of infecting several species of *Oryzae*. Clear symptoms of RYMV include severe leaf mottling, yellow-green streaking, decreased tillering, and stunting of plants during the vegetative stage. Reproductive stage symptoms include poor emergence of panicles and panicle sterility (Bakker, 1970). RYMV yield losses range from 10 to 100%, depending on the time of infection, ecology, viral strain, and the rice genotype. Plants that display severe symptoms during seedling and early vegetative stages often result in plant death (Bakker, 1974; Kouassi et al., 2005). In lowland ecologies, susceptible genotypes can be severely damaged in a short period of time during periods of intense disease activity. This has been observed in susceptible varieties grown in West African countries. For example, in Nigeria and Côte d'Ivoire, yield losses above of 90% have been reported in susceptible cultivars, Bouake 189 and FARO 29 (Onwughalu et al., 2011; Soko et al., 2016), while in Sierra Leone, losses of 82% were reported on varieties PN 623-3, TOX 516-12-SLR, and ROK 3 (Taylor et al., 1990). Most recently in Burkina Faso, losses of 84% were recorded on popular varieties, FKR56N, FKR62N, and TS2 (Traoré et al., 2015).

The prevalence of RYMV varies between rice-producing countries, probably because of multiple factors including transitions from subsistence production to large-scale intensive rice production, and the associated increase in the diversity of vectors involved in virus transmission. For example, the incidence and severity of RYMV in most of Uganda's rice-growing areas is between 50 and 75% under rainfed lowlands (Ochola and Tusiime, 2010), while in Burkina Faso, the incidence of the disease tends to be lower at 28% (Traoré et al., 2015). In Côte d'Ivoire, the incidence is higher during the dry season than during the rainy season while the opposite is the case in Nigeria (Heinrichs et al., 1997). In Niger, RYMV is generally sporadic and field infections are often found in patches (Sarra and Peters, 2003). High incidence of RYMV has been also reported in Burundi, Zimbabwe, Ethiopia, the Central African Republic, the Democratic Republic of Congo, and Zanzibar (Traoré et al., 2001; Abubakar et al., 2003; Hubert et al., 2013). The spread and severity of the disease in the Democratic Republic of Congo is attributed to changing agricultural patterns with most farmers increasingly cultivating rice in irrigated lowlands. Such changes create a conducive environment for RYMV vectors to multiply (Hubert et al., 2013), a trend that could increase transmission and create a risk of severe infections.

The response from the scientific community to the RYMV threat has been positive and has made progress. Yield losses have been addressed through adapting RYMV control measures to local situations. This includes crop improvement toward local production systems and utilization of specific agronomic practices including the use of varietal mixtures and pesticide sprays, early planting, destruction of previous plants, ratoons and volunteer crops, removal of infected plants, crop rotation, and optimum fertilizer application. These practices aim at disrupting the life cycle of the disease and improving crop health (Traoré et al., 2009). However, their use is limited and still ineffective, especially when the disease occurs in epidemic proportions. Genetic resistance is the best feasible option for economical and sustainable long-term RYMV management. Recent advances in genetics and molecular biology have contributed to the identification of RYMV resistance genes and quantitative trait loci (QTLs) that have been mapped and some cloned from *O. sativa* and *O. glaberrima* (Ndjiondjop et al., 1999; Ioannidou et al., 2003; Albar et al., 2006; Rakotomalala et al., 2008; Thiémélé et al., 2010;

Pidon et al., 2017). However, Traoré et al. (2006b) and Fargette et al. (2008a) have highlighted the nuisance associated with RYMV resistance management. The virus evolves rapidly, and resistance-breaking variants have been observed across SSA (Traoré et al., 2006a; Fargette et al., 2008a,b). So much work remains to be done to identify the best strategies to limit the prevalence and yield losses caused by RYMV. In this review, we present an update of RYMV genetics in relation to virus-rice interactions and discuss some interventions focusing on natural genetic resistance. In addition, we highlight the implications of using known genetic resistance in breeding for durable resistance to the virus in SSA.

RYMV GENOME STRUCTURE, GENE FUNCTION AND DIVERSITY

RYMV is a member of the genus *Sobemovirus* in the *Solemoviridae* family (Bakker, 1974; Hébrard et al., 2021). The virus capsid consists of 180 copies of 26 kDa coat protein (CP) subunits assembled in a T = 3 icosahedral structure with a positive-sense single-stranded RNA (+ssRNA) particle size of 25–28 nm in diameter (Bakker, 1974; Opalka et al., 2000; Qu et al., 2000). RYMV encodes a small genome of approximately 4,500 nucleotides, of these, roughly, 330 nucleotides are in non-coding regions (Yassi et al., 1994) (**Figure 1**). Additionally, the virus encapsidates a non-coding viroid like satellite RNA (satRNA) of about 220 nucleotides, which depends on a helper virus for replication. The satRNA plays no role during infection process (Tamm and Truve, 2000; Sõmera et al., 2015; Hébrard et al., 2021). The genome is a polycistronic RNA harboring five overlapping open reading frames (ORFs): ORF1, ORFx, ORF2a, ORF2b, and ORF3 (Yassi et al., 1994; Ling et al., 2013). ORF1 and ORF3 are more variable while ORF2a and ORF2b are quite conserved. Because of this, the genome size may vary depending on nucleotide diversity of ORFs. For instance, the Mali strain is about 4,450 nucleotides, and some Nigerian isolates are reported to be about 4,452 nucleotides. In ORF3, a few insertion-deletions involving basic amino acids occur depending on the strain (Fargette et al., 2004). Moreover, two non-coding regions of about 80 and 289 nucleotides, respectively, are adjacent to the furthest 5' and 3' ends of the genome (Yassi et al., 1994; Hébrard et al., 2008a). ORF1 is at the 5' end, and encodes the 17.8 kDa P1 protein of 157 amino acids. This protein is involved in viral accumulation and post-transcriptional gene silencing by suppressing the mechanisms of host RNA silencing (Siré et al., 2008; Lacombe et al., 2010). P1 is dispensable for the local movement and replication of RYMV but is essential for systemic infection (Brugidou et al., 1995; Bonneau et al., 1998; Nummert et al., 2017). At the 5' terminus of ORF1 is a viral genome-linked protein (VPg) instead of a cap while the 3' end of the viral genome is not polyadenylated (Hull, 1977; Yassi et al., 1994). ORFx, a newly assigned ORF, is embedded beneath the 5' end of ORF2. It encodes a replication protein, named protein X. Unlike in other *Sobemoviruses*, ORFx does not overlap with ORF1. Its translation initiates at a highly conserved CUG codon and proceeds through a leaky scanning and ribosomal frameshift mechanism (Ling et al., 2013). The next ORFs are the two overlapping ORF2a and ORF2b. ORF2a expresses VPg in the first 134 amino acids (Yassi et al., 1994; Fargette et al., 2004), which is pinpointed to influence the virulence against resistance conferred by two major genes (*RYMV1* and *RYMV2*) (Hébrard et al., 2008b; Pinel-Galzi et al., 2016). ORF2a also encodes a polyprotein protease P2a, and two additional proteins, P10 and P8, the functions of which have yet to be investigated. ORF2b encodes the (P2b) RNA-dependent RNA polymerase (RdRP) protein. ORF3 encodes the viral coat protein (CP) translated from the sub genomic RNA. The coat protein is responsible for cell-to-cell movement, virus packaging, and stability (Yassi et al., 1994; Bonneau et al., 1998; Opalka et al., 1998).

RYMV has a distinct geographic diversity (Fargette et al., 2004, 2008b), and the highest diversity is established in East Africa–the putative center of ancestry and diversification (Pinel-Galzi et al., 2015). Five serotypes (Ser1–Ser5) across Africa are distinguished based on serological typing (Konate et al., 1997; N'guessan et al., 2000). Molecular typing of the CP of these serotypes recognizes six strains including S1, S2, and S3 in West Africa and S4, S5, and S6 in East Africa. Nucleotide and amino-acid difference between East African

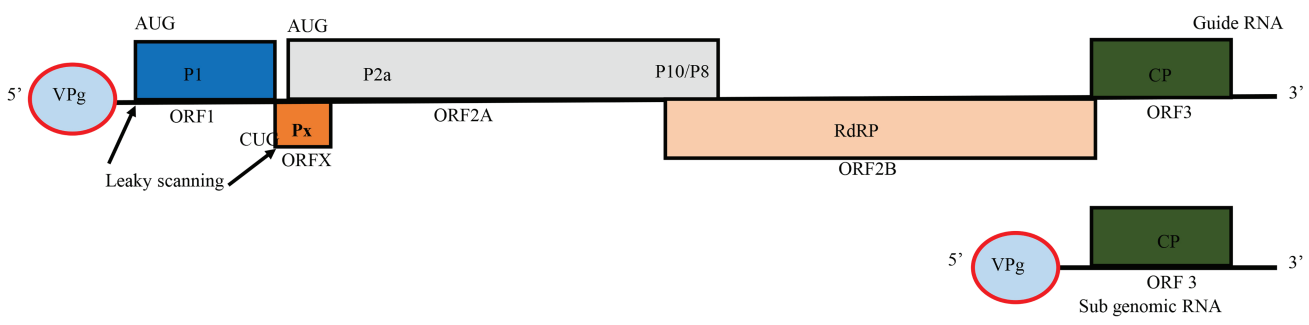

FIGURE 1 | Genome organization of Rice yellow mottle virus (RYMV). Boxes represent open reading frames (ORFs) and the encoded proteins in each ORF. VPg, viral genome-linked protein; P1, gene silencing suppressor protein; P2a, viral protease; P10/P8, polyproteins with no assigned function; RdRP, RNA dependent RNA polymerase; CP, major coat protein. The figure was adapted from Ling et al. (2013).

and West African strains can be up to 11%; however, at the nucleotide level, low variation within strain and within isolate is found (Pinel et al., 2000). Polymorphisms of amino-acids in the bipartite nuclear focusing motif of the R domain of the CP, and near the conserved position 151–154 of the S domain presumably determine differences and aggressiveness among the strains and isolates (Pinel et al., 2000). For instance, new Ugandan isolates were serotyped and grouped into Ser 4, based on polymorphisms in the amino acid sequences of CP gene (Uke et al., 2016). Recently, other variants in the S4, S6, and S1 subtypes have been identified (Adego et al., 2018). These serotypes are possibly segregated by polymorphisms in two amino acids: alanine vs threonine at position 115 and valine vs threonine at 191. These positions possibly localize in the antigenic sites and share an epitope placed within a conserved region. Thus, these polymorphisms may elucidate the cross-reactivity between RYMV isolates (Fargette et al., 2002a).

RYMV-HOST PLANT INTERACTION

RYMV is transmitted by about 12 insect vectors, which accelerate viral spread in most localities (Sere et al., 2008; Koudamilore et al., 2014). *Chrysomelid* beetles are the primary vectors that transmit the virus from its reservoirs in a semi-persistent manner (Bakker, 1970; Abo et al., 2000; Allarangaye et al., 2006). The virus can be found in the seed but no direct seed transmission has been definitively established in host plants (Konate et al., 2001; Allarangaye et al., 2006). It is unclear whether this is due to endogenous viral elements that have been reported to constitute footprints of previous infections by existing or ancient viruses (Maumus et al., 2014). Experimentally, RYMV is mechanically transmissible through sap inoculation. Other secondary forms of RYMV transmission include farming implements, wind, irrigation water, and animals (Traoré et al., 2009). Seedbed nurseries and infected crop stubble also serve as auxiliary sources of the virus (Traoré et al., 2006b; Uke et al., 2014).

Viral entry is facilitated through natural wounds caused by insect vectors and/or intercellular transfer as virion or viral ribonucleoproteins (Schoelz et al., 2011; Wang et al., 2015; Garcia-Ruiz, 2018). For compatible interaction, RYMV, like all plant viruses, must achieve both local and systemic infection in their hosts (van Loon, 1987). This infection process involves a sophisticated molecular interaction between the plant host factors and virus proteins (**Figure 2**). Compatible host proteins facilitate encapsidation, replication, translation, movement, and assembly. After the viral (+) RNA is released in the cytoplasm, replication is initiated. Like other *Sobemoviruses*, the mechanism of replication initiation of plus-and minus-strands in RYMV is still ambiguous, and needs to be further investigated (Tamm and Truve, 2000). However, recent studies suggest that the viral replication complex (VRC) replicates the nascent complementary negative sense RNA (−) using the primary +ssRNA. Subsequent (−) RNAs undergo translation and replication cycles yielding more (+) mRNAs. These are then used to produce new viral proteins and more (−) RNA and finally, the genome is enscapsidated to produce new virus particles (Souza, 2020). The new viral particles are transported cell-to-cell *via* the plasmodesmata to the vascular tissues for systemic spread (Mandadi and Scholthof, 2013; Heinlein, 2015). The systemic spread of RYMV occurs through xylem vessels in which large amounts of viral RNA accumulate and are then transported with solutes to new cells. RYMV disrupts the pit membranes in the xylem vessels, thus enabling the movement of virus particles into new cells (Opalka et al., 1998). To facilitate the active passage of virus particles to neighboring cells, the plasmodesmata must be modified with the help of host proteins. ORF1 and ORF3 play a key role in the modification of plasmodesmata (Bonneau et al., 1998; Nummert et al., 2017). Generally, two hypotheses explain plasmodesmata modification during viral transport (Schoelz et al., 2011; Reagan and Burch-Smith, 2020): the size exclusion limit and the removal of desmotubules and endoplasmic reticulum membranes (Schoelz et al., 2011; Reagan and Burch-Smith, 2020). RYMV uses the size exclusion limit strategy for movement to new cells (Opalka et al., 1998; Kouassi et al., 2006). RYMV particles can be localized in various plant cells, such as epidermis, nucleus vacuole, mesophyll, vesicles, bundle sheath, and vascular parenchymal cells, within 3–6 days post-infection (dpi; Opalka et al., 1998; Ndjiondjop et al., 2001), as well as in the chloroplast (Brugidou et al., 2002). Intracellularly, these viral particles occur in three isoforms described based on the presence of divalent ions and pH. The first is a stable compact form that is pH independent and has Ca^{2+}, the second is the stable transitional form dependent on acidic pH but devoid of Ca^{2+}, and the third is the unstable swollen form dependent on basic pH and lacks Ca^{2+} (Opalka et al., 1998; Brugidou et al., 2002). The viral particle stability depends on the stage of infection in the host, for instance, the transitional and swollen isoforms are more abundant during early infection, while the compact isoforms increase during late stages of infection (Brugidou et al., 2002).

In plant cells, the virus triggers host defense reactions that involve differential expression of genes that are regulated by various signaling pathways (Whitham et al., 2006). Transcriptomic studies using ESTs and cDNA-AFLP revealed differential activation of defense, metabolic, and photosynthesis pathways (Ventelon-Debout et al., 2003, 2008). In the partially resistant cultivar Azucena, in comparison with the susceptible IR64, RYMV induces expression of defense and stress related genes. Proteomic studies, using 2D-DIGE and LC-MS/MS to compare infected cell suspensions of the resistant cultivar IR64 with those of the partially resistant cultivar Azucena, further revealed protein profiles involved in metabolism, defense, and stress-related protein translation and synthesis (Ventelon-Debout et al., 2004). Delalande et al. (2005) identified three candidate proteins belonging to multigenic families including a phenylalanine ammonia-lyase, a mitochondrial chaperonin-60, and an aldolase C; however, the role of these proteins in RYMV infection remains to be validated. Further studies by Brizard et al. (2006), using SDS-PAGE and nano-LC-MS/MS

identified 223 differentially regulated proteins that were categorized into functional pathways comparable to those observed using 2D-DIGE. In an incompatible interaction, RYMV induces proteins in glycolysis pathway, defense-related proteins including superoxide dismutase (SOD) (Ventelon-Debout et al., 2004; Brizard et al., 2006). In contrast, there is a marked downregulation of SOD in susceptible cultivars (Ventelon-Debout et al., 2004). In addition, studies also reveal that there is an increased accumulation of HSP 70 in the susceptible cultivar IR64 during early RYMV stress compared to partially resistant Azucena (Ventelon-Debout et al., 2004). Expression of heat shock protein 70 (HSP70) is a common incidence in response to plant viral infections, though the function of HSP70 during viral infection is poorly understood (Aparicio et al., 2005). RYMV also induces translation and protein synthesis like ribosomal proteins, translation initiation, and elongation factors, protein disulfide isomerases, chaperone proteins, and proteins involved in protein turnover such as the 20S proteasome (Ventelon-Debout et al., 2004; Brizard et al., 2006). The role of these proteins during RYMV infection remains to be validated functionally.

While these studies provide a good view of the genes and proteins expressed during RYMV-rice interactions, no recent high throughput genome-based technologies, such as RNA-seq, have been used to study RYMV-rice interactions. To clarify the different transcriptomic responses between compatible and incompatible RYMV-rice interactions and to describe more genes involved in this process, RNA-seq based approaches ought to be applied.

GENETIC DETERMINANTS AND MECHANISMS OF QUALITATIVE RESISTANCE TO RYMV

Qualitative disease resistance genes show monogenic or near complete resistance and are thus called major genes (Nelson et al., 2018). Qualitative disease resistance can be described based on two models: gene-for-gene and the matching allele model (Fraile and García-Arenal, 2010). Gene-for-gene resistance involves activation of resistance proteins such as nucleotide-binding domain leucine-rich repeat proteins (NB-LRR), which play a role in the perception of pathogen invasion and activation of plant defense mechanisms. Resistant plants usually encode NB-LRR proteins which are normally genetically dominant (R genes) (Fraile and García-Arenal, 2010; Nelson et al., 2018) (**Figure 2**). The matching allele interaction/resistance is conferred by the absence of host factors (susceptibility factors) required for completion of the virus infection cycle (Moffett, 2009; Fraile and García-Arenal, 2010; Wang and Krishnaswamy, 2012). Some of the genes expressed in the matching allele model induce recessive resistance. Examples of recessive host factors include the eukaryotic-translation initiation factors (eIFs) such as eIF4E and eIF4G and their isoforms. Recessive resistance is the predominant form of resistance against plant viruses (Wang and Krishnaswamy, 2012; Hashimoto et al., 2016), and can be as a result of loss-of-function of susceptibility (*S* genes) (Wang and Krishnaswamy, 2012; Sanfaçon, 2015; Hashimoto et al., 2016; Garcia-Ruiz, 2018). Most of the genes conferring resistance against RYMV fall in this category. These include *RYMV1* (*Resistance* to the *yellow mottle virus1*) and *RYMV2* (Albar et al., 2006; Thiémélé et al., 2010; Orjuela et al., 2013; Pidon et al., 2017, 2020).

The first major gene to be found and most studied is *RYMV1*. *RYMV1* located on chromosome four and encodes eIF(iso)4G1. In a pro-viral interaction, eIF(iso)4G is recruited and directly interacts with VPg of RYMV for successful infection (Albar et al., 2006). In antiviral interactions, nonsynonymous mutations in eIF(iso)4G interfere with direct interaction with the VPg causing a resistant phenotype. These mutations may have occurred independently in *O. sativa* and *O. glaberrima*, each affecting the specificity of the allele/isolate interaction (Hébrard et al., 2010). The *RYMV1* locus harbors four alleles with point mutation or small deletions; including *rymv1-2*, the only allele identified in *O. sativa*, and *rymv1-3*, *rymv1-4*, and *rymv1-5*, the three alleles reported in *O. glaberrima* (Albar et al., 2006; Thiémélé et al., 2010). The resistance conferred by *rymv1-2* and *rymv1-4* is due to a substitution of a glutamic acid (E) for a lysine (K) at amino acid positions 309 and 321 of eIF(iso)4G, whereas, the resistance conferred by *rymv1-3* is characterized by a deletion of three amino acids at positions 322–324 in the central domain of eIF(iso)4G (Albar et al., 2006). A deletion in positions 313–315 in the central domain of eIF(iso)4G is responsible for the resistance conferred by *rymv1-5* (Thiémélé et al., 2010). Some rice accessions harboring *RYMV1* resistance exhibit complete resistance, and these are generally described as highly resistant accessions (**Table 1**).

The second *S* gene, *RYMV*2, was identified in the *O. glaberrima* accession Tog7291. *RYMV2* is predicted to be localized on chromosome 1, encodes a homolog of the *Arabidopsis CONSTITUTIVE EXPRESSION OF PATHOGENESIS RELATED GENE-5-1* (*CPR5-1*) (Thiémélé et al., 2010; Orjuela et al., 2013; Pidon et al., 2020). In rice, two *Arabidopsis CPR5* homologs are reported to be present, *CPR5-1* and *CPR5-2*. Resistance conferred by *CPR5* is linked to a point or nonsense mutation in the *CPR5-1* sequence (Orjuela et al., 2013). This gene encodes a transmembrane nucleoprotein in *Arabidopsis* and is known to regulate effector-triggered immunity by controlling the cell cycle and defense mechanisms. In response to the activation of immunoreceptors, *CPR5* undergoes a conformational switch from oligomer to monomer. In this process, loss of function occurs and leads to the release of cyclin dependent kinase inhibitors and the permeabilization of the nuclear pore complex, which activates constitutive resistance to several pathogens (Gu et al., 2016). Despite resistance against pathogens, this loss of function mutants usually come with detrimental phenotypes that are undesirable for crop improvement (Bowling et al., 1997; Pidon et al., 2020). Six frameshift or truncated alleles have been identified in *O. glaberrima* accessions harboring *RYMV2* (**Table 1**), interestingly, none of them display undesirable traits. Their activity is attributed to a partial functional redundancy of *CPR5-1*, suggesting that this gene is not a functional homolog

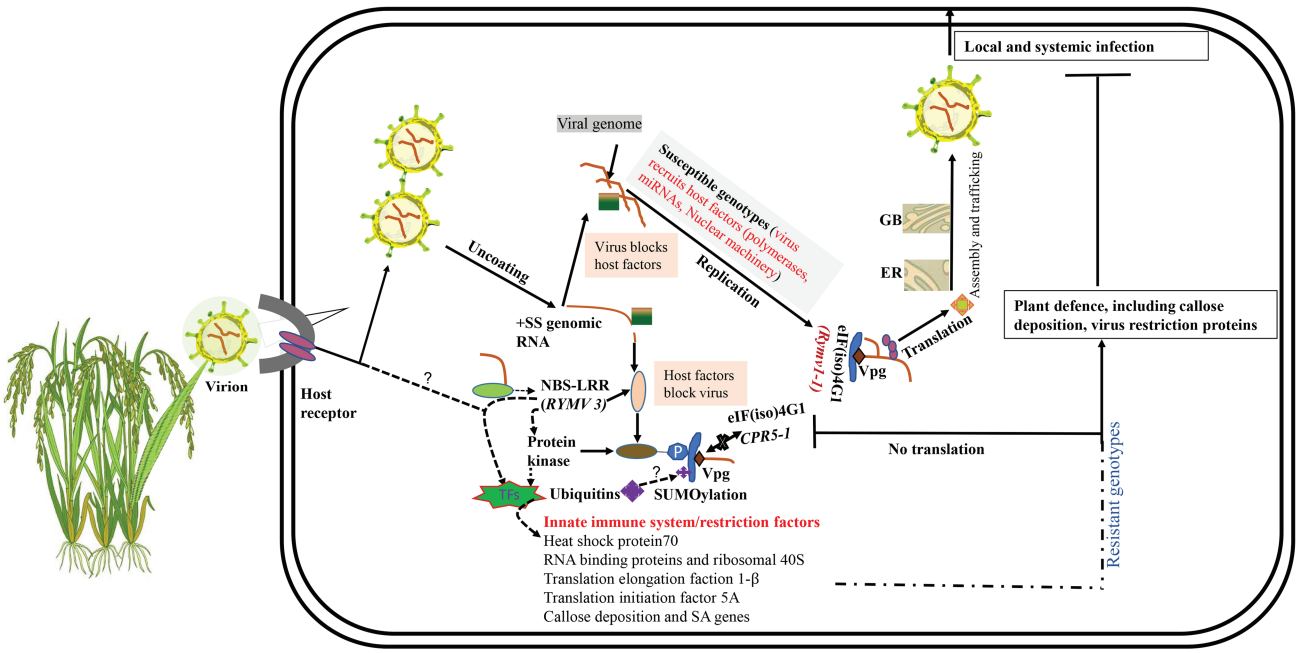

FIGURE 2 | Mechanisms of rice-RYMV interactions. Viruses rely on numerous interactions with the host cell to replicate and transmit. GB, Golgi body; ER, endoplasmic reticulum. Unknown hypotheses are indicated as "?." In a susceptible interaction, a virus attaches, un-coats, replicates, and expresses proteins, and then assembles and egresses. eIF(iso)4G1 encoded by *rymv1-1* (susceptibility allele) possesses altered sites that facilitates viral RNA Vpg binding for successful translation of viral proteins. In a resistant reaction, we hypothesize that when the virus enters the plant cell, viral RNAs or its associated molecules in the cytoplasm are recognized by NBS-LRR or unknown receptors. The signal is transmitted from NBS-LRR *via* transcription factors (TFs) to the nucleus where induced resistance genes that limit viral replication, translation, and movement are transcribed. NBS-LRR proteins could be activated by direct recognition of the viral RNA. The signal could also be transmitted *via* either protein kinase monomers or dimers upon binding to viral RNA, which phosphorylates eIF(iso)4G1, thereby leading to translation suppression. Ubiquitination and SUMOylation could also play a role in translation regulation of eIF(iso)4G1.

of *Arabidopsis CPR5*. The third major gene and the only R gene is NLR_{RYMV3}, or *RYMV3*, found in the *O. glaberrima* accessions Tog5307 and Tog5672. *RYMV3* maps on chromosome 11 and encodes for a NB-LRR (Pidon et al., 2017, 2020). The LRR proteins represent one of the most diverse and abundant classes of R-gene families in plants and can be variable even among closely related plants due to presence or absence of polymorphism (Dodds and Rathjen, 2010; Luo et al., 2012; Tan and Wu, 2012; Marone et al., 2013). At the *RYMV3* locus, three candidate alleles have been mapped: two alleles, $Nir_{RYMV3}R1$ and Nir_{RYMV3}-*x*, involve a substitution of one amino acid at position K779R and A823V, respectively. The resistance conferred by the third allele, NIr_{RYMV3}-*y*, is a result of a truncated protein in the LRR domain with 11 amino acid substitutions (Pidon et al., 2020). The molecular basis of NB-LRR gene resistance to virus infections is expressed in two forms: first, the hypersensitivity reaction restricts the virus to the primary infection site, and second, the extreme reaction, in which the intercellular movement of the virus is completely stopped (Dodds and Rathjen, 2010). Resistance mediated by *RYMV3* displays features of an extreme reaction with no symptoms expressed after infection (Pidon et al., 2020).

Collectively high genetic diversity for resistance has been identified among *O. glaberrima* genotypes compared to the commercially important species *O. sativa* (Albar et al., 2006; Thiémélé et al., 2010; Orjuela et al., 2013; Pidon et al., 2020) (**Table 1**). Among *O. sativa* accessions, only one major resistance gene has been found with two resistance alleles, while three major resistance genes, each with multiple alleles have been discovered in *O. glaberrima* accessions. Recessive genes (*RYMV1* and *RYMV2*) have less polymorphisms, which is attributed to conservative selection leading to low mutation rates. For instance, five and 10 non-synonymous mutations have been identified in *RYMV1* and *RYMV2*, respectively, whereas the R gene (*RYMV3*) is highly polymorphic with about 35 non-synonymous mutations identified (Pidon et al., 2020). These high mutation rates have been observed in all LRR genes due to selective pressure, which promotes the evolution of new receptors to counteract pathogens effectors (Mondragón-Palomino et al., 2002; Marone et al., 2013). This feature might be responsible for high allelic diversity in resistance loci of *O. glaberrima* (Pidon et al., 2020). A shorter evolutionary interaction between RYMV and *O. glaberrima* is however predicted as RYMV could have emerged only a few decades (Pinel-Galzi et al., 2015; Trovao et al., 2015; Pidon et al., 2020). Thus, the high variability of *RYMV3* gene is interesting, and might confer resistance to other pathogens.

The use of genetic resistance is an early prevention method to reduce the impact of viral diseases (Todorovska et al., 2009; Marone et al., 2013). However, the deployment of novel varieties harboring major genes is affected by the ability of pathogens to rapidly evolve and overcome such resistance. Most R genes are

TABLE 1 | List of the resistant accessions and details of the resistance genes and their alleles.

Gene	Host factor	Allele	Viral factor	RB[1] isolate	Source of resistance	Reference
		rymv1-2		S2, S4	Gigante, Bekarosaka	Albar et al., 2006; Rakotomalala et al., 2008
RYMV1	eIF(iso)4G	*rymv 1-3*	VPg	S4, S5, S6	Tog5681	Albar et al., 2006
		rymv1-4		S1, S2	Tog5463, Tog5672, Tog5438	Albar et al., 2006; Thiémélé et al., 2010
		rymv1-5		S2	Tog5674	Thiémélé et al., 2010
		rymv2-R1		S1, S2, S3	Tog6220, Tog6698, Tog7206, Tog7235, Tog10434, Tog7291, Tog7202,	Thiémélé et al., 2010; Orjuela et al., 2013; Pidon et al., 2020
RYMV2	*CPR5*	*rymv2-R2*	VPg		RAM 131, 1LG104, 3LG1178	
		rymv2-R3			Tog7456	
		rymv2-R4			Tog14367, Tog13943, Tog13709, Tog12401, Tog7197	Pidon et al., 2020
		rymv2-R5			SG32	
		rymv2-R6			Tog14361	
RYMV3	LRR	*NlrRYMV3R1*			Tog5307, Tog12086, Tog1260, Tog5474, Tog5286, Tog5747	Pidon et al., 2017, 2020
		Nlr_{RYMV3}-x			Tog5438, Tog5556	
		NlrRYMV3-y			Tog6220	

S1, serotype 1; S2, serotype 2; S3, serotype 3; S4, serotype 4; S5, serotype 5; S6, serotype 6; VPg, viral genome linked protein. [1]RB: resistance breaking isolates.

known to be race specific and only give resistance to a single or limited strain(s) of a given a pathogen (Burdon et al., 2014). The mechanisms of RYMV evolution responsible for its genetic diversity are presumably 2-fold: mutations (N'guessan et al., 2000) and recombination (Ochola et al., 2015; Ndikumana et al., 2017). Recombination analyses found that two new isolates, Ke101 and Ke105, evolved from homologous recombination between strains S4lv and S4ug recognized as emerging types from Western Kenya (Adego et al., 2018), whereas mutations in the central domains of the VPg or different regions of polyprotein P2a contribute to emergence RYMV variants that overcome major resistance genes (Hébrard et al., 2008b, 2010, 2018; Poulicard et al., 2014; Pinel-Galzi et al., 2016; Pidon et al., 2020).

Mutations in the VPg are predicted to develop in three sequential ways (Pinel-Galzi et al., 2007; Traoré et al., 2010; Poulicard et al., 2014). Pathway I occurs *via* the sequential substitution of arginine (A) with glycine (G) and glutamic acid (E); pathway II involves sequential mutations to valine (V) but coexists with isoleucine (I); and pathway III involves sequential mutations substituting arginine with tryptophan (W). Pathway I is more frequent and efficient, whereas II and III are isolate specific (Pinel-Galzi et al., 2007; Traoré et al., 2010). In addition, polymorphism at VPg codon 49 which involve either glutamic (E) or threonic (T) acid residues (E/T polymorphism) influences the virulence of RYMV isolates (Poulicard et al., 2012). This polymorphism involves three pathotypes. The first are the T-pathotypes, in which isolates with threonine (T) at codon 49 only break resistance in *O. glaberrima* accessions. T-pathotypes with substitutions at codons 41 and 52 of the VPg overcome resistance conferred by *rymv1-3* and *rymv1-5* alleles, respectively, while substitutions from threonine to alanine at position 43 overcome resistance of the *rymv1-4* allele. The T-pathotypes with substitutions at codon 804, exchanging phenylalanine for leucine in polyprotein P2a overcome *RYMV2*-mediated resistance (Pinel-Galzi et al., 2016) and *RYMV3* encoded resistance (Pidon et al., 2017), although the mechanism of resistance breakdown is not fully understood. The second are the E-pathotypes with a glutamic acid at codon 49 which overcome *rymv1-2* resistance in *O. sativa*. These pathotypes are polymorphic at codon 48 of VPg, and in avirulent isolates, a conserved arginine is present in this region. Substitutions of R48E and E309K in the VPg of E-pathotypes and eIF(iso)4G, respectively, provide direct interaction between the viral VPg and eIF(iso)4G (Pinel-Galzi et al., 2007; Hébrard et al., 2008b, 2010; Traoré et al., 2010). The third is a highly virulent pathotype suspected to overcome all known sources of resistance. The Hypervirulent T9-pathotype contains a mutation in the central domain of the VPg and was recently identified in West-Central Africa (Hébrard et al., 2018).

Geographically, the E-pathotypes are prevalent in East Africa while the T-pathotypes are common in West Africa. Similarly, the geographic clustering of rice accessions harboring resistance alleles in *RYMV1*, *RYMV2*, and *RYMV3* loci has been recently demonstrated (Pidon et al., 2020). Thus, the geographic specificity of isolates and resistance genes clearly indicates a pattern of adaptation which would guide the development and deployment of rice breeding products in SSA. Resistance coffered by *rymv1-5* and *RYMV3* are quite durable in both regions (Hébrard et al., 2018; Pidon et al., 2020), whereas resistance mediated by *rymv* 1-3, *rymv* 1-4 and *RYMV*2 might be effective in only East Africa. However, the high durability of rymv1-4 in Tog5672 than in Tog5438 suggests epistatic control of resistance.

GENETIC DETERMINANTS AND MECHANISMS OF QUANTITATIVE RESISTANCE TO RYMV

Quantitative disease resistance is controlled by multiple genes (minor genes) with small effects or quantitative trait loci (QTLs). Quantitative resistance is characterized by a reduced virus load in the plant tissues and a slow progression of disease development due to the weakened movement of the virus. Thus, because it does not show the dramatic breakdown observed with major R gene deployment, quantitative resistance is usually viewed as durable and consequently often used in a broad range of crops (Parlevliet, 2002; Burdon et al., 2014).

Quantitative resistance to RYMV is limited to the 1st week of infection, beyond which the disease progresses, virus titer increases, and symptoms reach levels comparable to those of susceptible varieties but with less loss of yield (Albar et al., 1998; Ioannidou et al., 2000). Quantitative resistance to RYMV has been identified mostly in tropical upland rice varieties such as Azucena and Moroberekan (*Japonica* subtypes) (Ghesquière et al., 1997; Ioannidou et al., 2003). Fifteen QTLs have been uncovered on seven chromosomal fragments. Using an Azucena × IR64 double haploid population, genetic mapping identified these QTLs on chromosomes 1, 2, 4, 7, 8, 9, and 12 (Boisnard et al., 2007). However, most of these QTLs co-localize with growth and development QTLs, except for those on chromosome 12, and are, therefore, difficult to target. The RYMV QTL on chromosome 12 is considered to be major (Ghesquière et al., 1997; Albar et al., 1998; Ioannidou et al., 2003; Boisnard et al., 2007). Epistatic interactions between QTLs on chromosomes 7 and 12 presumably play a vital role in the regulation of partial resistance to RYMV in Azucena (Pressoir et al., 1998; Ahmadi et al., 2001; Ioannidou et al., 2003), which might limit their usefulness in marker assisted selection (MAS) taken into consideration. Other partial resistance QTLs are probably in similar positions with the major RYMV resistance genes (Boisnard et al., 2007). For example, Orjuela et al. (2013) reported on the co-localization of QTL1 in a 151-kb interval of the RYMV2 gene, hence this QTL may combine complete and partial resistance. Genome-wide association analysis study (GWAS) involving various accessions of *O. glaberrima* also revealed considerable relationships between quantitative resistance and two known major resistance genes (Cubry et al., 2020). In the same study, several single nucleotide polymorphisms (SNPs) close to two major resistance genes *RYMV1* and *RYMV3* were identified. However, the SNPs associated with resistance conferred by *RYMV1* and *RYMV3* were not found in regions flanking any of the identified partial resistance QTLs indicating differences in genes and pathways of resistance (Cubry et al., 2020) suggesting the complex mechanism of partial resistance to RYMV in rice.

BREEDING FOR RYMV DURABLE RESISTANCE

Breeding for disease resistance has been the most sustainable way of crop improvement to avert potential crop yield losses due to plant viruses (Burdon et al., 2014; Mundt, 2014; Fuchs, 2017). Genetic resistance is durable if it is effective over time when deployed in an environment that is favorable for disease development (Johnson, 1981; Kobayashi et al., 2014). Resistance durability of a gene depends on the nature of resistance, pathogen variability, and environmental factors (Maule et al., 2007; Gómez et al., 2009; Fonseca and Mysore, 2019). These factors presumably influence the epidemiology of RYMV and complicate the deployment of control strategies across Africa (Traoré et al., 2009; Trovao et al., 2015).

The context of durable resistance depends on a given breeding programs, for instance, lasting resistance is critical when new varieties are released less frequently compared to programs that often release novel resistant varieties (Nelson et al., 2018). Generation of broad-spectrum resistance has been the focus of most breeding programs for RYMV resistance. Preliminary focus of breeding for RYMV resistance has been on the deployment of resistance derived from Gigante (*rymv1-2*), given its *O. sativa* background and high F1 hybrid fertility in cross combinations. Recently, *rymv1-2* allele was introduced into some elite cultivars, and several near-isogenic rice lines (NILs) were generated (Ndjiondjop et al., 2013). These NILs combine the *rymv1-2* allele and agronomically important traits. Efforts to pyramid RYMV major resistance genes and resistance QTLs through conventional breeding methods have proven futile (Ndjiondjop et al., 2013). This has been attributed to the recessive nature of resistance conferred by most RYMV genes. If a recessive gene is introduced into an elite variety by backcrossing, the theoretical segregation ratio between the heterozygotes with recessive resistance and homozygotes with no resistance gene is 1:1 in the first generation (Griffiths et al., 2012). At this stage, it is difficult to discriminate which individuals are the heterozygotes. The heterozygotes must be tested in the second generation, which requires more time and resources. However, the use of marker assisted breeding (MAB) would allow effective selection of rymv recessive alleles in the heterozygous state. No selfing or test crossing is needed to detect rymv alleles in populations, thus saving time and accelerating breeding progress.

The use of MAB would also provide opportunities to combine R and or S genes with QTLs that could provide durable and more resilient forms of resistance to RYMV. Thus, it is important to understand the impact of each of the RYMV major resistance genes alone or in combination with other resistance genes in the field before deployment. Combining the candidate QTLs with RYMV major resistance genes in a single genetic background would substantially enhance the durability of resistance as the partial resistance would delay the breakdown of the major resistance gene (Mundt, 2014; Fuchs, 2017). Thus, more QTLs for partial resistance should be identified and included in the breeding program in SSA to enhance the durability of *rymv1-2* and other major genes. Additional ways to improve durability of a major resistance gene is to combine them with another major gene (Rimbaud et al., 2018), especially those that interrupt the interaction with the conserved domains of the virus genome during the infection cycle. This would reduce the genetic adaptation of virulent variants to their environments and hosts (Fuchs, 2017). Pyramiding the recessive (*RYMV1*) and the dominant (*RYMV3*) resistance genes may provide much desired broad-spectrum resistance against RYMV and other pathogens in rice.

INTEGRATION OF NEW BREEDING TECHNIQUES FOR RYMV RESISTANCE

The continuous improvements in genomics and bioinformatics has a potential to speed up crop breeding (Batley and Edwards, 2016). Advances in genomic-assisted selection have become essential to facilitate the introduction of traits that may not be done using conventional breeding techniques. Molecular markers can be used to facilitate the selection of rare traits at early stages without phenotypic analysis, thus speeding up plant breeding and crop improvement (Varshney et al., 2005; Batley and Edwards, 2016).

The scope of MAS breeding for targeted introgression of RYMV resistance genes has been successfully demonstrated in SSA (Ndjiondjop et al., 2013). A number of SNP markers linked to *rymv1-2*, *rymv1-3*, *rymv1-4*, and *rymv1-5* alleles are now available (Albar et al., 2003; Thiémélé et al., 2010). Improvements in high-throughput genotyping have enhanced the identification of QTLs through GWAS. For instance, Cubry et al. (2020) observed a total of 2,199 SNPs, close to chromosomes 4 and 11 associated with *RYMV1* and *RYMV3* resistance, respectively. However, adoption and utilization of genomics-selection approaches in many breeding programs has remained low due to less know-how on genomic tools, and the cost involved in MAS (Ndjiondjop et al., 2013). However, given the current developments in refining SNPs associated with all RYMV major resistance genes at the International Rice Research Institute (IRRI), Institut de Recherche pour le Développement (IRD), and AfricaRice, it is likely that introgression of these genes through MAS will be more successful. These genes could also be pyramided with other biotic and abiotic stress resistance genes using anther culture techniques. Recently, successful crosses between *O. glaberrima* and Milyang23 (*O. sativa*) for resistance to multiple pathogens, such as RYMV, Bacterial leaf blight, Rice blast and Bacterial leaf streak, was demonstrated using anther culture techniques. Hybrids with combined resistance to these diseases were shown to be highly resistant to all four pathogens (Lamo et al., 2015).

Genetic engineering is another important strategy in crop improvement against plant viruses, considering the limited sources of natural resistance and the constraints related to the introduction of these genes to popular cultivars. RNA interference (RNAi) is one of the methods that has been explored to develop transgenic virus-resistant rice (Pinto et al., 1999; Sasaya et al., 2014; Kreuze and Valkonen, 2017). This approach involves the expression of hairpin RNA constructs in the host plant (Sanford and Johnston, 1985; Baulcombe, 1996; Brodersen and Voinnet, 2006), and it has shown success in generating RYMV resistant transgenic plants targeting the conserved P2a protein in the susceptible cultivar IR64 (Pinto et al., 1999). Additionally, genome editing is another approach with enormous potential to improve breeding for RYMV resistance. Genome editing tools, such as CRISPR-Cas9, are powerful techniques to facilitate crop improvement. CRISPR-Cas9 is based on introducing targeted mutations at specific sites by utilizing non-homologous end-joining to repair induced double-strand breaks (Belhaj et al., 2013; Haque et al., 2018; Kalinina et al., 2020). Full implementation of CRISPR-Cas9 technology is dependent on the identification of plant host factors which can be manipulated to limit virus proliferation (Kalinina et al., 2020). Some of these host factors have been demonstrated to interact directly with the viral RNA (Hyodo et al., 2014; Van Schie and Takken 2014; Garcia-Ruiz, 2018), although only a few of them have been identified to date. In rice, only *eIF(iso)G4*, *CPR-5* (Albar et al., 2006; Thiémélé et al., 2010), is known to interact with RYMV. This limited number of plant-interacting proteins, with experimental evidence, makes targeting specific host genes for gene modification difficult. Therefore, to provide more breeding options for RYMV resistance, additional susceptibility genes need to be identified and validated. Once validated, these genes can be modified using CRISPR-Cas9 to disrupt the interaction with viral proteins. This brings the susceptible host plant outside the host range of the virus, to confer resistance.

CONCLUSION

RYMV continues to cause losses to rice production in SSA due to lack of resistant elite cultivars. Considering the high adaptive potential of this virus and frequent resistance breakdown in rice cultivars, breeding for resistance and its durability should be given top priority in SSA. Encouraging news comes from recent knowledge on rice-RYMV interactions, which has enabled identification and isolation of three major resistance genes (*RYMV1*, *RYMV2*, and *RYMV3*), and the subsequent definition of geographic specificities of these genes and RYMV strains. There is need to build on these successes by further identifying the genomic localization of desired SNPs linked to the major resistance genes for use in genomic-assisted breeding. The speedy development of homozygous lines through double haploid breeding when coupled with MAS would be more effective for developing and deployment of durable RYMV resistant varieties. Parallel efforts are needed to identify additional genes and extensively screen host-virus protein interactors to identify and validate additional host factors that assist or suppress the virus. With these interaction factors identified, a reverse genetics approach could be used to identify novel host *S* genes that could be modified by genome editing to impair susceptibility. These short and long-term strategies will provide immediate products and build a large germplasm base and knowledge necessary to respond to future RYMV attacks.

AUTHOR CONTRIBUTIONS

PO wrote the first draft of the manuscript. GO helped to write and edited the manuscript. PO and GO drew the figures and tables. KG edited, supervised, and supported the writing. KN, TA, and OR edited all versions of the manuscript. All authors contributed to the article and approved the submitted version.

FUNDING

This work was funded by Belgian Directorate General for Development and Humanitarian Aid (DGD) and implemented by VLIR-UOS under grant number BE2017GMUKULA101.

ACKNOWLEDGMENTS

We gratefully thank Alice Kennedy, Molecular Biotechnology of Plants and Micro-organisms, KU Leuven, for her help in language editing.

REFERENCES

Abo, M. E., Alegbejo, M. D., Sy, A. A., and Misari, S. M. (2000). An overview of the mode of transmission, host plants and methods of detection of Rice yellow mottle virus. *J. Sustain. Agric.* 17, 19–36. doi: 10.1300/J064v17n01_04

Abubakar, Z., Ali, F., Pinel, A., Traoré, O., N'Guessan, P., Notteghem, J. L., et al. (2003). Phylogeography of Rice yellow mottle virus in Africa. *J. Gen. Virol.* 84, 733–743. doi: 10.1099/vir.0.18759-0

Adego, A. K., Poulicard, N., Pinel-Galzi, A., Mukoye, B., Fargette, D., Wéré, H. K., et al. (2018). Full-length genome sequences of recombinant and nonrecombinant sympatric strains of Rice yellow mottle virus from western Kenya. *Genome Announc.* 6, e01508–e01517. doi: 10.1128/genomeA.01508-17

Ahmadi, N., Albar, L., Pressoir, G., Pinel, A., Fargette, D., and Ghesquière, A. (2001). Genetic basis and mapping of the resistance to Rice yellow mottle virus. III. Analysis of QTL efficiency in introgressed progenies confirmed the hypothesis of complementary epistasis between two resistance QTLs. *Theor. Appl. Genet.* 103, 1084–1092. doi: 10.1007/s001220100642

Albar, L., Bangratz-Reyser, M., Hébrard, E., Ndjiondjop, M. N., Jones, M., and Ghesquière, A. (2006). Mutations in the eIF(iso)4G translation initiation factor confer high resistance of rice to Rice yellow mottle virus. *Plant J.* 47, 417–426. doi: 10.1111/j.1365-313X.2006.02792.x

Albar, L., Lorieux, M., Ahmadi, N., Rimbault, I., Pinel, A., Sy, A. A., et al. (1998). Genetic basis and mapping of the resistance to rice yellow mottle virus. I. QTLs identification and relationship between resistance and plant morphology. *Theor. Appl. Genet.* 97, 1145–1154. doi: 10.1007/s001220051003

Albar, L., Ndjiondjop, M.-N. N., Esshak, Z., Berger, A., Pinel, A., Jones, M., et al. (2003). Fine genetic mapping of a gene required for Rice yellow mottle virus cell-to-cell movement. *Theor. Appl. Genet.* 107, 371–378. doi: 10.1007/s00122-003-1258-4

Allarangaye, M. D., Traoré, O., Traoré, E. V. S., Millogo, R. J., Guinko, S., and Konaté, G. (2007). Host range of rice yellow mottle virus in Sudano-sahelian savannahs. *Pak. J. Biol. Sci.* 10, 1414–1421. doi: 10.3923/pjbs.2007.1414.1421

Allarangaye, M. D., Traoré, O., Traoré, E. V. S., Millogo, R. J., and Konaté, G. (2006). Evidence of non-transmission of Rice yellow mottle virus through seeds of wild host species. *J. Plant Pathol.* 88, 309–315. doi: 10.4454/jpp.v88i3.877

Aparacio, F., Thomas, C. L., Lederer, C., Niu, Y., Wang, D., and Maule, A. J. (2005). Virus induction of heat shock protein 70 reflects a general response to protein accumulation in the plant cytosol. *Plant Physiol.* 138, 529–536. doi: 10.1104/pp.104.058958

Bakker, W. (1970). Rice yellow mottle, a mechanically transmissible virus disease of rice in Kenya. *Neth. J. Plant Pathol.* 76, 53–63. doi: 10.1007/BF01974433

Bakker, W. (1974). Characterization and ecological aspects of rice yellow mottle virus in Kenya. *Agric. Res. Rep.* 829, 1-152.

Balasubramanian, V., Sie, M., Hijmans, R. J., and Otsuka, K. (2007). Increasing rice production in sub-Saharan Africa: challenges and opportunities. *Adv. Agron.* 94, 55-133. doi: 10.1016/S0065-2113(06)94002-4.

Batley, J., and Edwards, D. (2016). The application of genomics and bioinformatics to accelerate crop improvement in a changing climate. *Curr. Opin. Plant Biol.* 30, 78–81. doi: 10.1016/j.pbi.2016.02.002

Baulcombe, D. C. (1996). RNA as a target and an initiator of post-transcriptional gene silencing in trangenic plants. *Plant Mol. Biol.* 32, 79–88. doi: 10.1007/BF00039378

Belhaj, K., Chaparro-Garcia, A., Kamoun, S., and Nekrasov, V. (2013). Plant genome editing made easy: targeted mutagenesis in model and crop plants using the CRISPR/Cas system. *Plant Methods* 9:39. doi: 10.1186/1746-4811-9-39

Boisnard, A., Albar, L., Thiéméle, D., Rondeau, M., and Ghesquière, A. (2007). Evaluation of genes from eIF4E and eIF4G multigenic families as potential candidates for partial resistance QTLs to Rice yellow mottle virus in rice. *Theor. Appl. Genet.* 116, 53–62. doi: 10.1007/s00122-007-0646-6

Bonneau, C., Brugidou, C., Chen, L., Beachy, R. N., and Fauquet, C. (1998). Expression of the rice yellow mottle virus P1 protein in vitro and in vivo and its involvement in virus spread. *Virology* 244, 79–86. doi: 10.1006/viro.1998.9100

Bowling, S. A., Clarke, J. D., Liu, Y., Klessig, D. F., and Dong, X. (1997). The cpr5 mutant of arabidopsis expresses both NPR1-dependent and NPR1-independent resistance. *Plant Cell* 9, 1573–1584. doi: 10.1105/tpc.9.9.1573

Boyd, L. A., Ridout, C., O'Sullivan, D. M., Leach, J. E., and Leung, H. (2013). Plant-pathogen interactions: disease resistance in modern agriculture. *Trends Genet.* 29, 233–240. doi: 10.1016/j.tig.2012.10.011

Brizard, J. P., Carapito, C., Delalande, F., Van Dorsselaer, A., and Brugidou, C. (2006). Proteome analysis of plant-virus interactome: comprehensive data for virus multiplication inside their hosts. *Mol. Cell. Proteomics* 5, 2279–2297. doi: 10.1074/mcp.M600173-MCP200

Brodersen, P., and Voinnet, O. (2006). The diversity of RNA silencing pathways in plants. *Trends Genet.* 22, 268–280. doi: 10.1016/j.tig.2006.03.003

Brugidou, C., Holt, C., Ngon, A., Yassi, M., Zhang, S., Beachy, R., et al. (1995). Synthesis of an infectious full-length cDNA clone of rice yellow mottle virus andmutagenesis of the coat protein. *Virology* 206, 108–115. doi: 10.1016/S0042-6822(95)80025-5

Brugidou, C., Opalka, N., Yeager, M., Beachy, R. N., and Fauquet, C. (2002). Stability of rice yellow mottle virus and cellular compartmentalization during the infection process in *Oryza sativa* (L.). *Virology* 297, 98–108. doi: 10.1006/viro.2002.1398

Burdon, J. J., Barrett, L. G., Rebetzke, G., and Thrall, P. H. (2014). Guiding deployment of resistance in cereals using evolutionary principles. *Evol. Appl.* 7, 609–624. doi: 10.1111/eva.12175

Cubry, P., Pidon, H., Ta, K. N., Tranchant-Dubreuil, C., Thuillet, A.-C. C., Holzinger, M., et al. (2020). Genome wide association study pinpoints key agronomic QTLs in African rice *Oryza glaberrima*. bioRxiv [Preprint]. doi:10.1101/2020.01.07.897298

Das, G., and Rao, G. J. N. (2015). Molecular marker assisted gene stacking for biotic and abiotic stress resistance genes in an elite rice cultivar. *Front. Plant Sci.* 6:698. doi: 10.3389/fpls.2015.00698

Delalande, F., Carapito, C., Brizard, J. P., Brugidou, C., and Van Dorsselaer, A. (2005). Multigenic families and proteomics: extended protein characterization as a tool for paralog gene identification. *Proteomics* 5, 450–460. doi: 10.1002/pmic.200400954

Dodds, P. N., and Rathjen, J. P. (2010). Plant immunity: towards an integrated view of plant-pathogen interactions. *Nat. Rev. Genet.* 11, 539–548. doi: 10.1038/nrg2812

FAOSTAT (2018). *World Food and Agriculture: Statistical Pocketbook 2018*. Rome, 254.

Fargette, D., Konaté, G., Fauquet, C., Muller, E., Peterschmitt, M., and Thresh, J. M. (2006). Molecular ecology and emergence of tropical plant viruses. *Annu. Rev. Phytopathol.* 44, 235–260. doi: 10.1146/annurev.phyto.44.120705.104644

Fargette, D., Pinel, A., Abubakar, Z., Traoré, O., Brugidou, C., Fatogoma, S., et al. (2004). Inferring the evolutionary history of Rice yellow mottle virus from genomic, phylogenetic, and phylogeographic studies. *J. Virol.* 78, 3252–3261. doi: 10.1128/JVI.78.7.3252-3261.2004

Fargette, D., Pinel, A., Halimi, H., Brugidou, C., Fauquet, C., and Van Regenmortel, M. (2002a). Comparison of molecular and immunological typing of isolates of Rice yellow mottle virus. *Arch. Virol.* 147, 583–596. doi: 10.1007/s007050200008

Fargette, D., Pinel, A., Rakotomalala, M., Sangu, E., Traore, O., Sereme, D., et al. (2008b). Rice yellow mottle virus, an RNA plant virus, evolves as rapidly as most RNA animal viruses. *J. Virol.* 82, 3584–3589. doi: 10.1128/jvi.02506-07

Fargette, D., Pinel, A., Traoré, O., Ghesquière, A., and Konaté, G. (2002b). Emergence of resistance-breaking isolates of Rice yellow mottle virus during serial inoculations. *Eur. J. Plant Pathol.* 108, 585–591. doi: 10.1023/A:1019952907105

Fargette, D., Pinel-Galzi, A., Sérémé, D., Lacombe, S., Hébrard, E., Traoré, O., et al. (2008a). Diversification of Rice yellow mottle virus and related viruses spans the history of agriculture from the neolithic to the present. *PLoS Pathog.* 4:e1000125. doi: 10.1371/journal.ppat.1000125

Fonseca, J. P., and Mysore, K. S. (2019). Genes involved in nonhost disease resistance as a key to engineer durable resistance in crops. *Plant Sci.* 279, 108–116. doi: 10.1016/j.plantsci.2018.07.002

Food and Agriculture Organization of the United Nations (2010). The State of Food Insecurity in the World Addressing food insecurity in protracted crises 2010 Key messages. Available at: http://www.fao.org/docrep/013/i1683e/i1683e.pdf (Accessed April 22, 2021).

Fraile, A., and García-Arenal, F. (2010). "The coevolution of plants and viruses," in *Advances in Virus Research*. eds. J P. Carr and Gad Loebenstein (Oxford: Academic Press), 1–32.

Fuchs, M. (2017). Pyramiding resistance-conferring gene sequences in crops. *Curr. Opin. Virol.* 26, 36–42. doi: 10.1016/j.coviro.2017.07.004

Garcia-Ruiz, H. (2018). Susceptibility genes to plant viruses. *Viruses* 10:484. doi: 10.3390/v10090484

Ghesquière, A., Albar, L., Lorieux, M., Ahmadi, N., Fargette, D., Huang, N., et al. (1997). A major quantitative trait locus for rice yellow mottle virus resistance maps to a cluster of blast resistance genes on chromosome 12. *Phytopathology* 87, 1243–1249. doi: 10.1094/PHYTO.1997.87.12.1243

Gómez, P., Rodríguez-Hernández, A. M., Moury, B., and Aranda, M. (2009). Genetic resistance for the sustainable control of plant virus diseases: breeding, mechanisms and durability. *Eur. J. Plant Pathol.* 125, 1–22. doi: 10.1007/s10658-009-9468-5

Griffiths, A. J. F., Wessler, S. R., Caroll, S. B., and Doebley, J. (2012). *Introduction to Genetic Analysis. 10th Edn*. New York, NY: W. H. Freeman

Gu, Y., Zebell, S. G., Liang, Z., Wang, S., Kang, B. H., and Dong, X. (2016). Nuclear pore permeabilization is a convergent signaling event in effector-triggered immunity. *Cell* 166, 1526.e11–1538.e11. doi: 10.1016/j.cell.2016.07.042

Haque, E., Taniguchi, H., Hassan, M. M., Bhowmik, P., Karim, M. R., Śmiech, M., et al. (2018). Application of CRISPR/Cas9 genome editing technology for the improvement of crops cultivated in tropical climates: recent progress, prospects, and challenges. *Front. Plant Sci.* 9:617. doi: 10.3389/fpls.2018.00617

Hashimoto, M., Neriya, Y., Yamaji, Y., and Namba, S. (2016). Recessive resistance to plant viruses: potential resistance genes beyond translation initiation factors. *Front. Microbiol.* 7:1695. doi: 10.3389/fmicb.2016.01695

Hébrard, E., Fargette, D., and Konaté, G. (2008a). "Rice yellow mottle virus," in *Encyclopedia of Virology. 3rd Edn.* eds. B. W. J. Mahy and H. V. Van Regenmortel (Oxford: Academic Press), 485–490.

Hébrard, E., Pinel-Galzi, A., and Fargette, D. (2008b). Virulence domain of the RYMV genome-linked viral protein VPg towards rice rymv1-2-mediated resistance. *Arch. Virol.* 153, 1161–1164. doi: 10.1007/s00705-008-0087-9

Hébrard, E., Pinel-Galzi, A., Oludare, A., Poulicard, N., Aribi, J., Fabre, S., et al. (2018). Identification of a hypervirulent pathotype of Rice yellow mottle virus: a threat to genetic resistance deployment in West-Central Africa. *Phytopathology* 108, 299–307. doi: 10.1094/PHYTO-05-17-0190-R

Hébrard, E., Poulicard, N., Gérard, C., Traoré, O., Wu, H. C., Albar, L., et al. (2010). Direct interaction between the rice yellow mottle virus (RYMV) VPg and the central domain of the rice eIF(iso)4G1 factor correlates with rice susceptibility and RYMV virulence. *Mol. Plant-Microbe Interact.* 23, 1506–1513. doi: 10.1094/MPMI-03-10-0073

Hébrard, E., Poulicard, N., and Rakotomalala, M. (2021). "Rice yellow mottle virus (Solemoviridae)," in *Encyclopedia of Virology. 4th Edn.* eds. D. H. Bamford and M. Zuckerman (Oxford: Academic Press), 675–680.

Heinlein, M. (2015). Plant virus replication and movement. *Virology* 479–480, 657–671. doi: 10.1016/j.virol.2015.01.025

Heinrichs, E. A., Sy, A. A., Akator, S. K., and Oyediran, I. (1997). Seasonal occurrence of rice yellow mottle virus in lowland rice in cote d'ivoire. *Int. J. Pest Manag.* 43, 291–297. doi: 10.1080/096708797228591

Hubert, J. G., Pinel-Galzi, A., Dibwe, D., Cinyabuguma, E., Kaboré, A. D., Fargette, D., et al. (2013). First report of rice yellow mottle virus on rice in the Democratic Republic of Congo. *Plant Dis.* 97:1664. doi: 10.1094/PDIS-06-13-0650-PDN

Hull, R. (1977). The grouping of small spherical plant viruses with single RNA components. *J. Gen. Virol.* 36, 289–295. doi: 10.1099/0022-1317-36-2-289

Hyodo, K., Kaido, M., and Okuno, T. (2014). Host and viral RNA-binding proteins involved in membrane targeting, replication and intercellular movement of plant RNA virus genomes. *Front. Plant Sci.* 5:321. doi: 10.3389/fpls.2014.00321

Ioannidou, D., Lett, J. M., Pinel, A., Assigbétse, K., Brugidou, C., Ghesquière, A., et al. (2000). Responses of *Oryza sativa* japonica sub-species to infection with rice yellow mottle virus. *Physiol. Mol. Plant Pathol.* 57, 177–188. doi: 10.1006/pmpp.2000.0292

Ioannidou, D., Pinel, A., Brugidou, C., Albar, L., Ahmadi, N., Ghesquiere, A., et al. (2003). Characterisation of the effects of a major QTL of the partial resistance to Rice yellow mottle virus using a near-isogenic—line approach. *Physiol. Mol. Plant Pathol.* 63, 213–221. doi: 10.1016/j.pmpp.2003.12.005

Johnson, R. (1981). Durable resistance: definition of, genetic control, and attainment in plant breeding. *Phytopathology* 71, 567–568. doi: 10.1094/Phyto-71-567

Kalinina, N. O., Khromov, A., Love, A. J., and Taliansky, M. E. (2020). CRISPR applications in plant virology: virus resistance and beyond. *Phytopathology* 110, 18–28. doi: 10.1094/PHYTO-07-19-0267-IA

Kobayashi, K., Sekine, K.-T. T., and Nishiguchi, M. (2014). Breakdown of plant virus resistance: can we predict and extend the durability of virus resistance? *J. Gen. Plant Pathol.* 80, 327–336. doi: 10.1007/s10327-014-0527-1

Konate, G., Sarra, S., and Traore, O. (2001). Rice yellow mottle virus is seed-borne but not seed transmitted in rice seeds. *Eur. J. Plant Pathol.* 107, 361–364. doi: 10.1023/A:1011295709393

Konate, G., Traore, O., and Coulibaly, M. M. (1997). Characterization of rice yellow mottle virus isolates in Sudano-Sahelian areas. *Arch. Virol.* 142, 1117–1124. doi: 10.1007/s007050050146

Kouassi, N. K., Chen, L., Siré, C., Bangratz-Reyser, M., Beachy, R. N., Fauquet, C. M., et al. (2006). Expression of rice yellow mottle virus coat protein enhances virus infection in transgenic plants. *Arch. Virol.* 151, 2111–2122. doi: 10.1007/s00705-006-0802-3

Kouassi, N. K., N'Guessan, P., Albar, L., Fauquet, C. M., and Brugidou, C. (2005). Distribution and characterization of Rice yellow mottle virus: a threat to African farmers. *Plant Dis.* 89, 124–133. doi: 10.1094/PD-89-0124

Koudamilore, A., Nwilene, F. E., Silue, D., Togola, A., Oyetunji, O., Sere, Y., et al. (2014). Identification of insect vectors of Rice yellow mottle virus (RYMV) in Benin. *J. Entomol.* 11, 153–162. doi: 10.3923/je.2014.153.162

Kreuze, J. F., and Valkonen, J. P. (2017). Utilization of engineered resistance to viruses in crops of the developing world, with emphasis on sub-Saharan Africa. *Curr. Opin. Virol.* 26, 90–97. doi: 10.1016/j.coviro.2017.07.022

Lacombe, S., Bangratz, M., Vignols, F., and Brugidou, C. (2010). The rice yellow mottle virus P1 protein exhibits dual functions to suppress and activate gene silencing. *Plant J.* 61, 371–382. doi: 10.1111/j.1365-313X.2009.04062.x

Lamo, J., Cho, G., Jane, I., Dartey, P. K. A., James, E., Ekobu, M., et al. (2015). Developing lowland rice germplasm with resistance to multiple biotic stresses through anther culture in Uganda. *J. Korean Soc. Int. Agric.* 27, 415–420. doi: 10.12719/KSIA.2015.27.4.415

Ling, R., Pate, A. E., Carr, J. P., and Firth, A. E. (2013). An essential fifth coding ORF in the Sobemoviruses. *Virology* 446, 397–408. doi: 10.1016/j.virol.2013.05.033

Luo, S., Zhang, Y., Hu, Q., Chen, J., Li, K., Lu, C., et al. (2012). Dynamic nucleotide-binding site and leucine-rich repeat-encoding genes in the grass family. *Plant Physiol.* 159, 197–210. doi: 10.1104/pp.111.192062

Mandadi, K. K., and Scholthof, K. B. G. (2013). Plant immune responses against viruses: how does a virus cause disease? *Plant Cell* 25, 1489–1505. doi: 10.1105/tpc.113.111658

Marone, D., Russo, M. A., Laidò, G., De Leonardis, A. M., and Mastrangelo, A. M. (2013). Plant nucleotide binding site-leucine-rich repeat (NBS-LRR) genes: active guardians in host defense responses. *Int. J. Mol. Sci.* 14, 7302–7326. doi: 10.3390/ijms14047302

Maule, A. J., Caranta, C., and Boulton, M. I. (2007). Sources of natural resistance to plant viruses: status and prospects: review. *Mol. Plant Pathol.* 8, 223–231. doi: 10.1111/j.1364-3703.2007.00386.x

Maumus, F., Epert, A., Nogué, F., and Blanc, G. (2014). Plant genomes enclose footprints of past infections by giant virus relatives. *Nat. Commun.* 5:4268. doi: 10.1038/ncomms5268

Moffett, P. (2009). Mechanisms of recognition in dominant R gene mediated resistance. *Adv. Virus Res.* 75, 1–33. doi: 10.1016/s0065-3527(09)07501-0

Mondragón-Palomino, M., Meyers, B. C., Michelmore, R. W., and Gaut, B. S. (2002). Patterns of positive selection in the complete NBS-LRR gene family of *Arabidopsis thaliana*. *Genome Res.* 12, 1305–1315. doi: 10.1101/gr.159402

Mundt, C. C. (2014). Durable resistance: a key to sustainable management of pathogens and pests. *Infect. Genet. Evol.* 27, 446–455. doi: 10.1016/j.meegid.2014.01.011

N'guessan, P., Pinel, A., Caruana, M. L., Frutos, R., Sy, A., Ghesquì Ere, A., et al. (2000). Evidence of the presence of two serotypes of rice yellow mottle sobemovirus in Côte d'Ivoire. *Eur. J. Plant Pathol.* 106, 167–178. doi: 10.1023/A:1008792109954

Ndikumana, I., Pinel-Galzi, A., Fargette, D., and Hébrard, E. (2017). Complete genome sequence of a new strain of Rice yellow mottle virus from Malawi, characterized by a recombinant VPg protein. *Genome Announc.* 5, e01198–e01217. doi: 10.1128/genomeA.01198-17

Ndjiondjop, M. N., Albar, L., Fargette, D., Fauquet, C., and Ghesquière, A. (1999). The genetic basis of high resistance to rice yellow mottle virus

(RYMV) in cultivars of two cultivated rice species. *Plant Dis.* 83, 931–935. doi: 10.1094/PDIS.1999.83.10.931

Ndjiondjop, M. N., Albar, L., Sow, M., Yao, N., Djedatin, G., Thiemélé, D., et al. (2013). "Integration of molecular markers in rice improvement: a case study on resistance to Rice yellow mottle virus," in *Realizing Africa's Rice Promise*. eds. M. Wopereis, D. Johnson, N. Ahmadi, E. Tollens and A. Jalloh (Cotonou, Benin: CABI).

Ndjiondjop, M. N., Brugidou, C., Zang, S., Fargette, D., Ghesquiere, A., and Fauquet, C. (2001). High resistance to rice yellow mottle virus in two cultivated rice cultivars is correlated with failure of cell to cell movement. *Physiol. Mol. Plant Pathol.* 59, 309–316. doi: 10.1006/pmpp.2001.0368

Nelson, R., Wiesner-Hanks, T., Wisser, R., and Balint-Kurti, P. (2018). Navigating complexity to breed disease-resistant crops. *Nat. Rev. Genet.* 19, 21–33. doi: 10.1038/nrg.2017.82

Nummert, G., Sõmera, M., Uffert, G., Abner, E., and Truve, E. (2017). P1-independent replication and local movement of Rice yellow mottle virus in host and non-host plant species. *Virology* 502, 28–32. doi: 10.1016/j.virol.2016.12.007

Ochola, D., Issaka, S., Rakotomalala, M., Pinel-Galzi, A., Ndikumana, I., Hubert, J., et al. (2015). Emergence of rice yellow mottle virus in eastern Uganda: recent and singular interplay between strains in East Africa and in Madagascar. *Virus Res.* 195, 64–72. doi: 10.1016/j.virusres.2014.09.004

Ochola, D., and Tusiime, G. (2010). Survey on incidences and severity of Rice yellow mottle virus disease in eastern Uganda. *Int. J. Plant Pathol.* 2, 15–25. doi: 10.3923/ijpp.2011.15.25

Odongo, P. J., Kojima, N., Tsuboi, T., Asea, G., and Natsuaki, K. T. (2019). Evaluation of Ugandan rice cultivars for resistance against Rice yellow mottle virus. *Trop. Agric. Dev.* 63, 47–54. doi: 10.11248/jsta.63.47

Onwughalu, J. T., Abo, M. E., Okoro, J. K., Onasanya, A., and Sere, Y. (2011). Rice yellow mottle virus infection and reproductive losses in rice (*Oryza sativa* Linn.). *Trends Appl. Sci. Res.* 6, 182–189. doi: 10.3923/tasr.2011.182.189

Opalka, N., Brugidou, C., Bonneau, C., Nicole, M., Beachy, R. N., Yeager, M., et al. (1998). Movement of rice yellow mottle virus between xylem cells through pit membranes. *Proc. Natl. Acad. Sci. U. S. A.* 95, 3323–3328. doi: 10.1073/pnas.95.6.3323

Opalka, N., Tihova, M., Brugidou, C., Kumar, A., Beachy, R. N., Fauquet, C. M., et al. (2000). Structure of native and expanded Sobemoviruses by electron cryo-microscopy and image reconstruction. *J. Mol. Biol.* 303, 197–211. doi: 10.1006/jmbi.2000.4043

Orjuela, J., Thiémélé Deless, E. F., Kolade, O., Chéron, S., Ghesquiére, A., and Albar, L. (2013). A recessive resistance to rice yellow mottle virus is associated with a rice homolog of the CPR5 gene, a regulator of active defense mechanisms. *Mol. Plant-Microbe Interact.* 26, 1455–1463. doi: 10.1094/MPMI-05-13-0127-R

Parlevliet, J. E. (2002). Durability of resistance against fungal, bacterial and viral pathogens; present situation. *Euphytica* 124, 147–156. doi: 10.1023/A:1015601731446

Pidon, H., Chéron, S., Ghesquière, A., and Albar, L. (2020). Allele mining unlocks the identification of RYMV resistance genes and alleles in African cultivated rice. *BMC Plant Biol.* 20:222. doi: 10.1186/s12870-020-02433-0

Pidon, H., Ghesquière, A., Chéron, S., Issaka, S., Hébrard, E., Sabot, F., et al. (2017). Fine mapping of RYMV3: a new resistance gene to Rice yellow mottle virus from *Oryza glaberrima*. *Theor. Appl. Genet.* 130, 807–818. doi: 10.1007/s00122-017-2853-0

Pinel, A., N'Guessan, P., Bousalem, M., and Fargette, D. (2000). Molecular variability of geographically distinct isolates of Rice yellow mottle virus in Africa. *Arch. Virol.* 145, 1621–1638. doi: 10.1007/s007050070080

Pinel-Galzi, A., Dubreuil-Tranchant, C., Hébrard, E., Mariac, C., Ghesquière, A., and Albar, L. (2016). Mutations in rice yellow mottle virus polyprotein P2a involved in RYMV2 gene resistance breakdown. *Front. Plant Sci.* 7:1779. doi: 10.3389/fpls.2016.01779

Pinel-Galzi, A., Rakotomalala, M., Sangu, E., Sorho, F., Kanyeka, Z., Traoré, O., et al. (2007). Theme and variations in the evolutionary pathways to virulence of an RNA plant virus species. *PLoS Pathog.* 3:e180. doi: 10.1371/journal.ppat.0030180

Pinel-Galzi, A., Traoré, O., Séré, Y., Hébrard, E., and Fargette, D. (2015). The biogeography of viral emergence: Rice yellow mottle virus as a case study. *Curr. Opin. Virol.* 10, 7–13. doi: 10.1016/j.coviro.2014.12.002

Pinto, Y. M., Kok, R. A., and Baulcombe, D. C. (1999). Resistance to rice yellow mottle virus (RYMV) in cultivated African rice varieties containing RYMV transgenes. *Nat. Biotechnol.* 17, 702–707. doi: 10.1038/10917

Poulicard, N., Pinel-Galzi, A., Fargette, D., and Hébrard, E. (2014). Alternative mutational pathways, outside the VPg, of rice yellow mottle virus to overcome eIF(iso)4G-mediated rice resistance under strong genetic constraints. *J. Gen. Virol.* 95, 219–224. doi: 10.1099/vir.0.057810-0

Poulicard, N., Pinel-Galzi, A., Traoré, O., Vignols, F., Ghesquière, A., Konaté, G., et al. (2012). Historical contingencies modulate the adaptability of rice yellow mottle virus. *PLoS Pathog.* 8:e1002482. doi: 10.1371/journal.ppat.1002482

Pressoir, G., Albar, L., Ahmadi, N., Rimbault, I., Lorieux, M., Fargette, D., et al. (1998). Genetic basis and mapping of the resistance to rice yellow mottle virus. II. Evidence of a complementary epistasis between two QTLs. *Theor. Appl. Genet.* 97, 1155–1161. doi: 10.1007/s001220051004

Qu, C., Liljas, L., Opalka, N., Brugidou, C., Yeager, M., Beachy, R. N., et al. (2000). 3D domain swapping modulates the stability of members of an icosahedral virus group. *Structure* 8, 1095–1103. doi: 10.1016/S0969-2126(00)00508-6

Rakotomalala, M., Pinel-Galzi, A., Albar, L., Ghesquière, A., Rabenantoandro, Y., Ramavovololona, P., et al. (2008). Resistance to Rice yellow mottle virus in rice germplasm in Madagascar. *Eur. J. Plant Pathol.* 122, 277–286. doi: 10.1007/s10658-008-9282-5

Reagan, B. C., and Burch-Smith, T. M. (2020). Viruses reveal the secrets of plasmodesmal cell biology. *Mol. Plant-Microbe Interact.* 33, 26–39. doi: 10.1094/MPMI-07-19-0212-FI

Rimbaud, L., Papaïx, J., Rey, J. F., Barrett, L. G., and Thrall, P. H. (2018). Assessing the durability and efficiency of landscape-based strategies to deploy plant resistance to pathogens. *PLoS Comput. Biol.* 14:e1006067. doi: 10.1371/journal.pcbi.1006067

Sanfaçon, H. (2015). Plant translation factors and virus resistance. *Viruses* 7, 3392–3419. doi: 10.3390/v7072778

Sanford, J. C., and Johnston, S. A. (1985). The concept of parasite-derived resistance-deriving resistance genes from the parasite's own genome. *J. Theor. Biol.* 113, 395–405. doi: 10.1016/S0022-5193(85)80234-4

Sarra, S., and Peters, D. (2003). Rice yellow mottle virus is transmitted by cows, donkeys, and grass rats in irrigated rice crops. *Plant Dis.* 87, 804–808. doi: 10.1094/PDIS.2003.87.7.804

Sasaya, T., Nakazono-Nagaoka, E., Saika, H., Aoki, H., Hiraguri, A., Netsu, O., et al. (2014). Transgenic strategies to confer resistance against viruses in rice plants. *Front. Microbiol.* 4:409. doi: 10.3389/fmicb.2013.00409

Savary, S., Willocquet, L., Pethybridge, S. J., Esker, P., McRoberts, N., and Nelson, A. (2019). The global burden of pathogens and pests on major food crops. *Nat. Ecol. Evol.* 3, 430–439. doi: 10.1038/s41559-018-0793-y

Schoelz, J. E., Harries, P. A., and Nelson, R. S. (2011). Intracellular transport of plant viruses: finding the door out of the cell. *Mol. Plant* 4, 813–831. doi: 10.1093/mp/ssr070

Seck, P. A., Touré, A. A., Coulibaly, J. Y., Diagne, A., and Wopereis, M. C. S. (2013). "Africa's rice economy before and after the 2008 rice crisis," in *Realizing Africa's Rice Promise*. eds. M. Wopereis, D. Johnson, N. Ahmadi, E. Tollens and A. Jalloh (Cotonou, Benin: CABI), 24–34.

Séré, Y., Fargette, D., Abo, M. E., Wydra, K., Bimerew, M., Onasanya, A., et al. (2013). "Managing the major diseases of rice in Africa," in *Realizing Africa's Rice Promise*. eds. M. Wopereis, D. Johnson, N. Ahmadi, E. Tollens and A. Jalloh (Cotonou, Benin: CABI), 213–228.

Sere, Y., Sorho, F., Onasanya, A., Jobe, L., Darboe, S., Bojang, Y., et al. (2008). First report of Rice yellow mottle virus in rice in The Gambia. *Plant Dis.* 92:316. doi: 10.1094/PDIS-92-2-0316B

Siré, C., Bangratz-Reyser, M., Fargette, D., and Brugidou, C. (2008). Genetic diversity and silencing suppression effects of Rice yellow mottle virus and the P1 protein. *Virol. J.* 5:55. doi: 10.1186/1743-422X-5-55

Soko, D. F., Ayolie, K., Koffi, N. B. C., Tonessia, D. C., Sere, Y., Hilairekouakou, T., et al. (2016). Impact of eight isolates of Rice yellow mottle virus (RYMV) from Gagnoa (Côte d'Ivoire) on rice (*Oryza* sp) cultivars production. *Int. J. Biol. Chem. Sci.* 9:2459. doi: 10.4314/ijbcs.v9i5.17

Sõmera, M., Sarmiento, C., and Truve, E. (2015). Overview on Sobemoviruses and a proposal for the creation of the family sobemoviridae. *Viruses* 7, 3076–3115. doi: 10.3390/v7062761

Souza, P. F. N. (2020). Masters of manipulation: how do positive-sense RNA viruses employ plant proteins to replicate, move from cell to cell, and

overcome antiviral immunity? *J. Plant Dis. Prot.* 127, 425–440. doi: 10.1007/s41348-020-00342-w

Tamm, T., and Truve, E. (2000). Sobemoviruses. *J. Virol.* 74, 6231–6241. doi: 10.1128/JVI.74.14.6231-6241.2000

Tan, S., and Wu, S. (2012). Genome wide analysis of nucleotide-binding site disease resistance genes in *Brachypodium distachyon*. *Comp. Funct. Genomics* 2012:418208. doi: 10.1155/2012/418208

Taylor, D. R., Fofie, A. S., and Suma, M. (1990). Natural infection of rice yellow mottle virus disease (RYMV) on rice in Sierra Leone. *Int. Rice Res. newsl.* 15:19.

Thiémélé, D., Boisnard, A., Ndjiondjop, M. N., Chéron, S., Séré, Y., Aké, S., et al. (2010). Identification of a second major resistance gene to Rice yellow mottle virus, RYMV2, in the African cultivated rice species, *O. glaberrima*. *Theor. Appl. Genet.* 121, 169–179. doi: 10.1007/s00122-010-1300-2

Todorovska, E., Christov, N., Slavov, S., Christova, P., and Vassilev, D. (2009). Biotic stress resistance in wheat—breeding and genomic selection implications. *Biotechnol. Biotechnol. Equip.* 23, 1417–1426. doi: 10.2478/V10133-009-0006-6

Traoré, V. S. E., Néya, B. J., Camara, M., Gracen, V., Offei, S. K., and Traoré, O. (2015). Farmers' perception and impact of Rice yellow mottle disease on rice yields in Burkina Faso. *Agric. Sci.* 6, 943–952. doi: 10.4236/as.2015.69091

Traoré, O., Pinel, A., Fargette, D., and Konaté, G. (2001). First report and characterization of Rice yellow mottle virus in Central Africa. *Plant Dis.* 85:920. doi: 10.1094/PDIS.2001.85.8.920A

Traoré, O., Pinel, A., Hébrard, E., Dieudonné Gumedzoé, M. Y., Fargette, D., Traoré, A. S., et al. (2006a). Occurrence of resistance-breaking isolates of rice yellow mottle virus in West and Central Africa. *Plant Dis.* 90, 259–263. doi: 10.1094/PD-90-0259

Traoré, O., Pinel-Galzi, A., Issaka, S., Poulicard, N., Aribi, J., Aké, S., et al. (2010). The adaptation of Rice yellow mottle virus to the eIF(iso)4G-mediated rice resistance. *Virology* 408, 103–108. doi: 10.1016/j.virol.2010.09.007

Traoré, O., Pinel-Galzi, A., Sorho, F., Sarra, S., Rakotomalala, M., Sangu, E., et al. (2009). A reassessment of the epidemiology of Rice yellow mottle virus following recent advances in field and molecular studies. *Virus Res.* 141, 258–267. doi: 10.1016/j.virusres.2009.01.011

Traoré, O., Traoré, M. D., Fargette, D., and Konaté, G. (2006b). Rice seedbeds as a source of primary infection by Rice yellow mottle virus. *Eur. J. Plant Pathol.* 115, 181–186. doi: 10.1007/s10658-006-9004-9

Trovao, N. S., Baele, G., Vrancken, B., Bielejec, F., Suchard, M. A., Fargette, D., et al. (2015). Host ecology determines the dispersal patterns of a plant virus. *Virus Evol.* 1:vev016. doi: 10.1093/ve/vev016

Uke, A., Asea, G., and Natsuaki, K. (2016). Phylogenic analysis and serotyping of Rice yellow mottle virus strains in Uganda. *Trop. Agric. Dev.* 75, 81–88. doi: 10.11248/jsta.60.81

Uke, A., Tibanyendela, N., Ikeda, R., Fujiie, A., and Natsuaki, K. T. (2014). Modes of transmission and stability of Rice yellow mottle virus. *J. Plant Prot. Res.* 54, 363–366. doi: 10.2478/jppr-2014-0054

Valin, H., Sands, R. D., van der Mensbrugghe, D., Nelson, G. C., Ahammad, H., Blanc, E., et al. (2014). The future of food demand: understanding differences in global economic models. *Agric. Econ.* 45, 51–67. doi: 10.1111/agec.12089

van Loon, L. C. (1987). Disease induction by plant viruses. *Adv. Virus Res.* 33, 205–255. doi: 10.1016/S0065-3527(08)60319-X

Van Schie, C. C. N., and Takken, F. L. W. (2014). Susceptibility genes 101: how to be a good host. *Annu. Rev. Phytopathol.* 52, 551–581. doi: 10.1146/annurev-phyto-102313-045854

Varshney, R. K., Graner, A., and Sorrells, M. E. (2005). Genomics-assisted breeding for crop improvement. *Trends Plant Sci.* 10, 621–630. doi: 10.1016/j.tplants.2005.10.004

Ventelon-Debout, M., Delalande, F., Brizard, J. P., Diemer, H., Van Dorsselaer, A., and Brugidou, C. (2004). Proteome analysis of cultivar-specific deregulations of *Oryza sativa* indica and *O. sativa* japonica cellular suspensions undergoing Rice yellow mottle virus infection. *Proteomics* 4, 216–225. doi: 10.1002/pmic.200300502

Ventelon-Debout, M., Nguyen, T. T. H., Wissocq, A., Berger, C., Laudie, M., Piégu, B., et al. (2003). Analysis of the transcriptional response to Rice yellow mottle virus infection in *Oryza sativa* indica and japonica cultivars. *Mol. Gen. Genomics.* 270, 253–262. doi: 10.1007/s00438-003-0903-6

Ventelon-Debout, M., Tranchant-Dubreuil, C., Nguyen, T. T. H., Bangratz, M., Siré, C., Delseny, M., et al. (2008). Rice yellow mottle virus stress responsive genes from susceptible and tolerant rice genotypes. *BMC Plant Biol.* 8:26. doi: 10.1186/1471-2229-8-26

Wang, A., and Krishnaswamy, S. (2012). Eukaryotic translation initiation factor 4E-mediated recessive resistance to plant viruses and its utility in crop improvement. *Mol. Plant Pathol.* 13, 795–803. doi: 10.1111/j.1364-3703.2012.00791.x

Wang, Q., Ma, X., Qian, S., Zhou, X., Sun, K., Chen, X., et al. (2015). Rescue of a plant negative-strand RNA virus from cloned cDNA: insights into enveloped plant virus movement and morphogenesis. *PLoS Pathog.* 11:e1005223. doi: 10.1371/journal.ppat.1005223

Whitham, S. A., Yang, C., and Goodin, M. M. (2006). Global impact: elucidating plant responses to viral infection. *Mol. Plant-Microbe Interact.* 19, 1207–1215. doi: 10.1094/MPMI-19-1207

Yassi, M. N. A., Ritzenthaler, C., Brugidou, C., Fauquet, C., and Beachy, R. N. (1994). Nucleotide sequence and genome characterization of rice yellow mottle virus RNA. *J. Gen. Virol.* 75, 249–257. doi: 10.1099/0022-1317-75-2-249

Conflict of Interest: The authors declare that the research was conducted in the absence of any commercial or financial relationships that could be construed as a potential conflict of interest.

frontiers in Plant Science

METHODS
published: 03 September 2021
doi: 10.3389/fpls.2021.698573

Detection of Parietaria Mottle Virus by RT-qPCR: An Emerging Virus Native of Mediterranean Area That Undermine Tomato and Pepper Production in Southern Italy

Stefano Panno[1,2†], Andrea Giovanni Caruso[1†], Sofia Bertacca[1], Slavica Matić[3], Salvatore Davino[3,4] and Giuseppe Parrella[5*]*

[1] Department of Agricultural, Food and Forest Sciences, University of Palermo, Palermo, Italy, [2] Department of Biological, Chemical and Pharmaceutical Science and Technologies, University of Palermo, Palermo, Italy, [3] Institute for Sustainable Plant Protection, National Research Council (IPSP-CNR), Turin, Italy, [4] Consorzio di Ricerca sul Rischio Biologico in Agricoltura (Co.Ri.Bi.A.), Palermo, Italy, [5] Institute for Sustainable Plant Protection, National Research Council (IPSP-CNR), Portici, Italy

OPEN ACCESS

Edited by:
Yangrong Cao,
Huazhong Agricultural University, China

Reviewed by:
Edel Pérez-López,
Laval University, Canada
Jin Zhao,
Agricultural University of Hebei, China
Mengnan An,
Shenyang Agricultural University, China

***Correspondence:**
Salvatore Davino
salvatore.davino@unipa.it
Giuseppe Parrella
giuseppe.parrella@ipsp.cnr.it

[†] These authors have contributed equally to this work

Specialty section:
This article was submitted to Plant Pathogen Interactions, a section of the journal Frontiers in Plant Science

Received: 28 April 2021
Accepted: 29 July 2021
Published: 03 September 2021

Citation:
Panno S, Caruso AG, Bertacca S, Matić S, Davino S and Parrella G (2021) Detection of Parietaria Mottle Virus by RT-qPCR: An Emerging Virus Native of Mediterranean Area That Undermine Tomato and Pepper Production in Southern Italy. Front. Plant Sci. 12:698573. doi: 10.3389/fpls.2021.698573

Parietaria mottle virus (PMoV) is considered an emerging virus in many countries of the Mediterranean basin, especially on tomato and pepper crops. Symptoms on tomato leaves and fruits can be easily confused with those induced by cucumber mosaic virus (CMV) with necrogenic satellite RNA (CMV-satRNA), tomato spotted wilt virus (TSWV) or tomato mosaic virus (ToMV). Mixed infection of these viruses has been also reported in some tomato cultivars, with an increase in the complexity of the symptoms and severity of the disease. Although a specific serum and riboprobes have been produced, nowadays no sensitive diagnostic methods are available for the rapid PMoV detection. Here, we have developed a RT-qPCR assay with the aim to establish a more sensitive and specific method for PMoV detection. Specific primers and TaqMan probe were designed and *in silico* tested with all PMoV isolates available in GenBank. Moreover, this method was evaluated on tomato naturally infected samples from Sicily region (Italy). Results obtained showed that the RT-qPCR assay developed in this work is extremely sensitive, in fact, it is able to detect as few as 10 PMoV RNA copies in tomato total RNA; moreover, it will be a particularly valuable tool for early detection of PMoV. Furthermore, the analyzes on field samples show how this pathogen is increasingly present in tomato crops in the last years, helping to undermine the Italian horticultural sector.

Keywords: PMoV, RT-qPCR, emerging virus, early detection, field survey

INTRODUCTION

Vegetable crops represent one of the main sources of income and food worldwide. Among these crops of particular importance are tomatoes and peppers. Tomato (*Solanum lycopersicum* L., family *Solanaceae*) is a very important vegetable crop cultivated worldwide, with an area harvested of over five million hectares and a worldwide production of over 180 million tons (Food and Agriculture Organization of the United Nations (FAO), 2021). In the 2009–2019 decade, the global tomato

production increased by more than 25 million tons (Food and Agriculture Organization of the United Nations (FAO), 2021). Another important horticultural crop is the pepper (*Capsicum annuum* L., family *Solanaceae*), that is cultivated worldwide in almost two million hectares, with a total production of 38 million tons.

In Italy, tomato production in open field is mainly located in Apulia and Emilia-Romagna regions, whereas tomato production in protected conditions is primarily based in Sicily (Agri ISTAT, 2020).

In the Mediterranean basin, Italy represents the main access point for plant material to European countries, due to its central geographical position; this significantly increases the danger of introducing new pathogens, posing a serious risk to agriculture, biosecurity, and food production, jeopardizing the future of Italian horticulture (Panno et al., 2019c).

In the last decades, emerging and re-emerging viral diseases caused significant losses in the horticultural sector (Hanssen et al., 2010). In particular, Italian horticultural production has faced significant losses, due to the appearance or recrudescence of several viral diseases, including tomato yellow leaf curl virus (TYLCV), tomato yellow leaf curl Sardinia virus (TYLCSV) (Davino et al., 2009, 2012) and their recombinants (Panno et al., 2018), tomato spotted wilt virus (TSWV) (Panno et al., 2012), pepino mosaic virus (PepMV) (Davino et al., 2017b), tomato leaf curl New Delhi virus (ToLCNDV) (Panno et al., 2019b), tomato brown rugose fruit virus (ToBRFV) (Panno et al., 2019a, 2020b), and most recently, parietaria mottle virus (PMoV) (Parrella et al., 2020).

PMoV, genus *Ilarvirus* (subgroup 1), family *Bromoviridae*, was identified and characterized for the first time in 1987 in Turin province (northern Italy) in *Parietaria officinalis*, causing a typical mottling in leaves (Caciagli et al., 1989) and subsequently in tomato (Lisa et al., 1998) and pepper (Janssen et al., 2005) plants. PMoV belongs to the same subgroup of tobacco streak virus (TSV), the type member of the genus *Ilarvirus*, but these two viruses are not serologically correlated.

PMoV genome is composed of three positive sense single-stranded RNAs (Galipienso et al., 2009): the RNA1 (4.3 kb) encoding a putative replicase (p1); the RNA2 (2.3 kb) encoding a putative replicase (p2) and a protein of unknown function (2b) (Shimura et al., 2013); the RNA3 (2.7 kb) encoding the movement protein (MP) and the coat protein (CP) that is expressed through the sub-genomic RNA4 (Martìnez et al., 2014).

To date, PMoV has only been reported in a few countries of the Mediterranean basin, in particular Italy (Caciagli et al., 1989; Parrella et al., 2021), France (Marchoux et al., 1999), Greece (Roggero et al., 2000), and Spain (Aramburu, 2001). The real incidence of PMoV was often underestimated in the past, due to the confusion generated by similar symptoms, caused by TSWV, tomato mosaic virus (ToMV), cucumber mosaic virus (CMV) with the necrogenic satellite (satRNA), and to the lack of knowledge about this virus.

The symptomatology on tomato leaves consists of irregular necrotic lesions, coalescent and usually concentrated in the basal area; in addition, the necrotic lesions can perforate the leaf, which often appears deformed and curved (**Figure 1A**).

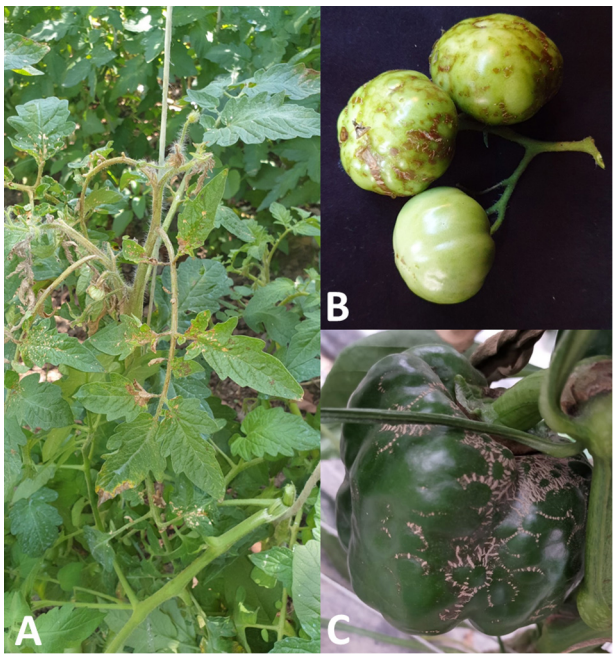

FIGURE 1 | Symptoms induced by PMoV in tomato and pepper: **(A)** basal irregular necrotic lesions of tomato leaflets, longitudinal necrotic stripes of the stem and necrosis of the apex; **(B)** greenish translucent rings and corky brownish rings on deformed tomato fruits; **(C)** brownish corky rings and fruits deformations in pepper.

The necrosis can progress to the leaf petiole and the stem, that often presents longitudinal necrotic stripes; in the worst cases, the stem apex necrotises and folds upon itself (Aramburu, 2001; **Figure 1A**). In tomato fruits the symptom consists in the pigmentation alteration: at the initial stage of infection, the fruits show greenish translucent rings, which become brownish, generally in relief, more or less corky and coalescent, causing fruit deformations (Galipienso et al., 2005; **Figure 1B**). On ripe and mature fruits, chlorotic rings associated to PMoV infection, have been also observed.

The symptoms on PMoV-infected pepper plants are very similar to symptoms described on tomato, consisting in corky necrotic stripes on the stems, corky rings and deformations on the fruits (**Figure 1C**), mosaic and basal necrosis on the leaves, causing in some cases the leaves perforation (Janssen et al., 2005).

PMoV can be passively transmitted by insects, such as thrips through the infected pollen (Aramburu et al., 2010).

Currently, the containment of PMoV dispersion can be implemented by early diagnosis and the application of preventive measures in crop management, reducing the introduction and subsequent spread in other countries. To date, there are no commercially available specific antibodies for the serological diagnosis of PMoV; the only currently available tool for PMoV identification is based on the end-point reverse transcription-polymerase chain reaction (RT-PCR) (Galipienso et al., 2008) and molecular hybridization techniques (Parrella et al., 2001, 2020; Galipienso et al., 2005). Consequently, it is necessary to develop

TABLE 1 | Forward, reverse primers and probe designed for RT-qPCR for the detection of PMoV.

Name	Genomic position	Referring sequence	Sequence 5′–3′	Length (nt)	Amplicon size (nt)
PMoV43 probe	1,392–1,413		FAM-CAGCGCAGGAATGCTCGCCGCG-TAMRA	22	
PMoV21F	1,370–1,389		CGGTGGACAAGTTTCGAACC	20	115
PMoV115R	1,464–1,484	KT005245	GGAAACCGGTATGACAGGTAC	21	
PMoV420F	1,769–1,788		GCACACGTACAAATGCCGAG	20	146
PMoV546R	1,895–1,914		GTCGAGAAATCGCAAACCAG	20	

In bold the primer pair with the lowest Ct value.

an alternative and more sensitive diagnostic methods for the PMoV early diagnosis. For this reason, the aim of the present work was to develop a sensitive and specific molecular method to detect PMoV in infected tomato and pepper plants, based on reverse transcription-quantitative polymerase chain reaction (RT-qPCR) with TaqMan® probe technique and estimate the dispersion of this pathogen in Southern Italy (Sicily).

MATERIALS AND METHODS

Source of Viral Material

One lyophilized PMoV isolate from tomato plant, named ST-1 (GenBank Acc. No. KP234349, Galipienso et al., 2015), stored in the plant virology laboratory of the University of Palermo, was used as source material for subsequent experiments. Total RNA from 100 mg of previously re-hydrated ST-1 isolate was extracted using a Plant RNA/DNA Purification Kit (Norgen Biotek Corp., ON, Canada), following the manufacturer's instructions. Total RNA concentration was determined in duplicate with NanoDrop 1000 spectrophotometer (Thermo Fisher Scientific, MA, United States) and used for cDNA synthesis. In the reverse transcription step (RT), the cDNA was obtained using the M-MLV Reverse Transcriptase (Thermo Fisher Scientific, MA, United States) in a 20 μL reaction volume containing 2 μL of total RNA and 100 pmol of the reverse primer PMoV-3R (5′-CACTCTTTACGTTGGCATCG-3′, position 1991–2010, Galipienso et al., 2008), according to the following cycling conditions: 42°C for 45 min and 95°C for 10 min. PCR was performed in 25 μL (final volume) containing 2 μL of the obtained cDNA, 20 mM Tris–HCl (pH 8.4), 50 mM KCl, 3 mM $MgCl_2$, 0.4 mM dNTPs, 100 pmol of the forward primer PMoV-2F (5′-AATCGAGACTTTCGCCAGGA-3′, position 865–884) and 100 pmol of the reverse primer PMoV-3R (Galipienso et al., 2008), 2U of Taq DNA polymerase (Thermo Fisher Scientific, MA, United States) and RNase free water to reach the final volume, according to the following cycling conditions: 95°C for 3 min; 40 cycles of 30 s at 95°C, 45 s at 55°C, 90 s at 72°C and a final elongation of 10 min at 72°C. The PCR was carried out in a MultiGene OptiMax thermal cycler (Labnet International Inc., NJ, United States). The obtained DNA products of expected size (1,146 nt) were confirmed by electrophoretic separation in a 1.5% agarose gel stained with SybrSafe (Thermo Fisher Scientific, MA, United States).

The obtained cDNA product using the PMoV-2F/PMoV-3R primer pair was cloned in the pGEM-T vector (Promega, WI, United States) following the manufacturer's instructions, and subsequently sequenced in both directions using an ABI PRISM 3100 DNA sequence analyzer (Applied Biosystems, CA, United States).

Primer and TaqMan® Probe Design

Multiple alignments using the ClustalX2 program (Larkin et al., 2007) were carried out using twenty PMoV CP sequences retrieved from GenBank database (Acc. No. KX866977, KP234349, KP234348, KP234347, KP234346, KP234343, KP234342, KP234341, KP234340, KP234339, KP234338, KP234337, KP234336, KP234335, KP234334, KP234333, KP234332, KP234331, KP234330, and KP234329).

Nucleotide identities between sequence pairs were estimated with the MEGA X program (Kumar et al., 2018), and two oligonucleotide primer pairs for RT-qPCR within the CP gene were designed using Vector NTI 11.5 (Thermo Fisher Scientific, MA, United States) (**Table 1**). Both sets of primers were tested, using the total RNA of ST-1 isolate with the concentration of ∼10 ng RNA/μL, by RT-qPCR with SYBR Green, in order to understand which primer pair has the lowest threshold cycle (Ct) value. The RT-qPCR was performed in a Rotor-Gene Q2plex HRM Platform Thermal Cycler (Qiagen, Hilden, Germany). The mixture consists in a 20 μL final volume, containing 1 μL of total RNA extract (ST-1), 1 μL of 0.5 mM of each primer, 10 μL of Master mix QuantiNova SYBR® Green PCR Kit (Qiagen, Hilden, Germany) and H_2O DEPC to reach the final volume.

Total RNA from a healthy tomato plant and water were used as negative control samples. Each sample was analyzed twice. Cycling conditions included reverse transcription at 45°C for 10 min, incubation at 95°C for 10 min, 40 cycles of 95°C for 5 s and 60°C for 10 s; the fluorescence was measured at the end of each cycle. Melting curve steps were added at the end of RT-qPCR as following: 95°C for 1 min, 40°C for 1 min, 70°C for 1 min and a temperature increase to 95°C at 0.5°C/s to record the fluorescence.

A specific PMoV TaqMan® probe (Eurofins Genomics, Luxembourg) was designed in a conserved domain within the region encompassed by the primers. The probe, with a length of 22 nucleotides, was 5′-labeled with the reporter dye FAM (6-carboxyfluorescein) and 3′-labeled with a non-fluorescent quencher (NFQ) TAMRA (**Table 1**). The predicted Tm values for PMoV primers and probe were 58 and 68°C, respectively, calculated with the prediction tool provided by Primer Express Software v3.0.1 (Thermo Fisher Scientific, MA, United States).

TABLE 2 | PMoV isolates used in this study.

ID sample	Isolate name	Original Host	Geographic coordinates	Sequence acc. num.
1	Sar-1	Tomato	N39°23′48″ E8°59′27″	MN782302
2	390	Tomato	N40°37′4″E14°22′56″	MW456562
3	391A	Tomato	N40°37′4″E14°22′56″	MW456563
4	316	Tomato	N40°50′2″E14°21′5″	na
5	317	Tomato	N40°50′2″E14°21′5″	na
6	305	Tomato	N40°32′28″E14°56′26″	na
7	306	Tomato	N40°32′28″E14°56′26″	na
8	307	Tomato	N40°32′28″E14°56′26″	na
9	Fri-1	Pepper	N40°56′57″ E14°0′29″	LT160068
10	Fri-2	Pepper	N40°56′57″ E14°0′29″	LT160070
11	Pap-1	Pepper	N40°49′33″E14°21′23″	LT160069
12	419	Pepper	N41°06′30″E13°56′48″	na
13	420	Pepper	N41°06′30″E13°56′48″	na
14	421	Pepper	N41°06′30″E13°56′48″	na
15	422	Pepper	N41°06′30″E13°56′48″	na

na, not applicable.

PMoV Genotype-Specific RT-qPCR Assay With TaqMan Probe

In order to test the RT-qPCR assay with TaqMan PMoV probe, fifteen PMoV isolates from tomato and pepper plants (eight tomato and seven pepper plants), stored at the plant Virology Laboratory of the Institute for Sustainable Plant Protection of National Research Council of Italy (IPSP-CNR), Portici section (Naples), were used (**Table 2**). Total RNA from these samples were extracted by using a Plant RNA/DNA Purification Kit (Norgen Biotek Corp., ON, Canada), following the manufacturer's instructions. In addition, another test was carried out with the most widespread viruses of the Mediterranean basin that affect tomato and pepper plants. In detail, the outgroup used to determine the RT-qPCR assay specificity was constituted by the following viral isolates: ToBRFV ToB-SIC01/19 isolate, ToCV (tomato chlorosis virus) Ragusa isolate, PepMV SIC2-09 isolate, CMV INU isolate, TSV (tobacco streak virus) ATCC isolate, TYLCV 8-4/2004 isolate, TYLCSV Sar-[IT:Sic:04] isolate, TICV (tomato infectious chlorosis virus) ART isolate, TSWV Turin isolate, and TMV and ToMV isolates supplied by Agdia, Inc., (Elkhart, IN, United States).

RT-qPCR was performed in a Rotor-Gene Q2plex HRM Platform Thermal Cycler in a reaction mix of 25 μL final volume, containing 5 μL of total RNA extract with the concentration of ∼10 ng RNA/μL, 0.5 μM of the forward primer PMoV21F and the reverse primer PMoV115R (the primer set that yielded the most sensitive detection for all PMoV isolates providing the lowest Ct values), 0.25 μM of TaqMan PMoV43 probe, 0.5 μL of RNase Inhibitor (Applied Biosystems, CA, United States), 12.5 μL of 2X QuantiNova Probe RT-PCR Master Mix, 0.25 μL of QN Probe RT-Mix, and H_2O DEPC water to reach final volume.

Two independent RT-qPCR assays were carried out. Each sample was analyzed in duplicate, moreover, the control samples in each test included total RNA purified from a healthy tomato plant, water instead of sample and at least two RNA transcripts (see below). The probe annealed specifically in an internal region of the PCR product amplified with primers PMoV21F and PMoV115R (primer pair that showed the lowest Ct value). The RT-qPCR conditions consisted in reverse transcription at 45°C for 10 min, enzyme denaturation at 95°C for 10 min, and 40 cycles of 95°C for 10 s and 60°C for 60 s; the fluorescence was measured at the end of each cycle. The mean (X) Ct value and the standard deviation (SD) for each sample were calculated from the four Ct values obtained.

Standard Curve

An external standard curve was obtained in order to determine the sensitivity of the RT-qPCR protocol. Serial dilutions of an *in vitro* synthesized positive-sense RNA transcript of the selected gRNA region were amplified using the RT-qPCR TaqMan assay. The template for the *in vitro* transcription was obtained using one ST-1 clone by conventional PCR amplification with the PMoV-3R primer and a modified PMoV-2F primer with the T7 promoter (Galipienso et al., 2008).

The obtained PCR product was transcribed *in vitro* with the HiScribe® T7 High Yield RNA Synthesis Kit (New England Biolabs, MA, United States) following the manufacturer's instructions.

Transcripts were purified with RNaid Spin kit (Bio101, CA, United States), treated twice with RNase free DNase (Turbo DNA-free from Ambion, TE, United States); their concentration was determined in duplicate with NanoDrop 1000 spectrophotometer (Thermo Fisher Scientific, MA, United States).

Ten-fold serial dilutions of the transcript in healthy tomato total RNA extract (10 ng/μL) containing 10^{10}–10^{1} copies were used in the RT-qPCR TaqMan assay. To ensure the absence of DNA template in transcript preparations, the assay was performed with and without the reverse transcriptase.

The RNA transcript concentration (pmol) in each dilution was calculated with the formula: micrograms of transcript RNA × (106 pg/1 μg) × (1 pmol/340 pg) × (1/number

TABLE 3 | Ct values obtained by RT-qPCR assay with TaqMan probe of fifteen PMoV isolates, two RNA transcripts, and other viruses used as outgroups.

Virus isolate	Ct ± SD
Sar-1	18.51 ± 0.2
390	24.98 ± 0.1
391A	22.22 ± 0.1
316	19.01 ± 0.3
317	18.77 ± 0.3
305	22.70 ± 0.2
306	21.89 ± 0.1
307	17.18 ± 0.2
Fri-1	21.09 ± 0.3
Fri-2	24.85 ± 0.1
Pap-1	17.69 ± 0.1
419	24.89 ± 0.3
420	18.50 ± 0.2
421	25.46 ± 0.1
422	26.86 ± 0.1
tRNA1	8.09 ± 0.1
tRNA2	8.51 ± 0.2
Healthy tomato plant tRNA	n.d.
Water	–
ToBRFV ToB-SIC01/19	n.d.
ToCV Ragusa	n.d.
PepMV SIC2-09	n.d.
CMV INU	n.d.
TSV ATCC	n.d.
TYLCV 8-4/2004	n.d.
TYLCSV Sar-[IT:Sic:04]	n.d.
TICV ART	n.d.
TSWV Turin	n.d.
TMV (Agdia, Inc.)	n.d.
ToMV (Agdia, Inc.)	n.d.

n.d., not detected.

of bases of the transcript), and the number of RNA copies was calculated using this concentration value and Avogadro's constant. The standard curve was obtained plotting the Ct values from two independent assays with four replicates per standard dilution vs. the logarithm of the RNA concentration dilution. The amplification efficiency was calculated from the slope of the corresponding curve using the formula $10^{(-1/\text{slope of the standard curve})}$, or the same formula × 100 (when given as a percentage value).

Comparison Between RT-qPCR and Conventional End-Point RT-PCR Techniques on Field Samples

A total of 130 tomato plants with and without typical symptoms induced by PMoV infection were collected in Sicily in month of June during the years 2018–2020. In detail, 40 leaf samples were collected in the 2018 (30 symptomatic and 10 asymptomatic samples), 40 leaf samples in the 2019 (30 symptomatic and 10 asymptomatic samples), and 50 samples leaf in the 2020 (35 symptomatic and 15 asymptomatic samples). The sampling areas selected were marked by GPS using the Planthology mobile application (Davino et al., 2017a). Each sample was placed in an extraction plastic bag (Bioreba, Kanton Reinach, Switzerland) containing 1 mL of extraction buffer (50 mM Tris pH 9.0, 150 mM LiCl, 5 mM EDTA), and homogenized with a HOMEX 6 homogenizer (Bioreba, Kanton Reinach, Switzerland). Healthy tomato plants used as negative controls were grown in a phytotron with a 16/8 hrs light/dark photoperiod, 27°C and 70–90% relative humidity. Total RNA from each sample was extracted by using a Plant RNA/DNA Purification Kit (Norgen Biotek Corp., ON, Canada), following the manufacturer's instructions, and the concentration was determined in duplicate with NanoDrop 1000 spectrophotometer (Thermo Fisher Scientific, MA, United States). In order to assess the presence/absence of PMoV, the collected samples were analyzed by conventional end-point RT-PCR (Galipienso et al., 2008). Subsequently, the same samples were analyzed in duplicate by RT-qPCR, following the protocol described previously, in order to confirm the validity of the technique developed in this work and to compare the results of the two diagnostic methods.

RESULTS

Source of Viral Material

The RT-PCR product of the ST-1 isolate used in this study showed the expected 1,146-bp size. The obtained sequence after cloning was trimmed in order to remove the external nucleotides, leaving only the coding region of the CP gene which showed a percentage identity of >99% with original ST-1 isolate (Galipienso et al., 2015).

Primer and TaqMan® Probe Design and Protocol Optimization

In **Table 1** are reported the two primer pairs and probe designed. The PMoV21F/PMoV115R primer pair showed lower Ct value (8.64 ± 0.2) compared to the PMoV420F/PMoV546R primer pair (9.02 ± 0.2) and were selected chosen as the best candidates together with the TaqMan PMoV43 probe for the subsequent analyses (Figure not shown). The optimal annealing/extension temperature was found at 60°C and it was selected for the RT-qPCR assay.

PMoV Genotype-Specific RT-qPCR Assay With TaqMan® Probe

As reported in **Table 3**, the two RNA transcripts, used as positive controls, gave the most sensitive signal with a Ct value ranging from 8.09 ± 0.1 to 8.51 ± 0.2 in the four different assays. The total RNA derived from all tested PMoV isolates (15) gave also positive signal with a Ct value that ranged from 17.18 ± 0.2 to 26.86 ± 0.1, (**Supplementary Figure 1**), while ToBRFV, ToCV, PepMV, CMV, TSV, TYLCV, TYLCSV, TICV, TSWV, TMV, and ToMV isolates used as outgroups did not give any signal. The qRT-PCR assay confirmed its specificity since it gave no signals from healthy tomato RNA extracts and water as well. As far as the repeatability and reproducibility of the assay is considered, it

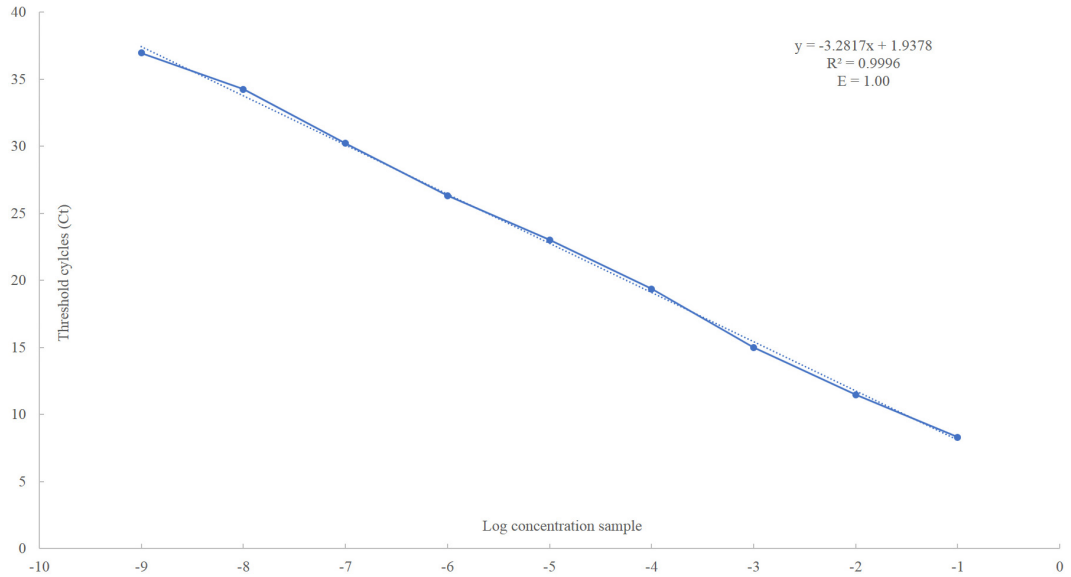

FIGURE 2 | Linear regression analysis, plotting the Ct value in the Y-axis vs. the logarithm of the starting RNA dilutions in the X-axis. Each plotted point represents the mean Ct value that was calculated from the four different experiments with two replicates. The calculated correlation coefficient (R^2) and amplification efficiency (E) values are indicated in each curve.

TABLE 4 | Number of samples and percentage of positive samples analyzed by end point RT-PCR and RT-qPCR during the years 2018–2020.

Sampling year	End point RT-PCR			RT-qPCR		
	Samples analyzed	Positive samples	% Positive sample	Samples analyzed	Positive samples	% Positive sample
2018	40	9	22.50	40	9	22.50
2019	40	13	32.50	40	14	35.00
2020	50	24	48.00	50	29	58.00
Total	130	46	35.38	130	52	40.00

was able to reliably amplify the 115-bp portion of PMoV CP gene in different experiments and laboratory conditions.

Standard Curve

The obtained standard curve covered a wide dynamic range (10 units of concentration) and showed a strong linear relationship, with a correlation coefficient of 0.9996 and 100% amplification efficiency (**Figure 2** and **Supplementary Figure 2**). The high sensitivity of the assay was achieved covering eight orders of magnitude of RNA concentration and enabling the detection of as few as 10^1 PMoV RNA copies in tomato total RNA.

Comparison Between RT-qPCR and Conventional End-Point RT-PCR Techniques on Field Samples

As reported in **Table 4**, **46** out of 130 samples resulted positive to PMoV by RT-PCR end- point, while 52 out of 130 samples give positive results to PMoV infection by RT-qPCR. In detail, the RT-qPCR showed an increase in detecting PMoV-positive samples, in fact the percentage of samples resulted positive were 40%, and 35.38% with RT-qPCR and conventional RT-PCR, respectively.

Regarding the difference in score between samples resulted positive at RT-PCR end-point and RT-qPCR, it is important to note that it concerns only asymptomatic samples (**Table 5**). Probably, this result is due to the low viral titer of asymptomatic samples. In **Table 5** are reported and compared the results obtained from the two independent analyses.

Regarding the PMoV spread dynamics in Sicily, during the 3 years of sampling, using the RT-qPCR assay, the incidence showed an upward trend from 22.5% in 2018 to 40% in 2020 (**Table 4**) in the area object of the survey, demonstrating an increase of PMoV infection of 17.5%.

DISCUSSION

Climate change, global trade and anthropic activities (and their consequences) seem to be closely related to the emergence of new viruses, triggering an increasing number of outbreaks and epidemics. In fact, emerging and re-emerging virus diseases represent a real threat for horticultural production, as has happened in recent years in southern Italy, with the ToLCNDV

TABLE 5 | Comparison of positive field samples to RT-qPCR with end point RT-PCR results.

Sampling year	ID sample	Symptomatic	End point RT-PCR results	RT-qPCR results	Ct value 1st test	Ct value 2nd test
	Sic 03/18	Yes	+	+	16.15	16.23
	Sic 09/18	Yes	+	+	13.84	12.98
	Sic 10/18	Yes	+	+	20.92	20.74
	Sic 15/18	Yes	+	+	21.59	22.03
2018	Sic 19/18	Yes	+	+	19.74	20.23
	Sic 20/18	Yes	+	+	17.63	18.13
	Sic 25/18	Yes	+	+	18.62	17.15
	Sic 31/18	Yes	+	+	29.76	31.48
	Sic 37/18	Yes	+	+	19.45	18.34
	Sic 07/19	Yes	+	+	18.95	17.03
	Sic 08/19	Yes	+	+	16.89	18.12
	Sic 11/19	Yes	+	+	15.96	16.42
	Sic 15/19	Yes	+	+	14.13	13.98
	Sic 20/19	Yes	+	+	15.18	15.73
2019	**Sic 24/19**	No	–	+	29.56	29.19
	Sic 25/19	Yes	+	+	18.30	17.99
	Sic 29/19	Yes	+	+	17.65	18.25
	Sic 32/19	Yes	+	+	28.74	28.23
	Sic 33/19	Yes	+	+	16.54	16.76
	Sic 34/19	Yes	+	+	27.68	29.01
	Sic 38/19	Yes	+	+	25.78	25.81
	Sic 39/19	Yes	+	+	23.98	22.37
	Sic 40/19	Yes	+	+	19.54	19.13
	Sic 03/20	Yes	+	+	17.62	17.25
	Sic 04/20	Yes	+	+	20.33	21.27
	Sic 06/20	No	–	+	30.52	30.11
	Sic 07/20	No	+	+	27.89	28.46
	Sic 08/20	Yes	+	+	15.98	16.00
	Sic 10/20	Yes	+	+	15.19	14.88
	Sic 13/20	Yes	+	+	22.89	22.24
	Sic 14/20	Yes	+	+	21.64	22.78
	Sic 16/20	Yes	+	+	22.13	22.47
2020	**Sic 19/20**	No	–	+	29.33	29.98
	Sic 23/20	Yes	+	+	24.53	23.89
	Sic 24/20	Yes	+	+	23.66	23.29
	Sic 26/20	Yes	+	+	18.58	19.01
	Sic 27/20	Yes	+	+	23.47	22.96
	Sic 28/20	No	–	+	30.06	29.15
	Sic 30/20	Yes	+	+	16.29	16.76
	Sic 31/20	Yes	+	+	18.77	18.59
	Sic 33/20	No	–	+	30.75	31.09
	Sic 34/20	Yes	+	+	13.74	13.27
	Sic 35/20	Yes	+	+	19.84	19.99
	Sic 38/20	Yes	+	+	22.78	22.01
	Sic 39/20	Yes	+	+	22.59	23.08
	Sic 40/20	No	–	+	29.68	30.23
	Sic 43/20	Yes	+	+	14.61	15.12
	Sic 44/20	Yes	+	+	21.56	21.43
	Sic 46/20	Yes	+	+	21.15	21.36

(Continued)

TABLE 5 | Continued

Sampling year	ID sample	Symptomatic	End point RT-PCR results	RT-qPCR results	Ct value 1st test	Ct value 2nd test
	Sic 48/20	Yes	+	+	19.60	20.12
	Sic 49/20	Yes	+	+	22.97	23.28
	Sic 50/20	Yes	+	+	19.74	20.11
	ST-1 clone	–	+	+	11.91	12.05
	Healthy plant	–	–	–	-	-

In bold the asymptomatic samples resulted negative to end point RT-PCR and positive to RT-qPCR.

dispersion (Panno et al., 2019b) and, more recently, with the emergence and subsequent rapid ToBRFV spread in Sicily (Panno et al., 2020a) which, in the last 2 years, has been seriously compromising tomato and pepper productions.

Numerous works have highlighted that climatic conditions changes are affecting the ecological impact of some plants, including *P. officinalis*, and thus could be in some extent responsible for increasing the PMoV incidence, substantially by enlarging the flowering period, and thus the pollen production (D'Amato and Cecchi, 2008).

Pathogen detection, identification and quantification are important in plant disease control, and must be accessible in all countries to ensure eco-sustainable crop production and food safety. For these reasons, it is essential to develop, in a plant disease surveillance context, new early diagnosis methods in order to control the pathogens (Ferriol et al., 2015; Puchades et al., 2017; Panno et al., 2020c). For this purpose, distinct parameters including environment conditions, genetic characteristics, transmission methods (Ferriol et al., 2013) and agronomical practices, such as organic amendment should be considered (d'Errico et al., 2019).

Specifically, as regard virus diseases, the detection is usually performed, when available, by serological tests such as double antibody sandwich enzyme-linked immunosorbent assay (DAS-ELISA) using polyclonal or monoclonal antibodies but, in most cases, the commercial ELISA tests unavailability and/or the low viral titer in nursery plants or during the early stages of virus infection, do not allow the reliable use of these techniques (Jacobi et al., 1998).

In detail, antigen-coated plate (ACP) ELISA and direct tissue blot immunoassay (DTBIA) using a polyclonal antiserum, non-isotopic tissue-printing hybridization (TPH) and dot-blot hybridization using a specific riboprobe, and one-step or two-steps RT-PCR end-point, are the diagnostic tests developed for the specific PMoV detection by some researchers so far (Roggero et al., 2000; Parrella et al., 2001, 2016; Galipienso et al., 2005, 2015; Parrella, 2020).

Nevertheless, serological methods have some limitations because PMoV is a poorly immunogenic, producing antiserum with a low titer, even against the homologous virus (Caciagli et al., 1989) and currently no commercial kits are available for the specific serological PMoV diagnosis. In addition, TSV and prunus necrotic ringspot virus (PNRSV), which belongs, respectively, to *Ilarvirus* subgroups I and III, react with PMoV isolates, although very weakly (Lisa et al., 1998).

The one-step RT-PCR end-point has been widely applied for the diagnosis and molecular characterization of PMoV isolates (Galipienso et al., 2005, 2008). The different diagnostic methods described above shows lack of information regarding the sensitivity and specificity, therefore, there is a current need for the development of a specific and sensitive methods for PMoV identification, which could also be usefully applied to epidemiological studies.

This study describes the development and evaluation of a RT-qPCR assay for the sensitive and specific PMoV detection which, in recent years, has increased its incidence in tomato and pepper crops in southern Italy. As reported in section "Results", the efficiency of PMoV detection in symptomatic and asymptomatic tomato samples from Sicily was higher with the RT-qPCR developed (52 out of 130 samples) compared to the conventional RT-PCR method (46 of 130 samples) described by Galipienso et al. (2008), with a sensitivity percentage increase of 4.62%. It is possible to note how the RT-qPCR assay developed in this study is more sensitive; this statement is also confirmed by the results of the sensitivity tests (see section "Standard Curve"), which showed that the developed technique is able to detect as few as 10 PMoV RNA copies in tomato total RNA.

Although it is difficult to compare the sensitivity of the PMoV RT-qPCR to the RT-qPCR assays for other ilarvirus species (Osman et al., 2014), as sensitivities are reported rarely in terms of target copy number, but in terms of sample dilution which are not directly comparable, however, a detection limit of approximately ten copies of target is consistent with assays for other, unrelated plant viruses (Agindotan et al., 2007; Gutierrez-Aguirre et al., 2009). In addition, field data demonstrate that the proposed RT-qPCR method being more sensitive, especially in asymptomatic samples, compared to those described so far for the PMoV early diagnosis, and it could represent a good and reliable tool to be applied in low viral titer conditions, during early stage of the disease, and in search for alternative hosts and latent infections.

In conclusion, the results obtained in the present study demonstrate the accuracy, specificity sensitivity, repeatability and reproducibility of the RT-qPCR assay developed for the diagnosis of PMoV in tomato and pepper plants. It is expected that the implementation of this RT-qPCR with TaqMan® probe assay will facilitate efficient and fast phytosanitary certification of nursery stock, when wide samples indexing is required, thereby decreasing the risk of further spread of this dangerous virus. Moreover, the method proposed can also be useful for other application and studies, where sensitivity, accuracy

and quantitative date are required, such as field survey, identification of natural virus reservoirs, and screening and characterization of resistances in germplasm.

DATA AVAILABILITY STATEMENT

The raw data supporting the conclusions of this article will be made available by the authors, without undue reservation.

AUTHOR CONTRIBUTIONS

SP designed and performed the experiments and bioinformatics analysis, analyzed the data, prepared figures and/or tables, authored the drafts of the manuscript, and approved the final draft. AC performed the experiments and bioinformatics analysis, analyzed the data, prepared figures and/or tables, and approved the final draft. SB performed the experiments and bioinformatics analysis, analyzed the data, and approved the final draft. SM analyzed the data, authored and reviewed drafts of the manuscript, and approved the final draft. SD conceived and designed the experiments, contributed to reagents, materials, and analysis tools, authored or reviewed drafts of the manuscript, and approved the final draft. GP conceived and designed the experiments, authored or reviewed drafts of the manuscript, and approved the final draft. All authors contributed to the article and approved the submitted version.

SUPPLEMENTARY MATERIAL

The Supplementary Material for this article can be found online at: https://www.frontiersin.org/articles/10.3389/fpls.2021.698573/full#supplementary-material

Supplementary Figure 1 | RT-qPCR assay with TaqMan® probe of fifteen characterized PMoV isolates and two RNA transcripts, using the PMoV21F/PMoV115R primer pair.

Supplementary Figure 2 | Standard curves prepared with 10-fold serial dilutions of *in vitro*-synthesized RNA transcripts from PMoV ST-1 clone using RT-qPCR with TaqMan probe.

REFERENCES

Agindotan, B. O., Shiel, P. J., and Berger, P. H. (2007). Simultaneous detection of potato viruses, PLRV, PVA PVX and PVY from dormant potato tubers by TaqMan realtime RT-PCR. *J. Virol. Methods* 142, 1–9. doi: 10.1016/j.jviromet.2006.12.012

Agri ISTAT (2020). *Benvenuto in I.Stat, la Banca Dati Completa per gli Esperti*. Available online at: http://dati.istat.it/ (Accessed April 6, 2021)

Aramburu, J. (2001). First report of *Parietaria mottle virus* on tomato in Spain. *Plant Dis.* 85:1210. doi: 10.1094/PDIS.2001.85.11.1210C

Aramburu, J., Galipienso, L., Aparicio, F., Soler, S., and López, C. (2010). Mode of transmission of *Parietaria mottle virus*. *J. Plant Pathol.* 92, 679–684.

Caciagli, P., Boccardo, B., and Lovisolo, O. (1989). *Parietaria mottle virus*, a possible new *Ilarvirus* from *Parietaria officinalis* (Urticaceae). *Plant Pathol.* 38, 577–584. doi: 10.1111/j.1365-3059.1989.tb01454.x

D'Amato, G., and Cecchi, L. (2008). Effects of climate change on environmental factors in respiratory allergic diseases. *Clin. Exp. Allergy* 38, 1264–1274. doi: 10.1111/j.1365-2222.2008.03033.x

Davino, S., Miozzi, L., Panno, S., Rubio, L., Davino, M., and Accotto, G. P. (2012). Recombination profiles between *Tomato yellow leaf curl virus* and *Tomato yellow leaf curl Sardinia virus* in laboratory and field conditions: evolutionary and taxonomic implications. *J. Gen. Virol.* 93, 2712–2717. doi: 10.1099/vir.0.045773-0

Davino, S., Napoli, C., Dellacroce, C., Miozzi, L., Noris, E., Davino, M., et al. (2009). Two new natural *Begomovirus* recombinants associated with the tomato yellow leaf curl disease co-exist with parental viruses in tomato epidemics in Italy. *Virus Res.* 143, 15–23. doi: 10.1016/j.virusres.2009.03.001

Davino, S., Panno, S., Arrigo, M., La Rocca, M., Caruso, A. G., and Bosco, G. L. (2017a). Planthology: an application system for plant diseases management. *Chem. Eng. Transact.* 58, 619–624. doi: 10.3303/CET1758104

Davino, S., Panno, S., Iacono, G., Sabatino, L., D'Anna, F., Iapichino, G., et al. (2017b). Genetic variation and evolutionary analysis of *Pepino mosaic virus* in Sicily: insights into the dispersion and epidemiology. *Plant Pathol.* 66, 368–375. doi: 10.1111/ppa.12582

d'Errico, G., Marra, R., Crescenzi, A., Davino, S., Fanigliulo, A., Woo, S. L., et al. (2019). Integrated management strategies of *Meloidogyne incognita* and *Pseudopyrenochaeta lycopersici* on tomato using a *Bacillus firmus*-based product and two synthetic nematicides in two consecutive crop cycles in greenhouse. *Crop Prot.* 122, 159–164. doi: 10.1016/j.cropro.2019.05.004

Ferriol, I., Rangel, E. A., Panno, S., Davino, S., Han, C. G., Olmos, A., et al. (2015). Rapid detection and discrimination of fabaviruses by flow-through hybridisation with genus-and species-specific riboprobes. *Ann. Appl. Biol.* 167, 26–35. doi: 10.1111/aab.12204

Ferriol, I., Rubio, L., Perez-Panadez, J., Carbonell, E. A., Davino, S., and Belliure, B. (2013). Transmissibility of *Broad bean wilt virus 1* by aphids: influence of virus accumulation in plants, virus genotype and aphid species. *Ann. Appl. Biol.* 162, 71–79. doi: 10.1111/j.1744-7348.2012.00579.x

Food and Agriculture Organization of the United Nations (FAO) (2021). *Food and Agriculture Data*. Available online at: http://www.fao.org/faostat/en/#home (Accessed April 6, 2021)

Galipienso, L., del Carmen Herranz, M., López, C., Pallás, V., and Aramburu, J. (2008). Sequence analysis within the RNA 3 of seven Spanish tomato isolates of *Parietaria mottle virus* (PMoV-T) reveals important structural differences with the *Parietaria* isolates (PMoV). *Eur. J. Plant Pathol.* 120, 125–135. doi: 10.1007/s10658-007-9200-2

Galipienso, L., Herranz, M. C., Pallas, V., and Aramburu, J. (2005). Detection of a tomato strain of *Parietaria mottle virus* (PMoV-T) by molecular hybridization and RT-PCR in field samples from north-eastern Spain. *Plant Pathol.* 54, 29–35. doi: 10.1111/j.1365-3059.2005.01109.x

Galipienso, L., Martínez, C., Willemsen, A., Alfaro-Férnandez, A., Font-San Ambrosio, I., Davino, S., et al. (2015). Genetic variability and evolutionary analysis of *Parietaria mottle virus*: role of selection and genetic exchange. *Arch. Virol.* 160, 2611–2616. doi: 10.1007/s00705-015-2550-8

Galipienso, L., Rubio, L., Lòpez, C., Soler, S., and Aramburu, J. (2009). Complete nucleotide sequence of a Spanish isolate of *Parietaria mottle virus* infecting tomato. *Virus Genes* 39, 256–260. doi: 10.1007/s11262-009-0388-4

Gutierrez-Aguirre, I., Mehle, N., Delic, D., Gruden, K., Mumford, R., and Ravnikar, M. (2009). Real-time quantitative PCR based sensitive detection and genotype discrimination of *Pepino mosaic virus*. *J. Virol. Methods* 162, 46–55. doi: 10.1016/j.jviromet.2009.07.008

Hanssen, I. M., Lapidot, M., and Thomma, B. P. H. J. (2010). Emerging viral diseases of tomato crops. *Mol. Plant Microbe Interact.* 23, 539–548. doi: 10.1094/MPMI-23-5-0539

Jacobi, V., Bachand, G. D., Hamelin, R. C., and Castello, J. D. (1998). Development of a multiplex immunocapture RT-PCR assay for detection and differentiation of tomato and tobacco mosaic tobamoviruses. *J. Virol. Methods* 74, 167–178. doi: 10.1016/S0166-0934(98)00086-X

Janssen, D., Sàez, E., Segundo, E., Martìn, G., Gil, F., and Cuadrado, I. (2005). *Capsicum annuum*–a new host of *Parietaria mottle virus* in Spain. *Plant Pathol.* 54:567. doi: 10.1111/j.1365-3059.2005.01195.x

Kumar, S., Stecher, G., Li, M., Knyaz, C., and Tamura, K. (2018). MEGA X: molecular evolutionary genetics analysis across computing platforms. *Mol. Biol. Evol.* 35, 1547–1549. doi: 10.1093/molbev/msy096

Larkin, M. A., Blackshields, G., Brown, N. P., Chenna, R., McGettigan, P. A., McWilliam, H., et al. (2007). Clustal W and clustal X version 2.0. *Bioinformatics* 23, 2947–2948. doi: 10.1093/bioinformatics/btm404

Lisa, V., Ramasso, E., Ciuffo, M., and Roggero, P. (1998). "Tomato apical necrosis caused by a strain of *Parietaria mottle ilarvirus*," in *Proceedings of the 9th Conference of the International Society for Horticultural Science*, (Torino: International Society for Horticultural Science), 3–5.

Marchoux, G., Parrella, G., and Gebre-Selassie Gognalons, P. (1999). Identification de deux *Ilarvirus* sur tomate dans le sud de la France. *Phytoma La Dèfense des vègètaux* 522, 53–55.

Martìnez, C., Coll-Bonfill, N., Aramburu, J., Pallàs, V., Aparicio, F., and Galipienso, L. (2014). Two basic (hydrophilic) regions in the movement protein of *Parietaria mottle virus* have RNA binding activity and are required for cell-to-cell transport. *Virus Res.* 184, 54–61. doi: 10.1016/j.virusres.2014.02.008

Osman, F., Al Rwahnih, M., and Rowhani, A. (2014). Improved detection of ilarviruses and nepoviruses affecting fruit trees using quantitative RT-qPCR. *J. Plant Pathol.* 96, 577–583. doi: 10.4454/JPP.V96I3.010

Panno, S., Caruso, A. G., Barone, S., Lo Bosco, G., Rangel, E. A., and Davino, S. (2020a). Spread of *Tomato brown rugose fruit virus* in Sicily and evaluation of the spatiotemporal dispersion in experimental conditions. *Agronomy* 10:834. doi: 10.3390/agronomy10060834

Panno, S., Caruso, A. G., Blanco, G., and Davino, S. (2020b). First report of *Tomato brown rugose fruit virus* infecting sweet pepper in Italy. *New Dis. Rep.* 41:20. doi: 10.5197/j.2044-0588.2020.041.020

Panno, S., Caruso, A. G., and Davino, S. (2018). The nucleotide sequence of a recombinant *Tomato yellow leaf curl virus* strain frequently detected in Sicily isolated from tomato plants carrying the *Ty-1* resistance gene. *Arch. Virol.* 163, 795–797. doi: 10.1007/s00705-017-3674-9

Panno, S., Caruso, A. G., and Davino, S. (2019a). First report of *Tomato brown rugose fruit virus* on tomato crops in Italy. *Plant Dis.* 103, 1443–1443. doi: 10.1094/PDIS-12-18-2254-PDN

Panno, S., Caruso, A. G., Troiano, E., Luigi, M., Manglli, A., Vatrano, T., et al. (2019b). Emergence of tomato leaf curl New Delhi virus in Italy: estimation of incidence and genetic diversity. *Plant Pathol.* 68, 601–608. doi: 10.1111/ppa.12978

Panno, S., Davino, S., Rubio, L., Rangel, E., Davino, M., García-Hernández, J., et al. (2012). Simultaneous detection of the seven main tomato-infecting RNA viruses by two multiplex reverse transcription polymerase chain reactions. *J Virol. Methods* 186, 152–156. doi: 10.1016/j.jviromet.2012.08.003

Panno, S., Matic, S., Tiberini, A., Caruso, A. G., Bella, P., Torta, L., et al. (2020c). Loop mediated isothermal amplification: principles and applications in plant virology. *Plants* 9:461. doi: 10.3390/plants9040461

Panno, S., Ruiz-Ruiz, S., Caruso, A. G., Alfaro-Fernandez, A., San Ambrosio, M. I. F., and Davino, S. (2019c). Real-time reverse transcription polymerase chain reaction development for rapid detection of *Tomato brown rugose fruit virus* and comparison with other techniques. *PeerJ* 7:e7928. doi: 10.7717/peerj.7928

Parrella, G. (2020). Sources of resistance in wild *Solanum* germplasm (section *lycopersicon*) to *Parietaria mottle virus*, an emerging virus in the Mediterranean basin. *Plant Pathol.* 69, 1018–1025. doi: 10.1111/ppa.13194

Parrella, G., Greco, B., and Troiano, E. (2016). Severe symptoms of mosaic and necrosis in bell pepper associated with *Parietaria mottle virus* in Italy. *Plant Dis.* 100:1514. doi: 10.1094/PDIS-02-16-0194-PDN

Parrella, G., Roggero, P., and Gallitelli, D. (2001). "Detection of *Parietaria mottle virus* by digoxigenin-labelled cRNA probe and RT-PCR," in *Proceedings of the 5th Congress of the European Foundation for Plant Pathology (EFPP): Biodiversity in Plant Pathology*, (Taormina), 219–220.

Parrella, G., Troiano, E., Cherchi, C., and Giordano, P. (2020). Severe outbreaks of *Parietaria mottle virus* in tomato in Sardinia, southern Italy. *J. Plant Pathol.* 102:915. doi: 10.1007/s42161-020-00492-8

Parrella, G., Troiano, E., Stinca, A., and Pozzi, M. I. (2021). Molecular and serological detection of *Parietaria mottle virus* in *Phytolacca americana*, a new host of the virus. *Phytopathol. Mediterr.* 60, 101–104. doi: 10.36253/phyto-12207

Puchades, A. V., Carpino, C., Alfaro-Fernandez, A., Font-San-Ambrosio, M. I., Davino, S., Guerri, J., et al. (2017). Detection of southern tomato virus by molecular hybridisation. *Ann. Appl. Biol.* 171, 172–178. doi: 10.1111/aab.12367

Roggero, P., Ciuffo, M., Katis, N., Alioto, D., Crescenzi, A., Parrella, G., et al. (2000). Necrotic disease in tomatoes in Greece and Southern Italy caused by the tomato strain of *Parietaria mottle virus*. *J. Plant Pathol.* 82:159. doi: 10.4454/jpp.v82i2.1157

Shimura, H., Masuta, C., Yoshida, N., Sueda, K., and Suzuki, M. (2013). The 2b protein of *Asparagus virus 2* functions as an RNA silencing suppressor against systemic silencing to prove functional synteny with related *Cucumoviruses*. *Virology* 442, 180–188. doi: 10.1016/j.virol.2013.04.015

Conflict of Interest: The authors declare that the research was conducted in the absence of any commercial or financial relationships that could be construed as a potential conflict of interest.

Publisher's Note: All claims expressed in this article are solely those of the authors and do not necessarily represent those of their affiliated organizations, or those of the publisher, the editors and the reviewers. Any product that may be evaluated in this article, or claim that may be made by its manufacturer, is not guaranteed or endorsed by the publisher.

frontiers in Plant Science

ORIGINAL RESEARCH
published: 21 September 2021
doi: 10.3389/fpls.2021.746543

Viral Strain-Specific Activation of Pathogen-Associated Molecular Pattern-Triggered Immunity Enhances Symptom Severity in Broad Bean Wilt Virus 2 Infection

*Soo-Jung Han[1], Boram Choi[2], Myung-Hwi Kim[1,3], Sun-Jung Kwon[2], Hae-Ryun Kwak[4] and Jang-Kyun Seo[1,2,3]**

[1]Department of International Agricultural Technology, Seoul National University, Pyeongchang, South Korea, [2]Institute of Green Bio Science and Technology, Seoul National University, Pyeongchang, South Korea, [3]Integrated Major in Global Smart Farm, Seoul National University, Seoul, South Korea, [4]Crop Protection Division, Rural Development Administration, National Institute of Agricultural Sciences, Wanju, South Korea

OPEN ACCESS

Edited by:
Giuseppe Parrella,
Institute for Sustainable Plant Protection of the National Research Council (IPSP-CNR), Italy

Reviewed by:
Dang Fengfeng,
South China Agricultural University, China
Nikon Vassilakos,
Benaki Phytopathological Institute, Greece

***Correspondence:**
Jang-Kyun Seo
jangseo@snu.ac.kr

Specialty section:
This article was submitted to Plant Pathogen Interactions, a section of the journal Frontiers in Plant Science

Received: 24 July 2021
Accepted: 24 August 2021
Published: 21 September 2021

Citation:
Han S-J, Choi B, Kim M-H, Kwon S-J, Kwak H-R and Seo J-K (2021) Viral Strain-Specific Activation of Pathogen-Associated Molecular Pattern-Triggered Immunity Enhances Symptom Severity in Broad Bean Wilt Virus 2 Infection. Front. Plant Sci. 12:746543. doi: 10.3389/fpls.2021.746543

Broad bean wilt virus 2 (BBWV2) is an emerging virus in various economically important crops, especially pepper (*Capsicum annuum* L.), worldwide. Recently, the emergence of various BBWV2 strains that induce severe symptoms has increased damage to pepper crops. While the symptomatic variations among virus strains should be associated with differences in the transcriptomic reprogramming of host plants upon infection, underlying molecular mechanisms and associated genes are largely unknown. In the present study, we employed transcriptome analysis to identify responsible host factors for symptom enhancement in the BBWV2-pepper pathosystem using two distinct BBWV2 strains, PAP1 (a severe strain) and RP1 (a mild strain). Comparative analysis of the differentially expressed genes (DEGs) revealed that various genes associated with pathogen-associated molecular pattern (PAMP)-triggered immunity (PTI) and ethylene signaling were significantly upregulated upon infection with the severe PAP1 strain, but not with the mild RP1 strain. Indeed, hormone analysis revealed that ethylene emission was significantly increased in pepper plants infected with PAP1. These observations imply that the activation of the PTI-associated defense responses reinforce symptom formation during BBWV2 infection in a virus strain-specific manner.

Keywords: broad bean wilt virus 2, symptom severity, PAMP-triggered immunity, ethylene, transcriptome analysis

INTRODUCTION

The symptom severity of crop diseases is closely related to productivity (Gaunt, 1995). Plant viruses are obligate intracellular parasites that disturb the normal activity of host cells, resulting in a wide range of symptoms. Different strains of plant viruses often induce symptoms with different severity in the host plants. Such symptomatic variation can be triggered by molecular interactions between the host and viral strain-specific factors, leading to transcriptome reprogramming of numerous genes involved not only in defense responses, but also in plant

development, physiology, and metabolism (Seo et al., 2018). In this regard, the identification of crucial host genes associated with symptomatic variation and their underlying molecular mechanisms can provide new insights into molecular plant physiological phenomena as well as symptom development.

Pepper (*Capsicum annuum* L.) is an economically important vegetable crop worldwide. However, commercial pepper production in many global areas continues to suffer from various viral diseases. While more than 100 viruses infect pepper plants worldwide (Kenyon et al., 2014), broad bean wilt virus 2 (BBWV2; genus *Fabavirus*, family *Secoviridae*) is an emerging virus in many global areas (Kwak et al., 2013a,b; Ferriol et al., 2014). The incidence of BBWV2 in pepper has increased rapidly over the past decade, because the virus can be easily transmitted by aphids and infect a wide range of plants, including various weed hosts that inhabit areas near pepper fields (Kwak et al., 2013a; Kim et al., 2014a). The BBWV2 genome is composed of two segments of positive-sense single-stranded RNAs, RNA1 (~5.8 knt) and RNA2 (~3.3 knt; Ferrer et al., 2011). Each RNA segment encodes a single open reading frame (ORF) that translates into a large polyprotein precursor. Proteolysis of the polyprotein precursor encoded by RNA1 yields five mature proteins: protease cofactor (Co-Pro), NTP-binding motif (NTBM), VPg, protease (Pro), and RNA-dependent RNA polymerase (RdRp). After the same processing, RNA2 expresses the following three mature proteins: movement protein (MP), large coat protein (LCP), and small coat protein (SCP; Ferrer et al., 2011).

Broad bean wilt virus 2 causes diverse symptoms in pepper, depending on the compatibility between pepper varieties and virus strains, including mild mosaic, malformation, stunting, and chlorosis (Kwak et al., 2013b, 2016). In a previous study, we generated infectious cDNA clones of two pathogenically different BBWV2 strains, namely pBBWV2-RP1 (a mild strain) and pBBWV2-PAP1 (a severe strain; Kwak et al., 2016). Using the chimeric viruses and amino acid substitution mutant viruses derived from pBBWV2-RP1 and pBBWV2-PAP1, we demonstrated that MP is the viral strain-specific factor that determines symptom severity in BBWV2 (Seo et al., 2017). In the present study, we employed comparative transcriptome analysis to gain a better understanding of the molecular mechanisms associated with the development of distinct symptoms caused by the two BBWV2 strains in pepper.

MATERIALS AND METHODS

Plant Growth and Virus Inoculation

Pepper (*Capsicum annuum* L. cv. Sinhong) and *Nicotiana benthamiana* plants were grown in an insect-free growth chamber in a cycle of 16 h light at 26°C and 8 h darkness at 24°C. Full-length infectious cDNA clones of two BBWV2 strains (RP1 and PAP1), as described in our previous study (Kwak et al., 2016), were used as the viral sources for each strain. Infectious cDNA clones of the virus strains were inoculated into the leaves of 2-week-old *N. benthamiana* plants by *Agrobacterium*-mediated infiltration (agroinfiltration), as previously described (Seo et al., 2009). Crude sap prepared from the symptomatic leaves of *N. benthamiana* infected with each virus strain was subsequently used for mechanical inoculation of pepper. Crude sap was rubbed onto leaves of 3-week-old pepper plants dusted with carborundum (400 mesh). After inoculation, the leaves were washed with sterile water.

Sample Preparation, Library Construction, RNA Sequencing, and Virus Detection

About 2 weeks after mechanical inoculation, symptomatic upper leaf samples were collected from nine individual plants infected with BBWV2-RP1 or PAP1, and frozen immediately in liquid nitrogen before use. Leaf samples from three individual plants were pooled together for RNA isolation. Thus, three biological replicate RNA samples were obtained for each experimental group. Similarly, leaf samples from uninoculated plants were used as healthy controls. Total RNA was extracted using the PureLink® RNA Mini Kit (Ambion, United States) and subjected to library construction using the Illumina TruSeq RNA Sample Preparation Kit v2 (Illumina, Inc., United States). Nine libraries were constructed and quantified with the KAPA library quantification kit (Kapa Biosystems, United States). Sequencing on an Illumina HiSeq2000 sequencer (Illumina, Inc., United States) was performed by TheragenEtex Inc. (Suwon, South Korea). To analyze virus accumulation levels in the systemically infected leaves, the same RNA preparations used for the RNA sequencing were subjected to quantitative real-time RT-PCR (qRT-PCR) using an iCycler iQ5 qRT-PCR detection system (Bio-Rad, United States) with the following specific primers: BBWV2-R1-RT-Fw (5'-TCACAGGTTATGCCG CTTGT-3') and BBWV2-R1-RT-Rv (5'-TCACTCGTCCCAAGC TGTTC-3') for BBWV2 RNA1 detection and UBI2-F (5'-TACCCTTCACCTTGTCCTCC-3') and UBI2-R (5'-GCCAT CCTCCAACTGTTTTC-3') for *ubiquitin2* mRNA detection. The *ubiquitin2* gene (*CA*.PGAv.1.6.scaffold337.91) was used as an internal reference to standardize the different samples. Three biological and technical replicates were used per sample.

Processing of mRNA Sequence Data

The Illumina pipeline filtrated raw sequence reads, which were then mapped to the reference transcripts of *C. annuum* cv. CM334 (Kim et al., 2014b) retrieved from the Pepper Genome Platform[1] using the RNA-seq mapping algorithm implemented in bowtie2 (v2.1.0) software (Langmead et al., 2009), allowing all aligning with a maximum of two mismatches. The raw data were deposited in the National Center for Biotechnology Information (NCBI) SRA database with BioProject accession number PRJNA751625. To eliminate bias caused by variations in sequencing depth, the number of mapped clean reads for each genes was measured and then normalized with the DESeq package in R software (Anders and Huber, 2010). Differentially expressed genes (DEGs) were identified by a ≤2-fold change in read coverage and a binomial test with a false discovery rate (FDR) ≤ 0.01. The FDR was applied to identify the threshold

[1]http://peppergenome.snu.ac.kr/

value of *p* for multiple tests and was calculated using DESeq. Correlation analysis and hierarchical clustering were performed to categorize the genes according to patterns of expression using the AMAP library in R (Lucas, 2014).

Gene Enrichment Analysis

Gene ontology (GO) analysis was performed to functionally annotate the DEGs based on the protein sequence similarity (e-value cutoff ≤ 1e-10) in the GO database (Ashburner et al., 2000). The number of DEGs assigned in each GO term was counted using the in-house scripts of SEEDERS Inc (Daejeon, South Korea). GO term enrichment was performed using the PANTHER overrepresentation test (Mi et al., 2013). Functional enrichment analysis was performed to assign biological relevance to the gene network modules using agriGO v2.0 (Tian et al., 2017). The Kyoto Encyclopedia of Genes and Genomes (KEGG) pathway was analyzed using the sequence similarity (e-value cut off ≤ 1e-10, identity ≥90) of pepper proteins in the KEGG database (Kanehisa and Goto, 2000).

DAB Staining

3,3'-diaminobenzidine (DAB) staining was performed to detect reactive oxygen species (ROS) as previously described (Wang et al., 2017). Briefly, upper uninoculated leaf samples were collected from the virus-infected and healthy plants at 14 days post-inoculation (dpi). The leaf samples were stained with 1 mg/ml DAB (Sigma, United States) by vacuum infiltration and incubated for 8 h at room temperature in the dark. The leaf samples were then destained with 90% ethanol. The destained samples were mounted in 50% glycerol and observed by light microscopy.

Ethylene Analysis

Ethylene production from virus-infected and healthy plants was measured at 14 dpi as described previously with minor modifications (Hou et al., 2018). Briefly, 5 g of the upper uninoculated leaves were sampled from three plants and placed in 400 ml glass jars for 5 h at 26°C in the dark. Next, 1 ml of the jar headspace gas sample was sampled and analyzed using a gas chromatograph equipped with a hydrogen flame ionization detector and an activated alumina column (Agilent Technologies, United States). Samples were compared to a standard of known concentration. The experiment was repeated three times, and data were averaged.

Engineering of the BBWV2 Viral Construct

The coding region of the *ethylene response factor 5* gene (*ERF5*; Gene ID: *CA*.PGAv.1.6.scaffold296.14) was amplified by RT-PCR using a primer pair (5'-GAAGATCTATGGATACTTCTTCACT AGAT-3' and 5'-GATCCTAGGTGAAACCAAAAGTTGAGAA AAACCA-3'; *Bgl*II and *Avr*II sites are shown in bold). The amplified fragments were digested with *Bgl*II and *Avr*II and cloned into pBBWV2-R2-OE (Choi et al., 2019), which was opened with *Bgl*II and *Avr*II. The resulting construct was named pBBWV2-RP1-R2-ERF5. For the agroinfiltration of pBBWV2-RP1-R2-ERF5, the plasmid DNA was first transformed into *Agrobacterium tumefaciens* strain EHA105, and agroinfiltration was subsequently performed as previously described (Choi et al., 2019).

Quantitative Real-Time PCR Validation

To validate the RNA sequencing data, the expression levels of *basic pathogenesis-related protein 1* gene (*CA*.PGAv.1.6.scaffold608.26), *ripening-related protein grip22* gene (*CA*.PGAv.1.6.scaffold631.48), *cysteine-rich receptor-like protein kinase 25* gene (*CA*.PGAv.1.6.scaffold674.24), *glycine-rich protein* gene (*CA*.PGAv.1.6.scaffold1405.6), *pathogenesis-related protein 3* gene (*CA*.PGAv.1.6.scaffold890.65), *WRKY transcription factor 70* gene (*CA*.PGAv.1.6.scaffold788.4), *ACC oxidase* gene (*CA*.PGAv.1.6.scaffold793.11), *LRR receptor-like serine/threonine-protein kinase* gene (*CA*.PGAv.1.6.scaffold1537.4), *ethylene responsive factor 5* gene (*CA*.PGAv.1.6.scaffold296.14), *chitin-binding lectin 1-like* gene (*CA*.PGAv.1.6.scaffold837.4), *ABC transporter B family member 11* gene (*CA*.PGAv.1.6.scaffold484.97), and *mitogen-activated protein kinase* gene (*CA*.PGAv.1.6.scaffold200.11) were analyzed using qRT-PCR. The *ubiquitin2* gene (*CA*.PGAv.1.6.scaffold337.91) was selected as an internal reference for the qRT-PCR experiments because this gene showed stable expression patterns across all treatments in the RNA sequencing results (data not shown). cDNA was synthesized from the same RNA preparations (DNase-treated) used for the RNA sequencing using Superscript III (Invitrogen, United States) with oligo dT primers. The resulting cDNA was subjected to qRT-PCR using an iCycler iQ5 qRT-PCR detection system (Bio-Rad, United States) with specific primers (listed in **Supplementary Table S1**). Three biological and three technical replicates were used per sample. qRT-PCR data were calculated as log2 fold changes and compared with log2 fold values obtained from the RNA sequencing.

RESULTS

Transcriptome Analysis of Symptomatic Variation Caused by Two Distinct BBWV2 Strains in Pepper

Two distinct BBWV2 strains, PAP1 and RP1, cause symptoms with different severity in pepper and *N. benthamiana*: BBWV2-PAP1 induced severe symptoms of mosaic, leaf malformation, and stunting in pepper and *N. benthamiana*, whereas BBWV2-RP1 caused no visible symptoms in pepper and very mild symptoms in *N. benthamiana* (**Figure 1**).

We sought to examine host genes associated with viral strain-specific symptoms in the BBWV2-pepper pathosystem. To this end, Illumina RNA sequencing was performed to examine the transcriptomic changes in pepper upon infection with BBWV2-PAP1 and RP1. We first analyzed viral RNA accumulation of each strain in the systemic leaves using qRT-PCR. The results showed no significant difference in viral RNA accumulation between the two BBWV2 strains (**Figure 2A**), suggesting that the symptomatic difference between the two BBWV2 strains was not due to differences in virus accumulation levels. The same RNA preparation was subjected to cDNA

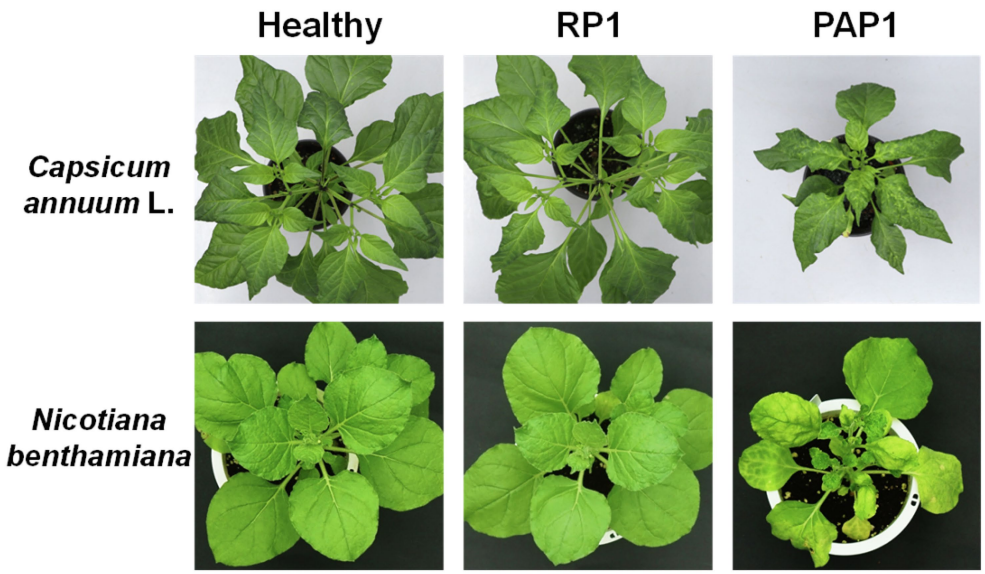

FIGURE 1 | Symptomatic responses of pepper (*Capsicum annuum* L.) and *Nicotiana benthamiana* plants upon infection with BBWW2 isolates PAP1 or RP1. BBWV2-RP1 induced no visible symptoms in pepper and very mild symptoms in *N. benthamiana*, whereas BBWV2-PAP1 caused severe disease symptoms in pepper and *N. benthamiana*.

library construction. Nine cDNA libraries (three for each sample) were sequenced by Illumina RNA sequencing. For mapping, we used a total of 35,884 reference transcripts of *C. annuum* cv. CM334 (Kim et al., 2014b). The Illumina pipeline filtered and trimmed the raw HiSeq reads, yielding approximately 81–86 million clean pair-end reads from each of the nine libraries (**Table 1**). The acquired reads were mapped on the reference pepper transcripts; this resulted in the mapping of approximately 83.6–92.81% of the nucleotides (**Table 1**). The nucleotide coverage for healthy, BBWV2-RP1, and BBWV2-PAP1 was 175, 164.68, and 168.45 times, respectively (**Table 1**).

Identification of DEGs in Response to Infection With BBWV2-PAP1 or RP1

The fragments per kilobase of exon per million fragments mapped (FPKM) value was used to normalize the expression levels of the mapped genes. DEGs were identified by statistically comparing the FPKM values of two samples using a 2-fold change in expression with the FDR $\leq$ 0.01. By comparing virus-infected samples to healthy samples, we identified 160 and 22 DEGs in response to infection with BBWV2-PAP1 and RP1, respectively (**Figure 2B**; **Supplementary Table S2**). When the DEGs were compared between the two infection conditions, a total of 147 genes were identified to be specifically expressed in response to BBWV2-PAP1 (upregulation of 141 genes and downregulation of six genes; **Figure 2C**; **Table 2**; **Supplementary Table S2**). Comparatively few genes were specifically affected upon infection with BBWV2-RP1 (upregulation of four genes and downregulation of five genes; **Figure 2C**; **Supplementary Table S2**). Hierarchical clustering of the total DEGs revealed six distinct groups based on the expression patterns in each infection condition (**Figure 2D**). For example, cluster 4 contained 19 genes upregulated by BBWV2-PAP1 infection but downregulated by BBWV2-RP1 infection.

Gene Ontology Analysis of Identified DEGs

For a better understanding of the DEGs associated with severe symptom development caused by BBWV2-PAP1, GO analysis was performed using the DEGs upregulated upon BBWV2-PAP1 infection. A total of 37 GO terms were significantly enriched by infection with BBWV2-PAP1 (**Supplementary Table S3**). Most BBWV2-PAP1-specific GO terms were associated with defense response and response to stimulus, e.g., systemic acquired resistance (GO:0009627), response to ethylene (GO:0009723), defense response to fungus (GO:0050832), response to salicylic acid (GO:0009751), innate immune response (GO:0045087), response to reactive oxygen species (GO:0000302), and immune response (GO:0006955). Hierarchical GO enrichment analysis using agriGO v2.0 further showed that the identified GO terms were highly correlated in a network context (**Figure 3**). The analysis also highlighted a few downstream GO terms, including defense response to fungus (GO:0050832), response to hormone (GO:0009725), and response to ethylene (GO:0009723), which are likely directly correlated to symptom development in response to BBWV2-PAP1 (**Figure 3**).

Important KEGG Pathways Influenced by BBWV2-PAP1 Infection

Kyoto encyclopedia of genes and genomes pathway analysis was performed to understand the relationship between DEGs and the associated pathways. KEGG analysis using the DEGs upregulated in response to BBWV2-PAP1 infection identified some of the highly ranked pathways, including plant–pathogen

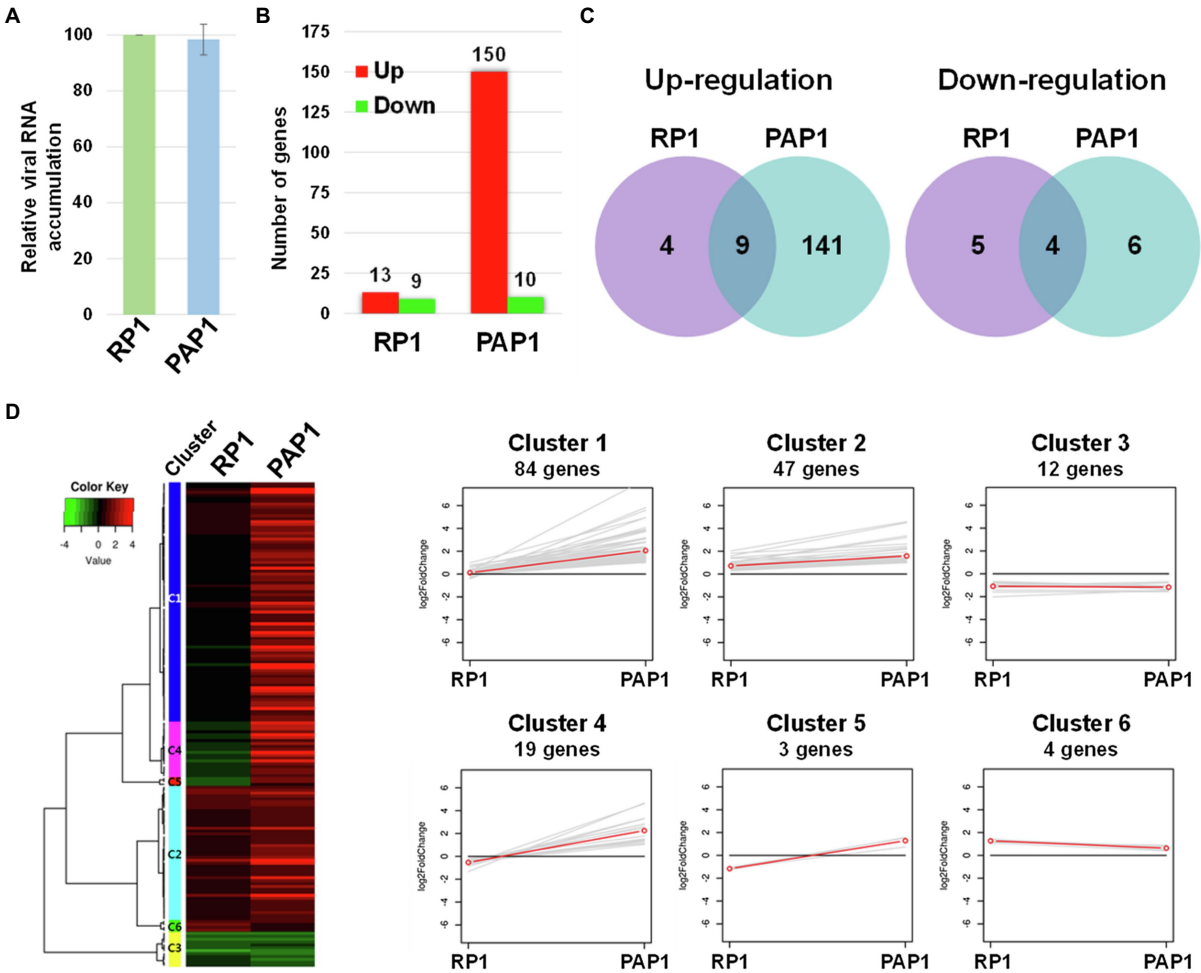

FIGURE 2 | Transcriptome analysis of distinct symptoms induced by two different BBWV2 strains in pepper. **(A)** Relative accumulation analysis of BBWV2-PAP1 and RP1 in pepper by quantitative real-time RT-PCR (qRT-PCR). Means ± SD from three independent experiments are shown and each column represents one group with nine plants; statistical analysis was performed using paired Student's *t*-tests to detect significant differences. **(B)** The number of DEGs identified by RNA sequencing of the transcriptomes in response to infection with BBWV2-PAP1 or RP1. The DEGs were identified by comparing the virus-infected samples to healthy samples using a 2-fold change in expression with a false discovery rate (FDR) of ≤0.01. Red and green bars indicate the numbers of up and downregulated DEGs, respectively. **(C)** Venn diagrams display the number of up or downregulated DEGs upon infection with each virus strain. **(D)** Hierarchical clustering of the identified DEGs. The heat-map was produced using a log scale of the fragments per kilobase of exon per million fragments mapped (FPKM) data obtained by RNA Sequencing. Red and green indicate up and downregulation, respectively. The linear graphs show the expression patterns of each cluster.

TABLE 1 | Read statistics for RNA sequencing of pepper plants infected with broad bean wilt virus 2 (BBWV2)-RP1 or PAP1.

Index	Healthy	BBWV2-RP1	BBWV2-PAP1
No. of trimmed reads (%)	80,988,234 (90.73%)	83,192,654 (91.68%)	85,958,586 (91.83%)
No. of mapped reads (%)	75,175,224 (92.82%)	70,481,206 (84.72%)	71,890,360 (83.63%)
No. of mapped nucleotides (%)	6,848,712,056 (92.81%)	6,444,797,133 (84.66%)	6,592,273,522 (83.62%)
Average coverage	175.00	164.68	168.45

interaction, metabolic pathways, plant hormone signal transduction, and pathways related to plant pigment metabolism (i.e., flavonoid biosynthesis, flavone and flavonol biosynthesis, and biosynthesis of secondary metabolites; **Table 3**). In particular, the most significant enrichment of upregulated DEGs was found in the KEGG pathway of plant–pathogen interaction (Pathway ID: cann04626; **Table 3**; **Figure 4A**). Various receptor-like protein kinase genes (**Figure 4B**), pathogen-associated molecular pattern (PAMP)-triggered immunity (PTI) signaling genes (**Figure 4C**), and pathogenesis-related protein genes (**Figure 4D**) involved in the KEGG pathway of plant–pathogen interaction were significantly upregulated in response to infection with BBWV2-PAP1. KEGG analysis also identified a few ethylene responsive transcription factor genes, including *ERF5*, in the plant hormone signal transduction pathway (Pathway ID: cann00943; **Figure 4E**). Our DEG analysis also revealed that key genes involved in ethylene biosynthesis (i.e., ACC oxidase genes) were significantly upregulated in response to infection

TABLE 2 | Top 30 upregulated differentially expressed genes (DEGs) upon infection with BBWV2-PAP1.

Gene ID	Seq. description	log2 fold change		*Arabidosis* homologous
		PAP1	RP1	
*CA.*PGAv.1.6.scaffold608.26	Basic pathogenesis-related protein 1	8.29	0.24	AT2G14580.1
*CA.*PGAv.1.6.scaffold631.48	Ripening-related protein grip22	5.82	–0.34	NA
*CA.*PGAv.1.6.scaffold674.24	Cysteine-rich receptor-like protein kinase 25	5.59	–0.15	AT4G05200.1
*CA.*PGAv.1.6.scaffold58.30	Nucleoside triphosphate hydrolases superfamily protein	4.95	–0.41	AT3G28580.1
*CA.*PGAv.1.6.scaffold1405.6	Glycine-rich protein	4.94	0.98	NA
*CA.*PGAv.1.6.scaffold890.65	Pathogenesis-related protein 3	4.60	–0.69	AT3G12500.1
*CA.*PGAv.1.6.scaffold575.21	CER1-like 1	4.59	2.03	AT1G02205.1
*CA.*PGAv.1.6.scaffold79.50	Glutathione S-transferase parC	4.50	1.59	AT1G78380.1
*CA.*PGAv.1.6.scaffold788.4	WRKY transcription factor 70	4.31	–0.79	AT3G56400.1
*CA.*PGAv.1.6.scaffold206.16	Pathogenesis-related protein 2	4.17	0.06	AT3G57260.1
*CA.*PGAv.1.6.scaffold793.11	ACC oxidase	4.07	–0.05	AT1G06620.1
*CA.*PGAv.1.6.scaffold647.6	LRR receptor-like serine/threonine-protein kinase GSO2-like	4.03	–0.42	AT5G46330.1
*CA.*PGAv.1.6.scaffold753.4	HYPER-SENSITIVITY-RELATED 4-like	3.92	0.60	AT3G50930.1
*CA.*PGAv.1.6.scaffold628.31	ABC transporter A family member 3	3.90	0.24	AT5G61700.1
*CA.*PGAv.1.6.scaffold1537.4	LRR receptor-like serine/threonine-protein kinase	3.82	0.17	AT3G47570.1
*CA.*PGAv.1.6.scaffold823.8	Ammonium transporter 2 member 2	3.73	–0.17	AT2G38290.1
*CA.*PGAv.1.6.scaffold242.12	Uncharacterized isomerase BH0283-like	3.35	1.05	AT4G02860.1
*CA.*PGAv.1.6.scaffold1134.9	Phosphoglycerate mutase-like	3.32	–0.61	AT3G05170.1
*CA.*PGAv.1.6.scaffold577.9	Cytochrome P450 CYP72A219-like	3.20	1.03	AT3G14690.1
*CA.*PGAv.1.6.scaffold628.32	ABC transporter A family member 2	3.19	0.09	AT3G47730.1
*CA.*PGAv.1.6.scaffold608.6	LRR receptor-like serine/threonine-protein kinase GSO1-like	3.13	0.76	AT1G71390.1
*CA.*PGAv.1.6.scaffold1592.1	COBRA-like protein 5	3.10	–0.10	AT5G15630.1
*CA.*PGAv.1.6.scaffold1110.29	G-type lectin S-receptor-like serine/threonine-protein kinase	3.08	0.40	AT4G27290.1
*CA.*PGAv.1.6.scaffold702.22	Senescence-specific cysteine protease SAG12	2.83	–0.39	AT5G45890.1
*CA.*PGAv.1.6.scaffold1152.14	Linoleate 9S-lipoxygenase 5-like	2.82	0.76	AT1G55020.1
*CA.*PGAv.1.6.scaffold702.24	Senescence-specific cysteine protease SAG39-like	2.82	–0.46	AT5G45890.1
*CA.*PGAv.1.6.scaffold954.24	AAA-ATPase-like	2.81	–0.19	AT3G28580.1
*CA.*PGAv.1.6.scaffold27.14	NRT1/PTR FAMILY 2.13-like	2.80	–0.13	AT1G69870.1
*CA.*PGAv.1.6.scaffold1218.1	Lipid transfer protein EARLI 1-like	2.77	0.22	AT4G12480.1
*CA.*PGAv.1.6.scaffold2870.1	LRR receptor-like protein kinase	2.64	–0.72	AT4G08850.1

with BBWV2-PAP1 (**Figure 4E**). Overall, our results revealed that the PTI and ethylene pathways were activated in BBWV2-PAP1-infectged pepper.

BBWV2-PAP1 Infection Increases ROS Accumulation and Ethylene Emission in Pepper

Pathogen-associated molecular pattern-triggered immunity response typically accompanies the accumulation of ROS and is sometimes associated with ethylene pathways (Peng et al., 2018). Because our transcriptomic analysis revealed that BBWV2-PAP1 infection activates PTI and ethylene pathways in pepper, we investigated whether ROS accumulation and ethylene production are enhanced in BBWV2-PAP1-infected leaf tissues. To detect ROS accumulation, DAB staining was performed on systemic leaves of the pepper plants infected with BBWV2-PAP1 or RP1. The leaves infected with BBWV2-PAP1 showed more intense staining than BBWV2-RP1-infected leaves (**Figure 5A**), indicating that ROS accumulation was specifically elevated by infection with BBWV2-PAP1 but not RP1.

To verify whether activation of the ethylene pathway leads to an increase in ethylene production in BBWV2-PAP1-infected pepper plants, ethylene emission was assessed for detached leaves infected with BBWV2-PAP1 or RP1. There was no significant difference in ethylene production in healthy and BBWV2-RP1-infected leaves (**Figure 5B**); however, ethylene production was considerably higher in BBWV2-PAP1-infected leaves than in BBWV2-RP1-infected leaves (**Figure 5B**). This implies that, consistent with the transcriptional upregulation of the ethylene pathway genes, BBWV2-PAP1 infection causes an increase in ethylene production in pepper.

Overexpression of *Ethylene Responsive Factor 5* Enhances Symptom Severity During BBWV2-RP1 Infection

Ethylene biosynthesis is strongly induced in PTI and plays an important role in defense responses (Yang et al., 2017; Peng et al., 2018). ERF5 functions as a positive regulators of ethylene-mediated immunity in *Arabidopsis* (Moffat et al., 2012; Son et al., 2012). Thus, we hypothesized that if the activation of ethylene signaling pathways is correlated with symptom severity in pepper infected with BBWV2, the ectopic overexpression of ERF5 would enhance symptom severity in pepper infected with BBWV2-RP1 (a mild strain). Testing this hypothesis required the overexpression of ERF5 in the pepper cells infected with BBWV2-RP1. For this, we utilized a viral vector system generated by engineering BBWV2-RP1 to overexpress foreign genes in pepper (Choi et al., 2019). Specifically, we engineered the BBWV2-RP1-based vector to overexpress ERF5 in the BBWV2-RP1-infected cells, and the resulting construct was

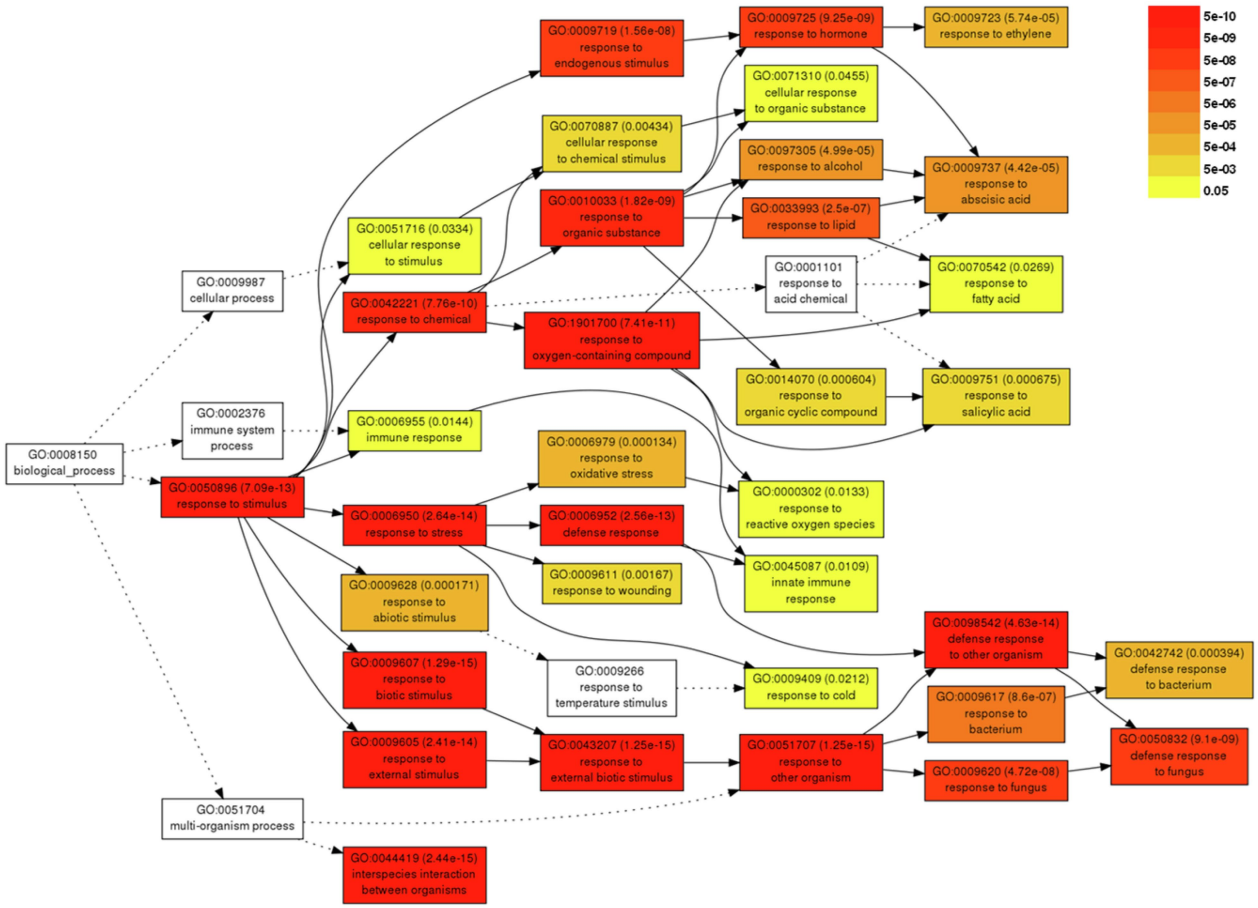

FIGURE 3 | Hierarchical tree graph of overrepresented gene ontology (GO) terms in response to BBWV2-PAP1. The graph was produced by singular enrichment analysis (SEA) using agriGO. Boxes in the graph represent GO terms labeled by GO number, statistical information, and term definition. The degree of color saturation in a box is proportional to the enrichment level of the term.

TABLE 3 | Top 10 Kyoto Encyclopedia of Genes and Genomes (KEGG) pathways enriched with upregulated DEGs when infected with BBWV2-PAP1.

Pathway	Pathway ID	DEGs	*p*
Plant–pathogen interaction	cann04626	37	0.000013
Metabolic pathways	cann00480	10	0.000386
Plant hormone signal transduction	cann00943	4	0.001894
Flavonoid biosynthesis	cann00905	3	0.007710
Amino sugar and nucleotide sugar metabolism	cann00520	4	0.045420
Biosynthesis of secondary metabolites	cann01040	4	0.045583
Flavone and flavonol biosynthesis	cann01212	3	0.049148
Protein processing in endoplasmic reticulum	cann00514	1	0.161728
Glycerophospholipid metabolism	cann00780	1	0.168753
Arginine and proline metabolism	cann00760	1	0.196282

named pBBWV2-RP1-R2-ERF5 (**Figure 6A**). To examine if the ERF5 overexpression affects symptom severity caused by BBWV2, pepper and *N. benthamiana* plants were infiltrated with a mixture of *Agrobacterium* cultures containing pBBWV2-RP1-R1 and pBBWV2-RP1-R2-ERF5. Interestingly, both plant species were systemically infected with the recombinant BBWV2 vector overexpressing ERF5 and developed severe symptoms of leaf malformation and stunting (**Figure 6B**). In particular, necrotic cell death responses were also observed in the systemically infected pepper leaves (**Figure 6B**). Therefore, our results revealed that the ethylene pathway-mediated responses specifically induced by BBWV2-PAP1 are associated with enhanced symptom severity in BBWV2 infection.

Quantitative Real-Time PCR Validation of RNA Sequencing Data

To validate the gene expression data from the RNA sequencing, the expression levels of 12 representative genes that significantly altered in response to virus infection were evaluated by qRT-PCR using the same RNA preparations used for RNA sequencing. The expression of target genes was normalized to that of the *ubiquitin2* gene (*CA*.PGAv.1.6.scaffold337.91) as an internal control. For each gene, relative expression levels were calculated and compared to the RNA sequencing results. In general, the qRT-PCR results for all of the tested genes were consistent with the RNA sequencing results (**Supplementary Table S4**).

A

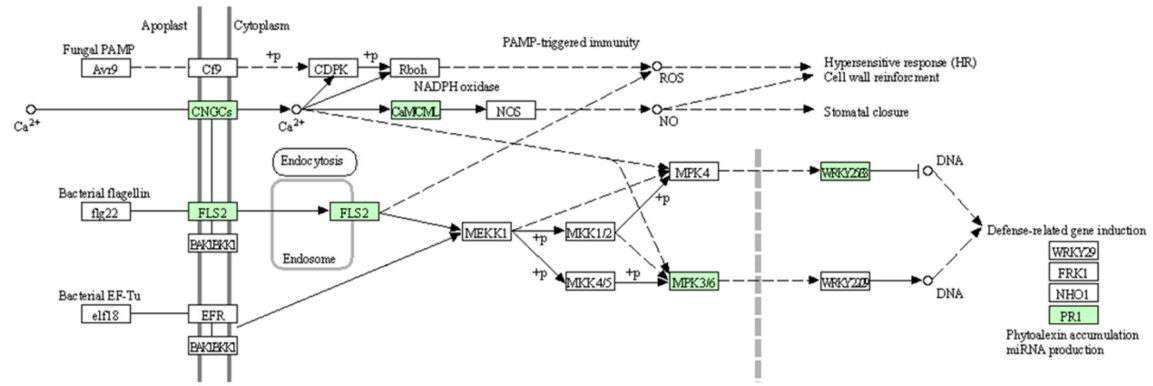

B

Receptor-like protein kinase genes

Gene ID	Seq. Description	log2 fold change		Arabidosis homologous
		PAP1	RP1	
CA.PGAv.1.6.scaffold674.24	Cysteine-rich receptor-like protein kinase 25	5.59	-0.15	AT4G05200.1
CA.PGAv.1.6.scaffold647.6	LRR receptor-like serine/threonine-protein kinase GSO2-like	4.03	-0.42	AT5G46330.1
CA.PGAv.1.6.scaffold1537.4	LRR receptor-like serine/threonine-protein kinase	3.82	0.17	AT3G47570.1
CA.PGAv.1.6.scaffold608.6	LRR receptor-like serine/threonine-protein kinase GSO1-lik2	3.13	0.76	AT1G71390.1
CA.PGAv.1.6.scaffold1110.29	G-type lectin S-receptor-like serine/threonine-protein kinase	3.08	0.40	AT4G27290.1
CA.PGAv.1.6.scaffold2870.1	LRR receptor-like protein kinase	2.64	-0.72	AT4G08850.1
CA.PGAv.1.6.scaffold162.126	G-type lectin S-receptor-like serine/threonine-protein kinase	2.48	-0.37	AT4G27290.1
CA.PGAv.1.6.scaffold1264.2	Somatic embryogenesis receptor kinase 2-like	1.51	-0.42	AT1G34210.1
CA.PGAv.1.6.scaffold1836.1	LRR receptor-like serine/threonine-protein kinase	1.49	-0.61	AT4G08850.1
CA.PGAv.1.6.scaffold222.21	LRR receptor-like serine/threonine-protein kinase	1.48	0.16	AT1G74170.1
CA.PGAv.1.6.scaffold404.77	Cysteine-rich receptor-like protein kinase 8	1.46	-0.06	AT4G23180.1
CA.PGAv.1.6.scaffold1372.17	LRR receptor-like serine/threonine-protein kinase	1.39	-0.43	AT5G46330.1
CA.PGAv.1.6.scaffold126.94	LRR-like serine/threonine/tyrosine-protein kinase	1.37	-0.08	AT2G31880.1
CA.PGAv.1.6.scaffold404.22	LRR receptor-like serine/threonine-protein kinase	1.32	-0.37	AT3G47570.1
CA.PGAv.1.6.scaffold610.39	Leaf rust 10 disease-resistance locus receptor-like protein kinase-like 4	1.26	0.14	AT1G25390.1
CA.PGAv.1.6.scaffold1334.11	G-type lectin S-receptor-like serine/threonine-protein kinase	1.22	0.27	AT4G27290.1
CA.PGAv.1.6.scaffold404.23	LRR-receptor-like serine/threonine-protein kinase	1.21	0.37	AT5G46330.1
CA.PGAv.1.6.scaffold649.17	G-type lectin S-receptor-like serine/threonine-protein kinase	1.14	-0.04	AT5G60900.1
CA.PGAv.1.6.scaffold1635.4	Receptor like protein kinase S.2-like	1.08	-0.11	AT2G32800.1
CA.PGAv.1.6.scaffold157.29	Putative receptor-like protein kinase	1.04	0.21	AT3G51550.1
CA.PGAv.1.6.scaffold1980.2	Receptor-like protein kinase	1.03	0.42	AT1G09970.1

-5 5

C

PTI signaling genes

Gene ID	Seq. Description	log2 fold change		Arabidosis homologous
		PAP1	RP1	
CA.PGAv.1.6.scaffold788.4	WRKY transcription factor 70	4.31	-0.79	AT3G56400.1
CA.PGAv.1.6.scaffold1018.1	WRKY transcription factor 70-like	1.58	-1.28	AT3G56400.1
CA.PGAv.1.6.scaffold239.2	Cyclic nucleotide-gated ion channel 1	1.53	-0.56	AT5G53130.1
CA.PGAv.1.6.scaffold337.71	Mitogen-activated protein kinase kinase kinase	1.45	0.96	AT4G26890.1
CA.PGAv.1.6.scaffold1656.15	Calcium-binding protein CML35	1.43	0.43	AT2G41410.1
CA.PGAv.1.6.scaffold200.11	Mitogen-activated protein kinase	1.39	-0.38	AT3G45640.1
CA.PGAv.1.6.scaffold474.19	WRKY transcription factor 25	1.21	0.51	AT2G38470.1

-5 5

D

Pathogenesis-related protein genes

Gene ID	Seq. Description	log2 fold change		Arabidosis homologous
		PAP1	RP1	
CA.PGAv.1.6.scaffold608.26	Basic pathogenesis-related protein 1	8.29	0.24	AT2G14580.1
CA.PGAv.1.6.scaffold890.65	Pathogenesis-related protein 3	4.60	-0.69	AT3G12500.1
CA.PGAv.1.6.scaffold206.16	Pathogenesis-related protein 2	4.17	0.06	AT3G57260.1
CA.PGAv.1.6.scaffold890.63	Pathogenesis-related protein 3	2.04	0.09	AT3G12500.1
CA.PGAv.1.6.scaffold837.22	Pathogenesis-related protein 2	1.78	0.12	AT4G16260.1
CA.PGAv.1.6.scaffold1306.1	Pathogenesis-related protein 3	1.67	0.55	AT3G12500.1
CA.PGAv.1.6.scaffold1306.3	Pathogenesis-related protein 3-like	1.26	0.11	AT3G04720.1
CA.PGAv.1.6.scaffold244.8	Pathogenesis-related protein 2-like	1.04	0.34	AT4G16260.1
CA.PGAv.1.6.scaffold495.19	Pathogenesis-related protein 3-like	1.03	0.29	AT3G54420.1

-5 5

E

Ethylene pathway genes

Gene ID	Seq. Description	log2 fold change		Arabidosis homologous
		PAP1	RP1	
CA.PGAv.1.6.scaffold793.11	ACC oxidase	4.07	-0.05	AT1G06620.1
CA.PGAv.1.6.scaffold247.16	Ethylene response factor 5-like	1.77	0.80	AT5G47230.1
CA.PGAv.1.6.scaffold397.73	ACC oxidase homolog 1-like	1.27	0.90	AT1G06620.1
CA.PGAv.1.6.scaffold296.14	Ethylene response factor 5	1.22	0.19	AT5G51190.1
CA.PGAv.1.6.scaffold291.8	Ethylene response factor 113-like	1.14	0.16	AT5G13330.1

-5 5

FIGURE 4 | Regulation of the genes involved in pathogen-associated molecular pattern (PAMP)-triggered immunity (PTI) upon BBWV2-PAP1 infection in pepper. **(A)** Kyoto Encyclopedia of Genes and Genomes (KEGG) pathway enrichment analysis. The DEGs upregulated upon BBWV2-PAP1 infection were mapped to the plant–pathogen interaction KEGG pathway (ID: cann04626). Green boxes represent genes upregulated upon BBWV2-PAP1 infection. **(B)** Receptor-like protein kinase genes upregulated upon BBWV2-PAP1 infection. **(C)** DEGs associated with PTI signaling. **(D)** Pathogenesis-related protein genes upregulated upon BBWV2-PAP1 infection. **(E)** DEGs associated with the ethylene pathway. The changes in gene expression were calculated using a log scale of the FPKM data obtained by RNA Sequencing. Red and green indicate up and downregulation, respectively.

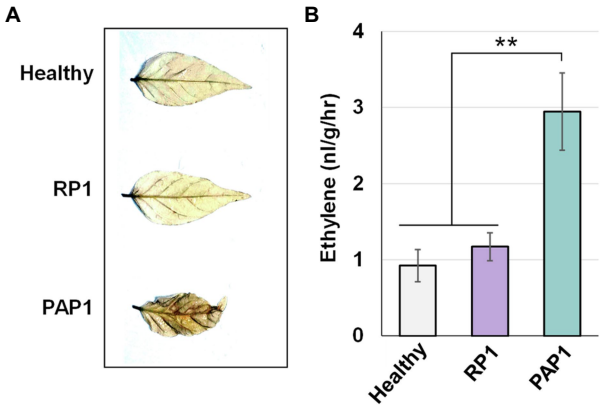

FIGURE 5 | Effect of BBWV2-PAP1 infection on reactive oxygen species (ROS) accumulation and ethylene production in pepper. **(A)** BBWV2-PAP1 infection increased ROS accumulation. Systemic leaves of pepper plants infected with BBWV2-PAP1 or RP1 were analyzed by 3,3'-diaminobenzidine (DAB) staining to visualize ROS accumulation. **(B)** BBWV2-PAP1 infection increased ethylene production. Ethylene emission from the upper uninoculated leaves of virus-infected and healthy plants was measured by gas chromatography. Means ± SD from three independent experiments are shown and each column represents one group with nine plants. Statistical analysis was performed using paired Student's *t*-tests to detect significant differences analyses (**$p < 0.01$).

This demonstrates that the changes in gene expression determined by the RNA sequencing were accurate.

DISCUSSION

Broad bean wilt virus 2 is an emerging virus in various economically important crops worldwide. BBWV2 has a wide host range, and the viral strains isolated from different hosts are genetically and pathogenically differentiated (Ferrer et al., 2011; Kwak et al., 2013a, 2016). Symptomatic variation among different virus strains in a host plant is primarily due to strain-specific viral proteins. Strain-specific viral proteins can have different activities to their original functions or interact with other proteins. In BBWV2, MP was identified as a strain-specific elicitor that determine symptom severity in pepper and *N. benthamiana* (Kwak et al., 2016; Seo et al., 2017); however, the molecular mechanisms and host genes involved in symptom development upon BBWV2 infection remain unknown.

Different symptoms induced by two different strains of BBWV2 (PAP1 and RP1) indicate that transcriptional responses must be different. Notably, BBWV2-RP1 induced no visible symptoms in pepper (**Figure 1**) while its replication level was similar to BBWV2-PAP1 (**Figure 2A**). Indeed, only a small number of DEGs were identified in pepper infected with BBWV2-RP1 (**Figures 2B,C**). On the other hand, BBWV2-PAP1 infection resulted in the upregulation of 150 DEGs (**Figure 2B**). Our GO term and KEGG pathway analyses revealed that many of the upregulated DEGs were PTI-associated genes, including receptor-like protein kinase genes, PTI signaling genes, and pathogenesis-related protein genes (**Figures 3, 4**).

Plant cells can recognize microbial invasions through the perception of PAMPs by pattern-recognition receptors (PRRs) localized on the plasma membrane, triggering the PTI activation (Peng et al., 2018). PTI involves a series of downstream defense responses, such as mitogen-activated protein kinase activation, ROS accumulation, plant hormone biosynthesis, and expression of pathogenesis-related proteins, resulting in the prevention of pathogen colonization (Peng et al., 2018). Our comparative transcriptome analysis revealed that PTI pathways can be activated in a virus strain-specific manner in pepper infected with BBWV2 (**Figure 4**). Many receptor-like protein kinase genes were specifically upregulated in response to BBWV2-PAP1 infection (**Figure 4B**). In plants, most surface PRRs are receptor-like protein kinases in plants (Wang et al., 2016). The *Arabidopsis* leucine-rich repeat receptor kinases FLAGELLIN SENSING 2 and EF-TU RECEPTOR, which can recognize bacterial flagellin and EF-Tu, respectively, are well-characterized PRRs (Zipfel, 2009; Tang et al., 2017). PAMP perception upregulates a number of receptor-like protein kinases, indicating that PTI increases the capacity for pathogen recognition (Zipfel et al., 2004, 2006).

Broad bean wilt virus 2-PAP1 infection also resulted in the upregulation of various PTI signaling genes, including *mitogen-activated protein kinase* (*CA*.PGAv.1.6.scaffold200.11), *WRKY transcription factor 70* (*CA*.PGAv.1.6.scaffold788.4), and *WRKY transcription factor 70-like* (*CA*.PGAv.1.6.scaffold1018.1; **Figure 4C**), which can lead to changes in the transcription of numerous genes involved in defense responses (Wang et al., 2016; Peng et al., 2018). Various pathogenesis-related protein genes were also upregulated in BBWV2-PAP1-infected pepper (**Figure 4D**). The *basic pathogenesis-related protein 1* gene (*CA*.PGAv.1.6.scaffold608.26) was highly upregulated in an incompatible interaction with *Xanthomonas campestris* pv. *vesicatoria* in pepper (Kim and Hwang, 2000). Interestingly, it was demonstrated that the upregulation of the *basic pathogenesis-related protein 1* gene was intrinsically associated with increased ethylene production (Kim and Hwang, 2000). In pepper, treatment with aminoethoxyvinylglycine (AVG), an inhibitor of ethylene biosynthesis, resulted in the suppression of *basic pathogenesis-related protein 1* gene expression, indicating that ethylene is an upstream regulator of this gene (Kim and Hwang, 2000). In addition, other ethylene-responsive pathogenesis-related protein genes, i.e., *pathogenesis-related protein 2* and *pathogenesis-related protein 3*, which encode β-1,3-glucanases and chitinase, respectively (van Loon et al., 2006b; Mazarei et al., 2007), were specifically upregulated in response to infection with BBWV2-PAP1 (**Figure 4D**). Therefore, our results suggest that PTI responses triggered by BBWV2-PAP1 infection are associated with ethylene signaling in pepper. Indeed, ethylene production and the pathway genes were significantly upregulated in pepper infected with BBWV2-PAP1 (**Figures 4E, 5B**).

Ethylene is one of the important regulating factors in disease responses as well as growth and development in plants (van Loon et al., 2006a; Huang et al., 2016). Accumulating evidence suggests that the involvement of ethylene signaling in defense responses is linked to the activation of ROS production (Mersmann et al., 2010; Yang et al., 2017). Similarly, BBWV2-PAP1 infection elevated ROS

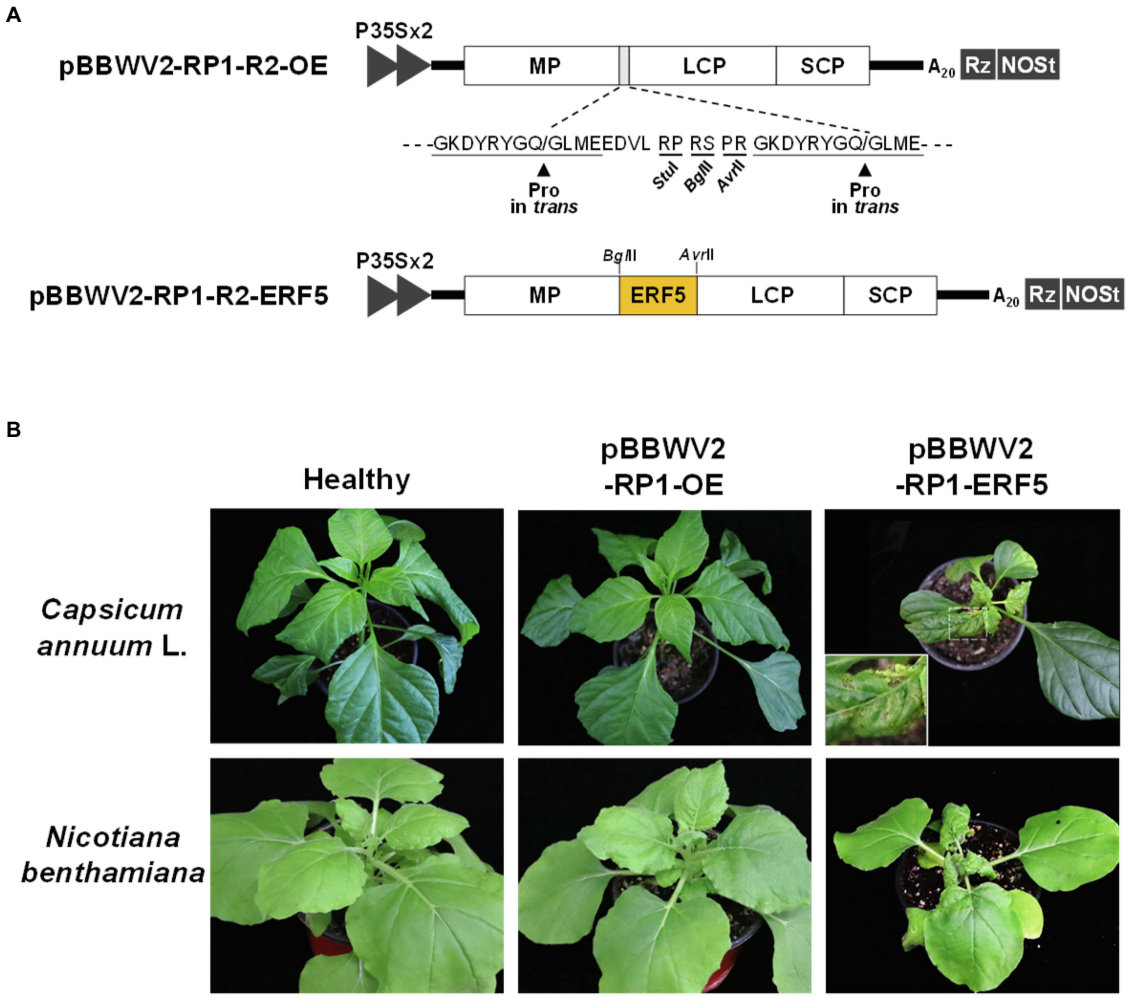

FIGURE 6 | Overexpression of *ethylene responsive factor 5* (*ERF5*) enhances symptom severity in pepper infected with the BBWV2 mild strain RP1. **(A)** Schematic representation of the BBWV2-RP1 RNA2 recombinant constructs. The *ERF5* gene was inserted between movement protein (MP) and large coat protein (LCP) to be expressed by proteolysis when the virus replicates. *In vivo* transcription of the BBWV2-RP1 RNA2 recombinant constructs is under the control of a double 35S promoter (P35SX2), a cis-cleaving ribozyme sequence (Rz), and a NOS terminator (NOSt). **(B)** Symptomatic responses in pepper and *N. benthamiana* plants upon infection with pBBWV2-RP1-ERF5. The inocula are indicated above each image. An enlargement of the boxed area is shown in the upper right panel.

accumulation as well as ethylene production in pepper (**Figure 5**). In defense responses, ROS can function as molecular signals to activate programmed cell death, thereby increasing symptom severity (Peng et al., 2018). Ethylene signaling has also been shown to positively regulate the FLS2 receptor accumulation in *Arabidopsis* (Mersmann et al., 2010), which is consistent with our observation that various receptor-like protein kinase genes were upregulated by BBWV2-PAP1 infection (**Figure 4A**). Ethylene signaling involves plant-specific transcription factors, such as ERFs, which regulate various responses to environmental stimuli (Muller and Munne-Bosch, 2015). While various ERFs have been well characterized recently, ERF5 was shown to activate ethylene-dependent defense genes, and its overexpression resulted in increased resistance to the necrotrophic pathogen *Botrytis cinerea* (Moffat et al., 2012). However, no visible phenotypic alterations were observed in transgenic tobacco plants that overexpress ERF5 (Fischer and Dröge-Laser, 2004). In this study, we demonstrated that overexpression of ERF5 can strongly enhance symptom severity in pepper even when infected with the mild BBWV2 RP1 strain (**Figure 6**). This further demonstrates that the ethylene signaling pathway is associated with the enhancement of symptom severity in BBWV2 infection.

A previous study showed that tobacco mosaic virus coat protein can be recognized as a PAMP to activate PTI and oxidative burst (Allan et al., 2001). Furthermore, for BBWV2, viral strain-specific MP was identified as a symptom severity determinant (Seo et al., 2017). In this study, we found that the viral strain-specific activation of PTI was associated with an increase in symptom severity in BBWV2 infection, that is, BBWV2 MP acts as a PAMP in a virus strain-specific manner. In this regard, it is interesting to consider how plant virus MP activates PTI because, in general, PTI is

activated upon the extracellular recognition of PAMPs by PRRs. BBWV2 MP is localized to plasmodesmata (PD), and forms tubule structures to facilitate virus cell-to-cell movement (Xie et al., 2016). PD are plasma membrane-lined channels that provide symplastic continuity between neighboring cells (Maule et al., 2011). PD membranes also contain various receptor proteins and receptor-like protein kinases (Faulkner, 2013). A previous study revealed that the interactions between viral MP and PD-located receptor-like proteins are crucial for tubule formation and virus cell-to-cell movement (Amari et al., 2010). Therefore, it is possible that BBWV2 MP may interact with PD-located PRRs, resulting in PTI signaling activation.

Disease symptom development is a complex physiological process involving large transcriptomic changes. Thus, analysis of the DEGs in plant–virus interactions is important to explore the molecular basis of various physiological phenomena in plants. The transcriptional responses in pepper were notably different after infection with the two different BBWV2 strains (PAP1 and RP1), which had different symptoms. Our comparative transcriptome analysis revealed molecular genetic clues for the increase in symptom severity upon infection with BBWV2-PAP1. Overall, our findings improve understanding of molecular mechanisms underlying disease symptom development in plants and provide a basis for the future exploration of the functions of pepper genes in fundamental plant physiology.

DATA AVAILABILITY STATEMENT

The original contributions presented in the study are publicly available. This data can be found here: National Center for Biotechnology Information (NCBI) BioProject database under accession number PRJNA751625.

AUTHOR CONTRIBUTIONS

J-KS designed the experiments and supervised the project. S-JH, S-JK, BC, M-HK, and H-RK performed the experiments. S-JH, S-JK, and J-KS analyzed the data and wrote and revised the manuscript. All authors contributed to the article and approved the submitted version.

FUNDING

This research was supported by grants from Agenda Program (PJ014878), and funded by the Rural Development Administration of Korea and Basic Science Research Program (NRF-2020R1I1A1A01072564) and the National Research Foundation of Korea. M-HK was supported by a graduate research fellowship from the Ministry of Education through the Brain Korea 21 Project (Global Smart Farm Division for Educating Innovative Human Resources).

SUPPLEMENTARY MATERIAL

The Supplementary Material for this article can be found online at: https://www.frontiersin.org/articles/10.3389/fpls.2021.746543/full#supplementary-material

Supplementary Table S1 | Primers used in this study for quantitative real-time PCR.

Supplementary Table S2 | Combined DEGs for infection with BBWV2-PAP1 or RP1.

Supplementary Table S3 | GO terms for up-regulated DEGs in response to BBWV2-PAP1 infection.

Supplementary Table S4 | Validation of RNA sequencing data by quantitative real-time PCR.

REFERENCES

Allan, A. C., Lapidot, M., Culver, J. N., and Fluhr, R. (2001). An early tobacco mosaic virus-induced oxidative burst in tobacco indicates extracellular perception of the virus coat protein. *Plant Physiol.* 126, 97–108. doi: 10.1104/pp.126.1.97

Amari, K., Boutant, E., Hofmann, C., Schmitt-Keichinger, C., Fernandez-Calvino, L., Didier, P., et al. (2010). A family of plasmodesmal proteins with receptor-like properties for plant viral movement proteins. *PLoS Pathog.* 6:e1001119. doi: 10.1371/journal.ppat.1001119

Anders, S., and Huber, W. (2010). Differential expression analysis for sequence count data. *Genome Biol.* 11:R106. doi: 10.1186/gb-2010-11-10-r106

Ashburner, M., Ball, C. A., Blake, J. A., Botstein, D., Butler, H., Cherry, J. M., et al. (2000). Gene ontology: tool for the unification of biology. The gene ontology consortium. *Nat. Genet.* 25, 25–29. doi: 10.1038/75556

Choi, B., Kwon, S. J., Kim, M. H., Choe, S., Kwak, H. R., Kim, M. K., et al. (2019). A plant virus-based vector system for gene function studies in pepper. *Plant Physiol.* 181, 867–880. doi: 10.1104/pp.19.00836

Faulkner, C. (2013). Receptor-mediated signaling at plasmodesmata. *Front. Plant Sci.* 4:521. doi: 10.3389/fpls.2013.00521

Ferrer, R. M., Ferriol, I., Moreno, P., Guerri, J., and Rubio, L. (2011). Genetic variation and evolutionary analysis of broad bean wilt virus 2. *Arch. Virol.* 156, 1445–1450. doi: 10.1007/s00705-011-0990-3

Ferriol, I., Ferrer, R. M., Luis-Arteaga, M., Guerri, J., Moreno, P., and Rubio, L. (2014). Genetic variability and evolution of broad bean wilt virus 1: role of recombination, selection and gene flow. *Arch. Virol.* 159, 779–784. doi: 10.1007/s00705-013-1868-3

Fischer, U., and Dröge-Laser, W. (2004). Overexpression of NtERF5, a new member of the tobacco ethylene response transcription factor family enhances resistance to tobacco mosaic virus. *Mol. Plant-Microbe Interact.* 17, 1162–1171. doi: 10.1094/MPMI.2004.17.10.1162

Gaunt, R. E. (1995). The relationship between plant-disease severity and yield. *Annu. Rev. Phytopathol.* 33, 119–144. doi: 10.1146/annurev.py.33.090195.001003

Hou, B. Z., Li, C. L., Han, Y. Y., and Shen, Y. Y. (2018). Characterization of the hot pepper (Capsicum frutescens) fruit ripening regulated by ethylene and ABA. *BMC Plant Biol.* 18:162. doi: 10.1186/s12870-018-1377-3

Huang, P. Y., Catinot, J., and Zimmerli, L. (2016). Ethylene response factors in *Arabidopsis* immunity. *J. Exp. Bot.* 67, 1231–1241. doi: 10.1093/jxb/erv518

Kanehisa, M., and Goto, S. (2000). KEGG: Kyoto encyclopedia of genes and genomes. *Nucleic Acids Res.* 28, 27–30. doi: 10.1093/nar/28.1.27

Kenyon, L., Kumar, S., Tsai, W. S., and Hughes, J. (2014). Virus diseases of peppers (Capsicum spp.) and their control. *Adv. Virus Res.* 90, 297–354. doi: 10.1016/B978-0-12-801246-8.00006-8

Kim, Y. J., and Hwang, B. K. (2000). Pepper gene encoding a basic pathogenesis-related 1 protein is pathogen and ethylene inducible. *Physiol. Plant.* 108, 51–60. doi: 10.1034/j.1399-3054.2000.108001051.x

Kim, S., Park, M., Yeom, S. I., Kim, Y. M., Lee, J. M., Lee, H. A., et al. (2014b). Genome sequence of the hot pepper provides insights into the evolution of pungency in Capsicum species. *Nat. Genet.* 46, 270–278. doi: 10.1038/ng.2877

Kim, M. K., Seo, J. K., Kwak, H. R., Kim, J. S., Kim, K. H., Cha, B. J., et al. (2014a). Molecular genetic analysis of cucumber mosaic virus populations infecting pepper suggests unique patterns of evolution in Korea. *Phytopathology* 104, 993–1000. doi: 10.1094/PHYTO-10-13-0275-R

Kwak, H. R., Kim, M. K., Lee, Y. J., Seo, J. K., Kim, J. S., Kim, K. H., et al. (2013a). Molecular characterization and variation of the broad bean wilt virus 2 isolates based on analyses of complete genome sequences. *Plant Pathol. J.* 29, 397–409. doi: 10.5423/PPJ.OA.03.2013.0036

Kwak, H. R., Kim, M. K., Nam, M., Kim, J. S., Kim, K. H., Cha, B., et al. (2013b). Genetic compositions of broad bean wilt virus 2 infecting red pepper in Korea. *Plant Pathol. J.* 29, 274–284. doi: 10.5423/PPJ.OA.12.2012.0190

Kwak, H. R., Lee, Y. J., Kim, J., Kim, M. K., Kim, J. S., Choi, H. S., et al. (2016). A determinant of disease symptom severity is located in RNA2 of broad bean wilt virus 2. *Virus Res.* 211, 25–28. doi: 10.1016/j.virusres.2015.09.018

Langmead, B., Trapnell, C., Pop, M., and Salzberg, S. L. (2009). Ultrafast and memory-efficient alignment of short DNA sequences to the human genome. *Genome Biol.* 10:R25. doi: 10.1186/gb-2009-10-3-r25

Lucas, A. (2014). AMAP: Another Multidimensional Analysis Package. R Package Version 0.8-12. Available at: http://CRAN.R-project.org/package=amap (Accessed April 4, 2016).

Maule, A. J., Benitez-Alfonso, Y., and Faulkner, C. (2011). Plasmodesmata—membrane tunnels with attitude. *Curr. Opin. Plant Biol.* 14, 683–690. doi: 10.1016/j.pbi.2011.07.007

Mazarei, M., Elling, A. A., Maier, T. R., Puthoff, D. P., and Baum, T. J. (2007). GmEREBP1 is a transcription factor activating defense genes in soybean and *Arabidopsis*. *Mol. Plant-Microbe Interact.* 20, 107–119. doi: 10.1094/MPMI-20-2-0107

Mersmann, S., Bourdais, G., Rietz, S., and Robatzek, S. (2010). Ethylene signaling regulates accumulation of the FLS2 receptor and is required for the oxidative burst contributing to plant immunity. *Plant Physiol.* 154, 391–400. doi: 10.1104/pp.110.154567

Mi, H., Muruganujan, A., and Thomas, P. D. (2013). PANTHER in 2013: modeling the evolution of gene function, and other gene attributes, in the context of phylogenetic trees. *Nucleic Acids Res.* 41, D377–D386. doi: 10.1093/nar/gks1118

Moffat, C. S., Ingle, R. A., Wathugala, D. L., Saunders, N. J., Knight, H., and Knight, M. R. (2012). ERF5 and ERF6 play redundant roles as positive regulators of JA/Et-mediated defense against Botrytis cinerea in *Arabidopsis*. *PLoS One* 7:e35995. doi: 10.1371/journal.pone.0035995

Muller, M., and Munne-Bosch, S. (2015). Ethylene response factors: a key regulatory hub in hormone and stress signaling. *Plant Physiol.* 169, 32–41. doi: 10.1104/pp.15.00677

Peng, Y., Van Wersch, R., and Zhang, Y. (2018). Convergent and divergent signaling in PAMP-triggered immunity and effector-triggered immunity. *Mol. Plant-Microbe Interact.* 31, 403–409. doi: 10.1094/MPMI-06-17-0145-CR

Seo, J. K., Kim, M. K., Kwak, H. R., Choi, H. S., Nam, M., Choe, J., et al. (2018). Molecular dissection of distinct symptoms induced by tomato chlorosis virus and tomato yellow leaf curl virus based on comparative transcriptome analysis. *Virology* 516, 1–20. doi: 10.1016/j.virol.2018.01.001

Seo, J. K., Kwak, H. R., Choi, B., Han, S. J., Kim, M. K., and Choi, H. S. (2017). Movement protein of broad bean wilt virus 2 serves as a determinant of symptom severity in pepper. *Virus Res.* 242, 141–145. doi: 10.1016/j.virusres.2017.09.024

Seo, J. K., Kwon, S. J., Choi, H. S., and Kim, K. H. (2009). Evidence for alternate states of cucumber mosaic virus replicase assembly in positive- and negative-strand RNA synthesis. *Virology* 383, 248–260. doi: 10.1016/j.virol.2008.10.033

Son, G. H., Wan, J., Kim, H. J., Nguyen, X. C., Chung, W. S., Hong, J. C., et al. (2012). Ethylene-responsive element-binding factor 5, ERF5, is involved in chitin-induced innate immunity response. *Mol. Plant-Microbe Interact.* 25, 48–60. doi: 10.1094/MPMI-06-11-0165

Tang, D., Wang, G., and Zhou, J. M. (2017). Receptor kinases in plant-pathogen interactions: more than pattern recognition. *Plant Cell* 29, 618–637. doi: 10.1105/tpc.16.00891

Tian, T., Liu, Y., Yan, H., You, Q., Yi, X., Du, Z., et al. (2017). AgriGO v2.0: a GO analysis toolkit for the agricultural community, 2017 update. *Nucleic Acids Res.* 45, W122–W129. doi: 10.1093/nar/gkx382

van Loon, L. C., Geraats, B. P., and Linthorst, H. J. (2006a). Ethylene as a modulator of disease resistance in plants. *Trends Plant Sci.* 11, 184–191. doi: 10.1016/j.tplants.2006.02.005

van Loon, L. C., Rep, M., and Pieterse, C. M. (2006b). Significance of inducible defense-related proteins in infected plants. *Annu. Rev. Phytopathol.* 44, 135–162. doi: 10.1146/annurev.phyto.44.070505.143425

Wang, L., Albert, M., Einig, E., Furst, U., Krust, D., and Felix, G. (2016). The pattern-recognition receptor CORE of Solanaceae detects bacterial cold-shock protein. *Nat. Plants* 2:16185. doi: 10.1038/nplants.2016.185

Wang, H., Seo, J. K., Gao, S., Cui, X., and Jin, H. (2017). Silencing of AtRAP, a target gene of a bacteria-induced small RNA, triggers antibacterial defense responses through activation of LSU2 and down-regulation of GLK1. *New Phytol.* 215, 1144–1155. doi: 10.1111/nph.14654

Xie, L., Shang, W., Liu, C., Zhang, Q., Sunter, G., Hong, J., et al. (2016). Mutual association of broad bean wilt virus 2 VP37-derived tubules and plasmodesmata obtained from cytological observation. *Sci. Rep.* 6:21552. doi: 10.1038/srep21552

Yang, C., Li, W., Cao, J., Meng, F., Yu, Y., Huang, J., et al. (2017). Activation of ethylene signaling pathways enhances disease resistance by regulating ROS and phytoalexin production in rice. *Plant J.* 89, 338–353. doi: 10.1111/tpj.13388

Zipfel, C. (2009). Early molecular events in PAMP-triggered immunity. *Curr. Opin. Plant Biol.* 12, 414–420. doi: 10.1016/j.pbi.2009.06.003

Zipfel, C., Kunze, G., Chinchilla, D., Caniard, A., Jones, J. D., Boller, T., et al. (2006). Perception of the bacterial PAMP EF-Tu by the receptor EFR restricts agrobacterium-mediated transformation. *Cell* 125, 749–760. doi: 10.1016/j.cell.2006.03.037

Zipfel, C., Robatzek, S., Navarro, L., Oakeley, E. J., Jones, J. D., Felix, G., et al. (2004). Bacterial disease resistance in *Arabidopsis* through flagellin perception. *Nature* 428, 764–767. doi: 10.1038/nature02485

Conflict of Interest: The authors declare that the research was conducted in the absence of any commercial or financial relationships that could be construed as a potential conflict of interest.

Publisher's Note: All claims expressed in this article are solely those of the authors and do not necessarily represent those of their affiliated organizations, or those of the publisher, the editors and the reviewers. Any product that may be evaluated in this article, or claim that may be made by its manufacturer, is not guaranteed or endorsed by the publisher.

frontiers in Microbiology

ORIGINAL RESEARCH
published: 03 November 2021
doi: 10.3389/fmicb.2021.773992

Interspecific Recombination Between Zucchini Tigre Mosaic Virus and Papaya Ringspot Virus Infecting Cucurbits in China

*Bin Peng[1], Liming Liu[1], Huijie Wu[1], Baoshan Kang[1], Zhangjun Fei[2,3] and Qinsheng Gu[1]**

[1]Zhengzhou Fruit Research Institute, Chinese Academy of Agricultural Sciences (CAAS), Zhengzhou, China, [2]Boyce Thompson Institute, Ithaca, NY, United States, [3]United States Department of Agriculture-Agricultural Research Service, Robert W. Holley Center for Agriculture and Health, Ithaca, NY, United States

Recombination drives evolution of single-stranded RNA viruses and contributes to virus adaptation to new hosts and environmental conditions. Intraspecific recombinants are common in potyviruses, the largest family of single-stranded RNA viruses, whereas interspecific recombinants are rare. Here, we report an interspecific recombination event between papaya ringspot potyvirus (PRSV) and zucchini tigre mosaic potyvirus (ZTMV), two potyviruses infecting cucurbit crops and sharing similar biological characteristics and close phylogenetic relationship. The PRSV-ZTMV recombinants were detected through small RNA sequencing of viruses infecting cucurbit samples from Guangxi and Henan provinces of China. The complete nucleotide (nt) sequences of the interspecific recombinant viruses were determined using overlapping RT-PCR. Multiple sequence alignment, recombination detection analysis and phylogenetic analysis confirmed the interspecific recombination event, and revealed an additional intraspecific recombination event among ZTMV populations in China. The symptoms and host ranges of two interspecific recombinant isolates, KF8 and CX1, were determined through experimental characterization using cDNA infectious clones. Surveys in 2017 and 2018 indicated that the incidences of the interspecific recombinant virus were 16 and 19.4%, respectively, in cucurbits in Kaifeng of Henan province. The identified interspecific recombinant virus between PRSV and ZTMV and the novel recombination pattern with the recombination site in HC-pro in *potyvirid* provide insights into the prevalence and evolution of ZTMV and PRSV in cucurbits.

Keywords: interspecific recombinant, zucchini tigre mosaic virus, papaya ringspot virus, cucurbits, evolution

OPEN ACCESS

Edited by:
Giuseppe Parrella, Institute for Sustainable Plant Protection of the National Research Council (IPSP-CNR), Italy

Reviewed by:
Jacques Davy Ibaba, University of KwaZulu-Natal, South Africa
Xifeng Wang, Institute of Plant Protection, Chinese Academy of Agricultural Sciences (CAAS), China

****Correspondence:***
Qinsheng Gu
guqinsheng@caas.cn

Specialty section:
This article was submitted to Virology, a section of the journal Frontiers in Microbiology

Received: *10 September 2021*
Accepted: *14 October 2021*
Published: *03 November 2021*

Citation:
Peng B, Liu L, Wu H, Kang B, Fei Z and Gu Q (2021) Interspecific Recombination Between Zucchini Tigre Mosaic Virus and Papaya Ringspot Virus Infecting Cucurbits in China. Front. Microbiol. 12:773992. doi: 10.3389/fmicb.2021.773992

INTRODUCTION

Cucurbits including watermelon (*Citrullus lanatus*), melon (*Cucumis melo*), cucumber (*Cucumis sativus*), zucchini (*Cucurbita pepo*), and pumpkin (*Cucurbita moschata*) are economically important fruit and vegetable crops worldwide. According to FAO statistics in 2018, China was the world's largest producer and consumer of major cucurbit crop products, exceeding 60% of production and consumption globally. Virus diseases pose a major threat to cucurbit crop production, and more than 90 species of viruses have been reported to infect cucurbits worldwide

(Liu et al., 2019b). So far, 15 potyviruses, one of the largest groups of plant viruses, have been reported to naturally infect cucurbits: Algerian watermelon mosaic virus (AWMV), clover yellow vein virus (ClYVV), cucurbit vein banding virus (CVBV), melon vein-banding mosaic virus (MVBMV), Moroccan watermelon mosaic virus (MWMV), papaya ringspot virus (PRSV), Sudan watermelon mosaic virus (SuWMV), turnip mosaic virus (TuMV), watermelon leaf mottle virus (WLMV), watermelon mosaic virus (WMV), wild melon vein banding virus (WMVBV), zucchini yellow fleck virus (ZYFV), zucchini yellow mosaic virus (ZYMV), zucchini tigré mosaic virus (ZTMV), and zucchini shoestring virus (ZSSV; Lecoq and Desbiez, 2012; Romay et al., 2014; Ibaba et al., 2016; Perotto et al., 2018; Moury and Desbiez, 2020). More than 30 viruses infect cucurbit crops in China, leading to a loss of nearly 4.2 billion dollars each year (Liu et al., 2019b).

Zucchini tigre mosaic potyvirus is a member of the genus *Potyvirus*, containing genomic RNA of ~10.3 kb in length, which encodes two ORFs, the pretty interesting potyvirus open reading frame (ORF; encoding protein PIPO) and a single major polyprotein that is cleaved into 10 mature proteins: protein 1 (P1), helper component-protease (HC-Pro), protein 3 (P3), 6-kDa peptide 1 (6K1), Cylindrical Inclusion protein (CI), 6-kDa peptide 2 (6K2), Viral Protein genome-linked (VPg), Nuclear inclusion A-protease (Nla-pro), Nuclear inclusion B (Nlb), and Coat protein (King et al., 2011; Romay et al., 2014). The PRSV cluster, first defined in 2008 (Yakoubi et al., 2008), contains a group of cucurbit-infecting potyviruses closely related to PRSV biologically, serologically and molecularly. So far, the cluster contains eight documented viruses: AWMV, MWMV, PRSV, SuWMV, WMVBV, ZSSV, ZTMV, and ZYFV (Desbiez et al., 2017). ZTMV, first described in Guadeloupe Island in the Caribbean region, is designated as the PRSV type T due to the differences from PRSV in serology and its symptoms of discoloration resembling a tiger stripe pattern on leaves of zucchini (Romay et al., 2014). According to phylogenetic analysis and sequence comparison, PRSV is the most closely related potyvirus with ZTMV, and their complete genomes share 66.8–68% nt sequence identities. Therefore, based on molecular and biological evidence, ZTMV has been proposed as a distinct potyvirus in the PRSV cluster (Quiot-Douine et al., 1986; Romay et al., 2014). ZTMV has been reported in three continents (Asia, Europe, and America) and in some Caribbean and Indian Ocean islands (Romay et al., 2014; Xiao et al., 2016; Desbiez et al., 2017; Abdalla and Ali, 2018; Wang et al., 2019). Based on phylogenetic analysis of the complete CP nt sequence, ZTMV isolates are classified into three subgroups: Asian, Indian Ocean, and American, related to their geographical origins (Romay et al., 2014). In 2014, the first Chinese isolate of ZTMV was reported in cucurbit plants from Yunnan province of China, which was identified as a major pathogen affecting cucurbit production in Yunnan province due to its wide distribution (Xiao et al., 2016). Moreover, two ZTMV isolates infecting wax gourd (*Benincasa hispida*) under accession number MN267689 and bitter melon (*Momordica charantia*) under accession number LC371337 have been detected in Guangdong and Taiwan provinces, respectively.

Numerous recombination events are involved in potyvirus evolution (Valli et al., 2007; Salvador et al., 2008). However, in a recombination analysis of 152 ORF sequences encoding polyprotein of potyvirus, only five interspecific recombination events were found, of which only two, WMV and SuWMV, were confirmed with experimental evidence (Gibbs et al., 2020). WMV is a recombinant between soybean mosaic virus (SMV) and bean common mosaic virus (BCMV; Desbiez and Lecoq, 2004), and SuWMV originated from an interspecific recombination event between a WMVBV and a MWMV (Desbiez et al., 2017). The junctions of these two recombination events are both in the coding region of P1, the first protein encoded by the potyvirus genome. P1 functions in biological processes such as virus replication, cell-to-cell movement, and systemic spread and stimulation of the gene silencing suppressor HC-Pro (Rohožková and Navrátil, 2011). In addition, previous studies have suggested that recombination site in the N-terminal of the P1 coding region of potyvirus could be less deleterious than that in other regions of the viral genomes, and therefore facilitate its adaptation to a wide range of host species (Valli et al., 2007; Salvador et al., 2008; Pasin et al., 2014; Desbiez et al., 2017).

In this study, three recombinant cucurbit-infecting ZTMV isolates identified in China are described and their biological properties were also investigated using infectious cDNA clones.

MATERIALS AND METHODS

Sample Collection

Sixty cucurbit leaf samples were collected in July 2017 and 2018 from Xinhuaying Town, Kaifeng City, Henan Province (35°29'31"N, 114°45'39"E) and in September 2017 from Anping Town, Cenxi County, Guangxi Zhuang Autonomous Region (23°7'10"N, 111°4'35"E). All samples, including six melon, 21 pumpkin and 33 watermelon leaf samples, exhibited virus-like symptoms such as mosaic, mottle, yellows, or crinkle (**Supplementary Table 1**). The collected samples preserved in dry ice were shipped to the lab and then stored at −80°C.

Small RNA Sequencing

Total RNA was extracted from frozen leaves using the RNAiso Plus kit (Takara, China) following the manufacturer's instructions. The quantity and integrity of total RNA were determined using a Qubit2.0 analyzer (Bioptic, China) and an Agilent 2100 Bioanalyzer (Agilent Technologies, United States), respectively. Seven small RNA (sRNA) mixtures (SR1-SR7), each pooled from 2 or 3 samples out of the 16 selected cucurbit samples according to the collected fields, hosts, and symptoms (**Supplementary Table 2**), were subjected to sRNA sequencing. Small RNA preparation and library construction, using the NEBNext® Small RNA Library Prep Set for Illumina® (NEB, United Kingdom), were performed following the manufacturer's instructions. Briefly, unique barcoded adaptors were added, RT-PCR was performed and the product was purified *via* polyacrylamide gel electrophoresis. sRNA libraries were sequenced on an Illumina NextSeq 500 system.

sRNA Read Processing and Analysis for Virus Identification

The adaptors of raw sRNA reads were removed using the perl script included in the VirusDetect package (Zheng et al., 2017). Cleaned sRNA reads, excluding short (<15 nt) and low-quality reads (<Q30), were subjected to virus detection using VirusDetect (V1.70), which performs reference-guided assembly by aligning sRNA reads to the known virus reference database (GenBank gbvrl) as well as *de novo* assembly using Velvet (Zerbino and Birney, 2008) with automated parameter optimization. Virus database v229 (included in VirusDetect package) was used as the virus reference sequences for the reference-guided assembly. Melon (Garcia-Mas et al., 2012), watermelon (Guo et al., 2013) and *Cucurbita moschata* (Sun et al., 2017) genomes were used to subtract sRNA reads derived from the cucurbit hosts.

Complete Genome Sequencing

According to the mapping of virus contigs assembled by VirusDetect to the reference genomes of ZTMV, a series of primers were designed to obtain the full genome sequence of ZTMV (**Supplementary Table 3**). RACE (rapid amplification of cDNA ends) was performed to determine the missing 5' and 3' end sequences of isolates using a SMARTer® RACE 5'/3' Kit (Clontech, United States) according to the manufacturer's instructions. The primer ZTMV-3utr, complementary to the 3' terminus of the genome of ZTMV, was used to generate cDNA by GoScript reverse transcriptase (Promega, United States). The 5' termini of KF17 and CX1 were determined by RACE using net primer sets 600R and 800R, respectively. The 5' and 3' terminus nt sequences of KF8 were successfully assembled from sRNA reads using VirusDetect (**Figure 1A**). The complete nt sequences of the three isolates (KF8, KF17, and CX1) of ZTMV were confirmed by Sanger sequencing of four segments derived from four overlapping RT-PCRs using four primer pairs (5utr&2400R, 2200F&4500R, 4500F&6700R, and 6700F&3utr shown in **Figure 2A**). Complete nt sequences of KF8 and CX1 isolates were further confirmed by one or two long-distance PCRs (LD-PCRs; primers pair shown in **Figure 2B**) and Sanger sequencing. Conventional PCRs, whose products were less than 3 kb, were performed using the 2 × Phanta Master Mix (Vazyme, China), and LD-PCRs, whose products were more than 3 kb, were done using the 2 × Phanta Max Master Mix (Vazyme, China). PCR products were cloned using the CV17-Zero Background pTOPO-Blunt Simple Cloning Kit (Aidlab, China) or into the pXT1 vector (Yao et al., 2011), and transformed into competent cells *Escherichia coli* Top10. Three independent clones or PCR products were selected for Sanger sequencing (Sangon, China). The assembly of the complete genome sequence was performed using the sequence assembly tools in the DNAMAN package (Version 8).[1] The prediction of ORF and translation of polyproteins were performed using the ORFfinder.[2] Identities of nucleotide sequences of the viral genome and UTR, as well as amino acid sequences of Polyprotein and 10 mature proteins, were derived from the multiple sequence alignments by Clustal Omega (Sievers and Higgins, 2014).

Recombination Analysis

Analyses of recombination of 13 viral genome sequences, including all 10 ZTMV available in GenBank and three PRSV complete sequences (Accession numbers and isolates names listed in **Figure 3**), were performed using RDP (version 4.8), which includes seven recombinant detection algorithms: RDP, GENECONV, BoosScan, MaxChi, Chimaera, SiScan, and 3Seq (Martin et al., 2015). We considered only the potential recombinant events with an average value of $p < 0.01$ in four or more recombinant detection algorithms.

Phylogenetic Analysis

According to the recombination pattern derived from the RDP analyses, the recombinant events were confirmed by phylogenetic analysis. Prior to the phylogenetic tree construction, jModelTest2 (Darriba et al., 2012) was used to select the best fitting evolution model for the alignment. Phylogenetic trees were constructed using MEGA X (Kumar et al., 2018) with the maximum-likelihood method and 500 bootstrap replicates, and visualized in iTOL.[3] All full-length sequences of ZTMV isolates retrieved from GenBank and determined in this study were included in the phylogenetic analysis. Meanwhile, three representative PRSV isolates and four *potyviruses* (AWMV, MWMV, SuWMV, and WMVBV) regarded as closely related to PRSV were used as the outgroup. The same phylogenetic analyses were applied to nt sequences of coding region of CP and CI, respectively.

Construction of Infectious cDNA Clones

Since the plant samples infected with ZTMV were also infected by other viruses including ZYMV and WMV, the isolation of ZTMV from these samples was performed with the construction of infectious cDNA clones. The samples 2017-kf08 and 2017-cx01, collected from Henan province and Guangxi Zhuang Autonomous Region, respectively, were propagated in zucchini (*Cucurbita pepo*) cv. Green Beauty plants. The extraction of RNA and synthesis of first cDNA were as described above. To construct infectious cDNA clones of ZTMV from sample 2017-kf08, two fragments of 6.7 and 3.6 kb in length were amplified using 5utrL&6739R and 6700F&3utrL primers pairs, respectively (**Supplementary Table 3**) by LD-PCR described above. For 2017-cx01, one fragment covering the genome sequence was amplified by LD-PCR using the 5utrL&3utrL. The two fragments from 2017-kf08 and one fragment from sample 2017-cx01 were assembled with the *Stu*I and *Sma*I-treated pXT1 vector (Yao et al., 2011) using ClonExpress MultiS one step cloning kit (Vazyme, China). The *Agrobacterium*-mediated inoculation method for cucurbit plants was as described in Liu et al. (2019a). Briefly, plasmids were introduced into *Agrobacterium tumefaciens* freeze-thawed with liquid nitrogen. After bacterial growth and induction, cell suspension of agrobacterium was injected into cotyledons of muskmelon.

[1] http://www.lynnon.com/

[2] https://www.ncbi.nlm.nih.gov/orffinder/

[3] https://itol.embl.de/

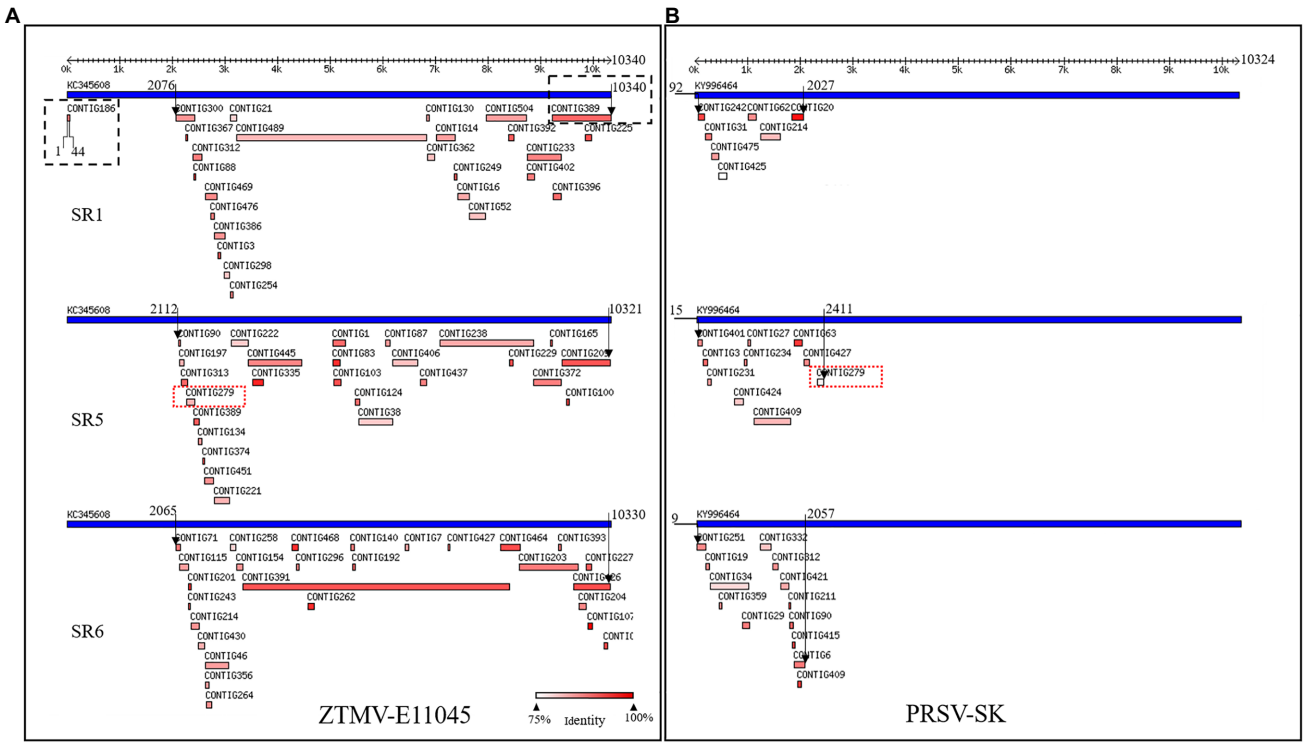

FIGURE 1 | Viruses identified from SR1, SR5, and SR6 samples using VirusDetect. **(A)** Alignments of assembled virus contigs to the ZTMV-E11045 genome. **(B)** Alignments of assembled virus contigs to the PRSV-SK genome. Blue tracks represent reference virus genomes, and red tracks represent assembled virus contigs. Double headed arrows with scales represent the length of genome. Black arrows represent range of contigs aligned with reference genome. Black dotted line box represents contigs aligned to the terminals of zucchini tigre mosaic potyvirus (ZTMV) reference genome. Red dotted line boxes represent contig279 from SR5 aligned to both ZTMV and PRSV reference genomes.

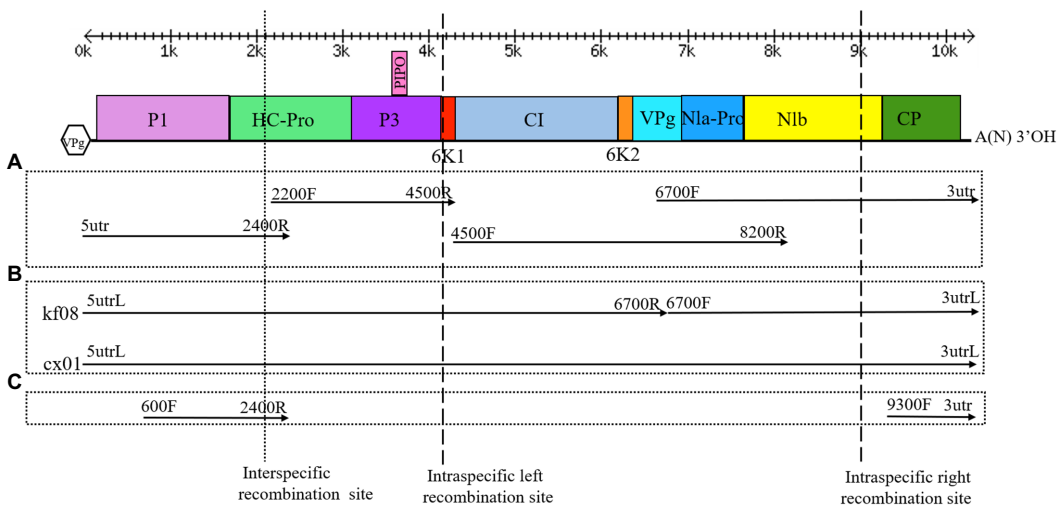

FIGURE 2 | Genome organization of ZTMV, detection of recombination isolates, cloning of complete genomes and construction of infectious cDNA clones. **(A)** Strategy of cloning the complete genomes. **(B)** Strategy of detection of recombination and construction of infectious cDNA clone. **(C)** Strategy of detection of recombination isolate of ZTMV from samples in field. Double-headed arrows with scales represent the length of the genome. Blackline represents the genome. Colored rectangles represent matured proteins derived from the large polyproteins. The Vpg in hexagon represents viral protein genome-linked. A(N)3'OH represents the polyA tail. Arrows represent the PCR fragments that were cloned. Primers used for amplifying the PCR fragments are indicated at the ends of each arrow. The cross of dotted line and the genome indicates the interspecific recombination point. The crosses of dash lines and the genome indicate the intraspecific recombination points.

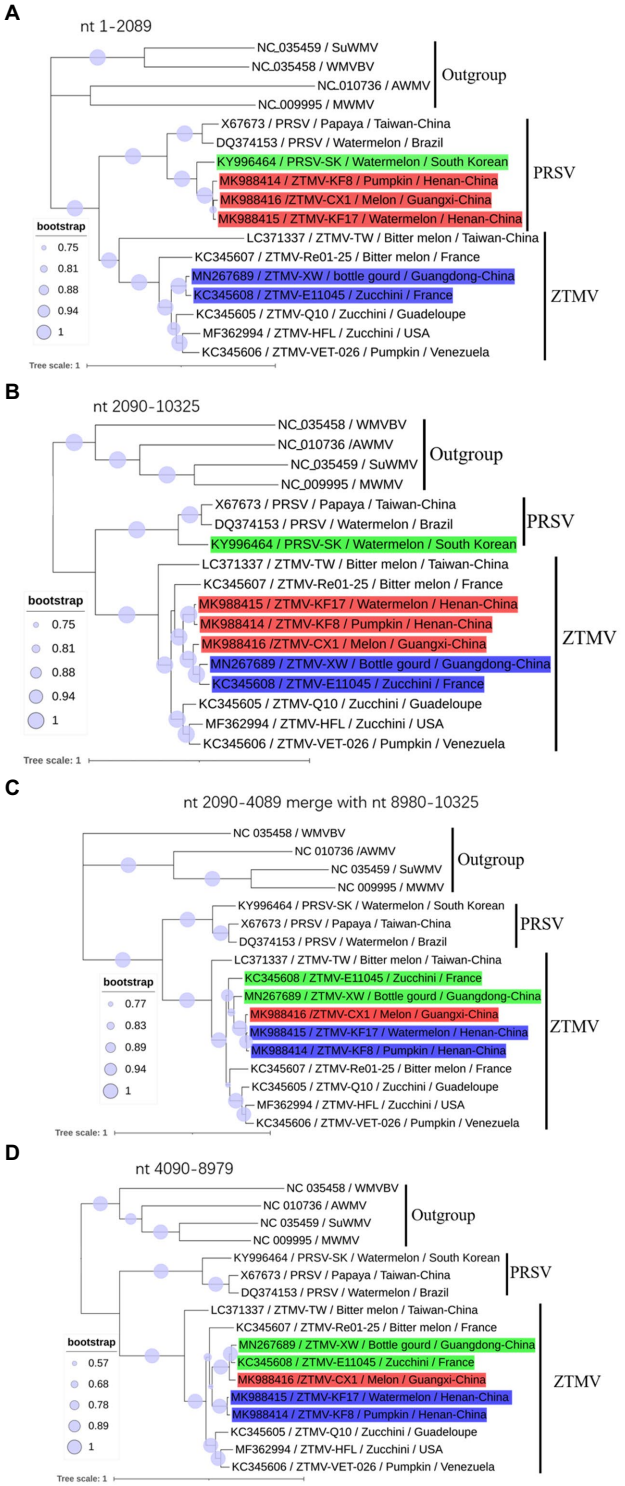

FIGURE 3 | Phylogenetic analysis of non-recombinant regions. **(A)** Phylogenetic tree based on nt 1–2,089 sequences; **(B)** Phylogenetic tree based on nt 2,090–10,325 sequences; **(C)** Phylogenetic tree based on nt 2,090–4,089 merged with nt 8,980–10,325 sequences. **(D)** Phylogenetic tree based on nt 4,089–8,079. Accession number, isolate name, host, and collected location are provided in nodes. Isolates with red, green, and blue backgrounds represent recombinant isolates, minor parents and major parents in the interspecific recombinant event, respectively.

Plants injected with *Agrobacterium* containing empty vector plasmid pXT1 were used as the negative control.

Validation of Infectivity

Each of the two infectious cDNA clones and the empty vector was inoculated on 10 melon plants. Inoculated plants were monitored until the occurrence of apparent symptoms or till 30 days post-inoculation. To confirm the presence of ZTMV in plants, two RT-PCR detections were carried out using primer pairs of 4500F&6400R and 8300F&3utr, respectively. Meanwhile, the RNA of ZTMV was detected with Northern dot-blot analysis using the DIG Northern Starter Kit (Roche, German). To synthesize the probe for dot-plot analysis, a RT-PCR product was obtained using the RNA from kf08 sample as the template and primers 9292F&T7_10064R, and then transcribed into RNA, which was labeled with DIG in an *in vitro* transcription reaction following the kit manual. For dot-plot analysis, in brief, total RNA extracted from 0.1 g fresh leaves of test plants was fixed in Hybond-N membranes at 120°C for 30 min. The fixed membranes were then hybridized with a DIG-labeled RNA probe and photographed using the Chemiluminescence imaging system (Tanon, China). The RNA from leaves infected by ZTMV in fields and non-inoculated leaves of plants injected with Agrobacterium with empty vector plasmid pXT1 were used as the positive and negative controls, respectively. Screening of other viruses infecting cucurbits, including ZYMV, WMV, PRSV, and CMV, was carried out with species-specific primers and commercial double-antibody sandwich enzyme-linked immunosorbent assay (DAS-ELISA) kit (Agdia, United States), to make sure that the tested cucurbit plants were free of these viruses. Conventional RT-PCR was performed as described above. DAS-ELISA was performed following the instructions, and the criterion used to demarcate the positive or negative results was determined according to Liu et al. (2017).

Validation of Aphid Transmissibility

One gram fresh leaves from melon plant inoculated by infectious cDNA clones were ground with 10 ml of 0.01 M PBS (pH 7.0). The prepared inocula were mechanically inoculated on cotyledons of 15 melon plants. The timing and symptoms were recorded after 5 days post inoculation (dpi) till the appearance of viral-disease symptoms. In March 2018, melon aphids, *Aphis gossypii* Glover (Hemiptera: Aphididae), were collected from symptomless melon, grown in a tunnel located in Zhengzhou, Henan province. After transfer to melon plants grown in air-conditioned insect-proof glasshouse with 18–24°C, 20 apterous aphids were maintained and propagated. Prior to aphid transmission tests, the aphids were validated as virus-free by DAS-ELISA and RT-PCR using commercial ELISA kit and species-specific primers for ZYMV, WMV, CMV, and PRSV. Before being transferred to symptomatic and systemically ZTMV-infected melon plants, the aphids were gently transferred into a petri dish by brush pen and starved for 30 min. The aphids were fed on ZTMV-infected melon for 5–10 min acquisition access periods followed by transfer to healthy melon plants (10–15 aphids per plant) for inoculation access periods of 24 h. Sulfoxaflor, a quick-acting insecticide against aphid, was applied to kill them. Fifteen melon plants were

aphid-inoculated with two ZTMV isolates. Virus-free aphids, fed on healthy melon plants, were transferred to another 10 melon plants as the healthy controls. The symptoms that developed were recorded. To detect the presence of ZTMV, the top young leaf was taken from each plant at 14 dpi and RT-PCR was carried out using ZTMV species-specific primers as described above.

Host Range Determination

Mechanical inoculation of 12 plant species, including seven *Cucurbitaceae* crops, five indicative plants and papaya (**Table 1**), was used to determine an experimental host range and symptoms for two isolates of ZTMV. The inocula were prepared and inoculated on cotyledons of cucurbit plants as described above. The top three fully expanded leaves of the five indicative plants (at the 6-leaf stage) and papaya (at the 8-leaf stage) were inoculated with the same inocula. At least10 plants of each species were used in the experiment. For inoculated plants at 30 dpi that showed no symptom, the absence of the virus was confirmed by RT-PCR. Plant inoculations were carried out with three independent repeats.

Detection of Recombinants by RT-PCR From Samples in the Field

Conventional RT-PCR was used for detection of ZTMV from 60 samples, collected in 2017 and 2018 (**Supplementary Table 1**), using two primer pairs, 600F&2400R that covered the interspecies recombination site, and 8300F&3utr (**Supplementary Table 3**), targeting partial P1-HC-pro region and CP coding region, respectively.

RESULTS

Small RNA Sequencing

After removing adapters, short and low-quality reads, we obtained 14,874,695–23,160,143 cleaned reads for each of the seven RNA mixture (SR1–SR7; **Supplementary Table 2**). Using these sRNA data, nine viruses were identified with the VirusDetect pipeline (Zheng et al., 2017), including ZYMV, WMV, ZTMV, PRSV, melon aphid-borne yellows virus (MABYV), *Cucumis melo* alphaendornavirus (CMEV), squash leaf curl china virus (SLCCV), melon yellow spot virus (MYSV), and *Citrullus lanatus* cryptic virus (CiLCV). Except for ZTMV and PRSV, the coverage of assembled contigs of all viruses against the corresponding reference genomes was greater than 95% (**Supplementary Table 2**). For the sRNA data of SR1, SR5, and SR6, 26, 26, and 27 contigs were aligned to the genome sequence of ZTMV E11045 isolate (Accession number KC345608), respectively, covering 78.6, 68.3, and 79.1% of the E11045 genome with an average sequence identity of 87.7, 88.7, and 92.2% (**Supplementary Table 4**). Except for one contig from SR1, which was aligned against nt 1–44 of the ZTMV-E11045 sequence, all contigs covered the range from about nt 2,000 to the 3' end of the genome. There was a about 2,000-nt gap from the 5' end to 2,000 nt where no contigs were aligned to the reference ZTMV genome (**Figure 1A**). Furthermore, 7, 10, and 13 contigs from SR1, SR5, and SR6, respectively, were aligned to the genome sequence of isolate PRSV-SK (Accession number KY996464). They covered 11.9, 16.7, and 17.6% of the PRSV-SK genome with sequence identities of 85.4, 87.1, and 88.5%, respectively. All these contigs only covered the 5' end to about 2,000 nt in the reference sequence (**Figure 1B**). Interestingly, contig279 from SR5 was not only aligned to PRSV with 80% identity but also to ZTMV with 85% identity.

Complete Sequencing and Sequence Alignment of KF8, KF17, and CX1

The ZTMV isolates from samples 2017-kf08, 2017-kf17, and 2017-cx01 were named as KF8, KF17, and CX1, respectively. The complete nt sequences of ZTMV-KF8, ZTMV-KF17, and ZTMV-CX1 were found to be 10,325,

TABLE 1 | Host ranges of ZTMV-KF8 and ZTMV-CX1 and symptoms of 13 plant species.

Host	Cultivar	ZTMV-KF8		ZTMV-CX1	
		Positive/total	Symptoms	Positive/total	Symptoms
Cucurbita pepo	Green beauty	10/10	M, Ma	10/10	M, Ma
Cucurbita moschata	Miben	6/10	B, Ma	7/10	B, Ma
Citrullus lanatus	Zhengkang No.2	8/10	M, Mo	5/10	M, Mo
Cucumis melo Makuwa	Qingtian	7/10	YS, Cu	10/10	YS, Cu
Cucumis melo	Queen	10/10	M	10/10	M
Cucumis sativus	Dongyu	6/10	MM	10/10	MM
Lagenaria siceraria	Yongzhen No.1	8/10	M, Ma	5/10	M
Nicotiana benthamiana	–	0/30	ns	0/30	ns
Nicotiana glutinosa	–	0/30	ns	0/30	ns
Nicotiana occidentalis	–	0/30	ns	0/30	ns
Chenopodium Amaranticolor	–	0/30	ns	0/30	ns
Chenopodium quinoa	–	0/30	ns	0/30	ns
Carica papaya	FZ No.1	0/30	ns	0/30	ns

M, mosaic; MM, mild mosaic; Mo, mottle; YS, yellow spot; Ma, malformation; B, blistering; Cu, curl; ns, no symptom. "positive" indicates the number of positive plants detected by RT-PCR; "total" indicates the number of total tested plants.

10,328, and 10,331 nucleotides in length, respectively, excluding the poly-(A) tail (**Supplementary Figures 1B**,**C**). They all presented a typical potyvirus genome organization, including a 5'-UTR, a single large ORF encoding a polyprotein, a motif for the PIPO protein and a 3'-UTR (**Figure 2**). The complete nucleotide sequences of KF8, KF17, and CX1 have been deposited in GenBank under accession numbers MK988414, MK988415, and MK988416, respectively. There were some variations in length of the genome, 5'-UTR, polyprotein and 3'-UTR comparing the three isolates with other ZTMV and two PRSV isolates from GenBank (**Supplementary Table 5**). The complete nt and aa sequences of KF8, KF17, and CX1 shared 91.4–97.8% and 97–98.3% identities between each other, 76.1–81.3% and 85.2–87.1% identities with other isolates of ZTMV from GenBank (excluding the HFL isolate from Hawaii), and less than 73.6 and 80.6% identities with the two isolates of PRSV (**Figure 4**). These results suggest that the three isolates, KF8, KF17, and CX1, should belong to ZTMV, according to the species demarcation criteria of *Potyviridae* (Wylie et al., 2017). The alignment information of nucleotide sequences of 5'- and 3'-UTRs and amino acid sequences of 10 mature proteins (P1, HC-pro, P3, 6K1, CI, 6K2, Vpg, Nla-pro, Nlb, and CP) of KF8 against those of KF17, CX1, other ZTMV isolates and two PRSV isolates is provided in **Supplementary Table 6**. There were two unexpected results in the 5'-UTR region and P1 protein. The 5'-UTR sequences of the KF8 isolate were both 97.6% identical to that of KF17 and CX1, and 52.4–65.9% identical to that of other seven ZTMV from GenBank, but 86.6 and 67.1% identical to that of PRSV-SK and the reference sequence of PRSV. Similarly, the amino acid sequence of P1 of the KF8 isolate was 94.2 and 92.3% identical to that of KF17 and CX1, 37.3–40.3% identical to that of other seven ZTMV from GenBank, while 83.4 and 64.4% identical to that of PRSV-SK and the reference sequence of PRSV (**Supplementary Table 6**). These results revealed that the three isolates could be recombinant isolates.

Recombination Analyses

Complete sequences of 10 ZTMV and three PRSV isolates were subjected to recombination analysis using RDP4 (Martin et al., 2015). Two strong independent recombination signals (value of $p < 10^{-11}$; **Table 2**), one interspecific (**Figure 5A**) and one intraspecific (**Figure 5B**), were identified by all seven methods used in RDP4. The three isolates, KF8, KF17, and CX1 from China, were regarded as interspecific recombination products, derived from a virus related of SK isolate of PRSV (Accession number KY996464) from south Korean and a virus related of ZTMV isolates E11045 from France (Accession number KC345608) or XW from Guangdong of China (Accession number MN267689; **Figure 5A**). The interspecific recombination junction was located in the genome of CX1 isolate at around position nt 2,089 within the HC-pro coding region (**Figure 2**). The front region of its complete sequence, including 5'-UTR, P1 and part of HC-Pro, was derived from PRSV, and other regions were derived from ZTMV. Another intraspecific recombination isolate, CX1, was derived from an intraspecific event (**Figure 5B**). The junctions were located in the CX1 genome at around nt 4,089 within the 6K1 coding region and nt 8,980 within the Nlb coding region (**Figure 2**). Full-length amplification using LD-PCR (**Figure 2B**) and Sanger sequencing of the KF8 and CX1 isolates further confirmed these two recombination events.

Phylogenetic Analysis

GTR + G + I substitution model, suggested by jModelTest2 (Darriba et al., 2012), was used for the phylogenetic tree construction based on nucleotide sequences. Phylogenetic analysis

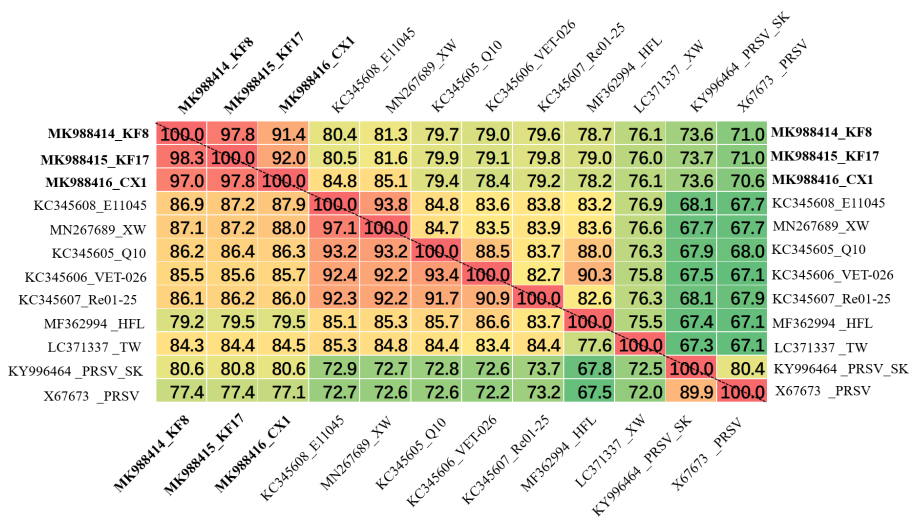

FIGURE 4 | Matrix of percent identity between the complete genome sequence (above the dotted-line) and polyprotein (below the dotted-line) of three recombination isolates and other ZTMV and two PRSV isolates.

of sequences from nt 1–2,089 (including 5'-UTR, coding regions of P1 and part of HC-pro) revealed that isolates KF8, KF17, and CX1 were clustered with the PRSV-SK isolate from South Korea within the PRSV clade (**Figure 3A**), while phylogenetic analysis of sequences from 2,090 to 10,325 (including coding regions of part of HC-pro and other proteins and 3'-UTR) clustered the three isolates into the ZTMV clade (**Figure 3B**). These results further verified that these three isolates are indeed interspecific recombinant viruses from PRSV and ZTMV. Furthermore, phylogenetic tree constructed using sequences from nt 2,090–4,089 combined with sequences from nt 8,980–10,325 revealed that the CX1 isolate was clustered with KF8 and KF17 (**Figure 3C**), whereas CX1 was clustered with ZTMV-E11045 and ZTMV-XW in the phylogenetic tree constructed using sequences from nt 2,090–4,089 combined with sequences from nt 4,090–8,979 (**Figure 3D**). These results also confirmed that the CX1 isolate was an intraspecific recombinant virus in the ZTMV population.

TABLE 2 | Recombination detected with the seven methods used in the RDP4 program.

Recombination detection methods	Interspecific recombination value of *p*	Intraspecific recombination value of *p*
RDP	3.9×10^{-151}	1.4×10^{-55}
GENECONV	1.3×10^{-112}	9.8×10^{-56}
BootScan	7.8×10^{-143}	3.1×10^{-57}
MaxChi	7.6×10^{-42}	5.3×10^{-26}
Chimaera	1.7×10^{-46}	2.6×10^{-29}
SiScan	3.7×10^{-62}	9.5×10^{-40}
3Seq	2.6×10^{-11}	1.3×10^{-11}

A phylogenetic tree (**Figure 6A**) constructed with the coding region of CP from 34 members (including 16 ZTMV isolates that are wrongly proposed as PRSV isolates in GenBank) of the ZTMV cluster showed that all isolates except PRSV-SHK-PM1 (accession number KY448325) and PRSV-Pak (accession number AB127935) were grouped into three subgroups: Asian, American, and the Indian ocean, related to their geographical origins (Romay et al., 2014). The Asian subgroup contained all five isolates from China (including three in this study), 12 from Myanmar, two from Indian and one from France. Furthermore, the phylogenetic tree (**Figure 6B**) constructed with nucleotide sequences of CI coding region from 27 members of the ZTMV cluster showed that the ZTMV cluster were grouped into three subgroups but different from the tree constructed with the nt sequences of CP. The Indian Ocean subgroup contained all isolates from Indian Ocean, and subgroup Asia contained the E11045 isolate from France and three isolates (TW, CX1, and XW) from southern of China. Subgroup America included all isolates from America. The four Chinese isolates, KF8 and KF17 from Henan province, and YJCH-NG1 (accession number KR259540) and YJCH-NG3 (accession number KR360723) from Yunnan province did not cluster with other Asian isolates but were more closely related to the subgroup America. Phylogeny based on nt sequences of Nla-pro was similar to

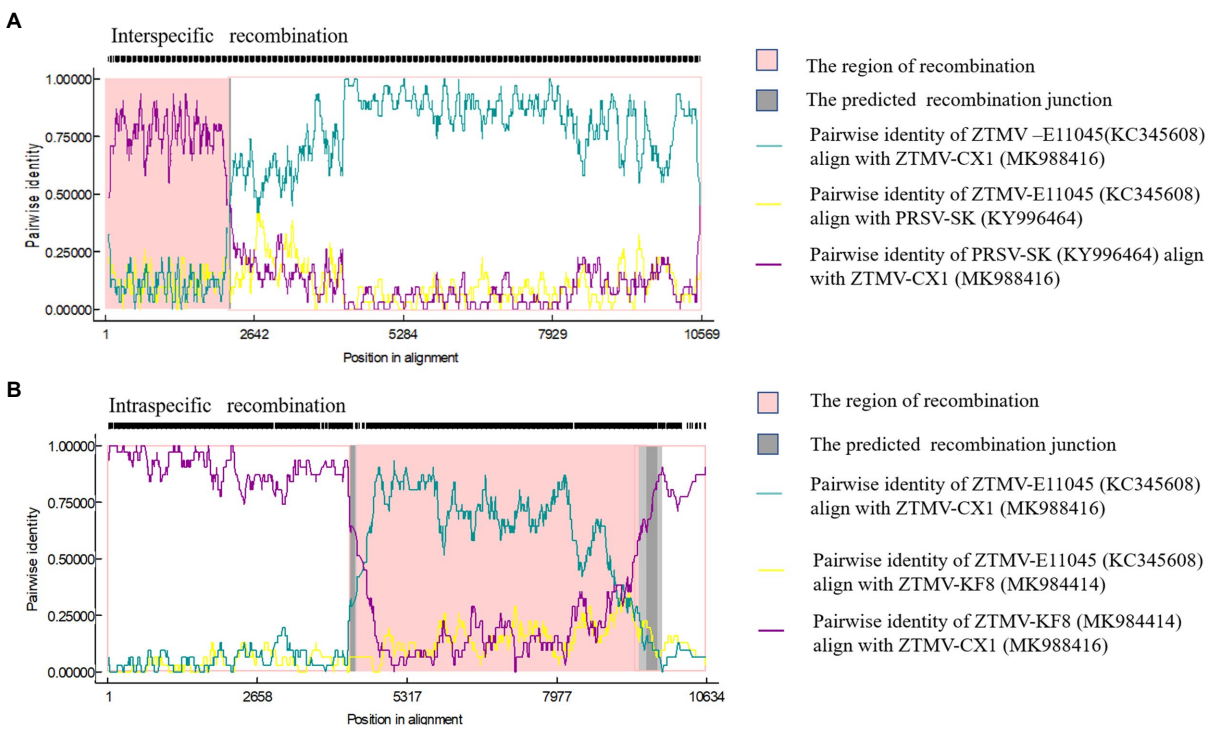

FIGURE 5 | Recombination in the ZTMV genome predicted by RDP4. **(A)** Nucleotide sequence identity along the genome of ZTMV-CX1, ZTMV-E11045, and PRSV-SK. **(B)** Nucleotide sequence identity along the genome of ZTMV-CX1, ZTMV-E11045, and ZTMV-KF8.

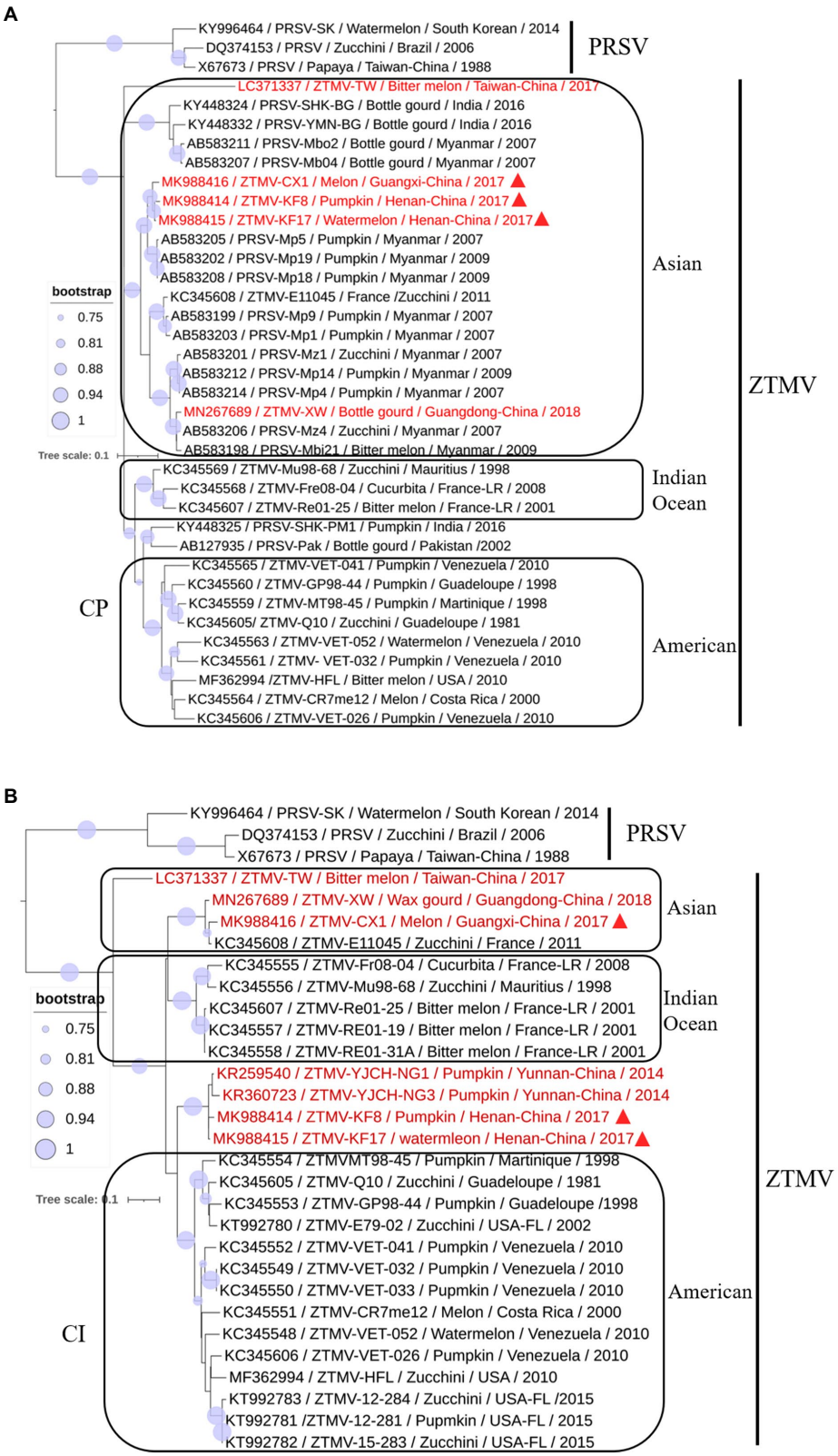

FIGURE 6 | Phylogenetic analysis of coding regions of CI **(A)** and CP **(B)**. Accession number, isolate name, host, collected location and collected year are provided in nodes. Isolates with red text represent ZTMV isolates from China and those marked by red triangles represent recombination isolates identified in this study.

that of CI. Phylogeny based on partial nt sequences of P3 showed that YSP-HG2 (accession number KU058173) and YSK-XHL2 (accession number KU058173), also from Yunnan of China, were grouped into a cluster with four isolates (KF8, KF17, CX1, and XW) from the mainland of China, similar to that in the CP tree (data not shown).

Construction and Characterization of Infectious cDNA Clones

KF17 and KF8 isolates, collected from the same field, had very high identity (97.8%) in their genome sequences (**Figure 4**). Therefore, we selected one of them, KF8, along with CX1, for biological characterizations. Two fragments, 6,575-bp and 3,633-bp in length, covered the complete sequence of ZTMV-KF8 (**Supplementary Figure 1C**), were amplified from cDNA with two primer pairs (5utrL&6700R and 6700F&3utrL, respectively) using LD-PCR. Both of them were synchronously cloned into a linearized pXT1 vector (**Supplementary Figure 1C**) by a homologous recombination reaction, resulting in constructing a plasmid, named pXT1-ZT-KF8, that contained a complete sequence of ZTMV-KF8. Another fragment, 10,395-bp in length (**Supplementary Figure 1C**), was obtained from amplifying cDNA of the ZTMV-CX1 isolate using the primer pair 5utrL&3utrL. The plasmid containing the complete sequence of ZTMV isolates CX1, named pXT1-ZT-CX1, was constructed. After 7 days post-inoculation (dpi), early symptoms, as well as mild mosaic or vine clearing were observed in the new non-inoculated upper leaves of melon plants injected by agrobacterium with pXT1-ZT-KF8 and pXT1-ZT-CX1 plasmid, respectively. At 14 dpi, obvious mosaic was shown on leaves of seven out of 10 of inoculated melon plants, but no symptoms could be observed on mock-inoculated plants (**Figure 7A**). The presence of ZTMV-KF8 and ZTMV-CX1 isolates in the plants was confirmed by RT-PCR and dot-blot hybridization (**Figure 7B**), and the absence of ZYMV, WMV, PRSV, and CMV was confirmed by RT-PCR using species-specific primers. The results of DAS-ELISA also revealed that the two isolates of ZTMV were not able to react against ZYMV, WMV, PRSV, and CMV antiserum. Two ZTMV isolates were successfully recovered from infectious cDNA clones, and the typical viral disease symptoms were shown after inoculation of them on melons.

Determination of Transmissibility and Host Ranges

After 14 days of mechanical inoculation with the sap of ZTMV-KF8 and ZTMV-CX1 isolates derived from infectious cDNA clones, 13 out of 15 and 10 out of 15 melon plants showed the viral disease symptoms as well as mosaic, respectively. Similarly, after 14 days of inoculation with the two isolates through aphid, all 10 of inoculated plants showed the symptoms same as ones of mechanical inoculation. The detection results of RT-PCR using ZTMV species-specific primers coincided with the presence of the symptoms.

After mechanical inoculation, systemic symptoms were observed in seven tested members of *Cucurbitaceae*. The two isolates of ZTMV produced mosaic or mottle in most *Cucurbitaceae*, chlorotic spots in orient melon, which was visible at 15 dpi and later developed into blistering in muskmelon and bottle gourd, curling in orient melon, and leaf deformations in zucchini, pumpkin and bottle gourd visible at 30 dpi (**Table 1** and **Supplementary Figure 2**). No systemic infection was detected in papaya and five indicator hosts, including three *Solanaceae* and two *Chenopodiaceae*, in three independent

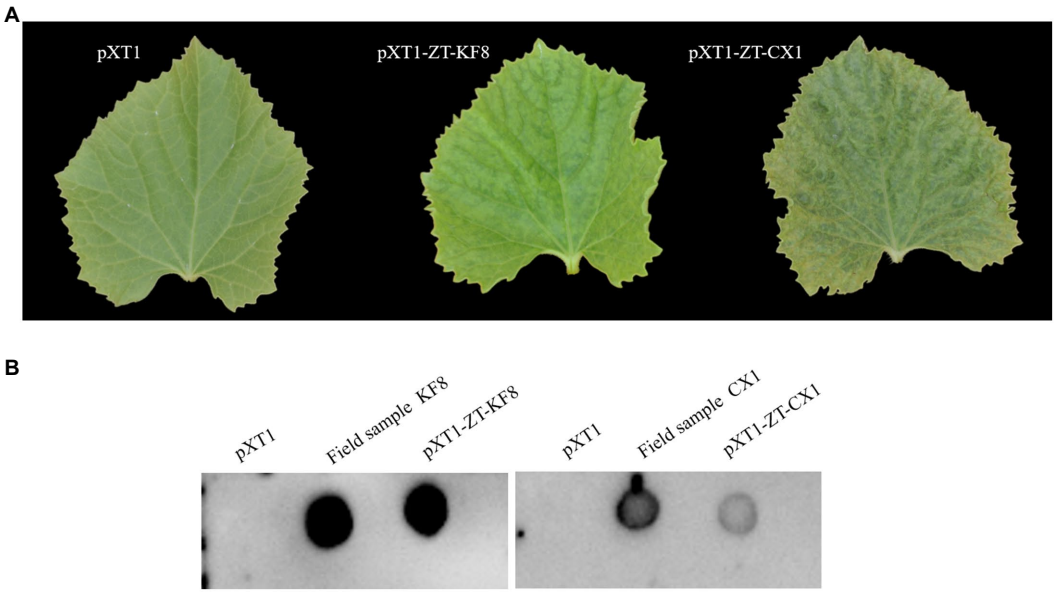

FIGURE 7 | Recovery of ZTMV from infectious cDNA clones. **(A)** Symptoms shown on the non-inoculated upper leaf at 14 dpi. **(B)** Detection of viral RNA of ZTMV by dot blot hybridization.

repeats. The negative results detected by RT-PCR coincided with the lack of systemic symptoms.

Prevalence of the Recombinants

RT-PCR was performed with two pairs of primers (600F&2400R and 9300F&3utr) for all samples collected from Guangxi and Henan provinces in 2 years. Twelve out of 60 (20%) were found positive for ZTMV, including two melons (2017-cx01 and 2017-cx02), one pumpkin (2017-kf08), and three watermelons (2017-kf17, 2017-kf23, and 2017-kf25) out of 29 cucurbit samples (four pumpkins, six melons, and 19 watermelons) collected in 2017, and five pumpkins (2018-kf17, 2018-kf18, 2018-kf19, 2018-kf120, and 2018-kf29) and one watermelon (2018-kf04) out of 31 cucurbit samples (17 pumpkins and 14 watermelons) collected in 2018. All PCR products were sequenced using Sanger dideoxy DNA sequencing. The nucleotide sequences of PCR products using the 600F&2400R primer pair (**Figure 2C** and **Supplemental Figure 1A**), covering the interspecific recombination site, were about 1,844 nt in length. The nt sequence identity between the two positive samples from Guangxi was 99.1%, and among all nine positive samples from Henan were above 98.2%. Sequences of PCR products obtained with the 9300F&3utr primer pair (**Supplemental Figure 1A**, bottom) were about 1,047 nt in length. Likewise, the nt sequence identity between the two positive samples from Guangxi was 99.4%, and among all nine positive samples from Henan were above 98.6%. Comparison of these sequences against the GenBank nucleotide database revealed that the former product of ZTMV isolate from 2017-kf08 shared the highest nucleotide sequence identity (approximately 85%) with PRSV (KY996464), while the latter product shared the highest nucleotide sequence identity (approximately 92%) with ZTMV (KC345608).

DISCUSSION

Zucchini tigre mosaic potyvirus has been detected in cucurbit crops grown in Asia, Europe, and America, as well as some Caribbean and Indian Ocean islands (Romay et al., 2014; Xiao et al., 2016; Desbiez et al., 2017; Abdalla and Ali, 2018; Wang et al., 2019); however, to date only seven complete genome sequences of ZTMV are available in GenBank (**Figure 3**). In China, ZTMV was first reported in pumpkin, zucchini, and cucumber of Yunnan province, located in southwestern China near Myanmar. The isolates of ZTMV from Yunnan, lack of complete genome sequences, only have four sequences of partial P3 and CI coding regions in GenBank. In recent years, two complete genome sequences of ZTMV isolates, one from bottle gourd in Guangdong and the other from bitter melon in Taiwan, have been deposited in GenBank under accession numbers MN267685 and LC371337, respectively. In this study, we identified and characterized interspecific recombination isolates of ZTMV from cucurbit crops (watermelon, pumpkin, and melon) in China using next-generation sequencing (NGS) and molecular approaches. As far as we know, our study is the first to detect and document the recombination isolates of ZTMV, which originated from a recombination event located in the coding region of HC-pro between ZTMV and PRSV. ZTMV has long been overlooked in cucurbit production, because it has the closest phylogenetic relationship with PRSV, shares the same host ranges and causes similar symptoms compared to other cucurbit-infecting potyviruses, including PRSV, ZYMV, and WMV (Romay et al., 2014). Due to the acquisition of molecular characteristics and the development of discriminating diagnostic tools for virus, such as PCR and NGS, ZTMV even the recombinant ZTMV isolates can now be readily distinguished from PRSV. In this study, we found that the host ranges and induced symptoms of the recombinant ZTMV isolates (**Table 1**) are indeed not significantly different from those of PRSV and ZTMV. According to the 2-year investigation in the same field in Kaifeng of Henan province in China (**Supplementary Table 1** and **Supplementary Figure 1A**), the interspecific recombination isolates have colonized cucurbits cultivated in the field and formed a stable virus entity with other cucurbit-infecting viruses, such as ZYVM, WMV, and CMV.

The three isolates are interspecific recombination viruses, with their minor parts of the genome derived from 5'-terminal region of PRSV (**Figure 5A**). However, we suggested that they should belong to ZTMV based on multiple alignments of complete nt and aa sequences of polyproteins (**Figure 4**), and according to species demarcation criteria for genus *Potyvirus* (Adams et al., 2005; Wylie et al., 2017). However, the amino acid sequence identities of CP between KF8 and ZTMV-HFL (72.4%) and between KF8 and ZTMV-XW (81.8%) were lower than those between KF8 and PRSV-SK (85.7%) and between KF8 and PRSV-X67673 (86.7%; **Supplementary Table 6**). Considering only the CP, according to the option species demarcation criterion of 80% amino acid identity (Adams et al., 2005), ZTMV could not be distinguished from PRSV. On the contrary, amino acid sequence identities of CI of KF8 with other 10 ZTMV isolates were 88.5–98.7, and 80.3 and 80.5% with PRSV-SK and PRSV-X67673, respectively. The option species demarcation criterion is 88% amino acid identity for CI (Adams et al., 2005). It has been discussed that ZTMV can be distinguished from PRSV using the coding region of CI more suitable than using the CP (Adams et al., 2005; Romay et al., 2014). A similar conclusion cloud be drawn from phylogenetic analysis based on CP nt sequences (**Figure 6A**), which indicated that some isolates collected from Asia (Myanmar, India, and Pakistan) between 2002 and 2016 that were designed as PRSV in GenBank, were clustered into the ZTMV group.

With the advance and reduced cost of NGS, it has a significant advantage in the discovery of novel viruses, identification of diverse strains and unravelling the virome of many crops compared to the conventional methods for virus detection (Villamor et al., 2019). In this study, our work was triggered by an apparent clue that suspected interspecific recombination isolates of ZTMV were present in cucurbits, suggested by the analysis of several sRNA sequencing data from field samples. The clue of the presence of interspecific recombination isolates should owe to the visual diagrams of contig mapping to the reference viral genome provided by VirusDetect (Zheng et al., 2017; **Figure 1**). In our previous work (Peng et al., 2019), the identification of an interspecific

recombination virus, zucchini aphid-borne yellows virus belonging to genus *polerovirus*, was also triggered by the analysis of an RNA-seq data using the VirusDetect pipeline. From our experience, it is feasible that interspecific recombination events could be identified from suitable NGS data using the pipeline, according to visual diagrams and associated information (range of coverage, depth etc. shown in **Supplementary Table 4**) provided by the pipeline. However, intraspecific recombination isolates could not be identified with NGS data using the pipeline, such as an intraspecific recombination event among ZTMV-CX1, ZTMV-KF8 and ZTMV-E11045 (**Figure 5B**).

RNA recombination is common and is one of the driving forces of evolution in potyvirus populations (Bujarski, 2013). A lot of intraspecies recombination events have been reported in potyviruses, but only two interspecies recombination events have been experimentally confirmed, namely WMV and SuWMV (Gibbs et al., 2020), and their breakpoints of recombination are both in the coding region of P1 (Desbiez and Lecoq, 2004; Desbiez et al., 2017). P1 is referred to as a mysterious protein of family *Potyviridae*, since it varies in length and sequence, and is deemed to be the key factor of potyviruses to adapt to various hosts and environments (Rohožková and Navrátil, 2011). Some studies indicate that genetic changes of the N-terminal of the P1 coding region have less lethal risk of recombinant isolates than other viral proteins (Valli et al., 2007; Desbiez et al., 2017). In this study, the breakpoints of recombinant ZTMV isolates are near the N'-terminal of HC-Pro (**Figure 1A**), and the genetic exchange involves whole P1 and part of HC-Pro. This recombinant pattern has not been found in potyviruses involving interspecific recombination but found in an intraspecific isolate of PRSV (Maina et al., 2019). The PRSV-XM isolate (accession number KY933061), collected from papaya in China, is a recombinant with PRSV-SK (KY996464) as a major parent with a minor 5'-terminal region (coding region of P1 and part of HC-Pro) of PRSV-HN-1, an isolate from Papaya in China. Besides the interspecific recombination, we also found an intraspecific recombination (**Figure 5B**) among the ZTMV population. CX1 isolate is a recombinant with the KF8 isolate as a major parent with the coding region of 6K1, CI, 6K2, VPg, Nla-pro, and part of Nlb of ZTMV-XW isolate. Both KF8 collected from Henan and CX1 isolate collected from Guangxi belong to ZTMV interspecific recombinant, whereas XW isolate collected from Guangdong and CX1 have the same geographical origin, both of which are in southern China. Henan is located in central China, more than 1,500 km away from Guangdong and Guangxi, and the climatic types are very different from each other. Identification of the intraspecific recombination indicated that long-distance genetic connectivity could have occurred among ZTMV populations in China.

Based on the phylogeny of CP nt sequences, the ZTMV population fell into three subgroups (namely the Asia, the America, and the Indian Ocean), related to their geographical origins (Romay et al., 2014). In this study, the same analysis based on the CP coding region (**Figure 6A**), was in accordance with the previous report (Romay et al., 2014), and the three interspecific isolates from China were grouped into the Asian group as expected. The E11045 isolate from France was grouped with other isolates from Asia. Romay et al. (2014) provided a possible explanation that the isolate E11045 invaded France by an accidental introduction. Another two isolates, one from India (accession number KY448345) and the other from Pakistan (accession number AB127935), were unexpectedly clustered between the India ocean subgroup and the American subgroup (**Figure 6A**). These results suggest that there is more genetic diversity in isolates from the South Asia subcontinent (India and Pakistan), which is consistent with the finding from a previous study (Castillo et al., 2011) that PRSV from India have the highest diversity of CP nt sequence. On the other hand, phylogenetic analysis on CI (**Figure 6B**) showed that the ZTMV of KF8, KF17 and other Yunnan isolates have a closer relationship with American isolates than with other Asian isolates. Similarly, an uncertain recombinant event (data not shown) was identified in the coding region of CI, 6K2, Vpg, and Nla-pro among KF8 isolate, CX1 isolate and VET-026 isolate (accession number KC345606) from Venezuela. These results implied that there could be genetic connections between Asian isolates and American isolates.

In this study, we identified and characterized interspecific recombinant viruses between zucchini tigre mosaic virus and Papaya ringspot virus in cucurbits. Despite the origin from interspecific recombination, we proposed that these viruses still belong to zucchini tigre mosaic virus according to their genome characteristics and biological features. We infer that the recombinant virus is epidemic in cucurbits with lower prevalence than other viruses (ZYMV, WMV etc.). In the future, we should develop efficient methods to monitor the incidence and damage of the recombinant ZTMV in cucurbits countrywide. On the other hand, our study provided new insights into the origin and evolution of ZTMV and PRSV.

DATA AVAILABILITY STATEMENT

The datasets presented in this study can be found in online repositories. The names of the repository/repositories and accession number(s) can be found in the article/**Supplementary Material**.

AUTHOR CONTRIBUTIONS

BP and QG contributed to conceptualization and writing. QG contributed to funding acquisition and supervision. BP contributed to investigation, sampling, and analysis of data. BP, LL, BK, and HW performed the experiment. ZF helped to perform the analysis of sRNA sequencing data and writing. All authors contributed to the article and approved the submitted version.

FUNDING

Financial support was provided by the China Agriculture Research System of MOF and MARA (CARS-25), and Central

Public-interest Scientific Institution Basal Research Fund (No. 1610192021401).

ACKNOWLEDGMENTS

We thank Cecile Desbiez from INRA for critical review of this manuscript, and Bixia Qin from Guangxi Academy of Agricultural Sciences and Zhiqiang Cheng from Kaifeng Academy of Agriculture and Forestry for their assistance in collecting samples.

SUPPLEMENTARY MATERIAL

The Supplementary Material for this article can be found online at: https://www.frontiersin.org/articles/10.3389/fmicb.2021.773992/full#supplementary-material

REFERENCES

Abdalla, O. A., and Ali, A. (2018). Molecular characterization reveals that squash chlorosis mottling virus and zucchini tigré mosaic virus are the same newly emerging potyvirus. *Arch. Virol.* 163, 777–780. doi: 10.1007/s00705-017-3657-x

Adams, M., Antoniw, J., and Fauquet, C. (2005). Molecular criteria for genus and species discrimination within the family Potyviridae. *Arch. Virol.* 150, 459–479. doi: 10.1007/s00705-004-0440-6

Bujarski, J. J. (2013). Genetic recombination in plant-infecting messenger-sense RNA viruses: overview and research perspectives. *Front. Plant Sci.* 4:68. doi: 10.3389/fpls.2013.00068

Castillo, X. O., Fermin, G., Tabima, J., Rojas, Y., Tennant, P., Fuchs, M., et al. (2011). Phylogeography and molecular epidemiology of papaya ringspot virus. *Virus Res.* 159, 132–140. doi: 10.1016/j.virusres.2011.04.011

Darriba, D., Taboada, G. L., Doallo, R., and Posada, D. (2012). jModelTest 2: more models, new heuristics and parallel computing. *Nat. Methods* 9:772. doi: 10.1038/nmeth.2109

Desbiez, C., and Lecoq, H. (2004). The nucleotide sequence of watermelon mosaic virus (WMV, Potyvirus) reveals interspecific recombination between two related potyviruses in the 5′ part of the genome. *Arch. Virol.* 149, 1619–1632. doi: 10.1007/s00705-004-0340-9

Desbiez, C., Wipf-Scheibel, C., Millot, P., Verdin, E., Dafalla, G., and Lecoq, H. (2017). New species in the papaya ringspot virus cluster: insights into the evolution of the PRSV lineage. *Virus Res.* 241, 88–94. doi: 10.1016/j.virusres.2017.06.022

Garcia-Mas, J., Benjak, A., Sanseverino, W., Bourgeois, M., Mir, G., González, V. M., et al. (2012). The genome of melon (*Cucumis melo* L.). *Proc. Natl. Acad. Sci. U. S. A.* 109, 11872–11877. doi: 10.1073/pnas.1205415109

Gibbs, A. J., Hajizadeh, M., Ohshima, K., and Jones, R. A. (2020). The potyviruses: an evolutionary synthesis is emerging. *Viruses* 12:132. doi: 10.3390/v12020132

Guo, S., Zhang, J., Sun, H., Salse, J., Lucas, W. J., Zhang, H., et al. (2013). The draft genome of watermelon (*Citrullus lanatus*) and resequencing of 20 diverse accessions. *Nat. Genet.* 45:51. doi: 10.1038/ng.2470

Ibaba, J., Laing, M., and Gubba, A. (2016). Zucchini shoestring virus: a distinct potyvirus in the papaya ringspot virus cluster. *Arch. Virol.* 161, 2321–2323. doi: 10.1007/s00705-016-2899-3

King, A. M. Q., Adams, M. J., Carstens, E. B., and Lefkowitz, E. J. (2011). *Virus Taxonomy: Ninth Report of the International Committee on Taxonomy of Viruse*. Amsterdam: Elsevier Academic.

Kumar, S., Stecher, G., Li, M., Knyaz, C., and Tamura, K. (2018). MEGA X: molecular evolutionary genetics analysis across computing platforms. *Mol. Biol. Evol.* 35, 1547–1549. doi: 10.1093/molbev/msy096

Lecoq, H., and Desbiez, C. (2012). "Viruses of cucurbit crops in the Mediterranean region: an ever-changing picture," in *Advances in Virus Research*. eds. K. Maramorosch, A. Shatkin and F. A. Murphy (San Diego, CA, USA: Elsevier), 67–126.

Liu, Y., Li, F., Zhang, S., Gao, X., Xie, Y., Zhang, A., et al. (2019b). Identification, distribution and occurrence of viruses in the main vegetables of China. *Sci. Agric. Sin.* 52, 239–261.

Liu, L., Peng, B., Zhang, Z., Wu, Y., Miras, M., Aranda, M. A., et al. (2017). Exploring different mutations at a single amino acid position of cucumber green mottle mosaic virus replicase to attain stable symptom attenuation. *Phytopathology* 107, 1080–1086. doi: 10.1094/PHYTO-03-17-0107-R

Liu, L., Xie, K., Tsekpuia, A. R., Peng, B., Liu, M., and Gu, Q. (2019a). Construction and biological characterization of an *Agrobacterium*-mediated infectious cDNA of squash mosaic virus. *Virus Res.* 274:197766. doi: 10.1016/j.virusres.2019.197766

Maina, S., Barbetti, M. J., Edwards, O. R., Minemba, D., Areke, M. W., and Jones, R. A. (2019). Genetic connectivity between papaya ringspot virus genomes from Papua New Guinea and Northern Australia, and new recombination insights. *Plant Dis.* 103, 737–747. doi: 10.1094/PDIS-07-18-1136-RE

Martin, D. P., Murrell, B., Golden, M., Khoosal, A., and Muhire, B. (2015). RDP4: detection and analysis of recombination patterns in virus genomes. *Virus Evol.* 1:1. doi: 10.1093/ve/vev003

Moury, B., and Desbiez, C. (2020). Host range evolution of potyviruses: a global phylogenetic analysis. *Viruses* 12:111. doi: 10.3390/v12010111

Pasin, F., Simón-Mateo, C., and García, J. A. (2014). The hypervariable amino-terminus of P1 protease modulates potyviral replication and host defense responses. *PLoS Pathog.* 10:e1003985. doi: 10.1371/journal.ppat.1003985

Peng, B., Kang, B., Wu, H., Liu, L., Liu, L., Fei, Z., et al. (2019). Detection and genome characterization of a novel member of the genus Polerovirus from zucchini (*Cucurbita pepo*) in China. *Arch. Virol.* 164, 2187–2191. doi: 10.1007/s00705-019-04217-w

Perotto, M. C., Pozzi, E. A., Celli, M. G., Luciani, C. E., Mitidieri, M. S., and Conci, V. C. (2018). Identification and characterization of a new potyvirus infecting cucurbits. *Arch. Virol.* 163, 719–724. doi: 10.1007/s00705-017-3660-2

Quiot-Douine, L., Purcifull, D., Hiebert, E., and De Mejia, M. (1986). Serological relationships and in vitro translation of an antigenically distinct strain of papaya ringspot virus. *Phytopathology* 76, 346–351. doi: 10.1094/Phyto-76-346

Rohožková, J., and Navrátil, M. (2011). P1 peptidase–a mysterious protein of family Potyviridae. *J. Biosci.* 36, 189–200. doi: 10.1007/s12038-011-9020-6

Romay, G., Lecoq, H., and Desbiez, C. (2014). Zucchini tigré mosaic virus is a distinct potyvirus in the papaya ringspot virus cluster: molecular and biological insights. *Arch. Virol.* 159, 277–289. doi: 10.1007/s00705-013-1798-0

Salvador, B., Saenz, P., YangÜez, E., Quiot, J. B., Quiot, L., Delgadillo, M. O., et al. (2008). Host-specific effect of P1 exchange between two potyviruses. *Mol. Plant Pathol.* 9, 147–155. doi: 10.1111/j.1364-3703.2007.00450.x

Sievers, F., and Higgins, D. G. (2014). Clustal omega. *Curr. Protoc. Bioinformatics* 48, 3.13.11–3.13.16. doi: 10.1002/0471250953.bi0313s48

Sun, H., Wu, S., Zhang, G., Jiao, C., Guo, S., Ren, Y., et al. (2017). Karyotype stability and unbiased fractionation in the paleo-allotetraploid Cucurbita genomes. *Mol. Plant* 10, 1293–1306. doi: 10.1016/j.molp.2017.09.003

Valli, A., Lopez-Moya, J. J., and Garcia, J. A. (2007). Recombination and gene duplication in the evolutionary diversification of P1 proteins in the family Potyviridae. *J. Gen. Virol.* 88, 1016–1028. doi: 10.1099/vir.0.82402-0

Villamor, D., Ho, T., Al Rwahnih, M., Martin, R., and Tzanetakis, I. (2019). High throughput sequencing for plant virus detection and discovery. *Phytopathology* 109, 716–725. doi: 10.1094/PHYTO-07-18-0257-RVW

Wang, D., Boluk, G., Quinto, E. A., Hamim, I., Borth, W. B., Melzer, M., et al. (2019). First report of zucchini tigre mosaic virus infecting bitter melon (*Momordica charantia*) in Hawaii. *Plant Dis.* 103:1047. doi: 10.1094/PDIS-08-18-1391-PDN

Wylie, S. J., Adams, M., Chalam, C., Kreuze, J., López-Moya, J. J., Ohshima, K., et al. (2017). ICTV virus taxonomy profile: Potyviridae. *J. Gen. Virol.* 98:352. doi: 10.1099/jgv.0.000960

Xiao, L., Li, Y., Tan, G., Lan, P., Zhong, L., Liu, Y., et al. (2016). First report of zucchini tigre mosaic virus infecting several cucurbit plants in China. *Plant Dis.* 100:1253. doi: 10.1094/PDIS-11-15-1318-PDN

Yakoubi, S., Lecoq, H., and Desbiez, C. (2008). Algerian watermelon mosaic virus (AWMV): a new potyvirus species in the PRSV cluster. *Virus Genes* 37, 103–109. doi: 10.1007/s11262-008-0237-x

Yao, M., Zhang, T., Tian, Z., Wang, Y., and Tao, X. (2011). Construction of *Agrobacterium*-mediated cucumber mosaic virus infectious cDNA clones and 2b deletion viral vector. *Sci. Agric. Sin.* 44, 3060–3068.

Zerbino, D. R., and Birney, E. (2008). Velvet: algorithms for de novo short read assembly using de Bruijn graphs. *Genome Res.* 18, 821–829. doi: 10.1101/gr.074492.107

Zheng, Y., Gao, S., Padmanabhan, C., Li, R., Galvez, M., Gutierrez, D., et al. (2017). VirusDetect: an automated pipeline for efficient virus discovery using deep sequencing of small RNAs. *Virology* 500, 130–138. doi: 10.1016/j.virol.2016.10.017

Conflict of Interest: The authors declare that the research was conducted in the absence of any commercial or financial relationships that could be construed as a potential conflict of interest.

The reviewer XW declared a shared affiliation with some of the authors, BP, LL, HW, BK, and QG to the handling editor at time of review.

Publisher's Note: All claims expressed in this article are solely those of the authors and do not necessarily represent those of their affiliated organizations, or those of the publisher, the editors and the reviewers. Any product that may be evaluated in this article, or claim that may be made by its manufacturer, is not guaranteed or endorsed by the publisher.

frontiers in Plant Science

ORIGINAL RESEARCH
published: 18 January 2022
doi: 10.3389/fpls.2021.798858

RNA-Seq Transcriptome Analysis Provides Candidate Genes for Resistance to *Tomato Leaf Curl New Delhi Virus* in Melon

Cristina Sáez[1], Alejandro Flores-León[1], Javier Montero-Pau[2], Alicia Sifres[1], Narinder P. S. Dhillon[3], Carmelo López[1]* and Belén Picó[1]**

[1] Institute for the Conservation and Breeding of Agricultural Biodiversity, Universitat Politècnica de València, Valencia, Spain, [2] Cavanilles Institute of Biodiversity and Evolutionary Biology, Universitat de València, Valencia, Spain, [3] World Vegetable Center, East and Southeast Asia, Research and Training Station, Kasetsart University, Nakhon Pathom, Thailand

OPEN ACCESS

Edited by:
Giuseppe Parrella,
Institute for Sustainable Plant Protection of the National Research Council (IPSP-CNR), Italy

Reviewed by:
Pranav Pankaj Sahu,
Academy of Sciences of the Czech Republic (ASCR), Czechia
Rui Shi,
North Carolina State University, United States

***Correspondence:**
Cristina Sáez
crisaesa@upvnet.upv.es
Carmelo López
clopez@upv.es
Belén Picó
mpicosi@btc.upv.es

Specialty section:
This article was submitted to Plant Pathogen Interactions, a section of the journal Frontiers in Plant Science

Received: 20 October 2021
Accepted: 29 November 2021
Published: 18 January 2022

Citation:
Sáez C, Flores-León A, Montero-Pau J, Sifres A, Dhillon NPS, López C and Picó B (2022) RNA-Seq Transcriptome Analysis Provides Candidate Genes for Resistance to Tomato Leaf Curl New Delhi Virus in Melon. Front. Plant Sci. 12:798858. doi: 10.3389/fpls.2021.798858

Tomato leaf curl New Delhi virus (ToLCNDV) emerged in the Mediterranean Basin in 2012 as the first DNA bipartite begomovirus (*Geminiviridae* family), causing severe yield and economic losses in cucurbit crops. A major resistance *locus* was identified in the wild melon accession WM-7 (*Cucumis melo* kachri group), but the mechanisms involved in the resistant response remained unknown. In this work, we used RNA-sequencing to identify disease-associated genes that are differentially expressed in the course of ToLCNDV infection and could contribute to resistance. Transcriptomes of the resistant WM-7 genotype and the susceptible cultivar Piñonet Piel de Sapo (PS) (*C. melo* ibericus group) in ToLCNDV and mock inoculated plants were compared at four time points during infection (0, 3, 6, and 12 days post inoculation). Different gene expression patterns were observed over time in the resistant and susceptible genotypes in comparison to their respective controls. Differentially expressed genes (DEGs) in ToLCNDV-infected plants were classified using gene ontology (GO) terms, and genes of the categories transcription, DNA replication, and helicase activity were downregulated in WM-7 but upregulated in PS, suggesting that reduced activity of these functions reduces ToLCNDV replication and intercellular spread and thereby contributes to resistance. DEGs involved in the jasmonic acid signaling pathway, photosynthesis, RNA silencing, transmembrane, and sugar transporters entail adverse consequences for systemic infection in the resistant genotype, and lead to susceptibility in PS. The expression levels of selected candidate genes were validated by qRT-PCR to corroborate their differential expression upon ToLCNDV infection in resistant and susceptible melon. Furthermore, single nucleotide polymorphism (SNPs) with an effect on structural functionality of DEGs linked to the main QTLs for ToLCNDV resistance have been identified. The obtained results pinpoint cellular functions and candidate genes that are differentially expressed in a resistant and susceptible melon line in response to ToLCNDV, an information of great relevance for breeding ToLCNDV-resistant melon cultivars.

Keywords: melon (*Cucumis melo* L.), ToLCNDV resistance, transcriptome (RNA-seq), DEG (differentially expressed genes), qPCR (quantitative polymerase chain reaction)

INTRODUCTION

Melon (*Cucumis melo* L.) is one of the major cucurbit crops cultivated worldwide and with large diversification. It is highly appreciated for its nutritional profile and its sweet and aromatic flavor, and its production generates large profits to farmers in developing and industrialized countries.

Despite years of selection and breeding, melon production around the globe is compromised by several pathogens and diseases. The occurrence of new viruses emerging in melon-growing regions is a major concern for farmers and seed producers because of the yield-limiting potential of these biological agents (Annu et al., 2019).

Tomato Leaf curl New Delhi virus (ToLCNDV) is a species of bipartite begomovirus (family *Geminiviridae*) naturally transmitted by the whitefly *Bemisia tabaci* (Gennadius) in a persistent manner. This virus has posed a major threat to melon crops in many countries of the Indian subcontinent since the earliest 2000s, but recently, a new recombinant strain has appeared in the Mediterranean basin that has generated a devastating disease to mainly melon and zucchini squash (*Cucurbita pepo*) crops (Juárez et al., 2014). The new strain was first identified in Spain, but all the isolates detected across the Mediterranean countries share a conserved genomic sequence (Juárez et al., 2014, 2019; Fortes et al., 2016; Panno et al., 2019). Consequently, the Mediterranean ToLCNDV strain has been designated as ToLCNDV-ES (Moriones et al., 2017).

Similar to the Asian strains, ToLCNDV-ES infection in melon results in severe symptomatology, including curling and distortion of leaves, green and yellow spotting conforming mosaic, and changes in leaf shape and stunting. Infection at young stages of the plant hampers growth and flowering with decreased or complete loss of fruit quality due to skin roughness, longitudinal cracking, and small fruit size, rendering them unmarketable (Panno et al., 2016). Melon production losses may reach 80% in greenhouse and open-field conditions if integrated control measures against the disease are not adopted (Messelink et al., 2020). For ToLCNDV-ES management, genetic resistance is the most efficient approach for farmers; it reduces the need for chemical treatments and, thus, is safer for producers, consumers, and the environment.

Melon accessions belonging to the Indian momordica, kachri, acidulous, and agrestis groups are reported to be resistant to begomoviruses (Yousif et al., 2007; McCreight et al., 2008; López et al., 2015; Pitrat, 2016; Romay et al., 2019; Martín-Hernández and Picó, 2021), and several QTLs associated with resistance have been identified in this germplasm (Sáez et al., 2017; Romay et al., 2019).

In previous works, we mapped a major gene with incomplete dominance conferring resistance to ToLCNDV-ES on chromosome 11 of the Indian wild melon accession WM-7 (kachri group, landrace originated from the semiarid region of Punjab state, India) (Roy et al., 2012; Sáez et al., 2017). However, two minor modifiers on chromosomes 2 and 12 modulate the response to this viral infection. Functional characterization of the genes located in these regions is required to enhance understanding of the molecular resistance mechanisms in WM-7 to ToLCNDV.

Transcriptome sequencing using RNA-seq technology has gained popularity to explore gene expression changes in cucurbit plants during viral infections (Li et al., 2017a; Sun et al., 2017, 2019; Lou et al., 2020). This tool offers a global view of expression changed during the basal defense response and helps to elucidate complex resistance mechanisms in plants through comparing gene expression upon infection in susceptible and resistant lines.

Transcriptome analysis and gene expression studies have been performed to evaluate interactions between ToLCNDV in solanaceous crops. Sahu et al. (2010) compare transcript levels between tomato genotypes tolerant and susceptible to ToLCNDV, finding induced genes in the tolerant genotype related to the cell cycle, transcription factors (TFs), DNA/RNA processing, and molecular signal and transport. The overexpression of two of the main candidate genes for resistance, a DEAD-box RNA helicase gene (*SlDEAD35*) and the 26S proteasome subunit RPT4a (*SlRPT4*), involved in the hypersensitive response and cell death, respectively, is associated with the inhibition of ToLCNDV infection and symptom expression (Sahu et al., 2016; Pandey et al., 2019). In pepper (*Capsicum annuum*) and potato (*Solanum tuberosum*) NBS-LRR genes are found induced in resistant genotypes after ToLCNDV infection (Kushwaha et al., 2015; Jeevalatha et al., 2017).

Román et al. (2019) measured expression differences of 12 candidate genes between a ToLCNDV resistant and a susceptible melon accession. Two genes, an a NAC TF and an actin related protein, were strongly induced in the susceptible genotype and were associated with disease development. Apart from those studies, global transcriptional and molecular characterization of ToLCNDV resistance in cucurbits has not been conducted.

In this study, we performed an RNA-seq assay to compare transcript levels between mock-inoculated and ToLCNDV-ES-infected melon plants between the resistant WM-7 genotype and a susceptible accession from day 0 to 12 days after treatment to identify candidate genes for resistance.

MATERIALS AND METHODS

Plant Material and Mechanical Inoculation

The ToLCNDV-resistant wild accession WM-7 (*C. melo*, kachri group) and the susceptible traditional Spanish cultivar Piñonet Piel de Sapo (PS) (*C. melo*, ibericus group) were used as plant materials in this study. WM-7 is an Indian accession (Roy et al., 2012), selfed in successive growing cycles to increase the level of homozygosity. Seeds of both accessions were disinfected in a 10% sodium hypochlorite solution for 1 min and washed twice with distilled water for 5 min. To ensure homogenous germination, all seeds were opened using forceps, placed over moistened cotton in Petri dishes and incubated in the dark at 37°C for 48 h. Seedlings were transplanted into pots containing commercial substrate (Humin-substrat N3, Neuhaus Klasmann-Deilmann, Germany) and growth in a climate chamber at 25°C and 60% relative humidity under a photoperiod of 16 h/8 h (day/night).

At the two true-leaves stage, 108 seedlings of both resistant and susceptible accessions were mechanically inoculated with ToLCNDV-ES following the procedure described in López et al. (2015). Symptomatic leaf tissue from zucchini plants agroinfiltrated with an infective ToLCNDV-ES clone (Sáez et al., 2016) was used as the inoculum source. The tissue was mashed in an iced mortar together with inoculation buffer in a 1:4 (*w:v*) proportion (López et al., 2015), and the mix was scrubbed with a cotton swab over one cotyledon and one true leaf, previously dusted with Carborundum 600 mesh. The same number of plants were mock-inoculated following the same protocol but rubbing with only inoculation buffer and Carborundum. Seedlings were cultivated for 20 days after mechanical inoculation (dpi) under controlled conditions as described above.

Sampling Design

At 0 dpi (two true-leaves stage), all expanded leaves of six healthy seedlings were sampled and used as the control treatment, maintaining seedlings alive with their apex intact. The remaining seedlings were mock- or virus-inoculated and sampled following the same procedure as the 0 dpi control but avoiding the inoculated leaves. Six different seedlings were sampled at each stage corresponding to 3, 6, 9, 12, 15, and 18 dpi. Samples were frozen immediately in liquid nitrogen before storage at −80°C. Once sampled, all plants were maintained until 20 dpi to test virus accumulation or absence by tissue-printing hybridization as described below. Then, the tissue of the six plants of each time point was pooled to a single sample. For each time point, three biological replicates were processed independently.

After evaluation of viral load by quantitative polymerase chain reaction (qPCR), samples of two biological replicates at 0, 3, 6, and 12 dpi were selected to be included in the RNA-seq assay, corresponding to a total of 28 samples (**Table 1**). The third replicate was included in qRT-PCR validation along with the two sequenced biological replicates.

Evaluation of Response to *Tomato Leaf Curl New Delhi Virus*

Symptoms of ToLCNDV were assessed in all plants at each sampling stage and at 20 dpi, according to the visual scale described in López et al. (2015), in which score 0 means absence of symptoms and score 4 very severe symptoms. Quantitative PCR (qPCR) was used to determine the viral titer evolution at the different stages analyzed (0, 3, 6, 9, 12, 15, and 18 dpi). Total DNA was extracted from each pooled sample of inoculated WM-7 and PS accessions in the three biological replicates using the Cetyltrimethyl ammonium bromide (CTAB) method (Doyle and Doyle, 1990). ToLCNDV amount was analyzed by qPCR in two technical replicates, following the same procedure described in Sáez et al. (2017).

Additionally, to verify the presence or absence of ToLCNDV infection in all plants at 20 dpi, tissue-printing hybridization by digoxigenin-labeled ToLCNDV-RNA probe was performed following the procedure described in Sáez et al. (2021).

RNA Extraction

The 28 samples of processed leaf tissue were sent to the Genomics4All Company (Universidad Politécnica de Madrid, Spain) for cDNA library construction. Total RNA extraction and DNAse treatment was performed with TURBO DNA-free™ kit (Ambion, Life technologies), following the manufacturer's protocol. RNA was purified with RNeasy Kit columns (Qiagen), and RNA integrity was checked on a Bioanalyzer 2100 (Agilent Technologies, Santa Clara, CA, United States) to ensure an RNA integrity number (RIN) score of ≥7. Total RNA (500 ng) were used to prepare RNA-seq libraries using the TruSeq Stranded mRNA Library Prep Kit (Illumina) according to the manufacturer's protocol.

For qRT-PCR validation, total RNA was isolated using 700 μL of Extrazol® EM30 (Blirt DNA, Gdansk, Poland), according to the manufacturer's specifications. Integrity was checked by 1% agarose gel electrophoresis, and purity and quantity were determined spectrophotometrically at 260 and 280 nm using a NanoDrop 1000 (Thermo Scientific, Waltham, MA, United States). Total RNA (1 μg) treated with PerfeCTa® DNase I (RNAse-free) (Quanta Biosciences, Gaithersburg, MD, United States) was used as template with the RevertAid™ First Strand cDNA Synthesis Kit (ThermoFisher Scientific) with Oligo dT primers.

RNA-Seq Data Analysis and Evaluation of Expression Differences

RNA-seq libraries were sequenced (single-end 50 pb) using a HiSeq 2500 Illumina (Illumina, CA, United States). Raw sequences were processed using Trimmomatic (Bolger et al., 2014) to remove adapters and low-quality reads. Quality of clean reads was checked by FastQC (Andrews, 2010).

Trimmed reads were mapped to the last version of the melon reference genome (v.4.0), recently updated and publicly available at the melonomics.net website (Castanera et al., 2020), using STAR v. 2.02.01 (Dobin et al., 2013). Subsequently, RSEM v. 1.3.1 was used to quantify the abundance of transcript reads assigned to each of the 28.299 genes included in the complete genome annotation according genome assembly v. 4.0 (Li and Dewey, 2011).

Clusters of genes sharing similar expression profiles across all samples were obtained by performing a weighted gene co-expression network analysis (WGCNA), using the R package WGCNA v.1.69 (Langfelder and Horvath, 2008). To test for statistical differences due to the effects of genotype, treatment, and time after inoculation, a generalized linear model using the cluster's eigengenes was performed. Kyoto Encyclopedia of Genes and Genomes (KEGG) enrichment analysis (Kanehisa and Goto, 2000) of genes that were significantly correlated at $p\text{-value} < 0.01$ with each gene cluster was performed using *clusterProfiler* (Yu et al., 2012).

Differentially expressed genes (DEGs) were detected using the DESeq2 package (version 1.26.0) (Love et al., 2014), comparing raw counts of samples at 3, 6, or 12 dpi against 0 dpi. Genes with *p-values* under 0.05 and $|\log2 \text{ (fold changes)}| \geq 1$ were considered as significant, assigning those presenting

TABLE 1 | Summary of the RNA-Seq experimental design, read alignment, and differentially expressed genes (DEGs).

Sample name	Inoculation treatment	Time point dpi	Replicate	Cleaned reads	Mapped reads	% Mapped reads	DEGs
WM-7_0dpi_1	Uninoculated	0	1	96,571,093	92,933,140	96.23	–
WM-7_0dpi_2		0	2	89,738,162	86,520,235	96.41	
WM-7_I3dpi_1	ToLCNDV inoculated	3	1	96,017,670	92,139,780	95.96	292
WM-7_I3dpi_2		3	2	90,412,987	87,094,110	96.33	
WM-7_B3dpi_1	Mock inoculated	3	1	97,337,221	93,893,779	96.46	
WM-7_B3dpi_2		3	2	90,083,950	53,101,818	58.95	
WM-7_I6dpi_1	ToLCNDV inoculated	6	1	95,502,062	88,222,091	92.38	354
WM-7_I6dpi_2		6	2	89,625,183	74,603,092	83.24	
WM-7_B6dpi_1	Mock inoculated	6	1	96,044,324	92,625,513	96.44	
WM-7_B6dpi_2		6	2	90,375,930	86,463,397	95.67	
WM-7_I12dpi_1	ToLCNDV inoculated	12	1	96,637,024	92,925,369	96.16	558
WM-7_I12dpi_2		12	2	90,324,017	86,939,559	96.25	
WM-7_B12dpi_1	Mock inoculated	12	1	97,444,807	94,078,242	96.55	
WM-7_B12dpi_2		12	2	91,063,342	87,570,888	96.16	
PS_0dpi_1	Uninoculated	0	1	102,027,470	95,339,552	93.44	–
PS_0dpi_2		0	2	90,578,076	87,236,559	96.31	
PS_I3dpi_1	ToLCNDV inoculated	3	1	95,503,001	91,778,653	96.1	404
PS_I3dpi_2		3	2	60,411,004	57,587,132	95.33	
PS_B3dpi_1	Mock inoculated	3	1	97,063,008	93,062,108	95.88	
PS_B3dpi_2		3	2	92,073,644	88,433,510	96.05	
PS_I6dpi_1	ToLCNDV inoculated	6	1	96,678,397	92,088,929	95.25	752
PS_I6dpi_2		6	2	93,655,611	89,233,728	95.28	
PS_B6dpi_1	Mock inoculated	6	1	96,653,614	92,903,742	96.12	
PS_B6dpi_2		6	2	91,746,137	88,232,317	96.17	
PS_I12dpi_1	ToLCNDV inoculated	12	1	95,935,797	92,131,302	96.03	981
PS_I12dpi_2		12	2	91,460,724	87,827,401	96.03	
PS_B12dpi_1	Mock inoculated	12	1	96,368,610	92,693,418	96.19	
PS_B12dpi_2		12	2	89,485,860	85,736,511	95.81	

Assigned name to each sample, their temporal and inoculation treatment, and replicates performed are shown. Proportion of uniquely clean reads mapped against the reference melon genome (v4.0), and differentially expressed genes comparing firstly with 0 dpi control and then between mock and ToLCNDV inoculated treatments are provided.

log2 (fold change) $\geq$ 1 to the "upregulated" group and those with values $\leq$ −1 to the "downregulated" group, compared to the 0 dpi stage.

Regarding the background "noise" encountered in previous time course transcriptomic experiments (Nueda et al., 2012) and with the view that eliminating as many false positives from the final data set is key (Conesa et al., 2016; Giacomini et al., 2018), we performed an additional filtering step to optimize and add ruggedness to our analysis. In this approach, the expression DEGs data sets obtained after comparing expression levels of 3, 6, and 12 dpi time points to 0 dpi were then further compared between mock and ToLCNDV inoculated samples at the same dpi stage, selecting those DEGs differing by at least $\pm$ 1.5 log2 (fold change) values between ToLCNDV and mock treatments. Thus, developmental changes of the melon plant along time are discarded, and DEGs obtained here must be attributed to ToLCNDV infection in each genotype.

Common DEGs at the different stages of the disease and those shared between genotypes were represented by Venn diagrams, displayed with the jvenn tool (Bardou et al., 2014), freely available at http://bioinfo.genotoul.fr/jvenn.

The Cucurbits Genomics Database (CuGenDB[1]) was employed to determine biological functions and pathways of the identified DEGs. GO term enrichment analysis was performed uploading DEGs lists, considering significantly enriched those with an adjusted *p-value* < 0.05.

Validation of Differentially Expressed Genes by Quantitative Polymerase Chain Reaction

To validate the RNA-Seq data, expression of seven candidate genes putatively associated to ToLCNDV resistance in melon was evaluated by qRT-PCR in six out of the seven time points sampled (0, 3, 6, 9, 12, and 18 dpi). Confirmation of the expression patterns of these seven genes was performed in the three biological replicates of mock and viral inoculated plants. cDNA for the validation experiment was prepared as described in section "RNA extraction."

PCR reactions were performed on a Roche LightCycler® 480 RT-PCR System (Roche Diagnostics, Rotkreuz, Switzerland)

[1]http://cucurbitgenomics.org/

using the FastStart Essential DNA Green Master (Roche Molecular Systems, Rotkreuz, Switzerland). Each qPCR reaction contained 1.5 μL of cDNA, 7.5 μL of FastStart Essential DNA Green Master (Roche Diagnostics, Rotkreuz, Switzerland) and 1.5 μL (10 μM) of each primer and of H_2O to a final volume of 15 μL. Primer design was made using Primer 3Plus software (Untergasser et al., 2007), and primer sequences are listed in **Supplementary Table 1**. The corresponding specific fragment was amplified in two technical replicates following these conditions: 95°C for 5 min, 40 cycles of 95°C for 15 s, 60°C for 30 s, and 72°C for 15 s. A melting curve analysis (60–95°C) was performed after the amplification to check specificity of the reaction. Expression levels were analyzed using relative quantitative accumulation by the $2^{(-\Delta\Delta Ct)}$ method (Schmittgen and Livak, 2008). As endogenous controls, the melon Peptidyl-prolyl *cis-trans* isomerase gene (Cyclophilin CYP7, MELO3C025848.2) (González-Ibeas et al., 2007), was used as a reference for the expression level of each candidate gene in every condition.

Transcript-Based Single Nucleotide Polymorphism Identification

To study the potential effect of genetic changes in coding regions, reads were aligned against the reference *C. melo* genome using *bowtie2* version 2.3.4.1 (Langmead and Salzberg, 2012), and variant-calling of Single Nucleotide Polymorphism (SNPs) and Indels was performed by Freebayes version 1.3.4 (Garrison and Marth, 2012), setting a minimum mapping quality cutoff of 40, minimum base quality of 20 and minimum minor allele frequency of 0.05. Variant annotation and its predicted functional effect on the transcript were made using SNPEff version 5.0e (Cingolani et al., 2012).

RESULTS

Assessment of WM-7 and PS Response to *Tomato Leaf Curl New Delhi Virus* Infection

All WM-7 plants inoculated with ToLCNDV remained symptomless throughout the assay (**Figure 1A**). Conversely, early mild symptoms (score 2) were identified in PS at 6 dpi on a small number of plants. This score increased at 9 dpi. At 12, 15, and 18 dpi all PS plants showed severe symptoms (scores from 3 to 4) including mosaic, curling, and yellowing (**Figure 1A**).

To quantify the relative viral accumulation of ToLCNDV in both WM-7 and PS after infection, a qPCR assay was performed, using healthy plants (0 dpi) as controls. ToLCNDV was identified at all stages in both genotypes except at 0 dpi. Viral accumulation was low in both WM-7 and PS at the early stage of 3 dpi, but significant differences were observed in the course of the disease (**Figure 1B**). Whereas WM-7 viral accumulation levels remained low until the end of the assay, viral load in PS continued to increase at 6 and 9 dpi, achieving the highest accumulation at 15 dpi (**Figure 1B**).

Qualitative viral titers at 20 dpi were determined by tissue-printing hybridization (data not shown). No signal was detected in control and mock-inoculated WM-7 and PS plants, whereas in all PS infected plants, there was a high level of ToLCNDV. Only some WM-7 plants exhibited slight hybridization signals, suggesting low viral titers.

According to these results, ToLCNDV was capable of initially infecting both resistant and susceptible genotypes. However, virus replication and/or movement were restricted in WM-7, whereas in PS, the infection became systemic after 6 dpi.

RNA Sequencing, Reads Alignment, and Weighted Gene Co-expression Network Analysis

Twenty-eight libraries were sequenced, generating almost 2.6 billion high-quality clean reads. On average, 94% of the clean reads were mapped to the melon reference genome (v4.0) unambiguously to a single locus (**Table 1**). Only in one sample, corresponding to the second replicate of ToLCNDV inoculated WM-7 at 6 dpi (WM7_I6dpi_Rep2), 58.95% of reads mapped to a single locus as a consequence of the high content of ribosomal RNA in this sample. This effect was corrected by the STAR outfilter multimap nmax function, selecting only those reads mapping to a single locus (**Table 1**). The 28 transcriptomes were further analyzed to compare gene expression of resistant and susceptible genotypes.

Weighted gene co-expression network analysis produced 21gene clusters (GCs) based on the expression profiles of the 28 samples (**Supplementary Figure 1**). Genes associated to each GC as well as KEGG and GO term enrichments are presented in **Supplementary Tables 2**, **3**, respectively. Some of the clusters clearly show a genotype-specific pattern of gene co-expression (e.g., GC 8, 16, and 21) or plant age (e.g., GC4 and 7). But only GCs 19 and 20 showed statistically significant differences regarding genotype × treatment × time (**Figure 2A** and **Supplementary Table 4**). Most upregulated genes within these GCs were enriched in KEGG pathways associated to plant–pathogen interaction, whereas those with an expression negatively correlated with the clusters were mainly classified in "Ribosome" and "Photosynthesis" ontologies (**Figure 2B**). Further, GO ontologies including upregulated co-expressed transcripts in GC19 and GC20 were "Transmembrane transport" in biological process and "ADP binding" and "Calmodulin binding" in molecular function (**Supplementary Table 3**). Conversely, "Hydrolase activity" and "GTP binding" of the molecular function class and "Chloroplast" and "Thylakoid" in the category cellular components included genes downregulated (**Supplementary Table 3**).

Differential Expression Analyses and Functional Classification by Gene Ontology Enrichment

In total, 1204 genes were differentially regulated in the resistant WM-7 genotype and 2137 genes in the susceptible PS genotype. The number of DEGs increased with the course of the disease for both genotypes (**Table 1**, gene lists are in **Supplementary Tables 5**, **6**). At 3 dpi, the lowest number of DEGs was observed for both WM-7 and PS. At this stage, all plants were asymptomatic and with low viral titers regardless the genotype.

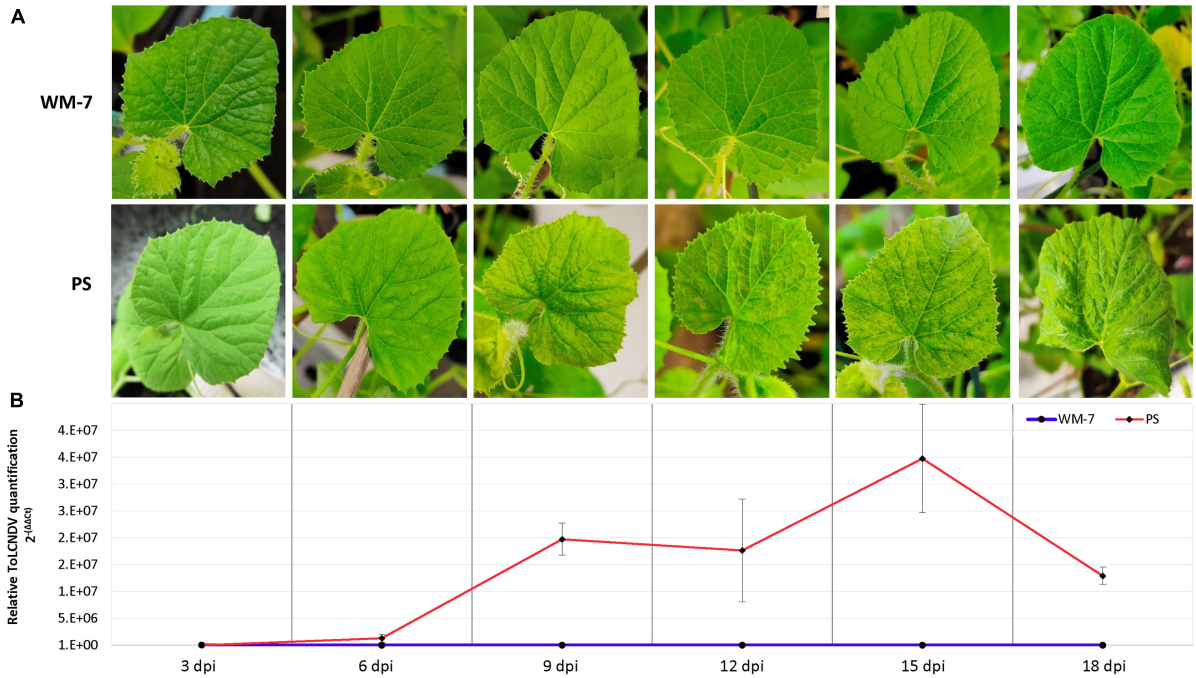

FIGURE 1 | Assessment of WM-7 and PS response to ToLCNDV-ES infection in the first total expanded apical leaf of each plant. Temporal evolution of symptomatology **(A)** and mean of viral titers **(B)** in WM-7 and PS.

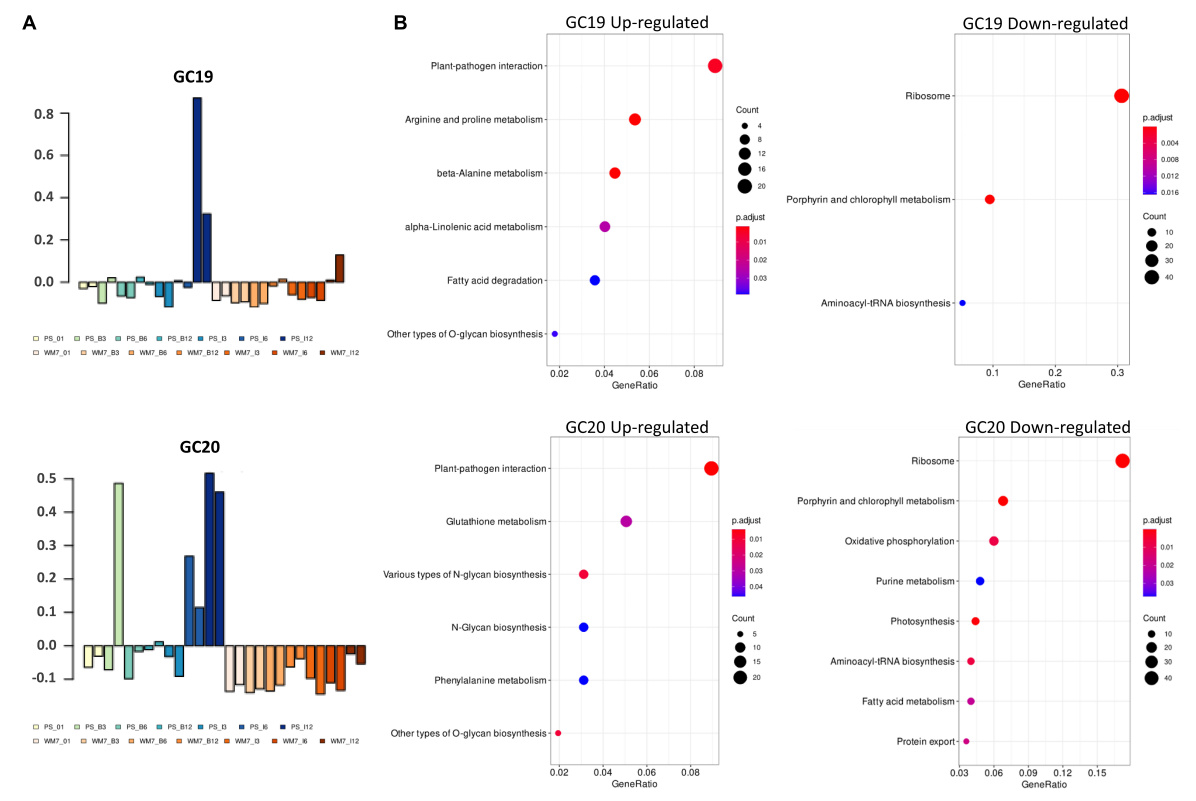

FIGURE 2 | Module eigengenes across samples for the gene clusters GC19 and GC20 **(A)**. KEGG enrichment profile of up- and down-represented genes within each cluster **(B)**. I: ToLCNDV inoculated; B: mock inoculated; 01: 0 dpi, 3: 3 dpi, 6: 6 dpi, 12: 12 dpi.

Interestingly, at all stages the number of DEGs was higher in PS than in WM-7, and both genotypes showed a different pattern of gene expression (**Figure 3**). Whereas the number of upregulated genes in PS plants increased markedly as infection progressed (159, 312, and 800 upregulated genes at 3, 6, and 12 dpi, respectively), in WM-7, this increase was less profound (146, 222, and 343 DEGs, respectively). Contrastingly, the number of downregulated genes in PS did not show this increasing pattern with a maximum at 6 dpi (245, 440, and 181 downregulated genes at 3, 6, and 12 dpi, respectively) although a slight increase was found in WM-7 (146, 132, and 215 DEGs). These results suggest that ToLCNDV infection causes a lower impact on the transcriptomic reorganization in WM-7 than in PS, consistent with similar studies comparing the response to begomoviruses in resistant and susceptible accessions (Allie et al., 2014; Zaidi et al., 2020).

PS and WM-7 shared 336 DEGs during ToLCNDV infection (**Figure 4A**). Interestingly, 56 of these DEGs had an opposite expression pattern with 26 induced in the susceptible genotype and repressed in the resistant and 30 upregulated in WM-7 but downregulated in PS (**Figure 4A** and **Supplementary Table 7**). Both sets of common DEGs include genes related to resistance to pathogens, host–pathogen systems, and components required to accomplish viral infection.

To further analyze and understand this response, an analysis of gene ontologies was performed, identifying GO terms of DEGs shared between the resistant and susceptible genotypes (**Figure 5**). Among the biological process group, those terms involved in chromosome organization and replication, metabolism, and conformation of DNA, contained DEGs that were induced at 3 dpi in PS but were repressed in WM-7 at 12 dpi. In the cellular component category, among the upregulated genes, those encoding membrane components were the most enriched in PS at 6 and 12 dpi. Although there were WM-7 membrane-associated genes overexpressed too, the number of these genes in PS was much greater than in the resistant genotype. A high number of upregulated genes in WM-7 concerned intracellular organelles; a group of these was repressed in PS at 6 dpi. Genes codifying proteins located in the nucleus or chromosome organization were induced in PS at 3 dpi but down-expressed at 6 dpi. By contrast, transcription of these genes in WM-7 was suppressed at 12 dpi. Although less in number represented, genes of the minichromosome maintenance protein complex (MCM) were repressed in WM-7 at 12 dpi and upregulated in PS at 3 dpi. MCM proteins interact with Rep protein of geminiviruses to facilitate their replication (Rizvi et al., 2015). Examining the GO terms concerning molecular components, those related with "binding" were the most enriched in PS, showing genes with highly altered expression patterns. Some genes related to DNA helicase activity were induced early in PS (3 dpi) but repressed at 12 dpi in WM-7.

Gene ontology terms including DEGs at 3 dpi in WM-7 and also in PS at any time point were not identified. REVIGO (Supek et al., 2011) was used to group similar GO term categories exclusively identified in WM-7 or PS but not in both lines. Scatterplots were constructed to present these results in **Supplementary Figure 2**. In total, 721 genes were exclusively found expressed in WM-7 and 1531 genes in PS (**Figure 4A**). In WM-7, nine of these genes showed differential expression at the three time points (**Figure 4B** and **Supplementary Table 8**), seven were upregulated, and two downregulated. A multiprotein-bridging factor 1c (MELO3C004553.2) on chromosome 5 showed the highest expression differences at 3, 6, and 12 dpi [log2 (fold change) of 3.525, 3.419, and 4.071, respectively]. A similar response was observed for a gene codifying a cysteine proteinase inhibitor (MELO3C002921.2) on chromosome 9. The cysteine proteinase inhibitor gene family has been described conferring resistance to viruses in plants (Gutiérrez-Campos et al., 1999; Gholizadeh et al., 2005). Two cysteine-rich receptor-kinase-like protein genes (CRKs) (MELO3C018796.2 on chromosome 1 and MELO3C002492.2 on chromosome 12) presented both strongly induced and repressed expression patterns at different stages in infected WM-7 plants. CRK involvement in pathogen resistance and cell death in plants has been well described (Lu et al., 2017; Yadeta et al., 2017; Quezada et al., 2019). Additionally, another nine genes related to heat stress responses were altered at some of the three stages, and a great number of photosynthetic genes had enhanced expression at 6 and 12 dpi (**Supplementary Table 5**). Another gene (MELO3C027682.2, chromosome 7) encoding a DNA-directed RNA polymerase, which has been associated with defense responses (Nemchinov et al., 2016), was also remarkably overexpressed at 6 and 12 dpi (**Supplementary Table 8**).

In PS plants, 10 genes were found to be DEGs at the three evaluated stages of ToLCNDV disease development (**Figure 4B** and **Supplementary Table 9**). The expression profiles of two of them, an accelerated cell death 6-like protein (MELO3C004399.2, chromosome 5) and a cysteine-rich receptor-like kinase (MELO3C018799.2, chromosome 1), were especially interesting as they were highly downregulated at 3 dpi but changed to be overexpressed at 6 and 12 dpi when this genotype developed symptoms and systemic infection of the virus, conversely to what was found in WM-7 for some of these types of genes.

Analysis of Differentially Expressed Genes in the Candidate Regions for Tomato Leaf Curl New Delhi Virus-ES Resistance

We focused our expression analyses on those genes included in the three candidate regions of the *C. melo* genome linked to the resistance to ToLCNDV-ES, at the major resistance QTL on chromosome 11, and on the minor QTLs on chromosome 2 and 12 (Sáez et al., 2017).

Transcription Changes on Chromosome 11

The main locus involved in the resistance identified in WM-7 was located in chromosome 11 between positions 30,112,560 and 30,737,924 bp. In this interval, seven genes were found to be differentially expressed in PS and three in WM-7 (**Table 2**).

Only one out of the seven genes in PS, a gene encoding a Glutaredoxin protein (MELO3C022339.2), was downregulated at 6 dpi; the other six genes were upregulated, especially at

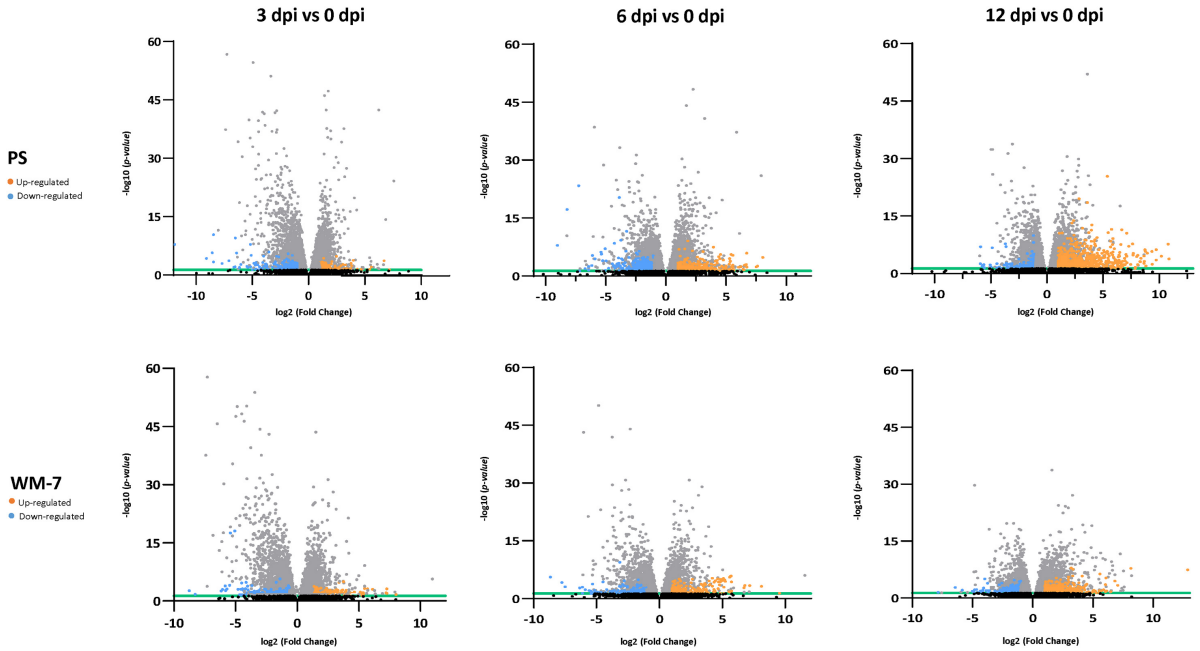

FIGURE 3 | Volcano plots display DEG distribution for each time point at 3, 6, and 12 dpi in both PS and WM-7. Orange dots represent the upregulated genes and blue dots downregulated genes. The *x*-axis correspond to log2 (fold change) and the *y*-axis to –log10 (*p*-adjusted). Black dots represent those DEGs not considered significant with *p*-adjusted $\geq$ 0.05 (green line shows the cutoff) and gray dots those DEGs differing from mock-inoculated treatments in 1.5 $<$ log2 (fold change) $>$ 1.5.

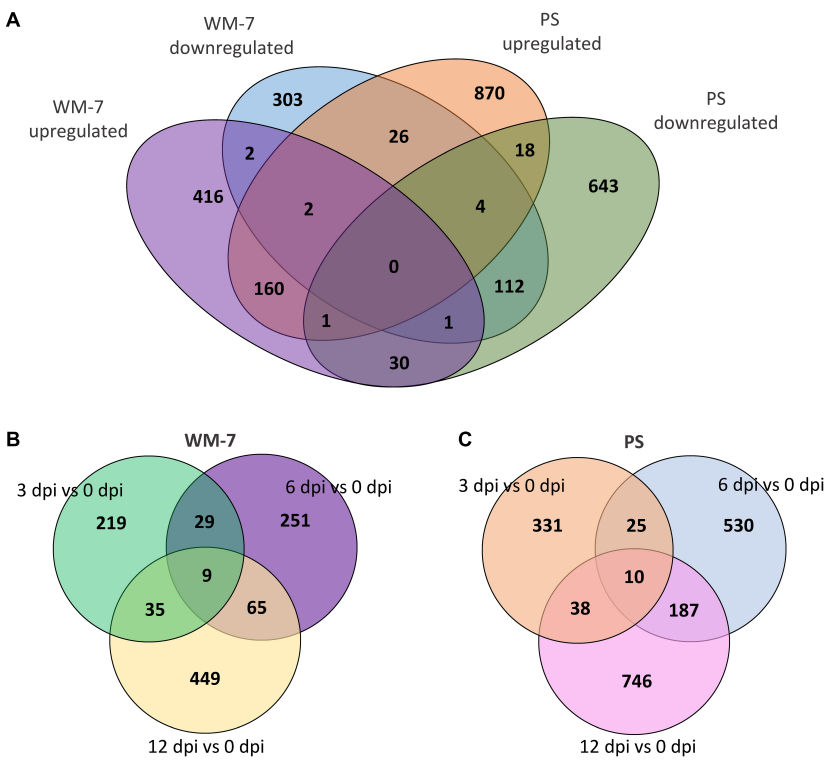

FIGURE 4 | Venn diagrams representing common and specific up and down DEGs identified in WM-7 and PS **(A)**; common and specific DEGs at 3, 6, and 12 dpi in WM-7 **(B)** and PS **(C)**.

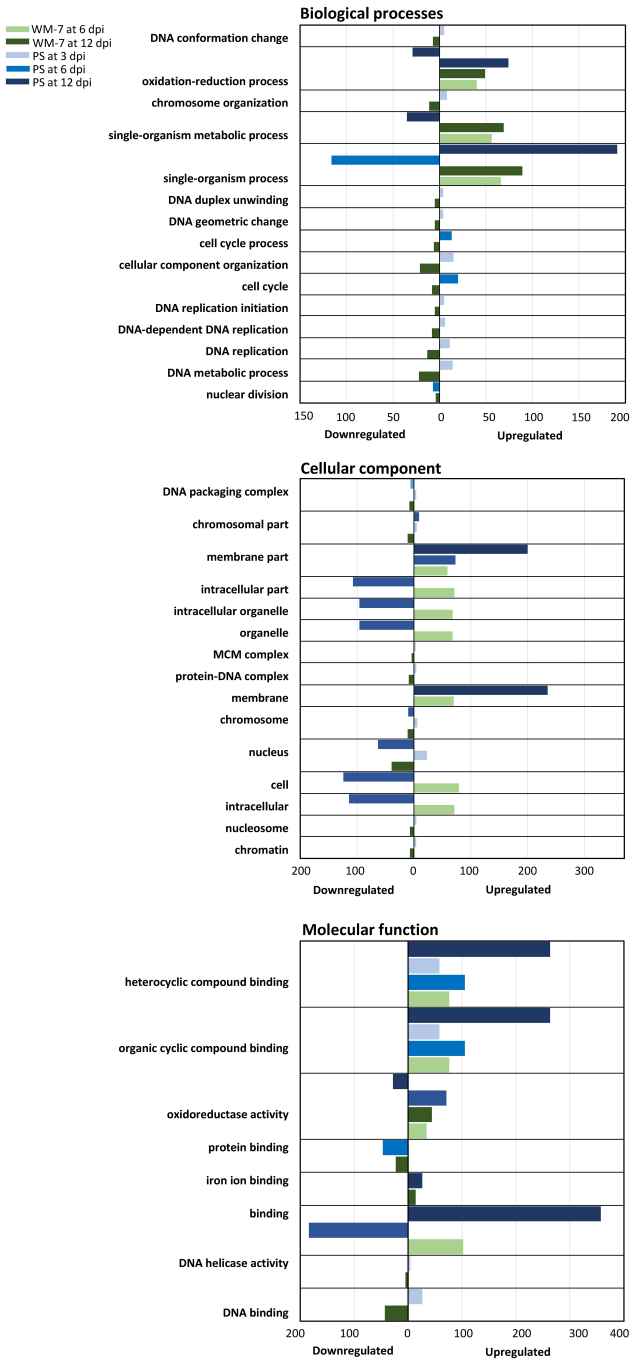

FIGURE 5 | Gene ontology (GO) classification. The number of upregulated or downregulated genes assigned to each class were calculated at 3, 6, and 12 dpi to WM-7 and PS and represented in colors according with the legend.

12 dpi. The highest induced expression was detected for a bidirectional sugar transporter SWEET (MELO3C022341.2) with a log2 (fold change) of 10.806. Genes with a lower induction were a proton pump-interactor 2-like isoform X2 (MELO3C022324.2), described as a plasma membrane regulator (Bonza et al., 2009), and an ethylene-responsive TF ERF113-like (MELO3C022358.2) protein family reported as induced in infected plants with TYLCV (Wu et al., 2019). Between the other three induced genes, MELO3C022365.2 and MELO3C022367 encode uncharacterized proteins, and MELO3C022300.2 is a probably inactive receptor-like protein kinase.

In WM-7, three DEGs identified in the candidate region for resistance of chromosome 11 were downregulated (**Table 2**).

A transmembrane protein, putative (MELO3C022327.2) was repressed at 3 and 6 dpi, whereas Auxin-responsive protein SAUR36 (MELO3C022337.2) was repressed only at the beginning of ToLCNDV-ES infection (3 dpi). Auxins and jasmonic acid (JA) pathways are interconnected, and both regulate defense response to begomoviruses, particularly to ToLCNDV in tomato (Ramesh et al., 2017; Vinutha et al., 2020). Further interesting was a downregulated at 12 dpi DNA primase large subunit (MELO3C022319.2), protein family associated with geminivirus replication (Gutierrez, 2000; Guilliam et al., 2015). DEGs identified in this region must be regarded as the main candidate genes implicated in triggering ToLCNDV infection and in the defense response in melon.

Transcription Changes on Chromosomes 2 and 12

Candidate regions for ToLCNDV-ES resistance in chromosomes 2 and 12 were larger than the region of the major QTL (Sáez et al., 2017), and hence, a larger list of DEGs was obtained for both regions (**Supplementary Table 10**).

In chromosome 2, many of the DEGs were TFs and disease-related proteins downregulated in PS at 3 dpi, but subsequently upregulated at 6 and 12 dpi. In the case of NAC (MELO3C017185.2) and bHLH35 (MELO3C017424.2) TFs, high induction was observed in PS after 6 dpi. A transmembrane protein (MELO3C017283.2) was highly induced at 12 dpi in PS, whereas at 3 dpi, a phosphoethanolamine *N*-methyltransferase (MELO3C017356.2) implicated in DNA methylation was upregulated. In WM-7, photosynthetic proteins were highly induced at 6 and 12 dpi.

A second QTL linked to ToLCNDV-ES resistance was mapped at the top of chromosome 12 (Sáez et al., 2017; **Supplementary Table 10**). In this region, a cytochrome P450 gene (MELO3C004742.2) was strongly repressed at 3 dpi in PS, whereas the gene Photosystem II protein D1 (MELO3C027714.2) located in the same region was over-expressed in WM-7 at 12 dpi.

Mitogen-activated protein kinases are proteins implicated in the signal pathway of JA biosynthesis and interact with MYC2. Overexpression of these proteins induces salicylic acid (SA) and JA gene expression and promotes TYLCV resistance (Li et al., 2017b). MELO3C026848.2 encodes a mitogen-activated protein kinase, which was downregulated in the susceptible genotype PS at the beginning of infection (3 dpi). Also located in this candidate region, a NAC-type TF (MELO3C004694.2) was highly induced in PS at 12 dpi, while a DNA-directed RNA polymerase II subunit E (MELO3C021758.2) was downregulated in WM-7 at 6 dpi.

Expression of Known Genes Related to Defense Response

To further investigate and identify candidate genes contributing to ToLCNDV resistance or susceptibility, we analyzed the expression profile of 70 R-genes of melon previously characterized by Islam et al. (2020) and other categories of genes related to the defense response in geminivirus infection, including gene silencing, pathogen-resistant proteins, and hormonal response.

R-genes

Of the characterized 70 R-genes in *C. melo*, 19 of them, distributed on chromosomes 1, 3, 4, 5, 7, 9, and 12 were differentially expressed in the susceptible genotype, whereas only three of them, located on chromosomes 4, 5, and 11, presented an altered expression in the resistant genotype (**Table 3**). In PS, all DEGs followed the same trend with repressed expression at 3 dpi but upregulation at 6 and 12 dpi. Similarly, in WM-7, one R-gene with LRR domain on chromosome 11 was strongly repressed at 6 dpi near the candidate region of resistance to ToLCNDV-ES described in Sáez et al. (2017), but the remaining two (MELO3C009694.2 and MELO3C004309.2) were upregulated at 12 dpi.

The expression pattern of other genes annotated with a resistance to pathogens function was also studied (**Table 4**). Most of these genes presented an altered expression pattern in PS as shown in the R-genes described above, whereas WM-7 exhibited a more diverse regulation pattern. In both genotypes, pathogenesis-related protein 1 (PR-1) family genes were altered. These proteins are the most abundantly produced when pathogens infect plants and have been considered as hallmarks of hypersensitive response and broad-spectrum systemic acquired resistance in association with salicylic acid (SA) (Balint-Kurti, 2019; Guerrero et al., 2020).

Some defense-related proteins were upregulated at 6 and 12 dpi in PS, including seven tobacco mosaic virus (TMV) resistance genes (chromosomes 5 and 9) and several TFs, such as NAC, MYB, bHLH, genes of hormonal response to ethylene, and a negative regulator of resistance protein (**Supplementary Table 9**).

Transcription Factors

In geminivirus infections, TFs involved in plant development are differentially regulated (Kumar, 2019). We searched for DEGs coding TFs, and 17 MYB were altered at all stages in both genotypes (**Supplementary Tables 5**, **6**). In PS, 23 DEGs were of WRKY type, and 16 were NAC TFs, all differentially regulated at mainly 6 and 12 dpi. Out of 16 NACs with altered expression, 12 were upregulated (**Supplementary Table 5**). Conversely, only four WRKY genes showed transcription changes in WM-7, one repressed at 3 dpi (**Supplementary Table 6**). In this genotype, there were also three altered NAC TFs; out of them, two were downregulated (**Supplementary Table 6**). Only one MYC-2 TF (MELO3C022250.2) was suppressed at 6 dpi in chromosome 11 of PS (**Supplementary Table 5**). MYC-2 belongs to the basic helix-loop-helix (bHLH) TF family and interacts with the BV1 protein of bipartite begomoviruses (Li et al., 2014). This protein directly regulates terpene transcription genes and mediates whitefly resistance achieving vector-virus mutualism. A member of the terpene cyclase/mutase genes family (MELO3C022374.2) was strongly suppressed in PS at 6 dpi but highly induced in WM-7 at 12 dpi (**Supplementary Table 7**). Similarly, 11 DEGs were bHLH in PS at 6 or 12 dpi (seven downregulated). In WM-7 plants, six bHLH genes were identified, all upregulated when compared with healthy controls. Therefore, ToLCNDV-ES generates a stronger readjustment of TF expression in PS than in WM-7.

TABLE 2 | Differentially expressed genes in the candidate region for ToLCNDV resistance of *C. melo* chromosome 11.

			Log2 (Fold Change)				
	Gen	Stage dpi	ToLCNDV inoculated	Mock inoculated	Start	End	Function
PS	MELO3C022339.2	6	–3.08	–	30,494,799	30,495,239	Glutaredoxin
	MELO3C022300.2	12	2.179	–	30,156,612	30,160,071	Probably inactive receptor-like protein kinase At2g46850
	MELO3C022324.2	12	1.888	–	30,394,274	30,397,789	Proton pump-interactor 2-like
	MELO3C022341.2	12	10.806	–	30,509,871	30,512,205	Bidirectional sugar transporter SWEET
	MELO3C022358.2	12	1.451	–	30,691,737	30,692,270	Ethylene-responsive transcription factor ERF113-like
	MELO3C022365.2	12	1.743	–	30,715,606	30,716,293	UPF0481 protein
	MELO3C022367.2	12	1.168	–	30,725,006	30,743,460	UPF0481 protein At3g47200
WM-7	MELO3C022327.2	3	–2.809	–	30,409,446	30,410,934	Transmembrane protein, putative
	MELO3C022337.2	3	–1.075	–	30,481,662	30,482,590	Auxin-responsive protein SAUR36
	MELO3C022327.2	6	–3.596	–	30,409,446	30,410,934	Transmembrane protein, putative
	MELO3C022319.2	12	–1.075	–	30,347,186	30,355,934	DNA primase large subunit

Hormones

Lipoxygenases (LOX) are essential enzymes required in the JA hormone synthesis (Wasternack and Song, 2017) and associated with systemic defense, hypersensitive response, and cell death when pathogens infect plants (Hwang and Hwang, 2010; Vicente et al., 2012). LOX genes differentially regulated have been reported after geminivirus infection (Góngora-Castillo et al., 2012; Allie and Rey, 2013). In the susceptible and resistant genotypes, 13 and 6 LOXs presented altered expression at all stages, respectively. Interestingly, all the genes coding these proteins were located in two clusters on chromosome 5 (**Supplementary Tables 5**, **6**). Among them, four were common DEGs to PS and WM-7 (MELO3C004244.2, MELO3C014630.2, MELO3C027325.2, and MELO3C031318.2) (**Supplementary Table 7**) and were induced early in the resistant genotype but suppressed in the susceptible melon.

Salicylic acid and JA pathways promote resistance to begomoviruses and also to heat stress, and both responses are mediated by common gene families (Tsai et al., 2019). The geminivirus coat protein interacts with heat shock proteins (HSPs) and recruits them to their own viral regulation, interfering with the host antiviral response (Gorovits et al., 2013; Gorovits and Czosnek, 2017; Jeevalatha et al., 2017; Kumar, 2019). HSP downregulation in resistant plants restricts begomovirus movement through plasmodesmata (Naqvi et al., 2017). However, out of 19 and 32 HSPs differentially regulated in PS and WM-7, 17 and 30 had a strong induction, respectively (**Supplementary Tables 5**, **6**).

Some defense-related proteins were upregulated at 6 and 12 dpi in PS, including genes of hormonal response to ethylene and a negative regulator of resistance protein (**Supplementary Table 9**).

Ubiquitination and Ubiquitin/Proteasome System Complex

In plants, ubiquitination contributes to resistance to geminivirus (Czosnek et al., 2013). RING-type E3 ubiquitin ligase and F-box genes are components of the proteasomal ubiquitination complex (UP) and have been described interacting with begomovirus infection (Correa et al., 2013). Nine RING-type E3 ubiquitin ligase genes were altered in PS, five of them downregulated and four induced, whereas only one RING-type E3 ubiquitin transferase (MELO3C003458.2) was repressed in WM-7 (**Supplementary Tables 5**, **6**). F-box genes were altered in both susceptible and resistant genotypes. In PS, eight F-box genes were induced and five underexpressed, and similarly, three F-box genes had repressed expression in WM-7 and four were induced (**Supplementary Tables 5**, **6**). F-box proteins regulate diverse cellular processes, including cell cycle transition, transcriptional regulation, and signal transduction, and mediate ubiquitination of proteins targeted for degradation by the proteasome, playing an essential role in many cellular processes.

RNA Silencing

As RNA silencing constitutes one of the major strategies to develop resistance against geminiviruses, we searched for DEGs involved in this mechanism.

Calmodulin proteins regulate the RNA-silencing machinery, and their induction increases geminivirus accumulation in plants (Chung et al., 2014). Calmodulin proteins can reduce the expression of RNA-dependent RNA polymerase (RDRs) proteins and interact with suppressor of gene silencing 3 (SGS3) and degrade it by autophagy. Despite the fact that Calmodulin binding was one of the enhanced GO categories in GC19 (see section "RNA sequencing, reads alignment and WGCNA"), we

TABLE 3 | Differentially expressed genes identified between the 70 R-genes of the melon genome characterized in Islam et al. (2020).

		log2 (Fold Change)						Gene				
		3 dpi		6 dpi		12 dpi						
		ToLCNDV inoculated	Mock inoculated	ToLCNDV inoculated	Mock inoculated	ToLCNDV inoculated	Mock inoculated	Chromosome	Start	End	Function	Functional disease resistance-related domains
PS	MELO3C023579.2			1.305	–	1.492	–	1	32,573,956	32,576,619	Disease resistance protein RGA2-like isoform X1	LRR
	MELO3C023578.2	–1.063	–					1	32,588,913	32,593,637	Disease resistance protein	NB-ARC
	MELO3C023441.2	–1.232	–					1	33,623,112	33,627,816	Receptor-kinase, putative	LRR
	MELO3C010826.2					3.548	–	3	28,214,790	28,218,285	Receptor-kinase, putative	LRR
	MELO3C010825.2					6.754	4.610	3	28,218,855	28,226,256	Receptor-kinase, putative	LRR
	MELO3C009693.2			1.112	–	1.407	–	4	28,945,912	28,948,344	Disease resistance protein	NB-ARC
	MELO3C009179.2			1.429	–			4	32,531,221	32,534,345	Receptor-kinase, putative	LRR
	MELO3C004289.2	–1.145	–			1.062	–	5	25,863,643	25,869,731	TMV resistance protein N-like	TIR-NBS-LRR
	MELO3C004303.2			1.697	–	1.664	–	5	26,036,017	26,040,632	TMV resistance protein N-like	LRR
	MELO3C004311.2			1.560	–	2.700	–	5	26,076,967	26,095,083	TMV resistance protein N-like	TIR-NBS-LRR
	MELO3C004313.2			2.177	–	1.771	–	5	26,106,563	26,109,785	TMV resistance protein N-like	TIR-NBS-LRR
	MELO3C017703.2	–1.062	–					7	24,126,814	24,129,634	Disease resistance protein RGA2-like	NB-ARC

(Continued)

TABLE 3 | (Continued)

		log2 (Fold Change)						Gene				
		3 dpi		6 dpi		12 dpi						
		ToLCNDV inoculated	Mock inoculated	ToLCNDV inoculated	Mock inoculated	ToLCNDV inoculated	Mock inoculated	Chromosome	Start	End	Function	Functional disease resistance-related domains
	MELO3C022146.2					2.410	–	9	744,523	750,028	TMV resistance protein N-like	TIR-NBS-LRR
	MELO3C022144.2			1.048	–	1.406	–	9	767,040	775,410	TMV resistance protein N-like	TIR-NBS-LRR
	MELO3C005450.2			2.717	–	3.153	–	9	20,427,143	20,430,013	LRR receptor-like kinase family protein	LRR
	MELO3C005451.2			5.330	–	7.293	3.030	9	20,434,381	20,437,380	LRR receptor-like kinase	LRR
	MELO3C002506.2			1.722	–	3.179	–	12	22,229,817	22,238,994	Receptor-like protein kinase	RLK
	MELO3C002504.2	–1.634	–			2.234	–	12	22,242,891	22,252,225	Cysteine-rich receptor-like protein kinase 28	RLK
	MELO3C002501.2					2.578	–	12	22,262,412	22,265,400	Cysteine-rich receptor-like protein kinase 26isoform X1	RLK
WM-7	MELO3C009694.2					1.795	–	4	28,938,791	28,941,261	Disease resistance protein	NB-ARC
	MELO3C004309.2					2.092	–	5	26,060,336	26,066,739	TMV resistance protein N-like	TIR-NBS-LRR
	MELO3C022449.2			–4.838	–			11	31,293,359	31,296,020	Receptor-like protein	LRR

Expression pattern of each gene is presented as log2 (fold change) at 3, 6, and 12 dpi stages. Physical position of genes according to v4.0 of melon genome, functional annotation, and disease resistance–related domain are included.

TIR-NBS-LRR: Toll/interleukin-1 receptor homology nucleotide-binding site leucine-rich repeat. Function: pathogen specificity and defense.

LRR: Leucine-rich repeat. Function: Recognition of pathogen and Plant Defense.

NB-ARC: Nucleotide-binding adaptor shared by APAF-1, R proteins and CED-4. Function: molecular switch in activating defenses.

RLK: Protein kinase. Function: Signaling and plant.defense.

TABLE 4 | Expression pattern of additional selected genes conferring resistance to pathogens.

		log2 (Fold Change)						Gene			
		3 dpi		6 dpi		12 dpi		Chr	Start	End	Function
		ToLCNDV inoculated	Mock inoculated	ToLCNDV inoculated	Mock inoculated	ToLCNDV inoculated	Mock inoculated				
PS	MELO3C018539.2					6.232	–	1	1,023,454	1,024,330	Pathogenesis-related protein 1-like
	MELO3C018540.2					4.757	–	1	1,030,810	1,031,348	pathogenesis-related protein 1-like
	MELO3C018544.2			1.148	–			1	1,042,545	1,043,212	Pathogenesis-related protein 1
	MELO3C018547.2					2.416	–	1	1,051,651	1,052,250	Pathogenesis-related protein 1
	MELO3C018878.2					3.820	–	1	3,559,447	3,560,191	Pathogen-induced protein CuPi1
	MELO3C023694.2					3.590	–	1	6,394,591	6,396,233	Pathogen-related protein
	MELO3C023578.2	–1.063	–					1	32,588,913	32,593,637	Disease resistance protein
	MELO3C017322.2	–1.803	–					2	24,275,353	24,280,275	LEAF RUST 10 DISEASE-RESISTANCE LOCUS RECEPTOR-LIKE PROTEIN KINASE-like 1.2 isoform X2
	MELO3C008149.2			1.310	–	2.130	–	3	1,163,259	1,172,229	LEAF RUST 10 DISEASE-RESISTANCE LOCUS RECEPTOR-LIKE PROTEIN KINASE-like 1.4 isoform X1
	MELO3C031443.2					1.049	–	5	18,385,406	18,392,554	TMV resistance protein N
	MELO3C004262.2			4.967	–	7.110	–	5	25,614,803	25,621,533	TMV resistance protein N-like
	MELO3C004265.2					–3.999	–	5	25,650,358	25,651,288	TMV resistance protein N-like isoform X2
	MELO3C004291.2			3.994	–	5.272	–	5	25,906,332	25,908,625	TMV resistance protein N-like
	MELO3C031332.2	6.714	4.701					5	26,375,103	26,376,034	Disease resistance protein
	MELO3C004354.2			1.032	–	1.137	–	5	26,592,987	26,596,766	CC-NBS-LRR resistance protein
	MELO3C004385.2					5.488	–	5	26,848,627	26,849,611	Pathogenesis-related protein PR-4-like
	MELO3C019482.2			–1.096	–			6	10,571,172	10,573,959	Pathogenesis-related thaumatin-like protein
	MELO3C016941.2					1.139	–	7	947,005	948,144	Protein ENHANCED DISEASE RESISTANCE 2
	MELO3C017692.2					4.161	–	7	24,081,397	24,084,555	Disease resistance protein RGA2-like
	MELO3C017703.2	–1.062	–					7	24,126,814	24,129,634	Disease resistance protein RGA2-like

(Continued)

TABLE 4 | (Continued)

		log2 (Fold Change)						Gene			
		3 dpi		6 dpi		12 dpi		Chr	Start	End	Function
		ToLCNDV inoculated	Mock inoculated	ToLCNDV inoculated	Mock inoculated	ToLCNDV inoculated	Mock inoculated				
	MELO3C033615.2			1.350	-	1.808	–	9	6,658,398	6,659,268	Disease resistance protein RGA2-like
	MELO3C029858.2	–1.042	–					9	20,748,481	20,749,427	NBS resistance-like protein
	MELO3C020880.2			–1.323	–			11	3,294,068	3,294,968	Pathogenesis-related protein 1
	MELO3C024731.2					3.364	–	11	7,170,632	7,173,642	Disease resistance protein RGA2-like
	MELO3C002084.2			2.412	–	2.657	–	12	24,991,237	24,991,695	Protein NEGATIVE REGULATOR OF RESISTANCE
WM-7	MELO3C018796.2	–2.636	–			–6.437	–	1	2,864,020	2,864,927	Cysteine-rich receptor-kinase-like protein
	MELO3C018540.2	5.297	–			5.506	–	1	1,030,810	1,031,348	Pathogenesis-related protein 1-like
	MELO3C018539.2					5.704	–	1	1,023,454	1,024,330	Pathogenesis-related protein 1-like
	MELO3C012701.2			1.438	–			1	21,798,030	21,798,830	Cysteine proteinase inhibitor
	MELO3C012702.2			1.869	–			1	21,826,195	21,827,118	Cysteine proteinase inhibitor
	MELO3C017497.2					5.171	–	2	22,319,516	22,320,537	Pathogenesis-related protein PR-1
	MELO3C008149.2					1.128	–	3	1,163,259	1,172,229	LEAF RUST 10 DISEASE-RESISTANCE LOCUS RECEPTOR-LIKE PROTEIN KINASE-like 1.4 isoform X1
	MELO3C031111.2	1.548	–	1.533	–			5	7,065,995	7,068,688	Negative regulator of systemic acquired resistance SNI1
	MELO3C004261.2					2.559	–	5	25,594,168	25,594,730	TMV resistance protein N-like
	MELO3C004309.2			2.056	–	2.092	–	5	26,060,336	26,066,739	LOW QUALITY PROTEIN: TMV resistance protein N-like
	MELO3C016128.2			–1.373	–			7	19,211,072	19,212,632	Pathogen-related protein
	MELO3C017071.2			1.514	–			7	123,638	125,187	Cysteine/Histidine-rich C1 domain family protein
	MELO3C022150.2					2.260	–	9	703,234	708,384	TMV resistance protein N-like
	MELO3C033944.2	–3.577	–7.025			–4.180	–	9	16,122,393	16,123,197	NBS-LRR type resistance protein
	MELO3C002921.2	1.250	–	1.610	–	1.477	–	9	7,641,728	7,642,167	Cysteine proteinase inhibitor
	MELO3C002492.2	4.266	–	3.409	–			12	22,299,334	22,300,624	Cysteine-rich receptor-like protein kinase 25

detected only four calmodulin DEGs downregulated at 3 dpi in PS and four upregulated at 6 and 12 dpi. In WM-7, just one calmodulin gene was induced at 12 dpi (**Supplementary Tables 5**, **6**). One autophagy protein (MELO3C031521.2) was also upregulated in WM-7 at 12 dpi.

Expression of two cytosine-specific methyltransferases (CMT3), implicated in transcriptional gene silencing (TGS), was altered in PS and WM-7 (**Supplementary Tables 5**, **6**). In the susceptible genotype, the gene MELO3C015649.2 on chromosome 2 encodes this kind of enzyme and was repressed at 6 dpi. Conversely, a gene with similar function (MELO3C026448.2, chromosome 10) was induced early at 3 dpi in WM-7. CMT3 also interacts with autophagy and ubiquitin pathways (You et al., 2019). Two cytosine-specific methyltransferases are also deregulated: one induced in WM-7 at 3 dpi (MELO3C026448.2) and one repressed in PS at 6 dpi (MELO3C015649.2) (**Supplementary Tables 5**, **6**). These enzymes have homology with MET1, also a methyltransferase involved in TGS.

Chromatin and histone methylation are mechanisms used by plants to regulate gene expression of invasive viral DNAs (Castillo-González et al., 2015). A histone-lysine *N*-methyltransferase (MELO3C025676.2) was induced in PS at 3 dpi, whereas the same gene was repressed in WM-7 at 12 dpi (**Supplementary Table 7**). In the resistant WM-7 genotype, two additional Histone-lysine *N*-methyltransferase genes, MELO3C011304.2 and MELO3C012115.2, were, respectively, induced and repressed at 12 dpi (**Supplementary Table 6**). A histone acetyltransferase coding gene (MELO3C011266.2) was also repressed at 3 dpi in this genotype. Additionally, in the course of assay, seven genes codifying histones appeared downregulated, and two were induced in the resistant accession. In PS (**Supplementary Table 5**), MELO3C022387.2 another histone-lysine *N*-methyltransferase was induced at 3 dpi in chromosome 11. A histone acetyltransferase and a histone demethylase (MELO3C018028.2 and MELO3C017723.2, respectively) were also repressed in this genotype at 6 dpi, and 10 genes coding histones were deregulated, five induced and five under-expressed. Reduction in transcript levels of genes related to histone is associated to suppression of chromatin organization and DNA methylation (Choi et al., 2015).

AGO4 reduces geminivirus infection by viral DNA methylation (Mallory and Vaucheret, 2010), but this protein may also be recruited by geminiviruses to enhance its transcription (Vinutha et al., 2018). ToLCNDV AC4 protein suppresses RNA silencing by interaction with the host argonaute 4 protein (AGO4) of tomato (Vinutha et al., 2018). Its ortholog protein in melon (MELO3C014440.2) was upregulated at 3 dpi in both susceptible and resistant genotypes.

RNA-dependent RNA polymerase play a key role impairing resistance to geminiviruses, amplifying RNA antiviral silencing (Prakash et al., 2020). In the melon genome, there are eight genes functionally annotated as RDRs and distributed by chromosomes 2, 9, and 10. Two of them were highly upregulated at 6 and 12 dpi in chromosome 9 of PS (MELO3C005284.2 and MELO3C005257.2). An additional one (MELO3C015406.2, chromosome 2) was also induced in this genotype at only 12 dpi. Changes of transcript level in these genes were not observed in the ToLCNDV-resistant genotype WM-7.

Numerous genes coding polymerase enzymes were deregulated in both resistant and susceptible genotypes (**Supplementary Tables 5**, **6**), but a DNA-directed RNA polymerase gene (MELO3C027682.2) was induced at 6 and 12 dpi in the WM-7 genotype.

Differentially Expressed Genes Validation by qRT-PCR

Seven genes were selected for qRT-PCR validation of the differential response observed in the 28 transcriptomes analysis. Six genes (MELO3C022319.2, MELO3C022313.2, MELO3C022315.2, MELO3C022322.2, MELO3C022327.2, and MELO3C022341.2) were located in the QTL region of chromosome 11 linked to the resistance to ToLCNDV and one gene on chromosome 9 (MELO3C005257.2), and both have been previously described in resistance to other begomoviruses.

Relative transcript accumulation observed for these genes by qPCR was correlated to the RNA-seq data (**Figure 6**). These results confirm the high reproducibility between replicates of the transcriptome analysis. MELO3C022327.2 coding a transmembrane protein putatively was the only gene in which low variances were observed between both analysis methodologies. Downregulation of this gene was identified by RNA-seq in only ToLCNDV-inoculated WM-7 samples at 3 and 6 dpi with log2 (fold change) of –1.075 and –3.596, respectively. However, qPCR analysis also detected high downregulation of this same gene in mock-inoculated WM-7 samples at similar levels to virus-inoculated plants. The small transcript level of this gene could be missed in sequencing assay but specifically amplified by qRT-PCR and overrepresented by the $2^{-\Delta\Delta Ct}$ method to determine the relative amount of expression.

Single Nucleotide Polymorphism Linked to Differentially Expressed Genes Associated With *Tomato Leaf Curl New Delhi Virus* Response

Out of 121,509 total genetic transcriptome-based variant positions found comparing WM-7 and PS, only 31,070 homozygous polymorphisms between both genotypes were considered in this study, excluding common variants (**Supplementary Table 11**). There were 128 variants located in the major candidate region in chromosome 11, and 951 and 847 were located within the QTL regions with a minor effect in chromosomes 2 and 12, respectively (**Supplementary Table 11**).

A predicted high impact over genes of the candidate region in chromosome 11 was not associated to any SNP. However, 23 SNPs had a moderate impact on 16 genes, causing a missense change that produces a different amino acid. Three of these SNPs were affecting a GYF domain-containing protein (MELO3C022336.2). A low effect was predicted in 46 SNPs producing in most cases synonymous variants, four of them located in DEGs coding for an Auxin-responsive protein SAUR36 (MELO3C022337.2), a Glutaredoxin protein (MELO3C022339.2), and an ethylene-responsive

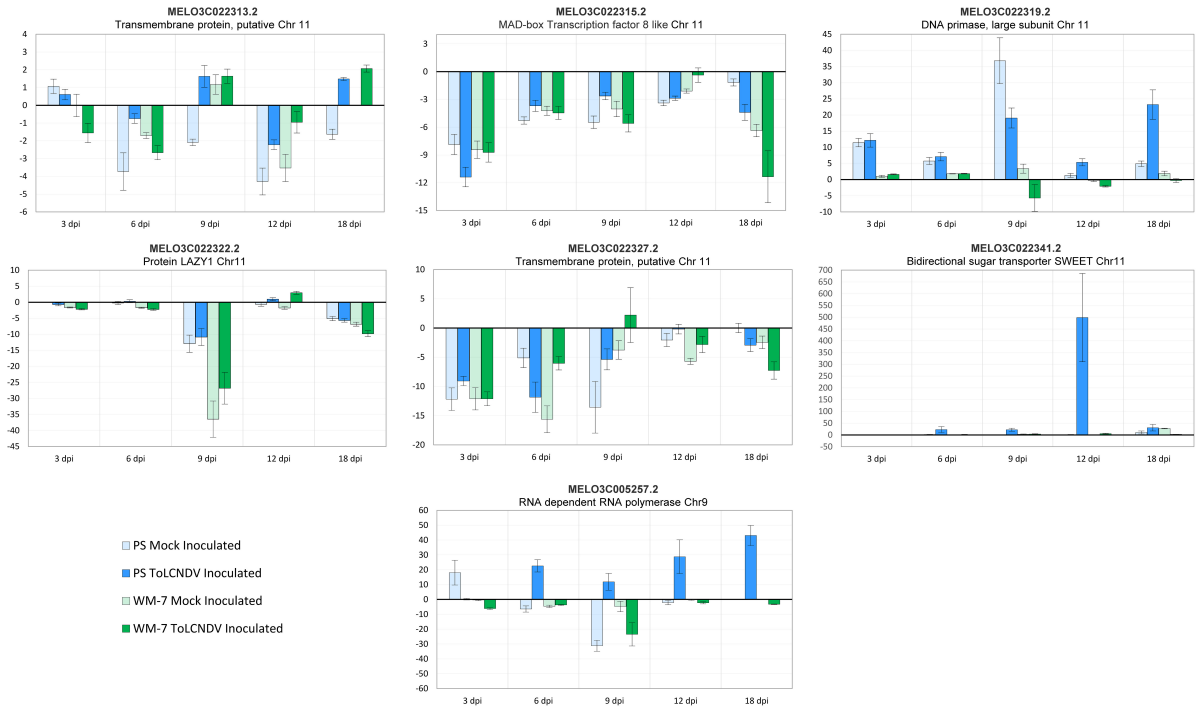

FIGURE 6 | Relative expression $2^{(-\Delta\Delta Ct)}$ of seven candidate genes for ToLCNDV resistance determined by qRT-PCR.

TF ERF113-like (MELO3C022358.2). In addition, three SNPs with low impact changed a region of the splice site of three genes (MELO3C022343.2 coding a Pyruvate dehydrogenase E1 component subunit beta, MELO3C022352.2 coding a coiled-coil domain-containing protein SCD2, and MELO3C022360.2 coding a Glycosyl transferase). The remaining SNPs identified within this region had a modifier effect, and therefore, their impact is difficult to predict. Four modifier SNPs interestingly affected two DEGs (**Supplementary Table 11**). In MELO3C022337.2, one SNP was a modifier of the 5′-UTR region. Conversely, in the DNA primase large subunit gene (MELO3C022319.2, down-regulated in WM-7), one SNP affected the 3′-UTR region and a second one had upstream predicted effect. Additional variants in DEGs with downstream effects or in heterozygosity were assumed to have a minimal impact in molecular functionality associated to ToLCNDV response.

In chromosome 2, there were six SNPs with high impact. Three of these variants caused a STOP codon in a 7SK snRNA methylphosphate capping enzyme (MELO3C024707.2) and in two unknown proteins (MELO3C017337.2 and MELO3C029555.2). Furthermore, one splice acceptor and intron variant hit the 5-formyltetrahydrofolate cyclo-ligase (MELO3C017137.2), whereas one insertion caused a frame shift in an unknown protein (MELO3C029754.2). However, the most significant variant conferring a high impact in a DEG of this region (25,433,111 bp) set a mutation of a stop codon into a non-stop codon and, moreover, hit a splice region of the TF bHLH47 (MELO3C017166.2), a gene upregulated in WM-7 at 12 dpi. Between the remaining DEGs of this region, in 40 genes, there were variants with moderate, low, or modifier impact. The upregulated gene in PS MELO3C017364.2 that encodes Ribosomal protein L19 was the DEG affected by the higher number of SNPs (22) in this region, including both missense variants and variants with impact on the 3′-UTR and 5′-UTR.

In the chromosome 12 candidate region, five SNPs had high impact (7,243,329, 9,455,480, 9,746,781, 10,176,940, and 15,255,896 bp), but only one (9,746,781 bp) was located on a DEG coding a splicing factor U2af small subunit B-like (MELO3C004799.2) upregulated in WM-7 at 6 dpi. In addition, this region included 48 DEGs affected by SNPs with moderate, low, or modifier impact, including DEGs described above, such as both DNA-directed RNA polymerases II and IV subunit 5A (MELO3C021758.2) and a Mitogen-activated protein kinase (MELO3C026848.2). It is worth highlighting that 17 SNPs generated different levels of impact on a serine carboxypeptidase-like protein (MELO3C004946.2), repressed in PS at 3 dpi. Moreover, in genes with not altered expression, six variants were within regions of the splice site, and three hit a splice donor or acceptor site, entailing predicted low and high impact, respectively.

DISCUSSION

ToLCNDV strains generate devastating damage in solanaceaous and cucurbitaceous crops, mainly in the Indian subcontinent and in the Mediterranean basin. Genetic resistance has been

previously identified in different species of both horticultural families, but characterization of the molecular mechanism regulating resistance is preferentially studied in *Solanaceaous* crops (Sahu et al., 2010, 2016; Kushwaha et al., 2015; Jeevalatha et al., 2017).

Recessive resistance or incomplete dominance to ToLCNDV is reported as the main inheritance model controlling the resistance in cucurbits (Sáez et al., 2017, 2020, 2021). In this study, we investigate the process of ToLCNDV infection in a resistant and susceptible *C. melo* genotype, trying to correlate resistance or susceptibility with changes in transcript expression patterns and comparing them at different temporal stages. The accession WM-7 is resistant to ToLCNDV, remaining symptomless till 30 days after mechanical inoculation, and this resistance is controlled by a major QTL in chromosome 11 with intermediate dominance and two additional QTLs in chromosomes 2 and 12 (López et al., 2015; Sáez et al., 2017; Romay et al., 2019). Using both approaches, time course infection and quantitative detection of viral load, we observed that virus replication in WM-7 takes place at the beginning of the infection, but its propagation and/or replication is impaired at early stages. Conversely, systemic infection and symptom development progresses in PS with an enhancement of ToLCNDV accumulation in the course of the disease. The behavior observed in WM-7 reflects a fast and time-persistent defense response.

We identified 10 candidate DEGs within the region covering the QTL for ToLCNDV resistance in chromosome 11, most of them associated with a defense response against geminiviruses. The expression of a glutaredoxin protein (MELO3C022339.2) is inhibited in PS at 6 dpi. This gene family is associated with JA-SA pathway (Li et al., 2017c), and moreover, MELO3C022339.2 is an ortholog to the Thioredoxin superfamily proteins of *A. thaliana*. Thioredoxin proteins are described as interacting with begomoviruses and also impairing resistance to potyviruses (Luna-Rivero et al., 2016; Liu et al., 2017; Mathioudakis et al., 2018). In response to TYLCV, thioredoxin and TCP proteins in tomato interact with TFs that regulate defense mechanisms (Huang et al., 2016). TCP TFs are linked to ubiquitination, SUMO, MYC2 pathways, lipooxygenases encoded at chloroplast, and JA biosynthesis and are proposed as responsible candidates for leaf curling during ToLCNDV infection in tomato (Schommer et al., 2008; Naqvi et al., 2010). Although a TCP20-like TF (MELO3C022331.2) is located within the candidate region for ToLCNDV resistance in chromosome 11 of C. melo, we have not identified expression changes during the viral infection course.

Within the same candidate region in chromosome 11, a bidirectional sugar transporter SWEET (MELO3C022341.2) is the gene with higher induction in the susceptible response of PS at 12 dpi. SWEET transporters facilitate sugar transference into the phloem and promote their transport (Chen, 2014). Some studies report transcription changes of SWEET genes in several crops after pathogens attack, including plant–begomovirus interactions (Antony et al., 2010; Chen, 2014; Chandran, 2015; Naqvi et al., 2017; Breia et al., 2020). In melon, plants infected with CMV accumulated more sugars in the phloem of leaves as result of the sucrose transporter effect (Gil et al., 2011). In cotton (*Gossypium* spp.), a SWEET transporter gene was downregulated in resistant plants after *cotton leaf curl disease* (CLCuD) infection (Naqvi et al., 2017), and involvement of sugar-signaling mechanisms has been observed in resistance plants to TYLCV (Sade et al., 2020). Out of the 24 genes coding for SWEET transporters in the *C. melo* genome, three DEGs of PS were located outside the QTL regions: on chromosome 12, MELO3C001650.2 was repressed at 12 dpi, whereas MELO3C005869.2 and MELO3C002381.2 were upregulated at 6 and 12 dpi in chromosomes 9 and 12, respectively.

Another DEG identified in this region encodes a DNA primase large subunit (MELO3C022319.2), which is downregulated in WM-7 after ToLCNDV inoculation, whereas in PS, it is induced. Interestingly, this gene is syntenic with the DNA primase gene in chromosome 8 of *Cucurbita moschata*, in which a mayor QTL controlling resistance to ToLCNDV has been identified (Sáez et al., 2020). Indeed, this is the only DEG shared between both syntenic regions in which we have also identified genetic polymorphisms between WM-7 and PS. Geminiviruses employ the host mechanism for triggering their own replication. Plant DNA primases are described as catalyst enzymes used in the first step of geminivirus replication (Saunders et al., 1992; Alberter et al., 2005). Thus, the reduced expression of MELO3C022319.2 in WM-7 likely contributes to disrupting transcription of ToLCNDV, which appears as a promising mechanism of resistance, developing a downstream defense response.

It is worth mentioning that the candidate region on chromosome 12 includes an NAC TF (MELO3C004694.2), highly induced in PS at 12 dpi. The same induction is reported for two NAC TF membranes upon ToLCNDV infection in tomato (Bhattacharjee et al., 2017) and, in prior works, Román et al. (2019) validates by qPCR a, NAC TF highly induced in PS accession. ToLCNDV accumulation and symptom severity seem to correlate with the expression of the NAC TF.

Most of the recessive genes involved in resistance to RNA plant viruses codify for eukaryotic translation initiation factors eIF4E/G, a protein complex that mediates recruitment of ribosomes, in which natural mutations lead to resistance by loss of function (Kachroo et al., 2017; Machado et al., 2017). In the case of begomoviruses, six *loci* are described conferring resistance to *Tomato yellow leaf curl virus* (TYLCV) in tomato, one has a recessive inheritance pattern (*ty-5*) (Anbinder et al., 2009; Hutton et al., 2012), and two of them have incomplete dominant control (*Ty-4* and *Ty-6*) (Yan et al., 2021). The *ty-5 locus* causes resistance by the loss of function of the messenger RNA surveillance factor Pelota (*Pelo*), which is involved in biosynthesis of ribosomes, and its dysfunction compromises the translational machinery and replication of begomoviruses (Lapidot et al., 2015). This gene is also reported in *Capsicum annuum* conferring resistance to mono and bipartite begomoviruses (Prins et al., 2019; Koeda et al., 2021). Furthermore, NIK1 (NSP-interacting kinase 1) or RIP (Ribosome-inactivating) proteins are associated with the prevention of the spread of geminiviruses through translational suppression or repression of components of the translational machinery, such as ribosomes (Hong et al., 1996; Zorzatto et al., 2015; Musidlak et al., 2017; Citores et al., 2021). In contrast to

what was expected, changes in the transcript level orthologous to these genes in melon after ToLCNDV infection were not identified in this study. However, an important number of genes related to ribosomal pathways were downregulated in WM-7. Moreover, the minor region modulating the response to ToLCNDV in chromosome 2 of *C. melo* includes a Ribosomal protein L19 (MELO3C017364.2) remarkably affected by a high number of SNPs, upregulated at 6 and 12 dpi in PS. As viruses require host enzymes for translation (Ignacio-Espinoza et al., 2020; Dong et al., 2021; Xiong et al., 2021), evolutionarily conserved genes involved in ribosome recruitment might be a plausible mechanism triggering the resistance response to ToLCNDV in melon.

Prior works suggest an interconnection between loss of function of translation factors and replication of the viral genomes, changes in the cell wall affecting viral movement and activation of immunity pathways (Sanfaçon, 2015; Ding et al., 2018). Indeed, geminiviruses not only recruit plant translational components, but also enhance their replication and spread using and relocalizing host genes involved in DNA replication and transcription (Preiss and Jeske, 2003; Kushwaha et al., 2017; Wu et al., 2019; Maio et al., 2020). The interference with this viral strategy is widely described conferring resistance to begomoviruses (Ullah et al., 2014; Chakraborty and Basak, 2018). In tomato, both 26S proteasomal subunit RPT4a (*SlRPT4*) and DEAD-box RNA helicase genes are described as interfering in ToLCNDV transcription and replication, respectively (Sahu et al., 2010, 2016; Pandey et al., 2019). In this study, none of their orthologs in melon showed differences in their transcription upon ToLCNDV infection. However, genes belonging to the RNA helicase gene family have altered expression in PS at all analyzed stages, and GO ontologies related to DNA conformation, replication, unwinding, cell cycle, DNA helicase activity, and MCM complex were enriched, including upregulated genes in PS that were repressed in WM-7. DNA helicases are required for strand separation during DNA replication. Their analogs, RNA helicases, are described as proteins hijacked by plant viruses to assist their replication (Ranji and Boris-Lawrie, 2010; Sharma and Boris-Lawrie, 2012). Although little research about host DNA helicases and geminiviruses has been reported, interaction between geminiviral proteins and DNA helicases is described as assisting DNA replication (Pradhan et al., 2017). Host DNA helicase proteins can be used by the virus to further strengthen the helicase activity of the geminiviral Rep protein and, therefore, generate unwinding and initiate the stem-loop formation on the viral DNA (Brister and Muzyczka, 1999; Kazlauskas et al., 2016). Furthermore, the MCM complex has a role in maintaining the minichromosome and is directly implicated with the initiation of DNA synthesis at replication origins (Forsburg, 2004; Bochman and Schwacha, 2008). There are reports pointing out the role of the MCM2 protein in geminivirus replication efficiency (Rizvi et al., 2015), but molecular mechanisms remain unknown (Cho et al., 2008; Suyal et al., 2013). Overall, induced DNA replication transcriptional pathways in PS are likely promoting ToLCNDV multiplication and systemic propagation.

To further analyze the changes of expression patterns regarding plant pathogen interaction between melon and ToLCNDV, we studied defense genes and pathways activated in similar pathosystems. In a recent work (Sharma et al., 2021), the *Sw5a* locus is reported as an R gene that recognizes ToLCNDV AC4 protein and restricts viral spread. Although the melon ortholog to this gene (MELO3C006780.2) is not differentially expressed in our system, it appears positively correlated to PS in CG19 and CG20, indicating that defense responses against ToLCNDV are not efficiently activated in this genotype. In addition, we identified other DEGs implicated in virus resistance distributed over the melon genome, most of them located in clusters at chromosomes 1, 5, and 9. The two largest NBS-LRR gene clusters in melon are located at chromosomes 5 and 9, where resistance to other cucurbit viruses has been mapped (Morata and Puigdomènech, 2017; Pérez-de-Castro et al., 2020). Chromosome 5 not only includes differentially regulated pathogenesis and R genes, but also lipoxygenase hormone biosynthesis genes induced in WM-7 and downregulated in PS. These hormones regulate cell death and JA biosynthetic routes and conduct lipid peroxidation as a response to pathogen infection (Hwang and Hwang, 2010). Plant–virus interaction studies evidence how geminiviruses regulate JA signaling, hijacking implicated genes and increasing susceptibility (Yan and Xie, 2015; Zhang et al., 2017; Guerrero et al., 2020). In this work, we identify transcriptional changes in JA genes required for resistance to viruses. MYC-2 TF (MELO3C022250.2), mitogen-activated protein kinases (MELO3C026848.2), and the terpene cyclase/mutase gene family (MELO3C022374.2) are downregulated in the susceptible genotype PS at the beginning of infection (3 and 6 dpi). Conversely, some of these genes are induced in WM-7 at same stages. In tomato (*Solanum lycopersicum*), induction of a mitogen-activated protein kinase 3 (*SlMPK3*) ortholog to MELO3C026848.2 here identified enhanced TYLCV resistance by an increase of SA/JA-gene expression as PR-1 or leucine aminopeptidases (Li et al., 2017b). Leucine aminopeptidases control the defense machinery in tomato, downstream of JA (Fowler et al., 2009). Here, we identify one gene (MELO3C004135.2) codifying this protein located on chromosome 5 of *C. melo*, highly induced in WM-7 at 3 dpi but downregulated in PS at 6 dpi (**Supplementary Table 7**). Additionally, we observed differential regulation at early stages of other genes, such as E3 ligases, LAF 1, and TFs participating in ubiquitination and photomorphogenesis, all interconnected with jasmonic signaling (Seo et al., 2001; Kazan and Manners, 2011; Lozano-Durán et al., 2011; Correa et al., 2013). Viral replication, cell-to-cell movement, and long-distance propagation are inhibited by SA and JA (Shang et al., 2011; Tsai et al., 2019). Thus, implication of all described genes in the JA pathway indicates either an interference or perhaps a recruitment of this route by ToLCNDV in PS as a strategy to increase the susceptible response at early stages. Instead, the opposite response shown over this hormonal pathway in WM-7 likely promotes resistance.

In chromosome 9, where the second larger R-gene cluster is located, two RDR genes were over-expressed in PS (MELO3C005284.2 and MELO3C005257.2) at 6 and 12 dpi. Those genes are orthologs to RDR1 (RDRα) of *Arabidopsis*

thaliana, involved in amplification of the gene silencing signal at the post-transcriptional level in virus infection (Qui et al., 2009; Willmann et al., 2011; Islam et al., 2018). RDRs are well described in the RNA silencing pathway, and their over-expression enhances resistance to begomoviruses, particularly to those of the tomato leaf curl viruses complex (Prakash et al., 2020). This function of RDR1 in geminivirus resistance is variable and depends on the virus species (Chen et al., 2010; Aregger et al., 2012). In *N. tabacum*, RDR1 is associated with recovery *tomato leaf curl Gujarat virus* (ToLCGV) infected plants, generating hypermethylation of the viral genome. However, in those *N. tabacum* plants infected with ToLCNDV, recovery is inhibited by AV2 viral protein, resulting in susceptible plants with high symptomatology and viral titers (Basu et al., 2018). In *N. benthamiana* a natural mutation of 72 bp insertion in the RDR1 gene promotes susceptibility to members of the *Tobamovirus* genus (Yang et al., 2004) and might be responsible for high susceptibility to numerous viruses observed in this species, including geminiviruses (Akhtar et al., 2011). In cucumber (*Cucumis sativus* L.), the RDR1 family has four subclasses (RDR1a, RDR1b, RDR1c1, RDR1c2). RDR1c1 and RDR1c2 are highly induced by geminivirus *squash leaf curl virus* (SLCV) in susceptible plants, but their expression level remains low in resistant plants (Leibman et al., 2018). Also, in *C. sativus*, RDR1 is notably induced by a viroid infection, suggesting the involvement of RDR1 in the antiviroid defense (Xia et al., 2017). Our results concerning RDR1 expression in resistant and susceptible melon genotypes follows a similar expression trend with very high expression in PS but unaltered in WM-7. However, polymorphic variations have not been identified in this work affecting any of these both genes.

A third RDR gene (MELO3C015406.2) was upregulated in PS in chromosome 2 at only 12 dpi. It is a RDR5 protein with a homologous sequence to the *Ty1/Ty3* gene conferring resistance to TYLCV by methylation of cytosines in the viral genome (Verlaan et al., 2013; Butterbach et al., 2014; Jackel et al., 2016; Gallego-Bartolomé et al., 2019). Despite their homology, MELO3C015406.2 was over-expressed in the susceptible genotype to ToLCNDV, conversely to what was expected, as *Ty1* expression is elevated in resistant lines (Verlaan et al., 2013). Tomato cultivars carrying *Ty1/Ty3* genes are described as displaying resistant behavior after ToLCNDV inoculation (Fortes et al., 2016; Hussain et al., 2019). However, the genetic background effect might modulate the effectiveness of *Ty1/Ty3* for resistance to ToLCNDV in tomato (Rai et al., 2013; Akhtar et al., 2019). In this work, we identify two SNPs generating missense variations in MELO3C015406.2, but QTLs linked to ToLCNDV resistance have not been mapped covering this region in previous works. Results obtained here suggest that infection of ToLCNDV induces and triggers the gene-silencing machinery in PS, but it is not efficient in controlling virus spread. Another approach to explain this behavior is that RDRs are targeted and induced by ToLCNDV, interfering with silencing mechanism for defense and deregulating host factors, which result in symptomatology display. Further studies must be conducted to characterize this process in begomovirus–cucurbits interaction.

In TGS, DNA methylation plays crucial role inhibiting viral DNA transcription and replication. Plant hosts with this pathway suppressed are strongly susceptible to geminiviruses (Raja et al., 2014). Besides RDRs, other genes involved in RNA silencing–based resistance to geminiviruses are identified with altered expression in this study, including histones, calmodulin proteins, AGO4, and methyltransferases. MET1 and CMT3 DNA methyltransferases are induced at early stages in WM-7 and repressed in PS after ToLCNDV inoculation. In geminivirus infection, Rep protein interacts with CMT3 and MET1 in *N. benthamiana* and *A. thaliana*, suppressing their expression and the maintenance of DNA methylation (Rodríguez-Negrete et al., 2013). A phosphoethanolamine *N*-methyltransferase (MELO3C017356.2) was upregulated in PS at early stages in the candidate region of chromosome 2. This protein has homology with the *S*-adenosyl-L-methionine-dependent methyltransferases of *A. thaliana.* Methylation of DNA is performed by cellular methyltransferases, using *S*-adenosyl methionine (SAM). *Arabidopsis* plants with mutated genes of SAM enzyme production are hypersensitive to geminiviruses (Mäkinen and De, 2019). *Beet severe curly top virus* (BSCTV) C2 protein interacts and inhibits SAM by decarboxylation, reducing methylation of the viral DNA and promoting infection (Zhang et al., 2011). C4 protein of *cotton leaf curl multan virus* (CLCuMuV) interacts with SAMS of *N. benthamiana*, reducing its activity and DNA methylation and promoting accumulation of CLCuMuV (Ismayil et al., 2018). Expression changes in PS of this kind of enzyme suggests its interaction with ToLCNDV even in susceptible response. DNA-directed RNA polymerases are components of the RNA-directed DNA methylation (RdDM) epigenetic process, mediating geminivirus silencing and conferring resistance (Jackel et al., 2016). Although several genes of this family are differentially expressed in both PS and WM-7 (**Supplementary Tables 5**, **6**), three DNA-directed RNA polymerases coding genes (MELO3C027682.2, MELO3C000330.2, and MELO3C028015.2 clustering together on chromosome 7) are highly induced only in WM-7 at 6 or 12 dpi.

Cell-to-cell movement and viral replication, encapsidation, and suppression of host defenses are essential steps in the infective cycle of plant viruses, and both are connected by means of cellular membranes (Levy and Tilsner, 2020). Components of membrane, membrane and transport activity GO categories were found enriched in DEGs in both susceptible and resistance genotypes. Interestingly, genes annotated in GO category "Thylakoid" GO in GC20. Induction of the chloroplast thylakoid membrane protein TMP14 in *N. benthamiana* increased disease symptom severity and virus accumulation of *Tomato Spotted Wilt Virus* (TSWV), evidencing that lack of this protein negatively affects viral infection (Zhan et al., 2021). In WM-7, the GO category "photosynthesis" was the most represented of the upregulated genes at 6 and 12 dpi. In plant–virus interactions, the chloroplast is strategically manipulated and damaged by viruses, affecting large proportions of genes (Bhattacharyya and Chakraborty, 2018; Rossitto de Marchi et al., 2020; Zhai et al., 2020).

Chlorosis and mosaics in *cucumber mosaic virus* (CMV) infected tobacco leaves (*Nicotiana tabacum*) are associated

with downregulation of photosynthetic and chloroplastic genes (Mochizuki et al., 2014), and similar genes had a reduced transcription in chlorotic tissues of watermelon [*Citrullus lanatus* (Thunb.) Matsum. & Nakai] systemically infected with *Cucumber green mottle mosaic virus* (CGMMV) (Sun et al., 2019). Among begomoviruses, transcriptional reprogramming caused by TYLCV infection in *N. benthamiana* generated an expression reduction of photosynthesis genetic pathways (Wu et al., 2019). Plant defense against virus infection usually involves high energetic costs for the host, for example, for antiviral RNA silencing. Consequently, multiple and complementary resistance mechanisms are activated to minimize this energy consumption (Souza et al., 2019). The high induction of chloroplastic and photosynthetic genes detected in WM-7 takes place at the stages when yellowing and mosaic symptoms are developed in PS. These genes could provide additional energy to the resistant plant cells to address the viral attack and avoid chloroplast damage and symptom development. Moreover, a repression of genes implicated with thylakoid membranes in WM-7 may indicate an additional obstacle to ToLCNDV to reach the photosynthetic machinery and components, increasing the resistance to this virus and protecting fruit yield in melon.

CONCLUSION

The data reported in this study demonstrate that ToLCNDV infection entails a complex and interconnected net of transcriptional rearrangements in melon. Our findings advance the molecular understanding underlying ToLCNDV infection in melon. Combining both DEGs and polymorphic SNP detection, we identify candidate genes linked to the three QTLs for resistance in WM-7. The lack or decrease in ToLCNDV replication is associated with the most promising candidate in chromosome 11, a DNA primase protein. Whereas in minor modifier regions of chromosomes 2 and 12, some of the described bHLH47 or NAC TFs, Mitogen-activated kinase, DNA-directed RNA polymerases, or alternative splicing events likely might act as potential factors triggering a transcriptomic cascade of genetic responses against viral infection. Although promising, further studies based on genome edition or induced gene silencing are required to functionally characterize these target genes.

DATA AVAILABILITY STATEMENT

The datasets presented in this study can be found in online repositories. The names of the repository/repositories and accession number(s) can be found below: NCBI SRA, PRJNA780428.

AUTHOR CONTRIBUTIONS

CS, BP, and CL conceived and designed the research. CS, CL, and AS performed the tests with ToLCNDV. CS, AF-L, and JM-P performed the bioinformatics analysis. CS and AS conducted the qPCR validation analysis. CS, CL, and BP conducted and wrote the manuscript with important contributions from JM-P, ND, and AS. All authors read and approved the final manuscript.

FUNDING

This work was supported by grants AGL2017-85563-C2-1-R and RTA2017-00061-C03-03 funded by MCIN/AEI/10.13039/501100011033 and by "ERDF A way of making Europe," by grant PID2020-116055RB-C21 funded by MCIN/AEI/10.13039/501100011033; and by PROMETEO projects 2017/078 and 2021/072 (to promote excellence groups) by the Conselleria d'Educació, Investigació, Cultura i Esports (Generalitat Valenciana).

ACKNOWLEDGMENTS

We thank Roland Schafleitner and Maureen Mecozzi for their helpful comments.

SUPPLEMENTARY MATERIAL

The Supplementary Material for this article can be found online at: https://www.frontiersin.org/articles/10.3389/fpls.2021.798858/full#supplementary-material

Supplementary Figure 1 | Gene expression patterns of the analyzed samples for each gene cluster. Eigengene values are represented across tissues.

Supplementary Figure 2 | Scatterplot showing grouped GO terms according to the most representative categories. Figures were generated using the REVIGO program loading the list of enriched GO terms of WM-7 and PS separately. Positive and negative numbers in both axes represent upregulated and downregulated genes, respectively.

Supplementary Table 1 | Primer sequences used in qPCR for DEG confirmation assay.

Supplementary Table 2 | Genes significantly correlated to each gene cluster (GC) at p-value < 0.01. Their functional description and ontology annotation are presented. Those genes with unavailable GO terms associated are shown as NA.

Supplementary Table 3 | GO terms and KEGG enrichments of the 21 gene clusters (GCs). KEGG and GO ontologies (BP, biological processes; MF, molecular function; CC, cellular component) include genes significantly correlated at p-value < 0.01.

Supplementary Table 4 | Significance (p-value) of each gene cluster (GC) after regression analyses using genotype, treatment, and time as factors.

Supplementary Table 5 | DEGs in WM-7 at 3, 6, and 12 dpi in ToLCNDV and mock-inoculated plants. Log2 (fold change) values, gene code, its genomic position in melon genome (v4.0) and functional annotation are shown.

Supplementary Table 6 | DEGs in PS at 3, 6, and 12 dpi in ToLCNDV and mock-inoculated plants. Log2 (fold change) values, gene code, its genomic position in melon genome (v4.0) and functional annotation are shown.

Supplementary Table 7 | Common DEGs upregulated in WM-7 and downregulated in PS at 3, 6, and 12 dpi. Log2 (fold change) values, gene code, its genomic position in melon genome (v4.0) and functional annotation are shown.

Supplementary Table 8 | Common DEGs at different stages (3, 6, and 12 dpi) after ToLCNDV inoculation in WM-7 genotype.

Supplementary Table 9 | Common DEGs at different stages (3, 6, and 12 dpi) after ToLCNDV inoculation in PS genotype.

Supplementary Table 10 | DEGs at 3, 6, and 12 dpi in the candidate regions of chromosomes 2 and 12 of PS and WM-7, conferring resistance to ToLCNDV.

Supplementary Table 11 | List of polymorphic transcript-based SNPs between WM-7 and PS with both alleles fixed in homozygosity. SNP position, reference and alternative alleles, genotype for each sample, affected genes, and putative impact of the SNP on the gene structure are shown. The reference allele is represented as 0 and the alternative allele as 1. Cells highlighted in yellow refer to DEGs. Horizontal lines in chromosomes 2, 11, and 12 delimit candidate regions considered in this study for ToLCNDV resistance.

REFERENCES

Akhtar, K. P., Akram, A., Ullah, N., Saleem, M. Y., and Saeed, M. (2019). Evaluation of *Solanum* species for resistance to tomato leaf curl New Delhi virus using chip grafting assay. *Sci. Hortic.* 256:108646. doi: 10.1016/j.scienta.2019.108646

Akhtar, S., Briddon, R. W., and Mansoor, S. (2011). Reactions of *Nicotiana* species to inoculation with monopartite and bipartite begomoviruses. *Virol. J.* 8:475. doi: 10.1186/1743-422X-8-475

Alberter, B., Rezaian, M. A., and Jeske, H. (2005). Replicative intermediates of tomato leaf curl virus and its satellite DNAs. *Virology* 331, 441–448. doi: 10.1016/j.virol.2004.10.043

Allie, F., Pierce, E. J., Okoniewski, M. J., and Rey, M. E. C. (2014). Transcriptional analysis of South African cassava mosaic virus-infected susceptible and tolerant landraces of cassava highlights differences in resistance, basal defense and cell wall associated genes during infection. *BMC Genomics* 15:1006. doi: 10.1186/1471-2164-15-1006

Allie, F., and Rey, M. E. C. (2013). Transcriptional alterations in model host, *Nicotiana benthamiana*, in response to infection by south African cassava mosaic virus. *Eur. J. Plant Pathol.* 137, 765–785. doi: 10.1007/s10658-013-0286-4

Anbinder, I., Reuveni, M., Azari, R., Paran, I., Nahon, S., Shlomo, H., et al. (2009). Molecular dissection of tomato leaf curl virus resistance in tomato line TY172 derived from *Solanum peruvianum*. *Theor. Appl. Genet.* 119, 519–530. doi: 10.1007/s00122-009-1060-z

Andrews, S. (2010). *FastQC: A Quality Control Tool for High Throughput Sequence Data*. Available online at: http://www.bioinformatics.babraham.ac.uk/projects/fastqc (accessed September 15, 2018).

Annu, P. K., Rani, R., and Rathi, A. S. (2019). Gemini viruses-emerging threat to crops. *J. Pharmacogn. Phytochem.* 8, 2006–2012.

Antony, G., Zhou, J., Huang, S., Li, T., Liu, B., White, F., et al. (2010). Rice xa13 recessive resistance to bacterial blight is defeated by induction of the disease susceptibility gene Os-11N3. *Plant Cell* 22, 3864–3876. doi: 10.1105/tpc.110.078964

Aregger, M., Borah, B. K., Seguin, J., Rajeswaran, R., Gubaeva, E. G., Zvereva, A. S., et al. (2012). Primary and secondary siRNAs in geminivirus-induced gene silencing. *PLoS Pathog.* 8:e1002941. doi: 10.1371/journal.ppat.1002941

Balint-Kurti, P. (2019). The plant hypersensitive response: concepts, control and consequences. *Mol. Plant Pathol.* 20, 1163–1178. doi: 10.1111/mpp.12821

Bardou, P., Mariette, J., Escudié, F., Djemiel, C., and Klopp, C. (2014). jvenn: an interactive Venn diagram viewer. *BMC Bioinformatics* 15:293. doi: 10.1186/1471-2105-15-293

Basu, S., Kumar Kushwaha, N., Kumar Singh, A., Pankaj Sahu, P., Vinoth Kumar, R., and Chakraborty, S. (2018). Dynamics of a geminivirus-encoded pre-coat protein and host RNA-dependent RNA polymerase 1 in regulating symptom recovery in tobacco. *J. Exp. Bot.* 69, 2085–2102. doi: 10.1093/jxb/ery043

Bhattacharjee, P., Das, R., Mandal, A., and Kundu, P. (2017). Functional characterization of tomato membrane-bound NAC transcription factors. *Plant Mol. Biol.* 93, 511–532. doi: 10.1007/s11103-016-0579-z

Bhattacharyya, D., and Chakraborty, S. (2018). Chloroplast: the Trojan horse in plant-virus interaction. *Mol. Plant Pathol.* 19, 504–518. doi: 10.1111/mpp.12533

Bochman, M. L., and Schwacha, A. (2008). The Mcm2-7 complex has in vitro helicase activity. *Mol. Cell* 31, 287–293. doi: 10.1016/j.molcel.2008.05.020

Bolger, A. M., Lohse, M., and Usadel, B. (2014). Trimmomatic: a flexible trimmer for Illumina sequence data. *Bioinformatics* 30, 2114–2120. doi: 10.1093/bioinformatics/btu170

Bonza, M. C., Fusca, T., Homann, U., Thiel, G., and De Michelis, M. I. (2009). Intracellular localisation of PPI1 (proton pump interactor, isoform 1), a regulatory protein of the plasma membrane H^+-ATPase of *Arabidopsis thaliana*. *Plant Biol.* 11, 869–877. doi: 10.1111/j.1438-8677.2008.00181.x

Breia, R., Conde, A., Pimentel, D., Conde, C., Fortes, A. M., Granell, A., et al. (2020). VvSWEET7 is a mono- and disaccharide transporter up-regulated in response to *Botrytis cinerea* infection in grape berries. *Front. Plant Sci.* 10:1753. doi: 10.3389/fpls.2019.01753

Brister, J. R., and Muzyczka, N. (1999). Rep-mediated nicking of the adeno-associated virus origin requires two biochemical activities, DNA helicase activity and transesterification. *J. Virol.* 73, 9325–9336. doi: 10.1128/JVI.73.11.9325-9336.1999

Butterbach, P., Verlaan, M. G., Dullemans, A., Lohuis, D., Visser, R. G., Bai, Y., et al. (2014). Tomato yellow leaf curl virus resistance by *Ty-1* involves increased cytosine methylation of viral genomes and is compromised by cucumber mosaic virus infection. *Proc. Natl. Acad. Sci. U.S.A.* 111, 12942–12947. doi: 10.1073/pnas.1400894111

Castanera, R., Ruggieri, V., Pujol, M., García-Mas, J., and Casacuberta, J. M. (2020). An improved melon reference genome with single-molecule sequencing uncovers a recent burst of transposable elements with potential impact on genes. *Front. Plant Sci.* 10:1815. doi: 10.3389/fpls.2019.01815

Castillo-González, C., Liu, X., Huang, C., Zhao, C., Ma, Z., Hu, T., et al. (2015). Geminivirus-encoded TrAP suppressor inhibits the histone methyltransferase SUVH4/KYP to counter host defense. *eLife* 4:e06671. doi: 10.7554/eLife.06671

Chakraborty, N., and Basak, J. (2018). Molecular and biochemical characterization of mungbean yellow mosaic India virus resistance in leguminous host *Vigna mungo*. *J. Plant Biochem. Biotechnol.* 27, 318–330. doi: 10.1007/s13562-018-0441-2

Chandran, D. (2015). Co-option of developmentally regulated plant SWEET transporters for pathogen nutrition and abiotic stress tolerance. *IUBMB Life* 67, 461–471. doi: 10.1002/iub.1394

Chen, H., Tamai, A., Mori, M., Ugaki, M., Tanaka, Y., Samadder, P. P., et al. (2010). Analysis of rice RNA-dependent RNA polymerase 1 (OsRDR1) in virus-mediated RNA silencing after particle bombardment. *J. Plant Pathol.* 76, 152–160. doi: 10.1007/s10327-010-0226-5

Chen, L. Q. (2014). SWEET sugar transporters for phloem transport and pathogen nutrition. *New Phytol.* 201, 1150–1155. doi: 10.1111/nph.12445

Cho, J. H., Kim, H. B., Kim, H. S., and Choi, S. B. (2008). Identification and characterization of a rice MCM2 homologue required for DNA replication. *BMB Rep.* 41, 581–586. doi: 10.5483/bmbrep.2008.41.8.581

Choi, H., Jo, Y., Lian, S., Jo, K. M., Chu, H., Yoon, J. Y., et al. (2015). Comparative analysis of chrysanthemum transcriptome in response to three RNA viruses: cucumber mosaic virus, tomato spotted wilt virus and potato virus X. *Plant Mol. Biol.* 88, 233–248. doi: 10.1007/s11103-015-0317-y

Chung, H. Y., Lacatus, G., and Sunter, G. (2014). Geminivirus AL2 protein induces expression of, and interacts with, a calmodulin-like gene, an endogenous regulator of gene silencing. *Virology* 460–461, 108–118. doi: 10.1016/j.virol.2014.04.034

Cingolani, P., Platts, A., Wang, L. L., Coon, M., Nguyen, T., Wang, L., et al. (2012). A program for annotating and predicting the effects of single nucleotide polymorphisms, SnpEff. *Fly* 6, 80–92. doi: 10.4161/fly.19695

Citores, L., Iglesias, R., and Ferreras, J. M. (2021). Antiviral activity of ribosome-inactivating proteins. *Toxins* 13:80. doi: 10.3390/toxins13020080

Conesa, A., Madrigal, P., Tarazona, S., Gomez-Cabrero, D., Cervera, A., McPherson, A., et al. (2016). A survey of best practices for RNA-seq data analysis. *Genome Biol.* 17:13. doi: 10.1186/s13059-016-0881-8

Correa, R. L., Bruckner, F. P., de Souza Cascardo, R., and Alfenas-Zerbini, P. (2013). The role of F-box proteins during viral infection. *Int. J. Mol. Sci.* 14, 4030–4049. doi: 10.3390/ijms14024030

Czosnek, H., Eybishtz, A., Sade, D., Gorovits, R., Sobol, I., Bejarano, E., et al. (2013). Discovering host genes involved in the infection by the tomato yellow leaf curl virus complex and in the establishment of resistance to the virus using tobacco rattle virus-based post transcriptional gene silencing. *Viruses* 5, 998–1022. doi: 10.3390/v5030998

Ding, W., Wu, J., Ye, J., Zheng, W., Wang, S., Zhu, X., et al. (2018). A Pelota-like gene regulates root development and defence responses in rice. *Ann. Bot.* 122, 359–371. doi: 10.1093/aob/mcy075

Dobin, A., Davis, C. A., Schlesinger, F., Drenkow, J., Zaleski, C., Jha, S., et al. (2013). STAR: ultrafast universal RNA-seq aligner. *Bioinformatics* 29, 15–21. doi: 10.1093/bioinformatics/bts635

Dong, H. J., Zhang, R., Kuang, Y., and Wang, X. J. (2021). Selective regulation in ribosome biogenesis and protein production for efficient viral translation. *Arch. Microbiol.* 203, 1021–1032. doi: 10.1007/s00203-020-02094-5

Doyle, J. J., and Doyle, J. L. (1990). Isolation of plant DNA from fresh tissue. *Focus* 12, 13–15.

Forsburg, S. L. (2004). Eukaryotic MCM proteins: beyond replication initiation. *Microbiol. Mol. Biol. Rev.* 68, 109–131. doi: 10.1128/mmbr.68.1.109-131.2004

Fortes, I. M., Sánchez-Campos, S., Fiallo-Olivé, E., Díaz-Pendón, J. A., Navas-Castillo, J., and Moriones, E. (2016). A novel strain of tomato leaf curl New Delhi virus has spread to the Mediterranean basin. *Viruses* 8:307. doi: 10.3390/v8110307

Fowler, J. H., Narváez-Vásquez, J., Aromdee, D. N., Pautot, V., Holzer, F. M., and Walling, L. L. (2009). Leucine aminopeptidase regulates defense and wound signaling in tomato downstream of jasmonic acid. *Plant Cell* 21, 1239–1251. doi: 10.1105/tpc.108.065029

Gallego-Bartolomé, J., Liu, W., Kuo, P. H., Feng, S., Ghoshal, B., Gardiner, J., et al. (2019). Co-targeting RNA polymerases IV and V promotes efficient de novo DNA methylation in *Arabidopsis*. *Cell* 176, 1068–1082.e19. doi: 10.1016/j.cell.2019.01.029

Garrison, E., and Marth, G. (2012). Haplotype-based variant detection from short-read sequencing. *arXiv* [Preprint]. arXiv:1207.3907

Gholizadeh, A., Santha, I. M., Kohnehrouz, B. B., Lodha, M. L., and Kapoor, H. C. (2005). Cystatins may confer viral resistance in plants by inhibition of a virus-induced cell death phenomenon in which cysteine proteinases are active: cloning and molecular characterization of a cDNA encoding cysteine-proteinase inhibitor (celostatin) from *Celosia cristata* (crested cock's comb). *Biotechnol. Appl. Biochem.* 42, 197–204. doi: 10.1042/BA20050029

Giacomini, D. A., Gaines, T., Beffa, R., and Tranel, P. J. (2018). Optimizing RNA-seq studies to investigate herbicide resistance. *Pest Manag. Sci.* 74, 2260–2264. doi: 10.1002/ps.4822

Gil, L., Yaron, I., Shalitin, D., Sauer, N., Turgeon, R., and Wolf, S. (2011). Sucrose transporter plays a role in phloem loading in CMV-infected melon plants that are defined as symplastic loaders. *Plant J.* 66, 366–374. doi: 10.1111/j.1365-313X.2011.04498.x

Góngora-Castillo, E., Ibarra-Laclette, E., Trejo-Saavedra, D. L., and Rivera-Bustamante, R. F. (2012). Transcriptome analysis of symptomatic and recovered leaves of geminivirus-infected pepper (*Capsicum annuum*). *Virol. J.* 9:295. doi: 10.1186/1743-422X-9-295

González-Ibeas, D., Blanca, J., Roig, C., González-To, M., Picó, B., Truniger, V., et al. (2007). MELOGEN: an EST database for melon functional genomics. *BMC Genomics* 8:306. doi: 10.1186/1471-2164-8-306

Gorovits, R., and Czosnek, H. (2017). The involvement of heat shock proteins in the establishment of tomato yellow leaf curl virus infection. *Front. Plant Sci.* 8:355. doi: 10.3389/fpls.2017.00355

Gorovits, R., Moshe, A., Ghanim, M., and Czosnek, H. (2013). Recruitment of the host plant heat shock protein 70 by tomato yellow leaf curl virus coat protein is required for virus infection. *PLoS One* 8:e70280. doi: 10.1371/journal.pone.0070280

Guerrero, J., Regedanz, E., Lu, L., Ruan, J., Bisaro, D. M., and Sunter, G. (2020). Manipulation of the plant host by the geminivirus AC2/C2 protein, a central player in the infection cycle. *Front. Plant Sci.* 11:591. doi: 10.3389/fpls.2020.00591

Guilliam, T. A., Keen, B. A., Brissett, N. C., and Doherty, A. J. (2015). Primase-polymerases are a functionally diverse superfamily of replication and repair enzymes. *Nucleic Acids Res.* 43, 6651–6664. doi: 10.1093/nar/gkv625

Gutierrez, C. (2000). DNA replication and cell cycle in plants: learning from geminiviruses. *EMBO J.* 19, 792–799. doi: 10.1093/emboj/19.5.792

Gutiérrez-Campos, R., Torres-Acosta, J. A., Saucedo-Arias, L. J., and Gomez-Lim, M. A. (1999). The use of cysteine proteinase inhibitors to engineer resistance against potyviruses in transgenic tobacco plants. *Nat. Biotechnol.* 17, 1223–1226. doi: 10.1038/70781

Hong, Y., Saunders, K., Hartley, M. R., and Stanley, J. (1996). Resistance to geminivirus infection by virus-induced expression of dianthin in transgenic plants. *Virology* 220, 119–127.

Huang, Y., Zhang, B. L., Sun, S., Xing, G. M., Wang, F., Li, M. Y., et al. (2016). AP2/ERF transcription factors involved in response to tomato yellow leaf curly virus in tomato. *Plant Genome* 9, 1–15. doi: 10.3835/plantgenome2015.09.0082

Hussain, Z., Lata, S., Kumar, P., Kumar, S., and Tomar, B. S. (2019). *Recessive Behavior of Ty-3 Gene for ToLCNDV Disease Resistance in Tomato (Solanum lycopersicum L.). Congress Communication*. Available online at: https://www.researchgate.net/profile/Kumar_Sumit3/publication/340476078_Recessive_behavior_of_Ty-3_gene_for_ToLCNDV_disease_resistance/links/5e8bf9c2a6fdcca789fbec50/Recessive-behavior-of-Ty-3-gene-for-ToLCNDV-disease-resistance.pdf (accessed May 4, 2020).

Hutton, S. F., Scott, J. W., and Schuster, D. J. (2012). Recessive resistance to tomato yellow leaf curl virus from the tomato cultivar Tyking is located in the same region as Ty-5 on chromosome 4. *Hortscience* 247, 324–327. doi: 10.21273/HORTSCI.47.3.324

Hwang, I. S., and Hwang, B. K. (2010). The pepper 9-lipoxygenase gene CaLOX1 functions in defense and cell death responses to microbial pathogens. *Plant Physiol.* 152, 948–967. doi: 10.1104/pp.109.147827

Ignacio-Espinoza, J. C., Laperriere, S., Yeh, Y. C., Weissman, J., Hou, S., Long, A., et al. (2020). Ribosome-linked mRNA-rRNA chimeras reveal active novel virus-host associations. *bioRxiv* [Preprint]. doi: 10.1101/2020.10.30.332502

Islam, M. R., Hossain, M. R., Jesse, D., Jung, H. J., Kim, H. T., Park, J. I., et al. (2020). Characterization, identification and expression profiling of genome-wide R-genes in melon and their putative roles in bacterial fruit blotch resistance. *BMC Genet.* 21:80. doi: 10.1186/s12863-020-00885-9

Islam, W., Noman, A., Qasim, M., and Wang, L. (2018). Plant responses to pathogen attack: small RNAs in focus. *Int. J. Mol. Sci.* 19:515. doi: 10.3390/ijms19020515

Ismayil, A., Haxim, Y., Wang, Y., Li, H., Qian, L., Han, T., et al. (2018). Cotton leaf curl multan virus C4 protein suppresses both transcriptional and post-transcriptional gene silencing by interacting with SAM synthetase. *PLoS Pathog.* 14:e1007282. doi: 10.1371/journal.ppat.1007282

Jackel, J. N., Storer, J. M., Coursey, T., and Bisaro, D. M. (2016). Arabidopsis RNA polymerases IV and V are required to establish H3K9 methylation, but not cytosine methylation, on geminivirus chromatin. *J. Virol.* 90, 7529–7540. doi: 10.1128/JVI.00656-16

Jeevalatha, A., Siddappa, S., Kumar, A., Kaundal, P., Guleria, A., Sharma, S., et al. (2017). An insight into differentially regulated genes in resistant and susceptible genotypes of potato in response to tomato leaf curl New Delhi virus-[potato] infection. *Virus Res.* 232, 22–33. doi: 10.1016/j.virusres.2017.01.015

Juárez, M., Rabadán, M. P., Martínez, L. D., Tayahi, M., Grande-Pérez, A., and Gómez López, P. (2019). Natural hosts and genetic diversity of the emerging tomato leaf curl New Delhi virus in Spain. *Front. Microbiol.* 10:140. doi: 10.3389/fmicb.2019.00140

Juárez, M., Tovar, R., Fiallo-Olivé, E., Aranda, M. A., Gosálvez, B., Castillo, P., et al. (2014). First detection of tomato leaf curl New Delhi virus infecting zucchini in Spain. *Plant Dis.* 98, 857–857. doi: 10.1094/PDIS-10-13-1050-PDN

Kachroo, A., Vincelli, P., and Kachroo, P. (2017). Signaling mechanisms underlying resistance responses: what have we learned, and how is it being applied? *Phytopathology* 107, 1452–1461. doi: 10.1094/PHYTO-04-17-0130-RVW

Kanehisa, M., and Goto, S. (2000). KEGG: Kyoto encyclopedia of genes and genomes. *Nucleic Acids Res.* 28, 27–30. doi: 10.1093/nar/28.1.27

Kazan, K., and Manners, J. M. (2011). The interplay between light and jasmonate signaling during defense and development. *J. Exp. Bot.* 62, 4087–4100. doi: 10.1093/jxb/err142

Kazlauskas, D., Krupovic, M., and Venclovas, Č (2016). The logic of DNA replication in double-stranded DNA viruses: insights from global analysis of viral genomes. *Nucleic Acids Res.* 44, 4551–4564. doi: 10.1093/nar/gkw322

Koeda, S., Onouchi, M., Mori, N., Pohan, N. S., Nagano, A. J., and Kesumawati, E. (2021). A recessive gene *pepy-1* encoding Pelota confers resistance to begomovirus isolates of PepYLCIV and PepYLCAV in *Capsicum annuum*. *Theor. Appl. Genet.* 134, 2947–2964. doi: 10.1007/s00122-021-03870-7

Kumar, R. V. (2019). Plant antiviral immunity against geminiviruses and viral counter-defense for survival. *Front. Microbiol.* 10:1460. doi: 10.3389/fmicb.2019.01460

Kushwaha, N., Singh, A. K., Basu, S., and Chakraborty, S. (2015). Differential response of diverse solanaceous hosts to tomato leaf curl New Delhi virus infection indicates coordinated action of NBS-LRR and RNAi-mediated host defense. *Arch. Virol.* 160, 1499–1509. doi: 10.1007/s00705-015-2399-x

Kushwaha, N. K., Mansi, and Chakraborty, S. (2017). The replication initiator protein of a geminivirus interacts with host monoubiquitination machinery and stimulates transcription of the viral genome. *PLoS Pathog.* 13:e1006587. doi: 10.1371/journal.ppat.1006587

Langfelder, P., and Horvath, S. (2008). WGCNA: an R package for weighted correlation network analysis. *BMC Bioinformatics* 9:559. doi: 10.1186/1471-2105-9-559

Langmead, B., and Salzberg, S. (2012). Fast gapped-read alignment with Bowtie 2. *Nat. Methods* 9, 357–359. doi: 10.1038/nmeth.1923

Lapidot, M., Karniel, U., Gelbart, D., Fogel, D., Evenor, D., Kutsher, Y., et al. (2015). A novel route controlling begomovirus resistance by the messenger RNA surveillance factor Pelota. *PLoS Genet.* 11:e1005538. doi: 10.1371/journal.pgen.1005538

Leibman, D., Kravchik, M., Wolf, D., Haviv, S., Weissberg, M., Ophir, R., et al. (2018). Differential expression of cucumber RNA-dependent RNA polymerase 1 genes during antiviral defence and resistance. *Mol. Plant Pathol.* 19, 300–312. doi: 10.1111/mpp.12518

Levy, A., and Tilsner, J. (2020). Creating contacts between replication and movement at plasmodesmata – a role for membrane contact sites in plant virus infections? *Front. Plant Sci.* 11:862. doi: 10.3389/fpls.2020.00862

Li, B., and Dewey, C. N. (2011). RSEM: accurate transcript quantification from RNA-Seq data with or without a reference genome. *BMC Bioinformatics* 12:323. doi: 10.1186/1471-2105-12-323

Li, R., Weldegergis, B. T., Li, J., Jung, C., Qu, J., Sun, Y., et al. (2014). Virulence factors of geminivirus interact with MYC2 to subvert plant resistance and promote vector performance. *Plant Cell* 26, 4991–5008. doi: 10.1105/tpc.114.133181

Li, X., An, M., Xia, Z., Bai, X., and Wu, Y. (2017a). Transcriptome analysis of watermelon (*Citrullus lanatus*) fruits in response to cucumber green mottle mosaic virus (CGMMV) infection. *Sci. Rep.* 7:16747. doi: 10.1038/s41598-017-17140-4

Li, Y., Qin, L., Zhao, J., Muhammad, T., Cao, H., Li, H., et al. (2017b). SlMAPK3 enhances tolerance to Tomato yellow leaf curl virus (TYLCV) by regulating salicylic acid and jasmonic acid signaling in tomato (*Solanum lycopersicum*). *PLoS One* 12:e0172466. doi: 10.1371/journal.pone.0172466

Li, Z., Feng, Z., Maeli, M., Jian, Y., and Sheng, Y. H. (2017c). Jasmonate signaling and manipulation by pathogens and insects. *J. Exp. Bot.* 68, 1371–1385.

Liu, Q., Liu, H., Gong, Y., Tao, Y., Jiang, L., Zuo, W., et al. (2017). An atypical thioredoxin imparts early resistance to sugarcane mosaic virus in maize. *Mol. Plant.* 10, 483–497. doi: 10.1016/j.molp.2017.02.002

López, C., Ferriol, M., and Picó, M. B. (2015). Mechanical transmission of tomato leaf curl New Delhi virus to cucurbit germplasm: selection of tolerance sources in *Cucumis melo*. *Euphytica* 204, 679–691. doi: 10.1007/s10681-015-1371-x

Lou, L., Su, X., Liu, X., and Liu, Z. (2020). Transcriptome analysis of *Luffa cylindrica* (L.) Roem response to infection with cucumber mosaic virus (CMV). *Gene* 737:144451. doi: 10.1016/j.gene.2020.144451

Love, M. I., Huber, W., and Anders, S. (2014). Moderated estimation of fold change and dispersion for RNA-seq data with DESeq2. *Genome Biol.* 15:550. doi: 10.1186/s13059-014-0550-8

Lozano-Durán, R., Rosas-Díaz, T., Gusmaroli, G., Luna, A. P., Taconnat, L., Deng, X. W., et al. (2011). Geminiviruses subvert ubiquitination by altering CSN-mediated derubylation of SCF E3 ligase complexes and inhibit jasmonate signaling in *Arabidopsis thaliana*. *Plant Cell* 23, 1014–1032. doi: 10.1105/tpc.110.080267

Lu, S., Faris, J. D., and Edwards, M. C. (2017). Molecular cloning and characterization of two novel genes from hexaploid wheat that encode double PR-1 domains coupled with a receptor-like protein kinase. *Mol. Genet. Genomics* 292, 435–452. doi: 10.1007/s00438-017-1287-3

Luna-Rivero, M. S., Hernández-Zepeda, C., Villanueva-Alonzo, H., Minero-García, Y., Castell-González, S. E., and Moreno-Valenzuela, O. A. (2016). Expression of genes involved in the salicylic acid pathway in type h1 thioredoxin transiently silenced pepper plants during a begomovirus compatible interaction. *Mol. Genet. Genomics* 291, 819–830. doi: 10.1007/s00438-015-1148-x

Machado, J. P. B., Calil, I. P., Santos, A. A., and Fontes, E. P. B. (2017). Translational control in plant antiviral immunity. *Genet. Mol. Biol.* 40, 292–304. doi: 10.1590/1678-4685-GMB-2016-0092

Maio, F., Helderman, T. A., Arroyo-Mateos, M., van der Wolf, M., Boeren, S., Prins, M., et al. (2020). Identification of tomato proteins that interact with Replication initiator protein (Rep) of the geminivirus TYLCV. *Front. Plant Sci.* 11:1069. doi: 10.3389/fpls.2020.01069

Mäkinen, K., and De, S. (2019). The significance of methionine cycle enzymes in plant virus infections. *Curr. Opin. Plant Biol.* 50, 67–75. doi: 10.1016/j.pbi.2019.03.002

Mallory, A., and Vaucheret, H. (2010). Form, function, and regulation of ARGONAUTE proteins. *Plant Cell* 22, 3879–3889. doi: 10.1105/tpc.110.080671

Martín-Hernández, A. M., and Picó, B. (2021). Natural resistances to viruses in cucurbits. *Agronomy* 11:23. doi: 10.3390/agronomy11010023

Mathioudakis, M. M., Khechmar, S., Owen, C. A., Medina, V., Ben Mansour, K., Tomaszewska, W., et al. (2018). A thioredoxin domain-containing protein interacts with pepino mosaic virus triple gene block protein 1. *Int. J. Mol. Sci.* 19:3747. doi: 10.3390/ijms19123747

McCreight, J. D., Liu, H.-Y., and Turini, T. A. (2008). Genetic resistance to cucurbit leaf crumple virus in melon. *Hortscience* 43, 122–126. doi: 10.21273/HORTSCI.43.1.122

Messelink, G. J., Calvo, F. J., Marín, F., and Janssen, D. (2020). "Cucurbits," in *Integrated Pest and Disease Management in Greenhouse Crops*, eds M. L. Gullino, R. Albajes, and P. C. Nicot (Cham: Springer International Publishing), 537–566. doi: 10.1007/978-3-030-22304-5_19

Mochizuki, T., Ogata, Y., Hirata, Y., and Ohki, S. T. (2014). Quantitative transcriptional changes associated with chlorosis severity in mosaic leaves of tobacco plants infected with cucumber mosaic virus. *Mol. Plant Pathol.* 15, 242–254. doi: 10.1111/mpp.12081

Morata, J., and Puigdomènech, P. (2017). Variability among *Cucurbitaceae* species (melon, cucumber and watermelon) in a genomic region containing a cluster of NBS-LRR genes. *BMC Genomics* 18:138. doi: 10.1186/s12864-017-3529-5

Moriones, E., Praveen, S., and Chakraborty, S. (2017). Tomato leaf curl New Delhi virus: an emerging virus complex threatening vegetable and fiber crops. *Viruses* 9:264. doi: 10.3390/v9100264

Musidlak, O., Nawrot, R., and Goździcka-Józefiak, A. (2017). Which plant proteins are involved in antiviral defense? Review on in vivo and in vitro activities of selected plant proteins against viruses. *Int. J. Mol. Sci.* 18:2300. doi: 10.3390/ijms18112300

Naqvi, A. R., Haq, Q. M., and Mukherjee, S. K. (2010). MicroRNA profiling of tomato leaf curl New Delhi virus (tolcndv) infected tomato leaves indicates that deregulation of mir159/319 and mir172 might be linked with leaf curl disease. *Virol. J.* 7:281. doi: 10.1186/1743-422X-7-281

Naqvi, R. Z., Zaidi, S. S. E. A., Akhtar, K. P., Strickler, S., Woldemariam, M., Mishra, B., et al. (2017). Transcriptomics reveals multiple resistance mechanisms against cotton leaf curl disease in a naturally immune cotton species, *Gossypium arboreum*. *Sci. Rep.* 7:15880. doi: 10.1038/s41598-017-15963-9

Nemchinov, L., Boutanaev, A., and Postnikova, O. (2016). Virus-induced gene silencing of the RPC5-like subunit of RNA polymerase III caused pleiotropic effects in *Nicotiana benthamiana*. *Sci. Rep.* 6:27785. doi: 10.1038/srep27785

Nueda, M. J., Ferrer, A., and Conesa, A. (2012). ARSyN: a method for the identification and removal of systematic noise in multifactorial time course microarray experiments. *Biostatistics* 13, 553–566. doi: 10.1093/biostatistics/kxr042

Pandey, S., Muthamilarasan, M., Sharma, N., Chaudhry, V., Dulani, P., Shweta, S., et al. (2019). Characterization of DEAD-box family of RNA helicases in tomato provides insights into their roles in biotic and abiotic stresses. *Environ. Exp. Bot.* 158, 107–116. doi: 10.1016/j.envexpbot.2018.11.018

Panno, S., Caruso, A. G., Troiano, E., Luigi, M., Manglli, A., Vatrano, T., et al. (2019). Emergence of tomato leaf curl New Delhi virus in Italy: estimation of incidence and genetic diversity. *Plant Pathol.* 68, 601–608. doi: 10.1111/ppa.12978

Panno, S., Iacono, G., Davino, M., Marchione, S., Zappardo, V., Bella, P., et al. (2016). First report of tomato leaf curl New Delhi virus affecting zucchini

squash in an important horticultural area of southern Italy. *New Dis. Rep.* 33:6. doi: 10.5197/j.2044-0588.2016.033.006

Pérez-de-Castro, A., López-Martín, M., Esteras, C., Garcés-Claver, A., Palomares-Ríus, F. J., Picó, M. B., et al. (2020). Melon genome regions associated with TGR-1551-derived resistance to cucurbit yellow stunting disorder virus. *Int. J. Mol. Sci.* 21:5970. doi: 10.3390/ijms21175970

Pitrat, M. (2016). "Melon genetic resources: phenotypic diversity and horticultural taxonomy," in *Genetics and Genomics of Cucurbitaceae*, Vol. 20, eds R. Grumet, N. Katzir, and J. Garcia-Mas (Cham: Springer Nature), 25–59. doi: 10.1007/7397_2016_10

Pradhan, B., Van Tien, V., Dey, N., and Mukherjee, S. K. (2017). *Molecular Biology of Geminivirus DNA Replication. Viral Replication, 2-35 Avid Science.* Available online at: https://www.researchgate.net/profile/Tien-Vu-6/publication/316456253_Molecular_Biology_of_Geminivirus_DNA_Replication/links/5906ecf0aca272116d333677/Molecular-Biology-of-Geminivirus-DNA-Replication.pdf (accessed December, 2021).

Prakash, V., Singh, A., Singh, A. K., Dalmay, T., and Chakraborty, S. (2020). Tobacco RNA-dependent RNA polymerase 1 affects the expression of defence-related genes in *Nicotiana benthamiana* upon tomato leaf curl Gujarat virus infection. *Planta* 252:11. doi: 10.1007/s00425-020-03417-y

Preiss, W., and Jeske, H. (2003). Multitasking in replication is common among geminiviruses. *J. Virol.* 77, 2972–2980. doi: 10.1128/jvi.77.5.2972-2980.2003

Prins, M. W., Van Enckevort, L. J. G., and Versluis, H. P. (2019). *Geminivirus Resistant Plants. U.S. Patent No. 2020/0392530 A1*. Wageningen, NL: International application published under the patent cooperation treaty (PCT).

Quezada, E. H., García, G. X., Arthikala, M. K., Melappa, G., Lara, M., and Nanjareddy, K. (2019). Cysteine-rich receptor-like kinase gene family identification in the *Phaseolus* genome and comparative analysis of their expression profiles specific to mycorrhizal and rhizobial symbiosis. *Genes* 10:59. doi: 10.3390/genes10010059

Qui, X., Bao, F. S., and Xie, Z. (2009). Small RNA deep sequencing reveals role for *Arabidopsis thaliana* RNA-dependent RNA polymerases in viral siRNA biogenesis. *PLoS One* 4:e4971. doi: 10.1371/journal.pone.0004971

Rai, N., Sahu, P., Gupta, S., Reddy, M. K., Ravishankar, K., Singh, M., et al. (2013). Identification and validation of an ISSR marker linked to tomato leaf curl New Delhi virus resistant gene in a core set of tomato accessions. *Vegetable Sci.* 40, 1–6.

Raja, P., Jackel, J. N., Li, S., Heard, I. M., and Bisaro, D. M. (2014). Arabidopsis double-stranded RNA binding protein DRB3 participates in methylation-mediated defense against geminiviruses. *J. Virol.* 88, 2611–2622. doi: 10.1128/JVI.02305-13

Ramesh, S. V., Sahu, P. P., Prasad, M., Praveen, S., and Pappu, H. R. (2017). Geminiviruses and plant hosts: a closer examination of the molecular arms race. *Viruses* 9:256. doi: 10.3390/v9090256

Ranji, A., and Boris-Lawrie, K. (2010). RNA helicases: emerging roles in viral replication and the host innate response. *RNA Biol.* 7, 775–787. doi: 10.4161/rna.7.6.14249

Rizvi, I., Choudhury, N. R., and Tuteja, N. (2015). Insights into the functional characteristics of geminivirus rolling-circle replication initiator protein and its interaction with host factors affecting viral DNA replication. *Arch. Virol.* 160, 375–387. doi: 10.1007/s00705-014-2297-7

Rodríguez-Negrete, E., Lozano-Durán, R., Piedra-Aguilera, A., Cruzado, L., Bejarano, E. R., and Castillo, A. G. (2013). Geminivirus Rep protein interferes with the plant DNA methylation machinery and suppresses transcriptional gene silencing. *New Phytol.* 199, 464–475. doi: 10.1111/nph.12286

Román, B., Gómez, P., Picó, B., López, C., and Janssen, D. (2019). Candidate gene analysis of tomato leaf curl New Delhi virus resistance in *Cucumis melo*. *Sci. Hortic.* 243, 12–20. doi: 10.1016/j.scienta.2018.07.005

Romay, G., Pitrat, M., Lecoq, H., Wipf-Scheibel, C., Millot, P., Girardot, G., et al. (2019). Resistance against melon chlorotic mosaic virus and tomato leaf curl New Delhi virus in melon. *Plant Dis.* 103, 2913–2919. doi: 10.1094/PDIS-02-19-0298-RE

Rossitto de Marchi, B., Kinene, T., Krause-Sakate, R., Boykin, L. M., Ndunguru, J., Kehoe, M., et al. (2020). Genetic diversity and SNP's from the chloroplast coding regions of virus-infected cassava. *PeerJ* 8:e8632. doi: 10.7717/peerj.8632

Roy, A., Bal, S. S., Fergany, M., Kaur, S., Singh, H., Malik, A. A., et al. (2012). Wild melon diversity in India (Punjab state). *Genet. Resour. Crop Evol.* 59, 755–767. doi: 10.1007/s10722-011-9716-3

Sade, D., Sade, N., Brotman, Y., and Czosnek, H. (2020). Tomato yellow leaf curl virus (TYLCV)-resistant tomatoes share molecular mechanisms sustaining resistance with their wild progenitor *Solanum habrochaites* but not with TYLCV-susceptible tomatoes. *Plant Sci. Int. J. Exp. Plant Biol.* 295:110439. doi: 10.1016/j.plantsci.2020.110439

Sáez, C., Ambrosio, L. G. M., Miguel, S. M., Valcárcel, J. V., Díez, M. J., Picó, B., et al. (2021). Resistant sources and genetic control of resistance to ToLCNDV in cucumber. *Microorganisms* 9:913. doi: 10.3390/microorganisms9050913

Sáez, C., Esteras, C., Martínez, C., Ferriol, M., Dhillon, N. P., López, C., et al. (2017). Resistance to tomato leaf curl New Delhi virus in melon is controlled by a major QTL located in chromosome 11. *Plant Cell Rep.* 36, 1571–1584. doi: 10.1007/s00299-017-2175-3

Sáez, C., Martínez, C., Ferriol, M., Manzano, S., Velasco, L., Jamilena, M., et al. (2016). Resistance to tomato leaf curl New Delhi virus in *Cucurbita* spp. *Ann. Appl. Biol.* 169, 91–105.

Sáez, C., Martínez, C., Montero-Pau, J., Esteras, C., Sifres, A., Blanca, J., et al. (2020). A major QTL located in chromosome 8 of *Cucurbita moschata* is responsible for resistance to tomato leaf curl New Delhi virus. *Front. Plant Sci.* 11:207. doi: 10.3389/fpls.2020.00207

Sahu, P. P., Rai, N. K., Chakraborty, S., Singh, M., Chandrappa, P. H., Ramesh, B., et al. (2010). Tomato cultivar tolerant to tomato leaf curl New Delhi virus infection induces virus-specific short interfering RNA accumulation and defence-associated host gene expression. *Mol. Plant Pathol.* 11, 531–544. doi: 10.1111/j.1364-3703.2010.00630.x

Sahu, P. P., Sharma, N., Puranik, S., Chakraborty, S., and Prasad, M. (2016). Tomato 26S proteasome subunit RPT4a regulates ToLCNDV transcription and activates hypersensitive response in tomato. *Sci. Rep.* 6:27078. doi: 10.1038/srep27078

Sanfaçon, H. (2015). Plant translation factors and virus resistance. *Viruses* 7, 3392–3419. doi: 10.3390/v7072778

Saunders, K., Lucy, A., and Stanley, J. (1992). RNA-primed complementary-sense DNA synthesis of the geminivirus African cassava mosaic virus. *Nucleic Acids Res.* 20, 6311–6315. doi: 10.1093/nar/20.23.6311

Schmittgen, T. D., and Livak, K. J. (2008). Analyzing real-time PCR data by the comparative CT method. *Nat. Protoc.* 3, 1101–1108. doi: 10.1038/nprot.2008.73

Schommer, C., Palatnik, J. F., Aggarwal, P., Chételat, A., Cubas, P., Farmer, E. E., et al. (2008). Control of jasmonate biosynthesis and senescence by miR319 targets. *PLoS Biol.* 6:e230. doi: 10.1371/journal.pbio.0060230

Seo, H. S., Song, J. T., Cheong, J. J., Lee, Y. H., Lee, Y. W., Hwang, I., et al. (2001). Jasmonic acid carboxyl methyltransferase: a key enzyme for jasmonate-regulated plant responses. *Proc. Natl. Acad. Sci. U.S.A.* 98, 4788–4793. doi: 10.1073/pnas.081557298

Shang, J., Xi, D. H., Xu, F., Wang, S. D., Cao, S., Xu, M. Y., et al. (2011). A broad-spectrum, efficient and nontransgenic approach to control plant viruses by application of salicylic acid and jasmonic acid. *Planta* 233, 299–308. doi: 10.1007/s00425-010-1308-5

Sharma, A., and Boris-Lawrie, K. (2012). Determination of host RNA helicases activity in viral replication. *Methods Enzymol.* 511, 405–435. doi: 10.1016/B978-0-12-396546-2.00019-X

Sharma, N., Sahu, P. P., Prasad, A., Muthamilarasan, M., Waseem, M., Khan, Y., et al. (2021). The *Sw5a* gene confers resistance to ToLCNDV and triggers an HR response after direct AC4 effector recognition. *Proc. Natl. Acad. Sci. U.S.A.* 118:e2101833118. doi: 10.1073/pnas.2101833118

Souza, P., García-Ruíz, H., and Carvalho, F. (2019). What proteomics can reveal about plant-virus interactions? Photosynthesis-related proteins on the spotlight. *Theor. Exp. Plant Physiol.* 31, 227–248. doi: 10.1007/s40626-019-00142-0

Sun, X., Wang, Z., Gu, Q., Li, H., Han, W., and Shi, Y. (2017). Transcriptome analysis of *Cucumis sativus* infected by cucurbit chlorotic yellows virus. *Virol. J.* 14:18. doi: 10.1186/s12985-017-0690-z

Sun, Y., Fan, M., and He, Y. (2019). Transcriptome analysis of watermelon leaves reveals candidate genes responsive to cucumber green mottle mosaic virus infection. *Int. J. Mol. Sci.* 20:610. doi: 10.3390/ijms20030610

Supek, F., Bošnjak, M., Škunca, N., and Šmuc, T. (2011). REVIGO summarizes and visualizes long lists of gene ontology terms. *PLoS One* 6:e21800. doi: 10.1371/journal.pone.0021800

Suyal, G., Mukherjee, S. K., Srivastava, P. S., and Choudhury, N. R. (2013). *Arabidopsis thaliana* MCM2 plays role(s) in mungbean yellow mosaic India

virus (MYMIV) DNA replication. *Arch. Virol.* 158, 981–992. doi: 10.1007/s00705-012-1563-9

Tsai, W. A., Weng, S. H., Chen, M. C., Lin, J. S., and Tsai, W. S. (2019). Priming of plant resistance to heat stress and tomato yellow leaf curl Thailand virus with plant-derived materials. *Front. Plant Sci.* 10:906. doi: 10.3389/fpls.2019.00906

Ullah, R., Akhtar, K. P., Moffett, P., Mansoor, S., Briddon, R. W., and Saeed, M. (2014). An analysis of the resistance of *Gossypium arboreum* to cotton leaf curl disease by grafting. *Eur. J. Plant Pathol.* 139, 837–847. doi: 10.1007/s10658-014-0437-2

Untergasser, A., Nijveen, H., Rao, X., Bisseling, T., Geurts, R., and Jack, A. M. (2007). Leunissen: Primer3Plus, an enhanced web interface to Primer3. *Nucleic Acids Res.* 35, W71–W74. doi: 10.1093/nar/gkm306

Verlaan, M. G., Hutton, S. F., Ibrahem, R. M., Kormelink, R., Visser, R. G., Scott, J. W., et al. (2013). The tomato yellow leaf curl virus resistance genes *Ty-1* and *Ty-3* are allelic and code for DFDGD-class RNA–dependent RNA polymerases. *PLoS Genet.* 9:e1003399. doi: 10.1371/journal.pgen.1003399

Vicente, J., Cascon, T., Vicedo, B., Garcia-Agustin, P., Hamberg, M., and Castresana, C. (2012). Role of 9-lipoxygenase and alpha-dioxygenase oxylipin pathways as modulators of local and systemic defense. *Mol. Plant* 5, 914–928. doi: 10.1093/mp/ssr105

Vinutha, T., Kumar, G., Garg, V., Canto, T., Palukaitis, P., Ramesh, S. V., et al. (2018). Tomato geminivirus encoded RNAi suppressor protein, AC4 interacts with host AGO4 and precludes viral DNA methylation. *Gene* 678, 184–195. doi: 10.1016/j.gene.2018.08.009

Vinutha, T., Vanchinathan, S., Bansal, N., Kumar, G., Permar, V., Watts, A., et al. (2020). Tomato auxin biosynthesis/signaling is reprogrammed by the geminivirus to enhance its pathogenicity. *Planta* 252:51. doi: 10.1007/s00425-020-03452-9

Wasternack, C., and Song, S. (2017). Jasmonates: biosynthesis, metabolism, and signaling by proteins activating and repressing transcription. *J. Exp. Bot.* 68, 1303–1321. doi: 10.1093/jxb/erw443

Willmann, M. R., Endres, M. W., Cook, R. T., and Gregory, B. D. (2011). The functions of RNA-dependent RNA polymerases in *Arabidopsis*. *Arabidopsis Book* 9:e0146. doi: 10.1199/tab.0146

Wu, M., Ding, X., Fu, X., and Lozano-Durán, R. (2019). Transcriptional reprogramming caused by the geminivirus tomato yellow leaf curl virus in local or systemic infections in *Nicotiana benthamiana*. *BMC Genomics* 20:542. doi: 10.1186/s12864-019-5842-7

Xia, C., Li, S., Hou, W., Fan, Z., Xiao, H., Lu, M., et al. (2017). Global transcriptomic changes induced by infection of cucumber (*Cucumis sativus* L.) with mild and severe variants of Hop stunt viroid. *Front. Microbiol.* 8:2427. doi: 10.3389/fmicb.2017.02427

Xiong, W., Lan, T., and Mo, B. (2021). Extraribosomal functions of cytosolic ribosomal proteins in plants. *Front. Plant Sci.* 12:607157. doi: 10.3389/fpls.2021.607157

Yadeta, K. A., Elmore, J. M., Creer, A. Y., Feng, B., Franco, J. Y., Rufian, J. S., et al. (2017). A cysteine-rich protein kinase associates with a membrane immune complex and the cysteine residues are required for cell death. *Plant Physiol.* 173, 771–787. doi: 10.1104/pp.16.01404

Yan, C., and Xie, D. (2015). Jasmonate in plant defense: sentinel or double agent? *Plant Biotechnol. J.* 13, 1233–1240. doi: 10.1111/pbi.12417

Yan, Z., Wolters, A. M. A., Navas-Castillo, J., and Bai, Y. (2021). The global dimension of tomato yellow leaf curl disease: current status and breeding perspectives. *Microorganisms* 9:740.

Yang, S. J., Carter, S. A., Cole, A. B., Cheng, N. H., and Nelson, R. S. (2004). A natural variant of a host RNA-dependent RNA polymerase is associated with increased susceptibility to viruses by *Nicotiana benthamiana*. *Proc. Natl. Acad. Sci. U.S.A.* 101, 6297–6302. doi: 10.1073/pnas.0304346101

You, W. J., Feng, Y. R., Shen, Y. H., Chen, Y. R., Chen, T. Y., and Fu, S. F. (2019). Silencing of NbCMT3s has pleiotropic effects on development by interfering with autophagy-related genes in *Nicotiana benthamiana*. *Plant Cell Physiol.* 60, 1120–1135. doi: 10.1093/pcp/pcz034

Yousif, M. T., Kheyr-Pour, A., Gronenborn, B., Pitrat, M., and Dogimont, C. (2007). Sources of 536 resistance to watermelon chlorotic stunt virus in melon. *Plant Breed.* 126, 422–427. doi: 10.1111/j.1439-0523.2007.01366.x

Yu, G., Wang, L., Han, Y., and He, Q. (2012). ClusterProfiler: an R package for comparing biological themes among gene clusters. *OMICS* 16, 284–287. doi: 10.1089/omi.2011.0118

Zaidi, S. S., Naqvi, R. Z., Asif, M., Strickler, S., Shakir, S., Shafiq, M., et al. (2020). Molecular insight into cotton leaf curl geminivirus disease resistance in cultivated cotton (*Gossypium hirsutum*). *Plant Biotechnol. J.* 18, 691–706. doi: 10.1111/pbi.13236

Zhai, Y., Peng, H., Neff, M. M., and Pappu, H. R. (2020). Emerging molecular links between plant photomorphogenesis and virus resistance. *Front. Plant Sci.* 11:920. doi: 10.3389/fpls.2020.00920

Zhan, J., Shi, H., Li, W., Zhang, C., and Zhang, Y. (2021). NbTMP14 is involved in tomato spotted wilt virus infection and symptom development by interaction with the viral NSm protein. *Viruses* 13:427. doi: 10.3390/v13030427

Zhang, L., Zhang, F., Melotto, M., Yao, J., and He, S. Y. (2017). Jasmonate signaling and manipulation by pathogens and insects. *J. Exp. Bot.* 68, 1371–1385. doi: 10.1093/jxb/erw478

Zhang, Z., Chen, H., Huang, X., Xia, R., Zhao, Q., Lai, J., et al. (2011). BSCTV C2 attenuates the degradation of SAMDC1 to suppress DNA methylation-mediated gene silencing in *Arabidopsis*. *Plant Cell* 23, 273–288. doi: 10.1105/tpc.110.081695

Zorzatto, C., Machado, J. P. B., Lopes, K. V., Nascimento, K. J., Pereira, W. A., Brustolini, O. J., et al. (2015). NIK1-mediated translation suppression functions as a plant antiviral immunity mechanism. *Nature* 520, 679–682. doi: 10.1038/nature14171

Conflict of Interest: The authors declare that the research was conducted in the absence of any commercial or financial relationships that could be construed as a potential conflict of interest.

Publisher's Note: All claims expressed in this article are solely those of the authors and do not necessarily represent those of their affiliated organizations, or those of the publisher, the editors and the reviewers. Any product that may be evaluated in this article, or claim that may be made by its manufacturer, is not guaranteed or endorsed by the publisher.

frontiers | Frontiers in Microbiology

TYPE Original Research
PUBLISHED 21 September 2022
DOI 10.3389/fmicb.2022.943382

OPEN ACCESS

EDITED BY
Toufic Elbeaino,
International Centre for Advanced Mediterranean Agronomic Studies, Italy

REVIEWED BY
Abdolbaset Azizi,
University of Kurdistan, Iran
Ho-jong Ju,
Jeonbuk National University, South Korea

*CORRESPONDENCE
Aflaq Hamid
falak19@gmail.com

SPECIALTY SECTION
This article was submitted to Microbe and Virus Interactions with Plants, a section of the journal Frontiers in Microbiology

RECEIVED 13 May 2022
ACCEPTED 29 August 2022
PUBLISHED 21 September 2022

CITATION
Rashid S, Wani F, Ali G, Sofi TA, Dar ZA and Hamid A (2022) Viral metatranscriptomic approach to study the diversity of virus(es) associated with Common Bean (*Phaseolus vulgaris* L.) in the North-Western Himalayan region of India. *Front. Microbiol.* 13:943382. doi: 10.3389/fmicb.2022.943382

Viral metatranscriptomic approach to study the diversity of virus(es) associated with Common Bean (*Phaseolus vulgaris* L.) in the North-Western Himalayan region of India

Shahjahan Rashid[1], Farhana Wani[1], Gowhar Ali[2], Tariq A. Sofi[1], Zahoor Ahmed Dar[2] and Aflaq Hamid[1]*

[1]Department of Plant Pathology, Sher-e-Kashmir University of Agricultural Sciences & Technology of Kashmir, Srinagar, India, [2]Department of Genetics and Plant Breeding, Sher-e-Kashmir University of Agricultural Sciences & Technology of Kashmir, Srinagar, India

Plant viruses are a major threat to legume production worldwide. In recent years, new virus strains have emerged with increasing frequencies in various legume cropping systems, which demands the development of cutting-edge virus surveillance techniques. In this study, we surveyed the common bean fields of Kashmir valley for virus infection using a total of 140 symptomatic and non-symptomatic leaf samples collected from different locations. The genetic diversity of viruses was examined by high-throughput sequencing (HTS) with three viruses being identified, namely, Bean Common Mosaic Virus (BCMV), Bean Common Mosaic Necrosis Virus (BCMNV), and Clover Yellow Vein Virus (ClYVV). BCMNV and ClYVV are new reports from India. *De novo* assembly of transcriptome constructed near-complete genomes of these viruses. RT-PCR results confirmed the presence of these viruses with an emerge incidence of 56. 4% for BCMV, 27.1% for BCMNV and 16.4 for ClYVV in the valley. Several samples were found to contain multiple virus infections with BCMV being the most predominant. Recombination events were detected in the genomes of BCMV and ClYVV, but not BCMNV. Phylogenetic and pairwise identity matrix evidence suggests viral import from multiple countries. Our results demonstrate that HTS followed by multiplex PCR assay is a simple, rapid, and reliable approach for simultaneous diagnosis of plant viruses.

KEYWORDS

next generation sequencing, BCMV, BCMNV, ClYVV, multiplex PCR, recombination, phylogenetic analysis

Introduction

Plants are vulnerable to various disease-causing pathogens, namely, fungi, bacteria, viruses, and nematodes. Viruses particularly can have a significant negative impact on the quality and yield of various agricultural crops (Jones et al., 2017). Every year crop losses due to viral diseases cost billions of dollars (Rubio et al., 2020). Among the different pulse crops susceptible to viruses, the common bean (*Phaseolus vulgaris L.*) is the most widely grown legume crop worldwide, namely, in India. Annually, around 31 million tonnes of dry bean grains are produced worldwide and India is among the countries with the largest production of dry beans (FAOSTAT., 2021). Common bean is locally called "Rajmash" and is an important part of the regional diet as it has high nutritional attributes. Being high in minerals, fibers, and a cheap source of protein, beans are used instead of meat in developing and under-developed countries which makes it a "grain of hope" for poor communities and is also called "Poor Man's Meat" (Zargar et al., 2017; Celmeli et al., 2018; Choudhary et al., 2018; Nadeem et al., 2021).

Common bean in the natural environment is threatened by an attack of multiple pathogens, especially viruses. It has been found susceptible to more than 70 viruses (Morales, 1986) and more than 30 viruses have been well characterized (Matthews, 1982; Hall, 1991; Loebenstein and Thottappilly, 2004). The majority of plant viruses have RNA as their genetic material and some have DNA (Kesanakurti et al., 2016). The most devastating RNA viral pathogens that infect common bean are Bean common mosaic virus (BCMV) and Bean common mosaic necrosis virus (BCMNV) in the genus potyvirus, family potyviridae (Worrall et al., 2015). Other examples of well-known common bean viral pathogens with genome as RNA are Bean yellow mosaic virus (BYMV), Clover yellow vein virus (ClYVV), Soybean mosaic virus (SMV), Cucumber mosaic virus (CMV), and Cowpea aphid-borne mosaic virus (CABMV) Potyvirus. Some DNA viruses are also reported to infect common beans such as Bean golden mosaic virus (BGMV), and Bean golden yellow mosaic virus (BGYMV). These viruses readily transmit via seed or insect vectors or by both and cause significant yield losses to the crop (Garrido-Ramirez and Sudarshana, 2000; Bonfim et al., 2007; Larsen et al., 2008; Worrall et al., 2015; Wainaina et al., 2019).

International trade, rapid climate change, and ability of viruses to rapid evolution have resulted in the frequent appearance of new viruses (Rubio et al., 2020). In recent years, new sophisticated technologies have opened new avenues in the detection of viruses and viroids. HTS is a broad-spectrum diagnostic screening approach employed for plant virus detection in 2009 (Adams et al., 2009; Kreuze et al., 2009). Since then various nucleic acid inputs have been used for library preparation using ribosomal RNA-depleted total RNA, small RNAs, total RNA, mRNA, and double-stranded RNA for HTS. The use of HTS has made it possible to detect not only known viruses but also novel/non-target viral pathogens for which other diagnostics are not available yet (Xu et al., 2019). The HTS is a broad-spectrum diagnostic tool in which prior knowledge of viral pathogens is not needed, as it enables the sequencing of all the genomic material in the sample (Adams et al., 2009; Maree et al., 2018; Gaafar et al., 2020). Unlike traditional virus diagnostic approaches which are based on observational, serological, and molecular methods which target only known pathogens and depend on prior knowledge of the pathogens being tested (Gaafar et al., 2020).

In addition, a mixed viral infection of crop plants occurs commonly in nature as a consequence of successive vector inoculations (Rubio et al., 2020). During these conditions, it becomes difficult to understand the disease etiology. HTS technique has provided us with a powerful tool to reveal the etiology of latent infections and unknown diseases and for the detection and identification of virome of infected plants (Barba et al., 2014).

Early identification of the viral pathogen is essential for limiting the spread of viral diseases as well as combating their negative effects on the yield of agricultural crops (Akinyemi et al., 2016). Accurate diagnosis and proper identification are the basic steps for managing any viral disease (Chiquito-Almanza et al., 2017). Using HTS 15 viruses were identified from common beans, namely, Southern bean mosaic virus (SBMV) and Tomato leaf curl Uganda virus for the first time in Tanzania (Mwaipopo et al., 2018). In Kenya, two cryptic double-stranded RNA viruses Phaseolus vulgaris endornavirus 1 (PvEV-1) and Phaseolus vulgaris endornavirus 2 (PvEV-2) beside Bean common mosaic necrosis virus (BCMNV), and Cucumber mosaic virus (CMV) were identified by using Illumina RNA-seq (Mutuku et al., 2018).

Although common bean is grown in several regions of India, there are only a few reports where attempts have been made to detect bean virus pathogens. Also, these studies were based on classical virus detection techniques. In this study, we used the viral metatranscriptomic approach by using Illumina high-throughput RNA sequencing to profile the virome of common bean that showed diverse virus-like symptoms. This is the first virome analysis of common beans from India. We identified three viruses by using a bioinformatics pipeline; two viruses are the first reports from India in common bean. Our study will be helpful in the production of disease-free seed stock in certification programs and the development of disease management strategies.

Materials and methods

Survey and collection of samples

In the early summer of 2020, a survey was conducted in Jammu and Kashmir, India, to determine the viral community

present in common beans. The area was divided into three regions South, Central, and North Kashmir. In each region, 5–10 fields of common bean were selected randomly for the collection of leaf samples. Common bean leaf samples collected during field surveys exhibited mosaic, necrosis, venial necrosis, puckering, leaf distortion, stunted growth, and upward and downward curling symptoms (Figure 1). Samples were collected from every selected field in RNAlater (Thermo Fisher Scientific Inc.). A total of 140 leaf samples of common bean were collected from Kashmir valley (Table 3). Some asymptomatic samples were also collected. Collected samples were stored at−80 C prior to further analysis.

RNA isolation, library preparation, and sequencing

Total RNA was extracted from leaf samples by grinding the samples in liquid nitrogen using the mortar pestle or TissueLyser and the fine tissue powder was immediately transferred into the Eppendorf tube 1.5µl and placed in liquid nitrogen. Total RNA was isolated from leaf samples using TRIzol reagent (Thermo Fisher Scientific Inc). The pellets were centrifuged and washed following RNA precipitation, wash was discarded and pellets were air dried and then dissolved in 30–50µl of nuclease-free water. RNA samples were checked for their quality and quantity using a NanoDrop 2000c UV-vis spectrophotometer (Thermo Fisher Scientific Inc.) and Agarose gel electrophoresis (1% Agarose Gel) containing TAE buffer. Out of 140 samples, RNA isolated from 14 samples (four from South, four from North, and six from Central Kashmir) were pooled to form a single sample and sent for virome analysis at Nucleome Biotech, Hyderabad, India for sequencing total RNA using HTS technology. The pooled sample was subjected to a preliminary quality check (QC) at Nucleome Biotech and the total RNA of the sample was quantified and qualified by using Agarose Gel Electrophoresis (1% Agarose Gel) and Qubit® 3.0 Fluorometer (Thermo Fisher Scientific Inc.). One microgram total RNA was used for library preparation. Ribosomal RNA was removed from total RNA using Ribo-Zero Magnetic Kit (Epicentre, Madison, WI, USA). HTS library preparations were constructed according to the manufacturer's protocol (NEBNext II RNA Library Prep Kit for Illumina®). Ready-to-run final libraries were quantified using a Qubit 3.0 Fluorometer (Thermo Fisher Scientific Inc.) using a DNA HS assay kit (Thermo Fisher Scientific Inc.) following the manufacturer's protocol. To identify the insert size of the library, we queried it on TapeStation 4150 (Agilent) utilizing highly sensitive D1000 ScreenTape (Agilent) following manufacturer's protocol. Libraries were sequenced by Illumina high-throughput sequencer with paired-end sequencing strategy. The qualified libraries were fed into Illumina sequencers NovaSeq 6000, S4 Flow Cell (2 x 150bp Read Length) after pooling according to their effective concentration and expected data volume.

Bioinformatic analysis

The Raw data from Illumina Sequencer was obtained in a FASTQ format which contains sequenced reads and corresponding sequencing quality information (Cock et al., 2010). For virome reconstruction and virus identification, the raw reads obtained from high-throughput sequencing were trimmed, and filtered to remove low-quality reads and adapter sequences using Fastp version 2.8 (Chen et al., 2018). Guanine–cytosine (GC) content, Phred quality scores (Q20 and Q30), and sequence duplication level were calculated. Reads that passed the quality filtering were used for downstream analysis. Clean reads were assembled de novo by using assembly software Trinity version 2.10.0 (Henschel et al., 2012), Spades (Prjibelski et al., 2020), and Rnabloom (Nip et al., 2020) with the default setting to create the complete genome assemblies. The taxonomic profiling of high-throughput sequencing of assembled contigs was performed by Kaiju version 1.7.3 (Menzel et al., 2016) using the NCBI reference sequence database and the Krona tool was used to visualize the results.

Identification of viruses

The contigs obtained after de novo assembly were subjected to Blastn and Blastx of GenBank database (NCBI) (https://www.ncbi.nlm.nih.gov/) to confirm the viral/viriod sequences present in the assembled library. Contigs that mapped with the individual viral genome sequences from the NCBI were used to identify candidate viruses present in analyzed common bean samples. The open reading frame (ORF) of the identified viruses was found using the ORF finder NCBI (https://www.ncbi.nlm.nih.gov/orffinder/).

Pairwise and phylogenetic analysis

The assembled viral genomes identified in this study from HTS were subjected to Blastn search of the NCBI database to retrieve the corresponding homologous genomes. Only the complete genomes that mapped with the assembled viral genomes in the present study were used to determine the pairwise identity and phylogenetic relationship. The genomes were trimmed to equal sizes and aligned using the ClustalW multiple alignment program in BioEdit version 7.2.5 (Hall, 1999). Pairwise nucleotide identities were calculated using the sequence demarcation tool (SDTv1.2) (Muhire et al., 2014) and identity scores were generated using color coded matrix. Maximum likelihood method was used to establish the

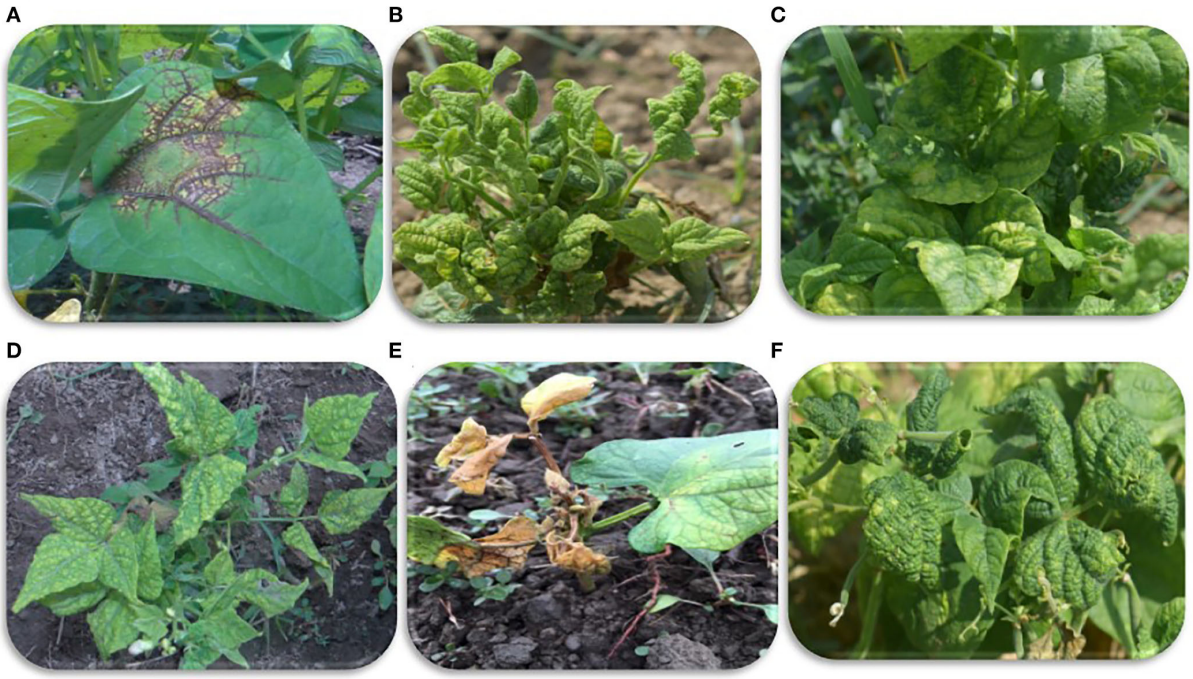

FIGURE 1
Viral symptoms on common beans observed during sample collection. **(A)** Veinal necrosis. **(B,D,F)** Mosaic and severe leaf deformities, **(C)** mosaic and puckering, and **(E)** mosaic and leaf necrosis.

phylogenetic relationship among the aligned sequences at 1000 replications for each bootstrap value in the MEGA X software (Kumar et al., 2018).

Recombination analysis

Sequences used for pairwise and phylogenetic analysis were used for the detection of recombination events like the potential recombinant sequences, number of recombination events, major and minor parent, and recombination breakpoints, by using the recombination detection program (RDP) v.4.85 (Martin et al., 2015) with default settings. RDP uses different recombination detecting programs like RDP, GENECONV, Chimaera, MaxChi, BOOTSCAN, SISCAN, 3Seq, and LARD to generate evidence of recombination. Recombination events supported by three or more algorithms present in RDP with significant P-values were considered positive events.

Data availability

Four near-complete viral genomes were deposited in GenBank, including two BCMVs (accession no. MW675689 and MW675688), one BCMNV (OK094708), and one ClYVV (MW675690).

Confirmation of identified viruses by RT-PCR

The presence of viruses identified by HTS was confirmed initially by RT-PCR by extracting the total RNA from samples used for HTS library preparation. The complementary DNA (cDNA) synthesis was done using RevertAid First Strand cDNA Synthesis Kit (Thermo Fisher Scientific Inc.) following the manufacturer's instructions with slight modification. Specific primers for each virus were designed based on highly conserved regions using Primer3Plus software (https://www.bioinformatics.nl/cgi-bin/primer3plus/primer3plus.cgi). The RT-PCR was performed in 25 μl reactions containing 12.5 μl of GoTaq Green Master Mix (2X) (Promega), 2 μl of template cDNA, 1 μl of each forward and reverse primer (10 μM), and 8.5 μl of nuclease-free water. The PCR program used for all the viruses was the same with an initial denaturation step of 95°C for 2 minutes, followed by 35 amplification cycles of 95°C for 30 seconds, 55°C for 30 seconds, 72°C for 1 minute, and final extension at 72°C for 10 minutes. The amplicons were resolved on 1 % agarose gel (containing TAE buffer) with 1Kb

ladder (Thermo Fisher Scientific Inc.) as molecular marker stained with ethidium bromide (Thermo Fisher Scientific Inc.) and first visualized on UV-transilluminator and then further analyzed on gel documentation system to capture gel images. The amplicons of each virus were sequenced for reconfirmation using Sanger sequencing (Biokart India Pvt. Ltd.).

RT-PCR-based incidence of identified viruses

All the collected samples (140) maintained at −80 °C were used to determine the distribution and incidences of identified viruses in the Kashmir valley by using RT-PCR. Total RNA extracted from these samples was subjected to RT-PCR as explained above. RT-PCR-based incidence was calculated as the percentage of plant samples infected with viruses.

Multiplex PCR

The multiplex PCR was optimized for the simultaneous detection of three identified viruses in this study. Samples having co-infection of all the identified viruses were used as positive control and healthy plant samples as a negative control for multiplex PCR. The total volume of the multiplex PCR reaction mixture was 25 μl containing four different primer sets and 12.5 μl GoTaq Green Master Mix (2X) (Promega). The primers used in uniplex PCR were also used in multiplex PCR. For the optimization and standardization of multiplex PCR, designed primer with different volumes from the working solution of 10μM concentrations (0.4, 0.5, 0.6, 0.8 μl) at varied annealing temperatures (50, 52, 55, and 58°C) was used. Amplification by multiplex PCR was performed at the initial denaturation step of 95°C for 2 minutes followed by 35 amplification cycles of denaturation at 95°C for 30 s, varied annealing temperatures (50, 52, 55, and 58°C) for 30 s, extension at 72°C for 1 min, and final extension temperature of 72°C for 10 min. The amplicon was electrophoresed in a 1% agarose gel (containing TAE buffer) with 1Kb ladder (Thermo Fisher Scientific Inc.) as a molecular marker run on 80 V for 1 h stained with ethidium bromide and visualized on UV transilluminator.

The total RNA isolated from infected plant samples had a concentration of 400 ng/ μl. To evaluate the sensitivity of multiplex PCR, the cDNA containing all the viruses was diluted 10-folds (10^{-1} to 10^{-8}) using nuclease-free water. Each dilution was used as a template for PCR to determine sensitivity.

Finally, the multiplex PCR assay standardized was validated on several common bean samples collected from the field.

Results

Virus identification and transcriptome assembly

The pooled RNA passed the quality control (QC) and showed an RNA integrity number (RIN) of 7.3. To guarantee the reliability of the data, QC was performed at each step of the procedure. A total of 16.9 GB of sequence data was obtained from Illumina sequencing of constructed cDNA libraries with 111783988 raw reads and 16879382188 bases. After trimming, we obtained 12051150320 bases with quality scores of Q30 and 49% GC content. *De novo* assembly of clean reads was performed using three different assemblers Trinity, Spades, and RNABloom generated 39837, 37429, and 50704 sequences, respectively, with N50 values for contigs ranging from 558 to 835 bp.

The contigs assembled were blasted against the virome database to determine the virus-associated contigs. Contigs that showed similarities with plant viruses were identified as BCMV, BCMNV, and ClYVV all belonging genus potyvirus, family potyviridae. A total of 50,315 to 58,778 virus-associated sequences were identified from these three assemblers, in which 16,781, 17,007, and 19,571 assembled sequences of BCMV, 16,759, 17,000, and 19,614 assembled sequences of BCMNV, and 16,775, 16,999, and 19593 assembled sequences of ClYVV were generated by Trinity, Spades, and RNABloom, respectively (Table 1). Taxonomic classification results showed that the majority of viral sequences were derived from BCMNV, representing 59% of total viral reads. BCMV and ClYVV were represented by 1% and 15% of total viral reads, respectively (Figure 2). The de novo assembly and Blastn results generated 18 partial/near-complete genomes of these viruses, including 10 genomes of BCMNV with the length between 308 and 9,967 nt, six genomes of BCMV with a size of 324 to 9964nt, and three genomes of ClYVV with lengths in the range from 227 to 9,759 nt (Supplementary Table 1).

RT-PCR confirmation of identified viruses

Viruses identified by HTS were confirmed by RT-PCR using specific primers for each virus against samples used for RNA-Seq. Four virus-specific primers designed based on highly conserved regions were used (Table 2). The presence of all three viruses was confirmed with an expected amplicon size of 442bp (BCMV 1), 661bp (BCMV 2), 834bp (BCMNV), and 1443bp (ClYVV). RT-PCR amplified virus-derived fragments were assessed on agarose gel (Figures 3A,B) and further confirmed by Sanger sequencing. Sequencing results showed 100% similarities with the contig sequences derived from the HTS data. Both the RT-PCR and HTS results indicated that all the viruses identified

TABLE 1 Descriptive statistics of assembled viral reads.

	Trinity			Spades			Rnabloom		
Virus strain	CYVV	BCMV	BCMNV	BCMV	CYVV	BCMNV	BCMV	CYVV	BCMNV
num_seqs	16775	16781	16759	17007	16999	17000	19571	19593	19614
sum_len	8468024	8552674	8456149	6869645	6877704	6878116	7919227	7857367	7910617
min_len	181	181	181	184	184	184	200	200	200
avg_len	504.8	509.7	504.6	403.9	404.6	404.6	404.6	401	403.3
max_len	20380	18822	20380	18012	18012	20379	18012	15738	16959
Q1	246	247	247	226	226	226	231	232	232
Q2	325	325	325	283	283	283	282	284	284
Q3	519	519	517	422	422	422	401	402	399
N50	584	594	582	429	430	430	405	402	402

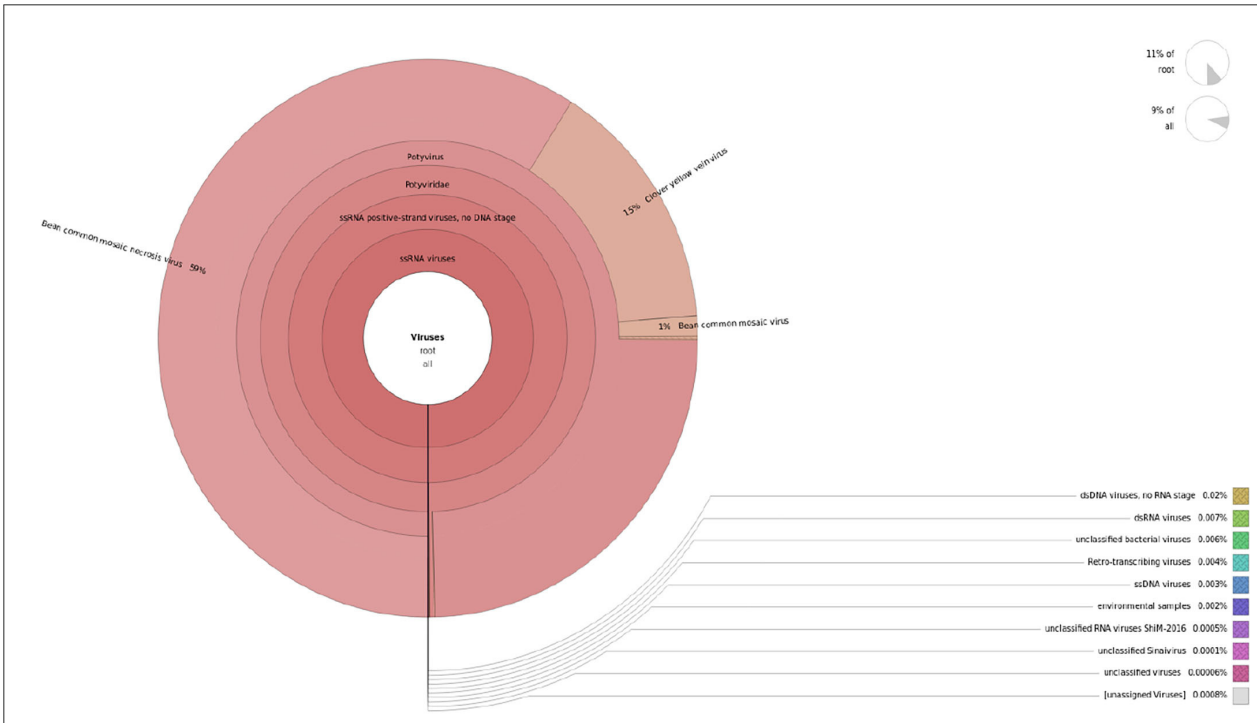

FIGURE 2
Krona representation of viral sequencing data obtained from Illumina.

by HTS were actually present in common bean samples sent for HTS sequencing.

Seventy-nine out of 140 samples were found positive for these viral pathogens, with BCMV, BCMNV, and ClYVV being present in all 79, 38, and 23 samples, respectively (Table 3). None of the asymptomatic samples showed the presence of these viruses. The majority of common bean samples showed positive reactions for more than one virus. The mixed infection rate was observed highest between BCMV and BCMNV. Among 79 samples, mixed infection was present in 44 samples. The BCMNV and ClYVV were always associated with BCMV and not a single sample was found in which only BCMNV or ClYVV was present. These were always present with BCMV in mixed infections as BCMV+ BCMNV + ClYVV or BCMV + BCMNV or BCMV + ClYVV.

RT-PCR of common bean samples from the Kashmir valley revealed the incidence of 56.42% for BCMV, 27.14% for BCMNV, and 16.42% for ClYVV. The highest incidence of all three viruses was observed from the field of SKUAST-K in the district Srinagar of central Kashmir. Of the 140 samples collected

TABLE 2 Primer designed and used in the present study.

S. No.	Primer Name		Primer Sequences 5′-3′ direction	Product Size (bp)
1	BCMV1	F1	TAGCTCACTTGGGGAATTGG	442
		R1	TGGATCAACAAAACGGATCA	
2	BCMV2	F1	GATTCTGGAGTGGGACAGGA	661
		R1	ATACTCGCCCTTCACAGCAT	
3	BCMNV	F1	ATGAACAGTGTGGCGAAGTG	834
		R1	GCTTTGTTGGGCTCTTCAAC	
4	ClYVV	F1	CAGTGCACCCAAGTCATGAG	1443
		R1	ACCTCACTTAGCTACTCTGTCAG	

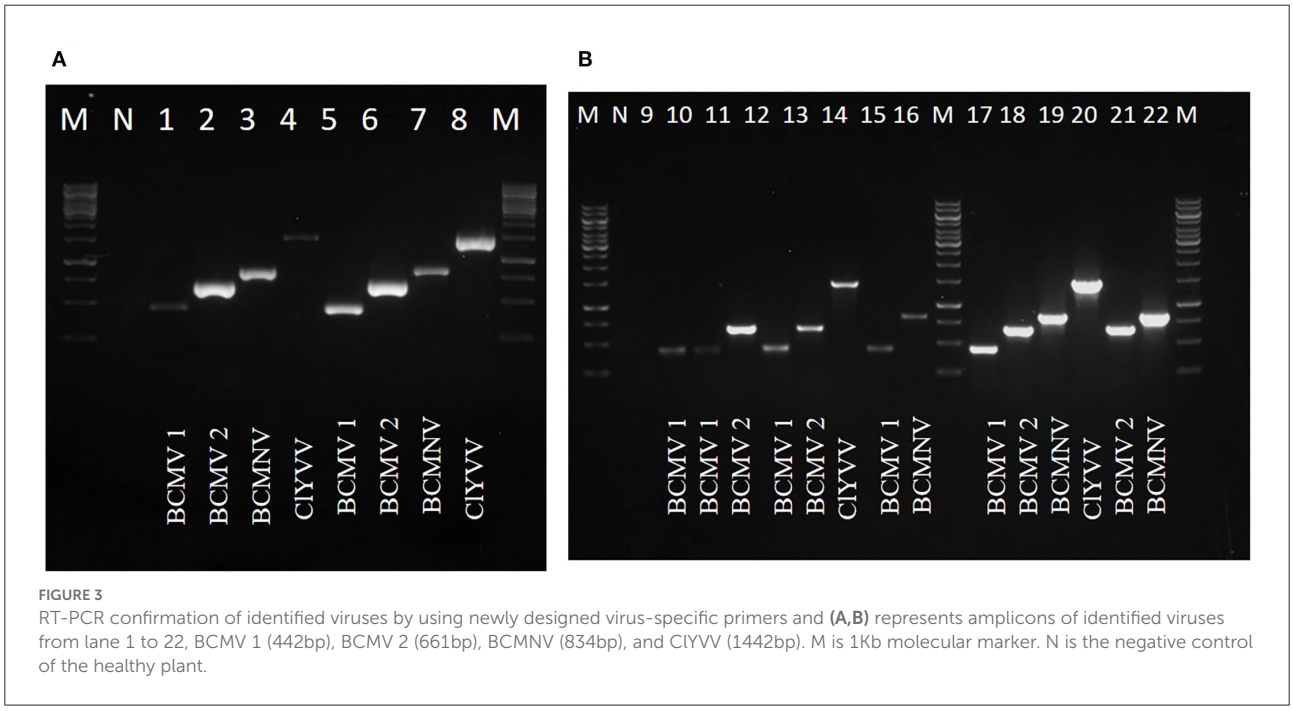

FIGURE 3
RT-PCR confirmation of identified viruses by using newly designed virus-specific primers and **(A,B)** represents amplicons of identified viruses from lane 1 to 22, BCMV 1 (442bp), BCMV 2 (661bp), BCMNV (834bp), and ClYVV (1442bp). M is 1Kb molecular marker. N is the negative control of the healthy plant.

from Kashmir, 43.57% samples had no viral infection. Results have also revealed that these viral pathogens were prevalent in all the different locations surveyed.

Genome organization, pairwise nucleotide comparison, and phylogenetic analysis of detected viruses

Two field BCMV isolates obtained from HTS were named BCMV 1 (MW675689) and BCMV 2 (MW675688), with genome sizes of 9964 and 9944 nt, respectively. The pairwise nucleotide identity between BCMV1 (Kash1) and BCMV2 (RU1) was 89%. The ORF of BCMV 1 comprises 9609 nt which encodes a predicted polyprotein of 3202 amino acids (aa). The two untranslated regions (UTR) in the 5' and 3' end of genomic RNA consisted of 127 nt and 238 nt, respectively (Table 4). The pairwise nucleotide identity of BCMV 1 with other similar BCMV isolates ranged from 83% to 94% (Figure 4A). The highest nucleotide identity of 94% was shared by sequences from the USA (KF919300, GQ219793, MH024843). The phylogenetic analysis showed a similar trend as indicated by pairwise analysis. The BCMV1 isolate clustered together with the six other BCMV isolates from the USA, Iran, and Tanzania in cluster III of the phylogenetic tree (Figure 5A).

In case of BCMV 2, the single polyprotein encodes for 3196 amino acids from 9591 nucleotide long ORF with 127 nt 5' UTR and 238 nt 3' UTR (Table 4). The pairwise nucleotide comparison found that BCMV 2 isolate showed 83% to 92% identity score range with known isolates in GenBank. The sequences from the USA (KF919298, KF919297, MH024843, GQ219793, KF919300) and Iran (MF498887) presented 92% identity scores with BCMV 2 isolate (Figure 4B). Similar results

TABLE 3 Distribution of viruses in Kashmir using RT-PCR.

S No.	Region	Districts	Site of Collection	No. of Samples Collected	No. of Samples Positive for Viruses			No. of Samples Negative for Viruses	No. of Multiple Infections
					BCMV	BCMNV	CYVV		
1	South Kashmir	Anantnag	Doru	10	5	2	1	5	2
			Zalangam	10	3	0	0	7	0
2		Pulwama	Kakapora	10	5	3	1	5	4
			Tikan	10	4	2	0	6	2
3	Central Kashmir	Srinagar	Noor bagh	10	7	3	2	3	4
			SKUAST-K	10	9	7	5	1	8
4		Budgam	Budgam	10	8	4	3	2	4
			Panzan	10	6	3	2	4	4
5		Ganderbal	Lar	10	6	2	2	4	3
			Prang	10	7	3	3	3	3
6	North Kashmir	Baramulla	Wadura	10	5	3	2	5	3
			Logripora	10	3	1	0	7	1
7		Kupwara	Cherkyoot	10	6	3	1	4	4
			Lalpora	10	5	2	1	5	2
		Total		140	79	38	23	61	44

TABLE 4 The genome size, organization, and accession numbers of viruses identified from common bean leaf samples from next-generation sequencing.

Virus name	Genome size (Kb)	5' UTR (nt)	Start codon	Stop codon	3'UTR	ORF size (Kb)	No. of amino acids	Accession no.
BCMV 1	10	127	128	9736	228	9.6	3202	MW675689
BCMV 2	10	125	126	9716	228	9.6	3196	MW675688
BCMNV	9.6	157	158	9373	228	9.2	3071	OK094708
ClYVV	9.8	286	287	9505	252	9.2	3072	MW675690

were reflected in phylogenetic analysis where BCMV 2 isolate clustered with isolates from the USA and Iran in cluster I (Figure 5B). The polyprotein comparison of BCMV 1 and BCMV 2 with the first 50 protein sequences in the NCBI GenBank revealed the percent identity of 87–98% and 89–94 %, respectively. Conserved domains of both the isolates of BCMV were also determined (Supplementary Figures 1A,B).

The near-complete genome of BCMNV obtained from HTS consisted of 9601 nt. The genomic RNA of BCMNV contained a single long ORF that starts at 158 nt and terminates at 9373 nt, encoding a single polyprotein of 3071 aa and 157 nt 5' UTR and 228 nt 3' UTR (Table 4). The polyprotein of BCMNV showed a similarity of more than 97% when compared with all other polyproteins of BCMNV available on NCBI. The conserved domains in BCMNV encoded protein were determined by using the conserved domain database (CDD) NCBI. The graphical results of the CD search obtained for BCMNV representing the whole viral genome are shown in Supplementary Figure 2A. This is the first near-complete genome sequence of BCMNV from India. The BCMNV isolate of the present study shared 96–99% pairwise identity with the other BCMNV isolates from NCBI GenBank. The isolates from Kenya (LC433691, MH169564, MH169566) and Zambia (MN987555) shared the highest pairwise nucleotide similarity of 99% (Figure 4C). Similar results were evident in phylogenetic analysis, where the identified BCMNV isolate formed a tight cluster with the above sequences in cluster I (Figure 5C).

The identified ClYVV isolate contained a genomic RNA of 9757nt including 5' (286 nt) and 3' (252 nt) UTR. The single large ORF of 9219 nt encodes a polyprotein of 3072 aa (Table 4). The polyprotein comparison of ClYVV shared more than 92% similarity with all other ClYVV protein sequences present on NCBI. Also, the functional CD of ClYVV was determined (Supplementary Figure 2B). This is the first

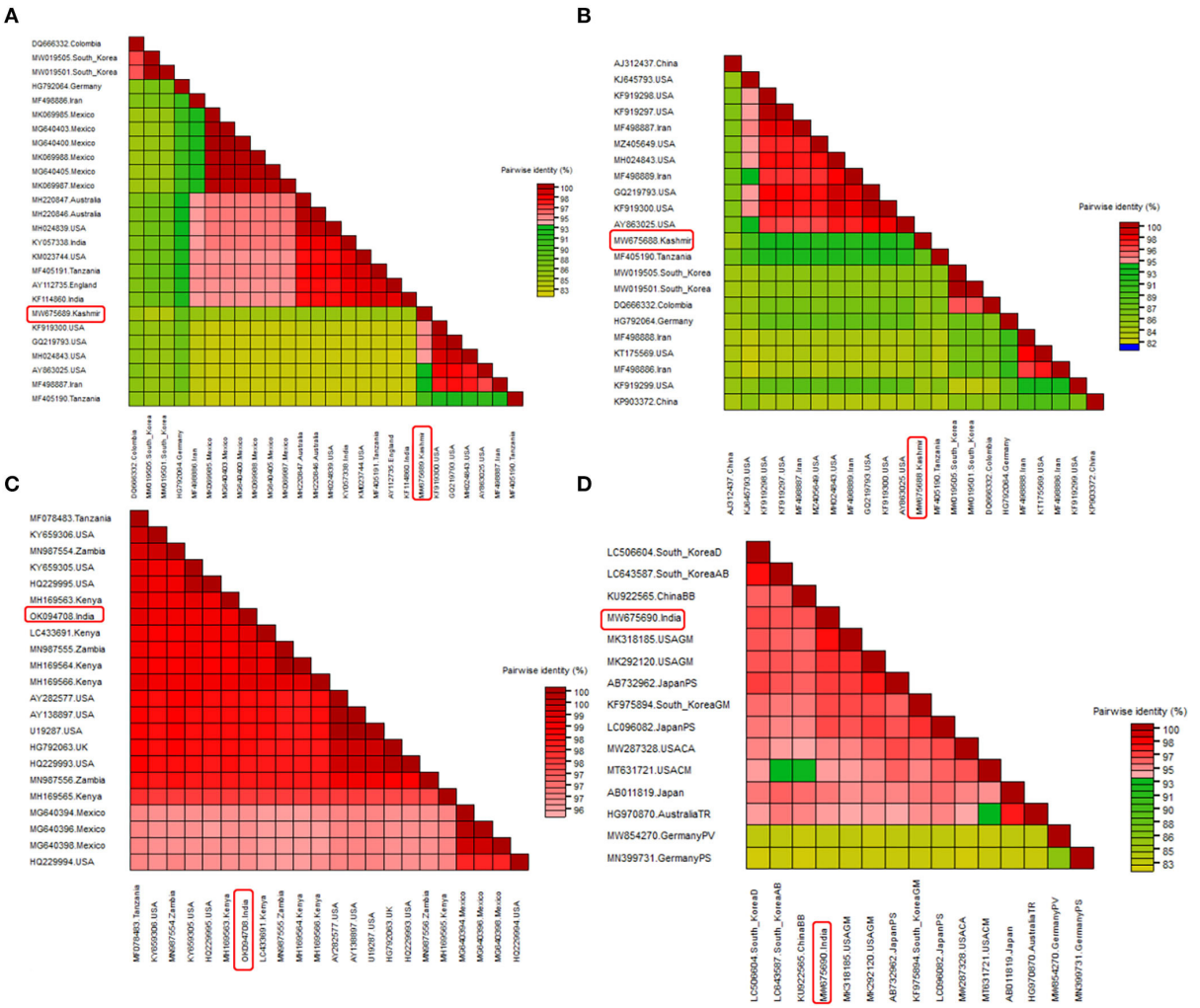

FIGURE 4
Pairwise nucleotide comparison of identified viruses along with closely related genomes obtained from GenBank NCBI database. Color coded matrix was generated using SDT. Each color in the matrix represents percent identity score. **(A)** Pairwise comparison of BCMV 1, **(B)** pairwise comparison of BCMV 2, **(C)** pairwise comparison of BCMNV, and **(D)** pairwise comparison of ClYVV.

report of ClYVV from India in common beans. The pairwise identity using SDT revealed that the reference sequence of USA (MK318185) showed more than 97% pairwise nucleotide identity (Figure 4D). In addition, phylogenetic analysis indicates that ClYVV recovered in this study was grouped in cluster I along with isolate from USA (MK318185) (Figure 5D).

To establish the inter-species phylogenetic relationship, a combined maximum likelihood phylogenetic tree was constructed using the available nucleotide and polyprotein sequences of all three viruses (Supplementary Figure 3). The 74 whole-genome sequences formed three highly supported clusters (I, II, III) representing 37 BCMV isolates (I), 22 BCMNV isolates (II), and 15 ClYVV isolates (III). BCMV isolates exhibited high diversity and variability with two sub-clusters (a and b) being classified. BCMV 1 and 2 were clustered closely in sub-cluster b along with genomes from Iran, the USA, China, and Tanzania. Also, the polyprotein sequences formed three clusters separating three viruses. But in contrast to nucleotide sequences, the two polyprotein sequences of BCMV isolates formed two separate sub-clusters (Supplementary Figure 4).

Recombination analysis

In potyviruses, recombination occurs frequently and is one of the major drivers that may affect the evolution of potyviruses (Zhou et al., 2014). The recombination events were detected in two isolates of BCMV and ClYVV identified in the current

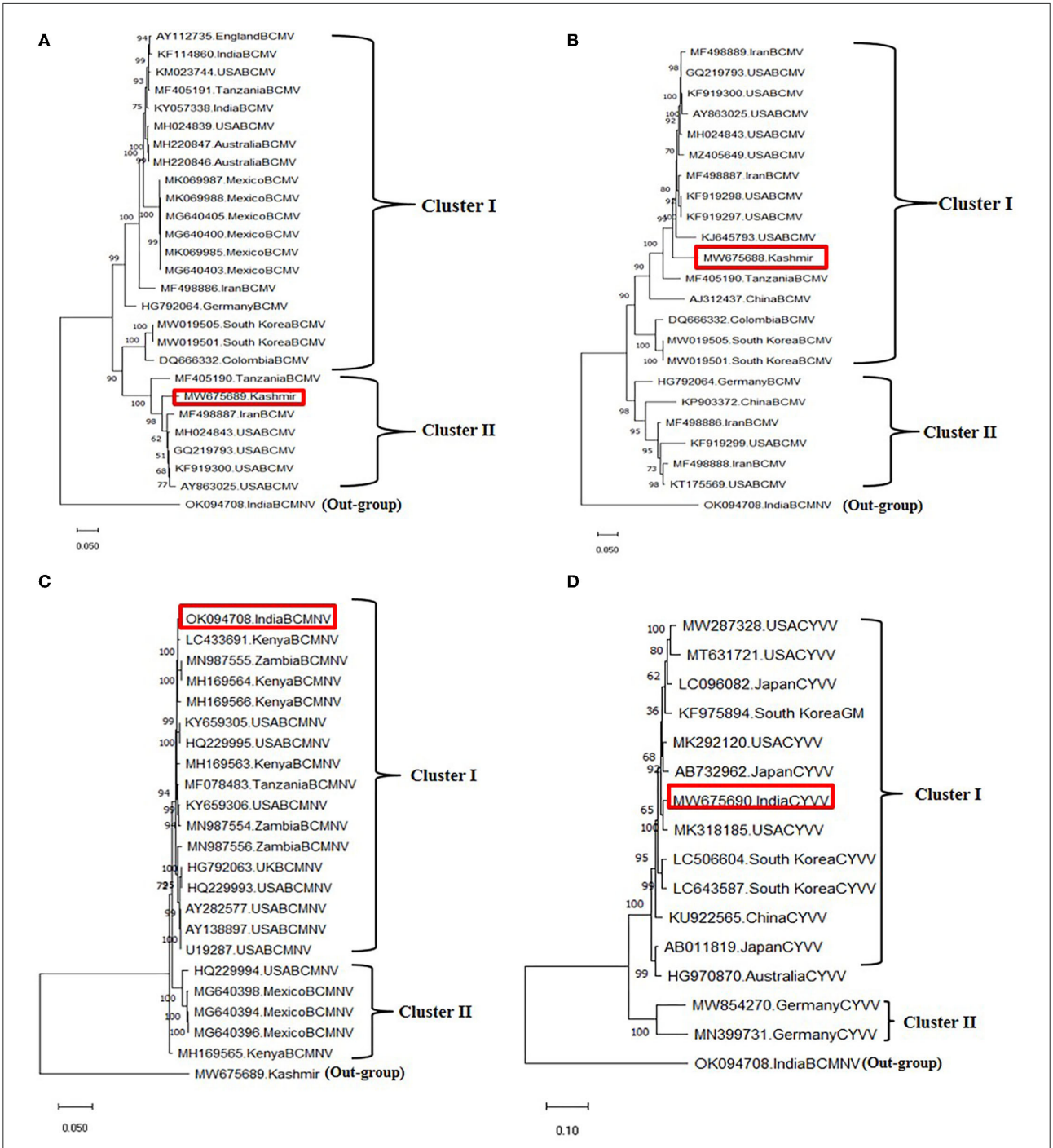

FIGURE 5
Phylogenetic analysis of identified viruses using whole genomes through maximum likelihood method using the MEGA X software. The scale indicates the number of substitutions per site. Highlighted in red in phylogeny represents the isolates of the present study. **(A)** Phylogenetic tree of BCMV 1, **(B)** phylogenetic tree of BCMV 2, **(C)** phylogenetic tree of BCMNV, and **(D)** phylogenetic tree ClYVV.

study. These recombination events were detected by three or more algorithms with associated P-values of $\leq 1.0x10^{-5}$. However, no traces of recombination were observed in the BCMNV isolate of the present study (Table 5, Figure 6).

Multiplex RT-PCR of identified viruses

It is important to develop the molecular diagnostics method for the detection of viruses infecting common beans. For that,

TABLE 5 The recombination events detected along with major and minor parents, p-value of viruses detected in common bean.

Virus Name	Event	Recombinant	Major parent	Minor parent	Break point start	Break point end	Methods						
							RDP	BOOTSCAN	GENECONV	MAXCHI	CHIMAERA	SISCAN	3Seq
							P-value						
BCMV 1	1	MW675689	HG792064 (Germany)	Unknown	20	1,947	2.278×10^{-210}	1.726×10^{-82}	1.154×10^{-265}	2.644×10^{-52}	3.477×10^{-18}	2.513×10^{-35}	1.927×10^{-10}
	2	MW675689	KF919300 (USA)	KM023744 (USA)	6,446	9,468	6.226×10^{-134}	1.025×10^{-133}	3.612×10^{-130}	5.988×10^{-44}	4.076×10^{-45}	3.635×10^{-52}	4.425×10^{-53}
	3	MW675689	MW019505 (South Korea)	Unknown	9,537	9,911	1.238×10^{-24}	–	6.008×10^{-21}	–	1.153×10^{-06}	2.937×10^{-17}	2.247×10^{-13}
BCMV 2	1	MW675688	Unknown	KF919298 (USA)	32	748	1.082×10^{-10}	3.769×10^{-05}	3.010×10^{-07}	4.346×10^{-13}	3.150×10^{-09}	3.628×10^{-15}	1.476×10^{-13}
	2	MW675688	MH024843 (USA)	Unknown	868	1,363	4.386×10^{-70}	7.988×10^{-64}	2.657×10^{-67}	2.860×10^{-21}	1.557×10^{-21}	2.024×10^{-19}	4.429×10^{-13}
	3	MW675688	KJ645793 (USA)	KT175569 (USA)	1,364	3,420	1.948×10^{-118}	5.766×10^{-106}	1.234×10^{-99}	7.000×10^{-36}	1.632×10^{-20}	8.279×10^{-33}	1.476×10^{-13}
	4	MW675688	MF498888 (Iran)	Unknown	9,627	10,011	1.311×10^{-24}	4.481×10^{-24}	7.536×10^{-27}	1.337×10^{-09}	8.326×10^{-07}	4.359×10^{-15}	1.476×10^{-13}
BCMNV							**No Recombination**						
ClYVV	1	MW675690	AB732962 (Japan)	AB011819 (Japan)	567	1,938	6.739×10^{-06}	$2.050\text{x}10^{-06}$-	–	5.113×10^{-09}	1.869×10^{-08}	3.070×10^{-10}	-
	2	MW675690	LC506604 (South Korea)	Unknown	2628	3,389	–	5.789×10^{-05}	–	1.009×10^{-05}	4.730×10^{-05}	–	–

10.3389/fmicb.2022.943382

FIGURE 6
Recombination events detected in identified viruses by using RDP. Position of our isolate is highlighted in red color. **(A)** Three recombination events detected in BCMV 1, **(B)** four recombination events detected in BCMV 2, **(C)** recombination was not found in BCMNV, and **(D)** two recombination events detected in ClYVV.

specific primers were designed against the identified viruses and the multiplex PCR was standardized. Samples with multiple infections confirmed by uniplex PCR (positive control) were used for the optimization of multiplex PCR assay. The various experiments showed that when different annealing temperatures ranging from 50°C to 58°C were used, optimum results with no unspecific bands were obtained at 55°C with 0.4 µl from a working solution of 10µM concentration of each primer pair. The designed primers successfully generated their respective amplicons only from infected samples. In case of cDNA from a healthy plant, no amplicon was observed. The results of multiplex PCR were visualized by using gel electrophoresis on the gel documentation system (Figure 7A).

The detection limit of multiplex PCR using a 10-fold serial dilution of cDNA showed positive results up to a dilution of 10^{-5} for both BCMV and ClYVV and 10^{-4} for BCMNV. All three viruses were detected simultaneously by multiplex PCR up to a dilution of 10^{-4}. To test the consistency and reproducibility of results with identical conditions, multiplex PCR was validated on several common bean samples infected with these viruses. All the viruses were identified from tested samples and the expected amplified fragments were visualized on 1% agarose gel (Figures 7B,C).

Discussion

Viral metatranscriptomics along with bioinformatic tools has revolutionized plant virus discovery, detection, genome sequencing, transcriptomics, ecology, and epidemiology (Barba et al., 2014). The application of HTS to plant viral diagnostics has resulted in a significant increase in the number and frequency of new viruses detected. This new technology not only detects viruses of known sequences but also identifies untargeted viral pathogens regardless of their genomic nature or structure (Ibaba and Gubba, 2020). Virome analysis investigates all the viral genomes present in plant tissues, as well as their complexity, replication, mutation, and changes in response to diverse environments (Jo et al., 2020). Recently, several HTS-based studies have intensively explored common beans infected by viruses in different countries (Nordenstedt et al., 2017; Mutuku et al., 2018; Mwaipopo et al., 2018; Alves-Freitas et al., 2019).

Our goal in this study was to survey common bean fields in Kashmir for virus infection and to investigate molecular variability and genetic diversity of identified viruses by using HTS and downstream molecular techniques. Symptomatic as well as non-symptomatic samples were collected in our study to ensure that potential cryptic viruses would not escape from

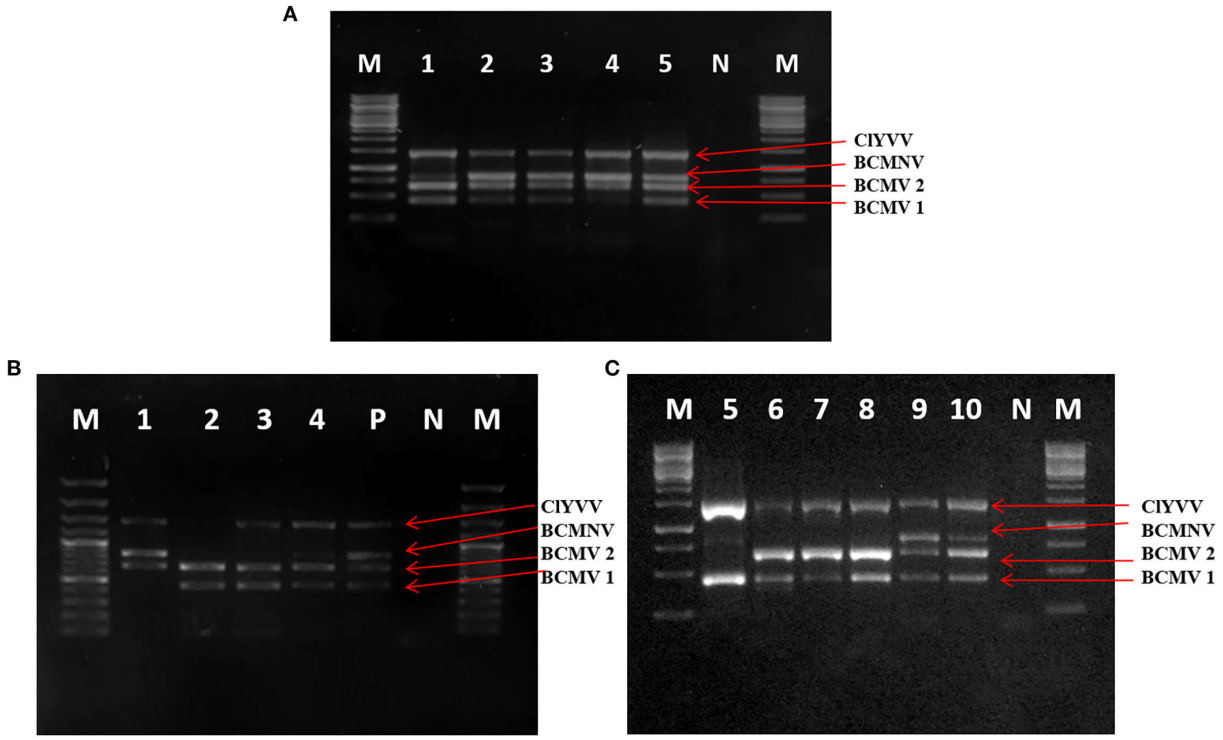

FIGURE 7
Optimization of multiplex PCR using specific primers of BCMV 1, BCMV 2, BCMNV, and ClYVV in RT-PCR assay. **(A)** Lane 1–5: PCR product using RNA with BCMV 1, BCMV 2, BCMNV, and ClYVV infection from positive control as a template for assay. **(B,C)** Simultaneous detection of bean viruses in multiplex RT-PCR by using RNA extracted from 10 field samples collected from SKUAST-K. Lanes 1–10 are amplified products of representative field samples. M is 1Kb molecular marker, P is positive control obtained from infected plants with all three viruses, and N is a negative control from a healthy plant.

detection. Sample pooling is an efficient way to balance virus identification and cost reduction. Ribosomal RNA-depleted total RNA was used for virome analysis. This method has been used successfully to detect both RNA and DNA viruses (Gaafar et al., 2020). Among the three viruses we identified, neither BCMNV nor ClYVV has been documented to occur in common bean fields of India before. BCMV occurrence in Kashmir was previously reported by Hamid et al. (2013). Our work represents the first viral metatranscriptomics study of infected common beans in India.

Mixed infection of plants by different viruses occurs commonly in nature as the consequence of successive vector inoculations (Rubio et al., 2020). We observe the association of BCMV to BCMNV or ClYVV infection in our study, indicating that mixed infections are not in the manner of random combinations. Some symptomatic samples in our study turned out to be RT-PCR negative. Their virus-infection-like symptoms could be due to nutrient deficiencies, deformities, and/or other injuries (Chiquito-Almanza et al., 2017). Fungal or bacterial infection of vascular tissues and roots may also resemble virus-caused symptoms (Nordenstedt et al., 2017). Most of the virus-infected samples were from the district of Srinagar, which could be due to the vector population difference affected by the altitudes (Myers et al., 2000). Consistent with previous surveys in India (Yaraguntaiah and Nariani, 1963) and particularly in Kashmir (Hamid et al., 2013), BCMV is the predominant common bean-infecting virus in Kashmir as revealed by our latest surveillance. BCMNV and ClYVV could be introduced just recently.

The genome sizes (~10 Kb) of the three viruses identified were similar to those of other potyviruses (Takahashi et al., 1997; Worrall et al., 2015). The pairwise nucleotide identities of potyvirus genomes from different species are generally lower than 76% (Adams et al., 2005). A sequence similarity greater than this value represents different isolates of the same species. Unlike BCMV or ClYVV, the BCMNV isolate we identified has less than 10% divergence from other known isolates. This is consistent with previous studies detecting low diversity among BCMNV isolates (Collins et al., 2019). The combined phylogenetic analysis detects higher diversity in BCMV isolates, which is also consistent with the previous study (Worrall et al., 2015). The similarity and close clustering of our identified

viruses with the isolates from the USA, Kenya, Tanzania, and Iran indicate that these viruses might have been introduced from the countries mentioned above (Collins et al., 2019; Sidharthan et al., 2020).

In potyviruses, recombination frequently occurs to serve as an important source of genetic variation (Seo et al., 2009; Zhou et al., 2014). Recombination also drives the genesis of new viral strains (Zhou et al., 2014; Worrall et al., 2015). Recombination rates in individual potyviruses could differ significantly (Revers et al., 1996). Feng et al. (2014) recently described a new recombinant strain RU-1M of BCMV, which causes temperature-independent necrosis in common bean plants harboring dominant I gene and recessive bc1 resistant gene. This study indicates that recombination may increase the threat of overcoming host resistance. The recombination events found in our BCMV and ClYVV isolates may facilitate their spread in Kashmir. Despite previously reported recombination in BCMNV (Larsen et al., 2005; Wainaina et al., 2019), no trace of recombination is found in the BCMNV isolate we reported in our study. The absence could be attributed to the founder effect caused by the initial introduction of low-diverse BCMNV variants to Kashmir (Seo et al., 2009).

Previous studies have shown the effectiveness of multiplex PCR in the simultaneous detection of three (Chiquito-Almanza et al., 2017), six (Cating et al., 2015), seven (Kwon et al., 2014; Zhao et al., 2015), eight (Kwak et al., 2014), and up to nine (Gambino, 2015) pathogens. The purpose of our optimization of multiplex PCR was to develop a robust, flexible, and accurate diagnostic tool for the detection of the identified viruses, as they produce similar symptoms and can be found within their hosts in multiple co-infections. Parameters posing challenges in multiplex PCR range from annealing temperature to master mix ingredients. Sensitivity of multiplex PCR was determined by the dilution of cDNA and all the viruses were amplified up to 10^{-4} dilution, indicating that these viruses can be detected simultaneously at lower concentrations of template cDNA. The optimized multiplex PCR assay developed in the present study can be used in virus diagnostic assays, seed certification, and crop improvement programs to obtain virus-free seed stocks.

The host resistance has been found to be the most efficient and economical option for managing the viral disease (Wagara and Kimani, 2007). In the present study, we found that common beans are infected by multiple viruses simultaneously, so the dominant I gene present in some bean cultivars may not be enough in conferring resistance against these viruses, being susceptible to BCMNV. The recessive resistant alleles available are strain specific to these viruses and, therefore, to provide broad resistance to the different strains of BCMNV and BCMV it is difficult to breed common bean cultivars using these genes individually. Thus, molecular markers can be used for pyramiding recessive genes (bc-u, bc-1, bc-1^2, bc-2, bc-2^2, and bc-3) along with the dominant I gene in order to develop the broadest resistance possible (Pasev et al., 2014).

Contribution to the field

The present study has shown that HTS assay is a valuable and powerful tool for the detection and identification of virome in common beans. This diagnostic approach has superior accuracy and sensitivity, which enables early identification of viral diseases, critical for limiting their spread. In our study, we utilized HTS-based method and identified three potyviruses from common beans, with BCMNV and ClYVV being reported for the first time from India. BCMV was found most prevalent virus followed by BCMNV and ClYVV. Since all three viruses are aphid transmitted in a non-persistent manner and BCMV and BCMNV are also seed transmitted, these viruses have the potential to cause epidemic along with vector transmission and can emerge as major constraints in bean production. So, there is a need to establish efficient control measures in developing countries to limit the spread and transmission of these identified viruses. We also developed a multiplex PCR protocol that can be used for the detection and diagnosis of these viruses and can also aid in seed certification, quarantine, and crop improvement programs to produce virus-free seed material. Our HTS-based viral metatranscriptomics analysis adds genomic information on viruses infecting beans, thereby enabling rapid response to emerging viral diseases of this crop.

Data availability statement

The datasets presented in this study can be found in online repositories. The names of the repository/repositories and accession number(s) can be found below: https://www.ncbi.nlm.nih.gov/, MW675689, MW675688, OK094708, and MW675690.

Author contributions

Conceptualization: AH. Methodology, software, writing-original draft preparation, and visualization: AH and SR. Validation: AH, SR, and ZD. Formal analysis: AH, SR, and GA. Investigation: AH, SR, GA, TS, and ZD. Resources, supervision, and funding acquisition: AH and ZD. Data curation: AH and HP. Writing–review and editing: AH, SR, GA, TS, and ZD. Project administration: AH. All authors contributed to the article and approved the submitted version.

Funding

This work has been funded by ICAR-IISS, Mau.

Conflict of interest

The authors declare that the research was conducted in the absence of any commercial or financial relationships that could be construed as a potential conflict of interest.

Publisher's note

All claims expressed in this article are solely those of the authors and do not necessarily represent those of their affiliated organizations, or those of the publisher, the editors and the reviewers. Any product that may be evaluated in this article, or claim that may be made by its manufacturer, is not guaranteed or endorsed by the publisher.

Supplementary material

The Supplementary Material for this article can be found online at: https://www.frontiersin.org/articles/10.3389/fmicb.2022.943382/full#supplementary-material

References

Adams, I. P., Glover, R. H., Monger, W. A., Mumford, R., Jackeviciene, E., Navalinskiene, M., et al. (2009). Next-generation sequencing and metagenomic analysis: a universal diagnostic tool in plant virology. *Mol. Plant Pathol.* 10, 537–545. doi: 10.1111/j.1364-3703.2009.00545.x

Adams, M. J., Antoniw, J. F., and Fauquet, C. M. (2005). Molecular criteria for genus and species discrimination within the family Potyviridae. *Arch. Virol.* 150,459–479. doi: 10.1007/s00705-004-0440-6

Akinyemi, I. A., Wang, F., Zhou, B., Qi, S., and Wu, Q. (2016). Ecogenomic survey of plant viruses infecting tobacco by next generation sequencing. *Virol. J.* 13,.1–12. doi: 10.1186/s12985-016-0639-7

Alves-Freitas, D. M., Pinheiro-Lima, B., Faria, J. C., Lacorte, C., Ribeiro, S. G., and Melo, F. L. (2019). Double-stranded RNA high-throughput sequencing reveals a new cytorhabdovirus in a bean golden mosaic virus-resistant common bean transgenic line. *Viruses* 11, 90. doi: 10.3390/v11010090

Barba, M., Czosnek, H., and Hadidi, A. (2014). Historical perspective, development and applications of next-generation sequencing in plant virology. *Viruses* 6, 106–136. doi: 10.3390/v6010106

Bonfim, K., Faria, J. C., Nogueira, E. O., Mendes, É. A., and Aragão, F. J. (2007). RNAi-mediated resistance to Bean golden mosaic virus in genetically engineered common bean (Phaseolus vulgaris). *Mol. Plant Microbe Interact.* 20,717–726. doi: 10.1094/MPMI-20-6-0717

Cating, R. A., Funke, C. N., Kaur, N., Hamm, P. B., and Frost, K. E. (2015). A multiplex reverse transcription (RT) high-fidelity PCR protocol for the detection of six viruses that cause potato tuber necrosis. *Am. J. Potato Res.* 92, 536–540. doi: 10.1007/s12230-015-9457-5

Celmeli, T., Sari, H., Canci, H., Sari, D., Adak, A., Eker, T., et al. (2018). The nutritional content of common bean (*Phaseolus vulgaris* L.) landraces in comparison to modern varieties. *Agronomy.* 8, 166. doi: 10.3390/agronomy8090166

Chen, S., Zhou, Y., Chen, Y., and Gu, J. (2018). fastp: an ultra-fast all-in-one FASTQ preprocessor. *Bioinformatics.* 35, 884–890. doi: 10.1093/bioinformatics/bty560

Chiquito-Almanza, E., Acosta-Gallegos, J. A., García-Alvarez, N. C., Garrido-Ramirez, E. R., Montero-Tavera, V., Guevara-Olvera, L., et al. (2017). Simultaneous detection of both RNA and DNA viruses infecting dry bean and occurrence of mixed infections by BGYMV, BCMV and BCMNV in the Central-west region of Mexico. *Viruses*9, 63. doi: 10.3390/v9040063

Choudhary, N., Hamid, A., Singh, B., Khandy, I., Sofi, P. A., Bhat, M. A., et al. (2018). Insight into the origin of common bean (*Phaseolus vulgaris* L.) grown in the state of Jammu and Kashmir of north-western Himalayas. *Genet. Resour. Crop Evol.* 65, 963–977. doi: 10.1007/s10722-017-0588-z

Cock, P. J., Fields, C. J., Goto, N., Heuer, M. L., and Rice, P. M. (2010). The Sanger FASTQ file format for sequences with quality scores, and the Solexa/Illumina FASTQ variants. *Nucleic Acids Res.* 38, 1767–1771. doi: 10.1093/nar/gkp1137

Collins, M. B., Karakacha, W. H., Benard, M., and Milicent, N. A. (2019). First full length genome sequence of bean common mosaic necrosis virus (BCMNV) isolated from common bean in Western Kenya. *Int. J. Genet. Genomics.* 7, 132. doi: 10.11648/j.ijgg.20190704.18

FAOSTAT. (2021). *2021: FAO Statistical Databases.* Available online at: http://www.fao.org/faostat/

Feng, X., Poplawsky, A. R., Nikolaeva, O. V., Myers, J. R., and Karasev, A. (2014). Recombinants of bean common mosaic virus (BCMV) and genetic determinants of BCMV involved in overcoming resistance in common bean. *Phytopathology.* 104, 786–793. doi: 10.1094/PHYTO-08-13-0243-R

Gaafar, Y. Z., Herz, K., Hartrick, J., Fletcher, J., Blouin, A. G., MacDiarmid, R., et al. (2020). Investigating the pea virome in Germany—old friends and new players in the field(s). *Front. Microbiol.* 11. doi: 10.3389/fmicb.2020.583242

Gambino, G. (2015). Multiplex RT-PCR method for the simultaneous detection of nine grapevine viruses. In Plant Virology Protocols Humana Press, New York, NY, 39-47.

Garrido-Ramirez, E. R., Sudarshana, M. R. and Gilbertson, R. L. (2000). Bean golden yellow mosaic virus from Chiapas, Mexico: characterization, pseudorecombination with other bean-infecting geminiviruses and germ plasm screening. *Phytopathology.* 90, 1224–1232. doi: 10.1094/PHYTO.2000.90.11.1224

Hall, R. (1991). *Compendium of Bean Diseases.* St Paul (MN): APS Press Publishers. p. 102.

Hall, T. A. (1999). BioEdit: a user-friendly biological sequence alignment editor and analysis program for Windows 95/98/NT. *Nucl. Acids. Symp. Ser.* 41, 95–98.

Hamid, A., Ahmad, M., Padder, B. A., Shah, M. D., Saleem, S., Sofi, T. A., et al. (2013). Pathogenic and coat protein characterization confirming the occurrence of Bean common mosaic virus on common bean (Phaseolus vulgaris) in Kashmir, India. *Phytoparasitica.* 42, 317–322. doi: 10.1007/s12600-013-0362-5

Henschel, R., Lieber, M., Wu, L. S., Nista, P. M., Haas, B. J., and LeDuc, R. D. (2012). "Trinity RNA-Seq assembler performance optimization," in *Proceedings of the 1st Conference of the Extreme Science and Engineering Discovery Environment: Bridging from the extreme to the campus and beyond* (New York, NY: Association for Computing Machinery), 1–8. doi: 10.1145/2335755.2335842

Ibaba, J. D., and Gubba, A. (2020). High-throughput sequencing application in the diagnosis and discovery of plant-infecting viruses in Africa, a decade later. *Plants.* 9,1376. doi: 10.3390/plants9101376

Jo, Y., Kim, S. M., Choi, H., Yang, J. W., Lee, B. C., and Cho, W. K. (2020). Sweet potato viromes in eight different geographical regions in Korea and two different cultivars. *Sci. Rep.* 10, 1–16. doi: 10.1038/s41598-020-59518-x

Jones, S., Baizan-Edge, A., MacFarlane, S., and Torrance, L. (2017). Viral diagnostics in plants using next generation sequencing: computational analysis in practice. *Front. Plant Sci.* 8, (1770). doi: 10.3389/fpls.2017.01770

Kesanakurti, P., Belton, M., Saeed, H., Rast, H., Boyes, I., and Rott, M. (2016). Screening for plant viruses by next generation sequencing using a modified double strand RNA extraction protocol with an internal amplification control. *J. Virol. Methods* 23635–40. doi: 10.1016/j.jviromet.2016.07.001

Kreuze, J. F., Perez, A., Untiveros, M., Quispe, D., Fuentes, S., Barker, I., et al. (2009). Complete viral genome sequence and discovery of novel viruses by deep sequencing of small RNAs. A generic method for diagnosis, discovery and sequencing of viruses. *Virology* 388, 1–7. doi: 10.1016/j.virol.2009.03.024

Kumar, S., Stecher, G., Li, M., Knyaz, C., and Tamura, K. (2018). MEGA X: molecular evolutionary genetics analysis across computing platforms. *Mol. Biol. Evol.* 35, 1547. doi: 10.1093/molbev/msy096

Kwak, H. R., Kim, M. K., Shin, J. C., Lee, Y. J., Seo, J. K., Lee, H. U., et al. (2014). The current incidence of viral disease in Korean sweet potatoes and development of

multiplex RT-PCR assays for simultaneous detection of eight sweet potato viruses. *Plant Pathol. J.* 30, 416–424. doi: 10.5423/PPJ.OA.04.2014.0029

Kwon, J. Y., Hong, J. S., Kim, M. J., Choi, S. H., Min, B. E., Song, E. G., et al. (2014). Simultaneous multiplex PCR detection of seven cucurbit infecting viruses. *J. Virol. Methods* 206, 133–139. doi: 10.1016/j.jviromet.2014.06.009

Larsen, R. C., Miklas, P. N., Druffel, K. L., and Wyatt, S. D. (2005). NL-3 K strain is a stable and naturally occurring interspecific recombinant derived from bean common mosaic necrosis virus and bean common mosaic virus. *Phytopathology.* 95, 1037–1042. doi: 10.1094/PHYTO-95-1037

Larsen, R. C., Miklas, P. N., Eastwell, K. C., and Grau, C. R. (2008). A strain of Clover yellow vein virus that causes severe pod necrosis disease in snap bean. *Plant Dis*. 92, 1026–1032. doi: 10.1094/PDIS-92-7-1026

Loebenstein, G., and Thottappilly, G. (2004). Virus and virus-like diseases of major crops in developing countries. Dordrecht: Kluwer Academic Publishers. p. 840. doi: 10.1007/978-94-007-0791-7

Maree, H. J., Fox, A., Al Rwahnih, M., Boonham, N., and Candresse, T. (2018). Application of HTS for routine plant virus diagnostics: state of the art and challenges. *Front. Plant Sci*. 9,.1082. doi: 10.3389/fpls.2018.01082

Martin, D. P., Murrell, B., Golden, M., Khoosal, A., and Muhire, B. (2015). RDP4: Detection and analysis of recombination patterns in virus genomes. *Virus Evol.* 1. doi: 10.1093/ve/vev003

Matthews, R. E. F. (1982). Classification and nomenclature of viruses. Forth report of the international committee on taxonomy of viruses. *Intervirology* 17, 1–199. doi: 10.1159/000149278

Menzel, P., Ng, K. L., and Krogh, A. (2016). Fast and sensitive taxonomic classification for metagenomics with Kaiju. *Nat. Commun.* 7, 1–9. doi: 10.1038/ncomms11257

Morales, F. J. (1986). Virus disease of beans in the tropics. *Rev. Trop. Plant Pathol.* 3, 405–409.

Muhire, B. M., Varsani, A., and Martin, D. P. (2014). SDT: a virus classification tool based on pairwise sequence alignment and identity calculation. *PloS ONE.* 9, 108277. doi: 10.1371/journal.pone.0108277

Mutuku, J. M., Wamonje, F. O., Mukeshimana, G., Njuguna, J., Wamalwa, M., Choi, S. K., et al. (2018). Metagenomic analysis of plant virus occurrence in common bean (Phaseolus vulgaris) in Central Kenya. *Front. Microbiol.* 9, 2939. doi: 10.3389/fmicb.2018.02939

Mwaipopo, B., Nchimbi-Msolla, S., Njau, P. J., Mark, D., and Mbanzibwa, D. R. (2018). Comprehensive surveys of Bean common mosaic virus and Bean common mosaic necrosis virus and molecular evidence for occurrence of other Phaseolus vulgaris viruses in Tanzania. *Plant Dis.* 102,2361–2370. doi: 10.1094/PDIS-01-18-0198-RE

Myers, J. R., Mink, G. A., and Mabagala, R. (2000). "Surveys for Bean common mosaic virus in East Africa," in *Annual Report of the Bean ImprovementCooperative* (Washington, DC: Department of Agriculture), 13–14.

Nadeem, M. A., Yeken, M. Z., Shahid, M. Q., Habyarimana, E., Yilmaz, H., Alsaleh, A., et al. (2021). Common bean as a potential crop for future food security: an overview of past, current and future contributions in genomics, transcriptomics, transgenics and proteomics. *Biotechnol. Biotechnol. Equip*. 35, 758–786. doi: 10.1080/13102818.2021.1920462

Nip, K. M., Chiu, R., Yang, C., Chu, J., Mohamadi, H., Warren, R. L., et al. (2020). RNA-Bloom enables reference-free and reference-guided sequence assembly for single-cell transcriptomes. *Genome Res*. 30, 1191–1200. doi: 10.1101/gr.260174.119

Nordenstedt, N., Marcenaro, D., Chilagane, D., Mwaipopo, B., Rajamäki, M. L., Nchimbi-Msolla, S., et al. (2017). Pathogenic seedborne viruses are rare but Phaseolus vulgaris endornaviruses are common in bean varieties grown in Nicaragua and Tanzania. *PLoS ONE.* 12, 0178242. doi: 10.1371/journal.pone.0178242

Pasev, G., Kostova, D., and Sofkova, S. (2014). Identification of genes for resistance to Bean common mosaic virus and Bean common mosaic necrosis virus in snap bean (Phaseolus vulgaris L.) breeding lines using conventional and molecular methods. *J. Phytopathol*. 162, 19–25. doi: 10.1111/jph.12149

Prjibelski, A., Antipov, D., Meleshko, D., Lapidus, A., and Korobeynikov, A. (2020). Using SPAdes de novo assembler. *Curr. Protoc. Bioinform* 70,102. doi: 10.1002/cpbi.102

Revers, F., Le Gall, O., Candresse, T., Le Romancer, M., and Dunez, J. (1996). Frequent occurrence of recombinant potyvirus isolates. *J. Gen. Virol.* 77, 1953–1965. doi: 10.1099/0022-1317-77-8-1953

Rubio, L., Galipienso, L., and Ferriol, I. (2020). Detection of plant viruses and disease management: relevance of genetic diversity and evolution. *Front. Plant Sci*. 11, 1092. doi: 10.3389/fpls.2020.01092

Seo, J. K., Ohshima, K., Lee, H. G., Son, M., Choi, H. S., Lee, S. H., et al. (2009). Molecular variability and genetic structure of the population of Soybean mosaic virus based on the analysis of complete genome sequences. *Virology.* 393,91–103. doi: 10.1016/j.virol.2009.07.007

Sidharthan, V. K., Sevanthi, A. M., Jaiswal, S., and Baranwal, V. K. (2020). Robust virome profiling and whole genome reconstruction of viruses and viroids enabled by use of available mRNA and sRNA-Seq datasets in grapevine (Vitisvinifera L.). *Front. Microbiol*. 11,1232. doi: 10.3389/fmicb.2020.01232

Takahashi, Y., Takahashi, T., and Uyeda, I. (1997). A cDNA clone to clover yellow vein potyvirus genome is highly infectious. *Virus Genes.* 14, 235–243. doi: 10.1023/A:1007940028058

Wagara, I. N., and Kimani, P. M. (2007). Resistance of nutrient-rich bean varieties to major biotic constraints in Kenya. *Afr. Crop Sci. J.* 8, 2087–2090.

Wainaina, J. M., Kubatko, L., Harvey, J., Ateka, E., Makori, T., Karanja, D., et al. (2019). Evolutionary insights of Bean common mosaic necrosis virus and Cowpea aphid-borne mosaic virus. *Peer J.* 7, 6297. doi: 10.7717/peerj.6297

Worrall, E. A., Wamonje, F. O., Mukeshimana, G., Harvey, J. J., Carr, J. P., and Mitter, N. (2015). Bean common mosaic virus and Bean common mosaic necrosis virus: relationships, biology, and prospects for control. *Adv. Virus Res*. 93, 1–46. doi: 10.1016/bs.aivir.2015.04.002

Xu, Y., Li, S., Na, C., Yang, L., and Lu, M. (2019). Analyses of virus/viroid communities in nectarine trees by next-generation sequencing and insight into viral synergisms implication in host disease symptoms. *Sci. Rep*. 9, 1–12. doi: 10.1038/s41598-019-48714-z

Yaraguntaiah, R. C., and Nariani, T. K. (1963). Bean mosaic virus in India. *Indian J. Microbiol*. 3, 147–150.

Zargar, S. M., Mahajan, R., Nazir, M., Nagar, P., Kim, S.T., Rai, V., et al. (2017). Common bean proteomics: present status and future strategies. *J. Proteomics* 169, 239–248. doi: 10.1016/j.jprot.2017.03.019

Zhao, X., Liu, X., Ge, B., Li, M., and Hong, B. (2015). A multiplex RT-PCR for simultaneous detection and identification of five viruses and two viroids infecting chrysanthemum. *Arch. Virol*. 160, 1145–1152. doi: 10.1007/s00705-015-2360-z

Zhou, G. C., Wu, X. Y., Zhang, Y. M., Wu, P., Wu, X. Z., Liu, L. W., et al. (2014). A genomic survey of thirty soybean-infecting bean common mosaic virus (BCMV) isolates from China pointed BCMV as a potential threat to soybean production. *Virus Res*. 191, 125–133. doi: 10.1016/j.virusres.2014.07.029

frontiers | Frontiers in Microbiology

TYPE Original Research
PUBLISHED 29 September 2022
DOI 10.3389/fmicb.2022.955089

OPEN ACCESS

EDITED BY
Giuseppe Parrella,
Institute for Sustainable Plant Protection of the National Research Council (IPSP-CNR), Italy

REVIEWED BY
Eui-Joon Kil,
Andong National University, South Korea
Tomofumi Mochizuki,
Osaka Metropolitan University, Japan
Fan Li,
Yunnan Agricultural University, China

*CORRESPONDENCE
Rong Wang
rwang@implad.ac.cn;
wangrong1019@163.com

SPECIALTY SECTION
This article was submitted to Virology, a section of the journal Frontiers in Microbiology

RECEIVED 28 May 2022
ACCEPTED 12 September 2022
PUBLISHED 29 September 2022

CITATION
Li Y, Liu S, Guo K, Ding W and Wang R (2022) Virome of *Pseudostellaria heterophylla*: Identification and characterization of three novel carlaviruses and one novel amalgavirus associated with viral diseases of *Pseudostellaria heterophylla*.
Front. Microbiol. 13:955089.
doi: 10.3389/fmicb.2022.955089

Virome of *Pseudostellaria heterophylla*: Identification and characterization of three novel carlaviruses and one novel amalgavirus associated with viral diseases of *Pseudostellaria heterophylla*

Yong Li, Sai Liu, Kun Guo, Wanlong Ding and Rong Wang*

Institute of Medicinal Plant Development, Chinese Academy of Medical Sciences and Peking Union Medical College, Beijing, China

Pseudostellaria heterophylla is a traditional Chinese herbal medicine, which has been cultivated for hundreds of years. Viral diseases of *P. heterophylla* occur widely and limit the yield and quality of this medicinal plant. In this study, five leaf samples of *P. heterophylla* with typical viral symptoms were collected from four main producing regions that are distributed in Fujian, Guizhou, and Anhui Provinces in China and analyzed by next-generation sequencing. Comprehensive bioinformatics analyses revealed that nine viruses in five genera *Carlavirus*, *Potyvirus*, *Fabavirus*, *Cucumovirus*, and *Amalgavirus* infected *P. heterophylla*. Among these viruses, three novel and two known carlaviruses, tentatively designated *Pseudostellaria heterophylla* carlavirus 1, 2, and 3 (PhCV1, PhCV2, and PhCV3), Jasmine virus C isolate Ph (Ph-JVC) and Stevia carlavirus 1 isolate Ph (Ph-StCV1), respectively, were first identified in *P. heterophylla*. PhCV1-3 share a similar genomic organization and clear sequence homology with members in the genus *Carlavirus* and could potentially be classified as new species of this genus. One novel amalgavirus, tentatively designated *P. heterophylla* amalgavirus 1 (PhAV1), was first identified in *P. heterophylla.* It had a typical genomic organization of the genus *Amalgavirus*. In PhAV1, the +1 programmed ribosomal frameshifting, which is prevalent in most amalgaviruses, was identified and used in the expression of RNA-dependent RNA polymerase (RdRp). Combined with a phylogenetic analysis, PhAV1 could potentially be classified as new species of the genus *Amalgavirus*. In addition, multiple *Broad bean wilt virus 2* (BBWV2) variants, *Turnip mosaic virus* (TuMV), and *Cucumber mosaic virus* (CMV), which have been reported in *P. heterophylla*, were also detected in this study. The distribution of PhCV1-3, Ph-JVC, Ph-StCV1, TuMV, BBWV2, and CMV in four production regions in Fujian, Guizhou, and Anhui Provinces was determined. This study increased our understanding of *P. heterophylla* virome and provided valuable information for the development of a molecular diagnostic technique and control of viral diseases in *P. heterophylla*.

KEYWORDS

Pseudostellaria heterophylla, virome, next-generation sequencing, novel viruses, *Carlavirus*, *Amalgavirus*

Introduction

Pseudostellaria heterophylla (Miq.) Pax is also known as "Tai-zi-shen" or "Hai-er-shen" in China. It is a member of the family Caryophyllaceae and one of the most popular traditional Chinese herbal medicines. It can be used to treat spleen deficiency, anorexia, weakness after illness, and spontaneous perspiration symptoms (Pang et al., 2011; Sheng et al., 2011; Guo et al., 2014; Choi et al., 2017). *P. heterophylla* is widely distributed in northeastern Asia, including China, Japan, and Korea. In China, *P. heterophylla* has been cultivated for hundreds of years, and its commercial areas of production are primarily distributed in Guizhou, Fujian, Anhui, Shandong, and Jiangsu Provinces. Most of the *P. heterophylla* used in the medicinal commodity market is grown in Shibing County (in Guizhou Province), Zherong County (in Fujian Province), and Xuancheng City (in Anhui Province; Kang et al., 2016).

Pseudostellaria heterophylla primarily propagates asexually through root tubers, which facilitates the transmission of viral diseases across generations. The infections then spread to different regions through the transportation of seedlings. Owing to the long-term vegetative propagation of these plants, the incidence of viral diseases increases yearly, which can result in rates of infection as high as 90% or even 100% (Huang and Lin, 2004; Wang et al., 2022). Such severe infections reduce the yield and quality of *P. heterophylla*. *P. heterophylla* infected by virus(es) display symptoms, such as foliar mottles, mosaics, ringspots, and leaf malformations, as well as the dwarfing of plants. To date, TuMV (of the genus *Potyvirus,* family *Potyviridae*), BBWV2 (of the genus *Fabavirus*, family *Secoviridae*), CMV (of the genus *Cucumovirus*, family *Bromoviridae*), and *Tobacco mosaic virus* (TMV, of the genus *Tobamovirus*, family *Virgaviridae*) are the four viruses that have been reported to infect *P. heterophylla* (Song and Pu, 1991).

The genus *Carlavirus* of the family *Betaflexiviridae* comprises 61 confirmed species (ICTV).[1] Carlaviruses have a monopartite, single-stranded, and positive-sense RNA genome that ranges from 8.3 to 8.7 kb long. Their genomic RNAs encode six open reading frames (ORFs). ORF1 encodes a viral replicase (Rep) and three overlapping ORFs, including ORF2–ORF4, encode the triple gene block (TGB) proteins 1, 2, and 3 that facilitate the movement of viruses. ORF5 encodes the coat protein (CP), and ORF6 encodes a cysteine-rich protein (CRP; Adams et al., 2012a). CRP serves as an RNA silencing suppressor and a determinant of symptoms and/or pathogenicity (Deng et al., 2015; Fujita et al., 2018). Most carlaviruses are transmitted naturally by aphids in a non-persistent manner, while some of them are transmitted by whiteflies (*Bemisia tabaci*; Adams et al., 2012a). All the carlaviruses are mechanically transmissible (Adams et al., 2012a).

Amalgaviridae is a recently reported family of double-stranded RNA viruses that is an amalgam of the families *Partitiviridae* and *Totiviridae*, which encode proteins phylogenetically related to former, but their structure is more closely related to the latter (Martin et al., 2011; Krupovic et al., 2015). It contains two genera, *Amalgavirus* and *Zybavirus*. *Amalgavirus* includes nine viral species that infect plants (ICTV).[1] Putative amalgaviruses have also been reported in fungi and bryophytes (Koloniuk et al., 2015; Vendrell-Mir et al., 2021). These amalgaviruses are monopartite and have small dsRNA genomes that are 3.3–3.5 kb long and encode two partially overlapping ORFs. ORF1 encodes a putative CP with unclear function, which is similar to the nucleocapsid proteins of the genera *Phlebovirus* and *Tenuivirus* (Krupovic et al., 2015) or the replication factory matrix-like protein (Isogai et al., 2011). In most amalgaviruses, there is a +1 programmed ribosomal frameshifting (PRF) in ORF1. When it occurs, the codon frame changes from UUU_CGN (ORF1) to U_UUC_GNN (ORF2; underlining indicates the codon boundary; N, any nucleotide), which causes the fusion of ORF1 and ORF2, and encodes an RdRp (Nibert et al., 2016; Park et al., 2018). Members of this family are transmitted vertically by seeds and are not thought to be capable of efficient extracellular transmission unless mediated by an unknown vector (Martin et al., 2006; Sabanadzovic et al., 2009).

To identify the viral species that infect *P. heterophylla* and provide a reference for the diagnosis, prevention, and control of viral diseases of *P. heterophylla*, the virome of *P. heterophylla* was analyzed by next-generation sequencing (NGS), a rapidly developing technique for viral detection and diagnosis that is suitable for a variety of plants, animals, and fungi (Mu et al., 2018; Jo et al., 2020; Kondo et al., 2020; Zhang et al., 2020). The five libraries used for NGS were prepared with *P. heterophylla* leaf samples collected from four different geographic regions in Guizhou, Fujian, and Anhui Provinces in China. Three novel and two known carlaviruses, one novel amalgavirus, multiple BBWV2 variants, TuMV, and CMV that infect *P. heterophylla* were identified.

Materials and methods

Plant samples

Leaf samples were collected from symptomatic *P. heterophylla* and transported to the laboratory under conditions of low

1 https://talk.ictvonline.org/taxonomy/

temperature and humidity. The samples were stored at -80°C and used for paired-end RNA-Seq.

RNA extraction, NGS, and data processing

Total RNA was extracted from the leaf tissue using a mirVana™ microRNA (miRNA) Isolation kit (Ambion, Thermo Fisher Scientific, Waltham, MA, United States) and treated with an RNA Clean XP Kit (Beckman Coulter, Brea, CA, United States) and an RNase-Free DNase Set (QIAGEN GmbH, Hilden, Germany) according to the manufacturer's instructions. The quality and quantity of total RNA were measured using a NanoDrop spectrophotometer (Thermo Fisher Scientific) and Agilent2100 (Agilent Technologies, Santa Clara, CA, United States). After the removal of ribosomal RNA using a Ribo-Zero Magnetic Kit (Epicentre, Lucigen, Middleton, WI, United States), the libraries were built using a TruSeq RNA Sample Prep Kit (Illumina, San Diego, CA, United States). Barcoded libraries were paired-end sequenced on an Illumina HiSeq X platform according to the manufacturer's instructions.[2] Sequences of adaptors and low-quality traits were trimmed using the FASTX-Toolkit software,[3] and clean reads were assembled *de novo* using CLC Genomics Workbench 6.0.4 (Qiagen, Valencia, CA, United States) according to the scaffolding contig algorithm. The second assembly was then conducted using CAP3 software.[4] The final contigs were compared against the NCBI non-redundant (Nr) database using BLASTX with an *E*-value < $1e^{-5}$.

Recovery of viral genomes

The genome of new *P. heterophylla* viruses were obtained by overlapping reverse transcription (RT)-PCR and rapid amplification of cDNA ends-PCR (RACE-PCR). The primers used in RT-PCR and RACE-PCR were designed based on the viral contig sequences using Primer Premier 6 (PREMIER Biosoft, Palo Alto, CA, United States; Supplementary Table S1). A RACE-PCR assay was conducted using a SMARTer RACE 5′/3′ Kit (Clontech, Mountain View, CA, United States). The PCR amplicons were purified by a TIANgel Midi Purification Kit (Tiangen, Beijing, China) and cloned into the pMD18 or pUC19 Vector (TaKaRa, Dalian, China). The sequence of each amplicon was determined from both directions of more than five clones by the biotechnology company Tsingke (Beijing, China). The full-length genome of each virus was assembled from all amplicons of the virus using DNAMAN 6.0 (Lynnon Biosoft, Quebec City, Canada).

Sequence analysis and read assembly

Viral genome organizations were analyzed using the ORF finder program.[5] The conserved domains of ORFs were analyzed using the Conserved Domain Search Service on the NCBI website.[6] The multiple sequence alignment, conserved domains analysis of the RdRps and CRPs of carlaviruses, and prediction of the PRF motif in RdRp of amalgaviruses were performed using CLC Genomics Workbench 21.0.5 (Qiagen). Pairwise comparisons between viruses were performed using MAFFT program[7] and displayed by Sequence Demarcation Tool (SDT) software using a color-coded matrix (Muhire et al., 2014).

Phylogenetic analysis

Each of the new viruses and its closely related viruses retrieved from the NCBI databases were aligned using the ClustalW program. Phylogenetic analyses were performed using the maximum-likelihood method (carlaviruses and amalgaviruses) or the neighbor-joining method (BBWV2) with 1,000 bootstrap replicates in MEGA X (Kumar et al., 2018).

Results

Sample collection and symptom description

Five *P. heterophylla* leaf samples were collected from the four different main production regions of *P. heterophylla* in June of 2020 and 2021, including one sample in Shibing County (SB) and one sample in Danzhai (DZ) County in Guizhou Province, two samples in Zherong County (ZR-HB and ZR-GX) in Fujian Province and one sample in Xuancheng city (XC) in Anhui Province, in China (Figure 1A; Supplementary Table S2). The samples displayed typical viral symptoms, such as foliar mosaics, ringspots, mottles, and leaf malformations (Figures 1B–F). Each sample was used to generate a library for paired-end RNA-Seq. For simplicity, the libraries were named based on the geographical regions that the samples were collected from.

Transcriptome assembly and virus identification

A total of 59,932,792–142,685,292 trimmed reads were individually generated from five independent libraries

2 www.illumina.com
3 http://hannonlab.cshl.edu/fastx_toolkit/index.html
4 http://doua.prabi.fr/software/cap3
5 https://www.ncbi.nlm.nih.gov/orffinder
6 www.ncbi.nlm.nih.gov/Structure/cdd/wrpsb.cgi
7 https://mafft.cbrc.jp/alignment/server/

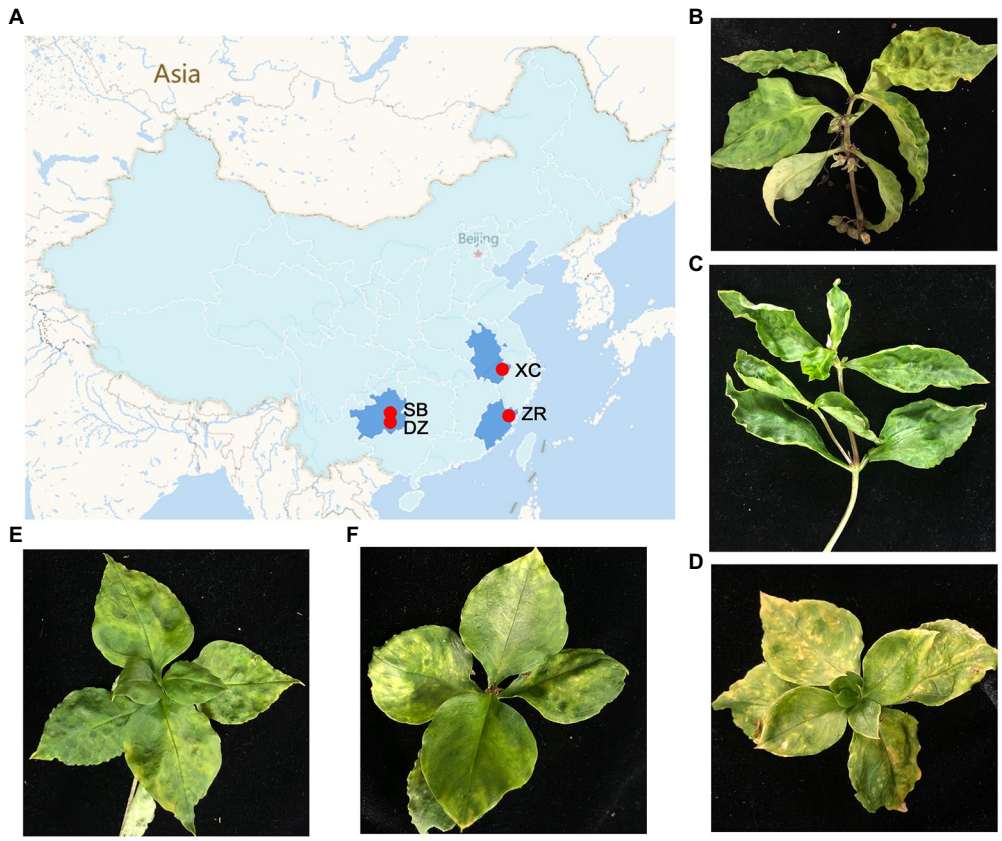

FIGURE 1
Geographical regions of the *Pseudostellaria heterophylla* samples collected in China and the leaf symptoms of *P. heterophylla* viral diseases. **(A)** A map that displays the four different geographical regions in China in which the *P. heterophylla* samples were collected. **(B–F)** Symptoms displayed on *P. heterophylla* leaves collected from SB, XC, ZR-HB, DZ, and ZR-GX, respectively. DZ and SB represent Danzhai County (DZ) and Shibing County (SB) in Guizhou Province, respectively. ZR-HB and ZR-GX represent Huangbai village (ZR-HB) and Gongxi village (ZR-GX) in Zherong County in Fujian Province, respectively. XC represents Xuancheng city (XC) in Anhui Province.

(Supplementary Table S3). Assembly of the clean reads generated 95,378 to 277,230 contigs that ranged from 200 to 10,252 nucleotides (nt) in size (Supplementary Table S3). A BLASTX analysis of the contigs revealed that 320 virus-related contigs representing five different viral taxa were obtained (Table 1). They included TuMV, BBWV2, carlaviruses, CMV, and the amalgaviruses. TuMV, BBWV2, and carlaviruses were identified in all five libraries. Approximately 94.06% (301 of 320) of the viral-related contigs, which were assembled from approximately 95.75% (150,587,101 of 157,276,057) viral-related reads, were homologous to the carlaviruses, TuMV or BBWV2 (Figures 2A,B; Table 1). Followed by CMV and the amalgaviruses, CMV was identified in the libraries ZR-HB and XC, and amalgaviruses were identified in the libraries ZR-HB, ZR-GX, DZ, and XC. Approximately 5.94% (19 of 320) of the viral-related contigs, which were assembled from approximately 4.25% (6,688,956 of 157,276,057) viral-related reads, were homologous to CMV or the amalgaviruses (Figure 2A,B; Table 1). TMV, a virus previously reported to infect *P. heterophylla* (Gao et al., 1993), was not identified in this study. Based on the viral-related reads, carlaviruses were the dominant viruses in the libraries DZ, ZR-HB, and ZR-GX; TuMV was the major virus in library SB, and BBWV2 was the major virus in library XC (Figure 2A; Table 1).

Turnip mosaic virus, CMV-II, and multiple BBWV2 variants were identified in *Pseudostellaria heterophylla*

The TuMV- and CMV-related contigs shared more than 96% nt sequence identity with TuMV and CMV in subgroup II (CMV-II). These results confirmed the presence of both viruses in *P. heterophylla*.

Six BBWV2 isolates were identified in *P. heterophylla*. One BBWV2 isolate was identified in libraries DZ and ZR-HB and designated BBWV2-DZ and -ZR-HB, respectively. Two BBWV2 isolates were identified in libraries XC and ZR-GX and designated BBWV2-XC1, -XC2, −ZR-GX1 and -ZR-GX2, respectively. Pairwise comparisons showed that the polyprotein encoded by RNA1 shared 73.41 to 98.15% nt sequence identities

TABLE 1 Information of the viral reads and contigs for the viruses identified in *Pseudostellaria heterophylla* in China.

Library name[a]	Contigs-related viruses	Number of viral reads	Percentage of viral reads (%)	Number of viral contigs	Percentage of viral contigs (%)	Viral contig lengths
DZ	Carlaviruses	12,601,625	54.0389	38	48.72	257–8,133
	BBWV2	10,321,512	44.2612	19	24.36	212–5,313
	TuMV	395,647	1.6966	19	24.36	225–9,947
	Amalgaviruses	751	0.0032	2	2.56	1,143-2,018
SB	TuMV	121,299	95.9158	6	13.95	456–4,994
	Carlaviruses	4,417	3.4927	20	46.51	262–8,647
	BBWV2	748	0.5915	17	39.53	201–5,944
ZR-HB	Carlaviruses	30,387,069	91.3997	52	54.17	262–8,647
	BBWV2	2,367,422	7.1208	33	34.38	207–5,944
	CMV	411,973	1.2392	3	3.13	2,171–3,365
	TuMV	79,744	0.2399	6	6.25	456–4,994
	Amalgaviruses	155	0.0005	2	2.08	1,289-1,670
ZR-GX	Carlaviruses	35,399,063	88.4569	31	58.49	246–10,252
	BBWV2	4,524,414	11.3058	14	26.42	227–6,800
	TuMV	94,656	0.2365	4	7.55	300–9,857
	Amalgaviruses	282	0.0007	4	7.55	474–1,125
XC	BBWV2	22,491,422	37.1358	17	34.00	218–7,246
	Carlaviruses	22,380,694	36.9530	14	28.00	203–9,049
	TuMV	9,417,369	15.5491	11	22.00	218–9,845
	CMV	6,274,568	10.3600	6	12.00	259–3,140
	Amalgaviruses	1,227	0.0020	2	4.00	1,404-2,019
Total		157,276,057		320		

[a]Library names are named based on the sampling regions. DZ and SB represent Danzhai County (DZ) and Shibing County (SB) in Guizhou Province, respectively. ZR-HB and ZR-GX represent Huangbai village (ZR-HB) and Gongxi village (ZR-GX) in Zherong County in Fujian Province, respectively. XC represents Xuancheng city (XC) in Anhui Province.

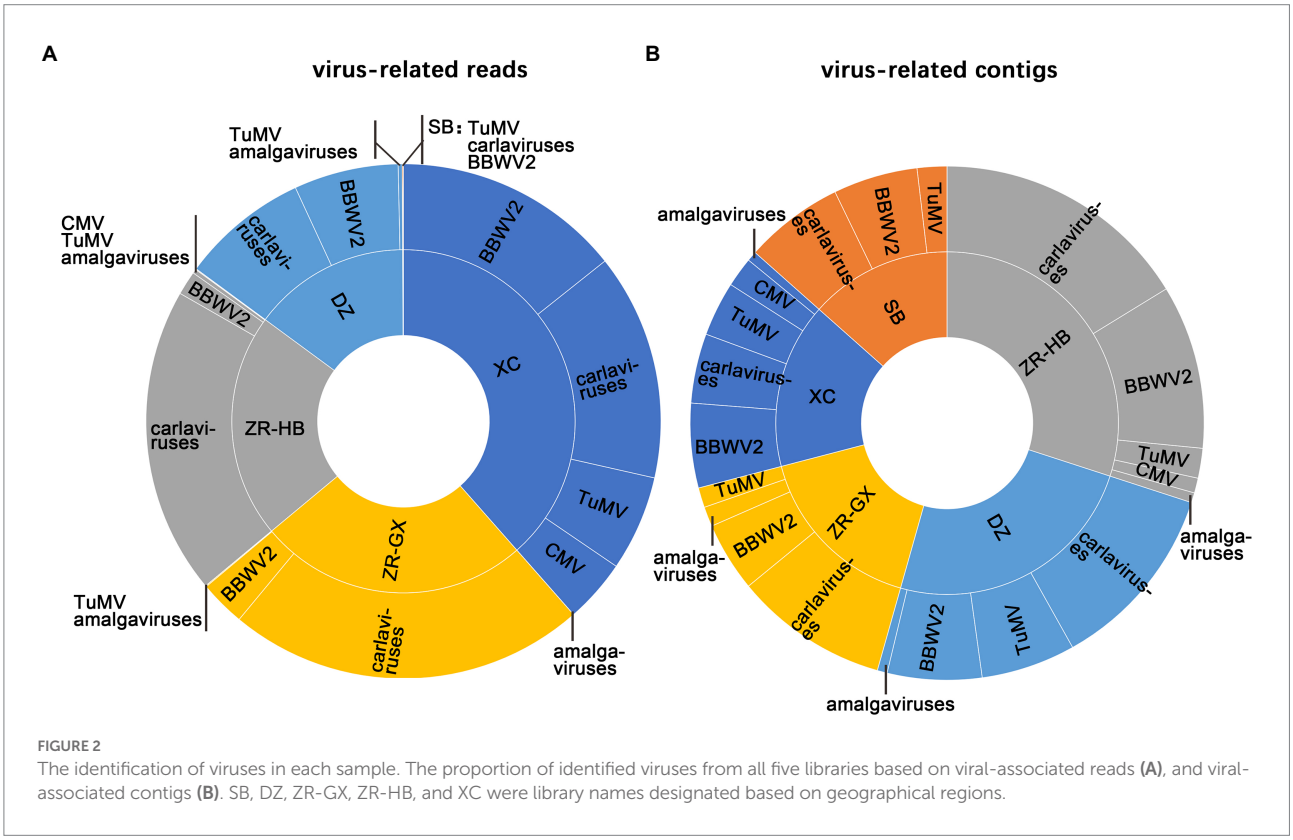

FIGURE 2
The identification of viruses in each sample. The proportion of identified viruses from all five libraries based on viral-associated reads **(A)**, and viral-associated contigs **(B)**. SB, DZ, ZR-GX, ZR-HB, and XC were library names designated based on geographical regions.

and 82.71 to 99.09% amino acid (aa) sequence identities with each other (Tables 2; Supplementary Table S4). The polyprotein encoded by RNA2 shared 70.12 to 98.18% nt sequence identities and 78.97 to 98.78% aa sequence identities with each other (Tables 2; Supplementary Table S4). Among them, RNA1 of ZR-GX1 and XC1 had lower nt identities (<75.66%) compared with the other reported BBWV2 isolates. RNA2 of ZR-GX1 and XC2 had low nt similarities (<74.19%) with the isolates reported (Table 2). The high proportion of nucleotide sequence changes did not result in significant changes in the aa sequences of the CP and Pro-Pol region, two indicators of the definition of new species (Sanfaçon et al., 2012). The Pro-Pol regions of ZR-GX1 and XC1 shared the highest aa sequence identities (89.81 and 87.04%, respectively) with that of the LNSY isolate (GenBank accession No. MN786954; Supplementary Table S4). The CP of ZR-GX1 and XC2 shared the highest aa sequence identities (85.31 and 85.81%, respectively) with that of the Yunnan (MW271032) and PC (MW939477) isolate, respectively (Supplementary Table S4). Since these sequence identity values are higher than the species demarcation threshold (80% aa sequence identity in Pro-Pol region or 75% aa sequence identity in CP) for the genus *Fabavirus* (Sanfaçon et al., 2012), these BBWV2 isolates cannot be defined as a new species in the genus *Fabavirus*. However, these results confirmed the variability of BBWV2 isolates in *P. heterophylla*.

A phylogenetic analysis based on the amino acid sequences of the Pro-Pol region of the polymerase showed that the BBWV2 isolates DZ, ZR-HB, ZR-GX2, and XC2 clustered closely with the isolates LN and LNSY, while the isolates ZR-GX1 and XC1 did not cluster (Figure 3).

Three novel and two known carlaviruses were identified in *Pseudostellaria heterophylla*

Carlavirus-related contigs were detected in all five libraries, and carlavirus-related reads accounted for the high proportions (91.40, 88.46, and 54.04%, respectively) of the viral-related reads in the ZR-HB, ZR-GX, and DZ libraries (Table 1). Three novel carlaviruses, PhCV1, PhCV2, and PhCV3, and two known carlaviruses, Ph-JVC and Ph-StCV1, were identified in this study. The genomic sequences of PhCV1, PhCV2, and PhCV3 were 8,744, 8,533, and 8,497 bp long, respectively, excluding the poly(A) tail at the 3′ end. Their genome organizations are typical of carlaviruses and contain six open reading frames (ORFs) that encode an Rep, three TGB proteins, a CP, and a CRP (Figure 4A; Adams et al., 2012a).

Six, five, and four domains were identified in the Rep of PhCV1, PhCV2, and PhCV3, respectively (Figure 4A). Viral methyltransferase (Mtr; pfam01660), viral helicase (Hel; cl26263), and RdRp (cl03049) domains were identified in the Rep of these three viruses (Figure 4A). Alkylated DNA repair protein (AlkB; cl21496) and DEAD-like helicase (D-Hel; cl28899) domains were identified in the Rep of PhCV1 and PhCV2 but not PhCV3 (Figure 4A). The carlavirus endopeptidase (Pep; cl05111) domain was identified in the Rep of PhCV1 and PhCV3 but not PhCV2 (Figure 4A). A conserved motif, $SGX_3TX_3NTX_{22}GDD$ (X, any aa residue), was identified near the C-terminus of the RdRp domain of these three carlaviruses (Figure 4B). Zinc finger-like motifs (ZFs), $CX_2CX_{12}CX_4C$, were identified in the CRPs of PhCV1, PhCV2, and PhCV3 (Figure 4C). Nuclear localization signals (NLSs), including

TABLE 2 Pairwise nucleotide sequence identities of the BBWV2 isolates identified in *Pseudostellaria heterophylla*.

Isolates[a]	Nucleotide identity (%) Polyprotein/Pro-Pol region (RNA1); coat protein (RNA2)					Most similar isolate at the nucleotide level /GenBank accession number/nucleotide sequence identities (%)
	ZR-GX2	ZR-HB	DZ	XC1	XC2	
BBWV2 RNA1						
ZR-GX1	75.10/76.54	75.22/76.39	74.46/76.39	74.10/75.00	75.08/75.93	LN/MK116519/75.66
ZR-GX2		98.15/97.69	81.98/83.56	73.78/75.85	97.82/97.45	LN/MK116519/90.28
ZR-HB			82.23/83.84	73.59/75.64	97.81/97.45	LN/MK116519/90.46
DZ				73.41/75.46	82.27/83.56	LN/MK116519/82.70
XC1					73.70/75.93	LNSY/MN786954/74.58
XC2						LN/MK116519/90.36
BBWV2 RNA 2						
ZR-GX1	72.08/74.61	72.41/74.00	72.55/74.94	72.42/74.72	71.47/74.00	PAP1/KC634010/74.19
ZR-GX2		79.72/81.61	97.78/97.56	98.15/98.17	70.24/73.61	IP/AB018698/93.50
ZR-HB			79.84/81.61	79.66/81.50	70.12/73.56	PC/MW939477/89.95
DZ				98.18/98.17	70.24/73.44	IP/AB018698/93.38
XC1					70.49/73.78	IP/AB018698/93.50
XC2						PC/MW939477/73.44

[a]ZR-GX1, ZR-GX2, ZR-HB, DZ, XC1, and XC2 represent the BBWV2 isolates isolated from the samples collected from Gongxi village (ZR-GX) and Huangbai village (ZR-HB) in Zherong County in Fujian Province, Danzhai County (DZ) in Guizhou Province, and Xuancheng city (XC) in Anhui Province, respectively.

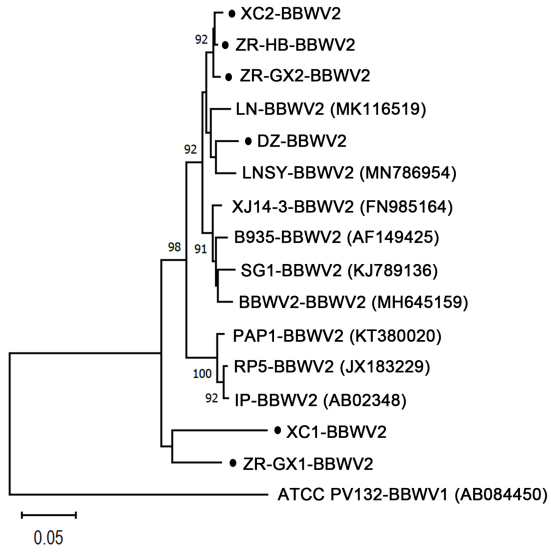

FIGURE 3
Phylogenetic relationships of BBWV2 isolates from *Pseudostellaria heterophylla* (ZR-GX1-, ZR-GX2-, ZR-HB-, DZ-, XC1-, and XC2-BBWV2) and the nine isolates that were the most similar to those of BBWV2 based on the amino acid sequences of the Pro-Pol region. The phylogenetic trees were constructed using the neighbor-joining method in MEGA X software with a bootstrap of 1,000 replicates. The black dots represent isolates identified in this study. ZR-GX1-, ZR-GX2-, ZR-HB-, DZ-, XC1- and XC2-BBWV2 represent the isolates isolated from the samples collected from Gongxi village (ZR-GX) and Huangbai village (ZR-HB) in Zherong County in Fujian Province, Danzhai County (DZ) in Guizhou Province, and Xuancheng city (XC) in Anhui Province, respectively.

RRRR or KKRR, were identified at aa 51–54 in the CRPs of PhCV1 and PhCV3 but not in the CRP of PhCV2 (Figure 4C).

A BLASTN analysis with the nucleotide sequence of genome revealed that PhCV1, PhCV2, and PhCV3 were the most similar to StCV1 (MW328723), Potato virus S (PVS, KC430335), and Tagetes carlavirus 1 (TaCV1, MW328722) with nt identities of 69.95% (55% query coverage), 69.75% (19% query coverage), and 71.15% (87% query coverage), respectively. Pairwise comparisons between PhCV1, PhCV2, PhCV3, Ph-JVC, Ph-StCV1, and 15 of the most similar carlaviruses were performed based on the nt and aa sequences of Rep and CP using MAFFT program and SDT software. The Reps of PhCV1, PhCV2, and PhCV3 shared 53.50–61.30%, 52.80–54.90%, and 53.70–66.90% nt sequence identities and 38.50–56.40%, 36.70–41.90%, and 39.20–72.20% aa sequence identities with Reps in the other aligned carlaviruses (Figures 5A,C; Supplementary Tables S5, S6). The CPs of PhCV1, PhCV2, and PhCV3 shared 47.80–66.40%, 46.10–58.30%, and 50.60–73.50% nt sequence identities and 25.70–67.10%, 24.20–50.50%, and 35.60–85.70% aa sequence identities with CPs in the other aligned carlaviruses (Figures 5B, D; Supplementary Tables S7, S8). The threshold for species demarcation of the genus *Carlavirus* is <72% nt sequence identity and <80% aa sequence identity between their CP or Rep. Since the CP and Rep of PhCV1 and PhCV2, Rep of PhCV3 meet the threshold, they can be recognized as new species of the genus *Carlavirus*.

Phylogenetic trees were constructed based on the aa sequences of the Reps and CPs of PhCV1-3, Ph-JVC, and Ph-StCV1, and 15 of the most similar carlaviruses were reported. *Apple stem pitting virus* (ASPV; MZ147984) was used as an outgroup. The phylogenetic tree based on Rep revealed that PhCV1 clusters closely with *Chrysanthemum virus B* (CVB); PhCV2 clusters closely with *Butterbur mosaic virus* (ButMV), and PhCV3 clusters closely with TaCV1 (Figure 4D). A similar result was obtained in the phylogenetic tree based on CP sequences (Supplementary Figure S1). These results demonstrate that PhCV1, PhCV2, and PhCV3 meet the criteria to be new species of the genus *Carlavirus*.

A novel double-strand RNA virus was identified in *Pseudostellaria heterophylla*

Amalgavirus-related contigs were identified in all five libraries except for SB. The genome of the novel amalgavirus, PhAV1, was 3,430 bp long and contained two partially overlapping ORFs in its positive strand (Figure 6A). ORF1 (nt 171–1,325) followed a short 5'-UTR of 170 nt and was predicted to encode a CP of 384 aa residues, with an estimated molecular weight of 43.3 kDa. A + 1 PRF motif sequence ^{999}UUU_CGN^{1,004} (underline indicates the codon boundary; N, any nucleotide) was found in the ORF1 of PhAV1 (Figure 6B). When the + 1 PRF event occurs, the codon frame changes from ^{999}UUU_CGU^{1,004} to ^{999}U_UUC_GUC^{1,005}, causing the fusion of ORF1 + 2 (nt 171–998, 1,000–3,336), which is predicted to encode RdRp with 1,054 aa residues, with an estimated molecular weight of 120.4 kDa. A BLASTP analysis showed that the CP of PhAV1 had the highest degree of identity (30.73% aa sequence) with that of *Phalaenopsis equestris* amalgavirus 1 (PeAV1; NC_040590), and RdRp of PhAV1 had the most identity (51.01% aa sequence) with that of *Cucumis melo* amalgavirus 1 (CmAV1; MH479774; Zhan et al., 2019). A phylogenetic analysis based on the aa sequences of the RdRp indicated that PhAV1 is in a clade with approved and putative amalgaviruses and in a different clade with *Zygosaccharomyces bailii virus Z* (ZbV-Z), the only species of the genus *Zybavirus* that infects fungi (Figure 6C). Within the amalgaviruses clade, PhAV1 clusters closely with a branch that includes three putative amalgaviruses, PeAV1 (Nibert et al., 2016), *Cucumis melon* amalgavirus 1 (CmAV1; Zhan et al., 2019), and rubber dandelion latent virus 1 (RdLV1; unpublished results; Figure 6C). These results demonstrate that PhAV1 could be a new species of the genus *Amalgavirus*.

The distribution of PhCV1-3, Ph-JVC, Ph-StCV1, TuMV, BBWV2, and CMV in *Pseudostellaria heterophylla*

To identify the incidence of these nine viruses in different *P. heterophylla* growing regions, 7, 16, 8, 12, and 12, *P. heterophylla* leaf samples were collected from ZR-GX, ZR-HB, SB, DZ, and XC,

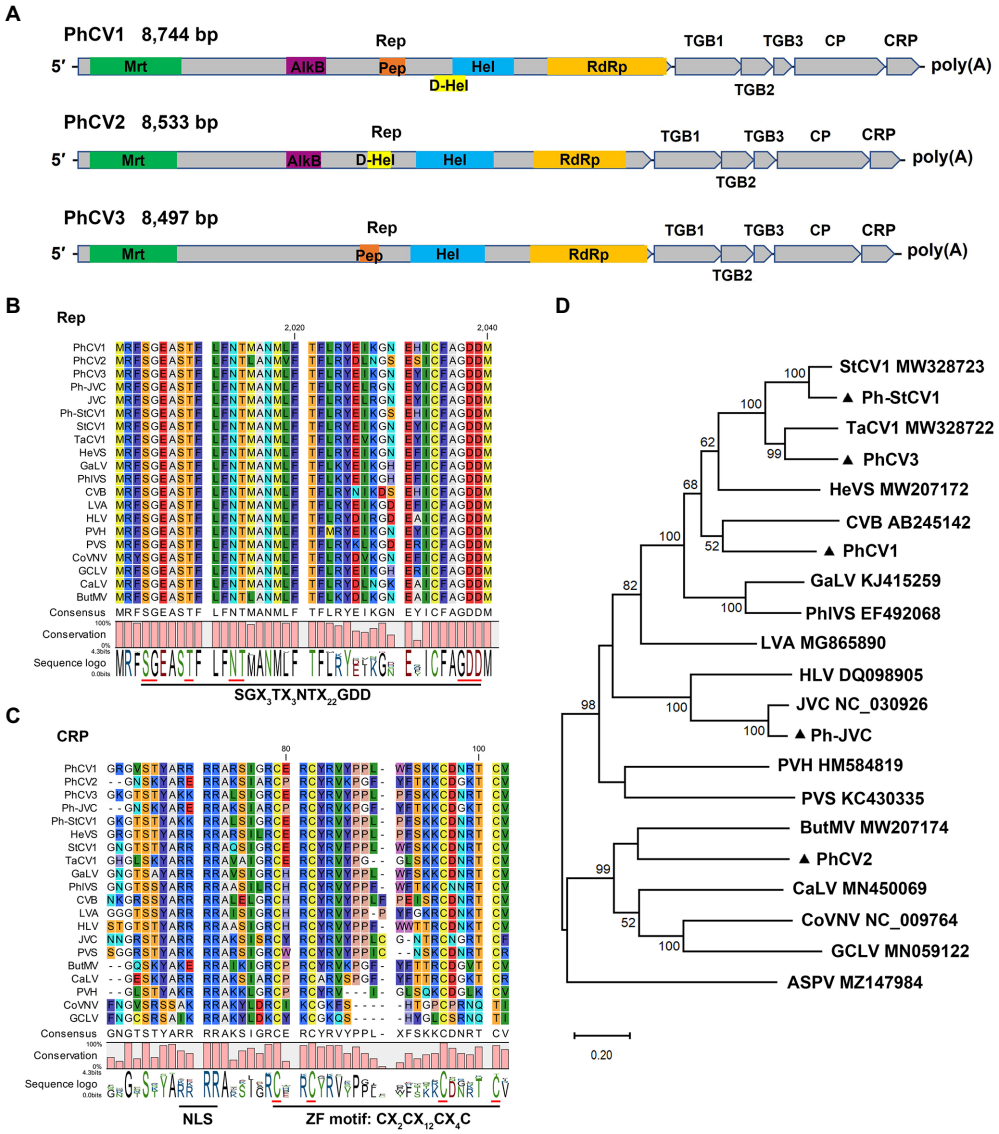

FIGURE 4
Characterization of three novel carlaviruses, pseudostellaria heterophylla carlavirus 1 (PhCV1), pseudostellaria heterophylla carlavirus 2 (PhCV2), and pseudostellaria heterophylla carlavirus 3 (PhCV3) isolated from *Pseudostellaria heterophylla* in China. **(A)** Genomic organization of PhCV1, PhCV2, and PhCV3. Rep, viral replicase; TGB, triple gene block; CP, coat protein; CRP, cysteine-rich protein; Mrt, methyltransferase; AlkB, alkylated DNA repair protein; Hel, viral helicase; D-Hel, DEAD-like helicase; Pep, Carlavirus endopeptidase; RdRp, RNA-dependent RNA polymerase. **(B)** Amino acid alignment between the conserved RdRp motifs of PhCV1, PhCV2, PhCV3, Ph-JVC, and Ph-StCV1 and 15 selected carlaviruses. **(C)** Amino acid alignment between NLS and ZF in the CRP of PhCV1, PhCV2, PhCV3, Ph-JVC, Ph-StCV1, and 15 selected carlaviruses. NLS, nuclear localization signal. ZF, zinc finger-like motif. **(D)** Phylogenetic analysis based on the amino acid sequences of the Rep of PhCV1, PhCV2, PhCV3, Ph-JVC, Ph-StCV1, and the 15 most similar carlaviruses, performed by the maximum-likelihood method in MEGA X software. Bootstrap values (1,000 replicates) are shown below the branches. The black triangles represent carlaviruses identified in this study.

respectively. Primers that specifically detect PhCV1, PhCV2, PhCV3, Ph-JVC, Ph-StCV1, TuMV, CMV, and RNA1 of BBWV2 were designed and are shown in Supplementary Table S1. The results showed that the detection rate of BBWV2 was the highest (78.18%), followed by TuMV (56.36%), PhCV1 (41.82%), and Ph-StCV1 (40.00%; Table 3). All eight viruses were detected in ZR-GX and ZR-HB in Fujian Province. BBWV2 (100%), TuMV (95.65%), and PhCV1 (65.22%) were present at higher levels (Figure 7; Supplementary Figure S2; Table 3). Except for PhCV2, all the viruses were detected in XC in Anhui Province with BBWV2 (83.33%), CMV (83.33%), and PhCV3 (83.33%) present at higher levels (Figure 7; Supplementary Figure S2; Table 3). Except for PhCV1 and PhCV3, all the viruses were detected in SB or DZ in Guizhou Province with BBWV2 (50.0%), PhCV2 (20.0%), and Ph-StCV1 (20.0%) present at higher levels (Figure 7; Supplementary Figure S2; Table 3). Due to the low content of PhAV1 (Table 1) and the long-term frozen storage of the cDNA samples, this virus was not detected in this experiment.

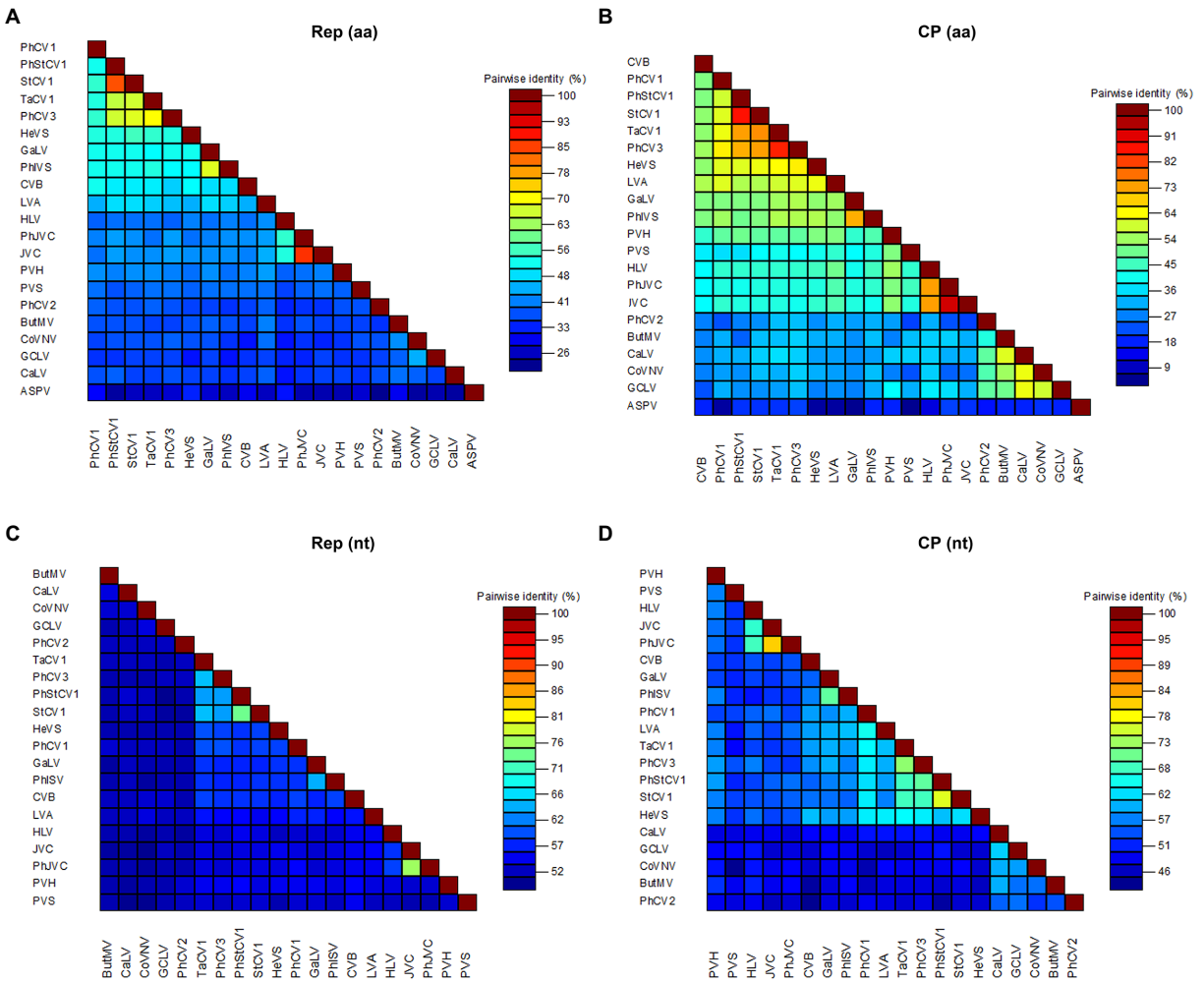

FIGURE 5
The pairwise identities plot of Reps and CPs in the genus of *Carlavirus* based on amino acid (aa) sequence **(A) (B)** and nucleotide (nt) sequence **(C) (D)** aligned by MAFFT and displayed by SDT software. Rep, viral replicase; CP, coat protein.

Discussion

Pseudostellaria heterophylla is one of the most popular traditional Chinese herbal medicines and has been cultivated for hundreds of years. Historically, viral infections have always resulted in important diseases that affect the production of *P. heterophylla*. In 1991, four viruses, including TuMV, BBWV2, CMV, and TMV, were reported to infect *P. heterophylla* (Song and Pu, 1991). To our knowledge, no other viruses have been reported to infect *P. heterophylla* in recent decades. Metagenomics based on NGS can be used to discover the biodiversity of plant viruses in nature (Roossinck et al., 2015). Therefore, we used NGS to detect viruses in *P. heterophylla*. Five samples collected from the different primary growing regions of *P. heterophylla* were analyzed, and the results revealed the presence of TuMV, CMV, BBWV2, five carlaviruses, including Ph-JVC, Ph-StCV1, PhCV1, PhCV2, and PhCV3, and one amalgavirus, PhAV1, in *P. heterophylla*. TuMV, CMV, and BBWV2 are three viruses known to infect *P. heterophylla*, and they have very wide host ranges (Song and Pu, 1991; Bujarski et al., 2012; Sanfaçon et al., 2012; Adams et al., 2012b). JVC and StCV1 are two known unclassified carlaviruses that were isolated from Arabian jasmine (*Jasminum sambac*) and stevia (*Stevia rebaudiana*), respectively. Based on informatic analyses of the genomic features and phylogeny, PhCV1, PhCV2, and PhCV3 were proposed to be new members of the genus *Carlavirus*, and PhAV1 was proposed to be a new member of the genus *Amalgavirus*. These data indicate that a rich diversity of viruses infect *P. heterophylla*.

The incidence of these nine viruses in different *P. heterophylla* growing regions was detected by RT-PCR (Supplementary Figure S2). The occurrence of *P. heterophylla* virus disease was very serious in Fujian, Anhui and Guizhou Provinces with incidences of 100, 91.67 and 75.0%, respectively. Of the 23 samples collected in Fujian Province, 22 were simultaneously infected with TuMV, BBWV2, and one or more carlavirus(es). Of the 12 samples collected in Anhui Province, 11 were simultaneously infected with CMV, BBWV2, and one or more carlavirus(es). A total of 20 samples were collected in

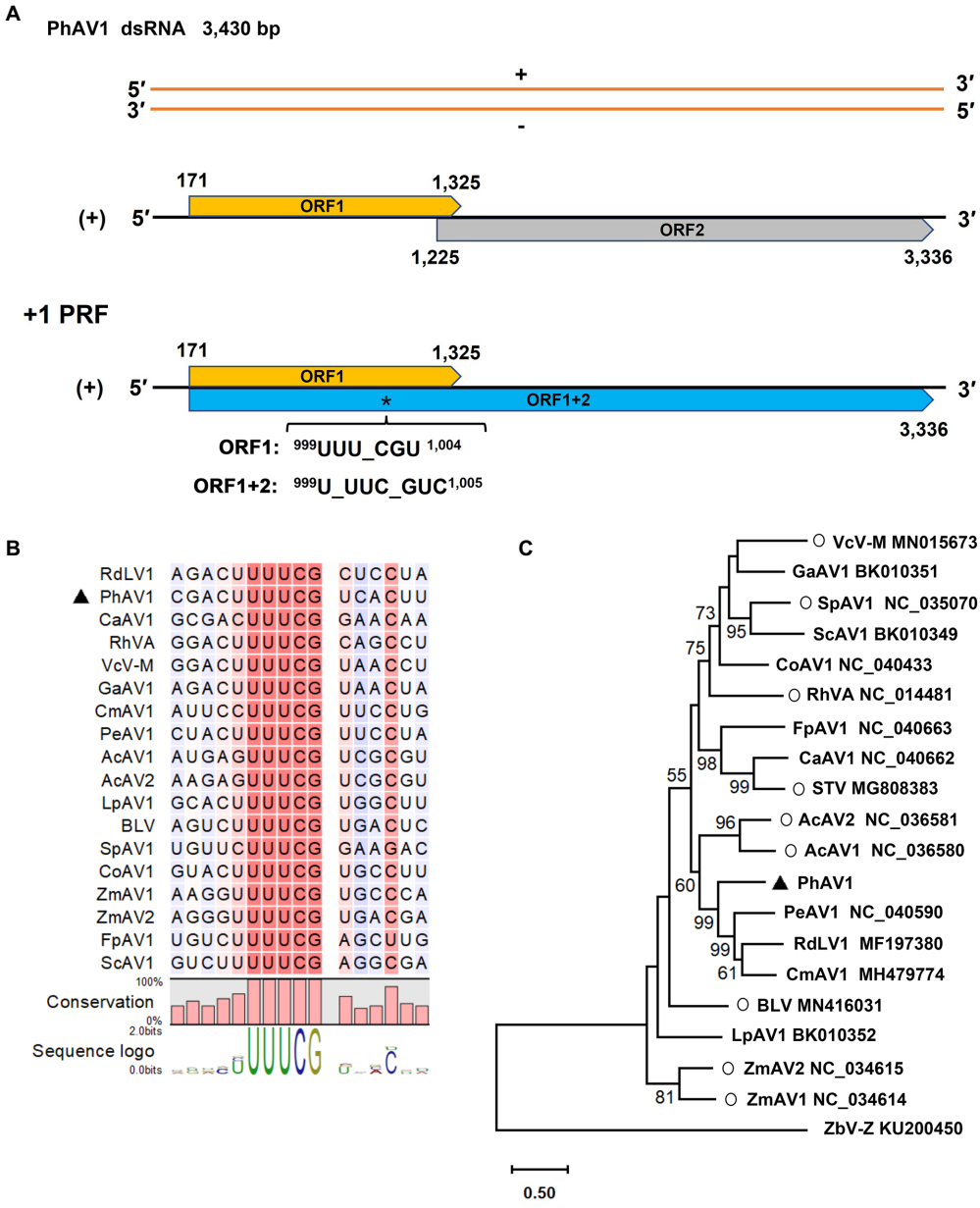

FIGURE 6
Characterization of a novel amalgavirus, pseudostellaria heterophylla amalgavirus 1 (PhAV1), isolated from *Pseudostellaria heterophylla* in China. Genomic organization of PhAV1 **(A)**, and the putative +1 programmed ribosomal frameshifting (PRF) motif of PhAV1 **(B)**. **(C)** A phylogenetic analysis based on the amino acid sequences of the RNA-dependent RNA polymerase (RdRp) of PhAV1, nine confirmed (marked with a circle) and nine putative species in the genus *Amalgavirus*, performed by the maximum-likelihood method in MEGA X. The black triangle represents the novel amalgavirus identified in this study.

Guizhou Province. One virus was detected in 10 samples, two in two samples, four in three samples, and no viruses were detected in five samples. This showed that severe viral infections in *P. heterophylla* were present in all three provinces, particularly in Fujian and Anhui Provinces. BBWV2 was the most common virus in the three provinces with an incidence of 100% in Fujian Province, 83.33% in Anhui Province, and 50.0% in Guizhou Province (Table 3). In addition, TuMV (95.65%) and PhCV1 (65.22%) were also common in Fujian Province, and CMV (83.33%) and PhCV3 (83.33%) were common in Anhui Province. The difference and similarity of pathogens of *P. heterophylla* virus disease in different planting regions may be related to regional differences and/or the long-distance transportation of seedlings.

Like other perennial herbs, *P. heterophylla* can germinate the following year through its seeds and root tubers. To preserve unique characters and the high yield of *P. heterophylla*, root tubers are mostly used for propagation and cultivation. Vegetative propagation using root tubers facilitates the transmission of

TABLE 3 RT-PCR analysis of the incidence of PhCV1, PhCV2, PhCV3, Ph-JVC, Ph-StCV1, TuMV, BBWV2, and CMV in *Pseudostellaria heterophylla* collected from five independent locations, including ZR-GX, ZR-HB, SB, DZ, and XC.

Viruses	Regions[a] (number of samples collected from this region)	ZR-GX (7)	ZR-HB (16)	ZR-GX+ ZR-HB (23)	SB (8)	DZ (12)	SB + DZ (20)	XC (12)	Total (55)
PhCV1	Number of positive samples (Positive ratio)	6 (85.71%)	9 (56.25%)	15 (65.22%)	0 (0)	0 (0)	0 (0)	8 (66.67%)	23 (41.82%)
PhCV2		3 (42.86%)	8 (50.00%)	11 (47.83%)	0 (0)	4 (33.33%)	4 (20.00%)	0 (0)	15 (27.27%)
PhCV3		1 (14.29%)	1 (6.25%)	2 (8.70%)	0 (0)	0 (0)	0 (0)	10 (83.33%)	12 (21.82%)
Ph-JVC		3 (42.86%)	6 (37.50%)	9 (39.13%)	0 (0)	3 (25.00%)	3 (15.00%)	4 (33.33%)	16 (29.09%)
Ph-StCV1		6 (85.71%)	6 (37.50%)	12 (52.17%)	1 (12.50%)	3 (25.00%)	4 (20.00%)	6 (50.00%)	22 (40.00%)
TuMV		7 (100%)	15 (93.75%)	22 (95.65%)	2 (25.00%)	1 (8.33%)	3 (15.00%)	5 (41.67%)	31 (56.36%)
BBWV2		7 (100%)	16 (100%)	23 (100%)	3 (37.50%)	7 (87.50)	10 (50.00%)	10 (83.33%)	43 (78.18%)
CMV		1 (14.28%)	1 (6.25%)	2 (8.70%)	0 (0)	1 (8.33%)	1 (5.00%)	10 (83.33%)	13(23.64%)

[a]Sample collection regions, DZ and SB represent Danzhai County (DZ) and Shibing County (SB) in Guizhou Province, respectively. ZR-HB and ZR-GX represent Huangbai village (ZR-HB) and Gongxi village (ZR-GX) in Zherong County in Fujian Province, respectively. XC represents Xuancheng city (XC) in Anhui Province.

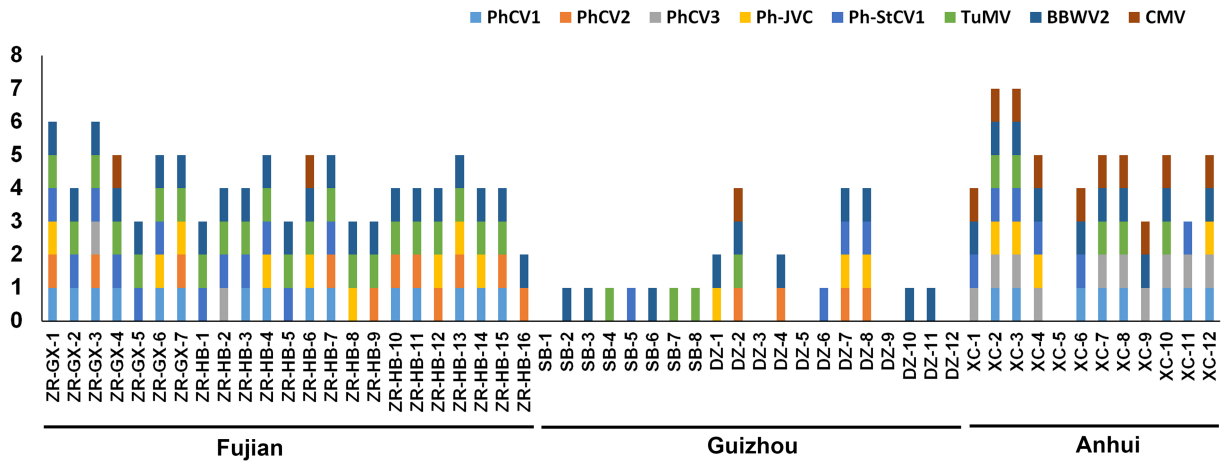

FIGURE 7
Distribution of PhCV1, PhCV2, PhCV3, Ph-JVC, Ph-StCV1, TuMV, BBWV2, and CMV in *Pseudostellaria heterophylla* collected from five independent locations, including ZR-GX, ZR-HB, SB, DZ, and XC.

viruses and viral-plant symbiosis and symbiogenesis (Roossinck, 2008). Viruses can also be transmitted from one plant to another through vectors, such as aphids, which often results in mixed infections. Most of the extant viruses, except for the amalgavirus, related to those identified from *P. heterophylla* in this study have specific vectors for their dispersal. TuMV and CMV can be transmitted by more than 80 species of aphids, including *Myzus persicae* and *Aphis gossypii* which are two efficient and important vectors (Shattuck, 1992; Wang et al., 1998; Palukaitis and García-Arenal, 2003); most fabaviruses and carlaviruses have also been demonstrated to be transmitted by *M. persicae* (Machado Caballero et al., 2009; Belliure et al., 2011; Sanfaçon et al., 2012; Adams et al., 2012a; Wang et al., 2019). As a result, the viral diseases of *P. heterophylla* are serious, and multiple virus infection is widespread. Amalgaviruses are not thought to be capable of efficient extracellular transmission; they are primarily transmitted vertically through seeds to maintain their levels and spread among host plants (Martin et al., 2011; Fukuhara et al., 2020). However, this did not affect the widespread existence of amalgaviruses in *P. heterophylla*. Long-term vegetative propagation could be responsible for the widespread existence of amalgaviruses in *P. heterophylla*.

Three new (PhCV1, PhCV2, and PhCV3) and two known (Ph-JVC and Ph-StCV1) carlaviruses were identified in *P. heterophylla* for the first time. Carlavirus-related reads accounted for high proportions (91.37, 88.45, and 54.03% respectively) in the ZR-HB, ZR-GX, and DZ libraries (Figure 2; Table 1), suggesting that carlaviruses are major viruses that infect *P. heterophylla*. Leaf malformation and whole plant stunting are the types of symptoms caused by carlaviruses (Fujita et al., 2018). The symptoms caused by carlaviruses in *P. heterophylla* could not be confirmed because such viruses usually combine with TuMV or BBWV2 to infect *P. heterophylla*, and they were identified in all five libraries. Previous studies have shown that the CRPs encoded

by carlaviruses play critical roles in determining symptoms and pathogenicity (Lukhovitskaya et al., 2013; Deng et al., 2015). The N-terminal region of CRPs, which contains conserved NLS and ZF motifs, determined the types of symptoms exhibited (Fujita et al., 2018). The CRPs of PhCV1, PhCV3, and Ph-StCV1 all contain NLS and ZF motifs, while the CRPs of PhCV2 and Ph-JVC contain the ZF motif but not the NLS one (Figure 4C). The association between symptoms and these conserved motifs merits further research.

Most of the putative amalgaviruses that have been recently identified were discovered by the analyses of a transcriptome dataset. Similarly, we identified PhAV1 in *P. heterophylla* by exploring its transcriptome. BLASTP and phylogenetic analyses based on the aa sequences of PhAV1 RdRp showed that PhAV1 clusters in the amalgaviruses clade. It displayed <51.01% aa sequence identity with the other amalgaviruses, indicating that PhAV1 could be a new species of the genus *Amalgavirus*. The +1 PRF is used in the expression of many genes of viruses, such as amalgaviruses, fijiviruses, and the influenza A virus (Firth and Atkins, 2009; Firth et al., 2012; Nibert et al., 2016). The shift site (^{999}UUUCG^{1,003}) of +1 PRF was identified in the ORF1 of PhAV1. This could result in the direction (+1) of the frameshifting that is involved in the expression of RdRp.

"BBWV2 exhibits a high genetic variation with sequence variants that are continuously distributed in a wide sequence space compared with most plant viruses. This sequence distribution (genetic structure) is not associated with geographic locations, suggesting long-distance gene flow, and it has been primarily shaped by negative selection and recombination (Ferrer et al., 2011)." Six isolates of BBWV2 were identified in *P. heterophylla,* and the RNA1 of isolates ZR-GX1 and XC1, RNA2 of isolates ZR-GX1 and XC2 shared a low degree of nt similarity (RNA1 < 75.66% and RNA2 < 74.19%) with other isolates in *P. heterophylla* and other isolates in the NCBI database (Table 2). Although these BBWV2 isolates did not meet the criteria for definition as new species, they confirmed the high genetic variation of BBWV2. Alternatively, they provide new genomic references for the molecular detection of BBWV2 in *P. heterophylla*.

In conclusion, this study is the first report of the complete nucleotide sequences of new viruses, including PhCV1, PhCV2, PhCV3, and PhAV1, that infect *P. heterophylla*. It is also the first report of the infection of *P. heterophylla* by JVC, StCV1, and multiple BBWV2 variants. The findings of this study provide useful information for the development of a molecular diagnostic technique to establish a more effective *P. heterophylla* viral disease control strategy.

Data availability statement

The datasets presented in this study can be found in online repositories. The names of the repository/repositories and accession number(s) can be found at: https://www.ncbi.nlm.nih.gov/genbank/, ON241319, ON241320, ON241321, ON241322, ON241323, ON241324, ON241325, ON241326, ON241327, ON241328, ON241329, ON241330, ON241331, ON241332, ON241333, ON241334, ON241335, ON241336.

Author contributions

RW and WD contributed to conception and design of the study, collected the samples and conducted the experiments. RW, YL, and SL performed the statistical analysis. RW, KG, YL, and SL discussed the results, drafted and revised the manuscript. All authors contributed to the article and approved the submitted version.

Funding

This work was supported by the Key project at central government level: The ability establishment of sustainable use for valuable Chinese medicine resources (2060302), CAMS Innovation Fund for Medical Sciences (CIFMS) (2021-I2M-1-032), and the National Natural Science Foundation of China (81873095).

Conflict of interest

The authors declare that the research was conducted in the absence of any commercial or financial relationships that could be construed as a potential conflict of interest.

Publisher's note

Supplementary material

The Supplementary material for this article can be found online at: https://www.frontiersin.org/articles/10.3389/fmicb.2022.955089/full#supplementary-material

SUPPLEMENTARY TABLE S5
Pairwise nucleotide identities of the Rep of PhCV1, PhCV2, PhCV3, Ph-JVC, Ph-StCV1, and the 15 most similar carlaviruses.

SUPPLEMENTARY TABLE S6
Pairwise amino acid identities of the Rep of PhCV1, PhCV2, PhCV3, Ph-JVC, Ph-StCV1, and the 15 most similar carlaviruses.

SUPPLEMENTARY TABLE S7
Pairwise nucleotide identities of the CP of PhCV1, PhCV2, PhCV3, Ph-JVC, Ph-StCV1, and the 15 most similar carlaviruses.

SUPPLEMENTARY TABLE S8
Pairwise amino acid identities of the CP of PhCV1, PhCV2, PhCV3, Ph-JVC, Ph-StCV1, and the 15 most similar carlaviruses.

References

Adams, M. J., Candresse, T., Hammond, J., Kreuze, J. F., Martelli, G. P., Namba, S., et al. (2012a). "Family Betaflexiviridae," in *Virus Taxonomy: Ninth Report of the International Committee on Taxonomy of Viruses*. eds. A. M. Q. King, M. J. Adams, E. B. Carstens and E. J. Lefkowitz (London: Elsevier Academic Press), 920–941.

Adams, M. J., Zerbini, F. M., French, R., Rabenstein, F., Stenger, D. C., and Valkonen, J. P. T. (2012b). "Family Potyviridae," in *Virus Taxonomy: Ninth Report Of The International Committee On Taxonomy Of Viruses*. eds. A. M. Q. King, M. J. Adams, E. B. Carstens and E. J. Lefkowitz (London: Elsevier Academic Press), 1069–1089.

Belliure, B., Amorós-Jiménez, R., Fereres, A., and Marcos-García, M. Á. (2011). Antipredator behaviour of *Myzus persicae* affects transmission efficiency of broad bean wilt virus 1. *Virus Res.* 159, 206–214. doi: 10.1016/j.virusres.2011.04.019

Bujarski, J., Figlerowicz, M., Gallitelli, D., Roossinck, M. J., and Scott, S. W. (2012). "Family Bromoviridae," in *Virus Taxonomy: Ninth Report Of The International Committee On Taxonomy Of Viruses*. eds. A. M. Q. King, M. J. Adams, E. B. Carstens and E. J. Lefkowitz (London: Elsevier Academic Press), 965–976.

Choi, Y. Y., Kim, M. H., Ahn, K. S., Um, J. Y., Lee, S. G., and Yang, W. M. (2017). Immunomodulatory effects of *Pseudostellaria heterophylla* (Miquel) Pax on regulation of Th1/Th2 levels in mice with atopic dermatitis. *Mol. Med. Rep.* 15, 649–656. doi: 10.3892/mmr.2016.6093

Deng, X. G., Peng, X. J., Zhu, F., Chen, Y. J., Zhu, T., Qin, S. B., et al. (2015). A critical domain of sweet potato chlorotic fleck virus nucleotide binding protein (NaBp) for RNA silencing suppression, nuclear localization and viral pathogenesis. *Mol. Plant Pathol.* 16, 365–375. doi: 10.1111/mpp.12186

Ferrer, R. M., Ferriol, I., Moreno, P., Guerri, J., and Rubio, L. (2011). Genetic variation and evolutionary analysis of broad bean wilt virus 2. *Arch. Virol.* 156, 1445–1450. doi: 10.1007/s00705-011-0990-3

Firth, A. E., and Atkins, J. F. (2009). Analysis of the coding potential of the partially overlapping 3' ORF in segment 5 of the plant fijiviruses. *Virol. J.* 6:32. doi: 10.1186/1743-422X-6-32

Firth, A. E., Jagger, B. W., Wise, H. M., Nelson, C. C., Parsawar, K., Wills, N. M., et al. (2012). Ribosomal frameshifting used in influenza a virus expression occurs within the sequence UCC_UUU_CGU and is in the +1 direction. *Open Biol.* 2:120109. doi: 10.1098/rsob.120109

Fujita, N., Komatsu, K., Ayukawa, Y., Matsuo, Y., Hashimoto, M., Netsu, O., et al. (2018). N-terminal region of cysteine-rich protein (CRP) in Carlaviruses is involved in the determination of symptom types. *Mol. Plant Pathol.* 19, 180–190. doi: 10.1111/mpp.12513

Fukuhara, T., Tabara, M., Koiwa, H., and Takahashi, H. (2020). Effect of asymptomatic infection with southern tomato virus on tomato plants. *Arch. Virol.* 165, 11–20. doi: 10.1007/s00705-019-04436-1

Gao, W., Zhang, J. S., Zhang, J. H., and Zhang, L. R. (1993). Detection and control of Taizishen mosaic virus. *Virol. Sin.* 8, 390–393.

Guo, R., Wei, W., Wang, Y., Li, K., Cui, X., Zhu, C., et al. (2014). Protective effects of radix Pseudostellariae extract against retinal laser injury. *Cell. Physiol. Biochem.* 33, 1643–1653. doi: 10.1159/000362947

Huang, Y., and Lin, C. (2004). Occurrence and control of Tizhi jinseng virus diseases in Mindong. *J. Ningde Teachers College (Nat. Sci.)* 16, 65–68.

Isogai, M., Nakamura, T., Ishii, K., Watanabe, M., Yamagishi, N., and Yoshikawa, N. (2011). Histochemical detection of blueberry latent virus in highbush blueberry plant. *J. Gen. Plant Pathol.* 77, 304–306. doi: 10.1007/s10327-011-0323-0

Jo, Y., Kim, S. M., Choi, H., Yang, J. W., Lee, B. C., and Cho, W. K. (2020). Sweet potato viromes in eight different geographical regions in Korea and two different cultivars. *Sci. Rep.* 10:2588. doi: 10.1038/s41598-020-59518-x

Kang, C. Z., Zhou, T., Guo, L. P., Huang, L. Q., Zhu, S. D., and Xiao, C. H. (2016). Ecological suitability and regionalization of *Pseudostellaria heterophylla* (Miq.) Pax ex Pax et Hoffm. In China. *Acta Ecol. Sin.* 36, 2934–2944. doi: 10.5846/stxb201409231880

Koloniuk, I., Hrabáková, L., and Petrzik, K. (2015). Molecular characterization of a novel amalgavirus from the entomopathogenic fungus *Beauveria bassiana*. *Arch. Virol.* 160, 1585–1588. doi: 10.1007/s00705-015-2416-0

Kondo, H., Fujita, M., Hisano, H., Hyodo, K., Andika, I. B., and Suzuki, N. (2020). Virome analysis of aphid populations that infest the barley field: the discovery of two novel groups of Nege/Kita-like viruses and other novel RNA viruses. *Front. Microbiol.* 11:509. doi: 10.3389/fmicb.2020.00509

Krupovic, M., Dolja, V. V., and Koonin, E. V. (2015). Plant viruses of the Amalgaviridae family evolved via recombination between viruses with double-stranded and negative-strand RNA genomes. *Biol. Direct* 10:12. doi: 10.1186/s13062-015-0047-8

Kumar, S., Stecher, G., Li, M., Knyaz, C., and Tamura, K. (2018). MEGA X: molecular evolutionary genetics analysis across computing platforms. *Mol. Biol. Evol.* 35, 1547–1549. doi: 10.1093/molbev/msy096

Lukhovitskaya, N. I., Solovieva, A. D., Boddeti, S. K., Thaduri, S., Solovyev, A. G., and Savenkov, E. I. (2013). An RNA virus-encoded zinc-finger protein acts as a plant transcription factor and induces a regulator of cell size and proliferation in two tobacco species. *Plant Cell* 25, 960–973. doi: 10.1105/tpc.112.106476

Machado Caballero, J. E., Lockhart, B. E., Mason, S. L., and Daughtrey, M. (2009). Identification and properties of a carlavirus causing chlorotic mottle of florists' hydrangea (*H. macrophylla*) in the United States. *Plant Dis.* 93, 891–895. doi: 10.1094/PDIS-93-9-0891

Martin, R. R., Tzanetakis, I. E., Sweeney, M., and Wegener, L. (2006). A virus associated with blueberry fruit drop disease. *Acta Hortic.* 715, 497–502. doi: 10.17660/ActaHortic.2006.715.76

Martin, R. R., Zhou, J., and Tzanetakis, I. E. (2011). Blueberry latent virus: an amalgam of the Partitiviridae and Totiviridae. *Virus Res.* 155, 175–180. doi: 10.1016/j.virusres.2010.09.020

Mu, F., Xie, J., Cheng, S., You, M. P., Barbetti, M. J., Jia, J., et al. (2018). Virome characterization of a collection of *S. sclerotiorum* from Australia. *Front. Microbiol.* 8:2540. doi: 10.3389/fmicb.2017.02540

Muhire, B. M., Varsani, A., and Martin, D. P. (2014). SDT: a virus classification tool based on pairwise sequence alignment and identity calculation. *PLoS One* 9:e108277. doi: 10.1371/journal.pone.0108277

Nibert, M. L., Pyle, J. D., and Firth, A. E. (2016). A +1 ribosomal frameshifting motif prevalent among plant amalgaviruses. *Virology* 498, 201–208. doi: 10.1016/j.virol.2016.07.002

Palukaitis, P., and García-Arenal, F. (2003). Cucumoviruses. *Adv. Virus Res.* 62, 241–323. doi: 10.1016/s0065-3527(03)62005-1

Pang, W., Lin, S., Dai, Q., Zhang, H., and Hu, J. (2011). Antitussive activity of *Pseudostellaria heterophylla* (Miq) Pax extracts and improvement in lung function via adjustment of multi-cytokine levels. *Molecules* 16, 3360–3370. doi: 10.3390/molecules16043360

Park, D., Goh, C. J., Kim, H., and Hahn, Y. (2018). Identification of two novel amalgaviruses in the common eelgrass (*Zostera marina*) and *in silico* analysis of the amalgavirus +1 programmed ribosomal frameshifting sites. *Plant Pathol. J.* 34, 150–156. doi: 10.5423/PPJ.NT.11.2017.0243

Roossinck, M. J. (2008). *Plant Virus Evolution*. Berlin: Springer Science & Business Media.

Roossinck, M. J., Martin, D. P., and Roumagnac, P. (2015). Plant virus metagenomics: advances in virus discovery. *Phytopathology* 105, 716–727. doi: 10.1094/PHYTO-12-14-0356-RVW

Sabanadzovic, S., Valverde, R. J., Martin, R., and Tzanetakis, I. (2009). Southern tomato virus: the link between the families Totiviridae and Partitiviridae. *Virus Res.* 140, 130–137. doi: 10.1016/j.virusres.2008.11.018

Sanfaçon, H., Iwanami, T., Karasev, A. V., van der Vlugt, R., Wellink, J., Wetzel, T., et al. (2012). "Family Secoviridae" in *Virus Taxonomy: Ninth Report Of The International Committee On Taxonomy Of Viruses*. eds. A. M. Q. King, M. J. Adams, E. B. Carstens and E. J. Lefkowitz (London: Elsevier Academic Press), 881–899.

Shattuck, V. I. (1992). The biology, epidemiology, and control of turnip mosaic virus. *Horticult. Rev.* 14, 199–238. doi: 10.1002/9780470650523.ch4

Sheng, R., Xu, X., Tang, Q., Bian, D., Li, Y., Qian, C., et al. (2011). Polysaccharide of radix pseudostellariae improves chronic fatigue syndrome induced by poly I: C in mice. *Evid. Based Complement. Alternat. Med.* 2011:840516. doi: 10.1093/ecam/nep208

Song, R., and Pu, Z. (1991). Studies of Taizishen (*Pseudostellaria heterophylla*) virus diseases. *Acta Agric. Shanghai* 7, 80–85.

Vendrell-Mir, P., Perroud, P. F., Haas, F. B., Meyberg, R., Charlot, F., Rensing, S. A., et al. (2021). A vertically transmitted amalgavirus is present in certain accessions of the bryophyte Physcomitrium patens. *Plant J.* 108, 1786–1797. doi: 10.1111/tpj.15545

Wang, R., Li, Y., Wei, R., Chen, B., Wang, T., and Ding, W. (2022). Investigation on the occurrence of virus diseases in the main producing areas of *Pseudostellaria heterophylla* in China. *Plant Prot.* 48, 204–210. doi: 10.16688/j.zwbh.2020584

Wang, R. Y., Powell, G., Hardie, J., and Pirone, T. P. (1998). Role of the helper component in vector-specific transmission of potyviruses. *J. Gen. Virol.* 79, 1519–1524. doi: 10.1099/0022-1317-79-6-1519

Wang, R. L., Zhu-Salzman, K., Elzaki, M. E. A., Huang, Q. Q., Chen, S., Ma, Z. H., et al. (2019). *Mikania micrantha* wilt virus alters insect vector's host preference to enhance its own spread. *Viruses* 11:336. doi: 10.3390/v11040336

Zhan, B., Cao, M., Wang, K., Wang, X., and Zhou, X. (2019). Detection and characterization of *Cucumis melo* crypticvVirus, *Cucumis melo* amalgavirus 1, and melon necrotic spot virus in *Cucumis melo*. *Viruses* 11:81. doi: 10.3390/v11010081

Zhang, S., Yang, L., Ma, L., Tian, X., Li, R., Zhou, C., et al. (2020). Virome of *Camellia japonica*: discovery of and molecular characterization of new viruses of different taxa in camellias. *Front. Microbiol.* 11:945. doi: 10.3389/fmicb.2020.00945

frontiers | Frontiers in Microbiology

TYPE Original Research
PUBLISHED 08 November 2022
DOI 10.3389/fmicb.2022.954460

OPEN ACCESS

EDITED BY
Shuofeng Yuan,
The University of Hong Kong,
Hong Kong SAR, China

REVIEWED BY
Ramón Gerardo Guevara-Gonzalez,
Universidad Autónoma de Querétaro,
Mexico
Dirk Janssen,
IFAPA Centro La Mojonera,
Spain

*CORRESPONDENCE
Giuseppe Parrella
giuseppe.parrella@ipsp.cnr.it

SPECIALTY SECTION
This article was submitted to Virology,
a section of the journal Frontiers in Microbiology

RECEIVED 27 May 2022
ACCEPTED 28 September 2022
PUBLISHED 08 November 2022

CITATION
Vo TTB, Troiano E, Lal A, Hoang PT, Kil E-J, Lee S and Parrella G (2022) ToLCNDV-ES infection in tomato is enhanced by TYLCV: Evidence from field survey and agroinoculation.
Front. Microbiol. 13:954460.
doi: 10.3389/fmicb.2022.954460

ToLCNDV-ES infection in tomato is enhanced by TYLCV: Evidence from field survey and agroinoculation

Thuy Thi Bich Vo[1], Elisa Troiano[2], Aamir Lal[1], Phuong Thi Hoang[1], Eui-Joon Kil[3], Sukchan Lee[1] and Giuseppe Parrella[2]*

[1]Department of Integrative Biotechnology, Sungkyunkwan University, Suwon, South Korea, [2]Institute for Sustainable Plant Protection, National Research Council (IPSP-CNR), Portici, Italy, [3]Department of Plant Medicals, Andong National University, Andong, South Korea

The tomato leaf curl New Delhi virus (ToLCNDV), a bipartite begomovirus (family *Geminiviridae*), poses a significant threat to various horticultural crops in many Asian and Mediterranean countries. Since its identification, the Asian strain of this virus has exhibited severe infectivity and caused high yield loss in tomato and cucurbit production in the Indian subcontinent and other parts of Asia. ToLCNDV-ES, a different strain of ToLCNDV, emerged recently in the Mediterranean Basin and caused significant outbreaks in *Cucurbitaceae* species but has shown low adaptation to tomatoes. In a field survey, tomato plants infected with this Mediterranean strain were not discovered. Nevertheless, the same field survey revealed that ToLCNDV-ES occurred in natural double infection with tomato yellow leaf curl virus (TYLCV) in tomato plants with an infection ratio of up to 50%. Moreover, results obtained from experiments where tomato plants agro-inoculated simultaneously with infectious clones of ToLCNDV-ES and TYLCV showed that ToLCNDV-ES was detected in tomatoes while synergized with TYLCV with infection ratios similar to those found under field conditions. Quantitative PCR data indicated the highest amount of ToLCNDV in co-infected plants and no significant change in TYLCV titers among the different mixed infections. Moreover, it was ascertained that not all begomoviruses can enhance the infectivity of Mediterranean ToLCNDV isolates in tomato plants. Our study reports a new finding regarding the ToLCNDV-ES response in tomato while synergized with TYLCV with evidence from both field and laboratory conditions.

KEYWORDS

geminiviruses, tomato, virus complementation, infectious clones, TYLCV, ToLCNDV

Introduction

Begomovirus, the largest genus in the family *Geminiviridae*, with 445 species, is a major cause of disease in numerous crops worldwide (Varma et al., 2011). Some begomoviruses are monopartite, with only one DNA component, or bipartite with two DNAs designated as DNA A and DNA B (Zerbini et al., 2017). Begomoviruses were mainly transmitted by

the whitefly *Bemisia tabaci*, however, recently seed transmission was also reported in several species including sweet potato leaf curl virus (Kim et al., 2015), tomato yellow leaf curl virus (TYLCV; Kil et al., 2016, 2017, 2018) despite some controversy (Pérez-Padilla et al., 2020), bitter gourd yellow mosaic virus (Manivannan et al., 2019), tomato leaf curl New Delhi virus (ToLCNDV; Sangeetha et al., 2018; Kil et al., 2020), dolichos yellow mosaic virus (Suruthi et al., 2018) and pepper yellow leaf curl Indonesia virus (Fadhila et al., 2020). Begomovirus infects abroad range of monocotyledonous and dicotyledonous plants, of which tomatoes are the most permissive hosts, the large-scale infection of which can result in severe economic losses (Hanssen et al., 2010).

ToLCNDV is an economically important member of the *Begomovirus* genus and has a bipartite genome structure (Moriones et al., 2017). ToLCNDV was initially reported in tomatoes in India approximately 25 years ago (Padidam et al., 1995) and then identified in cucurbits in the Mediterranean Basin in 2012 (Juárez et al., 2014; Mnari-Hattab et al., 2015; Panno et al., 2016; Parrella et al., 2018; Orfanidou et al., 2019). Along with *Solanaceae* and *Cucurbitaceae* (its host species), this virus has been reported to infect plants belonging to *Malvaceae, Fabaceae, Phyllanthaceae, Papaveraceae* and *Euphorbiaceae* families (Srivastava et al., 2016; Jamil et al., 2017; Venkataravanappa et al., 2018; Sharma et al., 2021). It is as a serious hindrance in the production of various crops in different countries because of its rapid infectivity and the extent of outbreaks it can cause.

Tomatoes are one of the most important crops with a high economic value, constituting up to 72% of the value of fresh vegetables produced worldwide (Hanssen et al., 2010). Its production is affected by numerous diseases, approximately 50% of which are caused by plant viruses. Databases revealed that tomatoes have the highest infection recorded for any plant; at least 312 viruses, satellite viruses, and viroid species are known to be able to infect them (Rivarez et al., 2021). The occurrence of TYLCV is a prevalent limiting factor for tomato production in many regions, including North Africa, East Asia, the Mediterranean, the Caribbean, and America (Mabvakure et al., 2016).

The isolates of ToLCNDV from Asian and Mediterranean countries (ToLCNDV-ES) are categorized as two different strains based on full-length sequences and performed distinct adaptations in tomato plants. The ToLCNDV Asian strain causes significant diseases in tomato with severe symptoms such as stunted or dwarfed growth; leaflets being curled upwards and inwards, slightly chlorotic and yellowish displays, crumpling, and mosaic/mottling (Singh et al., 2015). Despite this, the ToLCNDV-ES strains are mainly adapted to cucurbits and infect tomatoes with great difficulty; they have shown low field incidence in this plant (Yamamoto et al., 2021). In Spain, latent infection of ToLCNDV-ES (Fortes et al., 2016) and symptoms of slight leaf chlorotic mosaic (Ruiz et al., 2017), have been reported in tomato. Attenuated symptoms are correlated with low levels of ToLCNDV-ES accumulation in tomatoes, as opposed to the titers detectable in zucchini, especially with respect to the DNA B component. In addition, the transmission efficiency mediated by *B. tabaci* was significantly higher in zucchini (96%) than in tomatoes (2%). Overall, these features indicated that tomato is a less or not permissive host for ToLCNDV-ES (Simón et al., 2018). In fact, until now, after 7 years of ToLCNDV-ES monitoring in solanaceous and cucurbits crops (URCOFI project), this virus was never detected in tomato crops of continental Italy (in particular in Campania and Lazio regions), where the Italian subgroup I of ToLCNDV-ES isolates have been described so far (Panno et al., 2019). Interestingly, based on CP sequences, the Italian ToLCNDV-ES isolates are divided in two main subgroups: the subgroup I, grouping only Italian isolates (from Campania and Lazio regions) and the subgroup II, in which are grouped Spanish and Italian isolates, the latter only those from Sicily (Panno et al., 2019).

In a previous study, an infectious clone of ToLCNDV-ES that was obtained from a ToLCNDV-infected pumpkin plant, identified in Campania region (Southern continental Italy), was successfully constructed and its biological features were compared with that of an Asian strain, especially in cucurbits (Parrella et al., 2018; Vo et al., 2022).

In this study, we tested the infectivity of the ToLCNDV-ES Italian isolate *via* agroinoculation in different tomato cultivars using its infectious clone and demonstrated that this isolate was able to infect tomato plants (with a low viral titer) only when co-inoculated with TYLCV. These results confirmed previous observations made during a field survey in 2019–2020 in Italy of tomato crops that were naturally exposed to TYLCV and ToLCNDV-ES infections that were mediated by *B. tabaci*. The results showed that no ToLCNDV-ES infection was found in tomatoes, which is slightly different from the spread of ToLCNDV-ES isolates in Spain. The outcomes of inoculations of various mixes were also examined using infectious clones to determine whether TYLCV enhanced ToLCNDV-ES infection in tomatoes. Polymerase chain reaction (PCR) and quantitative PCR (qPCR) data indicated that ToLCNDV was detected, at a low ratio, only when co-inoculated with TYLCV. Other tomato-infected begomoviruses included tomato yellow leaf curl Kanchanaburi virus (TYLCKaV) and tomato leaf curl Joydebpur virus (ToLCJoV) did not induce ToLCNDV infection as TYLCV did. Our study highlights a new finding related to ToLCNDV-ES pathogenicity in tomato associated with TYLCV co-infection under both field and laboratory conditions. Apart from the findings obtained, our study prompts the identification of the key factors of ToLCNDV-ES emergence in tomatoes in future research.

Materials and methods

Field survey

A total of 71 tomato leaf samples, regardless of whether the plants showed symptoms or not, and 40 zucchini symptomatic leaf samples, were collected in 2019 and 2020 from a greenhouse (sampling site coordinates: 40°45 N, 14°25′E) in which tomato and zucchini were intercropped during the spring–summer period (Table 1). The first full expanded leaves from the apex of

both tomato and zucchini plants were sampled. In particular, 48 symptomatic and 23 symptomless tomato samples were collected (Table 1). Some tomato samples were taken from plants born spontaneously among the zucchini plants, most likely born from seeds originating from fallen fruits of the previous crop (Table 1 and Figure 1A). Samples were kept in a refrigerated field bag, transported the same day to the laboratory and immediately processed. The quantity necessary for DNA extraction was taken from each sample (see section "DNA extraction and PCR analysis"), and the remainder was dried in calcium chloride and stored at 5°C, with the aim of returning to the same sample for further investigation if it was necessary.

In the sampling location, TYLCV has been prevalent there since 2003 when it was first identified on tomatoes both by itself and in mixed infections with tomato yellow leaf curl Sardinia virus (TYLCSV; Parrella et al., 2006). In the following years, TYLCV was constantly found on this site on tomato cultivations, especially in the summer-autumn period. Instead, ToLCNDV-ES has been identified in the same site on cucurbits since 2017 (Panno et al., 2016; Parrella et al., 2018). During the survey of both crops, tomato and zucchini, showed obvious symptoms of geminivirus infection from early summer, coinciding with the increase in the population of *B. tabaci* (Figure 1A).

DNA extraction and PCR analysis

Total DNA was extracted from leaf tissue samples using the E.Z.N.A. Plant DNA kit (Omega Bio-tek, Norcross, GA). DNA concentration was determined with the BioSpectrometer basic (Eppendorf, United States), using the μCuvette G1.0 (Eppendorf, United States), and adjusted to a final concentration of about 50 ng/μL. Each DNA samples was then used for PCR analysis to detect TYLCV and ToLCNDV-ES.

Primers were designed manually from a multi alignment including the nucleotide sequences of the coat protein (CP) gene from representative Italian TYLCSV, TYLCV and ToLCNDV-ES isolates deposited in the National Center for Biotechnology Information (NCBI). The degenerated primer pair Gem1f (5'-AC KCCCGYMTCGAAGGTWCG-3′) and Gem2r (5'-GCATGM GTACAKGCCATATAC-3′) was selected in order to amplify a fragment of about 680 bp, comprising about 87% of the CP Open Reading Frame (ORF) of the three geminiviruses being studied. These primers were derived from primers TYCP1(+) and TYCP2(−), used previously for typing tomato yellow leaf curl viruses spreading in tomato crops in southern Italy (Parrella et al., 2005, 2006), in which, based on multi-alignment of Italian isolates of TYLCV, TYLCSV and ToLCNDV-ES of the CP genes, some additional degenerations were introduced in order to amplify also the Italian isolates of ToLCNDV-ES. Before use these primers for extensive field surveys, they were checked several times to detect the above geminiviruses by PCR end-point both in plants with simple/mixed infections and by using plasmids in which the CPs ORF of the three geminiviruses were cloned (not shown).

PCR amplification was performed in volumes of 25 μl, each containing 2.5 μl of the template genomic DNA, 12.5 pmol of each primer, 12.5 μl of GoTaqGreen Master Mix (Promega, United States) and 9.5 μl of sterile distilled water, using a Mastercycler Nexus X2 (Eppendorf, United States) thermocycler, under the following conditions: 3 min at 94°C as pre-denaturation, thermal cycling for 35 cycles (50 s at 94°C, 50 s at 55°C and 1 min at 72°C), and 10 min at 72°C as final extension. PCR products were visualized on 1.2% agarose gel and stained with ethidium bromide.

Geminivirus identification in tomato and *Bemisia tabaci* by restriction fragment length polymorphism of PCR products

The sequences of amplicons obtained, from tomato showing TYLCD syndrome, with Gem1f/Gem2r primer pairs corresponding with the geminiviruses TYLCSV, TYLCV, and ToLCNDV-ES (Italian isolates) were analyzed with MacVector software version 17.5.6 (Accelrys, Inc., United States) to obtain restriction maps, and a restriction fragment length polymorphism (RFLP)-based assay was developed. Under the conditions recommended by the supplier, 3 μl of purified PCR product was digested in a 10 μl mixture consisting of 5 U of *Ava*II (EURx, Gdańsk, Poland), 0.2 μl of 100× bovine serum albumin (BSA), 1 μl of the appropriate 10x restriction buffer (ONE buffer) and 5 μl of sterile distilled water. The digestion mixture was incubated at 37°C for 2 h, followed by heat-inactivation at 65°C for 20 min. The digested products were separated by 6% polyacrylamide gel electrophoresis (PAGE) and visualized by ethidium bromide staining. The *B. tabaci* specimens were checked for the presence of the three geminiviruses, following the same method described above for symptomatic tomatoes.

Identification of *Bemisia tabaci* genotype

A total of 10 *B. tabaci* adults were sampled from symptomatic tomato plants. Specimens were stored at −20°C in 95% ethanol until molecular proceedings were carried out. *B. tabaci* samples were genotyped using the method described previously (Parrella et al., 2012; Bertin et al., 2018, 2021). This method allows the identification of all the *B. tabaci* genotypes described so far in the Mediterranean basin by PCR-RFLP of the amplicon corresponding to the partial sequence of the cytochrome oxidase I gene (COI; Frohlich et al., 1999).

Construction of ToLCNDV and TYLCV infectious clones

Infectious clones of TYLCV and ToLCNDV-ES were obtained by constructing a tandem repeat fragment of the full-length viral DNA as previous described (Urbino et al., 2008).

10.3389/fmicb.2022.954460

TABLE 1 Synthesis of the results obtained performing the PCR-RFLP on the DNA extracted from 71 tomato plants in cultivation or spontaneously born among zucchini plants.

Sample	Variety/type	Date of sampling	Symptoms	PCR	RFLP results
1	Jama	04/11/19	Yes	+	TYLCV+ToLCNDV
2	Jama	04/11/19	Yes	+	TYLCV+ToLCNDV
3	Jama	04/11/19	No	–	n/a
4	Jama	04/11/19	Yes	+	TYLCV
5	Jama	04/11/19	Yes	+	TYLCV
6	Jama	02/11/20	Yes	+	TYLCV+ToLCNDV
7	Jama	02/11/20	Yes	+	TYLCV+ToLCNDV
8	Jama	02/11/20	Yes	+	TYLCV+ToLCNDV
9	Jama	02/11/20	Yes	+	TYLCV+ToLCNDV
10	Jama	02/11/20	Yes	+	TYLCV
11	Adelante	04/11/19	Yes	+	TYLCV+ToLCNDV
12	Adelante	04/11/19	Yes	+	TYLCV+ToLCNDV
13	Adelante	04/11/19	Yes	+	TYLCV+ToLCNDV
14	Adelante	04/11/19	Yes	+	TYLCV
15	Adelante	02/11/20	Yes	+	TYLCV+ToLCNDV
16	Adelante	02/11/20	Yes	+	TYLCV
17	Adelante	02/11/20	Yes	+	TYLCV
18	Adelante	02/11/20	Yes	+	TYLCV
19	Adelante	02/11/20	Yes	+	TYLCV+ToLCNDV
20	Adelante	02/11/20	Yes	+	TYLCV
21	spontaneous	02/11/20	Yes	+	TYLCV
22	spontaneous	02/11/20	Yes	+	TYLCV+ToLCNDV
23	spontaneous	02/11/20	Yes	+	TYLCV+ToLCNDV
24	spontaneous	02/11/20	Yes	+	TYLCV
25	spontaneous	02/11/20	Yes	+	TYLCV+ToLCNDV
26	spontaneous	02/11/20	Yes	+	TYLCV+ToLCNDV
27	spontaneous	02/11/20	Yes	+	TYLCV+ToLCNDV
28	spontaneous	10/11/20	Yes	+	TYLCV
29	spontaneous	10/11/20	No	–	n/a
30	spontaneous	10/11/20	No	–	n/a
31	spontaneous	10/11/20	No	–	n/a
32	spontaneous	10/11/20	Yes	+	TYLCV
33	spontaneous	10/11/20	Yes	+	TYLCV
34	spontaneous	10/11/20	No	–	n/a
35	San Marzano	10/11/20	Yes	+	TYLCV
36	San Marzano	10/11/20	Yes	+	TYLCV
37	San Marzano	10/11/20	Yes	+	TYLCV
38	San Marzano	10/11/20	No	–	n/a
39	San Marzano	10/11/20	No	–	n/a
40	San Marzano	10/11/20	Yes	+	TYLCV+ToLCNDV
41	spontaneous	19/11/20	No	–	n/a
42	spontaneous	19/11/20	Yes	+	TYLCV
43	spontaneous	19/11/20	Yes	+	TYLCV
44	spontaneous	19/11/20	No	–	n/a
45	spontaneous	19/11/20	Yes	+	TYLCV
46	spontaneous	19/11/20	Yes	+	TYLCV
47	spontaneous	19/11/20	Yes	+	TYLCV
48	spontaneous	19/11/20	Yes	+	TYLCV+ToLCNDV
49	spontaneous	19/11/20	Yes	+	TYLCV+ToLCNDV
50	spontaneous	19/11/20	Yes	+	TYLCV+ToLCNDV

(Continued)

TABLE 1 (Continued)

Sample	Variety/type	Date of sampling	Symptoms	PCR	RFLP results
51	spontaneous	19/11/20	Yes	+	TYLCV+ToLCNDV
52	spontaneous	19/11/20	Yes	+	TYLCV+ToLCNDV
53	spontaneous	19/11/20	Yes	+	TYLCV+ToLCNDV
54	spontaneous	19/11/20	No	–	n/a
55	spontaneous	19/11/20	No	–	n/a
56	spontaneous	19/11/20	No	–	n/a
57	spontaneous	19/11/20	No	–	n/a
58	spontaneous	19/11/20	Yes	+	TYLCV+ToLCNDV
59	spontaneous	19/11/20	No	–	n/a
60	spontaneous	19/11/20	No	–	n/a
61	spontaneous	19/11/20	No	–	n/a
62	spontaneous	19/11/20	Yes	+	TYLCV
63	spontaneous	19/11/20	No	–	n/a
64	spontaneous	19/11/20	Yes	+	TYLCV+ToLCNDV
65	spontaneous	19/11/20	No	–	n/a
66	spontaneous	19/11/20	Yes	+	TYLCV
67	spontaneous	19/11/20	No	–	n/a
68	spontaneous	19/11/20	No	–	n/a
69	spontaneous	19/11/20	No	–	n/a
70	spontaneous	19/11/20	No	–	n/a
71	spontaneous	19/11/20	No	–	n/a

Restriction profiles of each sample are shown in Figure 1. Underlined virus acronyms indicate virus samples that displayed faint bands in acrylamide gels and for which infection was further confirmed by specific qPCR (not shown). n/a=not applicable.

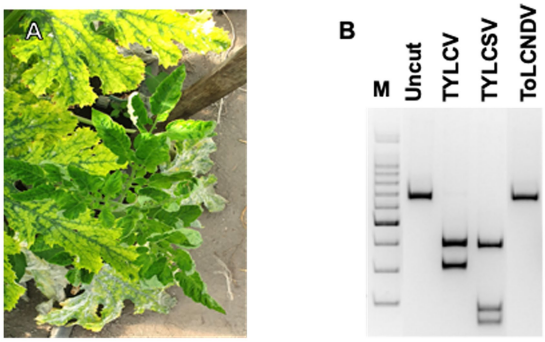

FIGURE 1
Virus detection on tomato plants: **(A)** symptomatic tomato plant, grown spontaneously among plants of a zucchini crop, also showing geminivirus symptoms; **(B)** PCR-RFLP based on *Ava*II digestions of the amplicons obtained by PCR with Gem1f/Gem2r primers on DNA extracted from tomato plants individually infected by the three geminiviruses.

To generate infectious clones of TYLCV, each partial fragment of approximately 1.6 kb and 1.4 kb was amplified by the newly designed primer sets (Supplementary Table S1) based on the genome of TYLCV isolate Goseong (Accession number: JN680149), and cloned into the pGEM T-easy vector (Promega, United States) to yield pGEM-TYLCV-0.6 mer/-0.5 mer. The cloned fragments were digested with *Sal*I, *Sph*I and *Bgl*II, and then ligated into the pCAMBIA 1303 vector to obtain the pCAMBIA-TYLCV-1.1 mer construct. The recombinant pCAM-TYLCV-1.1 mer was the used to transform the *Agrobacterium tumefaciens* strain GV3101 by electroporation. By using the same approach described, a ToLCNDV-ES infectious clone was successfully constructed in a previous study by using a ToLCNDV-ES Italian isolate from pumpkin (Parrella et al., 2018; Vo et al., 2022).

Agroinoculation and symptoms observation

For the single infection, *A. tumefaciens* containing each recombinant plasmid were grown in 20 ml of Luria-Bertani (LB) broth media supplemented with kanamycin (50 μg/ml), rifampicin (50 μg/ml), and gentamycin (50 μg/ml) for 24 h at 28°C and 200 rpm until it reached an optical density (OD) of 1.0 at 600 nm. Liquid culture were then inoculated into tomato through pinpricking method. For the co-inoculation test, cell cultures of *A. tumefaciens* that had been mixed separately with the two different infectious clones were centrifuged, and the pellet was plated at a ratio of 1:1 on LB medium with pH 5.7 for 2 h and contained 200 mm acetosyringone, 10 mm $MgCl_2$, and 10 mm MES. The activated *A. tumefaciens* cell culture was then used for agroinoculation of 3-week-old tomato plants *via* pinpricking of the main apical shoot (Sahu et al., 2010).

A total of 5 Italian cultivars of tomato (San Pedro, Roma VF, Principe Borghese, San Marzano 2, Sorrento), one Korean cultivar

(Seogwang), one TYLCV-resistant tomato cultivar (Bacchus), and the Moneymaker tomato lines were used in the single and co-inoculation tests. For each cultivar/line, 10 plants were agroinoculated and maintained in a growth chamber (16/8 h light/dark periods, at 22–28°C). All inoculated plants were observed daily, up to 3 weeks post-inoculation. The presence of ToLCNDV-ES and TYLCV in singly or double-inoculated plants was assessed by a PCR with specie-specific primer sets (Supplementary Table S1), and the symptomatology was recorded with a digital camera.

Determination of viral titer by qPCR

To determine the viral titer, qPCR was conducted on agroinoculated plants 21 days post-inoculation (dpi). Total DNA from the three plants was extracted using the DNeasy Plant Mini Kit (Qiagen, United States) and quantified using an Epoch microplate spectrophotometer (Biotek, Seoul, Korea). Equal amounts of genomic DNA (20 ng) were used as templates in the qPCR containing 5 µl of TB Green® Premix Ex Taq™ II (Tli RNAseH Plus; TaKaRa Bio, Japan), 1 µl of both TYLCV and ToLCNDV-ES qPCR primer sets (Supplementary Table S1), and sterile water, resulting in a final volume of 15 µl. The elongation factor-1α gene (EF-1α) was used as an internal control for the normalization of the amplification reactions (Wang et al., 2020) and each reaction was replicated three times.

The reaction conditions were as follows: pre-denaturation at 95°C for 10 min followed by 30 cycles (for TYLCV) and 35 cycles (for ToLCNDV-ES) of a denaturation step at 95°C for 10 s, an annealing step (at 58°C for TYLCV and, 60°C for ToLCNDV-ES) for 15 s, and an extension step at 72°C for 20 s. Data analyses were performed using the $2^{-\Delta\Delta Ct}$ method (Livak and Schmittgen, 2001). Statistical analyses were performed using the t-test using GraphPad Prism (GraphPad Software, United States).

Results

Identification of TYLCSV, TYLCV and ToLCNDV-ES by PCR-RFLP

The PCR results indicated that Gem1f/Gem2r primers were able to amplify each of the corresponding genomic regions of the three geminiviruses, giving a robust single amplicon of approximately 680 bp (not shown). Nevertheless, multi-alignment of the amplified genomic portions of the three viruses, encompassed by Gem1f/Gem2r primers, indicated that putative amplicons were slightly different, depending on the virus. The precise length of each amplicon was 680 bp for TYLCV, 677 bp for TYLCSV, and 674 bp for ToLCNDV-ES, corresponding to 87% of the CP ORF in all cases. However, these differences in amplicon lengths were not sufficient to differentiate the three geminiviruses, even when using PAGE. Instead, digestion of the amplicons with *Ava*II endonuclease provided a specific restriction profile for each of the Italian isolates of the three viruses, allowing them to be easily distinguished in both single and mixed infections (Figure 1B). This method was adopted to screen both tomato and *B. tabaci* samples, in order to identify the viral species associated to tomato (Figure 2) and vector (Figure 3B) during field survey.

Identification of *Bemisia tabaci* genotype and detection of geminiviruses in the vector

Based on the restriction profiles obtained after the digestion of the amplicon corresponding to the partial sequence of the COI gene (Parrella et al., 2012), all specimens analyzed belonged to the mitotype Q2 of the *B. tabaci* MED (Mediterranean) genotype (Figure 3A).

In the same specimens, TYLCV and ToLCNDV were also detected in all possible combination. ToLCNDV was detected alone in two specimens, while TYLCV in three specimens. The rest of the samples (50% of the specimens) showed the presence of both geminiviruses (Figure 3B).

ToLCNDV-ES infection was associated with TYLCV in field survey

The PCR-RFLP method described above was applied to check tomato samples for geminivirus infection during the field survey. The results are presented in Table 1 and Figure 2. A strong correlation was found between symptomatic plants and the presence of at least one geminivirus. TYLCSV was never found to be associated with symptomatic plants, whereas 48% of the tomato plants were individually infected with TYLCV (23 of 48 plants tested positive by PCR with Gem1f/Gem2r primers) and about 52% (25 plants out of 48 plants that had tested positive) were double-infected with both TYLCV and ToLCNDV-ES. No plant was infected by ToLCNDV-ES alone, and the remaining asymptomatic plants (23 out of 71 plants tested) were virus-free. Based on these results, ToLCNDV-ES infection in tomato was associated with the simultaneous presence of TYLCV. In some cases, when restriction digestion showed the presence of weak amplicons of TYLCV/ToLCNDV-ES in putative double-infected plants, the presence of both viruses was confirmed by qPCR as described previously (see section "Determination of viral titer by qPCR").

Coinoculation of TYLCV and ToLCNDV infection clones

The infectivity of single ToLCNDV and TYLCV clone were assessed by PCR and symptom observation after 3 weeks from agro-inoculation. All the tomato plants agroinoculated with TYLCV were positive in PCR and, with the exception of the TYLCV-resistant cultivar Bacchus, developed leaf curling

10.3389/fmicb.2022.954460

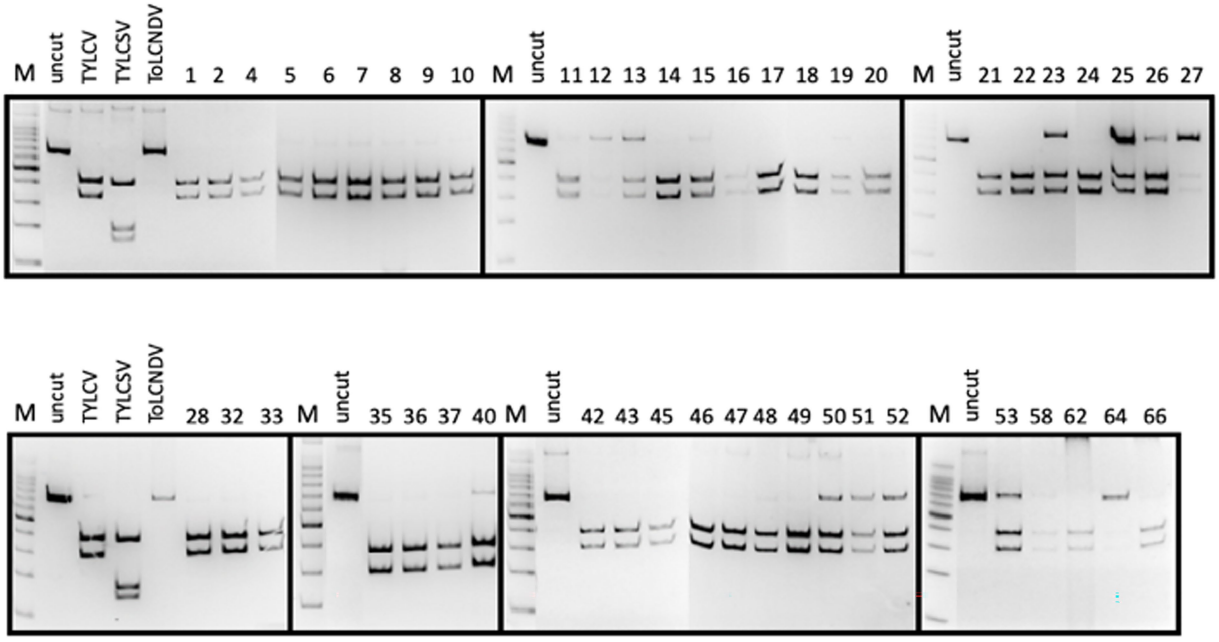

FIGURE 2
PCR-RFLP profiles obtained from each tomato plant sampled and checked for the presence of TYLC, TYLCSV, and ToLCNDV. The presence of viruses in samples showing weak fragments in acrylamide gels was further confirmed by specific qPCR (not shown).

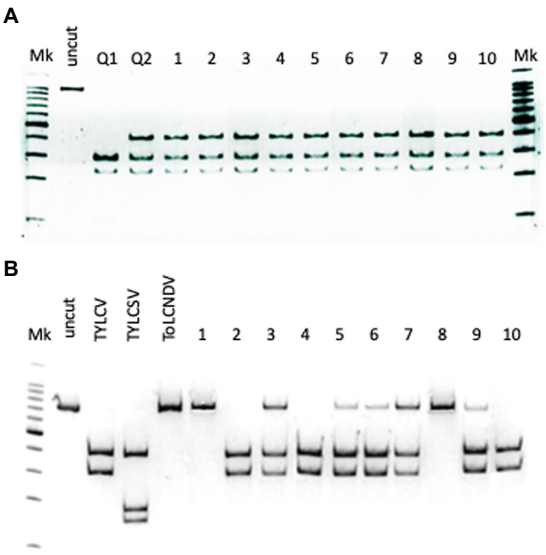

FIGURE 3
(A) Identification of the genotype in 10 *Bemisia tabaci* specimens sampled on tomato showing TYLCD, based on *Apo*I restriction of partial COI gene amplicons; lane Mk: ladder; lane uncut: undigested amplicon; lane Q1: restriction profile of the Q1 mitotype control; lane Q2: restriction profile of the Q2 mitotype control; lanes 1–10: restriction profiles of 10 *B. tabaci* specimens sampled, based on *Ava*II restriction of the amplicons corresponding to the partial CP of the three geminiviruses. **(B)** Identification of geminiviruses in the 10 *B. tabaci* sampled; lane Mk: ladder; lane uncut: undigested amplicon; lane TYLCV: control TYLCV amplicon; lane TYLCSV: control TYLCSV amplicon; lane ToLCNDV: control ToLCNDV amplicon; lanes 1–10: restriction profiles of the 10 *B. tabaci* specimens.

phenotype. No infection was found on tomatoes inoculated with ToLCNDV-ES alone (Table 2; Supplementary Figure S1). The same scenario was observed in the plants simultaneously inoculated with infectious clones of ToLCNDV-ES DNA A/B and TYLCV, where only the TYLCV-resistant cultivar Bacchus displayed a normal phenotype compared to control plants, while all the others, including Moneymaker, San Pedro, Roma VF, San Marzano and Sorrento, displayed leaf yellowing at 21 dpi in 10–50% of the plants, depending on the cultivar (Table 3). The San Pedro cultivar showed the highest infection rate (50%) of ToLCNDV-ES, whereas the other cultivars showed a lower infection ratio, ranging between 10 to 30% of co-inoculated plants. Moreover, symptoms severity in co-infected plants of the San Pedro cultivar were slightly higher than in plants with single TYLCV infection (Figure 4A). The Principe Borghese was the only tomato cultivar not infected by ToLCNDV-ES when co-inoculated with TYLCV. In ToLCNDV-ES positive plants, the PCR results showed the presence of the virus in different organs (including leaves, roots and stems) of each cultivar (Figure 4B). These results suggest that ToLCNDV-ES can replicate and move to other tissues inside co-infected tomatoes.

ToLCNDV detection on TYLCV susceptible and resistant tomato

To determine whether TYLCV enabled ToLCNDV-ES infection in tomato plants, mixed infections were applied to TYLCV-susceptible and resistant cultivars (i.e., San Pedro and Bacchus respectively). A single inoculation of TYLCV,

TABLE 2 Infectivity of single infections with ToLCNDV and TYLCV infectious clones on tomato.

Infectious clone	Cultivars	Infectivity	PCR	Symptoms
ToLCNDV	Moneymaker	0/9*	–	–
	Seogwang	0/9	–	–
	San Pedro	0/9	–	–
TYLCV	Moneymaker	9/9	+	Leaf curling, yellowing
	Seogwang	9/9	+	Leaf curling, yellowing
	San Pedro	9/9	+	Leaf curling, yellowing

*Number of infected plants/number of agroinoculated plants.

TABLE 3 Infectivity of ToLCNDV co-inoculated with TYLCV infectious clone on different tomato *via* PCR amplification and symptom observation at 21 dpi.

Tomato cultivars	Infectivity*			Symptoms
	TYLCV	ToLCNDV DNA A	ToLCNDV DNA B	
Bacchus**	9/10	0/10	0/10	No symptom
Seogwang	10/10	1/10	0/10	Leaf yellowing
Moneymaker	10/10	1/10	0/10	Leaf yellowing
San Pedro	10/10	5/10	0/10	Leaf yellowing
Roma VF	10/10	1/10	0/10	Leaf yellowing
Principe Borghese	10/10	0/10	0/10	Leaf yellowing
San Marzano	10/10	1/10	0/10	Leaf yellowing
Sorrento	10/10	3/10	0/10	Leaf yellowing

*Number of infected plants/number of agroinoculated plants.
**Reported as resistant to TYLCV mediated by the *Ty-1* gene.

ToLCNDV-ES DNA A and/or DNA B served as controls for comparison with the double infection test. After 3 weeks, in the susceptible tomato cultivar., TYLCV was detected by PCR in plants inoculated singly with TYLCV and in those inoculated with TYLCV and ToLCNDV-ES with both DNA or with each single DNA components (Figure 5A). Instead, in the same susceptible cultivar., ToLCNDV-ES DNA A was detected by PCR only in the plants, while the other tests showed the absence of ToLCNDV (Figure 5A). In addition, qPCR data indicated similar results (Figure 5B). The TYLCV titer was not different among infected plants (average relative TYLCV titer: 85.000), while the highest ToLCNDV-ES DNA A titer was recorded in the TYLCV/ToLCNDV-ES A-B condition (average relative ToLCNDV-ES titer: 450; Figure 5B). However, DNA B was not detected in any of the tested plants. The commercial TYLCV resistant cultivar showed weak infection of TYLCV and the absence of ToLCNDV-ES in all cases by PCR (Figure 6A) and qPCR (Figure 6B) analysis.

ToLCNDV infectivity with other begomoviruses in tomato

To check whether other begomoviruses, such as TYLCV, can also enable ToLCNDV-ES to infect tomato, a combination of ToLCNDV-ES and TYLCKaV and ToLCJoV was applied to the San Pedro cultivar. The results at 21 dpi showed no ToLCNDV-ES infection when co-inoculated with other begomoviruses. Plants exhibited yellow and leaf curl phenotypes under TYLCKaV co-infection but normal phenotypes under ToLCJoV (Figure 7A). These phenotypes were similar to those of single-infected plants. PCR results only showed TYLCKaV or ToLCJoV specific amplicons, while no amplicon was observed for ToLCNDV-ES (Figure 7B). These results show that not all begomoviruses are able to complement and help ToLCNDV-ES infect tomatoes.

Discussion

Whitefly transmitted viruses are emerging diseases of important food and fiber crops (Navas-Castillo et al., 2011). ToLCNDV is an economically important begomovirus transmitted by the whitefly *B. tabaci* and recently emerged in the Mediterranean area where it is causing major damage mainly in cucurbits (Fortes et al., 2016; Panno et al., 2016, 2019; Parrella et al., 2018). The Mediterranean ToLCNDV sequences were found to be genetically distant from the Asian strain and were classified as a different strain (ToLCNDV-ES). The two phylogenetically distantly groups of ToLCNDV isolates differ also for their pathogenicity in tomato and cucurbit crops, with ToLCNDV Asian isolates able to replicate efficiently in tomato, causing a clear viral disease syndrome, while ToLCNDV-ES isolates mainly adapted to infect cucurbits (Yamamoto et al., 2021).

ToLCNDV-ES caused yield losses of up to 20% in melon and 22% in zucchini crops in Almeria, Spain (Sáez et al., 2017; Crespo et al., 2020). In southern Italy, high incidences of disease (80–100%) have been reported in *C. moschata* crops in open fields (Parrella et al., 2018). Thus, ToLCNDV-ES has been listed in the Mediterranean region as a serious threat to cucurbit crops but not to tomatoes, since no significant outbreak of this virus has been recorded in tomato crops in this geographic area. In particular, ToLCNDV-ES was never detected in tomato in Italy so far. However, research regarding this pathogen characteristic should be continuously conducted to prevent future damage in non-permissive plants.

In this study, the infectious clone of ToLCNDV-ES isolated from Italy, belonging to subgroup I of ToLCNDV Italian isolates, showed no infectivity in tomatoes and coincided with the field observation data collected so far, since the first report of ToLCNDV in continental Italy (Parrella et al., 2018). Although the artificial infectious clone of the ToLCNDV-ES isolate used in our study showed a minor difference from previous reports of ToLCNDV identified in Spain (Fortes et al., 2016; Yamamoto et al., 2021), all the data obtained in the present study showed that tomatoes are non-permissive hosts for the subgroup I ToLCNDV-ES Italian isolate. Moreover, some results indicated that when TYLCV was impaired, ToLCNDV-ES could not infect tomatoes (see section "Coinoculation of TYLCV and ToLCNDV infection clones" and Figure 5).

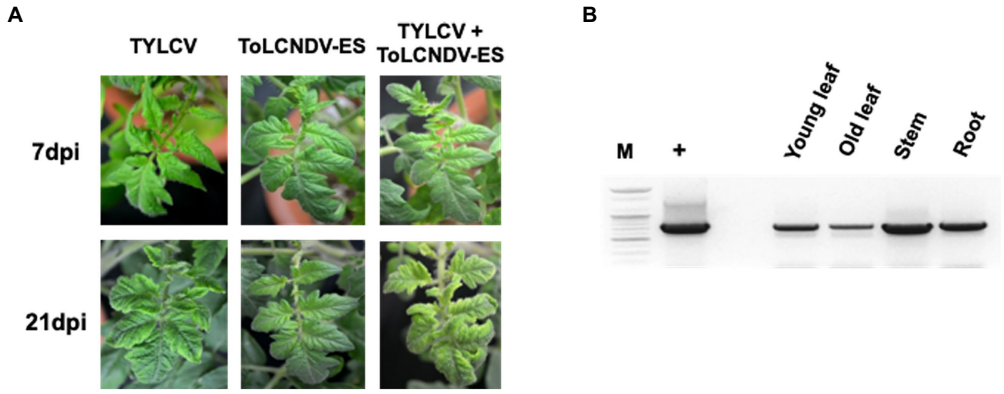

FIGURE 4
ToLCNDV appearance on co-inoculated tomato plants (San Pedro cultivar): **(A)** phenotype of single and co-inoculated tomato at 7 and 21 dpi. Leaf yellowing symptom was induced in TYLCV and co-inoculated plants, whereas ToLCNDV-ES inoculation displayed a normal phenotype. The symptom severity in co-infected plants was a little higher than a single TYLCV infection; **(B)** PCR results of ToLCNDV-ES on different organs including young leaf, old leaf, stem, and root of tomato. Lane M: ladder, lane +: positive control, lane –: negative control. DNA A of this virus was found in all tested tissues.

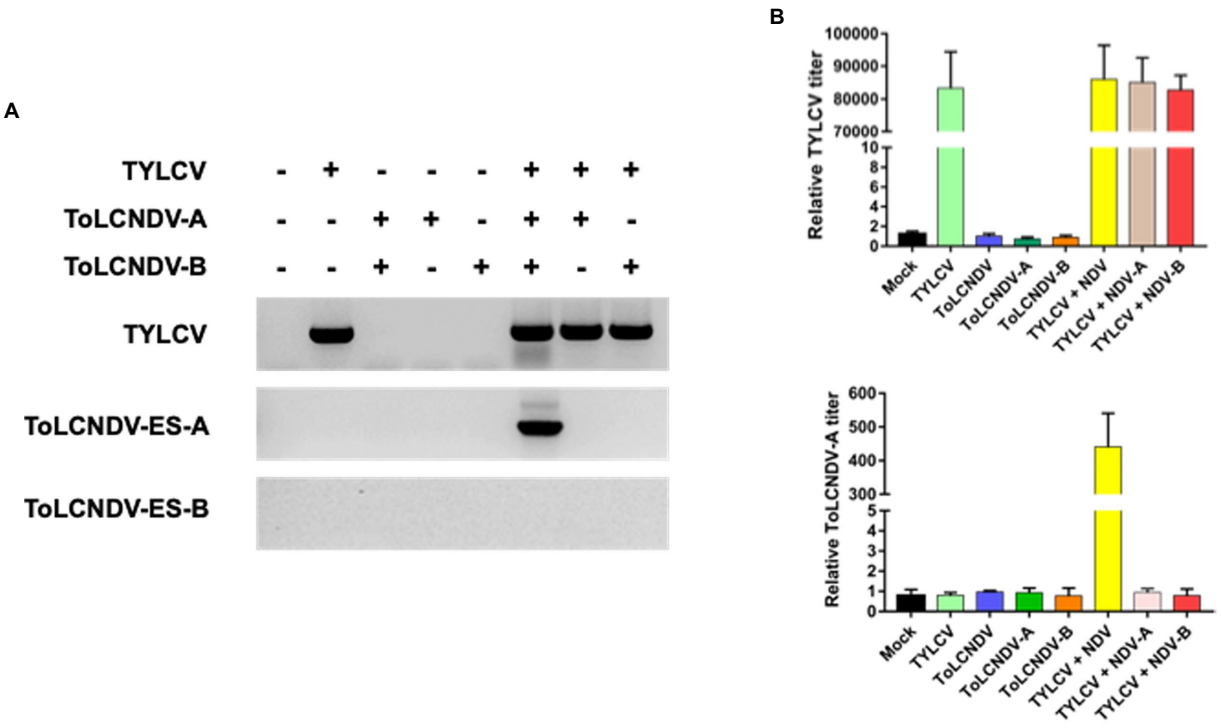

FIGURE 5
Co-inoculation result on TYLCV susceptible tomato (San Pedro cultivar): **(A)** PCR amplification results between TYLCV and ToLCNDV-ES component after 21 dpi. Seven mixed infections were tested at the same time under the presence (+) or absence (–) of different viral components. Only co-inoculated plants were positive for ToLCNDV-ES presence; **(B)** qPCR result for relative TYLCV and ToLCNDV-ES titers on co-inoculated plants. Titer in mock plants was normalized to 1. Relative viral titers were calculated by the $2^{-\Delta\Delta Ct}$ method. Statistical analysis by *t*-test (*p* value<0.05) indicated no significant difference in TYLCV amount among single and mixed infection plants, whereas the ToLCNDV-ES titer in co-infected tomato showed a significant difference.

Overall, data obtained from field and agroinoculation tests suggested also a possible different infectivity in tomato between subgroup I and subgroup II of Italian ToLCNDV isolates, with subgroup I unable to infect tomato even at subliminal mode. Similar results were also obtained in a previous study, concerning the different infectivity in cucurbits between the same ToLCNDV-ES Italian isolate and a ToLCNDV Pakistani isolate (Vo et al., 2022). Interestingly, the Italian subgroup I is phylogenetically more distantly

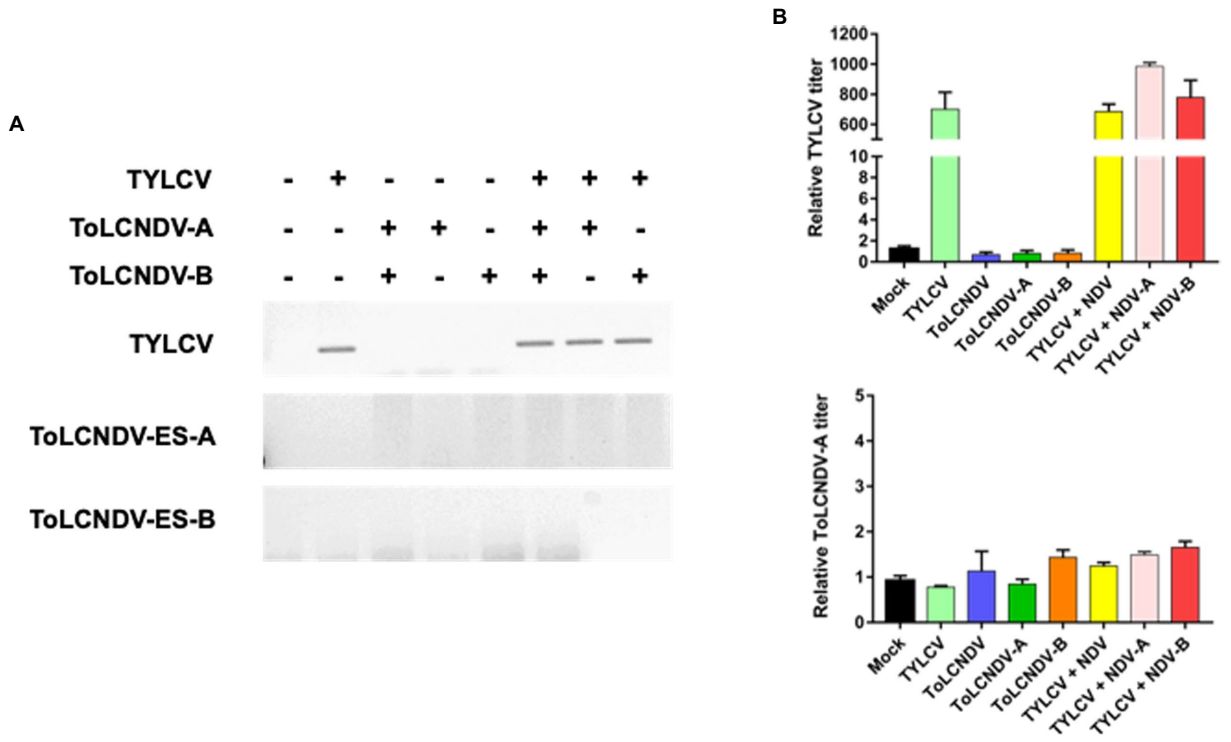

FIGURE 6
Mixed inoculation of TYLCV and ToLCNDV on TYLCV resistance tomato cultivar "Bacchus": **(A)** detection of the virus by PCR. In the resistance plants, TYLCV accumulation was reduced and no ToLCNDV was found in the association with the presence (+) or absence (–) of TYLCV; **(B)** relative TYLCV and ToLCNDV amounts on co-inoculated plants were conducted *via* qPCR. Titer in mock plants was normalized to 1. Co-inoculation between TYLCV and ToLCNDV-ES did not result in a significant change in the TYLCV titer compared to a single infection.

related to the ToLCNDV Asian strain than the Italian subgroup II of ToLCNDV isolates (Panno et al., 2019).

During field surveys, we found that tomato plants infected with ToLCNDV-ES (about 50% of symptomatic plants) correlate strictly with simultaneous presence of TYLCV, suggesting that TYLCV may enhance ToLCNDV infection in tomato (Table 1 and Figure 1). In 2014, Simón et al. (2017) conducted a field survey in southern Spain for tomato begomovirus infection by sampling 50 tomato plants showing tomato leaf curl disease (TYLCD). They found 41% of the plants infected by ToLCNDV-ES in double or complex infection with other begomoviruses, such as TYLCV, TYLCSV and tomato yellow leaf curl Axarquia virus (TYLCAxV). As observed in our experiments of agroinoculation, mixed infections of the tomato observed in southern Spain plants correlate with more severe symptoms than plants with single infection (Simón et al., 2017). Nevertheless, differently from our results, during field survey they found tomato plants infected by ToLCNDV, although in low percentage. This apparently difference between the results obtain after field survey in Spain and Italy could be explained considering that ToLCNDV-ES field isolate from Spain and those from Italy, in particular from Campania and Lazio regions (central Italy), belongs to two different subgroups of ToLCNDV isolates, with isolates belonging to subgroup I (from Campania and Lazio) which evolved more recently in south-central continental Italy, probably specializing prevalently in infecting cucurbits (Panno et al., 2019). Interestingly, during our survey we found that the *B. tabaci* genotype associated to TYLCD syndrome in tomato, belonged to the Q2 mitotype of the MED genotype. This finding is in complete agreement with previous results demonstrating, as results of an extensive survey on *B. tabaci* populations conducted in the same Italian region, a near complete displacement of the Q1 by the Q2 mitotype, especially in protected solanaceous crops (Parrella et al., 2014). Moreover, the displacement of the Q1 mitotype of *B. tabaci* correlated also with the disappearance of TYLCSV (Parrella et al., 2014). Thus, the data produced in the present work confirmed preliminary observation on the *B. tabaci* genotype and geminiviruses spreading in Campania region in solanaceous crops. Nevertheless, it must be considered that this scenario is different from that described in other countries of the Mediterranean basin. In Spain, the Q1 mitotype of *B. tabaci* is prevalent in the field and protected crops and, interestingly, also TYLCSV is routinely detected in tomato cultivations together with TYLCV, TYLCAxV and more recently with ToLCNDV (Moriones et al., 2017; Simón et al., 2017).

To confirm our findings related to 2019–2020 field surveys, experimental agroinoculation of ToLCNDV and TYLCV infectious clones was conducted in various tomato cultivars, and

the results were verified with that of the field reports. In addition, disease symptoms in double-infected plants were more severe than those in single infections. This implies that TYLCV and ToLCNDV-ES may have synergistic interactions in tomatoes. Several co-infection studies on the synergistic interaction between begomoviruses have been reported, and their synergism has led to increased symptom severity and significant economic impact of plant diseases. For examples, mix infection of pepper huasteco virus (PHV) and pepper golden mosaic virus (PepGMV) lead to increased their replication in tobacco (Méndez-Lozano et al., 2003). In addition, the two bipartite begomoviruses, PHV and tomato mottle Taino virus (ToMoTV), can complement infections in tomato and also pseudorecombine (Guevara-González et al., 1999).

Synergistic effects have also been observed during the interaction of begomoviruses with other distantly related viruses. The occurrence of TYLCV and tomato chlorosis virus (ToCV) co-infection has been on the rise and has promoted their spread in the field (Martínez-Zubiaur et al., 2008; Dai et al., 2017; Wei et al., 2018). Mixed infection of the Asian ToLCNDV strain with other viruses or satellites has also been reported (Shafiq et al., 2010; Sivalingam and Varma, 2012; Singh et al., 2016; Zaidi et al., 2017). These results imply that the satellite components can replace ToLCNDV DNA B in the movement of DNA A, resulting in more severe symptoms, whereas DNA A alone induced local infection and a mild disease phenotype. Similarly, in tomato plants agroinoculated with both TYLCV and ToLCNDV, only ToLCNDV DNA A was identified by PCR and qPCR in different tissues, including new leaves, shoots, and roots (Figure 3; Supplementary Figure S2), while, after co-inoculation of tomato plants, DNA B disappeared and was no longer detected in different parts of the plant. Such results would suggest that TYLCV favors the movement of ToLCNDV in the tomato plant, probably complementing the function of the movement protein carried by the DNA B. In double-infected plants, the ToLCNDV DNA A component was found in different tissues, but when we examined plants double-infected with TYLCV and others with only ToLCNDV DNA A, no evidence of ToLCNDV infection was observed. These results suggest that TYLCV proteins may assist ToLCNDV-ES DNA A replication as well as the replacement of the DNA B function of virus movement into the host, allowing ToLCNDV-ES to invade non-directly inoculated tomato plants tissues.

To our knowledge, this is the first report on the functional complementation and synergistic interaction between

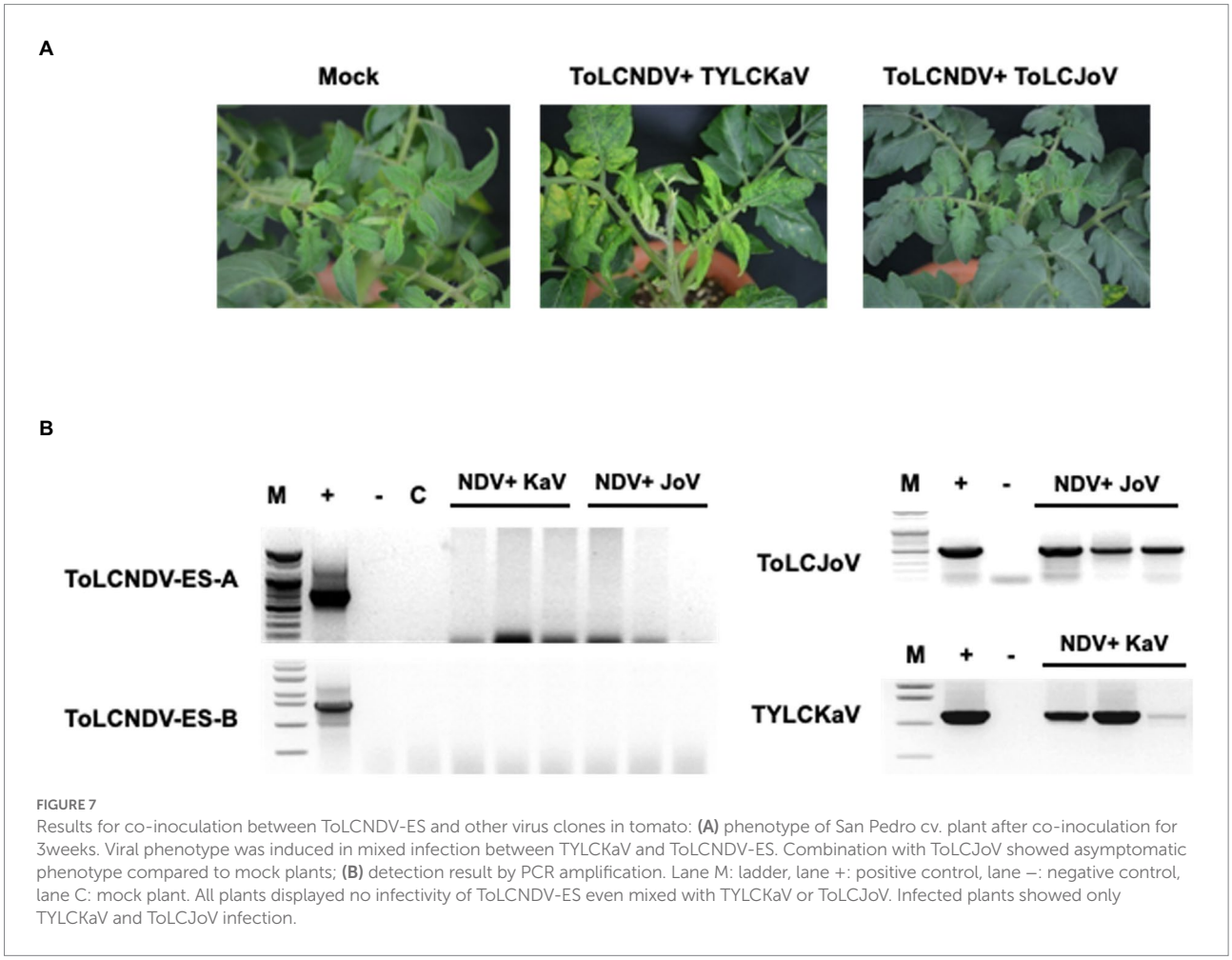

FIGURE 7
Results for co-inoculation between ToLCNDV-ES and other virus clones in tomato: **(A)** phenotype of San Pedro cv. plant after co-inoculation for 3weeks. Viral phenotype was induced in mixed infection between TYLCKaV and ToLCNDV-ES. Combination with ToLCJoV showed asymptomatic phenotype compared to mock plants; **(B)** detection result by PCR amplification. Lane M: ladder, lane +: positive control, lane –: negative control, lane C: mock plant. All plants displayed no infectivity of ToLCNDV-ES even mixed with TYLCKaV or ToLCJoV. Infected plants showed only TYLCKaV and ToLCJoV infection.

ToLCNDV-ES and other begomoviruses in the Mediterranean region. The ToLCNDV-ES Italian isolate in this study was only detected in double infection with TYLCV, which is associated with both components of ToLCNDV in the primary infection. Nevertheless, not all begomoviruses enhance ToLCNDV as TYLCV in mixed infections. We even tested co-infection with other monopartite (ToLCJoV) and bipartite (TYLCKaV) begomoviruses but neither of them had any positive effect on ToLCNDV infection. Thus, the synergistic relationship with TYLCV may play a key role in understanding the low or absent ToLCNDV-ES infectivity on tomato.

The complementation and synergistic effects in tomato caused by the double infection of ToLCNDV-ES and TYLCV can represent a new problem for tomato crops due to the following reasons: (a) in many countries of the southern Mediterranean area, two begomoviruses transmitted by the same vector are often present in the same cultivation areas of cucurbits and tomatoes; (b) symptoms observed on tomato plants by ToLCNDV-ES and TYLCV together were more severe than those induced by TYLCV alone; (c) there is always a risk that new recombinants with unknown phenotypes will be formed between two begomoviruses or a new viral species will be selected over time.

For these reasons, it is necessary to continue the monitoring and identification of viruses in the areas most at risk (e.g., where the two viruses coexist) and to adopt, when possible, some control measures such as the use of tomato genotypes that are resistant to TYLCV or ToLCNDV, in order to reduce the risk of selecting new recombinants from plants harboring mixed infections.

Conclusion

Our study provides a new finding on ToLCNDV-ES infection associated with TYLCV in tomatoes. The data reported from field and laboratory conditions demonstrate that the incidence of infection of a ToLCNDV-ES Italian isolate increases in case of contemporary infection with TYLCV as compared to single infections. Nevertheless, not all begomoviruses can enhance ToLCNDV-ES infection in tomato. Although further studies are needed to determine the molecular mechanisms that regulate ToLCNDV-ES infection in tomatoes, this finding highlights the risk of ToLCNDV-ES based on its increased pathogenicity in non-permissive hosts in combination with TYLCV, since both viruses are spreading or are already present in several Mediterranean countries.

Data availability statement

The original contributions presented in the study are included in the article/Supplementary material, further inquiries can be directed to the corresponding author.

Author contributions

GP conceived and developed the concept, supervised the experiments, and wrote the manuscript. TV, AL, PH, E-JK, and SL contributed to the data analysis and interpretation, discussions, and writing of the manuscript. TV, ET, and GP performed the experiments. All authors contributed to the article and approved the submitted version.

Funding

This work was supported under the framework of international cooperation program as part of a bilateral project managed by the National Research Foundation of Korea and the National Research Council of Italy (2017K2A9A1A06035325) and by the Campania Region-funded URCoFi project "Strengthening of the supervision activities and control of pests."

Acknowledgments

We sincerely want to thank the owners of the greenhouses, the brothers Aniello and Alfonso Patunzi-Polese from Torre del Greco (Naples), where the sampling of the material object of the work presented was carried out, for having patiently hosted us and for always being available for every need.

Conflict of interest

The authors declare that the research was conducted in the absence of any commercial or financial relationships that could be construed as a potential conflict of interest.

Publisher's note

Supplementary material

The Supplementary material for this article can be found online at: https://www.frontiersin.org/articles/10.3389/fmicb.2022.954460/full#supplementary-material

References

Bertin, S., Luigi, M., Parrella, G., Giorgini, M., Davino, S., and Tomassoli, L. (2018). Survey of the distribution of *Bemisia tabaci* (Hemiptera: *Aleyrodidae*) in Lazio region (Central Italy): a threat for the northward expansion of tomato leaf curl New Delhi virus (Begomovirus: *Geminiviridae*) infection. *Phytoparasitica* 46, 171–182. doi: 10.1007/s12600-018-0649-7

Bertin, S., Parrella, G., Nannini, M., Guercio, G., Troiano, E., and Tomassoli, L. (2021). Distribution and genetic variability of *Bemisia tabaci* cryptic species (Hemiptera: *Aleyrodidae*) in Italy. *Insects* 12:521. doi: 10.3390/insects12060521

Crespo, O., Robles, C., Ruiz, L., and Janssen, D. (2020). Antagonism of cucumber green mottle mosaic virus against tomato leaf curl New Delhi virus in zucchini and cucumber. *Ann. Appl. Biol.* 176, 147–157. doi: 10.1111/aab.12535

Dai, H., Cheng, L., Zhu, X., Liu, Y., and Zhao, J. (2017). Co-infections of tomato chlorosis virus and tomato yellow leaf curl virus transmitted by tobacco whitefly *Bemisia tabaci* to different tomato varieties. *J. Plant Protect.* 44, 453–459. doi: 10.13802/j.cnki.zwbhxb.2017.2016090

Fadhila, C., Lal, A., Vo, T. T., Ho, P. T., Hidayat, S. H., Lee, J., et al. (2020). The threat of seed-transmissible pepper yellow leaf curl Indonesia virus in chili pepper. *Microb. Pathog.* 143:104132. doi: 10.1016/j.micpath.2020.104132

Fortes, I. M., Sánchez-Campos, S., Fiallo-Olivé, E., Díaz-Pendón, J. A., Navas-Castillo, J., and Moriones, E. (2016). A novel strain of tomato leaf curl New Delhi Virus has spread to the Mediterranean basin. *Viruses* 8:307. doi: 10.3390/v8110307

Frohlich, D., Torres-Jerez, I., Bedford, I., Markham, P., and Brown, J. (1999). A phylogeographical analysis of the *Bemisia tabaci* species complex based on mitochondrial DNA markers. *Mol. Ecol.* 8, 1683–1691. doi: 10.1046/j.1365-294x.1999.00754.x

Guevara-González, R. G., Ramos, P. L., and Rivera-Bustamante, R. F. (1999). Complementation of coat protein mutants of pepper huasteco geminivirus in transgenic tobacco plants. *Phytopathology* 89, 540–545. doi: 10.1094/PHYTO.1999.89.7.540

Hanssen, I. M., Lapidot, M., and Thomma, B. P. J. M. P.-M. I. (2010). Emerging viral diseases of tomato crops. *Mol. Plant-Microbe Interact.* 23, 539–548. doi: 10.1094/MPMI-23-5-0539

Jamil, N., Rehman, A., Hamza, M., Hafeez, A., Ismail, H., Zubair, M., et al. (2017). First report of tomato leaf curl New Delhi virus, a bipartite begomovirus, infecting soybean (*Glycine max*). *Plant Dis.* 101:845. doi: 10.1094/PDIS-09-16-1267-PDN

Juárez, M., Tovar, R., Fiallo-Olivé, E., Aranda, M., Gosálvez, B., Castillo, P., et al. (2014). First detection of tomato leaf curl New Delhi virus infecting zucchini in Spain. *Plant Dis.* 98:857. doi: 10.1094/PDIS-10-13-1050-PDN

Kil, E.-J., Kim, S., Lee, Y.-J., Byun, H.-S., Park, J., Seo, H., et al. (2016). Tomato yellow leaf curl virus (TYLCV-IL): a seed-transmissible geminivirus in tomatoes. *Sci. Rep.* 6:19013. doi: 10.1038/srep19013

Kil, E.-J., Park, J., Choi, E.-Y., Byun, H.-S., Lee, K.-Y., An, C. G., et al. (2018). Seed transmission of Tomato yellow leaf curl virus in sweet pepper (*Capsicum annuum*). *Eur. J. Plant Pathol.* 150, 759–764. doi: 10.1007/s10658-017-1304-8

Kil, E.-J., Park, J., Choi, H.-S., Kim, C.-S., and Lee, S. (2017). Seed transmission of tomato yellow leaf curl virus in white soybean (*Glycine max*). *Plant Pathol. J.* 33, 424–428. doi: 10.5423/PPJ.NT.02.2017.0043

Kil, E.-J., Vo, T. T. B., Fadhila, C., Ho, P. T., Lal, A., Troiano, E., et al. (2020). Seed transmission of tomato leaf curl New Delhi virus from zucchini squash in Italy. *Plan. Theory* 9:563. doi: 10.3390/plants9050563

Kim, J., Kil, E.-J., Kim, S., Seo, H., Byun, H.-S., Park, J., et al. (2015). Seed transmission of sweet potato leaf curl virus in sweet potato (*Ipomoea batatas*). *Plant Pathol.* 64, 1284–1291. doi: 10.1111/ppa.12366

Livak, K. J., and Schmittgen, T. D. (2001). Analysis of relative gene expression data using real-time quantitative PCR and the 2(-Delta Delta C(T)) Method. *Methods* 25, 402–408. doi: 10.1006/meth.2001.1262

Mabvakure, B., Martin, D. P., Kraberger, S., Cloete, L., Van Brunschot, S., Geering, A. D. W., et al. (2016). Ongoing geographical spread of Tomato yellow leaf curl virus. *Virology* 498, 257–264. doi: 10.1016/j.virol.2016.08.033

Manivannan, K., Renukadevi, P., Malathi, V. G., Karthikeyan, G., and Balakrishnan, N. (2019). A new seed-transmissible begomovirus in bitter gourd (*Momordica charantia* L.). *Microb. Pathog.* 128, 82–89. doi: 10.1016/j.micpath.2018.12.036

Martínez-Zubiaur, Y., Fiallo-Olivé, E., Carrillo-Tripp, J., and Rivera-Bustamante, R. (2008). First report of tomato chlorosis virus infecting tomato in single and mixed infections with tomato yellow leaf curl virus in Cuba. *Plant Dis.* 92:836. doi: 10.1094/PDIS-92-5-0836C

Méndez-Lozano, J., Torres-Pacheco, I., Fauquet, C. M., and Rivera-Bustamante, R. F. (2003). Interactions between geminiviruses in a natural-ly occurring mixture: Pepper huasteco virus and Pepper golden mosaic virus. *Phytopathology* 93, 270-277. doi: 10.1094/PHYTO.2003.93.3.270

Mnari-Hattab, M., Zammouri, S., Belkadhi, M., Doña, D. B., Ben Nahia, E., and Hajlaoui, M. (2015). First report of tomato leaf curl New Delhi virus infecting cucurbits in Tunisia. *New Dis. Rep.* 31, 21–0588. doi: 10.5197/j.2044-0588.2015.031.021

Moriones, E., Praveen, S., and Chakraborty, S. (2017). Tomato leaf curl New Delhi virus: an emerging virus complex threatening vegetable and fiber crops. *Viruses* 9:264. doi: 10.3390/v9100264

Navas-Castillo, J., Fiallo-Olivé, E., and Sánchez-Campos, S. (2011). Emerging virus diseases transmitted by whiteflies. *Ann. Rev. Phytopathol.* 49, 219-48. doi: 10.1146/annurev-phyto-072910-095235

Orfanidou, C. G., Malandraki, I., Beris, D., Kektsidou, O., Vassilakos, N., Varveri, C., et al. (2019). First report of tomato leaf curl New Delhi virus in zucchini crops in Greece. *J. Plant Pathol.* 101:799. doi: 10.1007/s42161-019-00265-y

Padidam, M., Beachy, R. N., and Fauquet, C. M. (1995). Classification and identification of geminiviruses using sequence comparisons. *J. Gen. Virol.* 76, 249–263. doi: 10.1099/0022-1317-76-2-249

Panno, S., Iacono, G., Davino, M., Marchione, S., Zappardo, V., Bella, P., et al. (2016). First report of tomato leaf curl New Delhi virus affecting zucchini squash in an important horticultural area of southern Italy. *New Dis. Rep.* 33:6. doi: 10.5197/j.2044-0588.2016.033.006

Panno, S., Troiano, E., Luigi, M., Caruso, A. G., Mangli, A., Vatrano, T., et al. (2019). Tomato leaf curl New Delhi virus: an emerging pathogen that undermines the cultivation of zucchini squash in Italy. *Plant Pathol.* 68, 601–608. doi: 10.1111/ppa.12978

Parrella, G., Nappo, A. G., Manco, E., Greco, B., and Giorgini, M. (2014). Invasion of the Q2 mitochondrial variant of Mediterranean *Bemisia tabaci* in southern Italy: possible role of bacterial endosymbionts. *Pest Manag. Sci.* 70, 1514–1523. doi: 10.1002/ps.3686

Parrella, G., Scassillo, L., Crescenzi, A., and Nappo, A. G. (2006). Typing of tomato yellow leaf curl viruses and their vector in Italy. *Commun. Agric. Appl. Biol. Sci.* 71, 1229–1236.

Parrella, G., Scassillo, L., and Giorgini, M. (2012). Evidence for a new genetic variant in the *Bemisia tabaci* species complex and the prevalence of the biotype Q in southern Italy. *J. Pest. Sci.* 85, 227–238. doi: 10.1007/s10340-012-0417-2

Parrella, G., Sorrentino, D., Crescenzi, A., and Agosteo, G. E. (2005). Epidemics of TYLCSV and TYLCV in tomato crops in Calabria (Southern Italy). *Acta Hortic.* 789, 141–145. doi: 10.17660/ActaHortic.2008.789.19

Parrella, G., Troiano, E., Formisano, G., Accotto, G., and Giorgini, M. (2018). First report of tomato leaf curl New Delhi virus associated with severe mosaic of pumpkin in Italy. *Plant Dis.* 102:459. doi: 10.1094/PDIS-07-17-0940-PDN

Pérez-Padilla, V., Fortes, I. M., Romero-Rodríguez, B., Arroyo-Mateos, M., Castillo, A. G., Moyano, C., et al. (2020). Revisiting seed transmission of the type strain of Tomato yellow leaf curl virus in tomato plants. *Phytopathology* 110, 121–129. doi: 10.1094/PHYTO-07-19-0232-FI

Rivarez, M. P. S., Vučurović, A., Mehle, N., Ravnikar, M., and Kutnjak, D. (2021). Global advances in tomato virome research: current status and the impact of high-throughput sequencing. *Front. Microbiol.* 12:671925. doi: 10.3389/fmicb.2021.671925

Ruiz, L., Simon, A., Velasco, L., and Janssen, D. (2017). Biological characterization of tomato leaf curl New Delhi virus from Spain. *Plant Pathol.* 66, 376–382. doi: 10.1111/ppa.12587

Sáez, C., Esteras, C., Martínez, C., Ferriol, M., Dhillon, N. P., López, C., et al. (2017). Resistance to tomato leaf curl New Delhi virus in melon is controlled by a major QTL located in chromosome 11. *Plant Cell Rep.* 36, 1571–1584. doi: 10.1007/s00299-017-2175-3

Sahu, P. P., Rai, N. K., Chakraborty, S., Singh, M., Chandrappa, P. H., Ramesh, B., et al. (2010). Tomato cultivar tolerant to tomato leaf curl New Delhi virus infection induces virus-specific short interfering RNA accumulation and defence-associated host gene expression. *Mol. Plant Pathol.* 11, 531–544. doi: 10.1111/j.1364-3703.2010.00630.x

Sangeetha, B., Malathi, V., Alice, D., Suganthy, M., and Renukadevi, P. (2018). A distinct seed-transmissible strain of tomato leaf curl New Delhi virus infecting chayote in India. *Virus Res.* 258, 81–91. doi: 10.1016/j.virusres.2018.10.009

Shafiq, M., Asad, S., Zafar, Y., Briddon, R. W., and Mansoor, S. (2010). Pepper leaf curl Lahore virus requires the DNA B component of tomato leaf curl New Delhi virus to cause leaf curl symptoms. *Virol. J.* 7:367. doi: 10.1186/1743-422X-7-367

Sharma, J., Lager, P., and Kumar, Y. (2021). First report of tomato leaf curl New Delhi virus infecting *Ricinus communis*. *New Dis. Rep.* 44:e12053. doi: 10.1002/ndr2.12053

Simón, A., Ruiz, L., García, C., and Janssen, D. (2017). Identification of TYLCD-associated begomoviruses and ToLCNDV-ES co-infections in Spain. 15th congress of the Mediterranean Phytopathological Union, June 20-23, Córdoba, Spain. *Phytopathol. Mediterr.* 56:356.

Simón, A., Ruiz, L., Velasco, L., and Janssen, D. (2018). Absolute quantification of tomato leaf curl New Delhi virus Spain strain, ToLCNDV-ES: virus accumulation in a host-specific manner. *Plant Dis.* 102, 165–171. doi: 10.1094/PDIS-06-17-0840-RE

Singh, A. K., Kushwaha, N., and Chakraborty, S. (2016). Synergistic interaction among begomoviruses leads to the suppression of host defense-related gene expression and breakdown of resistance in chilli. *Appl. Microbiol. Biotechnol.* 100, 4035–4049. doi: 10.1007/s00253-015-7279-5

Singh, R., Rai, N., Singh, M., Saha, S., and Singh, S. (2015). Detection of tomato leaf curl virus resistance and inheritance in tomato (*Solanum lycopersicum* L.). *J. Agric. Sci.* 153, 78–89. doi: 10.1017/S0021859613000932

Sivalingam, P. N., and Varma, A. (2012). Role of betasatellite in the pathogenesis of a bipartite begomovirus affecting tomato in India. *Arch. Virol.* 157, 1081–1092. doi: 10.1007/s00705-012-1261-7

Srivastava, A., Kumar, S., Jaidi, M., Raj, S., and Shukla, S. (2016). First report of tomato leaf curl New Delhi virus on opium poppy (*Papaver somniferum*) in India. *Plant Dis.* 100:232. doi: 10.1094/PDIS-08-15-0883-PDN

Suruthi, V., Nakkeeran, S., Renukadevi, P., Malathi, V., and Rajasree, V. (2018). Evidence of seed transmission of dolichos yellow mosaic virus, a begomovirus infecting lablab-bean in India. *Virus Dis.* 29, 506–512. doi: 10.1007/s13337-018-0494-9

Urbino, C., Thébaud, G., Granier, M., Blanc, S., and Peterschmitt, M. (2008). A novel cloning strategy for isolating, genotyping and phenotyping genetic variants of geminiviruses. *Virol. J.* 5, 135–110. doi: 10.1186/1743-422X-5-135

Varma, A., Mandal, B., and Singh, M. K. (2011). "Global emergence and spread of whitefly (Bemisia tabaci) transmitted geminiviruses," in *The Whitefly, Bemisia tabaci (Homoptera:Aleyrodidae) Interaction with Geminivirus-Infected Host Plants.* ed. Thompson (Berlin: Springer), 205–292.

Venkataravanappa, V., Reddy, C. L., Saha, S., and Reddy, M. K. (2018). Recombinant tomato leaf curl New Delhi virus is associated with yellow vein mosaic disease of okra in India. *Physiol. Mol. Plant Pathol.* 104, 108–118. doi: 10.1016/j.pmpp.2018.10.004

Vo, T. T. B., Lal, A., Ho, P. T., Troiano, E., Parrella, G., Kil, E.-J., et al. (2022). Different infectivity of Mediterranean and Southern Asian tomato leaf curl New Delhi Virus Isolates in cucurbit crops. *Plants* 11:704. doi: 10.3390/plants11050704

Wang, B., Duan, H., Chong, P., Su, S., Shan, L., Yi, D. W., et al. (2020). Systematic selection and validation of suitable reference genes for quantitative real-time PCR normalization studies of gene expression in *Nitraria tangutorum*. *Sci. Rep.* 10:15891. doi: 10.1038/s41598-020-73059-3

Wei, L., Xiaobin, S., Xin, T., Yu, Z., Deyong, Z., Xuguo, Z., et al. (2018). Molecular identification of Tomato chlorosis virus and tomato yellow leaf curl virus in Yunnan Province. *Acta Hortic. Sin.* 45:552. doi: 10.16420/j.issn.0513-353x.2017-0735

Yamamoto, H., Wakita, Y., Kitaoka, T., Fujishiro, K., Kesumawati, E., and Koeda, S. (2021). Southeast Asian isolate of the tomato leaf curl New Delhi virus shows higher pathogenicity against tomato and cucurbit crops compared to that of the Mediterranean isolate. *Hort. J.* 90, 314–325. doi: 10.2503/hortj.UTD-269

Zaidi, S. S.-E.-A., Martin, D. P., Amin, I., Farooq, M., and Mansoor, S. (2017). Tomato leaf curl New Delhi virus: a widespread bipartite begomovirus in the territory of monopartite begomoviruses. *Mol. Plant Pathol.* 18, 901–911. doi: 10.1111/mpp.12481

Zerbini, F. M., Briddon, R. W., Idris, A., Martin, D. P., Moriones, E., Navas-Castillo, J., et al. (2017). ICTV virus taxonomy profile: geminiviridae. *J. Gen. Virol.* 98, 131–133. doi: 10.1099/jgv.0.000738

Frontiers in
Plant Science

Cultivates the science of plant biology and its applications

The most cited plant science journal, which advances our understanding of plant biology for sustainable food security, functional ecosystems and human health.

Discover the latest Research Topics

See more →

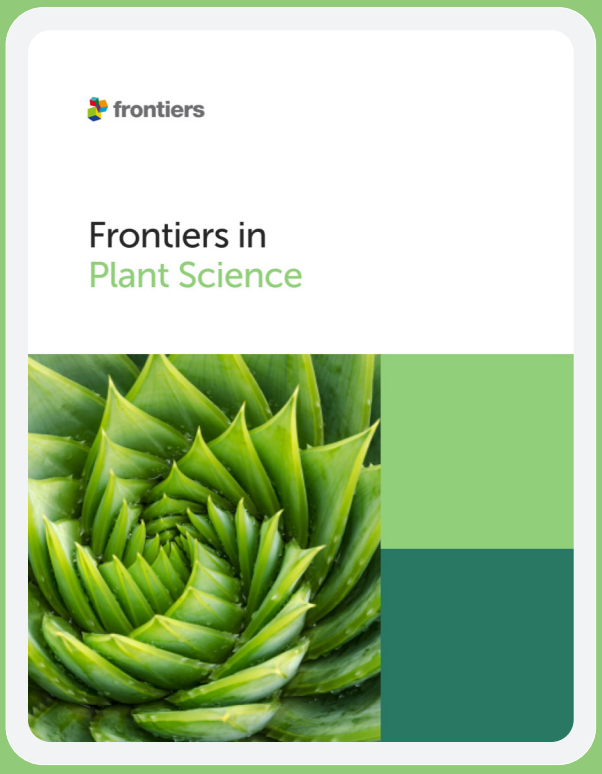

Frontiers

Avenue du Tribunal-Fédéral 34
1005 Lausanne, Switzerland
frontiersin.org

Contact us

+41 (0)21 510 17 00
frontiersin.org/about/contact